Andrey A. Radionov · Dmitrii V. Ulrikh ·
Svetlana S. Timofeeva ·
Vladimir N. Alekhin ·
Vadim R. Gasiyarov *Editors*

Proceedings of the 5th International Conference on Construction, Architecture and Technosphere Safety

ICCATS 2021

Springer

Lecture Notes in Civil Engineering

Volume 168

Lecture Notes in Civil Engineering (LNCE) publishes the latest developments in Civil Engineering - quickly, informally and in top quality. Though original research reported in proceedings and post-proceedings represents the core of LNCE, edited volumes of exceptionally high quality and interest may also be considered for publication. Volumes published in LNCE embrace all aspects and subfields of, as well as new challenges in, Civil Engineering. Topics in the series include:

- Construction and Structural Mechanics
- Building Materials
- Concrete, Steel and Timber Structures
- Geotechnical Engineering
- Earthquake Engineering
- Coastal Engineering
- Ocean and Offshore Engineering; Ships and Floating Structures
- Hydraulics, Hydrology and Water Resources Engineering
- Environmental Engineering and Sustainability
- Structural Health and Monitoring
- Surveying and Geographical Information Systems
- Indoor Environments
- Transportation and Traffic
- Risk Analysis
- Safety and Security

To submit a proposal or request further information, please contact the appropriate Springer Editor:

– Pierpaolo Riva at pierpaolo.riva@springer.com (Europe and Americas);
– Swati Meherishi at swati.meherishi@springer.com (Asia - except China, and Australia, New Zealand);
– Wayne Hu at wayne.hu@springer.com (China).

All books in the series now indexed by Scopus and EI Compendex database!

More information about this series at https://link.springer.com/bookseries/15087

Andrey A. Radionov · Dmitrii V. Ulrikh ·
Svetlana S. Timofeeva · Vladimir N. Alekhin ·
Vadim R. Gasiyarov

Editors

Proceedings of the 5th International Conference on Construction, Architecture and Technosphere Safety

ICCATS 2021

Springer

Editors
Andrey A. Radionov
South Ural State University
Chelyabinsk, Russia

Dmitrii V. Ulrikh
South Ural State University
Chelyabinsk, Russia

Svetlana S. Timofeeva
Irkutsk National Research State Technical
University
Irkutsk, Russia

Vladimir N. Alekhin
Ural Federal University named after
the first President of Russia B. N. Yeltsin
Ekaterinburg, Russia

Vadim R. Gasiyarov
South Ural State University
Chelyabinsk, Russia

Preface

The International Conference on Construction, Architecture and Technosphere Safety (ICCATS-2021) was organized by South Ural State University (national research university), Chelyabinsk, Irkutsk National Research Technical University, Irkutsk, and Ural Federal University named after the first President of Russia B. N. Yeltsin, Yekaterinburg, on September 5–11, 2021.

The conference program encompassed a wide range of topics and was divided into four parts: Industrial and Civil Engineering; Special and Unique Structures Construction; Urban Engineering and Planning; Engineering Structure Safety, Environmental Engineering and Environmental Protection.

The spread of the coronavirus COVID-19 made adjustments to our lives in this year, including the organization of our conference. Participants could take part in the conference as in a traditional face-to-face format and as format of video conference remotely.

The international program committee has selected totally 51 papers for publishing in Lecture Notes in Civil Engineering (Springer International Publishing AG).

On behalf of the organizing committee, we express appreciation to our colleagues who participated in the review procedure of the papers and especially thank members of international program committee, who helped us to organize this conference.

We express our gratitude to the participants for the active work at the conference sections and look forward to meeting at ICCATS-2022 next September in Sochi, Russia.

Chelyabinsk, Russia	Prof. Andrey A. Radionov
Chelyabinsk, Russia	Prof. Dmitriy V. Ulrikh
Irkutsk, Russia	Prof. Svetlana S. Timofeeva
Ekaterinburg, Russia	Prof. Vladimir N. Alekhin

Contents

**Engineering Structure Safety, Environmental Engineering and
Environmental Protection**

Industrial and Civil Engineering

Stability Analysis Method of Flat Rod Systems, Based on Forces Approximations

Yu. Ya. Tyukalov(✉)

Polytechnic Institute, Vyatka State University (PI of VSU), 36, Moskovskaya street, Kirov 610000, Russia

Abstract. The stability problems solution of plane rod systems by the finite element method based on the stresses is presented. The proposed method is based on a combination of the additional energy functional and the possible displacements principle. The algebraic equilibrium equations are included in the functional using Lagrange multipliers, which are the displacements of nodes. To solve stability problems, the functional considering the additional energy from longitudinal deformations arising from the bending of the rods. The buckling shape over the finite element region is approximated by a linear function. Two variants of internal forces approximations in the finite element length are considered: linear and piecewise constant. On the example of straight rods stability analysis, a circular arch, and a two-story frame for various finite element meshes, it is shown that the use of piecewise constant approximations of internal forces allows one to obtain the lower boundary of the critical forces. When using linear approximations of internal forces, the solution converges to the critical forces exact value from above and gives an upper bound of critical forces.

Keywords: Stability · Rod system · Forces approximations · Functional

1 Introduction

Determination of the critical load for various structures is the most important task in their research and design [1–11]. Many analytical and numerical methods have been developed to solve stability problems [12–18]. The widely used is the most universal finite element method, formulated since the Lagrange functional. When building a structure model using finite elements obtained with displacements approximations, we always use limited number of freedom degrees. As consequence, this method allows you to calculate critical load approximate value, which will be greater than exact value. In papers [19–28] there are presented the solutions of structural mechanic problems by the finite element method, which based on approximations of forces or stresses. The proposed method is based on a combination of the additional energy functional and the possible displacements principle and is an alternative to the finite element method which use displacements approximations.

2 Methods

Let us consider the application of the finite element method to solve the statics problems of plane rod systems (Fig. 1). The additional energy functional, in the absence of the specified displacements of nodes, will have the following form:

$$
\Pi^c = \sum_{i=1}^{n} \Pi \sum_{i}^{c} = \sum_{i=1}^{n} \left(\frac{1}{2} \int_0^{l_i} \frac{M(x)^2}{EI_i} dx + \frac{1}{2} \int_0^{l_i} \frac{N(x)^2}{EA_i} dx \right). \tag{1}
$$
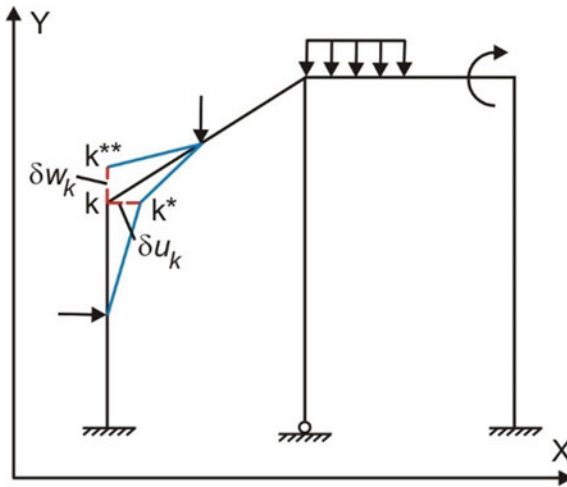
Fig. 1 Flat rod system. Possible displacements of node k

EI_i, EA_i are flexural and longitudinal stiffness of a rod; $M(x), N(x)$ are bending moment and longitudinal force; l_i is rod length; n is rods number.

Let us consider two variants of internal forces approximations along the finite element length: linear or piecewise constant (Fig. 2).
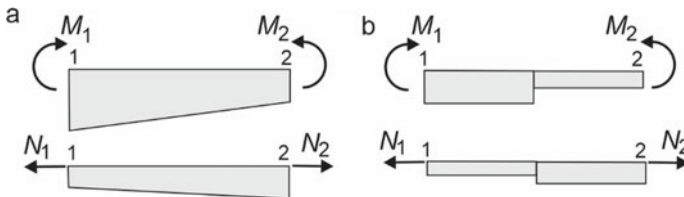
Fig. 2 Approximations of internal forces along the finite element length: **a** linear; **b** piecewise constant

Using the approximations of internal forces, we obtain an expression for the finite element additional energy in matrix form:

$$\Pi_i^c = \frac{1}{2} S_i^T D_i S_i, \quad S_i^T = \begin{pmatrix} M_1 & M_2 & N_1 & N_2 \end{pmatrix}. \tag{2}$$

$$D_i^L = \begin{bmatrix} \frac{l_i}{3EI_i} & \frac{l_i}{6EI_i} & 0 & 0 \\ \frac{l_i}{6EI_i} & \frac{l_i}{3EI_i} & 0 & 0 \\ 0 & 0 & \frac{l_i}{3EA_i} & \frac{l_i}{6EA_i} \\ 0 & 0 & \frac{l_i}{6EA_i} & \frac{l_i}{3EA_i} \end{bmatrix}, \quad D_i^C = \begin{bmatrix} \frac{l_i}{2EI_i} & 0 & 0 & 0 \\ 0 & \frac{l_i}{2EI_i} & 0 & 0 \\ 0 & 0 & \frac{l_i}{2EA_i} & 0 \\ 0 & 0 & 0 & \frac{l_i}{2EA_i} \end{bmatrix}. \tag{3}$$

S_i is the internal nodal forces vector of the finite element; S is the nodal forces vector for the entire system. The finite element flexibility matrix is D_i. For the case of linear approximations, this matrix is D_i^L and for piecewise constant approximations, it is D_i^C. Note that unknown nodal forces are assumed to be independent for each finite element. Therefore, the global vector size of unknown nodal forces will be *4n*. The global flexibility matrix for the entire system, and its inverse, will have a block-diagonal form:

$$D = \begin{bmatrix} D_1 & & & \\ & D_2 & & \\ & & \ddots & \\ & & & D_n \end{bmatrix}, \quad D^{-1} = \begin{bmatrix} D_1^{-1} & & & \\ & D_2^{-1} & & \\ & & \ddots & \\ & & & D_n^{-1} \end{bmatrix}. \tag{4}$$

Using (4), we obtain the expression for the entire system additional energy:

$$\Pi^c = \frac{1}{2} S^T D S. \tag{5}$$

Let us consider the nodes possible linear displacements and, in accordance with the possible displacements principle, compose the equilibrium equations for the finite element in the local coordinate system $X_1 0 Y_1$ (Figs. 3, 4).
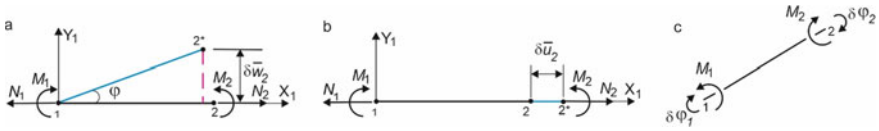
Fig. 3 Possible displacements of the node 2 in the local coordinate system: **a** transverse; **b** longitudinal; **c** in the form of nodal sections rotations

We write the possible displacements principle in the following form:

$$\sum_{i \in \Omega_i} \left(\delta \overline{U}_{i,j} + \delta \overline{V}_{i,j} \right) = 0, \quad j = \delta w, \delta u, \delta \varphi. \tag{6}$$

Ω_i is the set of finite elements adjacent to node *i*; δw, δu, $\delta \varphi$ are possible displacements of node *i*; $\delta \overline{U}_{i,j}$ is the finite element deformations energy with a possible displacement of the *i* node in the direction *j*; $\delta \overline{V}_{i,j}$ is the possible work of external forces with a
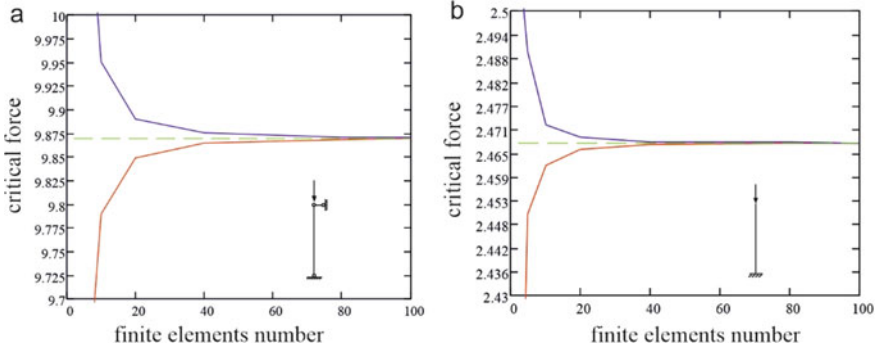
Fig. 4 a Simple hinge supported rod; **b** cantilever rod

possible displacement of the *i* node in the direction *j*. The nodes equations equilibrium can be written in the following matrix form:

$$F - LS = 0. \tag{7}$$

The matrix L can be called the local equilibrium matrix. F is the global vector of external forces. Using the Lagrange multipliers, we include the equilibrium Eqs. (7) in the functional (5):

$$\Pi^c = \frac{1}{2}S^T D S + y^T (F - L S). \tag{8}$$

When solving stability problems, it is necessary add to functional an additional energy of longitudinal deformations, arising due to the rod bending. Longitudinal deformations due to bending are determined by the expression:

$$\varepsilon_w = \frac{1}{2}\left(\frac{dw}{dx}\right)^2. \tag{9}$$

The transverse displacements function of a finite element axis at loss of stability, in the local coordinate system, will be approximated by the linear function.

$$w(x) = \overline{w}_1\left(1 - \frac{x}{l_i}\right) + \overline{w}_2\frac{x}{l_i}. \tag{10}$$

$\overline{w}_1, \overline{w}_2$ are transverse displacements of finite element nodes in the local coordinate system.

Using (10), the additional energy functional for solving the stability problem will have the following form:

$$\Pi^c = \frac{1}{2}S^T D S + \frac{1}{2}\lambda y^T G y - y^T L S. \tag{11}$$

The matrix G is formed from matrices of finite elements:

$$G_i = \frac{(N_1 + N_2)}{2l_i} \begin{bmatrix} \cos^2\varphi & -\sin\varphi\cos\varphi & 0 & -\cos^2\varphi & \sin\varphi\cos\varphi & 0 \\ -\sin\varphi\cos\varphi & \sin^2\varphi & 0 & \sin\varphi\cos\varphi & -\sin^2\varphi & 0 \\ 0 & 0 & 0 & 0 & 0 & 0 \\ -\cos^2\varphi & \sin\varphi\cos\varphi & 0 & \cos^2\varphi & -\sin\varphi\cos\varphi & 0 \\ \sin\varphi\cos\varphi & -\sin^2\varphi & 0 & -\sin\varphi\cos\varphi & \sin^2\varphi & 0 \\ 0 & 0 & 0 & 0 & 0 & 0 \end{bmatrix}. \quad (12)$$

N_1, N_2 are the longitudinal forces at the beginning and end of the finite element. In expression (11), the parameter λ is introduced that can be interpreted as safety factor of stability. The minimum of functional (35) corresponds to the existence of a deflected equilibrium form of the structure. Equating the functional derivatives with respect to vectors S and y, we obtain the matrix equations system:

$$-Ky + \lambda Gy = 0, \quad K = LD^{-1}L^T. \quad (13)$$

To determine the critical parameter value, we use the reverse iteration method:

$$\begin{cases} \text{introduce vector } y_0, \ i = 0; \\ \text{cycle } i = i + 1; \\ Ky_i = Gy_{i-1}; \\ y_{max} = \max|y_{i,j}|, \ j = 1..n; \\ \lambda_{cr,i} = \frac{1}{y_{max}}; \\ y_i = \frac{1}{y_{max}} y_i; \\ y_i = \frac{y_i + y_{i-1}}{2}; \\ \text{end of cycle, if } \frac{|\lambda_{cr,i} - \lambda_{cr,i-1}|}{\lambda_{cr,i}} \le \varepsilon. \end{cases} \quad (14)$$

In (14) y_{max} is the element maximum modulus of the nodal displacement vector y_i. Value of ε determines the accuracy of the critical parameter calculating.

3 Result and Discussion

According to the method proposed above, the critical forces for straight rods were determined for various options for ends fixing. To simplify the analysis, the bending stiffness and the rods length were taken equal to one.

The calculation results are shown in Figs. 4 and 5, where the horizontal dashed lines indicate the critical forces exact values. The red line corresponds to piecewise constant approximations of the internal forces, the blue line show to linear ones. The graphs in Figs. 4 and 5 are plotted according to the values given in Table 1.

Also, calculation of stability for the circular arch with hinged fixed supports (Fig. 6) was performed. The load on the arch was assumed to be uniformly distributed and directed radially. Arch radius is 4 m., $q = 1$ kN/m^2, $EA = 1000$ kN, $EI = 10$ kN/m^2. The stability safety factor was determined by dividing the arch into 8.16, 32 and 64 finite elements.
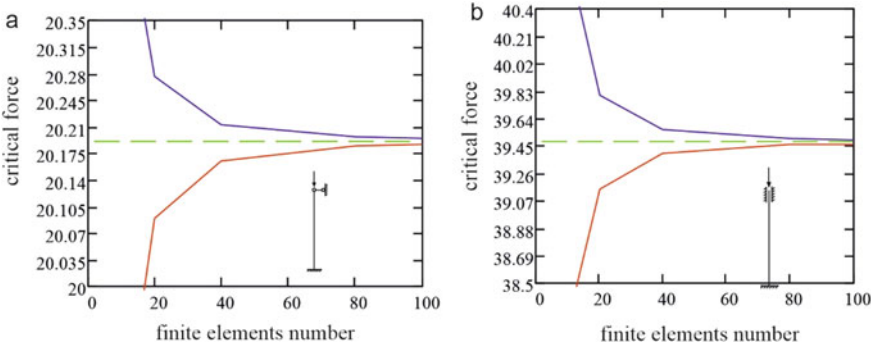
Fig. 5 **a** The rod with clamped end and simply hinges support; **b** the rod with clamped ends

The calculation results for the circular arch are shown in Fig. 7. Blue line (numeral is 1) corresponds to internal forces linear approximation, red line (numeral is 2)—piecewise constant, green line (numeral is 3)—FEM calculation results in displacements according to LIRA—SAPR program.

Analysis of the calculation results shows that the use of piecewise constant approximations of internal forces leads to the convergence of the critical forces (loads) calculated values to exact values strictly from below. That allows you to obtain a solution with the margin of construction stability. At the same time, in comparison with the finite element method in displacements, it is necessary to use a finer mesh. It should be borne in mind that the solution in displacements is more "rigid" and converges to the exact value from above, as in the case of using linear approximations of internal forces according to the proposed method. It is known that when the mesh is refined, the stresses in the region of the finite element will tend to constant values, therefore, for the convergence of solutions, it is necessary to provide the representation of constant values for the corresponding stresses. This condition is performed when we use the proposed method of stability analysis. Functional (8) can be formed to solve stability problems for plates, shells, and arbitrary combined systems.

4   Conclusion

For the problems of plane rod systems stability, the solving method, based on the additional energy functional and the possible displacements principle, is proposed. On the example of straight rods stability analysis for various finite element meshes, it is shown that the use of piecewise constant approximations of internal forces allows one to obtain the lower boundary of the critical forces.

When using linear approximations of internal forces, the solution converges to the critical forces exact value from above and gives an upper bound of critical forces. Using two variants of forces approximation makes it possible to determine the boundaries of the interval in which the critical force exact value is located and to estimate the approximate solution.

Table 1 Critical forces for the straight rods

Figure	Approximation	Finite elements number								Exact value
		2	4	5	10	20	40	80	100	
Figure 4a	Linear	12.0	10.4	10.2	9.951	9.8999	9.8746	9.8709	9.8704	9.8696
	Piecewise constant	8.0	9.38	9.55	9.789	9.8493	9.8645	9.8683	9.8688	
Figure 4b	Linear	3.0	2.50	2.49	2.472	2.4687	2.4677	2.4675	2.4675	2.4674
	Piecewise constant	2.0	2.41	2.45	2.462	2.4661	2.4671	2.4673	2.4674	
Figure 5a	Linear	27.4	22.4	21.6	20.53	20.275	20.212	20.196	20.194	20.191
	Piecewise constant	12.0	17.8	18.6	19.79	20.089	20.165	20.184	20.187	
Figure 5b	Linear	48.0	48.0	44.9	40.79	39.804	39.560	39.498	39.491	39.478
	Piecewise constant	16.0	32.0	34.6	38.20	39.155	39.397	39.458	39.465	
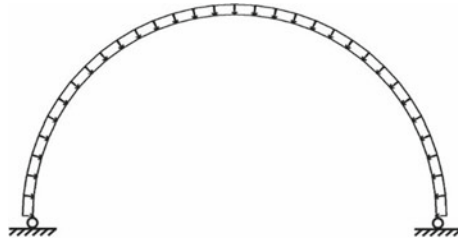
Fig. 6 The circular arch
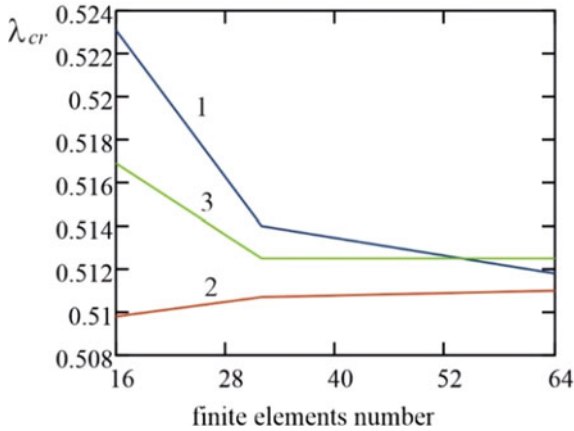
Fig. 7 Safety factors of stability λ_{cr} for the circular arch

References

1. Zhu ZC, Luo YF, Xiang Y (2018) Global stability analysis of spatial structures based on Eigen-stiffness and structural Eigen-curve. J Constr Steel Res 141:226–240. https://doi.org/10.1016/j.jcsr.2017.11.003
2. Yu M, Xu H, Ye J, Chi Y (2018) A unified interaction equation for strength and global stability of solid and hollow concrete-filled steel tube columns under room and elevated temperatures. J Constr Steel Res 148:304–313. https://doi.org/10.1016/j.jcsr.2018.05.026
3. Zhao Y-P, Li L, Jin M (2020) Stability of the bifurcation point and the initial post-buckling of an elastic column with a flexible support. Int J Solids Struct 193–194:593–600. https://doi.org/10.1016/j.ijsolstr.2020.02.038
4. Serpik IN (2017) Flat rod systems : optimization with overall stability control. 8:181–192. https://doi.org/10.18720/MCE.76.16
5. Polit O, Merzouki T, Ganapathi M (2018) Elastic stability of curved nanobeam based on higher-order shear deformation theory and nonlocal analysis by finite element approach. Finite Elem Anal Des 146:1–15. https://doi.org/10.1016/j.finel.2018.04.002
6. Pezeshky P, Mohareb M (2018) Distortional lateral torsional buckling of beam-columns including pre-buckling deformation effects. Comput Struct 209:93–116. https://doi.org/10.1016/j.compstruc.2018.08.010

7. Pelayo F, López-Aenlle M, Ismael G, Fernández-Canteli A (2017) Buckling of multilayered laminated glass beams: Validation of the effective thickness concept. Compos Struct 169:2–9. https://doi.org/10.1016/j.compstruct.2017.01.040

8. Ma T, Xu L (2020) Shear deformation effects on stability of unbraced steel frames in variable loading. J Constr Steel Res 164:105811. https://doi.org/10.1016/j.jcsr.2019.105811

9. Liu Y, Hang Z, Zhang W et al (2020) Analytical solution for lateral-torsional buckling of concrete-filled tubular flange girders with torsional bracing. Adv Civ Eng 2020. https://doi.org/10.1155/2020/4340381

10. Li P, Liang C, Yuan J, Qiao K (2018) Stability of steel columns stiffened by stays and multiple crossarms. J Constr Steel Res 148:189–197. https://doi.org/10.1016/j.jcsr.2018.05.020

11. Lalin VV, Rybakov VA, Diakov SF et al (2019) The semi-shear theory of V.I. Slivker for the stability problems of thin-walled bars. Mag Civ Eng 87:66–79. https://doi.org/10.18720/MCE.87.6

12. Lalin V V, Dmitriev AN, Diakov SF (2019) Nonlinear deformation and stability of geometrically exact elastic arches. Mag Civ Eng 89:39–51. https://doi.org/10.18720/MCE.89.4

13. Khudayarov BA, Ruzmetov KS, Turaev FZ et al (2020) Numerical modeling of nonlinear vibrations of viscoelastic shallow shells. Eng Solid Mech 8:199–204. https://doi.org/10.5267/j.esm.2020.1.004

14. Karpov V V. (2019) Mixed form equations for ribbed shells of a general type and their solutions. PNRPUMechanics Bull 116–134. https://doi.org/10.15593/perm.mech/2019.2.09

15. Debski H, Rozylo P, Wysmulski P (2020) Stability and load-carrying capacity of short open-section composite columns under eccentric compression loading. Compos Struct 252:112716. https://doi.org/10.1016/j.compstruct.2020.112716

16. Batista M (2019) Stability of elastic column with spring supports at both clamped ends. Int J Solids Struct 169:72–80. https://doi.org/10.1016/j.ijsolstr.2019.04.009

17. Batista M (2015) On stability of elastic rod planar equilibrium configurations. Int J Solids Struct 72:144–152. https://doi.org/10.1016/j.ijsolstr.2015.07.024

18. Abdikarimov RA, Khudayarov B (2014) Dynamic stability of viscoelastic flexible plates of variable stiffness under axial compression. Int Appl Mech 50:389–398. https://doi.org/10.1007/s10778-014-0642-x

19. Tyukalov YY (2019) Calculation method of bending plates with assuming shear deformations. Mag Civ Eng 85:107–122. https://doi.org/10.18720/MCE.85.9

20. Tyukalov YY (2019) Equilibrium finite elements for plane problems of the elasticity theory. Mag Civ Eng 91:80–97. https://doi.org/10.18720/MCE.91.8

21. Tyukalov YY (2017) The functional of additional energy for stability analysis of spatial rod systems. Mag Civ Eng 70:18–32. https://doi.org/10.18720/MCE.70.3

22. Tyukalov YY (2018) Refined finite element of rods for stability calculation. Mag Civ Eng 79:54–65. https://doi.org/10.18720/MCE.79.6

23. Tyukalov YY (2019) Finite element model of Reisner's plates in stresses. Mag Civ Eng 5:61–78. https://doi.org/10.18720/MCE.89.6

24. Tyukalov YY (2018) Finite element models in stresses for plane elasticity problems. Mag Civ Eng 77:23–37. https://doi.org/10.18720/MCE.77.3

25. Tyukalov YY (2018) Finite element models in stresses for bending plates. Mag Civ Eng 82:170–190. https://doi.org/10.18720/MCE.82.16

26. Tyukalov YY (2019) Calculation of circular plates with assuming shear deformations. In: IOP conference series: materials science and engineering. https://doi.org/10.1088/1757-899X/687/3/033004

27. Tyukalov YY (2020) Method of plates stability analysis based on the moments approximations. Mag Civ Eng 95:90–103. https://doi.org/10.18720/MCE.95.9
28. Tyukalov YY (2018) Calculation of bending plates by finite element method in stresses. In: IOP conference series: materials science and engineering. https://doi.org/10.1088/1757-899X/451/1/012046

Dynamic Analysis of an Elastic Plate Resting on a Nonlinear Fractional-Order Viscoelastic Pasternak Foundation and Subjected to Moving Load

M. Shitikova$^{(\boxtimes)}$ and A. Krusser

Research Centre On Dynamics of Solids and Structures, Voronezh State Technical University, 84, 20-Letija Oktjabrja Str., Voronezh 394006, Russia
`mvs@vgasu.vrn.ru`

Abstract. The problem of the nonlinear vibrations of an elastic plate resting on a viscoelastic foundation subjected to moving load is becoming increasingly widespread nowadays. In the present paper, the damping features of the nonlinear viscoelastic foundation are described by the fractional derivative Pasternak-type standard linear solid model. Assuming that only two natural modes of vibrations strongly coupled by the internal resonance are excited, the method of multiple time scales in conjunction with the expansion of the fractional derivative in terms of a small parameter has been utilized for solving nonlinear governing equations of motion. The governing set of equations is obtained for determining nonlinear amplitudes and phases in the case of forced vibrations of the plate under concentrated load moving along the edge of the plate, when the internal resonance 1:1 is combined with the external resonance. The expressions for defining coefficients depending on the vibration mode numbers are presented for simply supported case of boundary conditions of the plate.

Keywords: Nonlinear vibrations · Viscoelastic foundation · Pasternak model · Fractional derivative · Moving load

1 Introduction

The dynamics of beams and plates resting on viscoelastic foundations have been investigated during the past several decades. In order to describe the interactions between constructions and foundation, various models have been proposed. The study of the behavior of a plate resting on a viscoelastic foundation subjected to moving load is becoming increasingly widespread nowadays. This problem could find many engineering applications, such as aircraft–runway interaction or vehicle–road interaction, pavement-foundation system, dynamics of the helipad system, ship deck (especially aircraft carriers), soil-foundation system of offshore structures, railway track system, reinforced warehouse floor, etc. [1].

The problem of dynamic response of the rectangular plate supported by viscoelastic foundations and subjected to moving loads has drawn much interest among researchers [2–9]. Thus, Wu et al. analyzed the dynamic responses of nonuniform rectangular Kirchhoff–Love plate with various boundary conditions subjected to different moving loads using the finite element method (FEM) [2]. Taheri and Ting used Green's function to develop an algorithm for analysis of the transient response of elastic plates on the linear viscoelastic foundation with arbitrary boundary conditions and subjected to moving loads [3]. Zaman et.al. modeled the pavement-foundation system in [4] by a series of thick plate elements supported by discrete springs and dashpots at the nodal points representing the viscoelastic foundation, in order to evaluate the dynamic response of concrete pavements subjected to moving aircraft loads. Li et al. investigated the dynamic response of a thin simply-supported (SSSS) plate on an integer-order viscoelastic foundation subjected to moving loads at changing velocities, using the modal superposition method [5]. The behavior of stiffened plate resting on the viscoelastic Kelvin-Voigt foundation subjected to moving loads is studied in [6] by cell-based smoothed three-node Mindlin plate element. A rectangular plate subjected to a concentrated moving load was considered in [7], in so doing the viscoelastic properties of the foundation were defined by the Kelvin–Voigt model of Winkler type. Luong et al. (2018) studied the dynamic response of a thick plate on a Kelvin-Voigt foundation subjected to moving load using Moving element method [8]. The dynamic response of functionally graded plate on a two-parameter viscoelastic Pasternak foundation subjected to moving harmonic load was analyzed in [9] by using the moving element method.

Nowadays, fractional derivative Winkler-type or Pasternak-type models of viscoelastic foundations are of great interest among researchers, due to the important role of the fractional calculus in dynamic problems of structural mechanics [10, 11]. In the literature there are several reports on the research of dynamic response of plates on the fractional viscoelastic foundations subjected to moving loads [1, 12, 13]. Thus, Wei et al. [12] analytically studied the dynamic behavior of a simply-supported plate on the fractional derivative Kelvin–Voigt viscoelastic foundation of Winkler-type, subjected to dynamic forces from railway vehicles. The numerical simulation results show that the vertical vibration levels of high-speed vehicle–track coupled system calculated with the fractional Kelvin–Voigt model for rail pads in the time domain are apparently higher than those calculated with the ordinary Kelvin–Voigt model. Nonlinear vibration of a plate on the generalized foundation driven by random excitation is investigated in [13]. The dynamic behavior of the thin plates resting on a fractional Kelvin-Voigt viscoelastic foundation with four types of boundary conditions subjected to a moving point load is investigated in [1]. The effects of the orders of derivative, foundation parameters, and the velocity or acceleration of the moving load on the dynamic response of the plate-foundation system are studied. The results show that the damping of the foundation system increases with increasing the order of the fractional derivative, which leads to a decrease in the dynamic response.

To the best of the author's knowledge, most of the research papers on the dynamic response of the plates on fractional viscoelastic foundations subjected to moving load are considered in the linear formulation of the problem. Although, nonlinear dynamic response of isotropic thin rectangular plate under step function loads is analyzed in

[14], but in this case foundation is considered to be elastic, described by the Winkler, Pasternak and nonlinear Winkler models. Thus, in the present paper, nonlinear vibrations of a rectangular simply supported plate under a moving point load, resting on a nonlinear viscoelastic Pasternak-type foundation, the damping features of which are described by the fractional derivative standard linear solid model, is studied for the case of the one-to-one internal resonance using the fractional derivative expansion method.

2 Problem Formulation

Let us consider nonlinear vibrations of a simply supported elastic plate in a viscoelastic medium, resting on a viscoelastic foundation (Fig. 1). The dynamic behaviour of the system is described by the von Karman equation in terms of the plate's lateral deflection $w = w(x, y, t)$ and the Airy's stress function ϕ:

$$D\nabla^4 w + \rho h \frac{\partial^2 w}{\partial t^2} - \frac{\partial^2 w}{\partial x^2}\frac{\partial^2 \phi}{\partial y^2} - \frac{\partial^2 w}{\partial y^2}\frac{\partial^2 \phi}{\partial x^2} + 2\frac{\partial^2 w}{\partial x \partial y}\frac{\partial^2 \phi}{\partial x \partial y}$$
$$= P\delta(x - g(t))\delta(y - 0.5b) - F_1 - F_2 \tag{1}$$

$$\nabla^4 \phi = Eh\left[\left(\frac{\partial w}{\partial x \partial y}\right)^2 - \frac{\partial^2 w}{\partial x^2}\frac{\partial^2 w}{\partial y^2}\right] \tag{2}$$
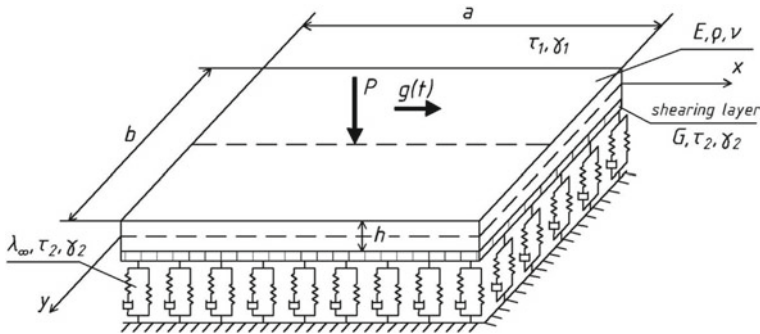
Fig. 1 Plate on a viscoelastic foundation subjected to a moving point load

where $D = Eh^3/12(1 - v^2)$ is the plate's cylindrical rigidity, E and v are the elastic modulus and Poisson's ratio of the plate's material, respectively, h and ρ are its thickness and density, t is the time, P is the magnitude of the force moving along the x-axis, δ is the Dirac delta function, $g(t)$ is the function which determines the instantaneous load positions, $g(t) = Vt$ or $g(t) = u_0 t \pm 0.5at^2$ for a load moving with constant velocity or acceleration/deceleration, respectively. Besides, $g(t)$ must satisfy condition $0 \leq g(t) \leq a$. Here, $F_1 = æ_1 \tau_1^{\gamma_1} D_{0+}^{\gamma_1} w$ is the damping force of the viscoelastic medium possessing the retardation time τ_1 and damping coefficient $æ_1$, which is modeled by

the viscoelastic Kelvin-Voigt model with the Riemann–Liouville derivative $D_{0+}^{\gamma_1}$ of the fractional order γ_1 $(0 < \gamma_1 \leq 1)$ [11, 15]

$$D_{0+}^{\gamma} x(t) = \frac{d}{dt} \int_0^t \frac{x(t - t')dt'}{\Gamma(1 - \gamma)t'^{\gamma}} \quad (0 < \gamma = \gamma_1 \leq 1) \tag{3}$$

and $\Gamma(1-\gamma)$ is the Gamma function, F_2 is the reaction force of the nonlinear viscoelastic foundation described by the fractional derivative Pasternak-type model

$$F_2 = \tilde{\lambda}w + kw^3 - G\,\tau_2^{\gamma_2}D_{0+}^{\gamma_2}\,\nabla^2 w \tag{4}$$

where $\nabla^2 = \partial^2/\partial x^2 + \partial^2/\partial y^2$ is the Laplace operator, G is the shear modulus, k is a nonlinear parameter, and τ_2 is the retardation time of the viscoelastic foundation.

Let us assume, following [16], that the compliance operator of a viscoelastic foundation is described by the standard linear solid model with the Riemann–Liouville fractional derivative D_{0+}^{γ} (3) with $\gamma = \gamma_2$:

$$\tilde{\lambda} = \lambda_{\infty}\left[1 - \nu_{\varepsilon}\frac{1}{1 + \tau_2^{\gamma}D_{0+}^{\gamma_2}}\right] \tag{5}$$

where λ_{∞} is the coefficient of instantaneous compliance of the foundation, $\nu_{\varepsilon} = \Delta\lambda\lambda_{\infty}^{-1}$, $\Delta\lambda = \lambda_{\infty} - \lambda_0$ is the defect of the compliance, i.e., the value characterizing the decrease in the compliance operator from its non-relaxed value to its relaxed value.

Considering a simply supported plate, the following boundary conditions should be added to the set of Eqs. (1) and (2) at each edge:

$$\text{at}\ \ x = 0\ \text{and}\ a, \quad w = \frac{\partial^2 w}{\partial x^2} = 0; \quad \text{at}\ y = 0\ \text{and}\ b, \quad w = \frac{\partial^2 w}{\partial y^2} = 0 \tag{6}$$

In order to identify the possibility of the occurrence of the internal resonance during nonlinear vibrations of a plate based on a viscoelastic foundation and to carry out its subsequent analysis, suppose that only two natural modes of vibrations with numbers $m_1 n_1$ и $m_2 n_2$ are excited. Then the deflection of the plate could be represented in the following form:

$$w(x, y, t) = x_1(t)\sin\frac{\pi m_1 x}{a}\sin\frac{\pi n_1 y}{b} + x_2(t)\sin\frac{\pi m_2 x}{a}\sin\frac{\pi n_2 y}{b}$$
$$= x_1(t)W_{m_1 n_1}(x, y) + x_2(t)W_{m_2 n_2}(x, y) \tag{7}$$

where $x_i(t)$ $(i = 1, 2)$ are generalized displacements, and $W_{m_i n_i}(x, y)$ are the eigen functions.

Substituting the proposed solution (7) in (2), taking into account the boundary conditions (6) and integrating with account for the orthogonality conditions of sines, we

obtain the stress function in the following form:

$$\phi(x, y, t) = Eh\left[\sum_i \sum_p \sum_q \phi_{ipq} X_{ip} Y_{iq} x_i(t)^2\right.$$

$$\left. + \frac{1}{4}\left(B^2 M_{11} N_{21} + C^2 M_{21} N_{11} - A^2 M_{11} N_{11} - D^2 M_{21} N_{21}\right) x_1(t) x_2(t)\right] \quad (8)$$

where $\xi = \frac{b}{a}$, $\eta_i = \frac{m_i}{n_i}$, $i = 1, 2$, $X_{ip} = \cos\frac{\pi p m_i x}{a}$, $Y_{iq} = \cos\frac{\pi q n_i y}{b}$, $\phi_{i02} = \frac{\xi^2 \eta_i^2}{32}$, $\phi_{i20} = \frac{1}{32\xi^2 \eta_i^2}$, $M_{1p} = \cos\frac{\pi p(m_1+m_2)x}{a}$, $M_{2p} = \cos\frac{\pi p(m_1-m_2)x}{a}$, $N_{1q} = \cos\frac{\pi q(n_1+n_2)y}{b}$, $N_{2q} = \cos\frac{\pi q(n_1-n_2)y}{b}$, $A^2 = \frac{\xi^2(m_1 n_2 - m_2 n_1)^2}{[(m_1+m_2)^2\xi^2+(n_1+n_2)^2]^2}$, $B^2 = \frac{\xi^2(m_1 n_2 + m_2 n_1)^2}{[(m_1+m_2)^2\xi^2+(n_1-n_2)^2]^2}$, $C^2 = \frac{\xi^2(m_1 n_2 + m_2 n_1)^2}{[(m_1-m_2)^2\xi^2+(n_1+n_2)^2]^2}$, $D^2 = \frac{\xi^2(m_1 n_2 - m_2 n_1)^2}{[(m_1-m_2)^2\xi^2+(n_1-n_2)^2]^2}$.

Substituting the assumed two-term expansion for the deflection function of the plate (7) and the corresponding stress function in the equation of motion of the plate (1) resting on the nonlinear viscoelastic Pasternak-type foundation yields the following set of nonlinear differential equations with respect to the generalized displacements:

$$\ddot{x}_1 + \omega_1^2 x_1 + \alpha_1 x_1^3 + \alpha_2 x_1 x_2^2 + \varepsilon^2 \mu_1 D_{0+}^{\gamma_1} x_1 - \varepsilon^2 \mu_2 \, \ni_\gamma^* \, (\tau_2^{\gamma_2}) x_1 + \varepsilon^2 \mu_3 D_{0+}^{\gamma_2} x_1 = P_1(t) \quad (9)$$

$$\ddot{x}_2 + \omega_2^2 x_2 + \alpha_3 x_2^3 + \alpha_4 x_2 x_1^2 + \varepsilon^2 \mu_1 D_{0+}^{\gamma_1} x_2 - \varepsilon^2 \mu_2 \, \ni_\gamma^* \, (\tau_2^{\gamma_2}) x_2 + \varepsilon^2 \mu_3 D_{0+}^{\gamma_2} x_2 = P_2(t) \quad (10)$$

where $P_i(t) = \frac{\int_0^a \int_0^b P\delta(x-g(t))\delta(y-0.5b)W_{m_i n_i}(x,y)dxdy}{\rho h \int_0^a \int_0^b [W_{m_i n_i}(x,y)]^2 dxdy}$, ε is a small dimensionless parameter, μ_i are finite values, $\varepsilon^2 \mu_1 = \frac{E_0 \tau_1^{\gamma_1}}{\rho h}$, $\varepsilon^2 \mu_2 = \frac{\lambda_\infty v_\varepsilon}{\rho h}$, $\varepsilon^2 \mu_3 = \frac{G \tau_2^{\gamma_2} \pi^2}{\rho h b^2}(\xi^2 m_i^2 + n_i^2)$, $\ni_\gamma^* (\tau_2^{\gamma_2}) = \frac{1}{1+\tau_2^{\gamma_2} D_{0+}^{\gamma_2}}$ is the Rabotnov dimensionless fractional operator [17], $\omega_i^2 = \Omega_i^2 + \frac{\lambda_\infty}{\rho h}$ $(i = 1,2)$ are vibration frequencies of the mechanical system "plate + viscoelastic foundation", and Ω_i^2 are the natural frequencies of the linear vibration of the plate defined as

$$\Omega_i^2 = \frac{Eh^2}{12\rho(1-v^2)}\nabla^4 W_{m_i n_i}(x,y) = \frac{E\pi^4 h^2}{12\rho(1-v^2)b^4}\left(\xi^2 m_i^2 + n_i^2\right)^2 \quad (11)$$

and α_i are the coefficients depending on the vibration mode numbers, defined as follows

$$\alpha_1 = -\frac{E}{2\rho ab}\pi^4 \int_0^a \int_0^b K_{11}^2 L_{11}^2 \left[\frac{m_1^4}{a^4}Y_{12} + \frac{n_1^4}{b^4}X_{12}\right]dxdy - \frac{9k}{16\rho h}, \quad (12)$$

$$\alpha_3 = -\frac{E}{2\rho ab}\pi^4 \int\limits_0^a \int\limits_0^b K_{21}^2 L_{21}^2 \left[\frac{m_2^4}{a^4}Y_{22} + \frac{n_2^4}{b^4}X_{22}\right] dxdy - \frac{9k}{16\rho h}, \tag{13}$$

$$\alpha_2 = -\frac{E}{2\rho ab}\pi^4 \int\limits_0^a \int\limits_0^b \left\{ K_{11}L_{11}\left[\frac{m_1^2 m_2^2}{a^4}Y_{22} + \frac{n_1^2 n_2^2}{b^4}X_{22}\right]\right.$$

$$+ \frac{2m_2^2}{a^2b^2}K_{21}L_{21}M_{11}\left[-A^2(n_1+n_2)^2 N_{11} + B^2(n_1-n_2)^2 N_{21}\right]$$

$$+ \frac{2m_2^2}{a^2b^2}K_{21}L_{21}M_{21}\left[-D^2(n_1-n_2)^2 N_{21} + C^2(n_1+n_2)^2 N_{11}\right]$$

$$+ \frac{2n_2^2}{a^2b^2}K_{21}L_{21}N_{11}\left[B^2(m_1-m_2)^2 M_{21}\right.$$

$$\left.-A^2(m_1+m_2)^2 M_{11}\right]$$

$$+ \frac{2n_2^2}{a^2b^2}K_{21}L_{21}N_{21}\left[-D^2(m_1-m_2)^2 \cos M_{11} + C^2(m_1+m_2)^2 M_{21}\right]$$

$$- \frac{4m_2 n_2}{a^2b^2}X_{21}Y_{21}(m_1+m_2)S_{11}\left[-A^2(n_1+n_2)T_{11} + B^2(n_1-n_2)T_{21}\right]$$

$$\left.- \frac{4m_2 n_2}{a^2b^2}X_{21}Y_{21}(m_1-m_2)S_{21}\left[-D^2(n_1-n_2)T_{21} + C^2(n_1+n_2)T_{11}\right]\right\}K_{11}L_{11}dxdy, \tag{14}$$

$$\alpha_4 = -\frac{E}{2\rho ab}\pi^4 \int\limits_0^a \int\limits_0^b \left\{ K_{21}L_{21}\left[\frac{m_1^2 m_2^2}{a^4}Y_{12} + \frac{n_1^2 n_2^2}{b^4}X_{12}\right]\right.$$

$$+ \frac{2m_1^2}{a^2b^2}K_{11}L_{11}M_{11}\left[-A^2(n_1+n_2)^2 N_{11} + B^2(n_1-n_2)^2 N_{21}\right]$$

$$+ \frac{2m_1^2}{a^2b^2}K_{11}L_{11}M_{21}\left[-D^2(n_1-n_2)^2 N_{21} + C^2(n_1+n_2)^2 N_{11}\right]$$

$$+ \frac{2n_1^2}{a^2b^2}K_{11}L_{11}N_{11}\left[B^2(m_1-m_2)^2 M_{21}\right.$$

$$\left.-A^2(m_1+m_2)^2 M_{11}\right]$$

$$+ \frac{2n_1^2}{a^2b^2}K_{11}L_{11}N_{21}\left[-D^2(m_1-m_2)^2 M_{21} + C^2(m_1+m_2)^2 M_{11}\right]$$

$$- \frac{4m_1 n_1}{a^2b^2}X_{11}Y_{11}(m_1+m_2)S_{11}\left[-A^2(n_1+n_2)T_{11} + B^2(n_1-n_2)T_{21}\right]$$

$$\left.- \frac{4m_1 n_1}{a^2b^2}X_{11}Y_{11}(m_1-m_2)S_{21}\left[-D^2(n_1-n_2)T_{21} + C^2(n_1+n_2)T_{11}\right]\right\}K_{21}L_{21}dxdy, \tag{15}$$

$$K_{ip} = \sin\frac{\pi p m_i x}{a}, \quad L_{iq} = \sin\frac{\pi q n_i y}{b}, \quad S_{1p} = \sin\frac{\pi p(m_1+m_2)x}{a}, \quad S_{2p} = \sin\frac{\pi p(m_1-m_2)x}{a},$$

$$T_{1q} = \sin\frac{\pi q(n_1+n_2)y}{b}, \quad T_{2q} = \sin\frac{\pi q(n_1-n_2)y}{b}.$$

Taking the property the delta function into account

$$\iint \delta(x - x_0)\delta(y - y_0)f(x, y)\, dxdy = f(x_0, y_0) \tag{16}$$

and considering the case of the force moving with a constant velocity V

$$P \iint \delta(x - Vt)\delta(y - b/2) \sin\left(\frac{\pi m_i x}{a}\right) \sin\left(\frac{\pi n_i y}{b}\right) dxdy = P \sin\left(\frac{\pi m_i Vt}{a}\right) \sin\left(\frac{\pi n_i}{2}\right) \tag{17}$$

the governing Eqs. (9) and (10) are reduced to the following form:

$$\ddot{x}_1 + \omega_1^2 x_1 + \alpha_1 x_1^3 + \alpha_2 x_1 x_2^2 + \varepsilon^2 \mu_1 D_{0+}^{\gamma_1} x_1 - \varepsilon^2 \mu_2 \, \partial_\gamma^* \, (\tau_2^{\gamma_2}) x_1 + \varepsilon^2 \mu_3 D_{0+}^{\gamma_2} x_1$$
$$- 4\varepsilon^3 f_1 \sin \omega_{f_1} t = 0 \tag{18}$$

$$\ddot{x}_2 + \omega_2^2 x_2 + \alpha_3 x_2^3 + \alpha_4 x_2 x_1^2 + \varepsilon^2 \mu_1 D_{0+}^{\gamma_1} x_2 - \varepsilon^2 \mu_2 \, \partial_\gamma^* \, (\tau_2^{\gamma_2}) x_2 + \varepsilon^2 \mu_3 D_{0+}^{\gamma_2} x_2$$
$$- 4\varepsilon^3 f_2 \sin \omega_{f_2} t = 0 \tag{19}$$

where $\omega_{f_i} = \frac{\pi m_i V}{a}$ are circular frequencies, and $\varepsilon^3 f_i = \frac{P}{ab\rho h} \sin\left(\frac{\pi n_i}{2}\right)$.

3 Method of Solution

In order to solve the set of Eqs. (18–19), the method of multiple time scales [18, 19] could be utilized, according to which the generalized displacements $x_i(t)$ could be represented via the following expansion in two time scales T_0 and T_2:

$$x_i(t) = \varepsilon X_{i1}(T_0, T_2) + \varepsilon^2 X_{i2}(T_0, T_2) + \varepsilon^3 X_{i3}(T_0, T_2) + \dots \tag{20}$$

where $T_n = \varepsilon^n t$ are new independent variables, among them: $T_0 = t$ is a fast scale characterizing motions with the natural frequencies, and $T_2 = \varepsilon t^2$ is a slow scale characterizing the modulation of the amplitudes and phases of the modes with nonlinearity.

Recall that the first and the second time derivatives, as well as fractional derivative could be expanded in terms of the new time scales, respectively, as follows [19]:

$$\frac{d}{dt} = D_0 + \varepsilon^2 D_2 + \dots, \quad \frac{d^2}{dt^2} = D_0^2 + 2\varepsilon^2 D_0 D_2 + \dots \tag{21}$$

$$D_+^\gamma = \left(\frac{d}{dt}\right)^\gamma = \left(D_0 + \varepsilon^2 D_2 + \dots\right)^\gamma = D_0^\gamma + \varepsilon^2 \gamma D_0^{\gamma-1} D_2 + \dots \tag{22}$$

where $D_0 = \partial/\partial T_0$ and $D_2 = \partial/\partial T_2$.

Expansion of the Rabotnov dimensionless fractional operator in a Taylor series in terms of a small parameter has the form [20]:

$$\mathfrak{s}_\gamma^* (\tau^\gamma) = \frac{1}{1 + \tau^\gamma D_{0+}^\gamma} = (1 + \tau^\gamma D_{0+}^\gamma)^{-1} = \left[1 + \tau^\gamma (D_0^\gamma + \varepsilon^2 \gamma D_0^{\gamma-1} D_2)\right]^{-1}$$

$$= (1 + \tau^\gamma D_0^\gamma)^{-1} - \varepsilon^2 (1 + \tau^\gamma D_0^\gamma)^{-2} \tau^\gamma \gamma D_0^{\gamma-1} D_2 + ... \tag{23}$$

Substituting expansion (20) with account for relationships (21–23), after equating the coefficients at like powers of ε to zero, we are led to the following set of recurrence equations to various orders for the case of force driven vibrations under moving load:

to order ε

$$D_0^2 X_{11} + \omega_1^2 X_{11} = 0 \tag{24}$$

$$D_0^2 X_{21} + \omega_2^2 X_{21} = 0 \tag{25}$$

to order ε^3

$$D_0^2 X_{13} + \omega_1^2 X_{13} = -2D_0 D_2 X_{11} - \left(\overline{\mu}_1 D_0^{\gamma_1} - \overline{\mu}_2 (1 + \tau_2^{\gamma_2} D_0^{\gamma_2})^{-1} + \overline{\mu}_3 D_0^{\gamma_2}\right) X_{11}$$
$$- \alpha_1 X_{11}^3 - \alpha_2 X_{11} X_{21}^2 + 4f_1 \sin(\omega_{f_1} T_0) \tag{26}$$

$$D_0^2 X_{23} + \omega_2^2 X_{23} = -2D_0 D_2 X_{21} - \left(\overline{\mu}_1 D_0^{\gamma_1} - \overline{\mu}_2 (1 + \tau_2^{\gamma_2} D_0^{\gamma_2})^{-1} + \overline{\mu}_3 D_0^{\gamma_2}\right) X_{21}$$
$$- \alpha_3 X_{21}^3 - \alpha_4 X_{21} X_{11}^2 + 4f_2 \sin(\omega_{f_2} T_0) \tag{27}$$

where $\overline{\mu}_i = \frac{\mu_i}{\rho h}$ $(i = 1, 2)$.

The solution of linear Eqs. (24–25) has the form

$$X_{j1} = A_j(T_2) \exp(i\omega_j T_0) + \overline{A}_j(T_2) \exp(-i\omega_j T_0) \tag{28}$$

where $A_j(T_2)(j = 1, 2)$ are yet unknown functions and $\overline{A}_j(T_2)$ are conjugate functions with $A_j(T_2)$.

Substituting (28) in (26–27) yields

$$D_0^2 X_{13} + \omega_1^2 X_{13} = -2i\omega_1 D_2 A_1 \exp(i\omega_1 T_0)$$
$$- \left[\overline{\mu}_1 (i\omega_1)^{\gamma_1} - \overline{\mu}_2 (1 + \tau_2^{\gamma_2} (i\omega_1)^{\gamma_2})^{-1} + \overline{\mu}_3 (i\omega_1)^{\gamma_2}\right] A_1 \exp(i\omega_1 T_0)$$
$$- \alpha_1 [A_1 \exp(3i\omega_1 T_0) + 3\overline{A}_1 \exp(i\omega_1 T_0)] A_1^2$$
$$- \alpha_2 \Big\{ A_2^2 \exp[(\omega_1 + 2\omega_2) T_0]$$
$$+ 2A_2 \overline{A}_2 \exp(i\omega_1 T_0) + \overline{A}_2^2 \exp[i(\omega_1 - 2\omega_2) T_0] \Big\} A_1$$
$$+ \frac{2f_1}{i} \exp(i\omega_{f_1} T_0) + cc \tag{29}$$

$$D_0^2 X_{23} + \omega_2^2 X_{23} = -2i\omega_2 D_2 A_2 \exp(i\omega_2 T_0)$$

$$c - \left[\bar{\mu}_1(i\omega_2)^{\gamma_1} - \bar{\mu}_2(1 + \tau_2^{\gamma_2}(i\omega_2)^{\gamma_2})^{-1} + \bar{\mu}_3(i\omega_2)^{\gamma_2}\right] A_2 \exp(i\omega_2 T_0)$$

$$- \alpha_3 \left[A_2 \exp(3i\omega_2 T_0) + 3\bar{A}_2 \exp(i\omega_2 T_0)\right] A_2^2$$

$$- \alpha_4 \left\{ A_1^2 \exp[(2\omega_1 + \omega_2)T_0] \right.$$

$$+ 2A_1\bar{A}_1 \exp(i\omega_2 T_0) + \bar{A}_1^2 \exp[i(\omega_2 - 2\omega_1)T_0]\right\} A_2$$

$$+ \frac{2f_2}{i} \exp(i\omega_{f_2} T_0) + cc \tag{30}$$

The analysis of relations (29–30) shows that the case of the occurrence of internal resonance one-to-one is possible, when any two vibration frequencies from the plane of the plate are close to each other.

$$\omega_1 = \omega_2, \text{ and therefore, } \Omega_1 = \Omega_2 \tag{31}$$

combined with the external resonance:

$$\omega_{fi} = \omega_i \tag{32}$$

The condition for eliminating secular terms in Eqs. (29) and (30) with account for (31–32) leads to a set of two governing equations:

$$2i\omega_1 D_2 A_1 + \left[\bar{\mu}_1(i\omega_1)^{\gamma_1} - \bar{\mu}_2(1 + \tau_2^{\gamma_2}(i\omega_1)^{\gamma_2})^{-1} + \bar{\mu}_3(i\omega_1)^{\gamma_2}\right] A_1 + 3\alpha_1 A_1^2 \bar{A}_1$$

$$+ \alpha_2 \bar{A}_1 A_2^2 + 2\alpha_2 A_1 A_2 \bar{A}_2 - \frac{2f_1}{i} = 0 \tag{33}$$

$$2i\omega_2 D_2 A_2 + \left[\bar{\mu}_1(i\omega_2)^{\gamma_1} - \bar{\mu}_2(1 + \tau_2^{\gamma_2}(i\omega_2)^{\gamma_2})^{-1} + \bar{\mu}_3(i\omega_2)^{\gamma_2}\right] A_2$$

$$+ 3\alpha_3 A_2^2 \bar{A}_2 + \alpha_4 \bar{A}_2 A_1^2 + 2\alpha_4 A_2 A_1 \bar{A}_1 - \frac{2f_2}{i} = 0 \tag{34}$$

Multiplying (33) by $\bar{A}_1$ and (34) by $\bar{A}_2$, adding and subtracting the equations conjugate to them, and also representing functions and in their polar form

$$A_i = a_i e^{i\varphi_i} \quad (i = 1, 2) \tag{35}$$

where $a_i = a_i(T_2)$ and $\varphi_i = \varphi_i(T_2)$ are the functions of amplitudes and phases of vibrations, yield the following set of equations:

$$\left(a_1^2\right)^{\cdot} + s_1 a_1^2 + \omega_1^{-1}\alpha_2 a_1^2 a_2^2 \sin\delta + 2f_1\omega_1^{-1}\alpha_2 \cos\varphi_1 = 0 \tag{36}$$

$$\left(a_2^2\right)^{\cdot} + s_2 a_2^2 - \omega_2^{-1}\alpha_4 a_1^2 a_2^2 \sin\delta + 2f_2\omega_2^{-1}\alpha_2 \cos\varphi_2 = 0 \tag{37}$$

$$\dot{\varphi}_1 - \frac{1}{2}\lambda_1 - \frac{3}{2}\alpha_1\omega_1^{-1}a_1^2 - \alpha_2\omega_1^{-1}a_2^2 - \frac{1}{2}\alpha_2\omega_1^{-1}a_2^2\cos\delta + f_1(\omega_1\,\alpha_1)^{-1}\sin\varphi_1 = 0$$
(38)

$$\dot{\varphi}_2 - \frac{1}{2}\lambda_2 - \frac{3}{2}\alpha_3\omega_2^{-1}a_2^2 - \alpha_4\omega_2^{-1}a_1^2 - \frac{1}{2}\alpha_4\omega_2^{-1}a_1^2\cos\delta + f_2(\omega_2\,\alpha_2)^{-1}\sin\varphi_2 = 0$$
(39)

where $\delta = 2(\varphi_2 - \varphi_1)$ is the phase difference,

$$s_i = \bar{\mu}_1\omega_i^{\gamma_1-1}\sin\psi_1 + \bar{\mu}_2\omega_i^{-1}R_i\sin\Phi_i + \bar{\mu}_3\omega_i^{\gamma_2-1}\sin\psi_2$$

$$\lambda_i = \bar{\mu}_1\omega_i^{\gamma_1-1}\cos\psi_1 - \bar{\mu}_2\omega_i^{-1}R_i\cos\Phi_i + \bar{\mu}_3\omega_i^{\gamma_2-1}\cos\psi_2$$

$$\psi_i = \frac{1}{2}\,\pi\gamma_i \ \ (i=1,2), \quad R_i = \sqrt{1 + 2(\tau_2\omega_i)^{\gamma_2}\cos\psi_2 + (\tau_2\omega_i)^{2\gamma_2}},$$

$$\tan\Phi_i = \frac{(\tau_2\omega_i)^{\gamma_2}\sin\psi_2}{1 + (\tau_2\omega_i)^{\gamma_2}\cos\psi_2}$$
(40)

The set of Eqs. (36–39) is the governing one for the amplitudes and phases of nonlinear force driven vibrations of the elastic plate subjected to moving point load and resting on a nonlinear viscoelastic Pasternak-type foundation, damping features of which are defined by the fractional derivative standard linear solid model (5), when vibrations occur in a viscoelastic surrounding medium, properties of which are described by the fractional derivative Kelvin-Voigt model.

4 Conclusion

In the present paper, an analytical solution is presented for the problem of large amplitude vibrations of a simply supported elastic plate based on a nonlinear Pasternak viscoelastic foundation and subjected to moving point load. The compliance operator of the foundation is described by the fractional derivative standard linear solid model, while the damping properties of the surrounding environment are described by the Kelvin-Voigt model with the Riemann–Liouville fractional derivative. The proposed model of the viscoelastic foundation could be reduced to the Winkler, Pasternak and nonlinear Winkler-type models by equating the corresponding parameters of the foundation to zero. Applying the fractional derivative viscoelastic model allows one to control the damping properties of the external environment and the foundation by changing the fractional parameters, resulting in the expansion of the range of applicability of the solution obtained.

The Bubnov-Galerkin method is used to solve von Karman equations of motion with an assumed deflection shape function. The resulting set of equations is obtained for determining of nonlinear amplitudes and phases in the case of force driven vibrations under load moving with constant velocity, when the internal resonance 1:1 is combined with external resonance. The governing set of equations could be solved numerically using the approach proposed in [21].

References

1. Praharaj R, Datta N (2020) Dynamic response of plates resting on a fractional viscoelastic foundation and subjected to a moving load. Mech Based Des Struct Mach. https://doi.org/10.1080/15397734.2020.1776621
2. Wu J, Lee M, Lai T (1987) The dynamic analysis of a flat plate under a moving load by the finite element method. Int J Numer Methods Eng 24:743–762. https://doi.org/10.1002/nme.1620240407
3. Taheri M, Ting E (1989) Dynamic response of plate to moving loads: structural impedance method. Comput Struct 33(6):1379–1393. https://doi.org/10.1016/0045-7949(89)90478-1
4. Zaman M, Taheri M, Alvappillai A (1991) Dynamic response of a thick plate on viscoelastic foundation to moving loads. Int J Numer Anal Methods Geomech 15:627–647. https://doi.org/10.1002/nag.1610150903
5. Li M, Qian T, Zhong Y et al (2014) Dynamic response of the rectangular plate subjected to moving loads with variable velocity. J Eng Mech 140(4):06014001. https://doi.org/10.1061/(ASCE)EM.1943-7889.0000687
6. Dang-Trung H, Luong-Van H, Nguyen-Toi T et al (2017) Analysis of stiffened plates resting on viscoelastic foundation subjected to a moving load by a cell-based smoothed triangular plate element. Int J Struct Stab Dyn 17(1):1750011. https://doi.org/10.1142/S0219455417500110
7. Hien T, Lam N (2018) Vibration of functionally graded plate resting on viscoelastic elastic foundation subjected to moving loads. IOP Conf Ser Earth Environ Sci 143(1):012024. https://doi.org/10.1088/1755-1315/143/1/012024
8. Luong V, Cao T, Lieu Q et al (2020) Moving element method for dynamic analyses of functionally graded plates resting on Pasternak foundation subjected to moving harmonic load. Int J Struct Stab Dyn 20(01):2050003. https://doi.org/10.1142/S0219455420500030
9. Luong V, Cao T, Reddy J et al (2018) Static and dynamic analyses of Mindlin plates resting on viscoelastic foundation by using moving element method. Int J Struct Stab Dyn 18(11):1850131. https://doi.org/10.1142/S0219455418501316
10. Rossikhin YA, Shitikova MV (2009) New approach for the analysis of damped vibrations of fractional oscillators. Shock Vib 16:365–387. https://doi.org/10.1155/2009/387676
11. Rossikhin YA, Shitikova MV (2010) Application of fractional calculus for dynamic problems of solid mechanics: Novel trends and recent results. Appl Mech Rev 63(1):1–52. https://doi.org/10.1115/1.4000563
12. Wei K, Wang F, Wang P et al (2017) Effect of temperature-and frequency-dependent dynamic properties of rail pads on high-speed vehicle–track coupled vibrations. Veh Syst Dyn 55(3):351–370. https://doi.org/10.1080/00423114.2016.1267371
13. Hosseinkhani A, Younesian D (2018) Farhangdoust S (2018) Dynamic analysis of a plate on the generalized foundation with fractional damping subjected to random excitation. Math Probl Eng 2:1–10. https://doi.org/10.1155/2018/3908371
14. Dumir P (1988) Nonlinear dynamic response of isotropic thin rectangular plates on elastic foundations. Acta Mech 71:233–244. https://doi.org/10.1007/BF01173950

15. Samko S, Kilbas A, Marichev O (1993) fractional integrals and derivatives. Theory and applications. Gordon and Breach Science Publishers, Switzerland
16. Rossikhin YuA, Shitikova MV (2020) Fractional operator models of viscoelasticity. In: Altenbach H, Öchsner A (eds) Encyclopedia of continuum mechanics. Springer, Berlin, pp 971–982. https://doi.org/10.1007/978-3-662-55771-6_77
17. Rossikhin YuA, Shitikova MV (2014) Centennial jubilee of Academician Rabotnov and contemporary handling of his fractional operator. Fract Calc Appl Anal 17:674–683. https://doi.org/10.2478/s13540-014-0192-2
18. Nayfeh A (2003) Perturbation methods. Wiley, New York
19. Rossikhin YuA, Shitikova MV (1998) Application of fractional calculus for analysis of nonlinear damped vibrations of suspension bridges. J Eng Mech 124:1029–1036. https://doi.org/10.1061/(ASCE)0733-9399(1998)124:9(1029)
20. Rossikhin YA, Krusser AI, Shitikova MV (2017) Impact response of a nonlinear viscoelastic auxetic doubly curved shallow shell. In: Proceedings of the 24th International Congress on Sound and Vibration, London, United Kingdom, 23–27 July 2017
21. Shitikova MV, Kandu VV (2019) Force driven vibrations of fractionally damped plates subjected to primary and internal resonances. Eur Phys J Plus 134(9):423. https://doi.org/10.1140/epjp/i2019-12812-x

Vibrations of a Constructively Nonlinear System with One-Way Connections

A. N. Potapov and N. T. Tazeev[✉]

South-Ural State University, 76, Lenin Prospect, Chelyabinsk 454080, Russia

Abstract. The article explores the passive method for damping wind auto-oscillations of an aboveground gas pipeline. The method consists in installing a vibration damping device in one of the spans, which operates on the principle of one-way connection. This characterizes the system as structurally non-linear. Integration of the differential equation of motion of a finite-dimensional dissipative system is based on the developed algorithm, which is associated with the analysis of the matrix quadratic characteristic equation. This allowed to obtain an analytical form of the dynamic reaction of a dissipative system in the matrix form of the Duhamel integral, which does not require the spectral expansion of the solution. Internal friction of the material is considered using a non-proportional damping model. The efficiency of devices with one one-way connection (OWC) in the span (DDM-1) and with two OWC (DDM-2) is compared on different values of the cable compliance. The estimation of the accuracy of solving the differential equation of motion by constructing the residual vector is carried out.

Keywords: Aboveground gas pipeline · Auto-oscillations · Vibration damping · One-way connection · Natural mode · Stiffness matrix · Displacement

1 Introduction

The vibrations of the flexible type structures such as aboveground pipelines often occur phenomena of aerodynamic instability due to wind resonance. The aboveground gas pipeline vibrates in the vertical plane, i.e. in the direction perpendicular to the wind flow. This phenomenon is caused by the Karman vortex street effect. The phenomenon of aerodynamic instability in flexible systems with wind flow around a cylindrical surface is well described in the classical literature [1, 2].

For the occurrence of wind self-oscillations, the following conditions are necessary: the laminar nature of the wind flow, elimination of local turbulent phenomena, and a relatively high flexibility of the pipeline. It is known that the occurrence of wind self-oscillations is practically excluded for pipelines of medium (300–500 mm) and large (over 500 mm) diameters, but for pipelines of smaller diameter this phenomenon can be destructive [3].

Various approaches are used to solve practical problems of vibration damping. Some are aimed at changing the nature of the flow around a structure or the nature of the

oscillatory process [4–11] (active damping methods). Others are aimed at constructive limitation of vibration by changing the natural frequency [12–14] (passive methods). Moreover, most of the studies are focused mainly on the numerical simulation of the aerodynamic problem using simplified damping models.

An analytical method for solving problems of aerodynamic instability aboveground pipelines, conducted in the framework of the theory of temporal analysis, occupies a special place [15]. In articles [16, 17], To damp the oscillations of the gas pipeline, a device made in the form of a cable—one-way connection (OWC) is used. As a result, the aerodynamic problem becomes structurally nonlinear, because in the process of vibrations of the structure, its structural scheme changes.

This article analyzes the dynamic response of a gas pipeline design scheme in a non-stationary process. Within the framework of the theory of time analysis, a mathematical model of oscillations of a system with one and two connections has been created. This model allows us to consider the behavior of the system in different states: the state of the base model (BM) when the OWC is turned off and the state of the model with an additional connection (MAC) when the OWC is turned on. It should be noted that, the computational model will have different stiffness matrices in the states of BM and MAC.

The influence of a number of factors (cable stiffness, influence of the OWC location in the span relative to the supports) on the parameters of the dynamic response of the computational model was studied in the analysis of oscillations.

2 Methods

The equation of motion of an elastic discrete dissipative system (DDS) in the framework of the linear model of viscous resistance (1) and the initial conditions (2) of the dynamic problem are represented in the form:

$$M\ddot{Y}(t) + C\dot{Y}(t) + KY(t) = P(t) \tag{1}$$

$$Y_0 = Y(t_i), \dot{Y}_0 = \dot{Y}(t_i), \tag{2}$$

where $M = \text{diag}(m_1, \ldots, m_n)$, $C_j = C_j^{\mathrm{T}}$, $K_j = K_j^{\mathrm{T}} \in M_n(\mathbf{R})$—mass matrix, damping matrix and stiffness matrix; $Y(t)$, $P(t)$—displacement vector and external load vector. The index $j = 0, 1, \ldots$ considers the state of the design model on the time interval $t \in [t_i, t_{i+1}]$, where zero-index j of the corresponding matrices is omitted. Here t_i—is the OWC on/off time.

The construction of fundamental solutions of the homogeneous differential equation following from (1) is related to the matrix function $\Phi_j(t) = e^{S_jt}$ in which $S_j \in$) satisfies the characteristic matrix quadratic equation (MQE)—the equation of motion of natural forms $M_n(\mathbf{C}$:

$$MS_j^2 + C_jS_j + K_j = 0 \tag{3}$$

The spectra of the matrices S_j contains the internal dynamic characteristics of the DDS (damping coefficients, frequencies and forms of natural vibrations). The MQE

solution (3) has an analytical representation in the form of a root pair:

$$S_{j(1,2)} = M^{-1}(-C_j + V_j \pm U_j)/2 \tag{4}$$

where $V_j = -V_j^{\mathrm{T}}$, $U_j = U_j^{\mathrm{T}}$—skew-symmetric and symmetric matrices.

For an elastic DDS with low dissipation, the elements of the matrices V_j, U_j are real and imaginary, respectively, and therefore the matrix roots $S_{j(1,2)}$ are complex conjugate $(S_{j,1} = S_j, S_{j,2} = \overline{S}_j)$ [15]:

$$S_j = M^{-1}(-C_j + V_j + U_j)/2,$$

$$\overline{S}_j = M^{-1}(-C_j + V_j - U_j)/2 \tag{5}$$

The system response (vectors of displacements and velocities of DDS nodes) is written in the matrix form of the Duhamel integral [18]:

$$Y(t) = 2\mathrm{Re}\{Z(t)\}, \ \dot{Y}(t) = 2\mathrm{Re}\{S_j Z(t)\}, \tag{6}$$

$$Z(t) = \Phi_j(t - t_i)U_j^{-1}M(-\overline{S}_j Y_0 + \dot{Y}_0) + U_j^{-1}\int_{t_i}^{t} \Phi_j(t - \tau)^{\mathrm{T}}P(\tau)d\tau. \tag{7}$$

The first term in (6) expresses the reaction of the design model with free vibrations, the second term is the Duhamel integral—the reaction with forced vibrations.

The aerodynamic effect of the wind load is determined by the sine law:

$$P(t) = P_0 \sin(\theta t) \tag{8}$$

The amplitude value of the disturbing load acting in the node is calculated as the drag force to the static wind action of the calculated speed. The angular frequency is the number of vortices escaping from the pipe surface in 2π seconds:

$$\theta = \frac{0,2v}{d} \cdot 2\pi \tag{9}$$

Under conditions of constant wind speed ($\theta = $ const along the entire length of the computational model), the dynamic response (7) takes the form on the interval $t \in [t_i, t_{i+1}]$ [15]:

$$\left.\begin{array}{l} Z(t) = \Phi_j(t - t_i)U_j^{-1}M[-\overline{S}_j Y_0 + \dot{Y}_0] + U_j^{-1}\left[(S_j^{\mathrm{T}})^2 + \theta^2\right]^{-1}F(t)P_0, \\ F(t) = S_j^{\mathrm{T}}\left[\Phi_j(t - t_i)^{\mathrm{T}}\sin(\theta t_i) - E\sin(\theta t_i)\right] + \left[\Phi_j(t - t_i)^{\mathrm{T}}\cos(\theta t_i) - E\cos(\theta t_i)\right]\theta, \end{array}\right\} \tag{10}$$

where E—identity matrix.

The design scheme (Fig. 1) of the gas pipeline is a continuous multi-span beam, in which all spans (except for the central one) contain the same number of nodes (masses).
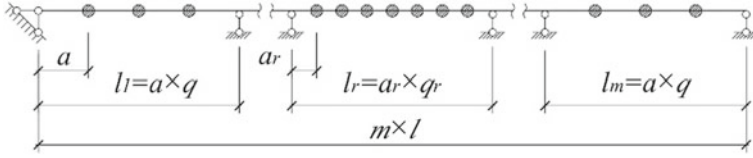
Fig. 1 Design scheme

In the central span, the number of nodes has been increased to improve the accuracy of the OWC placement. The number of degrees of freedom of the system is equal to the number of masses.

In the course of additional experimental studies [19], results were obtained that indicate a symmetric form of vibration of the beam when the one-way connection is located in the center of the span. The main premise was that the transient mode of the beam when the OWC is switched on (the cable is in a tense state) lasts a very short period of time (hundredths or thousandths of a second), which is many times less than the stay of the computational model in the BM state when the OWC is disabled. Since in the BM state the natural mode of vibrations of the beam axis is symmetric, then during the transition to the MAC state the natural mode of vibrations will also remain symmetric. In other words, due to the inertia of the beam in the new state, the system does not have time to change the type of symmetry of the vibration mode.

Activation and deactivation of connections is realized by changing the external (C_j, K_j) and internal (S_j, U_j) dynamic parameters of the system and changing the initial conditions (Y_0, $\dot{Y}_0$). In addition, when moving from interval $t \in [t_{i-1}, t_i]$ to interval $t \in [t_i, t_{i+1}]$, the time is changed from t_{i-1} to t_i.

In the case of a design model with one OWC in a span (DDM-1), Fig. 2a shows two possible states of the system (for $j = 0, 1$): BM and MAC. For a model with two OWC in a span (DDM-2), four possible states are considered ($j = 0, 1, 2, 3$): BM, MAC-1, MAC-2 and MAC-3 (Fig. 2b).
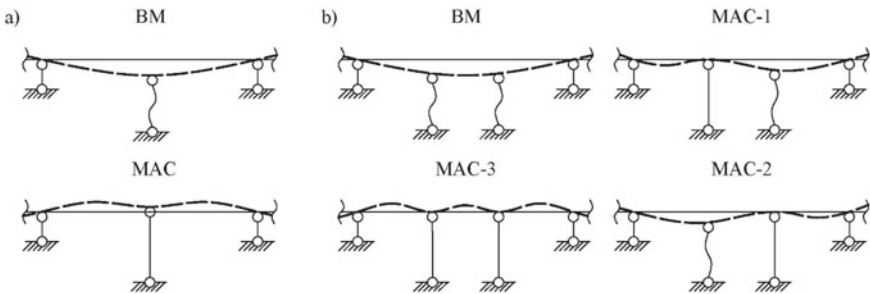
Fig. 2 Schemes of possible states of the design model: **a** with one OWC (DDM-1); **b** with two OWC (DDM-2)

In the case of a design model with two OWC in a span (DDM-2), their symmetrical location relative to the center of the span at the attachment points is considered: 19–21, 18–22 и 17–23 (Fig. 3).
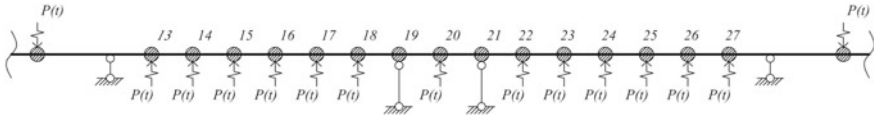
Fig. 3 Scheme of application of loads in the central span of DDM-2 (19–21)

Initial data for calculation: outer and inner diameters of the pipe, respectively $D = 219$ мм, $d = 209$ мм, elastic modulus $E = 2.1 \times 10^8$ kN/m^2, span length $l = 15$ m, number of spans $m = 9$, the number of elementary sections in the central span $q_1 = 16$, in another spans $q = 4$. Accordingly, the number of masses in the central span is 15, in other spans—3, the number of degrees of freedom $n = 39$. The tensile compliance of the cable takes values in the range $\delta_R \in [0.001, 0.1]$ m/kN. Logarithmic decrement $\delta = 0.07$. The wind speed at which the resonance occurs is $v = 2.951$ m/s.

3   Results

The results of computer simulation of the problem in MATLAB are graphs (oscillograms) of the parameters of the dynamic response of a constructively nonlinear dissipative system at a given time interval. These parameters are: displacements, velocities, accelerations, restoring (elastic), dissipative, inertial forces and the forces in the cables calculated in the design sections of the model.

The graph with a combination of various parameters is the most indicative and reflects the peculiarities of the system operation. Figure 4 shows a fragment of an oscillogram of displacements, restoring forces and forces in the cable, built for the 19th node, to which the left OWC is attached in the DDM-2 (19–21) system. As can be seen from the graph, during the OWC tension, the displacements $y_{19}(t)$ of this node (due to the compliance of the connection) become higher than the static equilibrium position. At this moment, the activation of elastic forces occurs due to the sharp transformation of kinetic energy into potential.

A comparative calculation of DDM-1 and DDM-2 was carried out with a minimum cable flexibility (0.001 m/kN) to compare the effectiveness of the ways for placing the OWC in the span. The maximum developed displacements of the masses of the central span were estimated for the entire period of oscillations. For this, the graphs of the maximum positive (upward) displacements were built, which, in fact, represent the enveloping diagrams of displacements (Fig. 5). The resulting graph shows that the level of fluctuations of the central span is most effectively suppressed in the DDM-2 with the OWC 19–21 location, that is, the closest to the center.

Figure 6 shows oscillograms of the maximum displacements of the base model, DDM-1 and DDM-2 (19–21) with a cable compliance of 0.01 m/kN at a 10-s interval. As can be seen from the graph, in DDM-2 the maximum displacement values are less
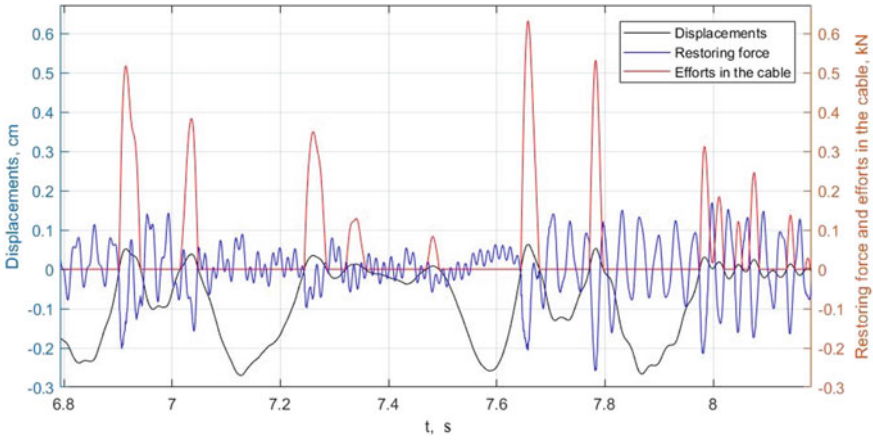
Fig. 4 Fragment of the oscillogram of displacements, restoring force and efforts in the cable at the attachment point of the left OWC
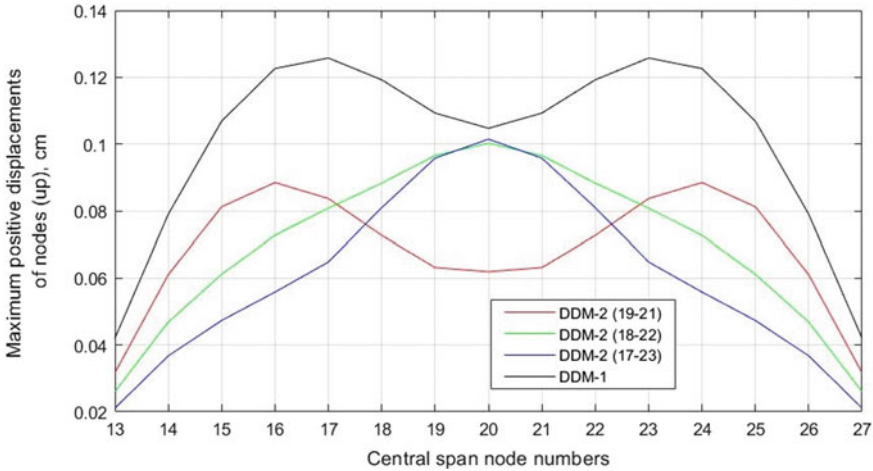
Fig. 5 Graph of the maximum positive vibration displacements of the nodes of the central span

than in DDM-1, and the maximum is reached earlier. Moreover, at the beginning of the process, the displacement in both models is higher than in the BM.

Figure 7 shows a graph of the maximum vibration displacements max$|y_i(t)|$ for models DDM-1, DDM-2 at different values of cable compliance (from 0.001 to 0.1 m/kN). According to the graph, the DDM-2 model (19–21) shows the maximum efficiency in almost the entire range of cable compliance values. The variant with the DDM-1 model shows the worst results in all cases. Moreover, a twofold increase in the rigidity (decrease in compliance) of the cable in DDM-1 does not give an advantage over DDM-2 in the effective range of rigidity (compliance range from 10^{-3} to 5×10^{-2} m/kN). In other
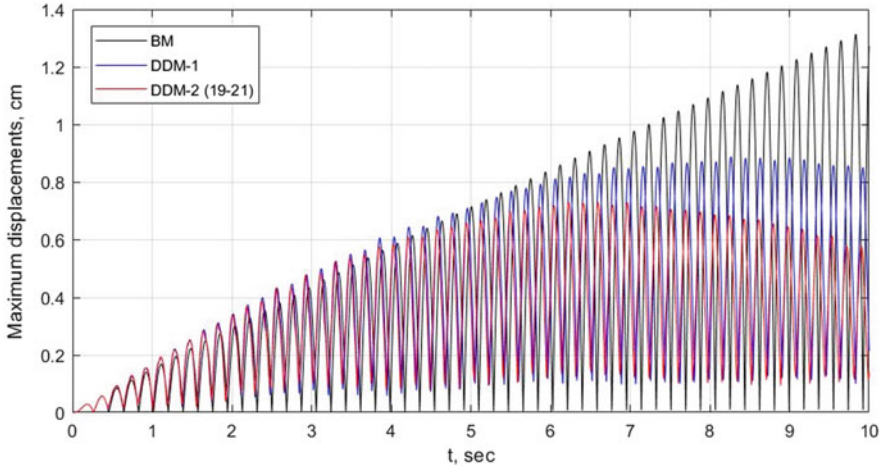
Fig. 6 Oscillograms of maximum modulus displacements BM, DDM-1, DDM-2 (19–21)

words, a single double-stiffness cable is not more efficient than two single-stiffness cable.
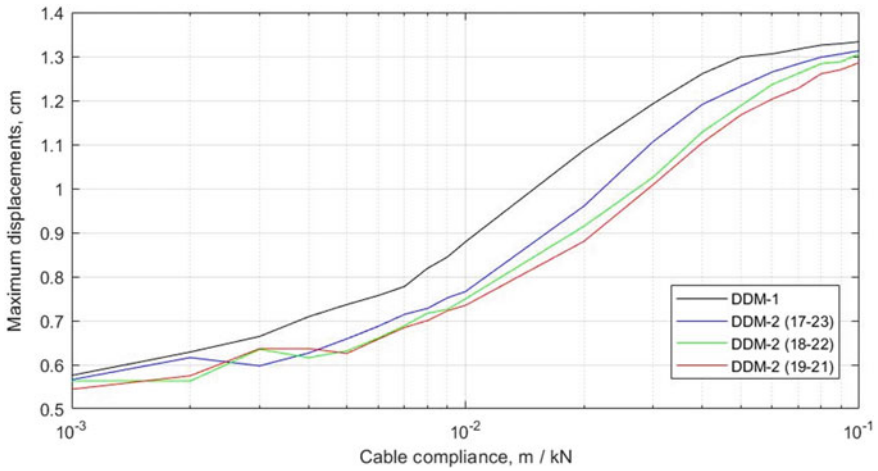
Fig. 7 Graph of the dependence of the maximum vibration displacements on the cable compliance in various models

To estimate the accuracy of solving the equation of motion (1), a residual vector was constructed $\Delta\varphi(t) = f(t) - P(t)$, where $f(t) = M\ddot{Y}(t) + C\dot{Y}(t) + KY(t)$ is the sum of inertial, dissipative and restoring forces on the left side of the equation; $P(t) = [p_j(t)]$—vector of external forces. Value $\Delta\varphi(t)$ is built for DDM-2 over the entire time interval, including the states of BM and MAC-2. The nature of the convergence of the solution (functions $f_j(t)$) to these functions $p_j(t)$ of the right-hand side of the equation

is shown on the oscillogram $\Delta\varphi_j(t)$ for the cable attachment point ($j = 7$) in Fig. 8. The accuracy of solving the differential equation of motion does not exceed the error limits $\varepsilon \leq 8{,}5 \times 10^{-13}$ kN.
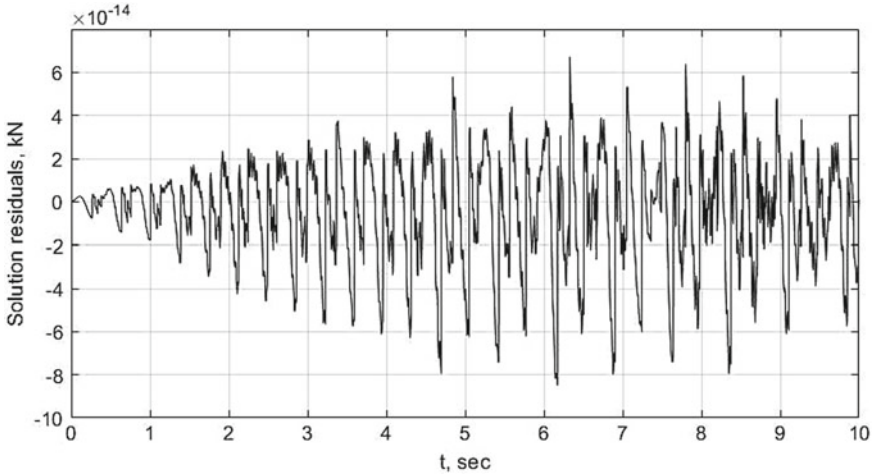
Fig. 8 Oscillogram of residuals $\Delta\varphi_7(t)$ of the solution of the equation of motion (1)

4 Conclusion

Based on the results of the study, the following conclusions were made:

1. The optimal way of placing the OWC for the DDM-2 (19–21—in the local numbering of the central span) has been obtained practically over the entire range of cable compliance values. With such an arrangement of connections, DDM-2 shows the best limitation of the amplitudes of the parameters of the dynamic response.
2. DDM-1 shows the worst results among all models. At the same time, a twofold increase in the rigidity of the cable in the DDM-1 model does not give an advantage over the DDM-2 by maximum displacements.
3. Computer simulation of the problem with one and two OWC showed a high efficiency of the damping device for the proposed oscillation model. The use of this model (within the framework of DDM-1 and DDM-2) will increase (optimize) placement step of vibration damping devices along the aboveground gas pipeline route and, thereby, reduce the number of these devices per one kilometer of the route compared to the model of vibrations with a skew-symmetric shape.

References

1. Bisplinghoff RL, Eshli H, Halfman RL (1955) Aeroelasticity. Massachusetts, Addison-Wesley Publishing Co, Cambridge
2. YaG P, Gubanova II (1967) Ustojchivost' i kolebaniya uprugih system (Stability and vibrations of elastic systems). Nauka Publ, Moscow
3. Tartakovsky GA (1967) Stroitel'naya mekhanika truboprovoda (Pipeline structural mechanics). "Nedra" Publ., Moscow
4. Wen-Li Chen, Guan-Bin Chen, Feng Xu et al (2020) Suppression of vortex-induced vibration of a circular cylinder by a passive-jet flow control. J Wind Eng Ind Aerodyn 1–13
5. Wang L, Jiang TL, Dai HL, Ni Q (2018) Three-dimensional vortex-induced vibrations of supported pipes conveying fluid based on wake oscillator models. J Sound and Vibr. 422:590–612
6. Potapov AN, Degtyareva NV et al (2007) Ustrojstvo dlya gasheniya rezonansnyh kolebanij truboprovoda (Pipeline resonance damping device). Patent RF № 2007109081, Bulletin № 25
7. Tkachenko IG, Shablya SG et al (2018) Ustrojstvo podavleniya vibracii (Vibration suppression device). Patent RF № 2018127117. Bulletin № 25
8. Minasyan MA, Minasyan AM (2014) Amortizator (Damper). Patent RF № 2014100557/11. Bulletin № 13
9. Antimonov VA, ZHukov BM et al (2013) Gasitel' vibracii (Vibration damper). Patent RF № 2013128975/07. Bulletin № 32
10. Akopyan LA, Beskrovnyj AYu et al (2017) Vibroizoliruyushchaya podveska truboprovoda (Vibration-isolating pipeline suspension). Patent RF № 2017137455. Bulletin № 29
11. Tkachenko IG, Shablya SG et al (2018) Ustrojstvo podavleniya vibracii (Vibration suppression device). Patent RF № 2018104385, Bulletin № 24
12. Bernshtejn MF, Il'ichev VA, Korenev BG et al (1984) Dinamicheskij raschet zdanij i sooruzhenij (Dynamic calculation of buildings and structures). Strojizdat, Moscow
13. Gabbai RD, Benaroya H (2005) An overview of modeling and experiments of vortex-induced vibration of circular cylinders. J Sound and Vibr 282:575–616
14. Kazakevich MI (1977) Aerodinamicheskaya ustojchivost' nadzemnyh i visyachih truboprovodov (Aerodynamic stability of overhead and overhead pipelines). "Nedra" Publ., Moscow
15. Potapov AN (2003) Dinamicheskij analiz diskretnyh dissipativnyh sistem pri nestacionarnyh vozdejstviyah (Dynamic analysis of discrete dissipative systems under nonstationary influences). SUSU Publ, Chelyabinsk
16. Degtyareva NV (2009) Postroenie aerodinamicheski ustojchivoj raschetnoj modeli nadzemnogo gazoprovoda s odnostoronnej svyaz'yu (Construction of an aerodynamically stable computational model of an elevated gas pipeline with a one-way connection). Bulletin of SUSU Ser Constru Archit 16:23–28
17. Potapov AN (2009) Vremennoj analiz modeli nadzemnogo gazoprovoda s odnostoronnimi svyazyami pri aerodinamicheskoj neustojchivosti (Time analysis of a model of an overground gas pipeline with one-way connections in case of aerodynamic instability). Bull SUSU Ser Constru Archit 16:23–28
18. Potapov AN (2017) Analiz kolebanij konstrukcij s vyklyuchayushchimisya svyazyami (Analysis of vibrations of structures with switching off connections). Bull SUSU Ser Constru Archit 17:38–48. https://doi.org/10.14529/build170105
19. Potapov AN, Tazeev NT, Amirova RR, Orlova OG (2021) Analiz kolebanij nadzemnogo gazoprovoda pri vetrovom rezonanse (Vibration analysis of an above-ground gas pipeline at wind resonance). Bull SUSU Ser Construction Archit 21:13–21. https://doi.org/10.14529/build210102

Study of the Stress-Strain State of Short Hollow Core Slabs Depending on the Width

A. Vasil'ev[1]([✉]) and Yu. Chudinov[2]

[1] Sholom-Aleichem Priamursky State University, 70, Shirokaya str., Birobidzhan 679015, Russia

[2] Komsomolsk-On-Amur State University, 27, Lenin str., Komsomolsk-on-Amur 681013, Russia

Abstract. The paper dwells on a numerical investigation of short hollow slabs of different width. The length of all specimens was 2400 mm. The calculations were performed analytically according to current technical documents, as well as by the ANSYS software package. In the software, loading was carried out subsequently with a stridden load application. Modern software packages are appropriate to use to study the stress-strain behavior of such constructions, using modern models and yield criteria based on incremental-iterative algorithms and general concepts of building mechanics, when solving physically nonlinear problems. The calculation data for the analytical approach are compared with the computational calculation based on the available Drucker–Prager yield criterion. The load-deflection curves for successive loading of specimens of different width are constructed on the basis of this model. The comparison of analytical and computational results of calculations was performed for the ultimate breaking load, maximum deflections, cracked condition, and in reinforcement stress at failure. It was found out the way in which the width of hollow slabs affects the value of the rupturing load for each square meter of the floor structure with a fixed reinforcement coefficient. What is more, it is shown that the specimens with a larger cross-section width and a larger number of voids had an ultimate load-bearing capacity. The stress-strain state in concrete was appreciated in the centre section of samples at various loading stages.

Keywords: Stress-strain state · Bilinear kinematic hardening · Drucker-Prager model · Bearing capacity · Deflection

1 Introduction

A hollow slab is a reinforced concrete slab where the voids reduce their own weight. Thereby, it increases the workload on the slab. At the production stage, light void formers are placed between the upper and lower reinforcement before placing the concrete mixture into the formwork in such slabs. The diameter of these voids is about two-thirds or three-quarters of the slab thickness They replace the concrete in the middle part of the slab. Hollow slabs were developed in the early twentieth century involving the use

of void formers in a cylinder or oval shape. Their use made it possible to reduce the self-weight of the slabs by 35% compared to solid slabs with no voids without sacrificing their load-bearing capacity [1].

Also, the use of prefabricated reinforced concrete panels allows you to quickly assemble the building and reduce the dead weight of the floor. Therefore, the use of such slabs is economical and allows the use of longer slabs for large spans.

The purpose of the research is to figure out in what way specimen width and reinforcement ratio influence the calculation data. However, the intricate shape of these constructions makes the calculations complicated and puts the cross-section into the shape of an I-beam to simplify it, considering the hollow slabs as I-beams.

1.1 Relevance, Scientific Relevance and Literature Review

Coincidently with the adoption of hollow-core slabs, various authors have made their efforts to study their structural behavior [2]. As a result, based on several experimental programs [3–7] the academic community managed to devise calculation methods, design standards, and instructions for hollow-core slab designing. The research of such slabs at normal temperature was also focused on in scientific papers [8–10]. In the research [11] of F. Algabas performed analytical and experimental studies of the structural behavior of prefabricated prestressed hollow reinforced concrete slabs reinforced with layered carbon fibre materials. Yuanli [12], Chan [13], Bennegadi [14] also studied the methods of reinforced slabs based on composites. The stress-strain state of reinforced concrete slabs with prestressed reinforcement was presented in the studies of Kankeri [15].

Vasiliev [16–18] observed the behavior of reinforced concrete slabs on load based on the models of reinforced concrete mechanics. The researchers that have been mentioned above developed and described it through actual software solutions and numerical computing.

1.2 Formulation of the Problem

The purpose of the study is to amend the section on Building Mechanics concerning the calculation of reinforced concrete hollow-core slabs having found out the influence of the specimen width and the reinforcement ratio on the calculation data. For these reasons, the authors need to.

- compare the numerical results obtained on the basis of the available Drucker–Prager yield criterion, and the analytical findings using conventional techniques.
- determine how much the width of hollow core reinforced concrete slabs affects the amount of limit load per square meter of the floor.
- make load–deflection curves in the case of gradual loading of specimens of different width based on this model.

2 Theoretical Part

2.1 Initial Data

In this paper, the authors deal with specimens with a length of 2400 mm. Each specimen was calculated with four width options: 1000 mm, 1200 mm, 1500 mm, 1800 mm, Fig. 1.
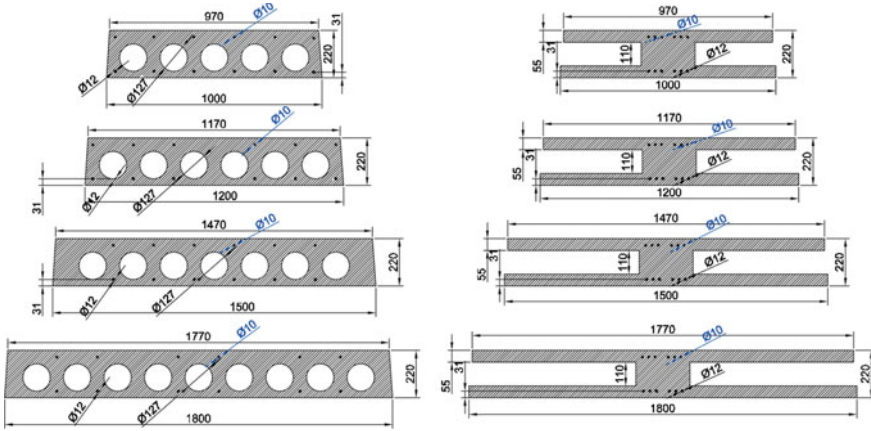
Fig. 1 The geometric dimensions of sections of samples under consideration

All the specimens were also taken with two variations of main reinforcement: single-layer reinforcement (6 rods with a diameter of 12 mm) in the tension side, or double-layer reinforcement: 6 rods in the upper and lower parts of the slab with diameters of 12 and 10 mm, respectively. The geometrical dimensions of the slab sections are shown in Fig. 1. The diameter of the voids in the specimens s 127 mm. The dimensions of the specimens in a natural and I-beam form are shown in Fig. 1.

The material properties are the following: A500 reinforcement design resistance in the tension side is $R_s = 435$ MPa; reinforcement design resistance in the compression region is $R_{sc} = 435$ MPa; design resistance of concrete compression is $R_b = 17$ MPa; the design resistance of the concrete split is $R_{bt} = 1.15$ MPa; characteristic strength of reinforcement split is $R_{bt\_ser} = 1.75$ MPa; characteristic strength of reinforcement compression is $R_{b\_ser} = 22$ MPa; concrete modulus of elasticity is $E_b = 3.25 \cdot 10^4$ MPa; elasticity modulus of reinforcement is $E_s = 2 \cdot 10^5$ MPa; the number of the main reinforcement rod in the tension side is $d = 0.012$ m;

2.2 Research Methods

Analytical calculations were performed according to the new code specification 63.13330. 2018. Concrete and reinforced concrete structures. The findings of the studies are breaking loads, deflections, cracking loads, stresses in the reinforcement during crack formation, and stresses in the reinforcement at fracture. The calculations were performed for a pure beam affected by a full-length distributed load (Fig. 2).

Numerical calculations were performed using a nonlinear stress–strain model with the ANSYS software solution. The reinforcement was modeled in in the form of rods consisting of cubic cells, based on the plasticity model with bilinear isotropic hardening. This indicates that when the yield strength of the reinforcing material was provided, the structure was not destroyed but was still able to resist loading until the ultimate strength of the material was exceeded as a result of its hardening. The E_{tan} tangent modulus here was 1000 MPa with a yield point of reinforcement of 435 MPa. For numerical
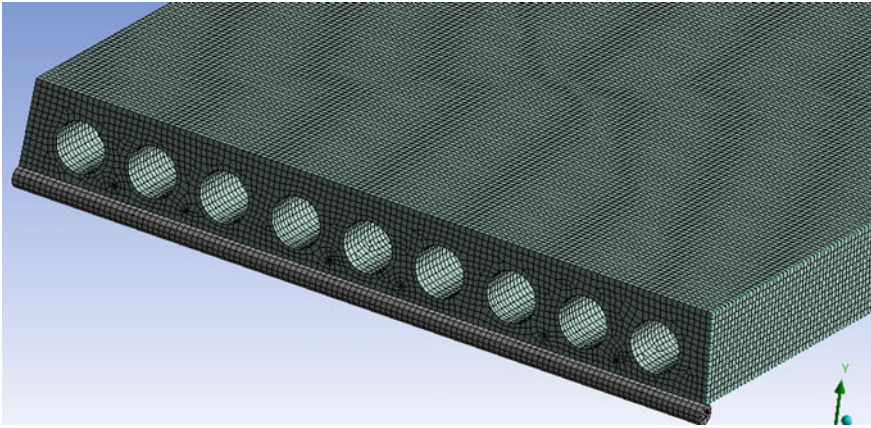
Fig. 2 Discrete slab model

calculations, the Drucker-Prager strength criterion was used [19] based on the limiting surface function [20, 21]. The general properties of the Drucker-Prager model in ANSYS are unconfined compressive strength $R_b = 16$ MPa, $R_{bt} = 1.15$ MPa are uniaxial tensile strength, $Rc = 17$ MPa are biaxial compressive strength. The load step in ANSYS was 5kN, 6kN, 7.5 kN, and 9 kN per second (this load intensity was evenly distributed over the entire cross-sectional area of the slab), respectively, for the specimens with a width of 1 m, 1.2 m, 1.5 m, and 1.8 m.

The cell size of the discrete model was 15 mm (See Fig. 2). The number of cells was from about 240,000 for a slab with a width of 1000 mm to 480,000 for a width of 1800 mm.

The supporting structures are cylindrical to prevent stress buildup in the places where the slab bearing rest. A destructible model was modeled (See Fig. 3a,b). It was being destructed when the reinforcement hit the ultimate stress limit in the tensile region after kinematic hardening with a maximum steel deformation of 0.011.

3 Research Results

Figure 4a shows load-deflection diagrams for specimens of different width. Wider slabs can have a lower load per square meter than slabs of smaller width. The reason for this is that the load per unit length on each reinforcement rod inevitably increases with a constant number of reinforcement in the cross-section and a larger effective range of the slabs. It leads to a faster stress increase in these rods. A similar trend can be monitored in the results of the analytical calculation (Table 1 and 2). Taking into account the changing cross-sectional area and the permanent area of the reinforcement in each section, the reinforcement ratio was 0.415%, 0.370%, 0.286, 0.245% respectively for the width of samples from 1000 to 1800 mm.

Let the authors take the ratio of the load per square meter to the percentage of reinforcement for the efficiency of the cross-section of the specimen of a given width. Figure 4b shows that a specimen with a width of 1800 mm has the largest load distributed
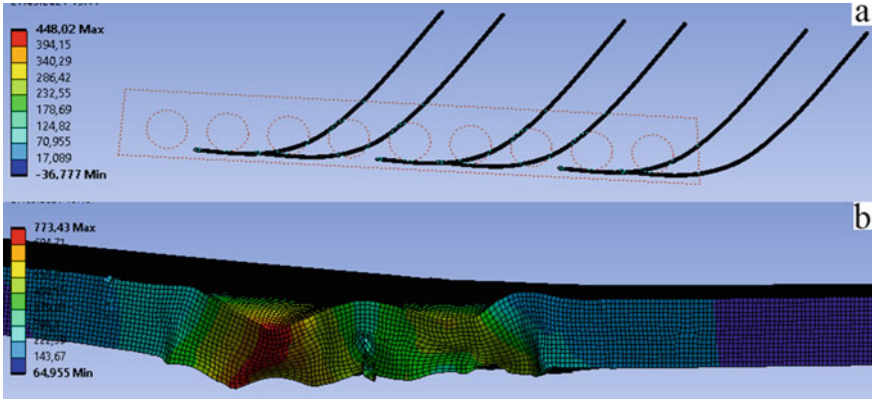
Fig. 3 The results of the stress–strain state in the ANSYS software: **a** axial stresses in the reinforcement in a state beyond the yield point, **b** ultimate deflections during sample failure
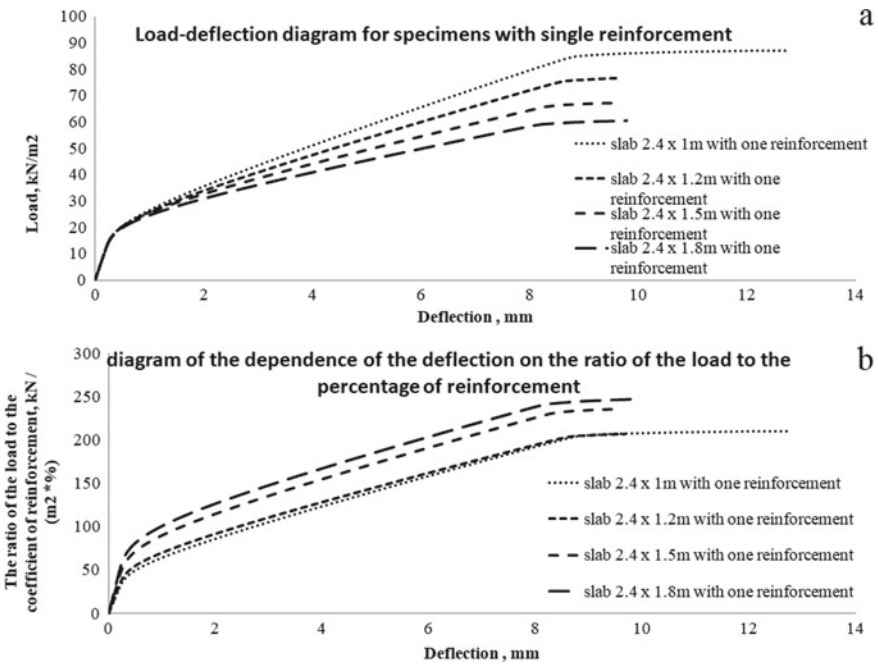
Fig. 4 Sample deflections: **a** from load per square meter of floor, **b** from the ratio of the load to the percentage of reinforcement

over the area about the reinforcement coefficient. The specimen of the largest width, according to this efficiency criterion, proved to be 4.5% better than the one with a width of 1500 mm and 16.2% better than those of 1000 and 1200 mm. Moreover, the specimens of 1000 and 1200 mm are something like equipotent when using the cross-section.

Figure 5 shows the results of normal stresses in the cross-sections of hollow slabs of different width depending on the depth of the section. As can be noted, the fastest increase in normal stresses is observed in the specimens of a larger width (due to a lower reinforcement coefficient) at the same load per square meter. This trend corresponds to Fig. 4a.
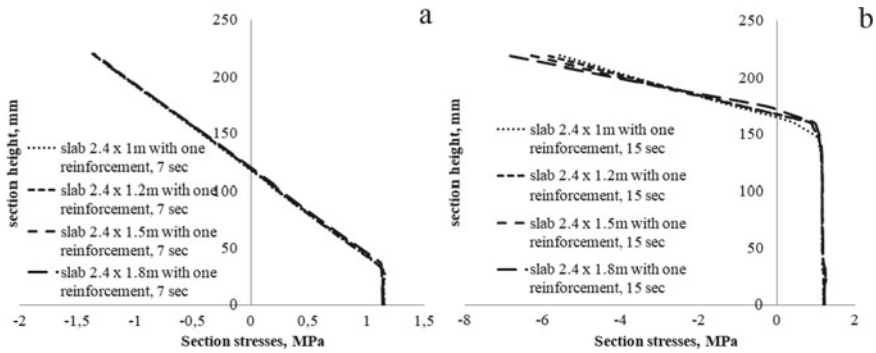
Fig. 5 Change in stresses in the middle of the slab section at different stages of loading: **a** 7 s, **b** 15 s

However, Fig. 5 a, b proves that the stresses do not grow if the load increases in the tensile region of the slab, being in the high yield strength. In addition to it, the stresses in the upper part have been steadily increasing. The stress diagram is a straight line due to the lack of time-dependent deformation in the compressive zone of the concrete. The main findings of the calculations are presented in Tables 1 and 2.

Table 1 Fracture load research results

Sample width (mm)	Breaking load (according to regulatory documents) [kN/m^2]	Breaking load, ANSYS (when the reinforcement reaches the yield point) [kN/m^2]	Breaking load, ANSYS (after reinforcement hardening) [kN/m^2]	Deviation of ANSYS results from analytical calculations (%)
1000	73.926	81.25	87	9.05
1200	62.1	71.67	76.69	13.35
1500	50.075	63.96	68.75	22.12
1800	41.949	57.08	60.5	26.4

Table 2 Study results for maximum deflections

Sample width (mm)	Maximum deflection (according to regulatory documents) [mm]	Maximum deflection ANSYS (when the reinforcement reaches the yield point) [mm]	Maximum deflection ANSYS (after reinforcement hardening) [mm]	Deviation of ANSYS results from analytical calculations (%)
1000	6.989	8.25	12.785	15.28
1200	6.466	7.93	9.67	18.46
1500	5.742	7.87	9.62	27.04
1800	5.131	7.7	9.78	33.35

Figure 6 shows the stresses in the reinforcement at various stages of loading. Obviously, the stresses in the reinforcement, in samples with a larger width, grow faster. It can be seen that, in connection with the reinforcement hardening at the last stages of loading (that is, using a diagram with bilinear isotropic hardening), at the end sections of each of the graphs, there is a slight stop in the growth of axial tensile stresses, with an increase in the acting load.
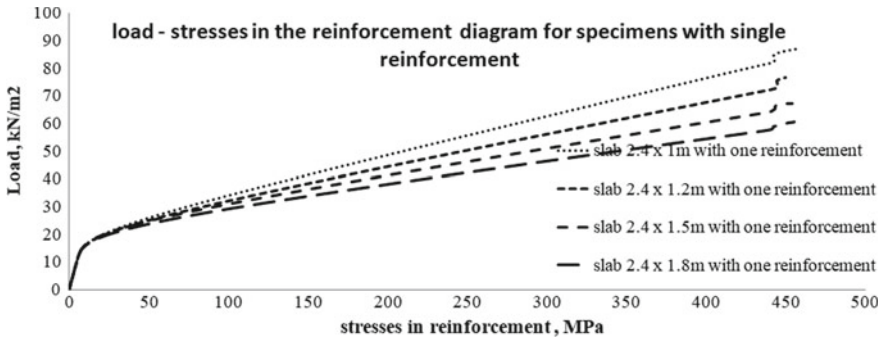
Fig. 6 Load—stresses in the reinforcement diagram for specimens with single reinforcement

As the Tables show that the results of deflections of numerical calculation according to the Drucker-Prager strength criterion differ from the results obtained by the standard method from 15 to 33% depending on the width of the specimens. This figure is also quite high for the load-bearing capacity and ranges from 9 to 26%.

At the same time, Table 1 presents two options for calculating the breaking load in ANSYS. This is the breaking load when the stress in the reinforcement corresponds to the yield point, as well as the destruction taking into account the reinforcement hardening. The second type of loss of bearing capacity was accompanied in the program by a sharp increase in slab deflections by tens of times, which was qualified as destruction.

Table 3 shows the results of the stress in the reinforcement as a result of the analytical calculation in comparison with the analogous results of the calculations in ANSYS. Based on the results of analytical calculations, it is obvious that with an increase in the width of the samples, the stress in the reinforcement during the formation of cracks in the slab increases. The deviations in the results of the reinforcement stress at fracture are from 4 to 7% in comparison with the calculation in the ANSYS software.

Table 3 Reinforcement stress results

Sample width (mm)	Cracking stress in reinforcement (according to regulatory documents) [MPa]	Stress in reinforcement at failure (according to regulatory documents) [MPa]	Stress in reinforcement at failure, ANSYS (MPa)	Deviation of ANSYS results from analytical calculations (%)
1000	226	477	457	− 4.37
1200	248	478	449	− 6.4
1500	285	485	454	− 6.82
1800	319	487	455	− 7.03

The results of the cracking load are presented in Table 4. At the same time, the calculations according to the traditional methods were carried out both taking into account elastic and taking into account inelastic deformations. As can be seen from the table, the deviation of the ANSYS results of the standard method varied from 16 to 28% depending on the width of the samples.

Table 4 Results of cracking load studies

Sample width (mm)	Cracking load taking into account elastic deformations (according to regulatory documents) [kN/m^2]	Cracking load taking into account Inelastic deformations (according to regulatory documents) [kN/m^2]	Cracking load, ANSYS (at the corresponding stresses in the reinforcement according to regulatory documents) [kN/m^2]	Deviation of ANSYS results from analytical calculations (%)
1000	35,078	43,847	52.5	16.48
1200	32,214	40,267	50.42	20.14
1500	29.444	36.805	49.76	26.03
1800	27.439	34.299	47.92	28.42

4 Conclusion

It is proved that the findings of calculating the stress-strain state of hollow slabs of different width according to the conventional method and the Drucker-Prager criterion have very significant differences up to 30% depending on the width of the specimens.

Nevertheless, the reviewed model allows the researchers to study the stress-strain state of a reinforced concrete element at various stages of loading, including when the reinforcement reached the yield point and begun to harden. The tables also prove that the load-bearing capacity per square meter decreases when the specimen width increases by a maximum of 43% when conventionally calculated with a maximum width difference from 1000 to 1800 mm and by 30% if numerically calculated using the Drucker-Prager model. For deflections, these figures are 26% and 6%, respectively.

It is obvious that the Drucker Prager Base model has quite serious deviations from the traditional method, especially in terms of breaking load and cracking load. However, the general trends coincide with the results of analytical calculations using the traditional method.

References

1. Mota M (2010) Voided slabs: then and now. Concr Int 32(10):41–45
2. Walraven JC, Mercx WPM (1983) The bearing capacity of prestressed hollowcore slabs. Heron 28:1–46
3. Becker RJ, Buettner DR (1985) Shear tests of extruded hollow core slabs. PCI J 30:40–54
4. Pajari M, Koukkari H (1998) Shear resistance of PHC slabs supported on beams. I: tests. J Struct Eng 9:1050–1061
5. Pisanty A (1992) The shear strength of extruded hollow-core slabs. Mater Struct 25:224–230
6. Karpenko NI, Mukhamediev TA, Petrov AN (1986) Iskhodnyye i transformirovannyye diagrammy deformirovaniya betona i armatury (Initial and transformed deformation diagrams of concrete and reinforcement). NIIZHB, Moscow, pp 7–25
7. Karpenko NI (1996) Obshchiye modeli mekhaniki zhelezobetona (General models of reinforced concrete mechanics). Stroyizdat, Moscow
8. Hegger J, Roggendorf T, Kerkeni N (2009) Shear capacity of prestressed hollow core slabs in slim floor constructions. Eng Struct 31:551–559
9. Lam D, Elliott KS, Nethercot DA (2000) Parametric study on composite steel beams with precast concrete hollow core floor slabs. J Constr Steel Res 54:283–304
10. Song JY, Elliott KS, Lee H et al (2009) Load distribution factors for hollow core slabs with in-situ reinforced concrete joints. Int J Concr Struct Mater 1:63–69
11. Elgabbas F, El-Ghandour AA, Abdelrahman AA et al (2010) Different CFRP strengthening techniques for prestressed hollow core concrete slabs: experimental study and analytical investigation. Compos Struct 92(2):401–411. https://doi.org/10.1016/j.compstruct.2009.08.015
12. Yuanli WU (2015) Shear strengthening of single web prestressed hollow core slabs using externally bonded FRP sheets. Electronic theses and dissertations. Windsor, Ontario, Canada
13. Chen GM, Chen JF, Teng JGl (2012) On the finite element modelling of RC beams shear-strengthened with FRP. J Constru Build Mater 32:13–26
14. Bennegadi ML, Sereir Z, Amziane Z (2013) 3D nonlinear finite element model for the volume optimization of a RC beam externally reinforced with a HFRP plate. J. Constru Build Mater 38:1152–1160

15. Kankeri P, Prakash S, Pachalla SKS (2018) experimental and numerical studies on efficiency of hybrid overlay and near surface mounted FRP strengthening of pre-cracked hollow core slabs. Structures 15:1–12
16. Vasilyev AS, Odinokova OA, Nazarova VP (2020) Investigation of the effect of reinforcing diaphragms ribbed panels on their carrying capacity. Mater Sci Forum 974:577–582
17. Vasilyev AS, Bazhenov RI, Gorbunova TN (2018) The influence of cross section shape on strengthening of hollow core slabs. Mater Sci Forum 931:24–29
18. Bai X, Zemlyak VL, Vasilyev AS et al (2020) Stressed-deformed state of ice crossings at the surface reinforcement of composite materials. J Mar Sci Appl 19(3):430–435
19. Drucker DC, Prager W (1952) Soil mechanics and plastic analysis for limit design. Quart Appl Math 2:157–165
20. Klovanich SF, Bezushko DI (2009) Metod konechnykh elementov v raschetakh prostranstvennykh zhelezobetonnykh konstruktsiy (Finite element method in the analysis of spatial reinforced concrete structures). Publishing House of Odessa National Maritime, Odessa University
21. Klovanich SF, Mironenko IN (2007) Metod konechnykh elementov v mekhanike zhelezobetona (Using Finite element method in reinforced concrete mechanics). ONMU, Odessa

Operation Analysis of the Main Arch-Cable-Stayed Systems When Operating Under Unevenly Distributed and Asymmetrically Working Loads

V. V. Dolgusheva(✉) and A. M. Ibragimov

National Research University Moscow State University of Civil Engineering (NRU MGSU), 26, Yaroslavskoye Shosse, Moscow 129337, Russia

Abstract. On account of the lack of detailed theoretical and experimental research of the arch-cable-stayed structures actual operation, the design and application of arch combined systems is limited. However, such systems have a number of advantages compared to simple arches: the combined systems survivability is higher, the combined systems consume less metal having the same geometrical parameters, high load-bearing capacity with relatively low weight, architectural expressiveness. The research aim is to compare the operation of the main arch-cable-stayed systems with symmetric and asymmetric load effects in a nonlinear setting. According to the calculation results in the Lira Sapr 2020 software package, the most dangerous load combinations, deformed schemes of arch systems, displacements, moments and forces are determined, the sections of arches and bowstrings are selected. From the point of view of the least effort, displacement and metal consumption, the arch systems with centrally concentrated stay cables and radially (fan-shaped) stay cables showed the best result out of the four considered systems.

Keywords: Combined systems · Arch- cable-stayed constructions

1 Introduction

On account of the construction growth of large-span public buildings with the use of metal structures, the search for a rational design solution is a topical task [1]. On the basis of the material consumption per square meter of the spanned area, often the solution to the task is the use of arch combined systems as part of load-bearing structures.

Arched combined systems, in contrast to simple arches, do not require the creation of massive support structures and foundations for the perception of the strut, since part of the spacer force is taken over by bowstrings, stay cables, racks and other auxiliary elements; require less material consumption due to better work on one-sided loads; have a smaller free space dimension, which reduces heating costs, in the case of a heated building.

Combined arch structures have a number of advantages compared to simple arches:

- The survivability of combined systems is higher than that of simple systems. Valerio De Biaggi notes that it is complex structures, such as combined systems, that have the least consequences of destruction under the work of beyond-design loads [2]. Due to the big number of combinations and elements, in complex constructions there is a more uneven redistribution of forces across the elements than in simple structures. "The survivability of one or another structural form is provided by the redistribution of forces between the structural elements and depends on its ability to connect" [3], thus, multi-connected structural systems are preferable to provide resistance to progressive collapse.
- The ability to reduce the calculated length of compressed-curved elements, improve the work in case of uneven loading, rationalize the work of stretched prestressed elements, reduce the boom of lifting the structure with the help of inserting stay cables, bowstrings, and additional rods into the structure.
- The ability to create complex, architecturally expressive spatial structures by combining elementary schemes [4] and varying parameters, such as the span, the boom lift, the slack of bowstrings, the number of additional elements, the material of the structure.
- With spans of more than 40 m, arches are more economical in terms of material consumption in comparison to beams and frames [5], and comparing to simple arches, combined arch systems have a lower material consumption with the same geometrical parameters (span, boom lifting height) [6].
- In arches with a system of high-strength inclined rods, it is possible to replace the suspensions in the operation mode of the structure [7].
- Combined structures have a high load-bearing capacity with a relatively low weight [8].
- Arch-cable-stayed combined systems work better with uneven loading [9].

More often, combined arch systems are used as load-bearing structures of a building in the form of an arch-cable-stayed structure.

Combined arch systems can be divided into 5 main types [10]:

- Hub type systems (Arches with centrally centered stay cables. The rods connect the points of the upper boom of the arch to the free center) see Fig. 1a;
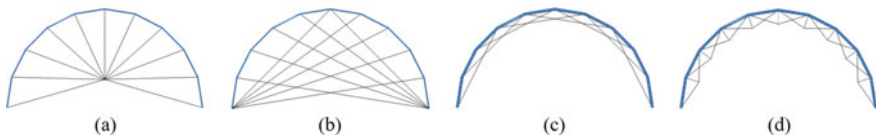
Fig. 1 a Arch № 1. Hud type system; **b** Arch № 2. Radial type system; **c** Arch № 3. Chord type system; **d** Arch № 4. Truss type system

- Radial type systems (Arches with radially (fan-shaped) placed stay cables. The stay cables connect the arch support point to one or more points of the arch boom) see Fig. 1b;
- Chord type systems (Stay cables are arch chords. In these systems, there is a fine balance between the degree of discretization of the arch boom and the degree of efficient operation provided by the connections) see Fig. 1c;
- Truss type systems (Are the most common solutions and have a greater variety in terms of the arrangement of elements. In all cases, the auxiliary elements repeat the shape of the arch) see Fig. 1d;
- Mixed systems (Such systems combine one or more of the systems above into a united structure to provide efficient operation in cases of various dominant loads).

On account of the lack of detailed theoretical and experimental research of the of the arch- shroud structures actual operation, the design and application of arch combined systems is limited.

The research aim is to compare the operation of the main arch-shroud systems with symmetric and asymmetric load effects in a nonlinear setting from the point of view of the least effort, displacement and metal consumption.

2   Materials and Methods

Source data. To compare the work of the main arch-cable-stayed systems, the loads for the III snow and I wind regions were taken, since according to the maps in Appendix E [11] these are the most common areas of the Russian Federation. The roof weight q = 300 (kg/m) was set as an evenly distributed load on the upper arch boom. Arches being more economical compared to beams and frames [5] at spans of more than 40 (m), the span L = 42 (m) was assumed to be a multiple of 3 (m). The lifting boom is taken from the proportion f/L = 1/2 as one of the "characteristic values of relative height". The type of arches is double-hinged. Double-hinged arches have a more favorable distribution of bending moments in their length, they are less sensitive to temperature exposures and settling of supports [12]. To create equal conditions, restrictions on the type of section for cables and the upper boom were imposed, so the type of section for cables was accepted according to GOST 3064-80 [13], and for the upper boom according to GOST 30245-2012 [14]. The upper boom of the considered arch-cable-stayed systems is a polygonal circular arch. The number of panels is determined according to the recommendations for arch calculations with an arbitrary number of rods [15]. In accordance with the recommendations for a span of L = 42 (m), it is necessary for the upper boom to be divided into 10 equal panels (Fig. 2).

Criteria for calculating and choosing sections. As the criteria for calculating and choosing sections, vertical and horizontal displacements were taken that do not exceed the maximum permissible values (for vertical displacements, fult = 0.13 (m); for horizontal displacements, hult = 0.103 (m) [11]), testing strength and stability with the action of a fore-and-aft force with a bend of the upper boom section [16], testing the tensile strength of the cable [17].

Modeling and calculation. The calculation of arch-cable-stayed systems was carried out in the Lira Sapr 2020 software package with the help of the finite element method.
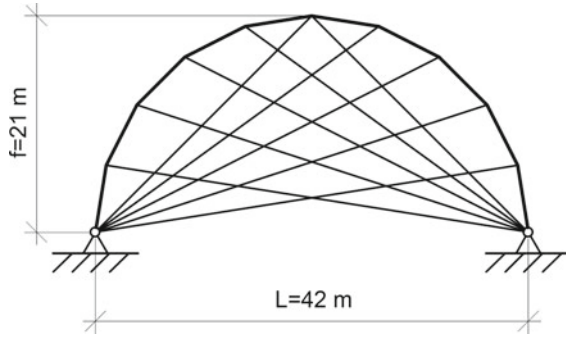
Fig. 2 Calculation scheme on the example of arch structure No. 2. (Radial type system)

The models are created in a flat formulation of the problem (three degrees of freedom: displacement along the x, z, rotation around the y axis) accounting for the physical and geometrical nonlinearity. The upper boom and the arch bowstrings are modeled with the help of finite element No.310 (geometrically nonlinear universal spatial rod-type finite element, thread). To calculate the nonlinear structure, the cables of the arch systems were divided into finite elements with a length of 0,5 0.5 (m), the upper boom of the arches was divided into finite elements with a length of ≈1 (m).

In the calculation scheme the following loads were enclosed:

- The dead weight of the arch system;
- Coating weight;
- Prestressing of bowstrings;
- Evenly distributed snow load;
- Unevenly distributed snow load;
- Static wind load on the X-axis;
- Static wind load against the X-axis;
- Ripple wind load on the X-axis;
- Ripple wind load against the X-axis.

The load values are determined in accordance with the requirements of SP 20.13330.2016 [11]. Ripple wind loads are defined in the software package on the basis of static wind loads as a dynamic impact. The prestress of the bowstrings was modeled by setting the temperature loads. Firstly, the maximum tensile force N_{max} of the bowstring was determined according to Eq. 1 [17], then the maximum temperature T_{max} which must be set to the bowstrings to receive the maximum permissible tensile force N_{max} was determined according to Eq. 2:

$$N_{\max} = \frac{\sum P_{un} \cdot m \cdot m_1}{\gamma_m} \tag{1}$$

$\sum P_{un}$ the whole value of the breaking force of the rope;
m, m_1 coefficients of working conditions;
γ_m coefficients of reliability.

$$T_{\max} = \frac{N_{\max}}{A \cdot \alpha \cdot E} \tag{2}$$

A calculated sectional area of all the wires;
α linear expansion coefficient;
E the elastic modulus of the steel rope.

The bowstrings were given the temperature load (prestress) which was not higher than Tmax and allowed to follow the criteria of calculating and choosing sections. Figure 3 shows the cables which were given prestressed voltage in kN.
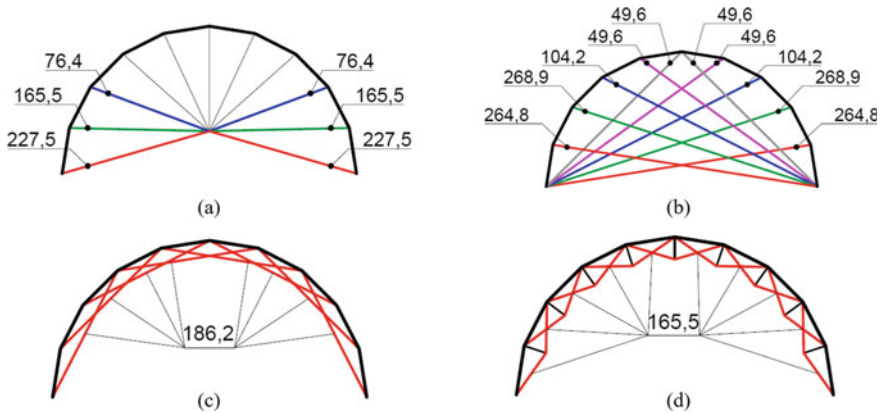
Fig. 3 Prestressed cables. The forces are shown in kN. **a** Arch № 1. Hud type system; **b** Arch № 2. Radial type system; **c** Arch № 3. Chord type system; **d** Arch № 4. Truss type system

The work of the arch structure without bowstrings in a linear setting was analyzed in order to determine the unfavorable combination of loads. The calculations were made on 12 calculated combinations of loads that had been formed in accordance with the requirements [11]. According to the results 2 most unfavorable combinations of loads were picked. The calculation of arch systems in a non-linear setting was made for one of the two picked unfavorable combinations, in particular for the combination in which the structure is affected by its own weight, the coating weight, prestressing, and uneven snow load. Figure 4 shows deformed schemes of the arch-cable-stayed systems.

3 Literature Review

In Russia, there is an increase in the construction of large-span public buildings with the use of metal structures [1]. When making an individual project, architects, designers, and builders try to create new and unique constructions. Unfortunately, due to the lack of research and experience in constructing new types of structures, errors occur in the design, installation, and operation, which lead to damages of buildings and structures.

Fig. 4 Deformed schemes. **a** Arch № 1. Hud type system; **b** Arch № 2. Radial type system; **c** Arch № 3. Chord type system; **d** Arch № 4. Truss type system

In this regard, the search for a rational design solution, providing the requirements of design and construction, is quite a topical task [7].

It often happens so that the solution to the task of structures rationalization when providing the requirements for the design of buildings is the use of arched combined systems as part of load-bearing structures. The application scope of arch systems is of a wide range: as part of load-bearing structures, arches are often used in extended buildings, such as sports complexes (ice rinks, basketball halls, skating centers, etc.), indoor markets, galleries or halls of shopping malls, warehouses, hangars, industrial buildings, railway stations, etc. Arch systems are very often used in the construction of bridges. The rational form of the arch at the given values of the load, span and boom lift is considered to be one that provides the necessary strength and resistance with the smallest volume [18, 19].

Combined arch systems have a wide variety of initial parameters: static scheme, span, boom lift, the outline of the plan, slack of bowstrings, location and number of additional rod-type elements, the material of structures, methods of design and installation [9]. Many researchers have considered the solution of this multifactorial task to be rationalization in different settings. The results of the research are given below.

V. G. Shukhov studied the problem of rationalization of types of rectilinear trussed rafters. The brochure [15] includes the solution in a linear setting of the following tasks for an arch-cable-stayed system with fan-shaped cables: the choice of the number of nodes and panels; the location of the balks; the determination of the distances between the trussed rafters; the choice of the outline of the upper boom if arch trussed rafters are with flexible rods; the determination of the most rational places for fixing the bowstrings; the search for the most rational structure on the basis of the criterion of minimum material consumption and coating weight.

Surovtsev B. A. studied the span structures of combined systems with a polygonal upper boom and inclined suspensions of the "rigid arch - rigid bowstring" type. The article shows the comparison of arch-cable-stayed bridges with vertically and inclined bowstrings [20]. The researcher comes to the conclusion that an arch with inclined stay cables forming a net works better under asymmetric loading; inclined bowstrings allow the load to be evenly distributed, so it helps reduce the values of the acting bending moments and forces of the section dimensions; the main forces in the arch and bowstrings are the longitudinal axial force.

Ibragimov an Kukushkin [21] compared five arch constructions, including an arch with fan-shaped bowstrings. According to the results of the research of the work of arch constructions with an evenly distributed load, the authors come to the conclusion that arched structure with stay cables has a good number of advantages: the steel consumption

for the arch with stay cables is noticeably less, such construction has the property of survivability, and the small size of the elements allows to reduce transportation costs. As a result of the rationalization of the dimensions of the boom lift and span for arches with a span of 18–36 m, the authors sum up that the rational boom lift equals from a quarter to a third of the span.

Researchers Tryanina N. Yu. and Testoedov P. S. mark the importance of arch systems with cable-stayed bowstrings and the existence of insufficiently studied problems related to their design and practical application. In the article [6], dedicated to comparing the work of several arch combined structures, the authors come to the following conclusions: the increase in the boom lift leads to the increase in the efficiency of installing inclined prestressed rods; inclined rods allow to align the absolute values of bending moments that help maximize the use of the load-bearing capacity of the arches, there is a decrease in the arch section stresses, that makes it possible to reduce the steel consumption per arch by up to 30%; it is mentioned that arches with centrally concentrated stay cables and fan-shaped stay cables are the most effective in terms of material consumption.

Nowadays, there is a number of research on individual arch-cable-stayed combined structures, but not all of the main types of arch-cable-stayed systems have been studied, this problem requires the attention of architects and engineers for the development of large-span arch construction. The results of scientific research in the field of structural mechanics, materials, construction and installation technology allow us to expand the use of arch-cable-stayed systems as long-span coverings. However, there are poorly studied problems related to their design and practical application:

- lack of detailed theoretical and experimental research of the actual operation of different arch-cable-stayed structures;
- lack of certain recommendations for the design and calculation of arch-cable-stayed systems;
- difficulties of reliable assessment of the strength of arched structures in real design;
- the lack of an effective solution to the problem of providing the strength of arch structures to progressive collapse;
- to solve the task of providing the safety of buildings and constructions, it is important to evaluate the design not only in the extreme, but also in extreme conditions that arise from new types of technological, natural and other beyond-design impacts.

It is necessary to improve the traditional methods and create new ones for assessing the survivability of a structural system [4] in order to implement the rational design solution, following the requirements of design and construction.

4   Results and Discussions

An arch without bowstrings was calculated in a linear and nonlinear setting in order to assess the influence of prestressed cables on the work and consumption of metal in the arch structure. The results of the calculations are shown in Table 1. The best indicators are highlighted with green colour in Table 1.

The conclusions, based on the received results, are as follows:

Table 1 The results of the calculations

№	Scheme name	Polygonal round arch	Polygonal round arch	Hud type system	Radial type system	Chord type system	Truss type system
	Scheme number	0.1	0.2	1	2	3	4
1	Calculation type	Linear calculation	Calculation accounting the physical and geometrical nonlinearity				
2	Maximum horizontal displacement hult (mm)	95,9	101	90,4	−72,3	96,3	102
3	Maximum vertical displacement fult (mm)	−75	−80,9	−109	90,8	−88	−89
4	Maximum fore-and-aft force force in the arch boom Nmax1 (kN)	−553,3	−552,3	−524,8	−726,9	−911,4	674,0
5	Maximum bending moment in the arch boom Mmax (kN·m)	−868,2 +644,5	−901,5 +662,2	−142,2 +144,2	−94,0 +70,3	−696,5 +498,4	−772,0 +501,3
6	Maximum lateral force in the arch boom Qmax (kN)	−132,4 +161,9	−134,4 +162,8	−70,5 +93,9	−82,3 +83,1	−107,9 +140,3	−110,9 +137,3
7	Maximum tension force in bowstrings Nmax2 (kN)	–	–	+265,9	+212,9	270,8	256,0
8	Selected section of the upper boom	Composite box 560x25	Composite box 560x25	Shape 250x10	Shape 250x10	Composite box 500x25	Composite box 500x25
9	Selected cable section	–	–	Ø11,5; Ø15,5; Ø27	Ø17; Ø27	Ø27	Ø27
10	Arch boom weight (t)	28,87	28,87	4,77	4,77	25,78	26
11	Cable weight (t)	–	–	0,40	0,88	0,55	0,44
12	Total construction weight	28,87	28,87	5,17	5,65	26,33	26,44
13	Reduced metal consumption (Proportion of total mass to span) (t/m)	0,687	0,687	0,123	0,135	0,627	0,630
14	Arch boom strength margin (based on the test results) %	–	64	14	43	65	61
15	Upper boom stability margin (based on the test results) %	–	64	24	52	65	61

- the result of calculating the arch in a linear and non-linear setting is different for displacements by 7,9%, for forces by 3,8%. To receive a more valid result it is necessary to calculate the arch combined systems in a nonlinear setting [5];
- the smallest vertical displacements are seen in scheme No.2, the smallest horizontal displacements (among the arch-cable-stayed systems) are seen in scheme No.3;
- the lowest fore-and-aft forces in the upper boom are seen in scheme No. 1, and the minimum moments and lateral forces and bowstring tensions are seen in scheme No.2;
- according to the metal consumption of the upper boom, schemes No.1 and No.2 are the most economical of the shown schemes, and scheme No.1 is more economical in terms of the metal consumption on ropes. According to the shown metal consumption, arch No.1 is the least expensive;
- in the considered arch structures, due to the specified criteria for calculating and choosing sections in all the schemes, and, in terms of strength and stability, the upper boom sections have a big margin. This shows the possibility of choosing more efficient sections and reducing metal consumption. However, the ropes used for the calculation do not allow to reduce the section of the upper boom (when reducing the sections of the upper boom, the tension in the ropes reaches the breaking force).

5   Conclusions

According to the results of the comparison of the main arch-stay-cabled combined systems, conclusions can be made as follows:

- it is necessary to calculate the combined arch systems in a nonlinear setting to get a more exact result;
- the most favourable arches, from the point of view of the least number of displacements, force and metal consumption, are the arch with centrally concentrated stay cables and the arch with fan-shaped stay cables;
- for further research, it is necessary to repeat the numerical study, but to consider arch-cable-stayed systems with a smaller span and at different proportions of the lift boom and span to receive more complete information about the arch systems operation, and to perform research of these systems survivability.

Arch-cable-stayed combined systems are a fancy-framed, architecturally expressive, constructively practical, low-cost material consumption (economical) solution to the task of overlapping large spans, providing the fulfillment of architectural, structural requirements and requirements for structural strength and safety. Nevertheless, in the sphere of arch combined systems there are a lot of unsolved problems that need the application of architectural and engineering actions. These problems are: the performance of numerical and full-scale experiments to identify the actual work of combined arch systems; the design of recommendations for constructing and calculating arch-cable-stayed structures; the problem of providing the stability of arch-cable-stayed systems; the study of resistance to progressive collapse.

There is another possible way to solve the problems mentioned above: the creation of scientific works on different types of arch-cable-stayed systems, which study the rationalization of the arch construction geometry, the study of the tension deformed condition and survivability of the combined system with the creation of new calculation methods, numerical and full-scale experiments are carried out, as the result of which it is possible to indicate the actual work of arch construction. According to the results of the performed research, it is possible to systematize the results, to elaborate the recommendations for the design of arch combined constructions.

References

1. Eremeev PG (2013) Sovremennye stadiony. Opyt proektirovaniya i vozvedeniya metallicheskih konstrukciy pokrytiy. Raschyot i proektirovanie metallicheskih konstrukciy (Modern stadiums. Experience in the design and construction of metal structures for coatings. Calculation and design of metal structures). Nauchno-prakticheskya konferencia, posvyashchyonnaya

100-letiyu so dnya rozhdeniya professora E.I. Beleni "Raschet i proektirovanie metallich-eskih konstrukciy", Moscow State University of Civil Engineering, 2013, Sbornik dokladov nauchno-prakticheskoy konferencii, ELS, ACEU, pp 72–83

2. De Biaggi V (2015) Povyshenie zhivuchesti sooruzheniy s pomoshch'yu uslozhneniya kon-struktivnyh skhem (Increasing the survivability of structures by increasing the complexity of structural schemes). Vestnik TGASU 4:92–100

3. Tryanina NY, Samokhvalov IA (2018) Issledovanye voprosa zhivuchesty setchatogo kupola (Investigation of the question of the survivability of the mesh dome). Privolzhskiy nauchniy zhurnal 1:15–18

4. Muschanov VF, Vishnyakova NA (2018) Sravnitel'ny analiz effektivnosti konstruktivnyh resheniy bol'sheprolyotnogo pokrytiya na krivolineynom plane (Comparative analysis of the effectiveness of design solutions for a large-span pavement on a curved plan). Metallicheskie konstrukcii 24:6–15

5. Kiselev DB (2009) Rabota kombinirovannoy arochnoy sistemy s uchyotom geometrich-eskoy nelinejnosti i posledovatel'nosti montazha (Combined arch system operation tak-ing into account geometric nonlinearity and installation sequence). Dissertaciya, AO "NIC"Stroitel'stvo"

6. Tryanina NY, Karzanov MA (2011) Issledovanie raboty arochnyh konstrukciy s sistemoy naklonnyh tyag (Tensile fabric surface formfinding control). Privolzhskiy nauchniy zhurnal 2:16–19

7. Kolyushev IE, Skornik OG, Tarbaev NA (2006) Primenenie vantovyh tekhnologiy v prolyot-nyh stroeniyah razlichnyh staticheskih system (Application of cable-stayed technologies in spans of various static systems). Transport Rossiyskoy Federacii. Zhurnal o nauke, praktike, ekonomike 5:49–52

8. Tryanina NY, Testoedov PS (2015) Research of the survivability of steel reticulate coverings. Privolzhskiy nauchniy zhurnal 1:9–15

9. Kiselev DB (2006) Arochno-vantovye kombinirovannye konstrukcii. Chislennye i eksper-imental'nye issledovaniya (Combined (hybrid) arch-cable structures. Numeric and experi-mental researches). Sovremennoe i grazhdanskoe promyshlennoe stroitel'stvo 2(1):17–27

10. Burford NK, Smith FW, Gengnagel C (2009) The evolution of arches as lightweight struc-tures—a history of empiricism and science. In: Proceedings of the Third International Congress on Construction History, Cottbus

11. SR 20.13330.2016 Nagruzki i vozdejstviya (Loads and impacts)

12. Lebedeva NV (2006) Fermy, arki, tonkostennye prostranstvennye konstrukcii (Trusses, arches, thin-walled spatial structures). Izdatel'stvo "Arhitektura-S", Moscow

13. GOST 3064-80 Kanat odinarnoy svivki tipa TK konstrukcii 1x37(1+6+12+18) (One lay rope type TK construction 1x37 (1+6+12+18). Dimensions). Standardinform, Moscow

14. GOST 30245-2012 Profili stalnye gnutye zamknutye svarnye kvadratnye dlya stroitelnyh kon-strukciy (Steel bent closed welded square and rectangular section for building. Specifications). Standardinform, Moscow, 2014

15. Shukhov VG (1977) Izbrannye trudy. Stroitel'naya mekhanika (Selected Works. Structural mechanics). NAUKA, Moscow, pp 102–139

16. SR 16.13330.2017 Stalnye konstrukcii (Steel structures)

17. SR 35.13330.2011 Mosty i truby (Bridges and pipes)

18. Kiselev VA (1964) Racional'nye formy arok i podvesnyh system (Rational forms of arches and suspension systems). Gos. izd. lit. po str. i arh., Moscows

19. Streletsky NS, Streletsky DN (1964) Proektirovanie i izgotovlenie ekonomichnyh metal-licheskih konstrukciy (Design and manufacture of economic metal structures). Stroyizdat, Moscow

20. Suvorovtsev BA (2017) Osobennosti proektirovaniya proletnyh stroeniy mostov kombinirovannyh sistem s gibkimi podveskami (Features of design of bridges span structures of the combined systems with flexible inclined suspension brackets). Sovremennye tekhnologii. Analiz. Modelirovanie 1:219–224

21. Ibragimov AM, Kukushkin IS (2014) Sravnitel'niy analiz variantov konstruktivnyh resheniy pologih arochnyh pokrytiy zdaniy (Comparative analysis of design options for shallow arched roofs of buildings). Vestnik MGSU 3:59–66

22. Niroumand H, Zain MF, Jamil M (2011) Bridge architecture in Japan. Int J Phys Sci 6(17):4302–4310

23. Niroumand H, Zain MF, Jamil M (2012) Bridge Architecture in Malaysia. Int J Environ Sci Dev 3(3):311–314

24. Stoyanova I (2015) The iron-glass roof of the Milan Gallery Vittorio Emanuele II: knowing the past, understanding the present and preservation for the future. Struct Stud Repairs Maintenance Heritage Architec XIV:78 (WIT Press)

25. Savor Z, Bleiziffer JZ (2008) Long span concrete arch bridges of Europe. Chinese-croation joint colloquium. Long arch bridges. Brijuni Islands, pp 171–180

Development of Flexible Joint
for Beam-to-Column Abutment

M. P. Son, G. G. Kashevarova, and A. D. Zemlyanukhin[✉]

Perm National Research Polytechnic University, 109, Kuibyshev St, Perm 614107, Russia
a_zemlyanukhin@bk.ru

Abstract. When designing buildings with a metal bearing frame, the design of joints is one of the most complex problems. Russian regulations adopt the division of joints into absolutely stiff and ideal hinged joints which is quite conditional. In fact, the joints are flexible, and neglecting it can result in design errors. The existing design and calculation methods are labor-intensive and not always correct. The article considers the structure of a flexible joint for the beam-to-column abutment. The joint base is a flange connection operated by the elastoplastic pattern. At the flange calculation the authors use the method of division into simple T-parts. Other connection parts (column wall, flange, etc.) with a negligibly small strain are not taken into account in the flexibility calculations. It reduces the analytical calculation complexity to a minimum. The joint proposed allows redistributing bending moments on the beam bearings and span. As a result the beam bearing capacity improves in comparison with a hinged or stiff abutment. The analytical calculation for the connection is added with the finite element design model. The authors compared the results of analytical and numerical calculations.

Keywords: Flange connection · Elastic connection · T-beam

1 Introduction

The braced frame is one of the most widespread building structural designs. When designing similar frames, longitudinal beam to column joints is generally designed either as absolutely stiff or ideal hinge joints. In fact, joints can be flexible which is confirmed by numerous research. Such a characteristic is one of the most important ones for a joint. Thus, for example, papers [1, 2] study the methods of joint reinforcement with various stiffeners and stiffening plates. The use of similar structural components reduces joint flexibility but the joint cannot be made as absolutely stiff in compliance with the Eurocode classification [3]. The joint flexibility negligence can cause significant errors in the frame static design.

The research of joint stiffness and strength characteristics in construction structures are also relevant today. Depending on the flexibility value the joint can be considered conditionally hinged or absolutely stiff. In Russia, when designing a stiff joint, one tends to eliminate even the smallest rotation of the beam bearing section. By the series 2.440-2 (1989) the flange connections of frame joints reinforce a set of structural parts: stiffeners,

haunches, companion flanges, etc. Judging by the research [4–8], including numerical and natural tests, one can draw the conclusion that connection reinforcement leads to the stiffness increase but reduces the connection stress–strain properties. The absence of potential plasticity reduces the connection ability to dissipate the oscillations caused by seismic loads, for example. Thus, in Northridge (USA) after the earthquake more than 150 metal frames were destroyed in the longitudinal beam-column joints [9]. The destruction was of a fragile nature and was caused by a high joint stiffness. Analyzing the defects that occurred, one can conclude bolt connections are more stable as compared with welded connections while flexible joints have the advantage over the stiff ones [3, 10].

European regulations allow designing flexible joints. In addition, Eurocode 8 binds the designers to stipulate oscillation dissipation areas on seismic impact when designing buildings. Structurally, such a solution can be provided for either in the beam-column joint or on the beam itself, for example, a local reduction of beam flanges in the proximity of column connection [10–20].

According to EN (1993-1-8-2009), the joint flexibility calculation is possible by means of a live experiment, mathematic modeling or a component method of joint design. A component method is based upon the joint representation as a set of components [3]. The bearing connection capacity is generally defined by the bearing capacity of its main components. Joint flexibility is defined as a set of flexibilities of "springs" connected successively and in parallel (Fig. 1). At joint design one can apply linear elastic or elasto-plastic calculation methods. As a result, it is possible to obtain the dependence "beam moment—rotation angle" (M-φ).
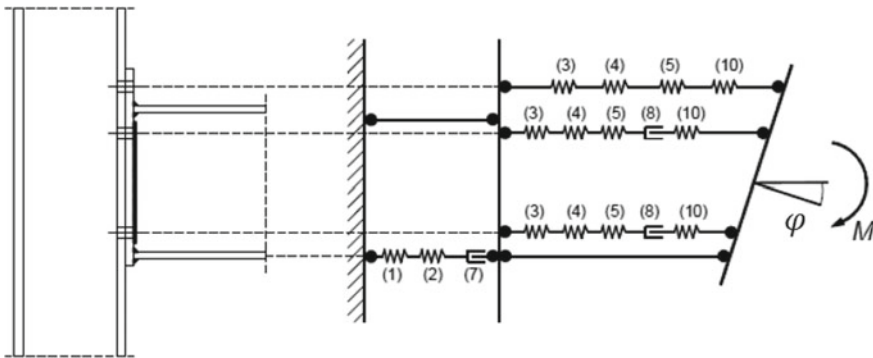
Fig. 1 Joint components by Eurocode

Basing upon the component method and finite element method a component finite element method (CFEM) was developed where main components (section walls and flanges) are modelled by component elements while other components are calculated by EN formulas. The research of CFEM calculation result correctness is provided in paper [1], numerical models are compared with full-size models' tests. The main comparison criteria are the limit perceived moment and the rotation angle of the beam section. The

bearing capacity calculation showed good convergence with the results of live experiments; the error was 5–14%. The strain calculation showed insufficient flexibility of the numerical models applied: rotation angle values were 25–90% lower than those obtained in the course of the experiment. The component method use for joint calculation and design is rather labor-intensive and cannot provide a guaranteed result. Mathematic modelling in the volume finite elements is also labor-intensive and requires verification by a live experiment. The only veracious engineering tool for flexible joint calculation remains the live experiment conduct.

The most important EN provision referred to cl.2.5, 5.2.2.1, 6.4, etc. can be stated as follows: design parameters can be obtained either on the basis of experimental data or appropriate design model verified by test results.

Since 2017 the Perm National Research Polytechnic University (PNRPU) laboratory have conducted comprehensive research of beam to column abutment joint. The scientists prepared a design model which was further verified with experimental data [4, 6, 7]. The basic principles of design model calculation were used in this research as well. The purpose of the research is to develop a flexible joint with an analytical description made in the simplest possible terms.

2 Development of a New Type of Flexible Joint

As it has been mentioned, one should take into account joint flexibility, especially for specific buildings. Yet, the flexibility calculation is a labor-intensive problem. There is a need of developing an engineering method, analytical calculation of flexible connections, for designing the joint without conducting numerical or live experiments, and the joint operation mechanics should be as simple as possible.

Consider the longitudinal beam with the double-T section connected to the columns with flexible joints and evenly loaded with a distributed load. The optimal stiffness of this joint is that at which the longitudinal beam metal consumption will be the least. I.e., the moment distribution will have similar module values of bending moments in the beam span and bearings. In particular:

$$M_c = M_{sup}| = \frac{q \cdot l^2}{16} \tag{1}$$

where M_{sup}—moment in the beam span, M_c—moment on the beam bearings (Fig. 2).

The bearing stiffness for obtaining such a distribution of beam moments can be calculated on the basis of the beam static design.

$$c = \frac{6 \cdot E \cdot I_x}{l} \tag{2}$$

here c—bearing stiffness, E—elasticity module, I_x—moment of inertia, l—beam span. Denoting i as the beam relative stiffness equal to $\frac{E \cdot I_x}{l}$, the required bean joint flexibility fixed by flexible joints will be defined by the following ratio:

$$c = 6 \cdot i \tag{3}$$
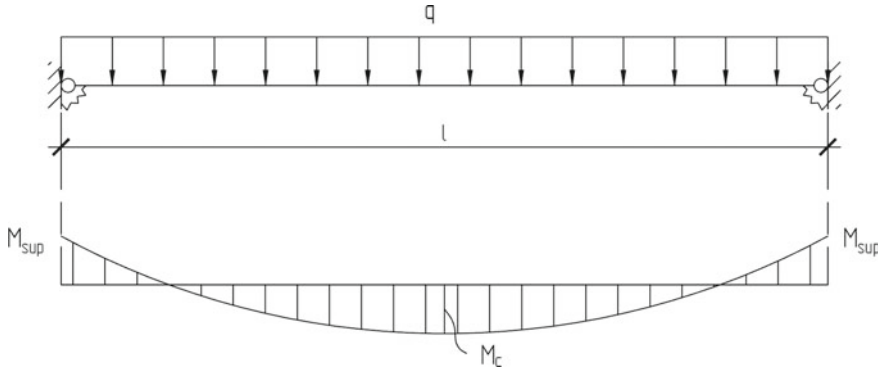
Fig. 2 Beam design model

The joint should have a significant initial stiffness $c \geq 6 \cdot i$, otherwise the design moment value in the joint will not be achieved.

It is a rather complex problem to implement a flexible joint with a fixed stiffness (linear diagram for strain under load). A number of random factors occur which are capable of impacting the design stiffness. For building structures it is possible to apply joints with a marked yielding area. The applicability of these solutions is confirmed by a set of research and construction practice. The effort under which the transition to plasticity occurs is selected structurally depending on the bearing moment M_{sup}. The required joint flexibility should provide the possibility of bearing section rotation by the angle defined by the formula:

$$\theta_{on} = \frac{M_{sup}}{6 \cdot i} \tag{4}$$

As a main joint component use a flanged connection calculated by the method of decomposition into simple flange T-elements (Fig. 3). These factors were selected as variable ones. The bearing capacity of the flanged connection is formed by the bearing capacities of its separate parts (T-flanges) which are the minimum of three possible failure options. For a flexible joint apply the failure scheme No. 1 as schemes No. 2 and 3 cause fragile destruction. In its turn, scheme No. 1 is characterized by a plastic failure form. The bolt bearing capacity should be sufficient for the failure implementation by the first scheme of the limit state. The secondary joint components capable of increasing the flexibility (such as column wall strain, bolt extension, column flange bent) will not be included in the calculation. The joint design should be made in such a way that the impact of secondary components on the general joint flexibility is negligibly small. This is reached by the installation of stiffeners and stiffening plates in the column and beam section.

T-flange can be considered as two rigidly restrained beams, the span (Figs. 3.1, 4). The transition to a plastic state occurs near the bolts and legs of welded seams. The effort under which a T-flange transits to a plastic state can be obtained as follows.

$$P_{fl.} = \frac{l \cdot R_y \cdot t^2}{e} \tag{5}$$
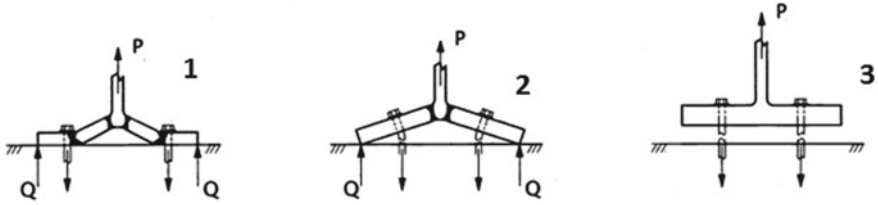
Fig. 3 Types of failure of the T-shaped flanged connection
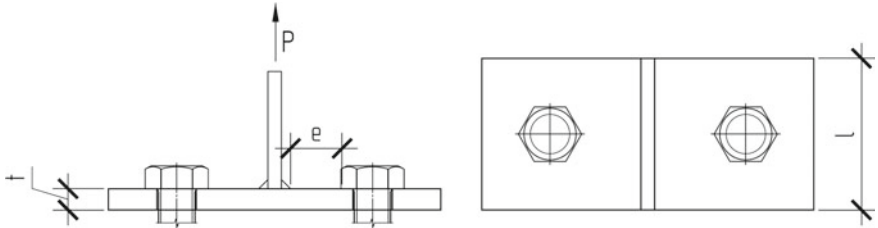
Fig. 4 The design scheme for T-shaped flanges

here R_y—steel yield strength, l—flange width, e—distance from the bolt edge to the welded seam leg, t—flange thickness.

The required bearing capacity of the extended T-flange is defined on the basis of the beam moment at the support and should be restricted by a bearing capacity of the element to which is fixed (an upper flange for a T-beam).

$$P_{fl.} = \frac{M_{sup.}}{h_b - t_{s.}} < t_{s.} \cdot b \cdot R_y \qquad (6)$$

where h_b—beam height, $t_{s.}$—beam flange thickness, b—beam flange thickness, R_y—steel yield strength. The T-flange dimensions and thickness, bolt distance are selected on the basis of the required bearing capacity with the $t/e = 0.3{:}0.35$ ratio that has been obtained earlier [6].

3 Flexible Joint Operation Under Load

The flexible joint for beam fixing presented in the paper is a flanged plate fastened by bolts and a support bracket bearing the compression and transverse stresses. An upper (extended) flange is welded to the beam in the flange area only. Transverse stress is translated through a support bracket. Joint flexibility is implemented in the beam extended area at plastic strain occurrence in a T-flange. The compressed beam area translates the effort via the contact action between a lower plate and the column flange (Fig. 5).

The load-bearing capacity of the girder varies with the type of nodes used. The maximum load-bearing capacity is achieved for scheme No. 4 (Fig. 6) with equal bending
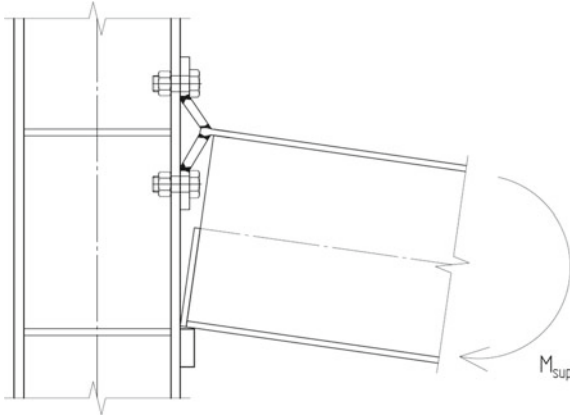
Fig. 5 The design scheme for flange connection

moments in the span and on the support. The load-bearing capacity of the suggested node is limited by the load-bearing capacity of the I-beam shelf. Thereafter, the maximum load-bearing capacity of the I-beam 30, which is fixed according to scheme No. 3 (Fig. 6), will be 67 kN/m.
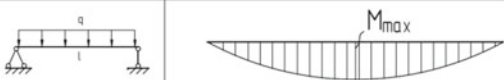
N⁰	Design scheme		M_{max}	q[kN/m] I30
1		M_{max}	$ql^2/8$	37 кN/m
2		M_{max}	$ql^2/12$	55 кN/m
3		M_{sup} M_{max}	$ql^2/8-M_{sup}$	67 кN/m
4		M_{max} M_{max}	$ql^2/16$	73 кN/m

Fig. 6 The load-bearing capacity of the I30 beam depending on the type of support

4 Numerical Test of the Beam Fixed by Flexible Joints

For this research the authors prepared a design beam model with a 6 m span (Fig. 7) fixed with T-flanges. As limit conditions the authors take a rigid fastening of plates contacting with a flange, hinged fastening of vertical displacement of a beam support bracket, beam

unfastening in the span from the plane. The design model is made in Ansys Workbench. To describe metal non-linear properties the authors use a bilinear Prandtl diagram, the yield strength 345 MPa.
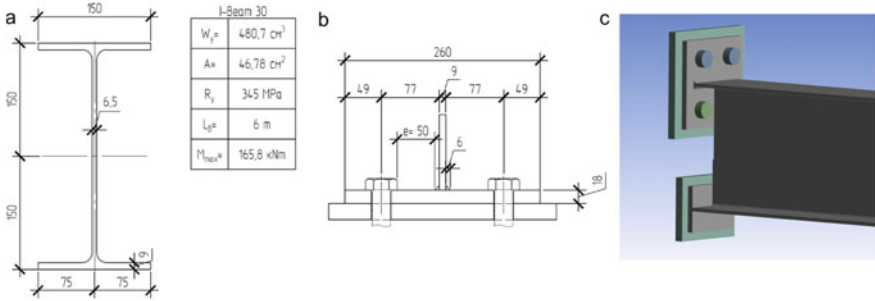
Fig. 7 a Beam section; **b** taken T-connection; **c** flexible joint structure

The joint works by an elastoplastic scheme: up to the design load M_{sup} it works in a linear elastic way, at more than M_c—as a plastic hinge (Fig. 3). The angle to which the section must rotate is defined by the formula (4):

$$\theta_{sup} = \frac{M_{sup}}{6 \cdot i} = 0.01 \, rad$$

Correspondingly, the strain caused the transition of a T-flange should be equal to:

$$\Delta_z = \theta_{sup} \cdot h_b = 0.01 \cdot 300 = 3 \, mm$$

where h_b—beam height.

The selection of flange parameters should be made on the basis of the required effort relying on the strength uniformity of bending moments in the span and on the beam bearing (6). Limit by a T-beam flange bearing capacity:

$$P_{fl.} = \frac{M_{sup.}}{h_b - t_{s.}} = \frac{165.8}{0.3 - 0.009} = 570 \, kN$$

$$P_{fl.} < t_{s.} \cdot b \cdot R_y = 0.009 \cdot 0.15 \cdot 345 \cdot 10^3 = 466 \, kN$$

The design effort is 466 kN on the basis of which define the required values of flange thickness and the distance e in the formula (5) setting the ratio $t/e = 0.3{:}0.35$. As a result the effort necessary for the flange to transit to the plastic strain will be equal to:

$$P_{fl.} = \frac{l \cdot R_y \cdot t^2}{e} = \frac{0.21 \cdot 345 \cdot 10^3 \cdot 0.018^2}{0.05} = 469 \, kN$$

The analytical solution of a bearing capacity of a T-flange is checked with the help of calculational experiments of the joint (Fig. 7) submodel in the software package Ansys. As a result the authors obtained the diagram "force–displacement" (Fig. 8). The T-flange

transition to plastic strain occurs under the load of 400 kN, the load at 3 mm displacement is 470 kN which, allowing for the error, correlates well with the analytical solution. The advantage of this connection is the range at which the T-flange is capable of providing an ultimate moment. The real joint structure will include initial defects, a wide range (0.5–5 mm in compliance with the diagram) at which the T-flange is capable of providing a design effort; in addition, such range will allow neutralizing excess joint flexibility.
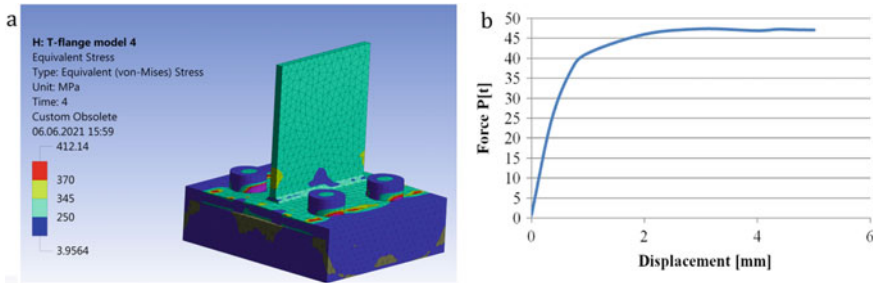
Fig. 8 **a** Equivalent von Mises equivalent stresses for a submodel of a flexible joint, first image; **b** dependency diagram "force–displacement"

The beam bearing capacity in the design model was defined at the conditions of plastic strain occurrence in the span and on the beam bearings. The upper flange longitudinal displacement was 3.2 mm which confirms the effort in the T-flange reached 470 kN. The maximum load as a result of calculation equaled 67 kN/m which is 22% higher than the design bearing capacity of a rigidly fixed beam with such a section (Fig. 9).
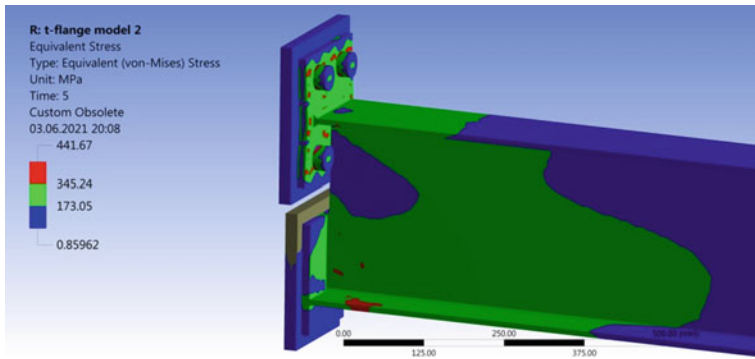
Fig. 9 Equivalent von Mises equivalent stresses for a rigidly fixed beam under 70 kN/m

5 Conclusions

- A new design solution that is characterized by simplicity of calculation and installation is proposed for a flexible beam assembly with a column.

- The node engineering calculation method which successfully correlates with the results of the numerical experiment is shown. The numerical models themselves were constructed according to the results of field experiments.
- The proposed joint of beams and columns allows to redistribute the bending moments along the length of the beam. The maximum load on the beam fixed on the proposed nodes is 1.22 times bigger than the calculated load-bearing capacity of a rigid beam of this section and 1.8 times higher than for a pivotally fixed beam.

References

1. Eduarte J (2018) Design of prequalified European beam-to-column connections for moment resistant frames with component based finite element method. Dissertation, Czech Technical University of Prague, p 69
2. Chung S-T, Morris RL (1978) Isolation and characterization of plasmid deoxyribonucleic acid from Streptomyces fradiae. In: Abstracts of the 3rd international symposium on the genetics of industrial microorganisms, University of Wisconsin, Madison, 4–9 June 1978
3. EN 1993-1-8 EN1993 3 (2005) Design of steel structures part 1.8: Design of joints CEN
4. Son MP (2018) Experimental studies of strength flanged connections. Struct Mech Eng Constr Build 14:348–356
5. Son M (2018) Parallel experiments of numerical and full-scale models of flange joints of the beam-column type. IOP Conf Ser: Mater Sci Eng 456:012092
6. Kashevarova GG, Son MP, Zemlyanukhin AD Design and modeling of a T-stub flange connection. Modern technologies in construction. Theory and practice
7. Shardakov I, Shestakov A, Son M (2018) Beam to column flange connection: from elasticity to destruction. Proc Struct Integr 13:1324–1329. https://doi.org/10.1016/j.prostr.2018.12.278
8. Khang T Huong, Gung H Nguyen (2018) Discussion about effecting of stiffener in four bolts in a row end plate connection for long span and heavy load steel structures in Vietnam. IOP Conf Ser: Earth Environ Sci 143. https://doi.org/10.1088/1755-1315/143/1/012028
9. Schippers JD (2012) A design procedure for bolted top-and-seat angle connections for use in seismic applications. In: CONNECTION VII 7th international workshop on connections in steel structures, Timisoara RO, p 173
10. Joints in Steel Construction Moment Connections (1997), p 233
11. Son MP (2018) Influence of the flange thickness for stress-strain state and the behaviour of the flange connection in the units of the beam-to-column. Struct Mech Anal Constr 5:11–16
12. Hunn ZD et al (2018) A finite element study of non-orthogonal bolted flange plate connections for seismic applications. Key Eng Mater 763:525–532
13. Chen X, Shi G (2016) Finite element analysis and moment resistance of ultra-large capacity end-plate joints. J Constr Steel Res 126:153–162. https://doi.org/10.1016/j.jcsr.2016.07.013
14. Swanson JA (2002) Ultimate strength prying models for bolted T-stub connections. Eng J 39(3):136–147
15. Meng B, Zhong W, Hao J (2018) Anti-collapse performances of steel beam-to-column assemblies with different span ratios. J Constr Steel Res 140:125–138
16. Fakih KAl, Chin SC, Doh SI (2018) Behavior of double-web angles beam to column connections. IOP Conf Ser: Mater Sci Eng 342
17. Sumner EA, Murray TM (2003) Behaviour and design of multi-row extended end-plate moment connections. In: Proceedings of international conference advances in structures
18. Cerfontaine F, Jaspart JP (2002) Analytical study of the interaction between bending and axial force in bolted joints. Eurosteel Coimbra

19. Undermann D, Schmidt B (2005) Moment resistance of bolted beam to column connections with four bolts in each row. In: Proceedings of IV European conference on steel and composite structures
20. Sumner EA (2003) Unified design of extended end-plate moment connections subject to cyclic loading. Dissertation for the degree of Doctor of philosophy in civil engineering, p 209

Dynamic Finite Element Analysis of Plane Frame with Nonlinear Multi Freedom Constraints Subjected to Harmonic Load Using Penalty Function Method

Vu Thi Bich Quyen[(✉)], Dao Ngoc Tien, and Tran Thi Thuy Van

Hanoi Architectural University, Km 10, Nguyentrai, Hanoi, Vietnam
quyenvtb@hau.edu.vn

Abstract. This paper proposes a way to utilize the Penalty function method for treating the nonlinear multi freedom constraints in solving the dynamic problem of the plane frame under harmonic load using the finite element method. In the dynamic finite element analysis frame with nonlinear varying boundary constraints, the solving procedure is established depending on the mathematical technique of treating the nonlinear boundary condition. Generally, the mathematical technique for imposing nonlinear boundary constraints based on optimization methods. This research introduces an approach to use the penalty function method for treating the nonlinear multi freedom constraints in dynamic finite element analysis of plane frame. The modified dynamic equilibrium equation is constructed by extremizing the Hamiltonian function and converting a constrained problem into an unconstrained problem using the penalty function method. The incremental iterative algorithm is established for solving the dynamic equilibrium equation of the system under time-dependent harmonic force based on the combining Newmark integration method and Newton Raphson method. Based on the proposed algorithm the calculation program is written for investigating the dynamic response of plane frame with nonlinear multi freedom constraints subjected to harmonic load.

Keywords: Multi freedom constraints · Nonlinear boundary constraints · Penalty function method · Dynamic finite element analysis · Frame subjected to harmonic load

1 Introduction

Investigating the dynamic behavior of frame structures arise in many engineering practical design. Most of the proceeding works deals with finite element formulation for solving the dynamic problem of frame structures. Using the finite element method [1, 2], establishing the solution algorithm is an important step in the procedure of solving the vibration problem of frame structures. The solution algorithm of the vibration problem of frame structures based on finite element formulation is highly dependent on the boundary conditions implemented. In the dynamic finite element analysis frame with

nonlinear multi freedom constraints, the solving procedure is established depending on the mathematical technique of treating the nonlinear boundary condition. The nonlinear boundary constraints significantly increase the mathematical difficulty in developing the modified stiffness equation. For treating nonlinear dependent constraints the mathematical technique based on optimization methods generally is used [3–5]. Therein, the penalty augmentation method and the Lagrange multiplier adjunction method are better techniques suited to the implementation of nonlinear constraints. Both of these methods are based on a mathematical technique to convert constrained problems to unconstrained problems. The multiplier method has the advantage of being exact and providing directly the constraint forces but it renders the augmented stiffness matrix indefinite, an effect that may cause grief with some linear equation solving methods that rely on positive definiteness [6]. In contrast to the Lagrange multiplier method, the penalty function method is straightforward implementation and the positive definiteness is not lost but has a serious drawback in the difficulty of choice of weight values that balance solution accuracy with the violation of constraint conditions [7, 8]. In the published work [9], the author presented an algorithm for imposing the nonlinear multi freedom constraints in static analysis of frame using finite element method. This research introduces an approach to use the penalty function method for treating the nonlinear multi freedom constraints in dynamic finite element analysis of plane frame. The modified dynamic equilibrium equation is constructed by extremizing the Hamiltonian function and converting a constrained problem into an unconstrained problem using the penalty function method. The incremental iterative algorithm is established for solving the dynamic equilibrium equation of the system under time-dependent harmonic force based on the combining Newmark integration method and Newton Raphson method. Based on the proposed algorithm the calculation program is written for investigating the dynamic response of plane frame with nonlinear multi freedom constraints subjected to harmonic load.

2   Problem Formulation

For constructing a dynamic equilibrium equation of the frame system with nonlinear multi freedom constraints subjected to harmonic load consider the nth degree of freedom frame system shown in Fig. 1.

The nonlinear multi freedom constraints are expressed as below equation.

$$g(u) = \{g_1(u), g_2(u), \dots, g_m(u)\}^T = 0 \quad or \quad g_k(u) = 0, \ k = 1 \dots m.$$

Designating the followings:

$u = u(t) = \{u_1(t), u_2(t), \dots, u_n(t)\}^T$, $u \in R^n$ is the time-dependent vector of nodal displacement;

$\dot{u} = \frac{du}{dt}$, $\ddot{u} = \frac{d^2u}{dt^2}$ are the nodal velocity and acceleration vectors;

$M = diag\{m_1, m_2, \dots, m_n\}$ is the mass matrix of the finite element system;

K is stiffness matrix of the finite element analysis system;

$T = T(\dot{u})$, $V = V(u)$ are the kinetic and potential energy of the finite element analysis system;

$W = W(u)$ is work done by damping force P_D and external force (harmonic force) $P(t)$.
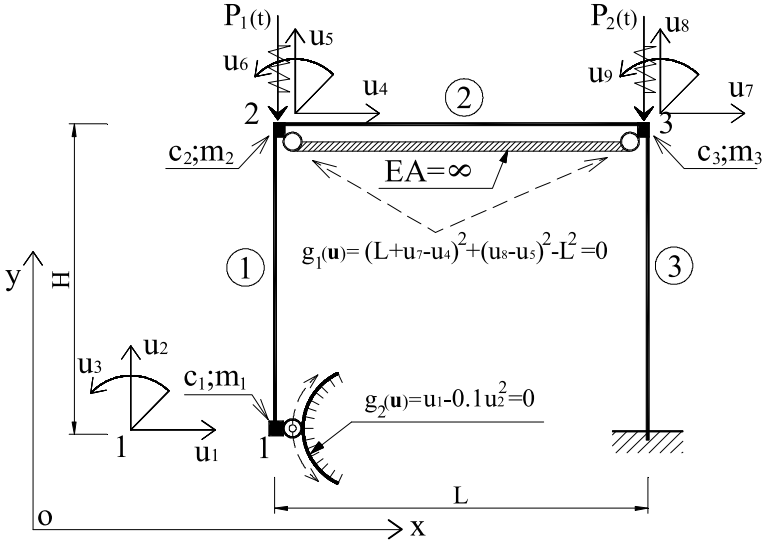
Fig. 1 Plane frame with nonlinear multi freedom constraints subjected to harmonic load

The kinetic and potential energy of the system can be computed as

$$T = T(\dot{u}) = \frac{1}{2}\dot{u}^T M \dot{u} \tag{1}$$

$$V = V(u) = \frac{1}{2}u^T K u \tag{2}$$

The work done by damping force and harmonic force can be calculated by the formula

$$W = W(u) = u^T (P_D + P(t)) \tag{3}$$

where $P_D = -C\dot{u}$ is Rayleigh damping force vector;

C is damping matrix of the finite element model;

$P = \{P_1(t), P_2(t), ..., P_n(t)\}^T$ is the vector of external forces (harmonic forces).

The motion of dynamical system $u = u(t)$ between two points at time interval $[t_0, t_1]$ is extremum for actual path followed by the system according to Hamilton's principle and can be written by the formula

$$H[u] = \int_{t_0}^{t_1} [T(\dot{u}) - V(u)]dt + \int_{t_0}^{t_1} W(u)dt \tag{4}$$

The system of dynamic equilibrium equations is obtained by developing the Euler equation describing motion for Eq. (4), expressing as

$$M\ddot{u} + C\dot{u} + Ku = P$$

The set of nonlinear multi freedom constraints is expressed as may be collected into nonlinear equations $g(u) = 0$. Incorporating nonlinear multi freedom constraints

and developing the modified equations can be done by minimization of the augmented potential energy function $H[\mathbf{u}]$ as

$$\min \left\{ H[u] : \quad g(u) = 0, \ u = u(t) \in R^n \right\} \tag{5}$$

Penalize objective function $Q[u, w]$ [3–5] with the penalty weight (or penalty element) w to convert the constrained extremal problem (5) into an unconstrained extremal problem (7) when the augmented potential energy function $Q[u, w]$ is extremal.

$$Q[u, w] = \int_{t_0}^{t_1} [T(\dot{u}) - V(u)]dt + \int_{t_0}^{t_1} W(u)dt$$
$$+ \int_{t_0}^{t_1} \frac{1}{2} w \sum_{k=1}^{m} g_k^2(u)dt = \int_{t_0}^{t_1} F(t, u, \dot{u})dt \tag{6}$$

when $F(t, u, \dot{u}) := [T(\dot{u}) - V(u)] + W(u) + \frac{1}{2} w \sum_{k=1}^{m} g_k^2(u)$.

$$\min \left\{ Q[u, w], \ u \in R^n \right\} \tag{7}$$

For the augmented function is minimizing $Q[u, w]$, the necessary and sufficient condition is satisfying the Euler equation as follows

$$\frac{\partial F(t, u, \dot{u})}{\partial u} - \frac{d}{dt} \left(\frac{\partial F(t, u, \dot{u})}{\partial \dot{u}} \right) = 0 \tag{8}$$

Adding $F(t, u, \dot{u})$ from Eq. (6) into Eq. (8), having

$$-\frac{d}{dt} \left(\frac{\partial T(\dot{u})}{\partial \dot{u}} \right) - \frac{\partial V(u)}{\partial u} + \frac{\partial W(u)}{\partial u} + w \sum_{k=1}^{m} g_k(u) \frac{\partial g_k(u)}{\partial u} = 0 \tag{9}$$

where $\frac{\partial g_k(u)}{\partial u} = \left\{ \frac{\partial g_k(u)}{\partial u_1}, \frac{\partial g_k(u)}{\partial u_2}, \dots, \frac{\partial g_k(u)}{\partial u_n} \right\}^T$, $k = 1 \dots m$.

Replacing the kinetic energy, potential energy, and work of finite element analysis system from the Eqs. (1—3) to the Eq. (9), getting

$$-M\ddot{u} - Ku + (P_D + P) + w \sum_{k=1}^{m} g_k(u) \frac{\partial g_k(u)}{\partial u} = 0 \tag{10}$$

Replacing Rayleigh damping force vector $P_D = -C\dot{u}$ to the Eq. (10), getting the modified system of dynamic equilibrium equations considering nonlinear multi freedom constraints as

$$M\ddot{u} + C\dot{u} + Ku - w \sum_{k=1}^{m} g_k(u) \frac{\partial g_k(u)}{\partial u} = P \tag{11}$$

Obviously, the equation system (11) is nonlinear multi-order differential equations due to nonlinear multi freedom constraints $g_k(u)$, $k = 1 \dots m$. Solving the nonlinear

differential equations requires using the iterative incremental step loading technique in finite element analysis. The incremental step loading equation system is expressed as

$$M\,\delta\ddot{u} + C\delta\dot{u} + \left[K - w\sum_{k=1}^{m}\frac{\partial}{\partial u}\left(g_k(u)\frac{\partial g_k(u)}{\partial u} \right) \right]\delta u = \Delta P \tag{12}$$

Expanding one component on the left-hand side of Eq. (12), getting

$$w\sum_{k=1}^{m}\frac{\partial}{\partial u}\left(g_k(u)\frac{\partial g_k(u)}{\partial u} \right)\delta u$$

$$= w\sum_{k=1}^{m}\left\{ \frac{\partial}{\partial u}\left(\frac{\partial g_k(u)}{\partial u} \right)g_k(u)\delta u + \frac{\partial g_k(u)}{\partial u}\left(\frac{\partial g_k(u)}{\partial u} \right)^T \delta u \right\} \tag{13}$$

Utilizing the Taylor series formula for a short δu to expand of equation $g_k(u) = 0$ around variable points, keeping the only linear term, getting $g_k(u) + \left(\frac{\partial g_k(u)}{\partial u} \right)^T \delta u = 0$, and replacing $g_k(u) = -\left(\frac{\partial g_k(u)}{\partial u} \right)^T \delta u$ to the Eq. (13), having

$$w\sum_{k=1}^{m}\frac{\partial}{\partial u}\left(g_k(u)\frac{\partial g_k(u)}{\partial u} \right)\delta u$$

$$= w\sum_{k=1}^{m}\left\{ -\frac{\partial}{\partial u}\left(\frac{\partial g_k(u)}{\partial u} \right)\left(\frac{\partial g_k(u)}{\partial u} \right)^T \delta u\,\delta u + \frac{\partial g_k(u)}{\partial u}\left(\frac{\partial g_k(u)}{\partial u} \right)^T \delta u \right\} \tag{14}$$

Neglecting the second-order infinitesimal value in the Eq. (14), getting

$$w\sum_{k=1}^{m}\frac{\partial}{\partial u}\left(g_k(u)\frac{\partial g_k(u)}{\partial u} \right)\delta u = w\sum_{k=1}^{m}\left\{ \frac{\partial g_k(u)}{\partial u}\left(\frac{\partial g_k(u)}{\partial u} \right)^T \right\}\delta u \tag{15}$$

Combining Eqs. (12) and (15), the incremental equation can be expressed as follows

$$M\,\delta\ddot{u} + C\delta\dot{u} + \left[K - w\sum_{k=1}^{m}\left\{ \frac{\partial g_k(u)}{\partial u}\left(\frac{\partial g_k(u)}{\partial u} \right)^T \right\} \right]\delta u = \Delta P \tag{16}$$

where w is penalty weight (or penalty element); $\delta u = \{\delta u_1, \delta u_2, \ldots, \delta u_n\}^T$ is the incremental nodal displacement; $\delta\ddot{u}$, $\delta\dot{u}$ are the incremental acceleration, incremental velocity vectors; $\frac{\partial}{\partial u}\left(\frac{\partial g_k(u)}{\partial u} \right) = \left[\frac{\partial^2 g_k(u)}{\partial u_i \partial u_j} \right]_{(nxn)} i, j = 1\ldots n$ is Hessian matrix of a function $g_k(u)$, $k = 1\ldots m$.

The system (16) can be written as below

$$M\,\delta\ddot{u} + C\delta\dot{u} + [K - K_W(u, w)]\delta u = \Delta P \tag{17}$$

In Eq. (17), this expression $K_W(u, w) = w \sum_{k=1}^{m} \left\{ \frac{\partial g_k(u)}{\partial u} \left(\frac{\partial g_k(u)}{\partial u} \right)^T \right\}$ is building based on nonlinear boundary constraints.

For solving nonlinear time-dependent Eqs. (17), Newmark's method [10] is employed in this research. Based on the Newmark integration method [10], the dynamic equation system in incremental form can be described as follows

$$
\begin{cases}
\delta \ddot{u} = \dfrac{1}{\beta \Delta t^2} \delta u - \dfrac{1}{\beta \Delta t} \dot{u} - \dfrac{1}{2\beta} \ddot{u} \\[2mm]
\delta \dot{u} = \dfrac{\gamma}{\beta \Delta t} \delta u - \dfrac{\gamma}{\beta} \dot{u} - \left(\dfrac{\gamma}{2\beta} - 1 \right) \Delta t \, \ddot{u}
\end{cases}
\tag{18}
$$

where: $(\gamma = 1/2, \beta = 1/4)$ according to Newmark's average acceleration method; $(\gamma = 1/2, \beta = 1/6)$ according to Newmark's linear acceleration method.

Adding $\delta \ddot{u}$, $\delta \dot{u}$ from Eq. (18) into Eq. (17), will be given Eq. (19)

$$
\left[K - K_W(u, w) + \frac{M}{\beta \Delta t^2} + \frac{\gamma C}{\beta \Delta t} \right] \delta u = \Delta P + M \left(\frac{1}{\beta \Delta t} \dot{u} + \frac{1}{2\beta} \ddot{u} \right)
$$
$$
+ C \left[\frac{\gamma}{\beta} \dot{u} + \left(\frac{\gamma}{2\beta} - 1 \right) \Delta t \, \ddot{u} \right] \tag{19}
$$

Designating in compact form as below $\overline{K}(u) = \left[K - K_W(u, w) + \frac{M}{\beta \Delta t^2} + \frac{\gamma C}{\beta \Delta t} \right]$ is the expanded tangent stiffness matrix including penalty weight; $\Delta \overline{P} = \Delta P + M \left(\frac{1}{\beta \Delta t} \dot{u} + \frac{1}{2\beta} \ddot{u} \right) + C \left[\frac{\gamma}{\beta} \dot{u} + \left(\frac{\gamma}{2\beta} - 1 \right) \Delta t \, \ddot{u} \right]$ is the expanded incremental load vector.

Witting the equation system (19) in compact form as follows

$$
\overline{K}(u) \delta u = \Delta \overline{P} \tag{20}
$$

In this work, establishing the incremental-iterative algorithm for solving the above problem is developed based on implementing the Newton Raphson technique [11–13].

3 Numerical Investigation

Investigating dynamic behavior of plane frame system with nonlinear multi freedom constraints subjected to harmonic load (shown in Fig. 2). All of the frame elements are made of the same material and have the same cross-sectional area. The parameters are given as follows:

$$
E = 2.10^4 (\text{kN/cm}^2), \ A = 60 \, \text{cm}^2, \ I = 3140 \, \text{cm}^4, \ L = 420 \, \text{cm}, \ H = 420 \, \text{cm}
$$

$$
P_4(t) = P(t) = 70. \sin(40\pi t) \ (\text{kN}); \ m_{1;2;3} = m = 50.10^{-5} \text{kNs}^2/\text{cm},
$$

$$
c_{1;2;3} = c = 10^{-2} \text{kNs/cm};
$$

The nonlinear multi freedom constraints can be is expressed as following functions.

$$
\begin{cases}
g_1(u) = (L + u_7 - u_4)^2 + (u_8 - u_5)^2 - L^2 = 0 \\
g_2(u) = u_1 - 0.1 u_2^2 = 0
\end{cases}
\quad or \quad g(u) = \{g_1(u), g_2(u)\}^T = 0
$$
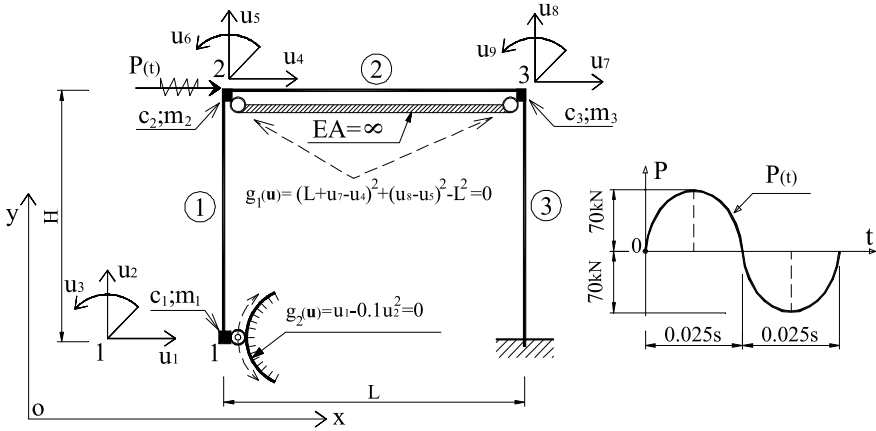
Fig. 2 Investigated frame system with nonlinear multi freedom constraints subjected to harmonic load

For determining dynamic behavior in the above-investigated frame the calculation program is written based on the proposed incremental-iterative algorithm. The Newmark's average acceleration method is employed in solving the dynamic equation of the frame system procedure using $\gamma = 1/2$; $\beta = 1/4$. The investigation time period is $[t_0, \ t_1] = [0, \ 0.5s]$ with time increment $\Delta t = 0.0025s$.

For investigating the convergence speed of the proposed method, the problem was solved with different options of weight values w, as following: $w_1 = 10^1, w_2 = 10^2, w_3 = 10^3, w_6 = 10^6$.

The calculation results of the dynamic analysis of the plane frame with nonlinear multi freedom constraints subjected to harmonic load are the displacement–time response and bending moment–time response (shown in Figs. 3, 4, 5) for different variants of weight values.
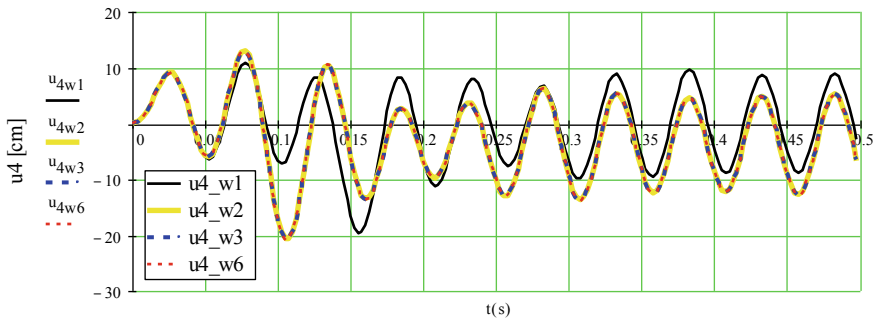
Fig. 3 Load–displacement equilibrium path ($u_4 - t$) in cases with the weight values $w_{1;2;3;6}$

Comments: The root convergence factor depends on the way to choose appropriate weights w and the solution will be converged faster in the case of increasing the weight
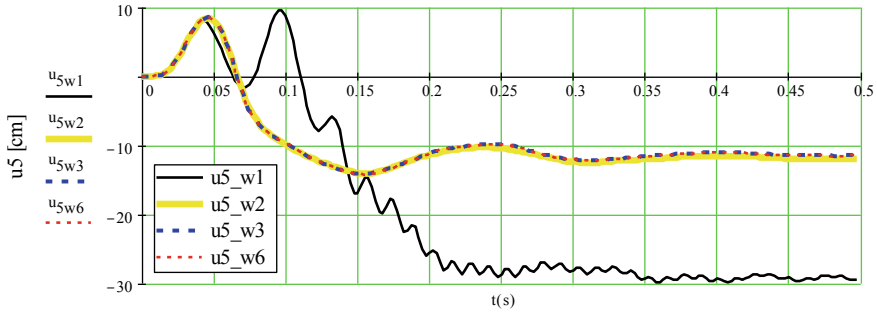
Fig. 4 Load–displacement equilibrium path ($u_5 - t$) in cases with the weight values $w_{1;2;3;6}$
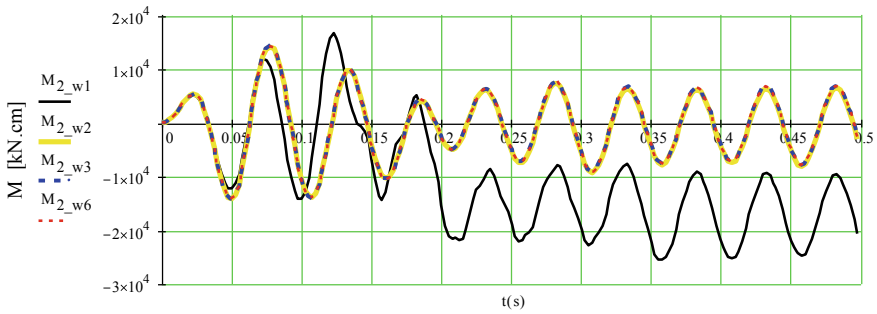
Fig. 5 Bending moment equilibrium path ($M_2 - t$) in cases with the weight values $w_{1;2;3;6}$

value. It will be better for convergence speed when selecting the initial value of penalty element approximately (or about) value of element stiffness.

4 Conclusions

The penalty function method is very easy for implementing the nonlinear boundary constraints in the solving procedure of structural dynamic problem. In this research, the modified dynamic equilibrium equation considering nonlinear multi freedom constraints had been successfully constructed by extremizing the Hamiltonian function and converting a constrained problem into an unconstrained problem. Results of the numerical investigation show the effectiveness of an established incremental iterative algorithm for solving the nonlinear time-varying equations in analyzing the dynamic response of the frame system subjected to the harmonic load.

References

1. Bathe KJ (2014) Finite element procedure. Prentice Hall
2. Zienkiewicz OC, Taylor RL (2014) The finite element method for solid and structural mechanics, 7th edn. Butterworth-Heinemann

3. Strodiot JJ (2002) Numerical methods in optimization. Namur, Belgium
4. Sun W, Yuan Y-X (2006) Optimization theory and methods—nonlinear programming. Springer
5. Rajesh KA (2015) Optimization: algorithm and application. Taylor & Francis Group
6. Quyen VTB, Tien DN, Huong NTL (2020) Treatment of nonlinear multi freedom boundary constraints in finite element analysis of frame system using Lagrange multiplier method. IOP Conf Ser: Mater Sci Eng 960:022076. https://doi.org/10.1088/1757-899X/960/2/022076
7. Quyen VTB, Tien DN, Dung NN (2020) A modified penalty function method for treating multi freedom constraints in finite element analysis of frames. J Phys: Conf Ser 1425:012097. https://doi.org/10.1088/1742-6596/1425/1/012097
8. Quyen VTB, Tien DN, Dat PV (2020) Treatment of multi freedom constraints in geometrically nonlinear stability analysis of truss structures using penalty function method. IOP Conf Ser: Mater Sci Eng 962:022069. https://doi.org/10.1088/1757-899X/962/2/022069
9. Quyen VTB, Tien DN, Dung NN, Khanh CQ (2020) Penalty function method for imposing nonlinear multi freedom and multi node constraints in finite element analysis of frame systems. IOP Conf Ser: Mater Sci Eng 869:052063. https://doi.org/10.1088/1757-899X/869/5/052063
10. Newmark NM (1959) A method of computation for structural dynamics. J Eng Mech Div ASCE 85:67–94
11. Crisfield MA (1981) Fast incremental/iterative solution procedure that handles snap-through. Comput Struct 13(1–3):55-62A
12. Crisfield MA (1997) Non-linear finite element analysis of solids and structures. Wiley 1–2:1997
13. Riks E (1972) The application of Newton's method to the problem of elastic stability. ASME J Appl Mech 39(4):1060–1066

Influence of the Chemical and Mineralogical Composition of Dolomites of Various Deposits on the Properties of MOC on Its Base

G. Averina[✉], V. Koshelev, and R. Zhivtcova

South Ural State University (National Research University), 76. Lenin Ave, Chelyabinsk
454080, Russia
`averinagf@susu.ru`

Abstract. The article discusses the relationship between some properties of magnesium composites based on binders based on dolomites from various deposits. Differences in the chemical and mineralogical composition of dolomite raw materials from different deposits of the Russian Federation are shown. The granulometric composition of samples of raw materials of the same fraction from different deposits has been investigated. The effect of dyeing oxide impurities on the color of magnesia composites has been established. The importance of the coloring oxides absence in raw materials for the production of binders used for the production of decorative building materials is indicated. An insignificant difference in compressive strength characteristics is shown depending on the quantitative content of magnesium oxide in the chemical composition of the raw material. The dependence of the strength characteristics on the granulometry of the raw material used has been established. Deposits with the most suitable raw materials for obtaining the most durable and decorative binders have been identified.

Keywords: Dolomite · Magnesium oxychloride cement (MOC) · Binder · Deposit · Chemical composition · Color · Compression strength

1 Introduction

The Dolomites and dolomitized limestones are very common sedimentary rocks. The composition of these rocks is represented by a double salt of magnesium, calcium and carbonic acid, as well as associated impurity minerals such as iron oxides, aluminum oxides, silica, calcite etc. [1–3].

It is generally accepted that there are several possible ways of the formation of dolomites and dolomite rocks. The Dolomites are often found in hydrothermal deposits and are associated with calcite. The Dolomites can also form when calcite is replaced under the influence of sea or ground waters and because of chemical precipitation from aqueous solutions or during the evaporation of water [4–6].

Due to the variety of ways of formation of this mineral and the rocks composed from it, their deposits are widespread throughout the world and on almost all continents.

The most famous and first developed deposit is located in the Dolomites Alps in Italy. Among the European countries in which dolomite deposits are present, Switzerland, Great Britain, Spain, Belarus and Ukraine also appear. In North America, a large deposit is located in the vicinity of Lake Ontario. In South America, dolomite deposits are found in Brazil and Mexico. In Africa, dolomites are found in the Republic of Namibia. In Asian countries there are dolomites in Kazakhstan, Uzbekistan and Tajikistan. A huge number of dolomite deposits are located on the territory of the Russian Federation, in the Lipetsk, Kemerovo, Buryatia, Bashkortostan, North Caucasus, Ural, Karelia and the Khabarovsk Territory [7–12].

Dolomite properties vary via deposit, due to the different combination of impurity minerals and the methods of formation. Differences can be found in color, density, strength, porosity, frost resistance, and even texture.

Depending on the specified properties, dolomites from each deposit have specific applications. One of the most popular ways to use dolomites is to make facing tiles from them [13, 14]. The Dolomites can also be used as a metallurgical flux and are in great demand in the glass industry [15–17]. Dolomite powder is an inexpensive and effective soil deoxidizer used in agriculture [18, 19]. Fine dolomite is used for the production of dry building mixtures as aggregates. Until recently, dolomite crushed stone was also often used in road construction, but due to updated national standards, this method of using dolomite rocks is not recommended today.

Another popular way of using dolomite rocks is to use them as a raw material for the production of binders for construction purposes. Various materials for finishing, flooring and partitions have been developed on the basis of dolomite binders. Their production is significantly more eco-friendly and energy efficient due to lower fuel consumption and reduced carbon dioxide emissions [20]. Composite materials based on magnesia oxychloride cement have a number of unique technical characteristics. They quickly gain high strength, have high abrasion resistance; also they are not susceptible to mold fungi, microbes and other types of aggressive biological medium. In addition, an extensive raw material base allows producing this material almost anywhere in the world.

Returning to the issue of varying the composition and properties of dolomites from different deposits, it is appropriate to assume that, depending on it, the properties of binders obtained on the basis of different dolomites will also differ.

Significant differences in the physical and mechanical properties of binders obtained on the basis of raw materials from different deposits can impose certain restrictions on the area of their use in the production of building materials.

Binders with low strength characteristics can only be used for the production of building mixtures and finishing materials that do not have a bearing capacity.

Binders with a low coefficient of water resistance must be used for the production of materials that are not exposed to moisture, including the effects of atmospheric precipitation.

The strength properties of binders and their resistance to water can be influenced by the presence of ferruginous compounds in the composition of the original rocks. Iron ions are able to integrate into the structure of minerals formed by the interaction of magnesium oxide with a solution of magnesium chloride. This modification increases the strength and water resistance of magnesia composites.

One of the characteristics that do not affect the performance properties of mineral binders for construction purposes, but of interest to the end user, is the color of the artificial stone obtained on their basis. Binders containing coloring impurities are not suitable for the production of most types of finishing building materials.

A large number of different chemical compounds can affect the color of a binder. In addition to the most common coloring compounds—iron and aluminum oxides, as well as carbonaceous chlorides, certain compounds of silicates, sulfides, sulfates, phosphates, tungstates, chromates, as well as oxides of some metals can have a significant effect on the color of the binder.

Less common, but strongly affecting the color of the binder, minerals that are natural inorganic pigments are:

- Glauconite ($(K, H_2O) (Fe^{3+}, Al, Fe^{2+}, Mg)_2[Si_3AlO_{10}](OH)_2 \times nH_2O$) is a natural clay mineral, at temperatures of 100–120 °C it loses adsorbed water, at 400–440 °C oxidizes Fe^{2+} to Fe^{3+}, at 440–510 °C. Composites with this compound has the shades of green.
- Mercury sulfide (α-HgS). At temperatures above 345 °C, it turns into β-HgS. The α-HgS modification gives the composites shades of red, the β-HgS modification paints the stone black.
- Arsenic sulfide (As_2S_3). The compound melts at 300–310 °C, boils at 707–723 °C, imparts yellow tints to the composite.
- Lead molybdate ($Pb [MoO_4]$) melts at 1060–1070 °C. The compound has a color spectrum ranging from yellow to brown.
- Ultramarine ($2 (Na_2O–Al_2O_3–3SiO_2)–Na_2S_4$), can impart rich shades of blue to the composite.
- Titanium dioxide (TiO2) is refractory, melts at 1975 °C. It is a white pigment.

The presence of titanium dioxide in the raw materials has a positive effect on the decorative properties of the finished product; the presence of other types of coloring oxides can reduce them. However, to obtain binders of a given shade, it is allowed to use the listed and other types of inert minerals as a pigment. It is recommended to introduce pigments by joint grinding with fired raw materials for the most uniform distribution. The amount of pigments introduced into the binder should not exceed 1–2% of the total weight of the finished product. But the content of even a small percentage of impurities in the form of traces of these minerals in raw rocks can unpredictably affect the color of the resulting binder.

The composition of impurities in dolomite rocks usually includes calcite, dolomite, iron and manganese carbonate, carbonaceous chloride and carbonaceous graphite matter.

The main aim of this paper is to study the properties of magnesium binders obtained on the basis of dolomite rocks from several deposits in the territory of the Russian Federation.

2   Materials and Research Methods

The Dolomites of the most popular deposits (Kovrovskoe, Satkinskoe, Temirtau and the Bosninskoe) were selected as samples.

The Kovrovskoe deposit is located in the Vladimir region near the village of Melekhovo. This deposit is represented by limestones and dolomites, which have an almost horizontal occurrence. The deposit belongs to the platform type, formed in marine conditions.

The Satkinskoe deposit is located on the western slope of the Southern Urals, in the Bashkir anticlinorium zone, near the town of Satka. The deposits are confined to the stratum of carbonate rocks (marble-like, brecciated dolomites, dolomitized limestones, limestones) of the Proterozoic Satka Formation. Magnesite deposits occur in dolomites, representing metasomatic formations formed under the influence of hot magnesium-containing solutions on carbonate layers. The formation includes marls, limestones, dolomites, shales, interlayers of marly dolomites and marly shales. The upper part of the formation contains magnesite deposits.

The Temirtau deposit is one of the largest deposits of Gornaya Shoria discovered in 1897. The deposit is located in the exocontact zone of the Telbes granitoid intrusion. Diorites, in contact with granites, experienced high-temperature contact metamorphism of the pyroxene-hornfels facies. The xenoliths of dolomite marbles contained in them were transformed into magnesian skarns among which dolomites and brucite marbles are found in the form of separate remnants.

Bosninskoe deposit is located on the right side of the Terek river, 17 km south of the town Ordzhonikidze. The geological structure of the Bosnian dolomite deposit involves the deposits of the Oxford and Kimmeridgian stages of the Upper Jurassic, represented by various limestones, sandy limestones, carbonated dolomites (in the upper part) limestones and dolomites. The rocks of the tiers have a monoclonal dip.

Dolomite samples from these deposits were tested to determine the mineralogical composition via differential thermal analysis. The chemical composition of these rocks was taken into account. The approximate chemical composition of the samples is shown in Fig. 1.
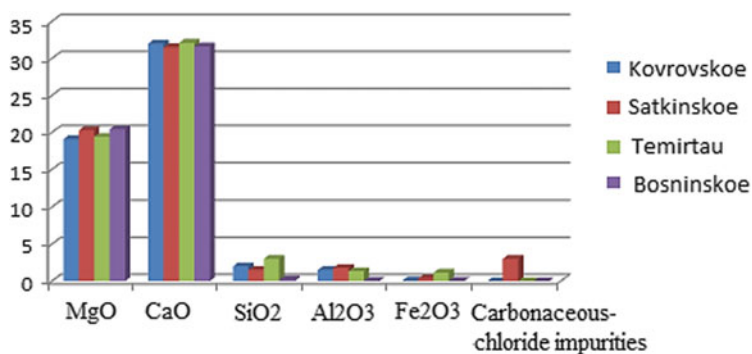
Fig. 1 The chemical composition of dolomites of various deposits, %

The binders were made from the rocks of these deposits by calcination with the decarbonization intensifier additives in a muffle furnace. The calcinated product was ground on a vibrating machine to a fineness of no more than 80 μm. For the binders

obtained in this way, the compression strength was determined on the 1st, 7th and 28th days of hardening and flexural strength was determined on the 7th and 28th days of hardening, as well as the color and uniformity of the volume change.

We also studied the granulometric composition of samples of raw materials from all deposits. All samples of dolomite rocks presented for analysis had a fraction of less than 5 mm. Differences in particle size distribution can significantly affect the quality of firing and the characteristics of the magnesium oxychloride cement [21]. The study of the particle size distribution was carried out using a set of standard sieves with the mesh size of 5, 2.5, 1.25, 0.63, 0.315 and 0.16 mm. Samples were dispersed on sieves and the partial and total residues on each sieve were calculated.

Strength characteristics were determined on the rectangular prisms shaped samples with a cross-sectional area of 4 × 4 cm and a height of 16 cm.

The color and light reflectance characteristics of the samples were determined using the photometer NR145 manufactured by the company "3nh". Using this device, it can be judged the prevalence of shades in the color range of samples. This characteristic is very important for magnesium oxychloride cements, since they are mainly used for decorative building materials—plasters and wall panels. The high coefficient of light reflection and the absence of pronounced shades allow using various types of coloring pigments to give the material a shade of any color.

The uniformity of the volume change was determined on a disc-shaped sample. The samples were hardened under normal conditions for a day. After that, the samples were placed in water, where they were kept for another day. If cracks did not appear on the surface of the samples during setting, due to exposure to water and after drying, it was assumed that the volume of the samples changes uniformly. This is one of the important indicator of the high-quality firing of dolomite in order to obtain a binder. In addition, the linear deformations of the samples were determined on instruments with dial indicators. Determination of linear deformations began after a day of hardening and ended when the average daily rate of change in the linear size of the sample differed from the average daily rate of the previous day by no more than 5%.

3   Research Part

The calculated content of dolomite in the composition of the studied samples of the above rocks is shown in Fig. 2.

It was found that all samples submitted for analysis meet the requirements for raw materials for the production of dolomite binders. However, in the rocks of the Kovrovskoye deposits and the Temirtau deposits, the dolomite content is 5–6% lower than the similar indicators of the Satkinskoye deposits and the Bosninskoye deposits.

Consequently, the presence of impurities, both inert and harmful, is more likely in the rocks of the Kovrovskoye deposit and the Temirtau deposit. With a correctly selected mode of firing the feedstock, calcite compounds can be attributed to inert impurities.

Then the granulometric compositions of dolomite samples from different deposits were determinate. The results of determining the granulometric composition of the samples are shown in Table 1.
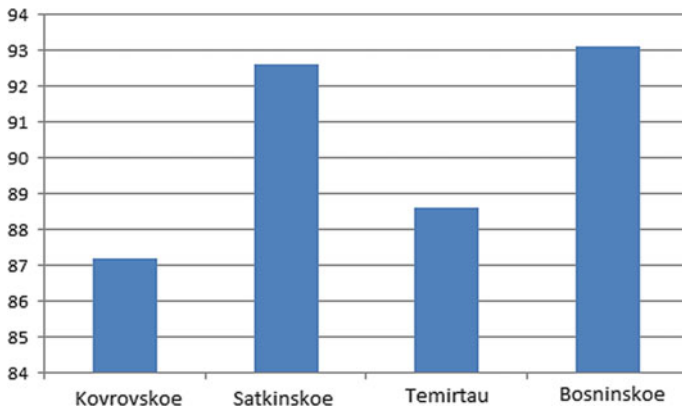
Fig. 2 Dolomite content in samples of raw material, %

In the course of the study, it was revealed that the largest amount of a fraction of more than 5 mm was found in the samples from the Kovrovskoe deposit, and the smallest in the samples from the Bosninskoe deposit. In the samples from the Bosninskoe deposit, one can also note the largest amount of dust-like fraction less than 0.16 mm. A high percentage of this fraction can adversely affect the quality of binders obtained on the basis of this raw material and increase the proportion of dust entrainment in the technological process. Equable granulometric composition is inherent in samples from the Satkinskoe and Bosninskoe deposits. In the sample from the Kovrovskoe deposit, there is practically no fraction of 0.63 mm. In the sample of the Temirtau deposit there is an insignificant amount of fractions of 2.5 and 1.25 mm.

The lack of continuous granulometry negatively affects the uniformity of the firing processes. Large and small grains are fired in different ways, because of which the magnesium oxide released during calcination crystallizes to different sizes. Dissimilarly crystallized magnesium oxide enters into a hydration reaction at different times and the growth of neoplasms can cause internal stresses in the body of the hardening and hardened composite. This fact can adversely affect the quality of the binders obtained.

Calcination was carried out until complete decarbonization of the magnesium component of dolomite.

Strength characteristics of samples showed the strength of magnesium composites, depending on the deposit of the source material, varies slightly (Table 2). At the same time, there is a direct dependence of strength on the content of magnesium oxide in the raw material.

All tested binders uniformly change their volume during hardening, which confirms the absence of cracks on the sample during they were kept in air and water. Samples were examined for cracks using optical instruments of a magnifying glass and an optical microscope. All samples had expansion deformations ranging 5–10 mm/m.

The color of the samples differs according to the chemical and mineralogical composition. Photographs of samples are shown in Fig. 3. The coefficients of light reflectance of the samples are given in Table 3.

Table 1 Granulometric composition of the samples from different deposits

Deposit	Residues on each sieve (%)														
	5 mm		2.5 mm		1.25 mm		0.63 mm		0.315 mm		0.16 mm	
	Partial	Total	Partial	Total	Partial	Total	Partial	Total	Partial	Total	Partial	Total
Kovrovskoe	10.2	10.2	12.1	22.3	17.9	40.2	0.6	40.8	20.7	61.5	13.3	74.8
Satkinskoe	3.1	3.1	14.8	17.9	10.1	28.0	14.4	42.4	21.7	64.1	16.6	80.7
Temirtau	5.5	5.5	1.2	6.7	0.9	7.6	22.9	30.5	33.8	64.3	22.0	86.3
Bosninskoe	2.4	2.4	10.6	13.0	14.1	27.1	18.6	45.7	11.6	57.3	12.6	69.9

Table 2 Strength characteristics of binders based on dolomites from different deposits

Deposit	1 day Compressive strength	7 days		28 days	
		Flexural strength	Compressive strength	Flexural strength	Compressive strength
Kovrovskoe	12.1	9.8	74.4	10.0	76.3
Satkinskoe	15.3	9.9	81.2	10.2	83.1
Temirtau	11.6	7.2	70.7	9.7	73.0
Bosninskoe	15.9	10.1	82.4	11.0	84.5
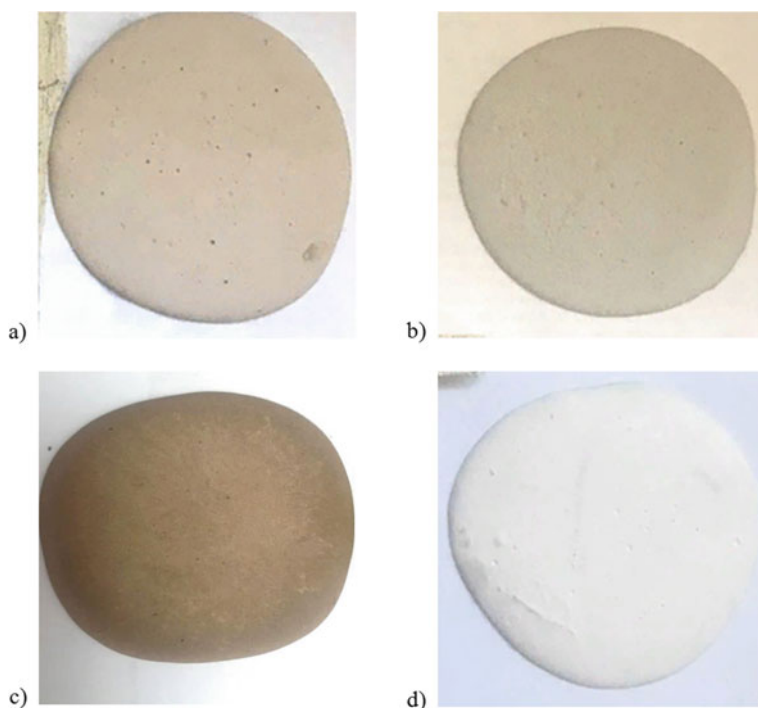
Fig. 3 Different sample colors **a** Kovrovskoe deposit; **b** Satkinskoe deposit; **c** Temirtau deposit; **d** Bosninskoe deposit

Table 3 Optical indicators of samples of magnesia stone

Deposit	Light reflectance coefficient (%)	Spectrum b+/b− (yellow/blue)	Spectrum a+/a− (red/green)
Kovrovskoe	86	14.18	3.34
Satkinskoe	73	8.86	1.59
Temirtau	64	11.05	2.45
Bosninskoe	89	3.89	0.77

Samples based on dolomite from the Satkinskoe deposit have a gray tint, samples based on Kovrovskoe dolomite are yellowish, and samples based on dolomites from the Bosninskoe deposit are white with a slight deviation into the yellow spectrum. Samples based on the dolomites of the Temirtau deposit are deep brown. Thus, magnesium oxychloride cements obtained on the basis of dolomites from the Satkinskoe, Kovrovskoe and Temirtau deposits have individual pronounced color shades. This fact does not affect the technological properties of magnesia composites based on such binders. However, this makes them less attractive to a number of manufacturers of decorative building materials such as plasters and magnesia glass sheets. It is possible to increase the whiteness of the binder from the dolomites of the Kovrovskoye deposit using a white pigment—titanium dioxide. For binders based on dolomites of the Satka deposit and the Temirtau deposit, the use of a white pigment is impractical, but they can be painted in darker colors using pigments such as iron oxide or beta modification of mercury sulfide.

4   Conclusion

In the course of this study, the dependence of the main properties of magnesia composites on the chemical and mineralogical composition of raw materials was established. The largest amount of magnesium oxide is observed in dolomite samples from the Satkinskoe and Bosninskoe deposits. In the Temirtau, Satkinskoe and Kovrovskoe deposits there are a significant proportion of iron and aluminum oxide impurities, and carbonaceous chloride impurities are also present in the dolomites of the Satkinskoe deposit, which significantly affects the color of the rock and the binder powder obtained on its basis.

Largely, the content of free magnesium oxide and the presence of impurities affect the color of the hardened composites, rather than their strength characteristics. However, the strength characteristics are probably influenced by the uniformity of the grain size distribution of the raw materials used.

The most suitable raw material for obtaining decorative and durable building material from the considered ones is dolomite from the Bosninskoe deposit.

A large amount of dust particles in the raw materials of the Bosninskoe deposit can complicate the technological process. This problem can be solved using the wet granulation method. This method involves mixing finely ground dolomite particles with a solution of an additive intensifier of firing and forming the resulting mass into granules.

References

1. Fairbridge W (1957) The dolomite question. Columbia University, New York
2. Sibley D, Gregg J (1987) Classification of dolomite rock textures. J Sediment Res 6:967–975
3. Folk R, Land L (1975) Mg/Ca ratio and salinity: two controls over crystallization of dolomite. AAPG Bull 59:60–68
4. Land L (1985) The origin of massive dolomite. JGE 33:112–125
5. Radke B, Mathis R (1980) On the formation and occurrence of saddle dolomite. J Sediment Res 50:1149–1168
6. Baker P, Kastner M (1981) Constraints on the formation of sedimentary dolomite. Sci 213:214–216

7. Gianolla P, De Zanche V, Mietto P (1998) Triassic sequence stratigraphy in the Southern Alps (Northern Italy): definition of sequences and basin evolution. SEPM 60:719–747
8. Pfeil R, Read J (1980) Cambrian carbonate platform margin facies, Shady Dolomite, southwestern Virginia, USA. J Sediment Res 50:91–116
9. Shimmield G, Price N (1984) Recent dolomite formation in hemipelagic sediments off Baja California, Mexico. J Sediment Res 41:5–18
10. Kearsey T, Twitchett R, Newell A (2012) The origin and significance of pedogenic dolomite from the Upper Permian of the South Urals of Russia. Geol Mag 149:291–307
11. Tojo B et al (2007) Calcite–dolomite cycles in the Neoproterozoic Cap carbonates, Otavi Group, Namibia. Geol Soc Spec Publ 286:103–113
12. Gabellone T, Borromeo O, Consonni A, Geloni C, Albertini C, Bigoni F, Vercellino A. (2020) A multistep reactive convection model for the prediction of the dolomite bodies distribution in the Karachaganak field-Kazakhstan. In: International petroleum technology conference, Dhahran, Kingdom of Saudi Arabia
13. Zaycev VA (2006) Finishing building material. RUS Patent 2006100485/22, 10 Sept 2006
14. Andreenkov V (2001) Perspektivy ispolzovaniya nerudnogo syrya severo-vostoka Voronezh-skoj anteklizy dlya proizvodstva oblicovochnyh i dekorativno-otdelochnyh izdelij (Prospects for the use of nonmetallic raw materials in the north-east of the Voronezh anteclise for the production of facing and decorative and finishing products). Bull VSU Ser: Geol 11:161–170
15. Rumyantseva G, Nemenyonok B, Tribushevsky V, Gorbel I (2016) Magnezialnye flyusy i osobennosti ih ispolzovaniya pri plavke stali (Magnesial fluxes and features of their use in steel melting). Metall 1:31–37
16. Nakai Y et al (2013) Hot metal desulfurization behavior with dolomite flux. ISIJ Int 53:1020–1027
17. Prusti P, Barik K, Dash N, Biswal S, Meikap B (2021) Effect of limestone and dolomite flux on the quality of pellets using high LOI iron ore. Powder Technol 379:154–164
18. Lyubin P, Sokolova E, Gavrilenko A (2017) Ispolzovanie dolomitovoj muki v kachestve dobavki dlya uvelicheniya nesushchej sposobnosti gruntovogo osnovaniya (The use of dolomite powder as an additive to increase the bearing capacity of the soil base). Act Prob Tech Sci (in Rus and ab) 1:57–59
19. Wu J et al (2006) Effect of dolomite application on soil acidity and yield of rapeseed on yellow-red soil. Chin J Oil Crop Sci 28:55
20. Nosov VA (2014) Magnezial'noe vyazhushchee iz dolomitov i materialy na ego osnove (Magnesia binder from dolomites and materials based on it). Dissertation, Belgorod State Technological University named after V.G. Shukhova
21. Averina G, Koshelev V, Kramar L (2019) Combined roasting of raw materials modified by additives-intensifiers in form of low humidity sludge. IOP Conf Ser: Mater Sci Eng 687:022038

Filling of Epoxy Polymers as a Factor of Obtaining a Multi-component Composition with Improved Strength Properties

R. A. Burkhanova[✉], N. Yu. Evstafyeva, T. K. Akchurin, and I. V. Stefanenko

Volgograd State Technical University (VSTU), 1, Akademicheskaya St, Volgograd 400074, Russia

Abstract. The article investigates a filled two-component polymer system (FTPS). Being production wastes, dispersed abrasive particles (AP) (formulation I) and discrete carbon fibers (CF) (formulation II) were used as the filling and strengthening phase. The reasonability of the choice of the FTPS fillers was evaluated by the availability of the ingredients of secondary material resources in the region and their market value. An increase in the strength due to the dispersion of another phase (AP and CF), which is more stiff and durable than the main polymer, in the polymer matrix was understood as the strengthening of the FTPS polymer composition. The set of the indices of the FTPS mechanical properties varied depending on the shape of the filler particles. The mixing of the FTPS dry components of the formulations I and II was carried out under normal conditions at the laboratory of the Department of Construction Materials and Special Technologies. The obtained results indicate a positive effect of the FTPS modification. The introduction of the fillers and chemical additives results in an increase in the strength characteristics of the composition, which makes it possible to consider the developed FTPS formulation not only as waterproofing but also as strengthening, thereby expanding the area of its use.

Keywords: Filled two-component polymer system (FTPS) · Modified concrete · Abrasive particles · Carbon fibers · Tensile strength · Bending strength

1 Introduction

In order to improve the strength characteristics of the filled two-component polymer system (FTPS), it can be reinforced with a dispersed material of mineral and organic nature, which is followed by the formation of a new set of properties of the composition due to interfacial interactions at the polymer-solid interface. They primarily include adsorption or molecular interactions. They are responsible for adhesion at the interphase boundary, as well as for the physical, mechanical and other properties of filled systems. The interfacial interactions determine the specific features of the boundary layer structure, the nature of molecular packing, molecular mobility, morphology and other properties [1–3].

Particular attention is paid to the reinforcement of polymers contributing to the strengthening of structures. Combining the FTPS and fillers is an essential way to create advanced composite materials with a tailored set of properties differing from the properties of the initial components, which makes it possible to obtain materials with completely new technological or operational characteristics. For composite polymer materials, two types of strengthening are distinguished:

- highly filled systems in which the polymer serves to envelop the reinforcing elements (long fibers) and occupies a smaller volume in the composition (20–50%);
- low filled systems in which the properties of the composition are closer to those of the polymer base, and small amounts of fibers or dispersed particles (5–25%) are introduced as the strengthening phase.

In accordance with the generally accepted classification of fillers, the following types are most often used in heterophase polymer formulations: spherical elements; crystalline fillers; fibrous fillers; synthetic polymers forming a filamentary network structure [4–9].

The investigations of low filled FTPS systems are of scientific and practical interest. There, dispersed abrasive particles (AP) (formulation I) and discrete carbon fibers (CF) (formulation II), being production wastes, are used as the filling and strengthening phase.

2 Research Methods

The reasonability of the choice of the fillers for multi-component polymer system was evaluated by the availability of the ingredients of secondary material resources in the region and their market value.

Strengthening of polymers is determined by the presence of a filler and the emergence of certain structures in the filled polymers, which cause a change in the properties of the polymer. An increase in the strength due to the dispersion of another phase (AP and CF), which is more stiff and durable than the main polymer, in the polymer matrix was understood as the strengthening of the FTPS polymer composition. Thus, the strengthening is carried out through combining the polymer system and the filler system in a free state, which leads to the "averaging" of their properties. The set of indices of the FTPS mechanical properties can vary depending on the shape of the filler particles. For fibrous carbon fillers, the index of the ultimate tensile stress at break is the most important one since fibers in a composite polymer material work mainly in tension. Compression, bending and shear are critical for grained abrasive fillers, which work primarily in compression, but can also work in tension and shear.

The conducted investigations pursued the goal of choosing the optimal formulations of FTPS taking into account their filling with discrete carbon fibers (CF) and abrasive particles (AP). Secondary epoxy resin modified with phenol–formaldehyde resin was used as a polymer binder. Polymer coatings were applied to the specimens made of cement-sand mortar (W/C = 0.55). The mixing of the FTPS dry components of the formulations I and II was carried out under normal conditions at the laboratory of the Department of Construction Materials and Special Technologies. The polymerization reaction of the filled FTPS with curing proceeds within 10–16 h. The viability of the

FTPS at the temperature of 20–23 °C is 4 h, the viability of the mixtures decreases with an increase in the air temperature. It is recommended to use the composition at positive temperatures. The dry polymer mixture can be stored for up to 3 years if it is packed to be moisture-proof.

The best diluents for epoxy resins are glycidyl ethers: cresyl glycidyl ether, butyl glycidyl ether, phenyl glycidyl ether, furyl glycidyl ether and glycidyl ethers of α-branched synthetic fatty acids. However, their high toxic potential does not allow us to recommend these ethers for widespread use. In the course of the conducted investigations, ketone diluents were used since they are considered to be the best solvents for epoxy resins and epoxy-resin-based compositions; they are capable of dissolving large amounts of a copolymer. The solutions have low viscosity, they are stable during storage and do not degrade when large volumes of diluents are added. Ketones are non-corrosive and relatively non-toxic [10–12].

3   Results and Discussion

The test results of the strength characteristics of the filled FTPS compositions are presented in Table 1.

Table 1 Test results of the strength of the filled compositions of FTPS

Strength of specimens	Reference specimen	Formulations of the filled composition					
		Names of the fillers and their introduction % of the polymer base mass					
		AP (I)		CF (II)		AP + CF (1:1)	
		5	15	5	15	5	15
σ_{break}, MPa	2,3	2,4	2,3	3,6	4,1	4,3	5,3
σ_{comp}, MPa	36,3	40,0	40,3	37,8	38,8	52,8	58,8
σ_{bend}. MPa	13,3	14,1	14,8	24,1	25,4	27,8	29,9

An analysis of the test results (Table 1) demonstrated that an increase in the strength characteristics of the specimens with a polymer coating is typical of the FTPS filling with both abrasive particles and carbon fibers. The diagrams of changes in the strength characteristics of the filled polymer systems depending on the type of the filler are given in Figs. 1 and 2.

The formulations combining both fillers in the ratio of 1:1 exhibit the highest indices of strength characteristics. An increase in the amount of the fillers from 5 to 15% gives an average 5% increase in strength. In comparison with the reference filler-free specimen, the tensile strength at break increased by 60%, the compressive strength increased by 50%, and the bending strength increased by 30%.

One of the most common physicochemical phenomena occurring at the "filler–polymer" interface is wetting. Good wetting of the substrate surface is one of the necessary
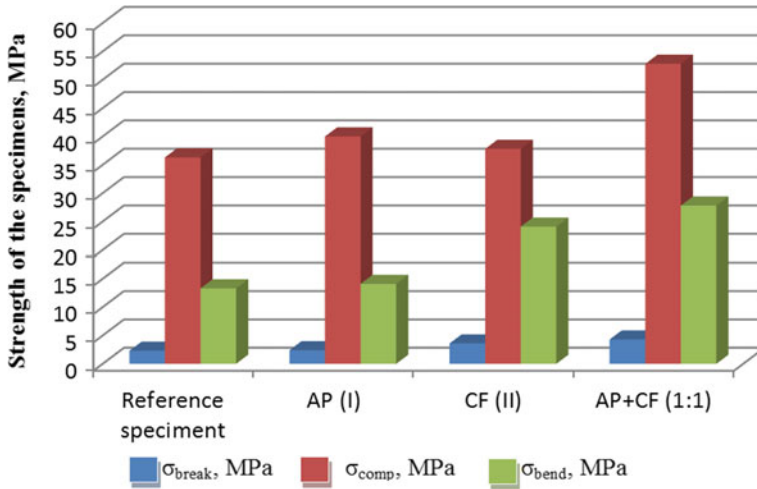
Fig. 1 Change in the strength characteristics of the specimens with FTPS coating depending on the type of the filler, at the filler content of 5%
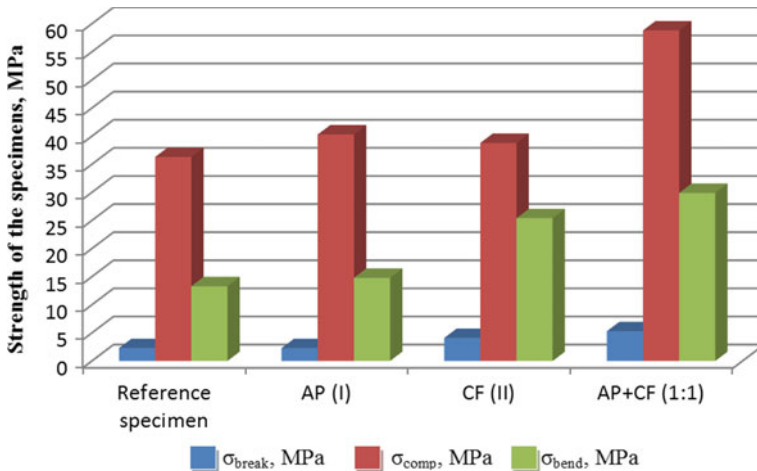
Fig. 2 Change in the strength characteristics of the specimens with FTPS coating depending on the type of the filler, at the filler content of 15%

conditions for obtaining a polymer composite material of a defect-free structure with high physico-mechanical properties.

Polyhydrosiloxanes (KOZh 136–41) were used as a chemical additive to enhance the adhesion characteristics of the FTPS, which were added in the process of the preparation of the polymer composition. The investigation of the effect of the additives on the adhesion of the FTPS polymer base to the substrate surface when applying the FTPS compositions to concrete with the aim of waterproofing and additional strengthening is of scientific and practical interest. From a theoretical point of view, the improved wetting

of the surfaces of the fillers and the substrate with the modified FTPS mixture can be explained as follows.

The surface-active agents introduced into the filled FTPS solution are adsorbed at the phase boundary, forming a monomolecular layer oriented in a strictly defined manner. These adsorbed layers change the balance of forces in the system and contribute to the reduction in the surface energy of the binder, which is a necessary condition for wetting [10–16].

In addition, the applied additive helps to reduce the viscosity of FTPS as a result of its interaction with particular chains and units of macromolecules. Through changing the conformation of the chains of the polymer base, the additive facilitates the formation of a dense oriented layer of them at the interface. This effect of the organic additives makes it possible to increase the number of contacts of macromolecules with the surface of the solid and enhance the adsorption interaction both in the system of polymer–substrate and in the system of filled polymer–substrate. This, in turn, improves the wetting of the contacting surfaces and contributes to the growth of adhesion. The results of the experiment are presented in Table 2 and in Figs. 3 and 4.

Table 2 Adhesion characteristics of the modified FTPS composition

Name of additive	Concentration c (%)	Contact angle of wetting σ, grad	Interfacial tension σ_1 (mJ/m^2)	Work of adhesion W_a, (mJ/m^2)	Work of cohesion W_c, (mJ/m^2)	Spreading coefficient S	Relative work of adhesion Z_a
FTPS	–	23,64	41,58	80,90	85,70	3,70	0,9629
KOZh 136–41	0,1	23,39	40,87	79,37	84,18	−3,54	0,9648
	0,5	22,75	38,84	75,53	80,00	−3,24	0,9663
	1,0	22,73	38,21	74,31	78,66	−3,17	0,9668
	3,0	22,70	38,11	73,44	77,76	−3,13	0,9689

When introduced into the formulation of the FTPS, the organosilicon fluid 136–41 significantly reduces the interfacial tension of the polymer mixture, being a surface-active agent (SAA) for it. With an increase in the SAA concentration, a regular decrease in the interfacial tension occurs. Thus, at the maximum concentration of KOZh 136–41 (3%), the interfacial tension decreases by 8.7%.

The processes taking place at the polymer-substrate interface are explained in terms of the adsorption theory of adhesion, which considers the adhesion to be a result of the activity of the forces of molecular interaction between the molecules of the adhesive substance and the substrate [17–22].

Being adsorbed at the phase boundary, the organosilicon fluid KOZh 136–41 helps to reduce the interfacial tension of the FTPS. The contact angle decreases, the wettability increases with a decrease in the work of adhesion (Table 2). The value of the relative work of adhesion of the composition is 0.9629–0.9689, which is close to unity. Consequently,
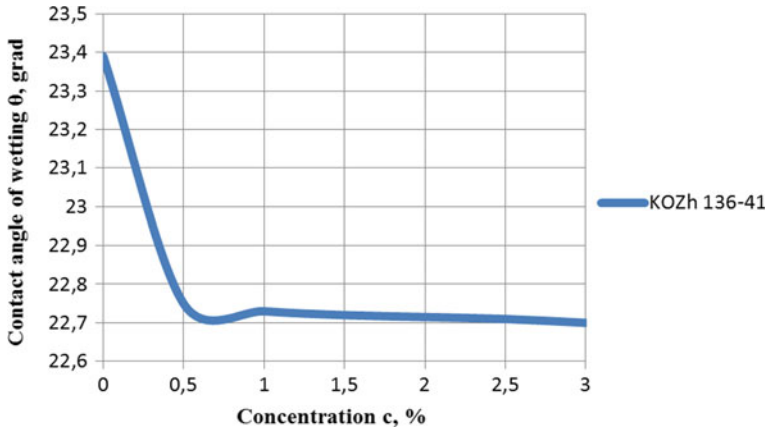
Fig. 3 Change in the contact angle of wetting of FTPS depending on the concentration of KOZh 136–41 modifier
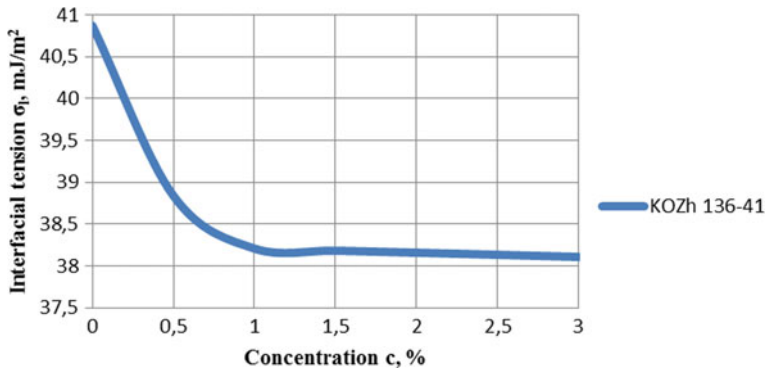
Fig. 4 Change in the interfacial tension of the FTPS depending on the concentration of KOZh 136–41 modifier

the values of the adhesion forces between the molecules of the polymer and the substrate approach to the values of the cohesion forces of the molecules of the polymer itself. This contributes to the formation of a material with a homogeneous, defect-free structure [23, 24].

However, the introduction of surface-active chemical additives affects not only the adhesion of the polymer coating to the base of a construction product or metal. The effect of the chemical additives on the change in the strength characteristics of the filled composition of the FTPS (AP + CF) was evaluated depending on the sequence of their introduction into the composition. Pretreatment of the surface of AP and CF with KOZh 136–41 and GKZh-10 additives significantly adds to the growth of strength characteristics. The surface of the fillers was treated with the 3% additive at the filler mixture content (AP + CF) of 5 and 15%. The results are presented in Table 3. The experimental results demonstrate (Table 3, Figs. 5 and 6) a change in the strength characteristics of the

coated specimens tending to grow due to the pretreatment of the surface of the fillers. The strength indices of the specimens increased (the values below the line, Table 3) by 10–15%, on average, in comparison with the specimens with non-modified surface of abrasive particles and carbon fibers.

Table 3 Test results of the strength of the filled compositions of FTPS

Strength of specimens	Formulations of the filled composition of FTPS			
	AP + CF (1:1)		AP + CF (1:1)	
	5	15	5	15
	KOZh 136–41 (3%)		GKZh-10 (3%)	
σ_{break}, MPa	4,5/5,2	5,5/6,1	4,5/4,9	5,5/5,8
σ_{comp}, MPa	53/61,2	59/65,3	53/60,7	59/63,9
σ_{bend}, MPa	28/32,8	30/33,6	28/30,8	30/32,6
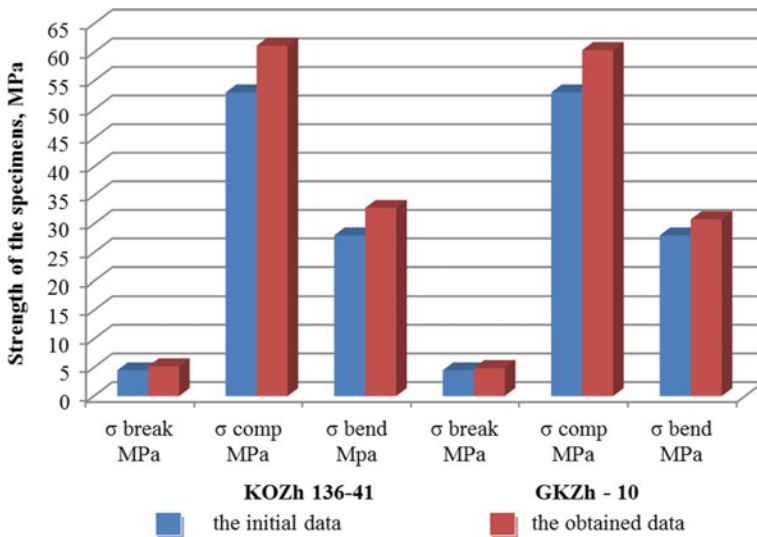
Fig. 5 Change in the strength characteristics of the specimens with the FTPS coating (formulation III, 5%), and in the type of the chemical additive (3%)

The effect of the surface modification of AP and CF fillers due to their pretreatment was assessed through the change in the indices of water permeability and water absorption. Several series of specimens with filled FTPS (AP + CF) and with unfilled polymer coating on all sides were manufactured. The water permeability was characterized as an ability of the coating to pass water or aqueous solutions. The essence of the method of the test without pressure was to determine the change in the mass of the coated specimen placed into an aqueous medium or solution and kept there for a selected period of time.
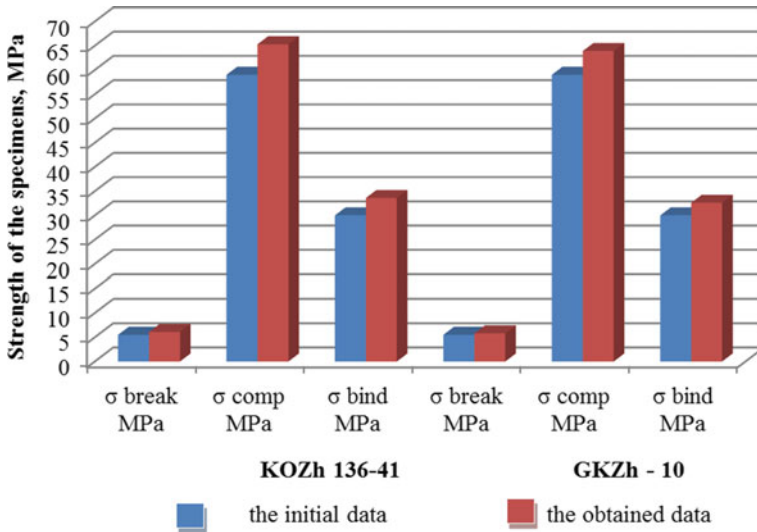
Fig. 6 Change in the strength characteristics of the specimens with the FTPS coating (formulation III, 15%), and in the type of the chemical additive (3%)

The specimens for the test are shown in Fig. 7a, b. The thickness of the coating was 300–350 μm.
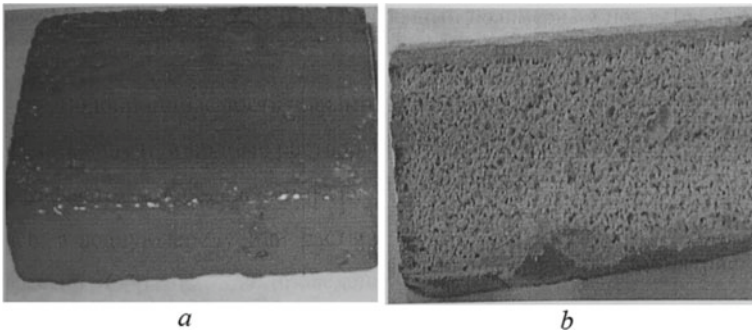
Fig. 7 Specimen with the FTPS coating for the tests. **a** General view of the specimen; **b** section view of the specimen

The authors carried out the quantitative assessment of the water permeability according to the average test indices calculated for each of the specimens according to the formula (1):

$$W = \frac{\Delta m}{F \cdot \tau}, \frac{g}{cm^2 \cdot days},$$ (1)

where $W\gamma$—water permeability of the coating; Δm—change in the mass of the coated specimen (g) over time—τ; F—area of the specimen, cm^2.

The test results are presented in Table 4. The application of the polymer composition to the surface of the specimens resulted in the twofold decrease in the water permeability. In the case of further exposure of the polymer-coated specimens to water, a decrease in the water permeability index and its stabilization were observed. The treatment of the filler surface with the chemical additive led to an additional decrease in the water permeability by 40% due to the formation of a denser structure of the filled composition and additional adhesion of the cement matrix to the modified surface of the fillers. The values of the water absorption indices of the specimens with the polymer coating without filler treatment (6.4%) and with the FTPS polymer coating with filler surface treatment (1.6%) were compared with the reference specimen without a coating (11.7%). The decrease in the index was from 2 to 7 times, respectively.

Table 4 Change in the water permeability ($\times 10^{-5}$) of the specimens depending on the time of exposure to water

Cement-sand specimen	Time of exposure to water, days			
	30	60	90	180
Without a coating	6,93	13,07	18,13	18,13
With a coating without filler treatment	3,30	2,67	2,53	2,21
With a coating with the filler treatment	2,35	2,23	1,82	1,79

4   Conclusions

Thus, the obtained results indicate a positive effect of the modification of the FTPS and the filler mixture surface with organosilicon fluids, which determines the sequence of the technological operations in the process of manufacturing of the filled polymer composition of FTPS. The introduction of the fillers and chemical additives leads to an increase in the strength characteristics of the composition, which makes it possible to consider the developed formulation of the FTPS not only as waterproofing but also strengthening, thereby expanding the area of its use. Low filled systems in which the properties of the composition are closer to those of the polymer base allow revealing and using the properties of the modified epoxy base to the fullest degree. The strengthening phases are introduced in small amounts in the form of short carbon fibers or dispersed abrasive particles (5–25%). For fibrous carbon fillers, the index of the ultimate tensile stress at break is the most important since fibers in a composite polymer material work mainly in tension. Compression, bending and shear are critical for grained abrasive fillers, which work primarily in compression, but can also work in tension and shear. In this regard, a necessity arises for a practical investigation of the effect of concrete base characteristics on the conditions of its joint work with the protective polymer coating. In this case, the performability and chemical resistance of concrete with polymer coatings depend on numerous factors.

References

1. Swaminatham V, Kildsig DO (2002) Polydisperse powder mixtures: effect of particle size and shape on mixture stability. Drug Dev Ind Pharm 28(1):41–48

2. Kats GS, Milevski DV (1981) Fillers for polymer composite materials. Khimiya, Moscow, p 736

3. Grozdov VG (2006) Strengthening of building structures. Publishing House KN+, St. Petersburg, p 232

4. Ngog Thanh Tran (2015) Fracture energy of ultra-high-performance fiber-reinforced concrete at high strain rates. Cem Concr Res 101(1):80–90

5. Rehbinder PA (2009) Physico-chemical mechanics of dispersed structures. Nauka Publ., Moscow, p 316

6. Khozin VG (2006) Modification of cement concretes with minor alloying additives. Stroitel'nye Mater 10:30–31

7. Chistov YuD, Krasnov MV (2010) Nanomodifiers in non-autoclaved aerated concrete. Concr Technol 7–8:68–71

8. Shmigalsky VN (1967) Determining the optimal ratio of fine and coarse aggregates. News of Higher Educational Institutions. Constr Archit 9:69–72

9. Mohammeda MK, Al-Hadithi AI, Mohammed MH (2019) Production and optimization of eco-efficient self compacting concrete SCC with limestone and PET. Constr Build Mater 197:734–746

10. Losev IP, Trostyanskaya EB (1960) Chemistry of synthetic polymers. Khimiya, Moscow, p 615

11. Lee H, Neville K (1967) Handbook of epoxy resins. In: Aleksandrov NV. Energy Publ., Moscow, p 415

12. Gadzhiev AM, Kurbanov RM, Khadzhishalapov GN (2017) The influence of the filler grain composition on the properties of the heat-resistant basaltic. Herald of Daghestan State Technical University. Tech Sci 44(3):146–155

13. Hongfang S, Li Z, Memon SA (2015) Influence of ultrafine $2CaO$ center dot SiO_2 powder on hydration properties of reactive powder concrete. Materials 8(9):6195–6207

14. Skazlic M, Skazlic Z, Majer J (2012) Application of high performance fibre reinforced shotcrete for tunnel primary support. In: Proceedings of the 10th international conference on shotcrete for underground support, pp 206–214

15. Shi XS, Collins EG, Zhao XL (2012) Mechanical properties and microstructure analysis of fly ash geopolymeric recycled concrete. J Hazard Mater 237:20–29

16. Sudarsana Rao H, Somashekaraiah HM, Ghorpade Vaishali G (2011) Strength and workability characteristics of fly ash based glass fibre reinforced high-performance concrete. Int J Eng Sci Technol 3(8):6266–6277

17. Evstafyeva NYu, Akchurin TK, Stefanenko IV (2018) Polymer systems of waterproofing and corrosion protection of building materials and structures. Bull Volgograd State Univ Archit Civ Eng. Ser: Civ Eng Archit 53(72):43–52

18. Evstafyeva NYu, Stefanenko IV, Akchurin TK (2020) Modification of concrete with polymer additives based on secondary resources. Mater Sci Forum 974:277–282

19. Evstafyeva NYu, Stefanenko IV, Akchurin TK (2019) Polymer protection system for construction products from the corrosive destruction. In: Proceedings of VII international scientific conference on resource-and-energy efficient technology in construction industry, Yuri Gagarin State Technical University of Saratov, pp 194–199

20. Gotlib EM (1988) On the role of adsorption interactions between binding agent and filler in the formation of phase structure and properties of filled epoxy polymers. Composite polymer materials: collection of scientific papers, p 4–8

21. Spiratos N (2015) Superplasticizers for concrete. Fundaments, technology and practice, Quebec, p 323
22. Balakrishna MN, Mohamad F, Evans R (2020) Durability of concrete with differential concrete mix design. Int Res J Eng Technol (IRJET) 7(4):696–701
23. Batrakov VG (2002) Modified concretes in contemporary construction practice. Ind Civ Eng 9:23–25
24. Al-Hadithi AI, Hilal NN (2016) The possibility of enhancing some properties of self-compacting concrete by adding waste plastic fibers. J Build Eng 8:20–28

Binding Agents of Autoclaved Hardening Based on Metallurgical Slags

F. L. Kapustin[1] and S. N. Pogorelov[2(✉)]

[1] Ural Federal University, 19, Mira Street, Ekaterinburg 620002, Russia
[2] South Ural State University, 76, Lenin Avenue, Chelyabinsk 454080, Russia
`pogorelovsn@susu.ru`

Abstract. The article presents a new technology for the manufacture of building products using binding agents of autoclaved hardening based on metallurgical slags. Three compositions of binders are proposed. The first composition based on decaying ferrochrome slag and finely ground nickel slag allows to increase the strength and reduce the cost of the binder in the manufacture of autoclave hardening products (silicate bricks) compared to traditional compositions. The second binder composition, including nickel slag and converter slag as a lime-containing component, was developed to increase the activity of the binder and showed an increase in the strength of the samples after heat treatment. The third composition of the binder, including converter slag and a silica additive, allows to increase the strength of autoclaved concrete products. The presented technology belongs to the construction materials industry and can be used in the manufacture of autoclave products at building factories.

Keywords: Autoclave products · Metallurgical slag · Ferrochrome slag · Nickel slag · Converter slag

1 Introduction

The construction materials industry has faced serious problems in improving the technical level of production, expanding the raw material base, assortment and improving the quality of products and, if possible, reducing its cost. Also, one of the main tasks that enterprises have to solve is to increase the strength characteristics of products [1]. One of the directions for improving product quality is the use of environmentally friendly or recycled materials, for example, for creating sustainable concrete and manufacturing products from it. These products may consist of fibers (for example, steel, polypropylene, carbon fibers), recycled materials (for example, tire rubber, crushed glass, plastic, industrial waste), and organic and inorganic elements, such as concrete aggregates and reinforcing elements [2–6]. Another direction is the use of waste from metallurgical industries as part of binders, such as ferrochrome slag, etc. [7].

Great potential exists for some slags to be used as mineral sources in cement manufacture [8]. Studies were carried out on the mechanical characteristics and resistance to

carbonization of concrete with total replacement of conventional aggregates by steel slag aggregates, containing no chemical admixtures. The steel slag concretes presented higher compressive strengths and reductions in carbonation depths up to 60% compared to conventional ones [9]. The influence of the high-temperature process on the microstructure and properties of industrial steel slag cement was also investigated. Experiments have shown that with the increase of temperature the flexural and compressive properties of cement gradually increased [10].

2   Relevance

The presented technology belongs to the construction materials industry and can be used in the manufacture of autoclave products at building factories.

The influence of the content of metallurgical slags in the composition of mixtures has been repeatedly considered in scientific articles. For example, in the article by Guryeva and Ilina [11], the results of research on the development of the production of ceramic bricks from low-melting high plasticity clay with the addition of nickel slags by plastic molding are presented. The dependence of the physical and mechanical properties of the brick on technological factors was also evaluated.

In the works of Platonov et al. [12] and Zubekhin and Dovzhenko [13], the authors aimed not only to develop new compositions of raw materials, but also to improve the quality of ceramic bricks based on low-grade clay raw materials with the use of secondary raw materials of electrometallurgical production. A similar task was set in the work of Yevtushenko and Ivanov [1].

In the work of Zyryanov and Khakimova [14], the question of the influence of the binder composition on the nature of concrete hardening was raised. These studies have shown that the kinetics of concrete hardening when using a composite binder is much more intense than concrete made on ordinary cement, and that concrete made using a composite binder has greater strength than is necessary for this brand, which allows you to save binders up to 40%.

The article Jena et al. [15] describes experimental studies of the effect of the ferrochrome slag use instead of coarse aggregates and jute fiber on various characteristics of concrete, for which 12 samples with different percentages of slags were made. The experimental outcome analysis depicts the concrete mix having 50–100% ferrochrome slag aggregates and 0.1% jute fibre has strength, physical and non-destructive parameters similar to those of normal concrete.

Priyatham et al. published a paper [16], which was devoted to the idea of using industrial waste in the production of concrete to fill the shortage of natural resources. The present experimental study shows the possibility of replacing a coarse aggregate with ferrochrome slag waste obtained in the metallurgical industry and cement with fly ash obtained from power plants for the production of concrete mixtures for many construction practices.

Lai et al. [17] studied the mechanical property and microstructure (mercury intrusion porosimetry and scanning electron microscope tests) of a total of 15 concrete mixes with different replacement ratios of coarse and fine aggregates using basic oxygen furnace steel slag. Results revealed that the optimum replacement ratios of coarse and fine

aggregates were 50% and 30%, respectively. Basic oxygen furnace steel slag aggregate improves mechanical behavior and microstructure of concrete.

Acharya and Patro [18] studied the bending behavior of reinforced concrete beams made of a coarse aggregate of air-cooled ferrochrome slag. In their work, the physical, chemical and mechanical properties of concrete on metallurgical slags were studied, and the experiment showed that the properties are much better than those of concrete with a natural coarse aggregate in the composition. The same question was raised by researchers from Oman Fares et al. in the review [19].

As the analysis of the articles shows, metallurgical slags can and should be used in the production of building materials, because this can not only improve the properties of products, but also save our planet from the storage of industrial waste and the exhaustion of natural resources. Also, the use of metallurgical slags allows you to reduce the cost of the finished product. However, in most cases, only one type of slag is used.

3 Statement of the Problem

The aim of the study was to determine the most tailored compositions of binders, including metallurgical slags (one or several), which will increase the strength of autoclave hardening products, increase the activity of the binder and reduce the cost. Three fundamentally different compositions of binders were selected.

3.1 The Composition of the Binder No. 1

To increase strength and reduce the cost of the binder it is suggested to use a binder that includes slacking ferrochrome slag and fine ground silica component (ground nickel slag) in the following ratio of ingredients: slacking ferrochrome slag—30–60 wt%; Nickel slag is 40–70 wt%.

Binder in the absence of lime and quartz sand has greater strength than with the addition of these components. In addition, the replacement of natural sand with waste from metallurgical production contributes to solving environmental problems.

This composition can be used by factories of wall building materials for the manufacture of autoclave products, for example, silicate bricks.

Autoclave hardening binders containing metallurgical slags, an activator and a finely ground silica component are known [19]. The closest to the proposed one is the binder, which includes,%: slacking ferrochrome slag 75, lime 5 and ground quartz sand 20. The disadvantage of the known binders is their low strength.

3.2 The Composition of Binder No. 2

To increase the activity of the binder, a composition containing nickel slag and a lime-containing component (converter slag) is proposed with the following component ratio: nickel slag—50–95 wt%; converter slag—5–50 wt%.

There are known slag binders with hardening activators in the form of lime or gypsum HL. There is also known as a binder containing nickel slag and a lime-containing component [20]. This binder is the closest to the invention in terms of its technical essence and the achieved result. However, the activity of such astringents is low.

3.3   The Composition of the Binder No. 3

The composition is proposed, which includes converter slag and silica additive in the following ratio: converter slag—60–90 wt%, silica additive—10–40 wt%.

As a silica additive, the binder may contain, for example, fine ground quartz sand.

There is a binder, which includes converter slag, an oxidizer and sodium chloride [21].

The closest to the proposed binder, which includes converter slag and a silica additive [20].

However, known binders have low strength.

4   The Theoretical Part

The problem of processing slag disposal areas of ferrous and non-ferrous metallurgy plants is the most urgent today, not only from the point of view of additional raw materials for the extraction of non-ferrous metals and iron, but also from the environmental one. The utilization of such raw materials in the last decade has become a national problem for many countries of the world due to the intensive growth of production and environmental pollution.

Metallurgical and phosphoric slags are good raw materials for the production of building materials. The spread of slags, although uneven, on the territory of the country makes their use even more effective, since the distance of transporting materials to construction objects is reduced. Ferrous metallurgy slags are used to the fullest extent, especially blast furnace slags. More than 50% of blast furnace slags are processed into granular.

The latest achievements and problems associated with the use of steel slags (converter, electric arc and low-temperature slags) as a substitute for cement and aggregate in cement concrete are presented in the review [22]. The results show that the cementing capacity of all steel slags in concrete is low and requires activation. However, taking into account environmental and economic aspects, steel slags can also be used as raw flour in the production of cement clinker.

As a filler, steel slag has good morphological and mechanical properties. A complete overview of the application of steel slags in cement-based composites and their characteristics is given in [23]. Durability studies on eco-friendly concrete mixes incorporating steel slag as coarse aggregates provided by Palankar et al. [24] showed The inclusion of steel slag aggregates slightly reduced the durability performance of alkali activated slag concrete and alkali activated slag fly ash concrete mixes. Therefore, it is important to optimize the mix design appropriately in order to guarantee the desired level of durability. The mixes containing steel slag aggregates may be aimed at higher compressive strength and lower water penetration as main characteristics. The promising mechanical performance and durability of cement-based composites prompt further research into the use of steel slag.

In this study, 3 types of slags were used in the binder compositions: ferrochrome, nickel and converter slags.

4.1 Ferrochrome Slag

Ferrochrome slag is formed as a by-product in the production of ferrochrome (FC) alloy, which consists mainly of chromium and iron, contains 50–70% chromium by weight and various amounts of iron, carbon and other elements. It is mainly produced in submersible electric arc furnaces at temperatures from 1500 to 1700 °C. FC production involves the production of a large amount of slag, which is called ferrochrome slag (FCS). The production of each 1 ton of FC gives 1.1–1.6 tons of FCS [25]. The exact number of FCS depends mainly on the feed materials.

The Chelyabinsk Electrometallurgical Combine is one of the largest Ural ferroalloy manufacturing enterprises. The production of 1 ton of alloy is accompanied by the production of 1.1–2.5 tons of slags. The ferrochrome self-decomposing slag stored in dumps is a dispersed powder with a specific surface area of 200 m^3/kg and is classified as a substance of the 3rd class of toxicity [26]. The composition of The Chelyabinsk Electrometallurgical Combine (ChEMK) slag is regulated by TU 14-5-295-99.

4.2 Nickel Slag

The depletion of known ore deposits and the continuous growth of non-ferrous metal production have aroused scientific and industrial interest in man-made waste from steel mills, considering this waste as a factor in reducing the cost of finished metal products when they are involved in the production process. The involvement of low-grade scrap and waste in the production of nickel alloys has increased by more than 1.5 times. As a result, the volumes of man-made waste—slags, slurries, dust, etc.—have significantly increased and a significant part of which is still not used, is stored in dumps, storage facilities, decanting tanks.

In the solid state dump nickel slags are partially processed by purely mechanical methods in order to extract the metal phase—cold shots. Nickel, cobalt and iron contained in these slags in the form of chemical compounds (sulfides and oxides) are not extracted, since this requires complex technological operations associated with fine grinding and remelting of dump slags.

Nickel is widely used in the steel industry for the production of special steel products that are resistant to corrosion, high-temperature oxidation and strong chemicals. This use accounts for approximately 65% of the total nickel production. Nickel is harder than iron, it is also used in the production of non-ferrous alloys and specialized industries, such as the aerospace industry and the production of nuclear reactors, which account for approximately 20% of the total use of nickel. Approximately 9% of nickel is used for electrotyping and 6% for other purposes, including coins and various chemicals containing nickel (INSG, 2014).

Primary nickel is extracted from nickel ores. However, more and more often large volumes of secondary nickel scrap are used for the production of secondary nickel or an additive to newly extracted nickel. Nickel occurs in nature mainly in the form of oxides, sulfides and silicates. Nickel ores are currently mined in about 20 countries on all continents, and are smelted or refined in about 25 countries (INSG, 2014). Primary nickel is produced and used in the form of ferronickel, nickel oxides and other chemicals,

as well as in the form of more or less pure metallic nickel. In the pyrometallurgical production of nickel, nickel slag is formed at the stages of melting and conversion.

The chemical composition of nickel slag is very siliceous, it can contain up to 50–55% silica and has a high magnesium content. Compared to copper slag, it contains less iron, lime and alumina [27].

4.3 Converter Slag

The main converter slag is a waste of the metallurgical industry during the production of steel in the converter. Just like air-cooled blast furnace slag, converter slag is slowly cooled due to natural cooling and water irrigation at the cooling site. Then it is processed and used for the production of various slags from cast iron and steel (converters). Approximately 110 kg of slag is formed for each ton of converter steel [28, 29].

The converter steel slag usually acts as an inert ingredient in construction due to the relatively low reactivity. However, its mineral composition results in a high reactivity in a CO_2 rich environment. Studies have been carried out on the use of modified by an ambient CO_2 pretreatment converter steel slag as the supplementary cementitious material in the design of eco-friendly ultra-high performance concrete by using a particle packing model. The results show that the incorporation of carbonated steel slag improves the cement hydration, enhance the formation of ettringite and C–S–H, while densify the microstructure compared to non-carbonated slag in eco-friendly ultra-high performance concretes [30].

The composition of steelmaking slags varies from one mill to another due to the use of different raw materials from each other. The chemical composition of the converter slag used in the proposed binder compositions is as follows (Table 1).

Table 1 The chemical composition of the converter slag

The chemical composition	%
CaO	50–55
MgO	1
Mn	4–6
$\Sigma FeO + Fe_2O_3$	18–22
SiO_2	14–18
Al_2O_3	0,5–1,5
CaF_2	2–4

5 Practical Significance, Suggestions and Case Studies, the Results of Experiments

5.1 The Composition of Binder No. 1

The process of preparing this substance consists in jointly grinding the ingredients to a specific surface area of 2800–3000 cm/g.

During the research, three variants of the proposed composition of the binder were prepared (Table 2).

Table 2 The content of slags in variants of the composition of the binder, wt%

	Ferrochrome slag ChEMK	Nickel slag
Variant 1	30	70
Variant 2	45	55
Variant 3	60	40

The substance of these compositions was mixed with sand aggregate in a ratio of 1:3 and moistened to 6%. Samples were made from the mixtures-cylinders with a diameter of 60 mm, which were subsequently subjected to autoclave treatment according to the regime $3 + 8 + 3$ h at a pressure of 8 atm. At the same time, control samples were made on a traditional lime-silica binder and sand aggregate taken in a ratio of 1:3. Compressive strength (binder 300–400 kg/cm^2).

The compositions of the molding mixtures and the test results of autoclaved samples are shown in Table 3.

Table 3 The compositions of the molding mixtures and the test results of autoclaved samples

Content of components (%)					Green strength (kp/cm^2)	Bulk weight (kg/ m^3)	Strength of an earth brick (kp/cm^2)
Ferrochrome slag	Nickel ground slag	Lime	Silica flour	Unground silica			
7.5	17.5	–	–	75	5	1950	250
11.0	14.0	–	–	75	7	1900	320
15.0	10.0	–	–	75	8	1860	280
7.5	–	6.5	11.0	75	12	1850	240

As Table 3 shows, a brick on a binder made of a mixture of ferrochrome and nickel slags has a strength of 20% higher than a brick on a binder made of ferrochrome slag with the addition of lime and silica flour.

5.2 The Composition of the Binder No. 2

The process of preparing this binder consists in mixed grinding or mixing before tempering in the specified proportion with pre-ground ingredients. The binder is subjected to autoclave treatment under a pressure of 8 atm. according to the regime $3 + 6 + 3$ h. The obtained samples were tested for strength.

The test results and the binder compositions are shown in Table 4.

Table 4 The binder compositions and the test results

The composition of the binder		Strength of samples after heat treatment at 174.5 °C kg/cm^2
Known	Proposed	
Nickel slag 90% + lime 10%		220
	Nickel slag 90% + converter slag 10%	479
	Nickel slag 70% + converter slag 30%	455

The proposed binder has a higher binder activity in comparison with the known, including lime.

5.3 The Composition of the Binder No. 3

One of the appropriate areas of application of the proposed substance is the production of silicate bricks and products made of autoclaved concrete. The process of preparing the proposed substance consists of the mixed grinding of converter slag with a silica additive or in mixing pre-ground ingredients in the specified proportion, followed by heat treatment in an autoclave according to the mode $3 + 6 + 3$ at a temperature of 174.5 °C.

The proposed binder is prepared from converter slag, ground to a specific surface of 4000 cm^2/g and finely ground quartz sand.

The physical and mechanical parameters of the proposed binder are shown in Table 5.

Table 5 The physical and mechanical parameters of the proposed binder

Time, day	The strength of the proposed binder, kp/cm^2 = 1 bar	
	90% converter slag + 10% quartz sand	70% converter slag + 30% quartz sand
7	685	711
28	771	727

6 Conclusions

Three compositions of binders are proposed. The first composition based on decaying ferrochrome slag and finely ground nickel slag allows to increase the strength and reduce the cost of the binder in the manufacture of autoclave hardening products (silicate bricks) compared to traditional compositions. The second binder composition, including nickel slag and converter slag as a lime-containing component, was developed to increase the activity of the binder and showed an increase in the strength of the samples after heat treatment. The third composition of the binder, including converter slag and a silica additive, allows to increase the strength of autoclaved concrete products.

References

1. Yevtushenko EI, Ivanov AS (2008) Razrabotka sostava mass dlya keramicheskogo kirpicha s ispolzovaniem metallurgicheskih shlakov (Development of the composition of masses for ceramic bricks using metallurgical slags). Fundam Res 11:84–85
2. Zamora S, Salgado R, Melendez-Armenta R, Herrera-May A, Sandoval-Herazo L (2021) Sustainable development of concrete through aggregates and innovative materials: a review. Appl Sci 11:629
3. Kirthika SK, Singh SK, Chourasia A (2020) Alternative fine aggregates in production of sustainable concrete—a review. J Clean Prod 268:122089. https://doi.org/10.1016/j.jclepro.2020.122089
4. Guo H, Shi C, Guan X et al (2018) Durability of recycled aggregate concrete—a review. Cement Concr Compos 89:251–259
5. Kiyanets A (2018) Prospects for application of magnesium binder in construction. IOP Conf Ser: Mater Sci Eng 451:012074
6. Siddika A, Abdullah Al Mamun M, Alyousef R et al (2019) Properties and utilizations of waste tire rubber in concrete: a review. Constr Build Mater 224:711–731
7. Dash MK, Patro SK (2021) Performance assessment of ferrochrome slag as partial replacement of fine aggregate in concrete. Eur J Env Civil Eng 25(4):635–654
8. Wang GC (2016) Slag use in cement manufacture and cementitious applications. In: Wang GC (ed) The utilization of slag in civil infrastructure construction. Woodhead Publishing, pp 305–337
9. Andrade HD, de Carvalho JMF, Costa LCB, Elói FP DF, e Silva KD DC, Peixoto RAF (2021) Mechanical performance and resistance to carbonation of steel slag reinforced concrete. Constr Build Mater 298:123910
10. Wang F, Xu M, Wang R, Yang C, Chen A, Li S, Song J, Yang X (2019) Effect of high temperature process on microstructure and properties of industrial steel slag cement. Key Eng Mater 814 KEM:413–418
11. Gur'eva VA, Il'ina AA (2021) Investigation of the properties of ceramic bricks with nickel slags by the least squares method. Stroitel'nye Mater (Constr Mater) 4:4–8 (in Russian). https://doi.org/10.31659/0585-430X-2021-790-4-4-8
12. Platonov A, Grechanikov A, Kovchur A, Kovchur S, Manak P (2015) Production of the ceramic brick with use of industrial wastes. Vestnik Vitebsk State Technol Univ 1(28):128–134

13. Zubekhin AP, Dovzhenko IG (2011) Povyshenie kachestva keramicheskogo kirpicha s prime-neniem osnovnyh staleplavil'nyh shlakov (Improving the quality of ceramic bricks using the main steelmaking slag). Stroitel'nye Mater (Constr Mater) 4:57–59

14. Zyryanov FA, Khakimova ESh (2011) Issledovanie aktivnosti kompozicionnogo vyazhushchego na osnove portlandcementa i samoraspadayushchegosya ferrohromovogo shlaka (Investigation of the activity of a composite binder based on Portland cement and self-decaying ferrochrome slag). Concr Technol 1–2:12–13

15. Jena B, Patra RK, Mukharjee BB (2021) Influence of incorporation of jute fibre and fer-rochrome slag on properties of concrete. Aust J Civ Eng. https://doi.org/10.1080/14488353.2021.1899601

16. Priyatham BP RV S, Chaitanya DV SK, Prasanna Kumar G (2021) Effect of ferrochrome slag and fly ash on the mechanical properties of concrete. IOP Conf Ser: Mater Sci Eng 1025:012024

17. Lai MH, Zou J, Yao B, Ho JCM, Zhuang X, Wang Q (2021) Improving mechanical behav-ior and microstructure of concrete by using BOF steel slag aggregate. Constr Build Mater 277:122269

18. Acharya PK, Patro SK (2021) Flexural behavior of reinforced cement concrete beams made with air-cooled ferrochrome slag coarse aggregate. Indian Concr J 95(2):56–63

19. Fares AI, Sohel KMA, Al-Jabri K, Al-Mamun A (2021) Characteristics of ferrochrome slag aggregate and its uses as a green material in concrete—a review. Constr Build Mater 294

20. Volzhenskij AV et al (1969) Betony i izdeliya iz shlakovyh i zol'nyh materialov (Concrete and products from slag and ash materials). Stroyizdat, Moscow

21. Bugg YuM (1965) Tekhnologiya vyazhushchih veshchestv (Binder technology). Moscow

22. Jiang Y, Ling T-C, Shi C, Pan S-Y (2018) Characteristics of steel slags and their use in cement and concrete—a review. Resour Conserv Recycl 136:187–197

23. Martins ACP, Franco de Carvalho JM, Costa LCB, Andrade HD, de Melo T V, Ribeiro JCL, Pedroti LG, Peixoto RAF (2021) Steel slags in cement-based composites: an ultimate review on characterization, applications and performance. Constr Build Mater 291:123265

24. Palankar N, Ravi Shankar AU, Mithun BM (2016) Durability studies on eco-friendly concrete mixes incorporating steel slag as coarse aggregates. J Cleaner Production 129:437–448

25. Kumar PH, Srivastava A, Kumar V, Majhi MR, Singh VK (2014) Implementation of indus-trial waste ferrochrome slag in conventional and low cement castables: effect of microsilica addition. J Asian Ceram Soc 2(2):169–175. https://doi.org/10.1016/j.jascer.2014.03.004

26. Sokol EV, Nigmatulina EN, Nokhrin DY (2010) Dust emission of chromium from chromite ore processing residue disposal areas in the vicinity of krasnogorskii village in Chelyabinsk oblast. Contemp Probl Ecol 3(6):621–630

27. Veselovskiy AA, Roshchin VE, Lajhan SA (2017) Chemical heat treatment of dumped nickel slags to recover nickel and iron. Bull South Ural State Univ. Ser Metall 17(4):22–31(in Russ.). https://doi.org/10.14529/met170402

28. Ruzavin AA (2018) Evaluation of PAO "Mechel" Steelmaking Slags Suitability for the Con-crete Production. Bull South Ural State Univ. Ser Constr Eng Archit 18(4):58–64 (in Russ.). https://doi.org/10.14529/build180409

29. Kourounis S, Tsivilis S, Tsakiridis PE, Papadimitriou GD, Tsibouki Z (2007) Properties and hydration of blended cements with steelmaking slag. Cem Concr Res 37(6):815–822. https://doi.org/10.1016/j.cemconres.2007.03.008

30. Liu G, Schollbach K, Li P, Brouwers HJH (2021) Valorization of converter steel slag into eco-friendly ultra-high performance concrete by ambient CO_2 pre-treatment. Constr Build Mater 280:122580

Prospects for the Use of Fly Ash from a Thermal Power Plant of the Kaliningrad Region in the Construction Industry

A. Zakharov, A. Puzatova[✉], M. Dmitrieva, and V. Leitsin

Immanuel Kant Baltic Federal University, 14, Nevskogo St, Kaliningrad 236016, Russia
asharanova@kantiana.ru

Abstract. The paper presents the results of a study of the prospects for the use of fly ash generated during the combustion of Kuznetsk coal at a new thermal power plant in the Kaliningrad region, for use in the construction industry as an additional binder to reduce the consumption of cement, or as a microfiller for concrete and mortars. The data on the chemical, mineralogical and fractional composition of the ash under study are presented, the images of the microstructure of the ash obtained using a scanning electron microscope are presented, and the fineness of the residue on the control sieve is determined. The index of ash activity was calculated on samples aged 28 days, data on the compressive strength of heavy concrete samples prepared with the replacement of a part of the cement with the studied ash are given. In accordance with the regulatory documents, classes and types of ash are determined, the possibility of its use in the construction industry as an additional binder in order to reduce the consumption of cement, or as a micro-filler for concrete and mortars.

Keywords: Fly ash · Coal industry · Waste · Thermal power plants · Construction · Concrete additive · Ecology

1 Introduction

In 2017, the construction of a coal-fired thermal power plant, which was named Primorskaya TPP, began in the Svetlovsky urban district of the Kaliningrad region. The power plant includes three steam power plants with a unit capacity of generating equipment of 65 MW, with a total installed capacity of 195 MW. Kuznetsk coal is used as fuel [1]. In December 2020–February 2021, the last third power unit was commissioned, and the station started operating at full capacity [2]. In this regard, the question arises about the use of waste from the operation of the Primorskaya TPP, namely, about the use of ash formed by burning a large amount of coal necessary to maintain the plant's design capacity. The storage of this waste in ash dumps carries a great burden on the ecology in the area of the station and on the healthy life of people living in villages and cities near the station.

Pollution of the environment by ash dumps occurs in several ways. Among them: surface erosion—air currents carry the upper layers of ash around the ash dump, while ash can settle on soils that do not belong to the ash dump, and water sources, migration of harmful substances along the soil profile can lead to pollution of underground, ground and surface waters.

The ash of thermal power plants may contain toxic substances, heavy metals and rare elements in a dispersed state, such as gallium, vanadium, germanium [3].

The results of the literature review show that the practice of using the secondary combustion product from thermal power plants is widespread throughout the world. In Western countries, the volume of waste use can reach 90%, in Russia this amount is about 10%. This shows the lag of our environmental development in this aspect from foreign colleagues, and also indicates the relevance of this topic.

The effectiveness of the use of fly ash is assessed positively by most literature sources, however, the same sources indicate that this material has some features that need to be further investigated for a better understanding of its work.

Fly ash is understood to mean only a certain part of all ash and slag waste—products of combustion of the energy industry. Namely, that part of it that settles in cyclones and electrostatic precipitators, and later accumulates in silos. Such ash removal is called "dry".

The main regulatory document regulating the use of such ashes is GOST 25818-2017 [4], which replaced the GOST 25818-91 developed by the Scientific Research Institute of Reinforced Concrete of the USSR State Construction Committee. The main change in this document, relatively old, is the appearance of an additional division of ashes into classes and subcategories by dispersion and loss on ignition (LI), as well as a new system for assessing the quality level of fly ash, assessing the stability of quality indicators, which will allow creating a full-fledged product at TPPs—commercial fly ash with stable properties [4].

Today, in accordance with the accepted normative literature and a large number of studies on this topic, it is customary to divide fly ash into the following types, categories and classes.

By the type of fuel burned: anthracite coal, hard coal, lignite coal. The type of fuel, the method and mode of its combustion, significantly affect the future characteristics of ash.

According to the purpose of fly ash, in accordance with GOST 25818-2017, they are divided into four types. Depending on such indicators as the percentage of basic elements, loss on ignition, sieve residue and specific surface area, ash is assigned its type and denoted by a Roman numeral. For example, type IV ash can be used for concrete and reinforced concrete products and structures operating in especially harsh conditions (hydraulic structures, roads, airfields, etc.). Also, these indicators may deviate from those given in GOST, if special studies justify the use of the studied ash.

Depending on the loss on ignition, fly ash is assigned a category denoted by Russian letters: A—LI less than 2%, Б—LI less than 5%, B—LI less than 9% and Г—LI more than 9%. This division will further simplify the selection of fly ash for their use in the cement industry, where LI the ash should not exceed 5% [5].

According to the fineness indicator—the residue on the sieve 45 µm, the ashes are subdivided into classes denoted by Arabic numerals: 1—the residue on the sieve is less than 15%, 2—more than 15% and less than 40%, and 3—more than 40%. According to GOST 25818-2017, the ash dispersion is also characterized by the residue on sieve No. 008 (80 µm). For fly ash, dispersion is a rather important indicator, since the nature of the influence of fly ash on the concrete mixture largely depends on its value. Reducing the range of fluctuations in the fractional composition of fly ash using various methods of particle separation is one of the promising directions for expanding the range of use of this type of waste, as well as improving the controllability of the effect reproducible by fly ash on concrete mixtures [6–8].

Speaking about the classification of fly ash, it is necessary to consider its chemical, as well as phase composition, because the possible direction of using this resource largely depends on them.

In terms of chemical composition, high-calcium (basic) and siliceous (acidic) ashes are distinguished. In this case, the main ashes exhibit hydraulic activity, and acidic pozzolanic ones. This is due to the different content of calcium oxide CaO in them, the increased content of which (more than 10%) allows the main ashes to have binder properties. At the same time, those ashes that contain less than 10% CaO are classified as acidic ashes. Siliceous ashes are allowed to be used in the production of cement, however, due to the instability of their properties, they rarely meet the requirements of GOST 31108-2016 "Cements for general construction", and additional processing of ashes to bring them to the required characteristics leads to additional costs and reduces the overall economic efficiency the use of ash cement [5, 9, 10].

The main and widespread methods of disposal of fly ash both in Russia and abroad are its use as a filler or an active component in the construction industry in the manufacture of heavy concrete of high strength, cellular concrete, mortar, heat-resistant concrete, silicate and clay bricks [11–22]. The purpose of this work is to study the properties of fly ash of Primorskaya TPP, the possibility of its classification in accordance with the current regulatory documents and an assessment of its applicability in construction, namely in the preparation of heavy concrete.

2 Materials and Methods

To establish the possibility of using fly ash from Primorskaya TPP in the construction industry, tests were carried out required to determine the compliance of these ashes with GOST 25818-2017 "Fly ash from thermal power plants for building concrete", as well as for their classification and for making assumptions about possible areas of its application.

The following tests were carried out:

- Investigation of the chemical composition and determination of loss on ignition of fly ash of Primorskaya TPP. It was carried out using the method of energy dispersive X-ray dispersion (ED-XRF) on an apparatus for X-ray fluorescence spectroscopy Epsilon 3 (Netherlands);

- The determination of the mineralogical composition of fly ash of Primorskaya TPP was carried out using an X-ray powder method on an X'pert MPD X-ray diffractometer (Netherlands) with a PW 3020 goniometer and an anode of an X-ray source Cu (Kα) and a graphite monochromator. The recorded diffraction patterns and their data were processed in the HightScore Pro software. The mineral phases were identified using the PCPDFWIN software version 1.30;
- The analysis of the particle size of fly ash of Primorskaya TPP was carried out on a Mastersizer 3000 with the modification of Hydro EV (Great Britain) using a laser diffraction method with a measurement range from 0.01 to 2 mm;
- Electron microscopy of fly ash at Primorskaya TPP using a Quanta 250 FEG by FEI scanning electron microscope (SEM), optical microscopy using an Olympus SZX16 stereomicroscope;
- The residue on a sieve No. 008 was determined in accordance with the methodology of GOST 310.2;
- The ash activity index in accordance with GOST 25818-2017 was determined by comparing the compressive strength at the age of 28 days according to Appendix D to the same standard. Samples-prisms measuring $40 \times 40 \times 160$ mm, made according to GOST 30744 from mortar mixtures of the control cement-sand and basic cement-ash-sand compositions, after reaching the design age, were tested for strength in compression and tensile bending. The tests were carried out in accordance with GOST 30744, holding the samples under normal conditions in accordance with GOST 10180. The ToniNORM installation with the ToniPRAX modification was used as a testing machine, designed to measure the force arising from deformation of the samples when determining the mechanical characteristics of building materials;
- The strength of ash–cement concrete was determined in compliance with the requirements and instructions of GOST 10180-2012 by measuring the minimum forces destroying the manufactured concrete samples in the form of cubes with a size of $100 \times 100 \times 100$ mm under their statistical loading with a constant rate of increase in the load, and then calculating the stresses under these efforts. Based on the known composition of the heavy concrete of the pile with the design strength class B25, 3 compositions with different fly ash content of the total weight of the binder were designed (0, 15 and 30%, Table 1).

3   Results and Discussions

3.1   Chemical Analysis and Loss on Ignition

The results of chemical analysis and determination of loss on ignition are presented in Table 2.

One of the most important indicators in chemical analysis is the content of calcium oxide (CaO). Since its content in the studied ash exceeds 10%, it can be attributed to the basic type. The amount of magnesium oxide (MgO) is less than 5% and does not limit the use of this ash. The sulfur trioxide (SO_3) content also does not exceed the lowest value of 3%.

Table 1 Consumption of materials for 1 m³ of concrete mix with different content of fly ash

The amount of fly ash by weight of the binder (%)	Cement (kg)	Sand (kg)	Coarse aggregate (kg)	Superplasticizer Stachement 2598 (kg)	Fly ash (kg)	Water (kg)
0	410	780	970	2.26	–	165
15	348.5	780	970	2.26	61.5	165
30	287	780	970	2.26	123	165

Table 2 Chemical composition and loss on ignition of fly ash of Primorskaya TPP

Element	Content (%)	Qualitative indicators for the 4th type of fly ash according to GOST 25818-2017	
		For acidic ash	For basic ash
Na_2O	–	3	<1.5
MgO	1.235	5	5
Al_2O_3	14.869	–	–
SiO_2	42.1	–	–
P_2O_3	0.79	<100 mg/kg*	<100 mg/kg*
SO_3	1.261	3	<3
K_2O	0.98	–	–
CaO	16.398	10	>10
CaO (free)	–	–	<2
TiO_2	1.199	–	–
Fe_2O_3	8.091	–	–
LI	12.54	A < 10; H < 5; L < 2	<3

* in terms of P_2O_5; A - anthracite coal; H - hard coal; L- lignite coal

3.2 Mineralogical Composition, Electron and Optical Microscopy

The results of the study of the mineralogical composition, electron and optical microscopy are presented in Figs. 1, 2 and 3.

As can be seen from the results of X-ray analysis, the crystalline phase of the Kaliningrad fly ash is mainly represented by such elements as quartz, magnetite and mullite. To a lesser extent, it contains hematite, calcite and limestone. In Fig. 2, microspheres are clearly visible, which make up the amorphous phase of fly ash and have a rounded shape.

Using an optical microscope, an image was obtained of large fractions of fly ash (>80 µm), which remained on the sieve when determining the residue on sieve No. 008 (Fig. 3). The picture shows a large amount of unburned fuel, which causes large loss
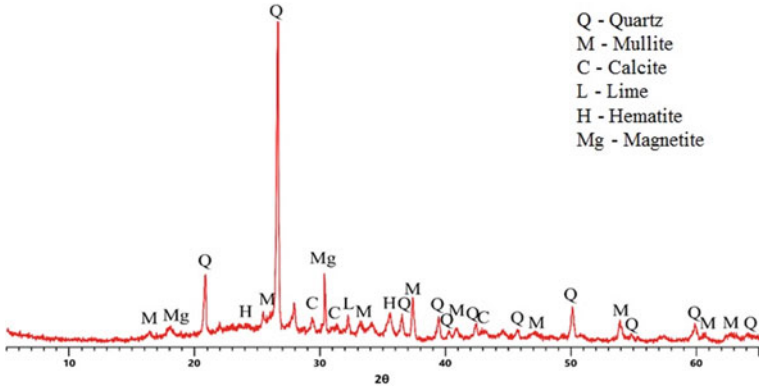
Fig. 1 The diffractogram of fly ash of Primorskaya TPP
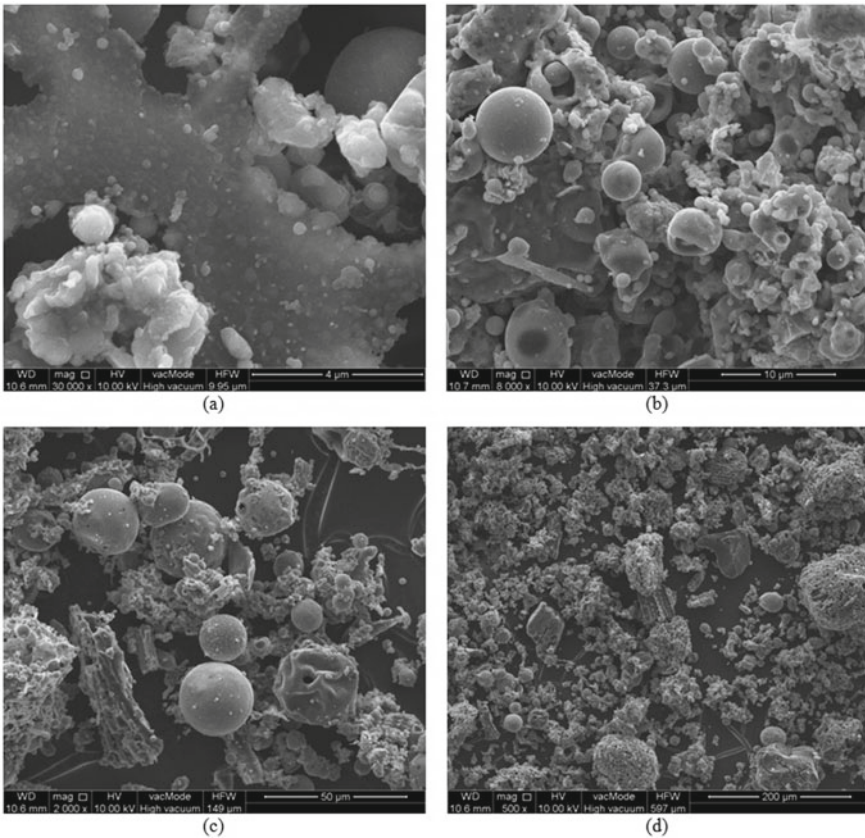
Fig. 2 Images of fly ash at Primorskaya TPP obtained with an electron microscope. Magnification ×30,000 (**a**), ×8000 (**b**), ×2000 (**c**), ×500 (**d**)
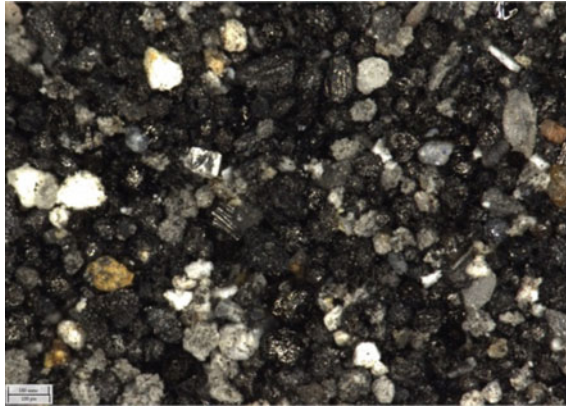
Fig. 3 Image of the residue on sieve No. 008 of fly ash of Primorskaya TPP. Magnification ×5

on ignition and a dark, ashy shade of fly ash, which is especially clearly visible during sieving, since fuel residues, having a larger size than crystals and microspheres, do not pass through the sieve when determining sieve residue No. 008.

3.3 Grain Size and Fractional Composition

The results of studying the grain size and fractional composition are shown in Figs. 4 and 5.
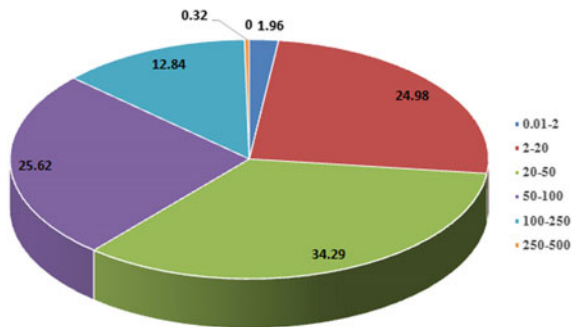
Fig. 4 Diagram of the distribution of the fractional composition of fly ash at Primorskaya TPP (particle size in microns)

Grain size studies have shown that about 85% of the fly ash mass has a size of less than 100 µm, which is a fairly good result and which subsequently affects the results of its sifting through a sieve.

3.4 Residue on Sieve No. 008

The results of determining the residue on sieve No. 008 during sieving are presented in Table3.
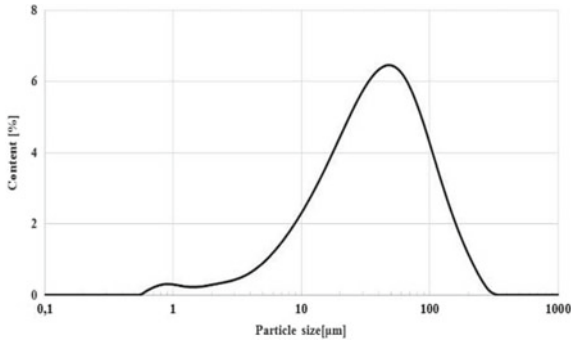
Fig. 5 Particle size distribution graph

Table 3 Sieve residue No. 008

Sifting number	Result (g)	The ratio to the initial mass of the sample (%)	Standard GOST 25818-2017 for the ash of the 4th type (%)
1	6.6	13.2	15
2	7	14	
Average	6.8	13.6	

After the first sieving, the total mass of ash remaining on the sieve was 6.6 g. During the second test, a residue of 7 g was obtained.

According to this indicator, the fly ash of Primorskaya TPP meets the highest requirements presented in GOST 25818-2017 for ashes of the 4th type, that is, suitable for use in concrete and reinforced concrete products and structures operating in especially harsh conditions. Also, relying on the test results and based on the provisions of Industry road methodology document 218.2.031-2013 [23], it can be attributed to highly dispersed ash.

3.5 Fly Ash Activity Index

The results of determining the ash activity index are presented in Table 4.

In accordance with paragraph 4.4.1 of GOST 25818-2017, the ash activity index 28 days after the manufacture of samples must be at least 75%. In this experiment, the activity index at 28 days of age was 61.9%. Thus, the fly ash of Primorskaya TPP does not meet this requirement.

3.6 Compressive Strength Properties

The results of strength tests are presented in Table 5 and in the graph in Fig. 6.

As can be seen from the results of the study, the strength of heavy concrete with the addition of fly ash from Primorskaya TPP instead of a part of the binder has a downward

Table 4 Strength of samples when determining the activity index

Sample marking *	Breaking load F (kN)	Working section area A (mm^2)	Strength at the age of 28 days R_{28} (MPa)
1C	16.6	2500	6.64
2C	19.6		7.84
3C	19		7.6
4C	16.9		6.76
5C	16		6.4
6C	18.9		7.56
1B	12.4		4.96
2B	11.4		4.56
3B	10		4
4B	11		4.4
5B	10		4
6B	11.4		4.56
Fly ash activity index (%)			61.9

*1C-6C—samples of the control composition (without fly ash)
1B-6B—samples of basic composition (with fly ash)

Table 5 Strength of samples of concrete cubes 100 × 100 × 100 mm

Sample marking**	Average density (kg/m^3)	Strength at the age of 3 days R_3 (MPa)	Strength at the age of 7 days R_7 (MPa)	Strength at the age of 28 days R_{28} (MPa)
1.0	2395.1	52.93	61.19	68.46
2.0		54.92	59.72	72.27
3.0		54.64	58.6	67.66
4.0		52.38	56.1	71.76
1.15	2367	52.59	57.4	68.73
2.15		51.89	58.33	70.12
3.15		51.84	55.79	68.58
4.15		53.43	57.4	65.51
1.30	2345	42.93	49.33	60.84
2.30		42.33	52.46	58.13
3.30		40.73	51.51	61.9
4.30		43.02	50.88	64.63

**1.0–4.0—samples without fly ash
1.15–4.15—samples with the addition of 15% fly ash
1.30–4.30—samples with the addition of 30% fly ash
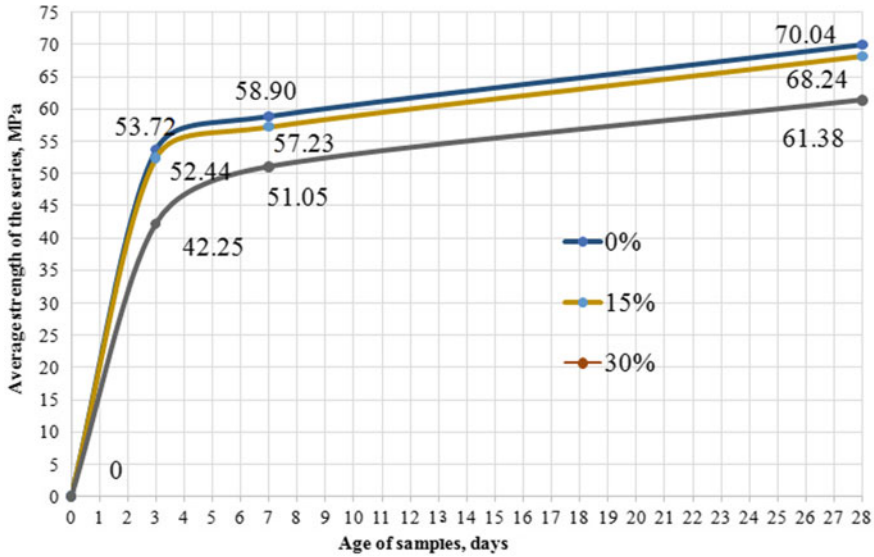
Fig. 6 The graph of the increase in the strength of concrete samples in a series depending on the age of the sample and the content of fly ash in it by the mass of the binder

trend. At the same time, the content of fly ash in the amount of 15%, lowering the strength of concrete by about 3%, does not affect this indicator as much as its content in a 30% dosage, where the strength value drops to 87% of the strength of the control samples.

4 Conclusion

In accordance with GOST 25818-2017, fly ash of the Primorskaya TPP of the Kaliningrad Region, by the type of fuel burned, is classified as coal (CO); by chemical composition— to the main; category by the number of losses on ignition—Г; in terms of dispersion—to highly dispersed ash.

Determination of the ash activity index showed that according to this indicator, fly ash of Primorskaya TPP does not meet the requirements of GOST 25818-2017 without additional processing. There is also a high rate of loss on ignition; the ash contains many particles of unburned fuel. To comply with GOST in this indicator for the main ash, it is recommended to increase the level of fuel combustion in order to obtain a reduced indicator for losses on ignition.

Fly ash of the Primorskaya termal power plant is promising for use in the construction industry in the Kaliningrad region. Further research is needed to accurately determine the conditions for the use of ash in the construction industry.

References

1. Primorskaya TES (Primorskaya TPP). http://irao-engineering.ru/ru/projects/primorskaya-tes/. Accessed 30 May 2021
2. Tretiy energoblok Primorskoy TES vveden v ekspluatatsiyu v dekabre 2020 (The third power unit of Primorskaya TPP was put into operation in December 2020). https://energybase.ru/news/industry/tretij-energoblok-primorskoj-tes-vveden-v-ekspluataciu-v-dekabre-2020-2021-02-15. Accessed 30 May 2021
3. Cherntsova AA, Olesik SM (2013) Otsenka zoloshlakovykh otkhodov kak istochnik zagryazneniya okruzhayushchey sredy i kak istochnik vtorichnogo syr'ya (Evaluation of ash and slag waste as a source of environmental pollution and as a source of secondary raw materials). Gornyy informatsionno-tekhnicheskiy byulleten', pp 230–243
4. GOST 25818-2017 (2017) Fly ash from thermal power plants for concrete. Technical conditions. Standartinform, Moscow
5. GOST 31108-2016 (2019) General construction cements. Technical conditions. Standartinform, Moscow
6. Kushnerova OA, Akimochkina GV, YeV F et al (2018) Odnostadiynoye aerodinamicheskoye razdeleniye zoly-unosa ot pylevidnogo szhiganiya uglya Ekibastuzskogo basseyna (One-stage aerodynamic separation of fly ash from pulverized coal combustion in the Ekibastuz basin). Khimiya tverdogo topliva 3:47–60
7. Petrik I, Khristich Y, Gubar VN et al (2018) Vliyaniye elektrostaticheskoy sepa-ratsii na dispersnost' zol-unosa TES (Influence of electrostatic separation on the dispersion of fly ash at TPP). Vestnik Donbasskoy natsional'noy akademii stroitel'stva i arkhitektury 4–2:203–208
8. Omirtayev BO (2020) Analiticheskiy obzor primeneniye zoly TETS v proizvodstve betona (Analytical review of the use of ash from Heating Electric Plants in the production of concrete). Molodoy uchenyy 3:25–28
9. Vatin NI, Petrosov DV, Kalachev AI et al (2011) Primeneniye zol i zoloshlakovykh otkhodov v stroitel'stve (The use of ash and ash-slag waste in construction). Inzhenerno-stroitel'nyy zhurnal 4:16–21
10. Mineral'nyye komponenty dlya proizvodstva tsementa (Mineral components for the production of cement). https://lafargeholcimrus.ru/advises/article/mineralnye-komponenty-dlya-proizvodstva-tsementa/. Accessed 30 May 2021
11. Gergichny Z (2014) Primeneniye zoly-unosa v sostave tsementa i betona (Application of fly ash in cement and concrete). In: Zoloshlaki TES: udaleniye, transport, pererabotka, skladirovaniye: Abstarct of V int. conf., Moscow, 24–25 Apr 2014
12. Zharov MA (2012) Perspektivy primeneniya tekhnogen-nykh otkhodov v sostavakh betonnykh smesey (Prospects for the use of man-made waste in the composition of concrete mixtures). In: Aktual'nyye problemy sovremennoy nauki: Abstarct of all-Russian scientific and practical conference, Stavropol university, Kislovodsk, 02–06 May 2012
13. Shalayev AG, Shalayeva MA, Antonenko NA (2020) Ispol'zovaniye zoly-unosa dlya resheniya problem sukhikh stroitel'nykh smesey (Using fly ash to solve problems with dry mixes). In: Novyye tekhnologii v uchebnom protsesse i stroitel'nom proizvodstve: Abstract of XVIII international scientific and technical conference, Ryazan Institute of Federal State Budgetary Education of Higher Education "Moscow Polytechnic University", Ryazan, 15–17 Apr 2020
14. Mangushev IF, Karamyshev IM, Golubeva YeA (2020) Effektivnost' ispol'zovaniya dobavok v betony na osnove otkhodov omskikh TETS (Efficiency of using additives in concrete based on waste of Omsk thermal power plants). In: Obrazovaniye, transport, innovatsii, stroitel'stvo: Abst. of III nat. scient. and prac. conf., SibADI, Omsk, 23–24 Apr 2020

15. Kharayev GI, Khanturgayeva GI (2020) Tekhnologiya utilizatsii letuchey zoly energetich-eskikh ugley (Coal Fly Ash Utilization Technology). In: Obrazovaniye i nauka. Tekhnich-eskiye nauki: Abstract of national scientific and practical conference, East Siberian State University of Technology and Management, Ulan-Ude, 13–17 Apr 2020

16. Lebedev MS, Shiman AA, Korreva Avedzho DV et al (2014) Nekotoryye voprosy primeneniya zol-unosa teplovykh elektrostantsiy v dorozhnykh asfal'-tobetonakh (Some issues of the use of fly ash from thermal power plants in road asphalt concrete). In: Naukoyemkiye tekhnologii i innovatsii. Abstract of Jubilee International Scientific and Practical Conference dedicated to the 60th anniversary of BSTU named after V.G. Shukhov, Belgorod State Technological University named after V.G. Shukhov, Belgorod, 09–10 Oct 2014

17. Chen Y, Guan L, Zhu S et al (2021) Foamed concrete containing fly ash: properties and application to backfilling. J Con Build Mat 273:121685. https://doi.org/10.1016/j.conbuildmat.2020.121685

18. Gao H, Wang W, Liao H et al (2021) Characterization of light foamed concrete containing fly ash and desulfurization gypsum for wall insulation prepared with vacuum foaming process. J Cons Build Mat 281:122411. https://doi.org/10.1016/j.conbuildmat.2021.122411

19. She W, Du Y, Zhao G et al (2018) Influence of coarse fly ash on the performance of foam concrete and its application in high-speed railway roadbeds. J Con Build Mat 170:153–166. https://doi.org/10.1016/j.conbuildmat.2018.02.207

20. Gökçe HS, Hatungimana D, Ramyar K et al (2019) Effect of fly ash and silica fume on hardened properties of foam concrete. J Con Build Mat 194:1–11. https://doi.org/10.1016/j.conbuildmat.2018.11.036

21. Chindaprasirt P, Rattanasak U (2011) Shrinkage behavior of structural foam lightweight concrete containing glycol compounds and fly ash. J Mat Des 32(2):723–727. https://doi.org/10.1016/j.matdes.2010.07.036

22. Amran M, Debbarma S, Ozbakkaloglu T (2021) Fly ash-based eco-friendly geopolymer concrete: a critical review of the long-term durability properties. J Con Build Mat 270:121857. https://doi.org/10.1016/j.conbuildmat.2020.121857

23. ODM 218.2.031-2013 (2014) Metodicheskiye rekomenda-tsii po primeneniyu zoly-unosa i zoloshlakovykh smesey ot szhiganiya uglya na teplovykh elektrostantsiyakh v dorozh-nom stroitel'stve (Methodical recommendations for the use of fly ash and ash-and-slag mixtures from coal combustion at thermal power plants in road construction). Federal Road Agency, Moscow

Influence of the Quantity and Time of Hardening Ash of Thermal Power Plants Formation of the Structure and Properties of Cement Stone

A. M. Makhmudov[1]([✉]), B. Ya. Trofimov[1], K. V. Shuldyakov[1], and B. R. Bokiev[2]

[1] South Ural State University, 76, Lenin Avenue, Chelyabinsk 454080, Russia

[2] Tajik Technical University Named After M. Osimi, 10, Academics Radzhabov Avenue, Dushanbe 734042, Tajikistan

Abstract. Currently, the durability of concrete is normalized by indirect indicators—the quality of the materials used, reinforcement and additives, the properties of the concrete mixture and its degree of compaction when molding reinforced concrete structures, the duration and parameters of concrete care. Regulatory documents, depending on the operating environment, regulate the maximum allowable value of W/C, the minimum allowable consumption of cement and the class of concrete for compressive strength. The main structural element of concrete is cement stone, the products of cement hydration provide its adhesive and cohesive properties and form a concrete conglomerate. Low basic calcium hydrosilicates form a cement gel—the densest and most durable component of cement stone. Modification of cement stone with water-reducing additives and microsilicon contributes to the formation of hydrosilicate phases in the form of an uncrystallized gel, a weakly crystallized gel-like C-S-H (I) phase with a ratio of C/S = 1,1–1,3, and individual inclusions of calcium hydroxide are observed.

Keywords: TPP ash · Cement stone · Pozzolan · Compressive strength · Structure of hydrated phases

1 Introduction

Concrete is the main building material that will be in demand and in the future will be produced using mainly CEM I and CEM II. Each ton of produced Portland cement leads to the emission of an average amount of CO_2 into the atmosphere—about 6% of all anthropogenic carbon emissions, which is harmful to the environment [1–4].

The basis of modern concrete technology is a cement matrix, which is characterized by low defectiveness and stability of the structure. The structure of the cementing matrix of concrete is the main determining factor of its basic physical and mechanical properties.

In recent years, one of the main challenges in the construction industry has been the demand for cement materials that can reduce carbon emissions, and most research has focused on reducing the use of cement or using cement substitutes.

Consequently, concrete should be made with as little cement as possible and practical. This can be achieved by replacing some of the cement with pozzolanic materials (industrial by-products) from thermal power plants and the metallurgical industry, especially fly ash and blast furnace slag.

The binding of $Ca(OH)_2$ as a product of hydrolysis of clinker minerals by active additives increases the degree of cement hydration, which, provided that an increase in water demand and, accordingly, porosity of concrete is prevented, leads to an increase in its strength. Active mineral additives, interacting with calcium hydroxide $Ca(OH)_2$, form low-basic hydrosilicates.

Despite the growing importance of renewable energy sources (geothermal, wind and solar energy), the share of coal in the global energy balance continues to grow. Therefore, the world production of coal ash is increasing, and there is an urgent need for its processing and disposal [5, 6].

In the processes of layer or flare burning of coal at thermal power plants (TPP), gaseous products and solid ash and slag waste—ash and slag-are formed. These are products of high temperature (1200–1700 °C) processing of the mineral part of the fuel [7–9].

Ash consists mainly of SiO_2, but may also contain significant amounts of Al_2O_3. The amount of CaO is limited, but varies greatly depending on the origin of the fly ash [10].

When ash is used in combination with Portland cement, the calcium hydroxide released during the hydrolysis of the calcium silicates of Portland cement reacts with the aluminosilicate glass present in the ash to form cementitious compounds with cohesive and adhesive properties. The products of these reactions, called pozzolanic products, are time dependent but generally have the same type and characteristics as the cement hydration products. However, pozzolanic reactions are much slower than cement hydration reactions [11–14].

Pozzolans reduce the amount of calcium hydroxide produced during cement hydration by forming a secondary gel of calcium silicate hydrate (CSH) with a lower Ca/Si ratio [15, 16].

Ash can vary greatly in its physical and chemical characteristics, so quality control is especially important. It is important to check the carbon content and the degree of crystallinity [17].

Some of the advantages of CEM I concrete with ash include improved workability, reduced permeability, increased ultimate strength, better surface finish, and reduced heat of hydration.

The ash in general, very heterogeneous, consists of mixtures of vitreous particles with different identifiable crystalline phases such as quartz, mullite and various iron oxides. However, the slow development of strength at the initial stage limits its further use in the field of civil engineering as a good environmentally friendly material.

In his research, Mehta [18] tested 11 types of fly ash from different sources and found that the calcium content and particle size distribution are decisive in determining the rate of strength development.

An increase in the degree of ash grinding increases its pozolanic activity and density. This has a positive effect on the strength and durability of concrete, reliably ash [19].

Replacing the cement with the original ash reduces the pore size of the cement paste, and the inclusion of crushed ash leads to a further decrease in the pores of the cement stone [20]. Studies show that the smaller the ash particle size, the higher its activity and hydration rate.

2 Materials and Methods of Research

At the Department of "Building Materials and Products" of SUSU, research was conducted to study the influence of the amount of ash on the formation of the structure and properties of cement stone.

This study used:

- Portland cement 52.5 N produced by Dyckerhoff Korkino cement with a true density of 3.1 g/cm^3, ND = 28.2%.
- ash of Troitsk SDPP. The chemical composition is shown in Table 1.

Table 1 Chemical composition of Portland cement and ash

Materials	Content of oxides, % by weight							
	SiO_2	Al_2O_3	Fe_2O	CaO	MgO	Na_2O	SO_3	loi
CEM I	19.9	5.1	4.5	63.2	1.6	0.5	3.0	0.9
Ash	62.53	28.75	4.1	7.64	2.61	2.35	0.2	0.61

Portland cement has the following mineralogical composition:
C_3S—64.2%; C_2S—10.0%; C_3A—6.3%; C_4AF—14.1%.

The fineness of grinding, normal density and setting time of cement and ash were determined according to GOST 310. 2,3-81.

To replace part of the Portland cement, 10, 20, 30 and 40% of the initial and crushed ash from the binder weight were used. The normal density (ND) of the cement paste is 28.2% with an increase in the amount of initial ash to 30%, ND decreases to 27.4%. In addition, cement paste ash has a normal density from 29.5 to 31.0%, which increases with increasing dispersion of crushed ash in mixtures.

The ball mill was used to reduce the size of the ash particles by impact and abrasion using steel balls.

From a mixture of CEM I and ash, a dough of normal density was prepared and cubes were molded with an edge of 20 mm. The samples were kept under normal conditions of hardening at a temperature of $20 \pm 20\,°C$ and a humidity of more than 95%. Compressive strength tests were performed according to GOST 10180-2012 at the age of 28, 42, 56 and 90 days.

To prevent the process of hydration and carbonation of the cement stone, the samples were pretreated with ethyl alcohol, further dried at 60 °C for 24 h, and ground in a mortar to pass through a sieve of 80 μm [21].

The content of Ca(OH)$_2$ in hydrated cement pastes was determined by thermogravimetric analysis (TGA).

X-ray phase analysis was used to obtain the mineral composition of cement samples with additives at the age of 90 days.

3 Results and Discussion

As a rule, ash reduces the strength at an early age, but the value of Rcs increases at a later age.

According to the data obtained (Table 2), the strength of the cement stone mainly depends on the curing time, the amount and dispersion of the ash. The results of the study show that at 28 and 42 days of normal hardening, the strength of cement stone with ash is lower than that of ash-free stone. At 56 days, the strength of the cement stone with the replacement of 10 and 20% with ash is higher than without it, and with 30–40% replacement it approaches the strength of the control samples. The strength of cement stone without ash at the age of 90 days of normal hardening was 97.6 MPa, and the maximum value up to 100 MPa was found at 20%. At 30% replacement, 98.5 MPa was obtained, which is lower than the maximum and higher than the ash-free one. However, at 40% replacement, a minimum strength value of 84.3 MPa was obtained.

Table 2 Strength characteristics of cement stone

Cement (%)	Ash (%)	Ground ash (%)	ND (%)	Compressive strength of cement stone (MPa)			
				28 day	42 day	56 day	90 day
100	–	–	28.2	92.15	94.18	94.88	97.63
90	10	–	28.2	89.27	92.65	95.78	98.72
80	20	–	28.0	80.97	90.88	94.42	100
70	30	–	27.5	77.64	89.0	91.8	98.42
60	40	–	28.5	70.22	73.95	76.0	84.35
90	–	10	29.5	91.81	94.53	99.13	100.33
80	–	20	30.0	91.5	94.45	100.77	101.2
70	–	30	30.5	90.77	91.78	98.82	102.42
60	–	40	31.0	83.77	85.0	86.28	96.83

The strength of cement stone with crushed ash exceeds the strength of ashless cement stone at the age of 42 days with 20% replacement, and at 56 days with 30%. In 90 days, when replacing cement with 40% crushed ash, the strength value is almost equal to the strength of the control one.

The significant improvement in the compressive strength of cement stone with ash is explained by the high pozzolanic activity of the ash and its ability to function as a microfiller.

The coefficient of variation in the strength of the samples is less than 5%.

The development of strength characteristics of samples of Portland cement cubes with different ash dosages is shown in Fig. 1.
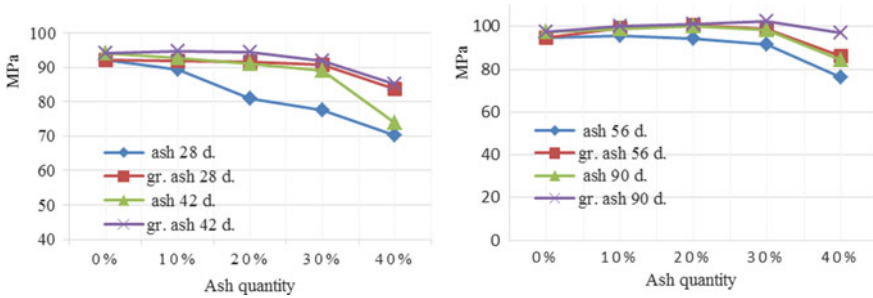
Fig. 1 Development of the compressive strength of cement stone without and with the replacement of part of the cement with ash, at the age of 28, 42, 56 and 90 days of normal hardening

The results show that replacing the cement with ash reduced the strength at an earlier age compared to the control samples. However, at a later age, they either gained high strength or very nearly reached the strength of the control samples of cement stone. Samples with 20 and 30% ash showed a higher increase in strength than those with 40% ash. The strength of the cement stone with crushed ash developed faster than that of the control stone.

The results show that replacing the cement with ash reduced the strength at an earlier age compared to the control samples. However, at a later age, they either gained high strength or very nearly reached the strength of the control samples of cement stone. Samples with 20 and 30% ash showed a higher increase in strength than those with 40% ash. The strength of the cement stone with crushed ash developed faster than that of the control stone.

Continuous hydration of the cement results in a constant increase in the $Ca(OH)_2$ content, but the pozzolanic reaction of the ash absorbs some $Ca(OH)_2$. According to the results obtained according to the DTA data (Fig. 2), replacing part of the cement with ash at the age of 90 days of normal hardening reduces the amount of portlandite. When replacing 30% with initial ash, the content of $Ca(OH)_2$ in the cement stone decreases to 7.03%, compared to ashless 9.95%, while replacing 40% with crushed ash reduces the amount of portlandite to 4.07%. This indicates that the pozzolanic activity of the crushed ash is higher than that of the original ash and that the crushed ash has a greater effect on cement hydration. Also, on the derivatograms at a temperature of 830–86 °C, an exothermic effect is observed, indicating the formation of a weakly crystallized phase C-S-H (I). The endothermic peak at about 920–950 °C in the DTA curves is caused by the decomposition of a small amount of $CaCO_3$.

C-S-H gel is not only the most common hydration product, but is also responsible for many important properties of the cement paste and therefore for the material in general. This is the densest phase, which bonds the hydration products and aggregate grains together, giving the material strength (Fig. 3).
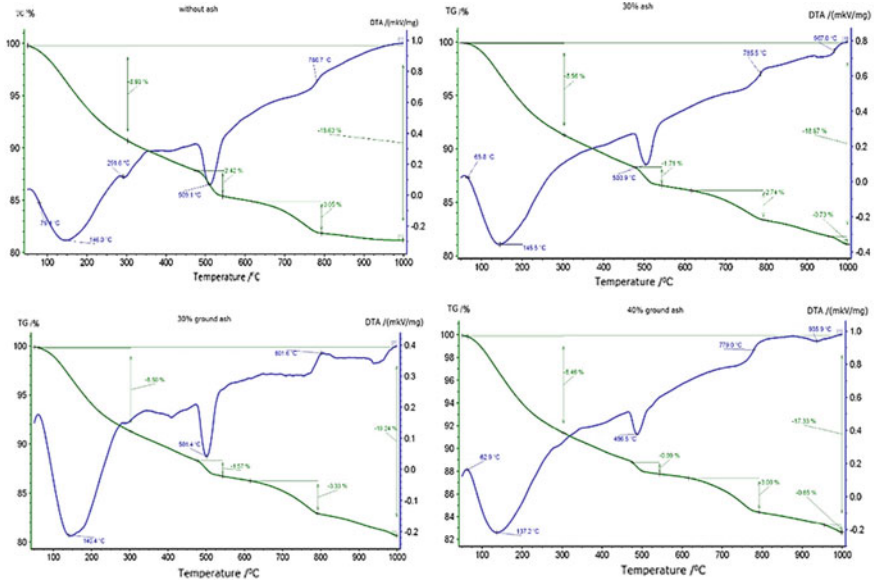
Fig. 2 Derivatography of cement stone without ash, 30% ash, 30 and 40% ground ash
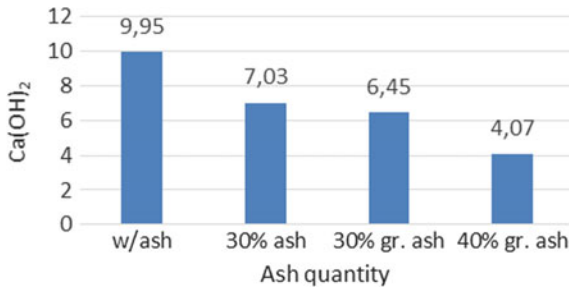
Fig. 3 Effect of ash quantity and dispersion on the Ca(OH)$_2$ content in cement stone
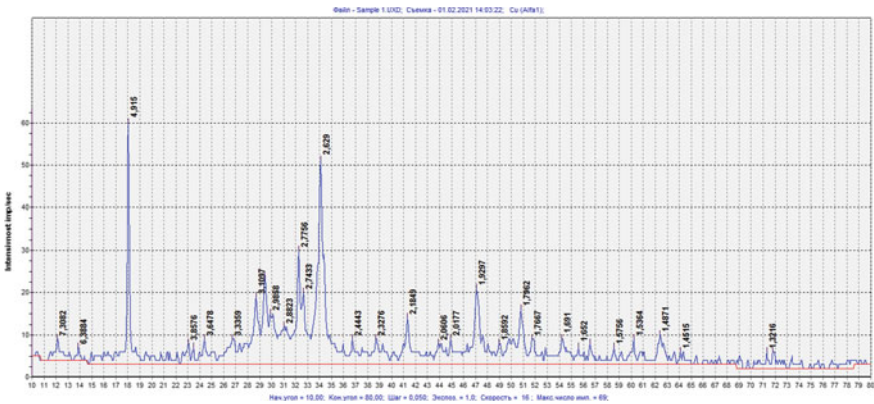
Fig. 4 X-ray of a cement stone without ash
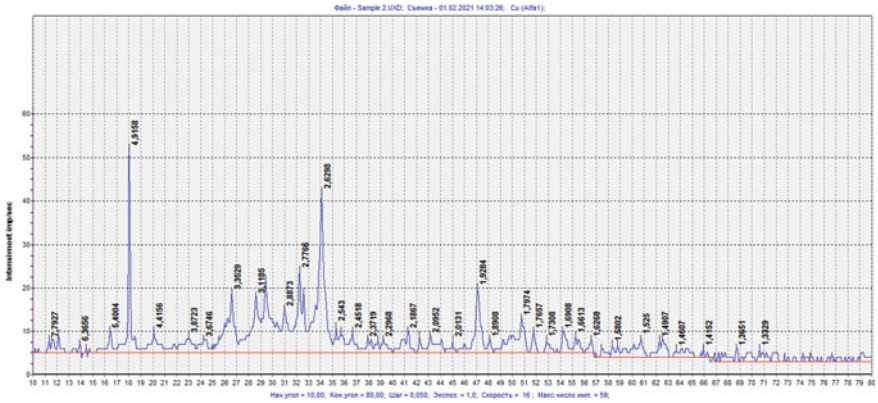
Fig. 5 X-ray of a cement stone with replacement of 30% ash
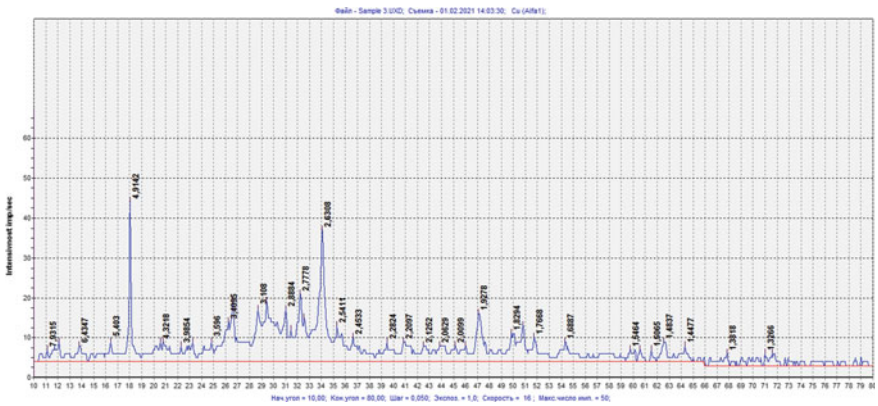
Fig. 6 X-ray of cement stone with replacement of 30% crushed ash

The development of the increase in the strength of cement stone is associated with the phase composition of hydrate neoplasms of cement.

On the X-ray image, the main part of the interplanar distances of the hydrate phases of the cement stone are: C–S–H(I) 12.5; 3.032; 2.09; 1.52 nm, C–S–H(II) 9.8; 4.92; 3.032; 2.883; 2.09; 1.728 nm, $Ca(OH)_2$ 4.92; 3.115; 2.63; 1.926; 1.796; 1.688; 1.485 nm, $C_5S_6H_5$ 2.747; 2.544; 2.186; 1.926; 1.76; 1.523; 1.36 nm.

X-ray diffraction patterns of samples of cement stone and with the addition of ash at the age of 90 days are shown in Figs. 4, 5 and 6.

$Ca(OH)_2$ intensity peaks appear at 2θ 18.07°, 28.75°, 34.13°, 47.12° and 50.85°. Replacing the cement with crushed ash more effectively reduces the $Ca(OH)_2$ intensity than the original ash. It is well known that the decrease in $Ca(OH)_2$ depends on the degree of the pozzolanic reaction. The factors influencing the pozzolanic reactivity are the dispersion and the content of the glassy phase in the ash. The finer ash had a larger surface area and increased pozzolanic reactivity than the original ash.

4   Conclusions

Based on the obtained experimental results, the following conclusions can be drawn:

Replacing part of the cement with ash reduces the compressive strength of the cement stone at an early age. At 30% replacement of cement with ash at the age of 90 days of normal hardening, the strength of the cement stone increases without ash, and at 30% replacement of cement with crushed ash, the strength is higher than that of the ash-free sample at the age of 56 days.

Replacing part of the cement with ash reduces the amount of $Ca(OH)_2$ due to the pozzolan reaction and improves the proportions of calcium hydrosilicate (C-S-H), which increases the strength, density, water resistance and overall durability of cement stone and concrete.

Due to the optimizing role of the crushed ash, the cement hydration process is accelerated, and the quantity, homogeneity and density of hydration products are improved.

Based on the results obtained, the dispersity and the CEM I ash substitution coefficient have a significant effect on the structure and properties of the cement stone.

References

1. Benhelal E, Rafiei A, Shamsaei E (2012) Green cement production: potentials and achievements. Int J Chem Eng 3:407–409
2. IEA, Technology Roadmap—cement. 2018. https://www.iea.org/reports/technology-roadmap-low-carbon-transition-in-the-cement-industry
3. Hsu S, Chi M, Huang R (2018) Effect of fineness and replacement ratio of ground fly ash on properties of blended cement mortar. Constr Build Mater 10:250–258
4. Mingaleeva GR, Dmitrienko IV, Zdorov AI, Nikolaev AN, JeV S, Afanas'eva OV (2013) Tehnologija poluchenija bikarbonata ammonija pri utilizacii vybrosov uglekislogo gaza cementnoj promyshlennosti Rossii i Ukrainy (Technology for producing ammonium bicarbonate in the utilization of carbon dioxide emissions from the cement industry in Russia and Ukraine). Mod Prob Sci Edu 5:1–8
5. Franus W, Wiatros-Motyka MM, Wdowin M (2015) Coal fly ash as a resource for rare earth elements. Environ Sci Pollut Res 22:9464–9474. https://doi.org/10.1007/s11356-015-4111-9
6. Hudjakova LI, Zaluckij AV, Paleev PL (2019) Ispol'zovanie zoloshlakovyh othodov teplovyh jelektrostancij XXI vek. (Use of ash and slag waste from thermal power plants XXI Century). Technosphere safet 4:290–306
7. Panibratov JuP, Staroverov VD (2011) K voprosu primenenija zol TJeS v betonah (On the issue of using ashes from thermal power plants in concrete). Concr Technol 2:43–47
8. Adeeva LN, Borbat VF (2009) Zola tjec perspektivnoe syr'e dlja promyshlennosti (Ash CHP is a promising raw material for industry). Bull Omsk Univ 2:141–145
9. Fomenko NA (2019) Primenenie okislennyh buryh uglej dlja povyshenija jekologicheskoj bezopasnosti utilizacii zoloshlakovyh othodov (The use of oxidized brown coal to improve the environmental safety of ash and slag waste disposal). Dissertation, National research technological university "MISiS"
10. Navdeep S, Shehnazdeep, Anjani B (2020) Reviewing the role of coal bottom ash as an alternative of cement. Constr Build Mater 233:117276
11. Joshi RC (2010) Fly ash—production, variability and possible complete utilization. Indian Geotech Conf 12:16–18

12. Korovkin MO, Petuhov AV (2017) Vysokoprochnye betony s vysokim soderzhaniem zoly Kansko-Achinskogo burougol'nogo bassejna (High-strength concrete with a high ash content of the Kansk-Achinsk brown coal basin). Eng Bull Don 1:106–112
13. Siddique R, Iqbal K (2011) Supplementary cementing materials, engineering materials. Springer, Berlin,Heidelberg, p 297
14. Volzhenskij AV, Burov JuS, Kolokol'nikov VS (1979) Mineral'nye vjazhushhie veshhestva (Mineral binders). Moscow, p 476
15. Lothenbach B, Scrivener K, Hooton RD (2011) Supplementary cementitious materials. Cem Concr Res 41:1244–1256
16. Parfenova LM (2013) Primenenie zol teplovyh jelektrostancij v betonah (Application of ashes of thermal power plants in concrete). Bull Polotsk State Univ 16:68–72
17. Mohammad ShA (2007) Effects of systematic increase of pozzolanic materials on the mechanical, durability, and microstructural characteristics of concrete. A thesis submitted for the degree of doctor of philosophy. Dissertation, University of New South Wales
18. Mehta PK (1985) Influence of fly ash characteristics on the strength of portland-fly ash mixtures. Cem Concr Res 15:669–674
19. Semsi Y, Hasan SA (2012) Effects of fly ash fineness on the mechanical properties of concrete. Sadhana—Indian Acad Sci 37:389–403
20. Davis RE, Carlson RW, Kelly HJW, Davis HE (2008) Properties of cements and concretes containing fly ash. J Am Concr Inst 33:577–611
21. Gorshkov VS, Timashev VV, Savel'ev VG (1981) Metody fiziko-himicheskogo analiza vjazhushhih veshhestv (Methods of physical and chemical analysis of binders). Moscow, p 335

The Study of the Stress State in Girders Braced with Carbon Fiber

A. O. Zhurbenko[✉] and M. V. Tabanyukhova

Novosibirsk State University of Architecture and Civil Engineering (Sibstrin), 113, Leningradskaya str, Novosibirsk 630008, Russia

Abstract. Currently, composite materials are intensively used in the construction industry. The high physical and mechanical parameters of carbon fibers help improve the carrying capacity of structures without losing useful space and increasing the net weight of buildings. One of the key research goals is the study of the strain and stress conditions of structure elements depending on the bracing option using various composites to select the best option. This work deals with the study of the stress state of carbon fiber braced girder models and the assessment of the impact bracing has on the redistribution of stress in the workpiece. We used the photoelasticity method to study the stress state in the experiments. This method allows for a visual representation of the stress and strain state of the object under investigation. During the tests, we obtained stress fields in the models of girders made of piezooptical materials for two workpiece load options. Girder models used in the work were made of E2 plexiglass. We reviewed three carbon fiber bracing options for workpieces. The girders were tested for symmetrical lateral bending, namely for simple and three-point bending. We used the photoelasticity method to obtain interference bands representing the fields of top shear stresses in the workpiece. Using the stress fields, we analyzed the stress state of the girder models and assessed the bracing options in terms of reducing the stress in the region of tension.

Keywords: Carbon fiber · Photoelasticity method · Model test · Stress state

1 Introduction

Carbon was discovered in 1880 by T. Edison and it was immediately introduced in various industries including manufacturing and construction. Carbon fibers were first used in construction practices in southern Germany in 1982. Carbon bands were used to reinforce a concrete bridge (Fig. 1) [1].

In Russia, carbon fibers were introduced in the construction practices in 2003 during the repair of the girders of an automobile bridge over the river Kirzhach. The reinforcement was required because of the cracks forming in the bridge span. The carbon fiber reinforcement method stipulates attaching robust carbon fibers to the surface of the structure to take some of the stresses and thus improve the carrying capacity of the element. Special construction-grade adhesives are used as the glue and they are often based on

Fig. 1 Bridge reinforcement modeling, Germany (1982)

epoxy resins or mineral binders. The advantages of this technology include the high resistance to external impacts and corrosion, easy application, and high durability of the reinforcement material layer. The drawbacks include the deterioration of the structure material near the reinforcing layer, and the flaking of the reinforcing layer over time [2]. Besides, some actions were performed to reinforce the bridge, including the installation of anchoring devices, the prestressing and fixation of carbon fiber fittings, the attachment of carbon bands on cracks and carbon fiber sheets to prevent the further deterioration of weakened regions (Fig. 2). Currently, the bridge over the river Kirzhach is in operation [3].

Fig. 2 Kirzhach bridge reinforcement layout

The problem of operating structures with various defects or oddly-shaped details is typical of the construction practices. This is due to the formation of stress and strain zones that should be taken into account [4]. Concrete, reinforced concrete, and stone structures

can be used even if they have cracks. To improve the calculation and design methods for such structures, it is necessary to further develop the applied fracture mechanics [5]. The complexity of contemporary structures makes it difficult to obtain the data on strain zones [6]. The presence of stress risers conditions the complex distribution of strains and the areas of their concentration. Concentration stands for a localized increase of stress, and it is assessed using the stress concentration factor [7].

Several researchers conducted experiments and determined that reinforced concrete objects braced with composite materials have better durability than those without bracing under the same dynamic load levels [8]. The reinforcement of main girders of concrete span structures using composite materials instead of metals results in a significant reduction of major repairs due to the low labor inputs required to perform the reinforcement and the relatively low overall cost of the materials used [9]. The optical methods are often used to study the mechanical properties of materials because they facilitate the complete field metering and provide a wide range of parameters obtained. There are many methods that fit this goal, such as interferometric methods, digital image correlation (DIC), infrared thermography (IRT), and photoelasticity [10]. Previously, the photoelasticity method was used to study the stress state of girder models with partial deterioration (kerf-cracks) before and after the application of a reinforcing carbon fiber layer, as well as to obtain stress fields and analyze the impact the reinforcing layer has on stress concentration near the crack tips [11]. Usually, stresses and their concentration are determined using the known deformations or by numerical integration of differential equations of balance [12]. Stress concentration is a localized increase of stress in structure elements due to the rapid shifts in cross-sections related to apertures, cuts, etc., that are referred to as stress risers. The degree of stress concentration is characterized by the concentration factor [13]. Stress concentration factors obtained using the experimental data allow us to assess the impact of the crack pitch and grouping on the stress state of the element [14]. The assessment of stress concentration factors can be useful in determining the durability of fiber composite coatings (carbon, cotton, and wood fibers, asbestos cement, glass fibers) [15].

Today, fiber materials, including carbon fibers, are not only used in repairs. They are also used to reinforced newly-produced structures. Researchers suggest applying reinforcements before the partial deterioration of structure elements, such as cracks, becomes evident to avoid the appearance of stress risers in tension zones. There are various requirements for structures and their elements. They must be durable, rigid, stable, reliable, and cost-efficient. The latter requirement contradicts all of the former ones because the presence of stress risers leads to the increased stress and thus to the increased consumption of the material needed to produce the structure. The reduction of stress concentration allows for producing structures that are reliable, high-quality, and more cost-efficient in terms of material consumption [16].

Structures and elements relying on girders are the most widely-used ones in the construction industry. They are very often used in industrial and civil engineering [17]. They could benefit from the development of cheaper and easier-to-mount reinforcement systems using various composites, such as carbon fibers, during the production stage [18]. Various reinforcement options using fiber materials may reduce the costs of specific construction materials while maintaining the mechanical parameters. This work focuses

on the study of the stress state in the elements of girder-based structures (simple and three-point bending) reinforced with carbon fibers. We used the photoelasticity method and implemented the research on the girder models made of optically responsive material.

2 Experimentation

Goal: the photoelastic analysis of the stress state of girder models reinforced with carbon fibers depending on the reinforcement option.

Objectives: producing workpieces of E2 plexiglass (B1 is the model of a non-reinforced girder, B2 is the girder model with reinforcements in the tension zone); obtaining stress fields in the models for the two load modes; analyzing the impact of the reinforcing carbon fiber layer on the stress state of the girder models and the redistribution of stresses in them due to the reinforcing layer; comparing the experimental results for various load modes and reinforcement options (simple and three-point bending).

In this research, the properties of plexiglass and carbon fiber play a crucial role. Carbon fiber plastic is a multilayer composite material made of sheets of carbon fibers coated by thermoreactive polymer (usually epoxy) resins. A key feature of polymer composites based on carbon fibers is the high anisotropy of their stress and strain properties. High durability and rigidity are obtained in composites with the unidirectional placement of continuous fibers [19]. Plexiglass is a thermoplastic vinyl polymer [20].

To conduct the experiments, we produced a batch of E2 plexiglass workpieces with carbon fiber reinforcements and without them. The sizes of girder models in millimeters, load modes, and carbon fiber reinforcement options are shown in Figs. 3 and 6. The models were tested for symmetrical lateral (simple and three-point) bending. The tests were carried out under direct radioscopy with crossed and parallel polarizers in white and green light (in this research, we used the color filter allowing us to obtain the green light with a wavelength of $\lambda = 541$ mmc). This algorithm was used for a more accurate determination of band order. When the stress gradient is high, the photoelasticity method has an error of up to 5% because it is difficult to determine the tenth fractions of the bands accurately. Figures 4, 5, 7, and 8 show photographs of interference bands (maximum shear stress fields in the plane) appearing in B1 and B2 girder models under simple and tree-point bending. The photographs shown in this work were made in white light, which allows for the visualization of interference bands with different colors depending on the band order. The order of the bands in the photographs is identified with numbers 0, 1, 2, etc. The highest band order values can be found in stress concentration zones, namely in the load application areas. This can be observed for both simple and three-point bending.

3 Model Testing for Simple Bending

Model B1 tested for simple bending features symmetrical interference bands relative to the horizontal axis. When reinforcing carbon fibers were introduced, line 0 (neutral fiber layer) shifts downwards to the tensioned fibers (Fig. 4). Figure 4a shows that the highest band order in the girder model without reinforcements was 3.5 under the load of 441 N. In the girder model reinforced with carbon fibers in the tensioned zone, the band order equaled 2 under the load of 589 N (Fig. 4b) and 3.3 in the compressed zone at
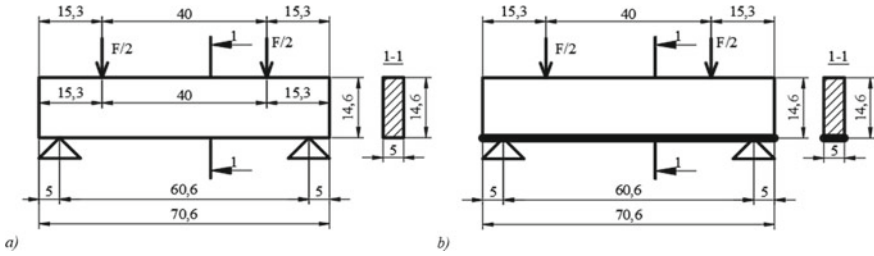
Fig. 3 The loading and reinforcement mode for girder models under simple bending: **a** girder model without reinforcements—B1; **b** girder model with carbon fiber reinforcement applied all over the lower plane—B2
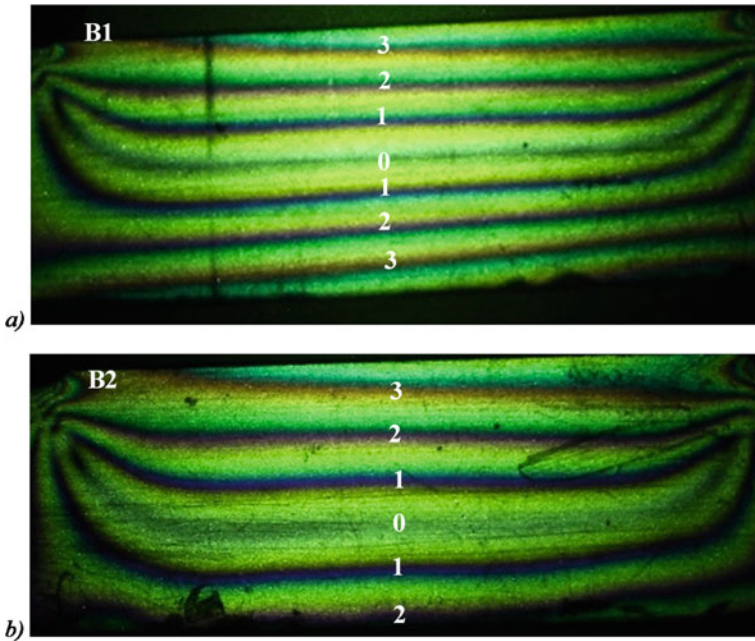
Fig. 4 Interference bands in girder models for simple bending: **a** B1 under a load of 441 N; **b** B2 under a load of 589 N

the top. The application of a reinforcing carbon fiber layer resulted in the redistribution of stresses. We must note that when there were fewer bands, the stress level was also lower. The comparison of test results under various loads—441 N (Fig. 4a) and 589 N (Fig. 4b) —shows that the reinforced B2 girder can take higher loads with the same stress levels (in the compressed zone, while in the tensioned zone the stress was lower) as the non-reinforced B1 girder. The application of carbon fibers reduces the stress in the tensioned zone (where the reinforcing layer is attached).

For visual comparison, Fig. 5 shows interference bands for B1 and B2 girder models under the same load of 441 N. In the reference girder (Fig. 5a), there are 3.5 bands
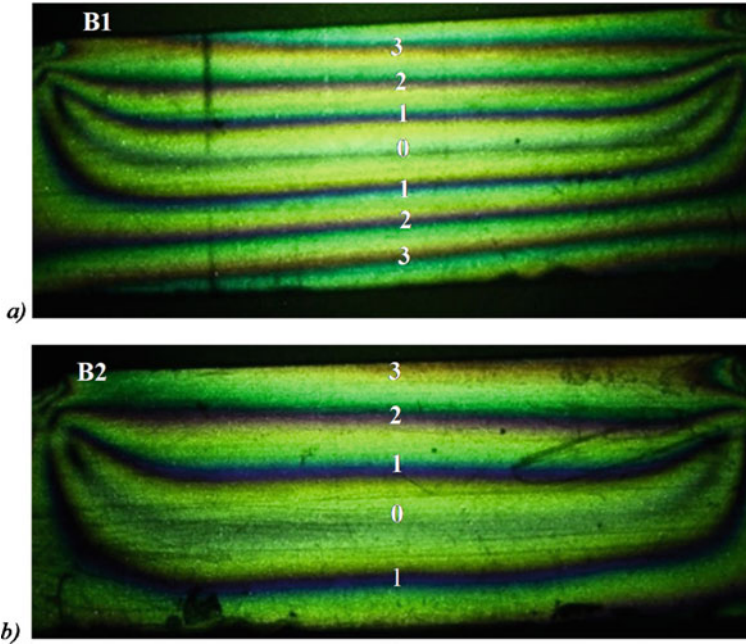
Fig. 5 Interference bands in girder models for simple bending under a load of 441 N: **a** B1 girder model; **b** B2 girder model
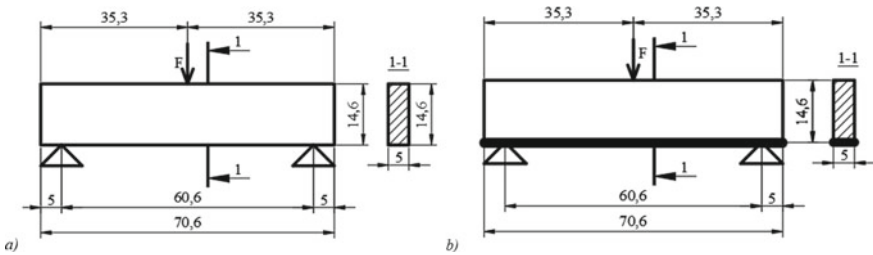
Fig. 6 The loading and reinforcement mode for girder models under symmetrical lateral bending: **a** girder model without reinforcements—B1; **b** girder model with carbon fiber reinforcement applied all over the lower plane—B2

on the outline, and they are symmetrical about the horizontal axis of the workpiece corresponding with the zero band order. In the reinforced girder, the outline only features bands with an order of 1.8 (at tension zone at the bottom) and 3 (at the compression zone at the top) (Fig. 5b). Stress redistribution is observed: the zero band shifts towards the tensioned zone that was reinforced with carbon fibers. In this case, the lower band order (1.8 and 3.5) in the reinforced girder model B2 (Fig. 5b) is significant compared to the non-reinforced B1 girder (Fig. 5a) under the same load of 441 N. The stress relief in the B2 girder model was 66% compared to the B1 model.
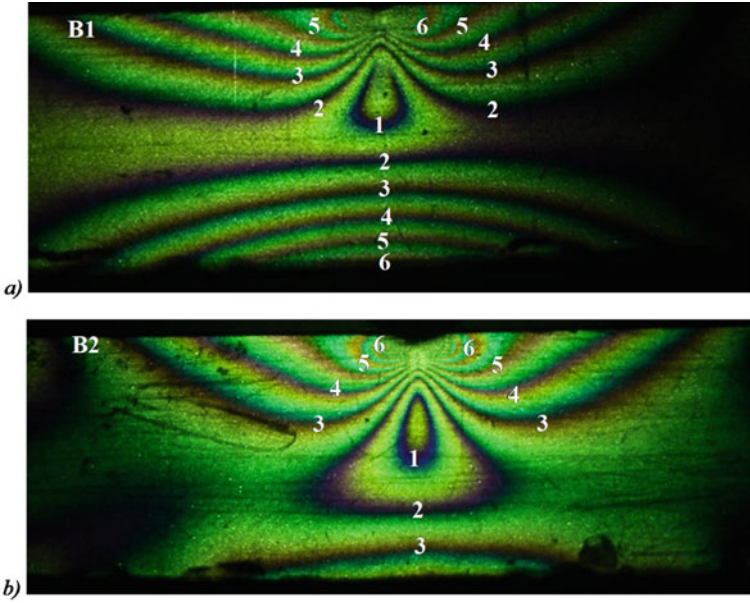
Fig. 7 Interference bands in girder models under symmetric lateral bending: **a** B1 under 245 N; **b** B2 under 343 N
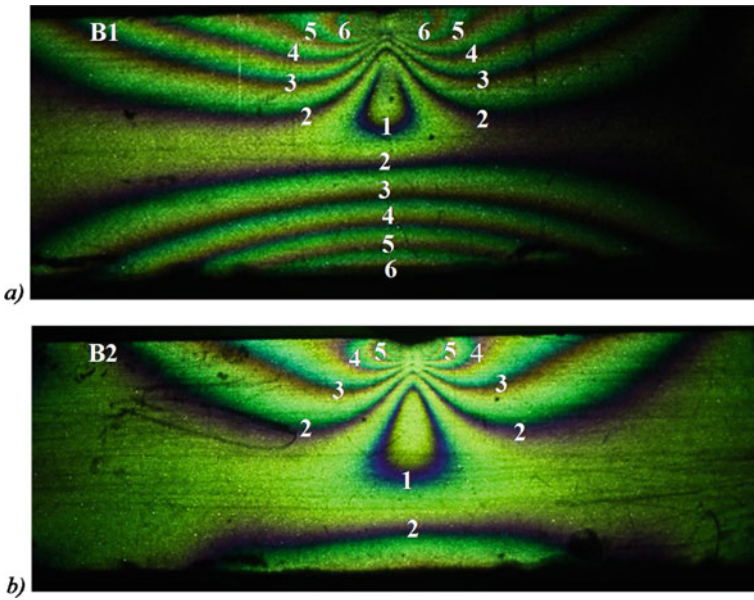
Fig. 8 Interference bands in girder models for symmetric lateral bending under 245 N: **a** girder model—B; **b** girder model—B2

4 Model Testing for Symmetrical Lateral Bending

Figure 6 shows loading modes for symmetrical lateral (three-point) bending of girder models with reinforcements and without them, as well as the workpiece dimensions in millimeters. We must note that the workpieces from the same batch were also tested for simple bending. The models were not stressed to destruction—in all of the experiments their material was in the elastic range of stress, which allowed for multiple experiment runs to specify the data obtained using the photoelasticity method.

Figure 7 shows the photographs of interference bands in girder models B1 and B2 under symmetric lateral bending (three-point). The band order is identified with numbers 0, 1, 2, etc. The highest band order is observed under the concentrated force. Within this research, the stress concentration caused by the point application of loads is insignificant. Therefore, stress fields shall be discussed relative to the tension zone.

Figure 7a shows that the girder model without reinforcements reached the highest band order of 6 in the tensioned zone under 245 N, while the carbon fiber reinforced girder model had just 3.8 bands in the tensioned zone under a higher load of 343 N (Fig. 7b). Thus, the introduction of the reinforcing layer of carbon fibers resulted in a significant reduction of stresses under higher loads.

For the visual comparison of the stress state of the girder models, Fig. 8 shows interference bands for B1 and B2 workpieces under the same load of 245 N. In the tensioned zone of the reference girder (Fig. 8a), the outline (barely) features a 6th order band, while the outline of the girder reinforced with carbon fibers only has the 2.8th order band (Fig. 8b). This signifies a significant reduction of stress in the tension zone due to the application of the reinforcing layer. The stress relief in the B2 girder model was 54% compared to the B1 model.

5 Results

We performed a photoelastic analysis of the stress state of girder models reinforced with carbon fibers under two loading modes (simple and three-point bending).

- We obtained the stress fields under simple and three-point bending for the E2 plexiglass girder model reinforced with carbon fibers in the tension zone and the one that was not reinforced.
- We analyzed the impact the reinforcing carbon fiber layer had on the stress state of the girder models. When comparing the stress state of B1 and B2 models, we observed a 66% reduction of stress for simple bending and a 54% reduction for three-point bending.
- The workpiece tests for simple and three-point bending produce similar results. The introduction of carbon fibers resulted in the redistribution stress and its reduction in the tension zone (for fibers reinforced with carbon fibers).

This work does not cover the impacts of the adhesive and carbon fiber layer thickness on the stress state of the model due to the increased cross-section. Due to the small height of the workpieces, this factor might be quite significant, which calls for a series of new

experiments to assess the influence of reinforcement (glue + carbon fibers) thickness on the stress state of the model. Besides, this research did not cover the shift of the neutral layer of fibers after the application of the reinforcing layer. This fact is interesting and it requires additional research and the analysis of publications dedicated to this topic.

References

1. Dmitriev VG, Salatov EK (2016) The use of carbon composites in renovating transport infrastructure buildings and. The introduction of modern structures and innovative technologies in track facilities 89:52–60
2. Tabanyukhova MV (2012) The study of the stress state of girders with a reinforcing layer of carbon fibers. Mekhanika kompozitsionnykh materialov i konstruktsii. 348:248–254
3. Ovchinnikov II, Ovchinnikov IG, Chesnokov GV, MIkhaldykin ES (2016) The analysis of experimental research on bracing reinforced concrete structures with polymer composites. Part 1. Russian experiments under static loads. Naukovedenie Internet J 324:130–131
4. Albaut GN, Baryshnikov VN, Pangaev VV et al (2003) Determining stress concentration factors in non-standard problems using the photoelastic methods. Phys Mesomech 195:91–95
5. Albaut GN, Kurbanov AB, Pangaev VV, Tabanyukhova MV (2004) The photoelastic study of stresses in elements with different singularities. Phys Mesomech 463:359–362
6. Neuber H, Hahn H (1967) The problem of stress concentration in academic research and engineering. Mechanics—a collection of translated works 380:109–131
7. Kazakova EA, Tabanyukhova MV (2019) Photoelastic analysis of the stress state of castellated girders. Des Constr Southwest State University 345:209–212
8. Nevolin DG, Smerdov DN, Smerdov MN (2017) Bracing reinforced concrete buildings and various structures with polymer composites: a monograph. USURT, Yekaterinburg 379:150–151
9. Tabanyukhova MV (2012) The study of the stress state of girders with a reinforcing layer of carbon fibers. Mekhanika kompozitsionnykh materialov i konstruktsii 324:248–254
10. Albaut GN, Kharinova NV (2005) Stress-strain study near cracks in rubber models by non-linear photoelasticity. In: 11th international conference on fracture, ICF11 vol 1070, pp 5010–5014
11. Tabanyukhova MV (2010) The reduction of stress in girders with defects. Defects in building and structures. In: Building structure reinforcement: proceedings of XIV research and methodology conference of Military Engineering and Technology Institute, vol 547, pp 104–108
12. Albaut GN, Akhmetyanov MKh, Kharinova NV (2010) The study of geometrically and physically non-linear problems of solid mechanics using the method of non-linear photoelasticity. Uchenye Zapiski Kazanskogo Universiteta. Series: Fiziko Matematicheskie Nauki 158:77–85
13. Zerkal SM, Kharinova NV (2019) The study of stress concentration in rubber plates with round apertures and rigid inclusions. Innov Life 350:119–125
14. Tabanyukhova MV (2018) Determining the stress concentration coefficients near kerfs imitating cracks. In: Structure theory; achievements and problems: proceedings of the III All-Russian research and practice conference, vol 256, pp 88–92
15. Albaut GN, Kharinova NV, Akhmetzyanov MK (2010) The study of the deformation of polyurethane bands with central kerf-crack using the non-linear photoelasticity method. Deformatsiya i Razrushenie materialov 147:42–45
16. Tabanyukhova MV (2019) The experimental study of the stress state of a perforated flat workpiece. In: XII All-Russian congress on the fundamental problems of theoretical and applied mechanics, vol 547, pp 202–204

17. Volik AR, Novikova TS, Svintsitsky AA (2018) The bracing of bend reinforced concrete workpieces with composite fabric. In: The architecture and construction industry: problems, prospects, innovations: the proceedings of the international research conference dedicated to the 50th anniversary of Polotsk State University, vol 365, pp 128–131
18. . Volik AR, Tsvetinsky II (2006) The work of reinforced laminated girders with different reinforcing materials and their placement options. Vestnik of Polotsk State University 130:21–25
19. Davydova IF, Kavun NS (2012) Glass fiber plastics as versatile composites. Aviat Mater Technol 345:253–260
20. Kablov EN, Kablov CLV, Babin AN et al (2016) The developments of All-Russian Scientific Research Institute of Aviation Materials in melt binders for polymer composites. Polym Mater Technol 278:37–42

Getting Gypsum Mixes Based on Construction Waste

M. D. Butakova[✉]

South Ural State University, 76, Lenin Prospekt, Chelyabinsk 454080, Russia
butakovamd@susu.ru

Abstract. Today one of the most pressing issues in the modern world is the rational waste management. Uncontrolled waste management leads to serious environmental consequences, in connection with which special legislative acts are adopted in all developed countries, regulating the integrated management of waste (collection, transportation, sorting, neutralization, processing, recycling, liquidation, burial, requirements for disposal sites, marking and storage regulations), which pose a danger to human health and the environment, on which life on Earth depends. The production of building materials, elements and products is associated with the formation of various types of waste. Manufacturing wastes are residues of raw and other materials, or semi-finished goods generated in the manufacturing process, which have completely or partially lost their useful physical properties. Products generated as a result of physical and chemical processing of raw materials, extraction and processing of mineral resources, the receipt of which is not the purpose of the production, can be considered production waste. Gypsum waste is generated in industrial gypsum plants. This waste consists of scrapped and substandard materials. Recycling this waste stream is usually part of the gypsum plant's waste prevention activities.

Keywords: Building materials · Construction waste · Recycling · Setting and hardening times · Strength

1 Introduction

At present, plaster is one of the most multi-functional finishing materials for ceiling and wall surfaces. One may see plastered surfaces practically in every building and in every room. The issue on the use of plasters, which perform not only the function of smoothing, but also of soundproofing and thermal insulation, is relevant.

Cement-based plasters, as a rule, are used for facades, finishing and heat insulation of humid premises. Plasters based on gypsum binder are used for internal works; unlike the cement-based ones, they have a number of positive properties: good molding capacity, uniform change of volume during hardening, and no need for compaction; fast strength generation, formation of favorable porous or capillary structure, which allows to regulate the humidity (positive effect on the room microclimate), insignificant density

and, as a result, high thermal-insulation capacity; high fire resistance; favorable behavior when drying, low equilibrium moisture; good workability, high vapor permeability, antiseptic properties and environmental friendliness, what is especially highly-valued when performing interior furnishing.

However, gypsum binder has significant downsides—short setting and hardening times, what complicates the work with plaster mixes based on this binder.

In order to obtain the required properties of the mortars, small amounts (up to 2% by mass of the binder) of chemicals are added to gypsum mixes. Additives are introduced to mortar at manufacturing plants or on construction sites. At the same time, it is important to take into consideration the fact that additives often function in a complex way. Usually, they provide for both the desirable and other additional effects. Thus, for instance, the majority of the setting retarders and accelerators have a negative effect on the final strength of gypsum products. Meanwhile, retarders often lead to shrinkage of the hardened gypsum binders, and accelerators that speed up the formation of rigid structure, on the contrary, cause certain expansion.

By using multi-functional additives it is possible to simultaneously improve many properties of gypsum binders. Such additives are composed of plasticizers, polymers, hardening regulators, water-repellent sealers, water-retaining and other admixes. Thus, for instance, it is possible to achieve the simultaneous change in the setting time by adding retarders or accelerators, and the flowability by using fluxing agents, increasing the surface hardness and decreasing the solubility in water.

Fluxing agents. Plasticizers (technical lignosulphonate (LST) and waste sulphite liquor), at a stable water-gypsum ratio, increase the cone flow value and the mortar flowability. This helps reduce the amount of water required to obtain a mortar with the set rheological properties, what determines the increase in strength. The most effective are super fluxing agents (super plasticizing agents (dry or liquid C-3)).

At a stable water-gypsum ratio, fluxing agents extend the setting time, and preserve or slightly shorten those in case of constant flowability. For example, super plasticizing agent in the amount of up to 1.5% by mass leads to slight extension of the setting time, and waste sulphite liquor tangibly slows down the setting in case of constant flowability.

Super plasticizing agents proportioned 0.5–1% by mass have the effect of increasing the strength of the hardened gypsum mortar in wet condition by 50–60%, and in dry condition by 30% if processing properties remain the same. The use of additives in the amount exceeding 1% by mass decreased the strength if the water-gypsum ratio is preserved [1–3].

Setting retarders. Since, in order to reduce the energy expenditures on burning, gypsum binders with short setting time are produced most often, then additives slowing down the setting time are especially in demand. At a stable water-gypsum ratio, the overwhelming majority of the setting retarders, besides the lime-containing products, slightly increase the flowability. Thanks to mild fluxing action there appears a possibility to reduce the water-gypsum ratio while preserving the required processing properties of the gypsum paste and the strength characteristics of the hardened paste. When using small amounts of additives, the compression strength decreases insignificantly; however, big amount of the setting retarders result in a tangible strength decrease. Thus, for instance, at the water-solids ratio equaling 0.75, the adding of citric acid of 0.16% by mass extends

the beginning of setting from 14 up to 140 min, while the tension strength under bending decreases by more than 90%.

The retarders based on calcium hydrate have a different effect: at a stable water-gypsum ratio, the strength increase is observed, and a slight decrease of the strength in case of constant flowability. Such retarders as borax, citric acid and its salts, waste sulphite liquor, and glue, decrease the expansion value at the hydration stage, while simultaneously increasing the diffusion rate of water in a gypsum product. This is explained by the change in the character of crystallization of calcium sulphate dihydrate under exposure to the setting retarders and, as a result, the increase in the capillary porosity. Special attention, when using the setting retarders, should be paid to limiting their amount, otherwise the will have a negative effect on such properties as strength, expansion, and capillary water absorption.

Setting accelerators. Setting accelerators are used in the production of thin-shell construction elements on installations with high performance and quick rotation of forms. Mostly, potassium sulphate and fine-grained gypsum stone (centers of crystallization) are used as setting accelerators. Just 0.5% by mass of potassium sulphate and fine-grained gypsum stone reduce the setting time by half. The intensity of action of calcium sulphate dihydrate increases with the decrease in the fineness of grinding. The setting accelerators increase the strength at early hardening stage. But as the age increases till complete drying out, a drop is observed in the strength of the gypsum binders with added setting accelerators as compared to the strength of the gypsum binders without the accelerators. This phenomenon is explained by the activation of recrystallization processes since it is manifested stronger if the amount of additives is increased. Meanwhile the decrease in the strength occurs thanks to the formation of big crystals, which have regular structure, intergrow less, and generate form bigger pores. Reasoning from this fact, the introduced setting accelerators should be limited to strictly necessary amount.

Most often, a combination of fluxing agents and setting time regulators is used. In this connection, it seems promising to use construction waste based on calcium sulphate dihydrate as the regulator of the setting and hardening times. This will allow to increase the volume of production of gypsum materials and products, and improve the quality of gypsum products, their strength and water resistance, what will significantly broaden the field of application of gypsum materials in construction.

In order to solve these complicated tasks, it is necessary to improve the existing technology and develop new principles of obtaining gypsum products both based on gypsum products, and from industrial gypsum waste using energy-conserving low-waste technologies.

Construction waste is the cheapest raw material for refabricating many materials. Recycling construction waste contributes to the manufacture of new building materials made from inexpensive recycled material.

Timely recycling avoids the annual increase in manufacturing waste. Disposal of construction and manufacturing waste helps save natural resources and money on the purchase and production of new materials. Proper recycling keeps the environment free from pollution, namely forests and fields that can serve as disposal sites. Recently, the pace of general construction has been increasing very rapidly, therefore, the need for

building materials, especially high-quality and inexpensive ones, will only increase. In view of this, research into the use of construction waste in the creation of building materials is relevant.

2 Main Part

Gypsum materials are composed of calcium sulphate dihydrate ($CaSO_4 \cdot 2H_2O$). Sulphate-reducing bacteria convert sulphates to toxic hydrogen sulphide; they die on contact with air, but a humid, airless, carbonaceous landfill environment is a good habitat for them. Thus, gypsum sent to disposal site will decompose, releasing hydrogen sulphide up to a quarter of its weight [4–9]. The issue of the use of calcium sulphate dihydrate waste in the production of building materials outside of recycling has not yet been fully explored.

The goal of this work was to study the possibility of using waste from producing gypsum materials in complex with plasticizer for the manufacture of light-weight plasters baseв on perlite aggregate.

The following input products were used in the work:

- G-5 gypsum binders
- Water
- Perlite aggregate
- Technical lignosulphonate (LST)
- Gypsum waste—ground calcium sulphate dihydrate ($CaSO_4 * 2H_2O$).

All materials meet the requirements of GOST [10–17]. Technical lignosulphonate (LST) was used as a plasticizer and retarder for the setting of gypsum binders.

Ground calcium sulphate dihydrate, a waste from the manufacture of gypsum materials, was introduced as crystallization centers of a gypsum binder (CC).

At the first stage, it was necessary to determine the effect of the additives on the setting and hardening times of the gypsum binder. The results obtained are shown in Table 1.

Group of gypsum binder in terms of setting time: normally hardening—B.

With an equal amount of tempering water, technical lignosulphonate (LST) causes an obvious increase in setting and hardening times, and crystallization centers (CC) cause a significant reduction in setting times.

Combined application of LST additive at a dosage of 0.8% and CC at a dosage of 10% slightly increases the setting time.

Further tests were connected with the establishment of the dependence of the strength indicators of gypsum stone in compression and bending on the dosage of the technical lignosulphonate (LST) plasticizer additive (Fig. 1).

With an increase in the LST content, there is a gradual decrease in the strength of the samples in comparison with the control sample without additives. At the same time, the plasticity and setting and hardening times significantly increase, therefore, the LST dosage of 0.8% was chosen for further research, since the priority for working with plasters is the duration of the setting and hardening times. Also the plaster mortar does

Table 1 Results of the test for determining the setting time of the gypsum dough of standard consistency

Composition	Initial set	Final set
Gypsum	10:40	14:20
Gypsum, LST 0.4%	16:30	20:00
Gypsum, LST 0.8%	20:00	24:15
Gypsum, CC 5%	8:00	13:00
Gypsum, CC 10%	6:45	11:30
Gypsum, LST 0.8%, CC 5%	12:15	18:30
Gypsum, LST 0.8%, CC 10%	12:00	17:45
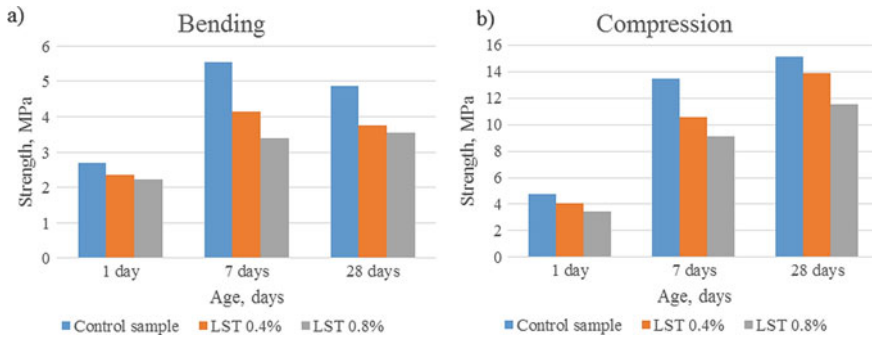
Fig. 1 Dependence of gypsum strength (MPa) on the amount of LST additive: **a** Bending; **b** compression

not bear a structural load—it is a self-supporting component, therefore, high strength is not its main indicator [18–21].

In order to exclude any side effects, the dependences of the strength indicators of gypsum stone in compression and bending on the dosage of gypsum waste—crystallization centers (CC) were investigated (Fig. 2).

It was found out that with the introduction of crystallization centers, samples with 10% of CC have the highest compressive strength at the age of 28 days. However, a repetition of the dependence of a slight decrease in bending strength by the 28th day of hardening was observed. This is associated with a sharp increase in the number of crystals and the formation of a sufficiently dense structure in the gypsum stone [22–25]. Further growth leads to the creation of close conditions and the appearance of stress centers, due to which the structure softens by the 28th day.

The joint introduction of 0.8% LST and crystallization centers (CC) showed that the increase in the strength value at the age of 28 days with 5% CC is practically the same as the value of the compressive strength of the control sample (Fig. 3).
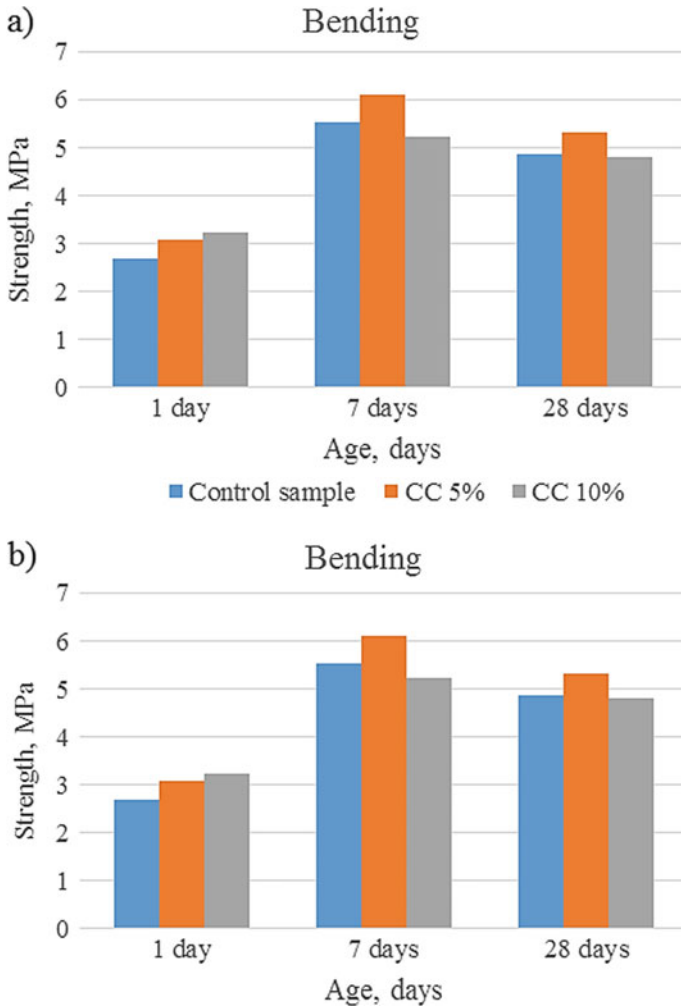
Fig. 2 Dependence of gypsum strength (MPa) on the amount of crystallization centers (CC): **a** Bending; **b** compression
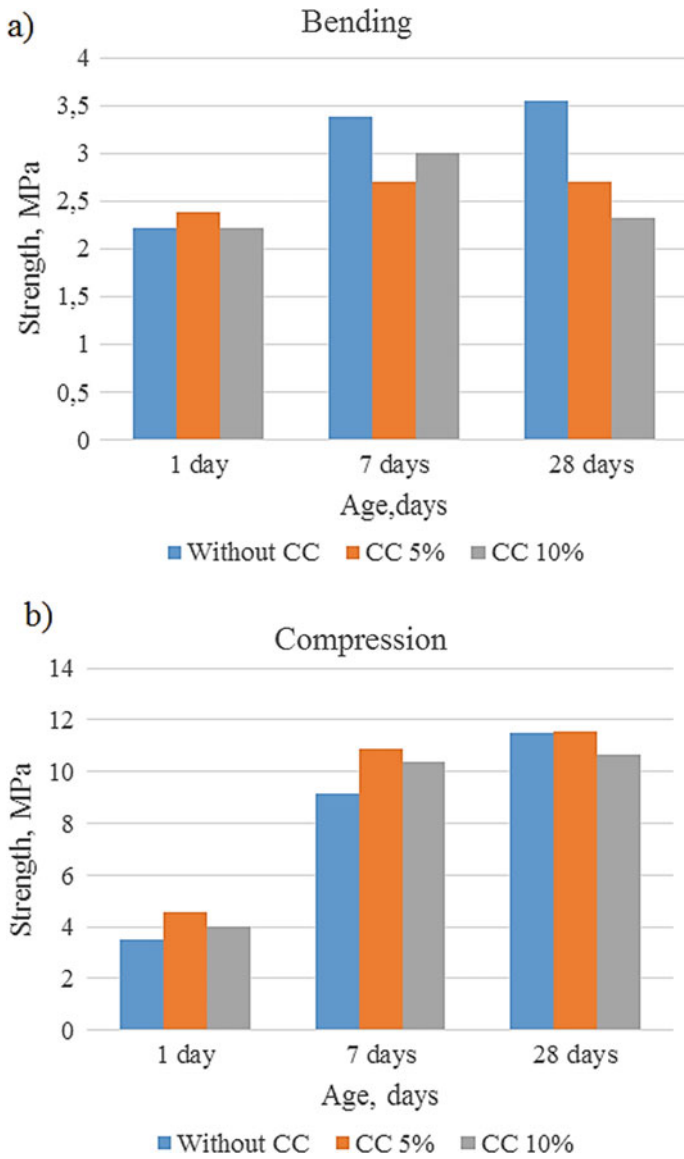
Fig. 3 Dependence of the strength of gypsum with the addition of LST 0.8% (MPa) on the amount of crystallization centers (CC): **a** Bending; **b** compression

And when the amount of CC is 10%, it does not change after 7 days, which is due to the fact that internal stress arises because of the formation of a sufficiently strong structure by 7 days, and further growth of crystals does not lead to an increase in strength, but leads to the appearance of internal stresses; the compressive strength does not increase and the bending strength decreases. When the amount of CC is 10%, the bending strength decreases from 7 to 28 days, and slightly increases during compression. A steady increase in strength is observed without crystallization centers. Crystallization centers were introduced to study the effect on the growth of strength when introduced together with the addition of the LST plasticizer. The expected increase in strength did not occur, therefore, the introduction of CC together with the LST plasticizer is meaningless.

It was also found that with an increase in the setting and hardening times (when using LST additive), the strength of the samples increases in the presence of CC, while the plasticity of the gypsum dough is the same (upon condition that the given water–solid ratio (W/S) is maintained).

The adhesion of plaster mortar to various bases (surfaces) is an important technical characteristics determining its ability to "adhere" and hold on to the surface of walls made of different materials for a long time. The adhesion strength of the hardened plaster mixes on gypsum binder to the base in accordance with GOST 31377-2008, clause 4.6.3 must be at least 0.3 MPa.

According to the experiment, the adhesion strength exceeds the values specified in GOST and is more than 3.3 and 3.2 MPa for brick and concrete, respectively (Table 2).

Table 2 Results of testing the adhesion bond strength (adhesion)

Composition	Adhesion bond strength (MPa)	
	Brick	Concrete
Gypsum, LST 0.8%, perlite 0.16 mm-flame-retardant	More than 3.2 Samples peel character—base material destruction	More than 3.3 Samples peel character—base material destruction

That is, the resulting mixture meets the requirements of GOST 31377 [26].

3   Conclusion

1. With an equal amount of tempering water, technical lignosulphonate (LST) causes an obvious increase in setting and hardening times of gypsum dough, while reducing the strength of the samples after hardening. Gypsum waste, which was used as a crystallization centre (CC), causes a significant reduction in the setting time, while increasing the strength of the hardened samples.

2. Combined application of LST additive at a dosage of 0.8% and CC at a dosage of 10% slightly increases the setting time, while decreasing the strength of the hardened samples.

3. As a result of the study of the effect of crystallization centers on the strength of plaster mixtures based on gypsum binder with LST additive on a perlite aggregate, it was revealed that the addition of crystallization centers (CC) in the amount of 5 and 10% does not have a positive effect on the strength of plaster mixtures on gypsum binder with LST additive on perlite aggregate, and also reduces the setting and hardening times of the mixture and increases the W/S ratio, when normal density is reached.

References

1. Skramtaev BG, Popov NA, Gerlivanov NA, Mudrov GG (1954) Construction materials. State Publishing House of Building Materials Literature, Moscow, p 643
2. Korneev VI, Zozulia PV, Medvedeva IN et al (2018) Technology of dry building mixtures textbook. Lan, St.Petersburg, p 372
3. Belov VV, Burianov AF, Iakovlev GI et al (2012) Modification of the structure and properties of building composites based on calcium sulfate. In: Burianov AF (ed) Monograph. De Nova Publishing House, Moscow, p 196
4. Baikov AA (1948) Proceedings in the field of binders and refractory materials. USSR Academy of Sciences Publishing House, Moscow, p 272
5. Borshchevskii AA, Ilin AS (1987) Mechanical equipment for the production of building materials and products. Higher School Publishing House, Moscow, p 368
6. Butt IuM, Sychev MM, Timashev VV (1980) Chemical technology of binders: university textbook. Higher School Publishing House, Moscow, p 472
7. Volzhenskii AV, Ferronskaia AV (1974) Gypsum binders and products. Stroyizdat Publishing House, Moscow, p 328
8. Garkavi MS (2005) Thermodynamic analysis of structural transformations in binding systems. Publishing House of Magnitogorsk State Technical University, Magnitogorsk, p 243
9. Gypsum Materials and Products (Production and Use). In: Ferronskaia AV (ed) (2004) Reference book. Publishing House of the International Association of Building Higher Education Institutions, Moscow, p 488
10. GOST 10832−2009 Expanded Perlite Sand and Crushed Stone (2011) Specifications. Standards Publishing House, Moscow, p 18
11. GOST 22023-76 Building Materials (2020) Methods of the microscopic quantitative analysis of structure. Standards Publishing House, Moscow, p 11
12. GOST 23732−2011 Water for Concrete and Building Mortar (2011) Specifications. Standards Publishing House, Moscow, p 12
13. GOST 24211−2008 International Standard Additives for Concrete and Building Mortar (2008) General specifications. Standards Publishing House, Moscow, p 12
14. GOST 25226−82 Perlite Raw Materials for the Production of Expanded Perlite (2020) Specifications. Standards Publishing House, Moscow, p 12
15. GOST 31376−2008 Dry Building Plasters Based on Gypsum Binder (2010) Testing methods. Standardinform, Moscow, p 15
16. GOST 125-2018 Gypsum Binders (2018) Specifications. Standardinform, Moscow, p 9
17. GOST 23789-2018 Gypsum Binders (2018) Testing methods. Standardinform, Moscow, p 11
18. Koroviakov VF (2003) Gypsum binders and their application in construction. J Russ Chem Bull 4:18–25
19. Kuznetsov AM (1963) Technology of binders and products textbook for University students. Higher School Publishing House, Moscow, p 456

20. Lesovik VS, Pogorelov SA, Strokova VV (2000) Gypsum binders and products textbook. Publishing House of Belgorod State Technological Academy of Building Materials, Belgorod, p 224
21. Sagdatullin DG, Morozov NN, Khozin VG (2009) Rheological characteristics of water suspensions of a composite gypsum binder and its components. J Bull Kazan State Univ Architect Eng 2(12):263–268
22. Sulimenko LM (2005) Technology of mineral binders and products University textbook. Higher School Publishing House, Moscow, p 334
23. Bazhenov IuM, Alimov LA, Voronin VV, Magdeev UKh (2008) Technology of concrete, building products and structures textbook. Publishing House of the International Association of Building Higher Education Institutions, Moscow, p 350
24. Chaus KV, Chistov ID, Labzina IuV (1988) Manufacturing technology of building materials, products and structures. Stroyizdat Publishing House, Moscow, 448 p
25. Shlenkin SS, Garkavi MS, Nova R (2007) Influence of plasticizers on the hardening of gypsum binder. J Build Mater 9:61–62
26. GOST 31377−2008 Dry Building Plasters Based on Gypsum Binder (2010) Specifications. Standardinform, Moscow, p 7

Using Linear Programming for Builder Brigades Optimization

V. D. Kudryavtseva[1(✉)], E. M. Litvinovsky[1,2], T. N. Shchelokova[3], and E. V. Tararushkin[1,3]

[1] Russian University of Transport, 9b9, Obrazcova Street, Moscow 127994, Russia
asp_doc@miit.ru
[2] Limited Liability Company «Build City», 3, 1, Argunovskaya Street, Moscow 129075, Russia
[3] National Research Moscow State University of Civil Engineering, 26, Yaroslavl highway, Moscow 129337, Russia

Abstract. The chapter presents a mathematical model for optimal assignment workers to building brigades. Model created using operations research theory. The assignment of a worker to brigades is carried out taking into account their classification and experience from the condition of maximizing the quality of their work. This model refers to the linear programming problem and is similar to the classic assignment problem. The difference between the presented model and the classic assignment problem lies in the presence of constraints associated with the wishes of the designers, as well as the lack of a limit on the number of brigades to which a worker is assigned. To solve the problem of assigning workers, the simplex method is used together with the branch and bound method to obtain integer solutions. We also presented an example to better understand the formation of model constraints and this example of modeling shows the impact of constraints on the formation of brigades. This model can find application in the organization of construction, especially when managing the construction of large buildings and structures. Using such a model by the designers help to reduce their time resources, reduce the labor intensity of work and better perform the assignment of workers to building brigades.

Keywords: Assignment · Worker · Qualification · Building brigade · Quality · Optimization · Liner programming

1 Introduction

Today, the quality of building construction is one of the main factors affecting their cost. The higher the requirement for the quality of construction, the higher their cost. In an economically competitive environment, construction management strives to generate high profits by optimizing the quality of construction. One of the ways to solve this problem is to use mathematical modeling methods [1].

During the development of a construction project, the assignment of employees to specific types of construction work is carried out by designers who rely on their

professional skills and experience. Sometimes the solutions of a construction designer may not meet the requirements of the most optimal assignment of builders. For small construction projects, such an assignment of workers in general does not affect the quality of construction. But in the design and construction of large buildings and structures, this method becomes inappropriate, since designers are faced with the analysis of large amounts of data that must be taken into account in order to make the best decision. In this case, there may be a problem with the objective of minimizing the construction cost. The solution to this problem is the creation and use of mathematical modeling methods to find the optimal composition of builder workers brigade with their subsequent implementation in the form of software. The main goal of mathematical models is to find the optimal composition of workers brigades, taking into account a larger number of types of worker and the qualifications of workers. The ability to assign workers or forbid them from working in the required brigades is also an additional optimization requirement. Using mathematical models allows better analyzing big data, reducing the time to solve the assignment problem, take into account the requirements for the qualifications and experience of workers when they are assigned to certain types of work and to brigades. Similar mathematical models for optimizing works team or crew are also used in such industries as railroad and aviation [2–11].

Also, such an optimization assignment of workers to brigades contributes to an increase in the safety of the building process by taking into account the qualifications of workers. The higher the qualifications of the worker, the higher the safety of the building process due to the availability of sufficient experience of the workers. The risk of negative phenomena in the production of work is influenced by many factors, which also include the qualifications of the worker. The reason for this in the human factor, or rather the indiscipline of the worker. At the same time, higher qualifications lead to less indiscipline.

This chapter presents a mathematical model for optimizing the assignment of the worker to brigades. Optimization is performed subject to the maximum quality of work, while considering the relative quality of work. The main mathematical method of the model is the linear programming method [12, 13] and a model similar to the classic assignment problem. The difference lies in the fact that the number of brigades for workers is unlimited and additional constraints, which make it possible to assign workers to the necessary brigades or forbid them from working in the necessary brigades. To obtain integer solutions of the model, the simplex method is used in combination with the branch and bound method.

2   Mathematical Model

Let us compose a mathematical model of the problem of the optimal assignment of workers to the brigades for construction work. Let it be necessary to form brigades for construction work with a certain number of workers, so that the quality of construction work at the facility is the highest possible. The brigades carry out the work sequentially.

Formulation of the model:

1. there are N types of workers of a building organization—brigade members assigned to certain types of work;

2. there are n_i workers of the i type, $i = \overline{1, N}$ (workers of various classifications (for instance, 2–5 grades)), then each worker is determined by a pair (i, j), where i is the type of worker, j is the ordinal number of the worker among workers of the i type, $j = \overline{1, n_i}$;

3. q_{ij}—qualification of a worker (i, j) (this includes work experience, skills of a worker, etc.), can take a value from the interval [0,1];

4. the worker's qualifications should depend on the worker's classification, therefore, a weight a_i is introduced, with which the qualifications of the i type of worker are taken into account (a_i can only take natural values), then the worker's qualification (i, j) is product-calculated: $a_i q_{ij}$, $i = \overline{1, N}, j = \overline{1, n_i}$;

5. the number of brigades, k, is set equal to M, thus $k = \overline{1, M}$;

6. b_i^k workers of the i type must be assigned to the brigade numbered k; the binary variable x_{ij}^k takes 1 if the worker (i, j) is assigned to the brigade k, and takes 0 otherwise, thus, there is a constraint in the mathematical model:

$$\sum_{j=1}^{n_i} x_{ij}^k = b_i^k, \tag{1}$$

where $i = \overline{1, N}, k = \overline{1, M}$.

7. some workers can be assigned to any type of work at the request of the designer; some workers can work on any kind of work at the request of the designer, i.e. in the formulation of the problem, constraints $x_{ij}^k = 1$ are possible for some sets i,j,k and constraints $x_{ij}^k = 0$ for some sets of i,j,k;

8. it should be possible for some workers to work together in any brigade, i.e. possible constraints:

$$x_{i_1 j_1}^k + x_{i_2 j_2}^k = 2 \tag{2}$$

for some numbers of brigade k and some pairs (i_1,j_1), (i_2,j_2).

The absolute quality of the k brigade is determined by the expression:

$$Q_{abs}^k = \sum_{i=1}^{N} \sum_{j=1}^{n_i} a_i q_{ij} x_{ij}^k \tag{3}$$

The maximum quality of the k brigade that can be achieved is given by the formula:

$$Q_{max}^k = \sum_{i=1}^{N} a_i b_i^k \tag{4}$$

Since the number of workers in the brigades can be different, to compare the quality of the brigades, it is necessary to use not absolute, but relative quality, which for the k brigade is determined by the ratio:

$$Q_{rel}^k = \frac{Q_{abs}^k}{Q_{max}^k} \tag{5}$$

The goal is to form the composition of the brigades so as to ensure the highest possible quality of all brigades. That is, it is necessary to consider the following objective function:

$$f(x) = \sum_k \frac{Q_{abs}^k}{Q_{max}^k} \rightarrow \max \tag{6}$$

The above model of the optimal assignment workers to brigades in the described setting is a linear programming problem. This formulation of the problem of assigning workers to building brigades differs from the classical formulation of the assignment problem. In particular, the formulation of the problem constraints related to the wishes of designers, namely: constraints of the form $x_{ij}^k = 1$ and $x_{ij}^k = 0$ some sets of I, j, k and constraints $x_{i_1j_1}^k + x_{i_2j_2}^k = 2$ for some numbers of brigade k and some pairs (i_1, j_1), (i_2, j_2). Also, in the general case, in the considered formulation of the problem, there are no restrictions on the number of brigades to which one or another worker can be assigned. It follows that the classical methods for solving the assignment problem, such as the Hungarian method [14–17], are not applicable to the problem of assigning workers to building brigades in the considered setting. The classical assignment problem, which is also a linear programming problem, is formulated as follows [18]:

$$\begin{cases} \sum_{i=1}^{n}\sum_{j=1}^{n} c_{ij}x_{ij} \rightarrow max \\ \sum_{j=1}^{n} x_{ij} = 1, i = \overline{1, n} \\ \sum_{i=1}^{n} x_{ij} = 1, j = \overline{1, n} \\ x_{ij}\epsilon\{0, 1\}, i = \overline{1, n}, j = \overline{1, n} \end{cases} \tag{7}$$

where c_{ij} measures the cost of assigning i to j.

3   Model Example

Let us consider an example of a linear programming problem for assigning workers to brigades in the above formulation.

Let $N = 3$ (three types (5, 3, 2 grades) workers), $n_1 = 4$ (in the first type, 4 workers), $n_2 = 6$, $n_3 = 8$ (in the second and third types, 6 and 8 workers, respectively). It is necessary to assign workers for three brigades ($k = 3$) from 5 workers, taking into account the maximization of the quality of work.

The vectors of qualifications for workers are as follows:

- vector of qualifications for workers of the 5th grade:

$$q_{1,j}^{\mathrm{T}} = \begin{bmatrix} 0.9 \\ 0.9 \\ 0.6 \\ 0.9 \end{bmatrix} \tag{8}$$

- vector of qualifications for workers of the 3rd grade:

$$q_{2,j}^{\mathrm{T}} = \begin{bmatrix} 0.7 \\ 0.7 \\ 0.5 \\ 0.3 \\ 0.6 \\ 0.7 \end{bmatrix} \tag{9}$$

- vector of qualifications for workers of the 2nd grade:

$$q_{3,j}^{\mathrm{T}} = \begin{bmatrix} 0.4 \\ 0.3 \\ 0.9 \\ 0.8 \\ 0.7 \\ 0.5 \\ 0.6 \\ 0.7 \end{bmatrix} \tag{10}$$

Thus, the qualifications matrix:

$$q_{i,j} = \begin{bmatrix} 0.9 & 0.9 & 0.6 & 0.9 & 0.0 & 0.0 & 0.0 & 0.0 \\ 0.7 & 0.7 & 0.5 & 0.3 & 0.6 & 0.7 & 0.0 & 0.0 \\ 0.4 & 0.3 & 0.9 & 0.8 & 0.7 & 0.5 & 0.6 & 0.7 \end{bmatrix} \tag{11}$$

Weight vector of qualifications:

$$a = \begin{bmatrix} 3 \\ 2 \\ 1 \end{bmatrix} \tag{12}$$

Each natural number in the weight vector of qualifications corresponds to the number of the worker's grade, so the number 3 corresponds to the 5th grade, the number 2 corresponds to the 3rd grade and the number 1 corresponds to the 2nd grade.

The vector of constraints is as follows:

$$b = \begin{bmatrix} 1 \\ 2 \\ 2 \end{bmatrix} \tag{13}$$

The objective function is formulated according to Eq. (6). Taking into account the pre-calculated coefficients of the variables, the function is calculated in the following form:

$$
\begin{aligned}
f(x) = {} & \frac{3}{10}x_{11}^1 + \frac{3}{10}x_{12}^1 + \frac{2}{10}x_{13}^1 + \frac{3}{10}x_{14}^1 + \frac{7}{60}x_{21}^1 \\
& + \frac{7}{60}x_{22}^1 + \frac{1}{12}x_{23}^1 + \frac{1}{20}x_{24}^1 + \frac{1}{10}x_{25}^1 + \frac{7}{60}x_{26}^1 \\
& + \frac{1}{15}x_{31}^1 + \frac{1}{20}x_{32}^1 + \frac{3}{20}x_{33}^1 + \frac{2}{15}x_{34}^1 + \frac{7}{60}x_{35}^1 \\
& + \frac{1}{12}x_{36}^1 + \frac{1}{10}x_{37}^1 + \frac{7}{60}x_{38}^1 + \frac{3}{10}x_{11}^2 + \frac{3}{10}x_{12}^2 \\
& + \frac{2}{10}x_{13}^2 + \frac{3}{10}x_{14}^2 + \frac{7}{60}x_{21}^2 + \frac{7}{60}x_{22}^2 + \frac{1}{12}x_{23}^2 \\
& + \frac{1}{20}x_{24}^2 + \frac{1}{10}x_{25}^2 + \frac{7}{60}x_{26}^2 + \frac{1}{15}x_{31}^2 + \frac{1}{20}x_{32}^2 \\
& + \frac{3}{20}x_{33}^2 + \frac{2}{15}x_{34}^2 + \frac{7}{60}x_{35}^2 + \frac{1}{12}x_{36}^2 + \frac{1}{10}x_{37}^2 \\
& + \frac{7}{60}x_{38}^2 + \frac{3}{10}x_{11}^3 + \frac{3}{10}x_{12}^3 + \frac{2}{10}x_{13}^3 + \frac{3}{10}x_{14}^3 \\
& + \frac{7}{60}x_{21}^3 + \frac{7}{60}x_{22}^3 + \frac{1}{12}x_{23}^3 + \frac{1}{20}x_{24}^3 + \frac{1}{10}x_{25}^3 \\
& + \frac{7}{60}x_{26}^3 + \frac{1}{15}x_{31}^3 + \frac{1}{20}x_{32}^3 + \frac{3}{20}x_{33}^3 + \frac{2}{15}x_{34}^3 \\
& + \frac{7}{60}x_{35}^3 + \frac{1}{12}x_{36}^3 + \frac{1}{10}x_{37}^3 + \frac{7}{60}x_{38}^3 \to \max
\end{aligned} \tag{14}
$$

Due to the fact that one brigade consists of 5 workers the system of constraints is set according to item 6 of the formulation of the model (Eq. 1):

$$
\begin{cases}
x_{11}^1 + x_{12}^1 + x_{13}^1 + x_{14}^1 = 1 \\
x_{21}^1 + x_{22}^1 + x_{23}^1 + x_{24}^1 + x_{25}^1 + x_{26}^1 = 2 \\
x_{31}^1 + x_{32}^1 + x_{33}^1 + x_{34}^1 + x_{35}^1 + x_{36}^1 + x_{37}^1 + x_{38}^1 = 2 \\
x_{11}^2 + x_{12}^2 + x_{13}^2 + x_{14}^2 = 1 \\
x_{21}^2 + x_{22}^2 + x_{23}^2 + x_{24}^2 + x_{25}^2 + x_{26}^2 = 2 \\
x_{31}^2 + x_{32}^2 + x_{33}^2 + x_{34}^2 + x_{35}^2 + x_{36}^2 + x_{37}^2 + x_{38}^2 = 2 \\
x_{11}^3 + x_{12}^3 + x_{13}^3 + x_{14}^3 = 1 \\
x_{21}^3 + x_{22}^3 + x_{23}^3 + x_{24}^3 + x_{25}^3 + x_{26}^3 = 2 \\
x_{31}^3 + x_{32}^3 + x_{33}^3 + x_{34}^3 + x_{35}^3 + x_{36}^3 + x_{37}^3 + x_{38}^3 = 2
\end{cases}
\tag{15}
$$

From item 7 of the formulation of the model, the system of constraints is defined as follows:

$$
\begin{cases}
x_{12}^1 = 0 \\
x_{12}^2 = 1 \\
x_{24}^1 = 0 \\
x_{33}^3 = 0
\end{cases}
\tag{16}
$$

This constraints can be interpreted as follows: for the first constraint the 2nd worker of the 1st type (5 grade) cannot be assigned to the 1st brigade; for the second constraint the 2nd worker of the 1st type (5th grade) cannot be assigned to the 2nd brigade; for the third constraint the 4th worker of the 2nd type (3rd grade) cannot be assigned to the 1st brigade; for the fourth constraint the 3rd worker of the 3rd type (2nd grade) cannot be assigned to the 3rd brigade.

From item 8 of the formulation of the model, the system of constraints is defined as follows (Eq. 2):

$$
\begin{cases}
x_{22}^2 + x_{24}^2 = 2 \\
x_{21}^3 + x_{25}^3 = 2
\end{cases}
\tag{17}
$$

For these constraints, the interpretations are as follows: for the first constraint the 2nd and 4th workers of the 2nd type (3rd grade) must be assigned to the 2nd brigade; for the second constraint the 1st and 5th workers of the 2nd type (3rd grade) must be assigned to the 3rd brigade.

Integer requirement:

$$
x_{ij}^k \in \{0, 1\},\ k = \overline{1, 3},\ i = \overline{1, 3},\ j_1 = \overline{1, 4},\ j_2 = \overline{1, 6},\ j_3 = \overline{1, 8},\ x_{ij}^k \in Z
\tag{18}
$$

As mentioned above, the problem cannot be solved by standard methods that are applicable to assignment problems. Therefore, for the present model, it is proposed to

solve the problem using the simplex method [19–24] in conjunction with the branch and bound method [24, 25] to obtain an integer solution. The simplex method is a general method for solving optimization problems in linear programming. The simplex solution process is iterative. The essence of the simplex method is the transition from one vertex of the polyhedron of feasible solutions to another vertex in order to optimize the objective function. For example, Fig. 1 shows the feasibility set for a 2-dimensional convex polyhedron with five vertices [24]. The objective function corresponds to a hyperplane that passes through a vertex. Optimality estimates correspond to deviations with respect to the hyperplane. When all optimality estimates are positive, then the objective function reaches its maximum. Figure 1 shows the feasibility set for a 2-dimensional convex polyhedron with five vertices [24–26].
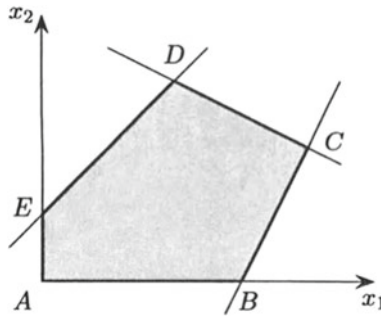
Fig. 1 A two dimensional convex polyhedron with five vertices [24]

For the problem of optimal assignment workers to building brigades, it is necessary to obtain integer values of the variables, and this must be done on the closed interval [0, 1]. In the general case, when solving a linear programming problem using the simplex method, we do not necessarily obtain an integer optimal solution; therefore, it becomes necessary to use integer programming. The general formulation of the integer programming problem differs from the general formulation of the linear programming problem by the presence of an additional constraint (the requirement of integer number). The problem of assignment workers to building brigades is a completely integer problem, i.e. the integer requirement applies to all variables. Moreover, this problem is a Boolean linear programming problem (BLP).

To obtain an integer solution to the assignment problem, it is necessary to use the branch and bound method. The branch and bound method is a combinatorial method for solving optimization problems. According to the general idea of the method, first, a linear programming problem with relaxed constraints corresponding to the original integer programming problem is solved, and its optimal solution X is found. Then select the basic variable x_i whose value β_i in the set X is not an integer. Since the interval $(\text{int}(\beta_i), \text{int}(\beta_i) + 1)$ does not contain integer values x_i, any valid integer value of this variable satisfies one of the inequalities: $x_i \leq \text{int}(\beta_i)$ or $x_i \geq \text{int}(\beta_i) + 1$. The addition of these inequalities into a linear programming problem with weakened constraints generates two new problems, the sets of feasible solutions of which do not intersect, that is, the original problem branches into two new problems, and the procedure of its

replacement by a set of two problems, equivalent to it in the sense of an optimal solution, is called branching processes. Taking into account the integer requirement in the process of branching makes it possible to exclude from consideration a part of the set of feasible solutions. Choosing any of the two problems generated by the original problem, solve the corresponding linear programming problem with weakened constraints. If the obtained solution satisfies the integer requirement, then it is the optimal solution to the generated integer programming problem. This solution is fixed as the best, no further branching of the considered problem is performed and the solution is passed to the solution of the second generated problem. Otherwise, the task forks into two new tasks. In the list of problems generated by the original integer programming problem, instead of the already considered one, two problems generated by it are added. This list has already included three problems, each of which is studied according to the same scheme as the first. As soon as an optimal solution to a linear programming problem with weakened constraints is obtained that satisfies the integer requirement, it is compared with the existing one (if any) and the best of them is fixed (in the sense of the optimal value of the objective function). The branching process is continued until each generated problem leads to an optimal solution satisfying the integer requirement, or until it is established that it is impossible to improve (in the sense of the optimal value of the objective function) the already fixed best solution. To increase the efficiency of the considered procedure, the concept of a boundary (the value of the objective function) is introduced, on the basis of which it is possible to determine the need for further branching of each of the problems generated by the original integer programming problem. A sketch example of the working principle of the branch and bound method is shown in Fig. 2. Branching in the tree occurs until the best solution is found in terms of the value of the objective function (green number). Variables corresponding to the maximum value of the objective function are the answer to the problem Fig. 2 also shows the case with an empty set (red number). In the case of an empty set, further branching is impossible.

In light of the above the algorithm for solving the problem of assigning workers to building brigades is reduced to the following stages:

1. Formation of the input parameters of the problem, the formation of the vector of constraints, the formation of the vector of values of the coefficients for unknown variables of the objective function.
2. Compilation of a simplex table for unknown variables, taking into account the previously formed vector of constraints and the vector of values of the coefficients for unknown variables of the objective function.
3. Elimination of unknown variables from the simplex table. The assignment of the excluded variables is carried out according to the constraints on items 7 and 8 from the formulation of the model (or problem).
4. Creating an auxiliary problem for calculating the initial admissible basic solution.
5. Solution of the auxiliary problem by the simplex method.
6. Solution of the original problem by the simplex method, taking into account the excluded variables and the basic variables found in 5.
7. Using the branch and bound method to obtain integer values of the set of feasible solutions.
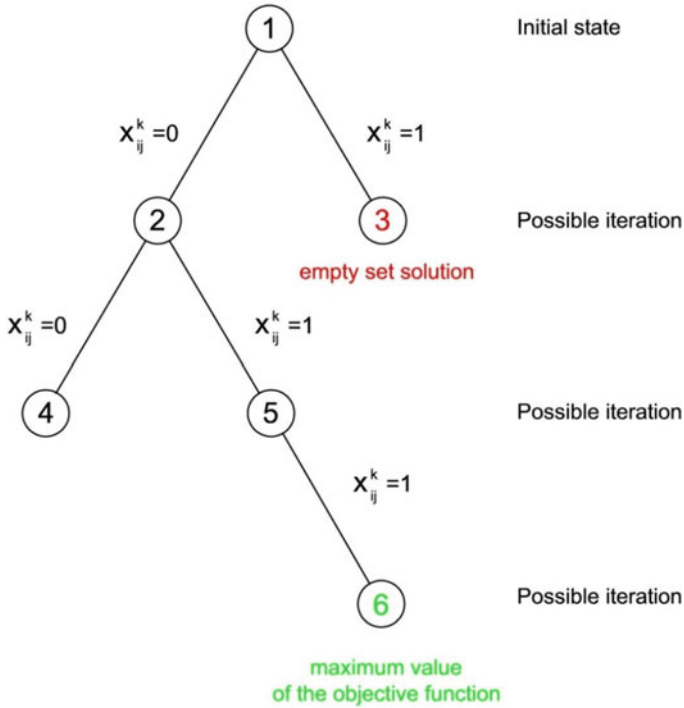
Fig. 2 Example branch and bound method diagram

Some items from the above list require a more detailed description. Due to the presence of constraints from items 7 and 8 from the formulation of the model, it becomes necessary to exclude variables. The exclusion of variables for a constraint of item 7 is performed as follows: if some variable satisfies the equality $x_{ij}^k = 0$, then this variable is excluded from the simplex table and at the same time is entered into the set of feasible solutions with the value 0. If some variable satisfies the equality $x_{ij}^k = 1$, then this variable is excluded from the simplex table and the excluded variable is entered into the set of feasible solutions with a value of 1, after which the constraint value from item 6 in the simplex table is reduced by 1 for the corresponding excluded variable. The exclusion of variables for the constraint from item 8 from the formulation of the model is performed as follows: if some variables satisfy the equality $x_{i_1j_1}^k + x_{i_2j_2}^k = 2$, these variables are excluded from the simplex table, and each excluded variable is entered into the set of feasible solutions with the value 1. After that, the value of the constraint from item 6 in the simplex table is reduced by 1 for each of the excluded variables.

To calculate the initial admissible basic solution for the original problem of assigning workers to building brigades it is necessary to compose and solve an auxiliary problem. The search for a solution to the auxiliary problem is performed by the simplex method, and if at the end of the calculations the value of the objective function is not equal to 0, then the set of all feasible solutions is empty.

When using the branch and bound method to solve the problem of assigning workers to building brigades, a peculiarity arises in relation to this problem, namely: if in the optimal solution of the original problem the variable x_{ij}^k turns out to be non-integer, then the first problem generated by the original problem differs from the original problem by adding a constraint of the form $x_{ij}^k = 0$, and the second problem generated by the original problem differs by adding a constraint of the form $x_{ij}^k = 1$. When a variable is branched, the variable should be excluded from the simplex table with the addition of the variable to the set of feasible solutions with the corresponding value (0 or 1). The process of excluding a variable is performed in accordance with the description of excluding a variable for constraints from item 7.

When excluding variables in accordance with the described algorithm, a situation may arise when one or several elements of the column of the right parts of the constraint system in the simplex table become negative. In this case, each such line of the simplex table must be multiplied by –1.

We created the computer code of the simplex method in combination with the method of boundaries and branches allows us to solve the above model of optimal assigning builder workers to brigades. The integer solution taking into account the maximum quality of work for example of assigning workers to brigades is presented in Table 1. As a result, it is noticeable that manual assignment due to the constraints from items 7 and 8 of the formulation of the model affects the composition of the formed brigades. For example, in the 2nd brigade for the worker of the 5th grade, worker number 2 in the qualification vector is assigned due to the prohibition of work in this brigade of the worker with the first number in the qualification vector. Also, in the 2nd brigade, the assignment of a worker of the 3rd grade with the lowest qualification (number 4 in the qualification vector) was made, which is also the result of manual assignment through a constraint from item 8 of the formulation of the model.

Table 1 Composition of brigades

Worker type	Workers numbers (j) from the vector of qualifications		
	Brigade number		
	1	2	3
Worker 5th grade	1	2	1
Worker 3rd grade	1	2	1
Worker 3rd grade	2	4	5
Worker 2nd grade	3	3	4
Worker 2nd grade	4	4	5

4 Conclusion

When planning and constructing buildings and structures, it is necessary to perform high-quality work at a minimal cost. One of the approaches to find a solution to this problem

is the use of mathematical models that allow you to find optimal solutions. Operations research theory is suitable for creating mathematical models that can help to obtain optimal solutions. This research provides a mathematical model for optimal assigning the composition of builder workers to the brigades. The formation of such brigades is carried out taking into account the classification of workers and their experience from the condition of maximizing the quality of their work. The model implies that the construction works are carried out sequentially by building brigades. This model is a linear programming problem and similar to the classical assignment problem, but unlike the latter, our model has additional constraints and there are no restrictions on the number of brigades to which one or another worker can be assigned. For these reasons, it is not possible to solve the proposed model with well-known algorithms such as the Hungarian method, etc. As methods for solving the mathematical model, it is proposed to use the simplex method in conjunction with the branch and bound method to obtain integer solutions. These methods are most efficient for obtaining integer solutions for this class of models. In this case, the algorithm includes an auxiliary problem, which is also solved by the simplex method.

This formulation of the model can find practical application in the management and organization of construction buildings and structures, especially when designing the construction of large projects. Using such models make it easier for the designer to find optimal solutions during the design. The model also provides the designer with the ability, through constraints, to assign workers to the required brigades, or, on the contrary, to forbid workers from working in brigades, either separately or together. The need for manual assignment of workers to brigades may arise for various reasons, such as the illness of a worker, dismissal of a worker, etc. The creation of software products based on similar optimization models allows to simplify the work of designer with big data and also reduces the appearance of incorrect decisions. Thus, the use of models for assigning workers to building brigades allows simplifying the work of the designer and reducing the time of his work. In addition, assigning workers to brigades, taking into account their qualifications and experience, not only improves the quality of construction production, but also leads to greater safety in the performance of their work due to the experience of workers. More skill and experience of workers leads to less indiscipline, which reduces the risk of unsafe situations.

References

1. Syrcova ED (1972) Matematicheskiye metody v planirovanii i upravlenii stroitel'nym proizvodstvom. Uchebnoye posobiye. Moscow, Vysshaya shkola
2. Caprara A, Fischetti M, Toth P, Vigo D, Guida PL (1997) Algorithms for railway crew management. Math Program 79(1):125–141
3. Caprara A, Toth P, Vigo D, Fischetti M (1998) Modeling and solving the crew rostering problem. Oper Res 46(6):820–830
4. Abbink EJW, Albino L, Dollevoet T, Huisman D, Roussado J, Saldanha RL (2011) Solving large scale crew scheduling problems in practice. Public Transp 3(2):149–164
5. Suyabatmaz AÇ, Şahin G (2015) Railway crew capacity planning problem with connectivity of schedules. Transp Res Part E: Logistics Transp Rev 84(C):88–100. https://doi.org/10.1016/j.tre.2015.10.003

6. Klabjan D, Johnson EL, Nemhauser GL, Gelman E, Ramaswamy S (2001) Solving large airline crew scheduling problems: random pairing generation and strong branching. Comput Optim Appl 20(1):73–91. https://doi.org/10.1023/A:1011223523191
7. Gershkoff I (1989) Optimizing flight crew schedules. Interfaces 19(4):29–43. https://doi.org/10.1287/inte.19.4.29
8. Chu HD, Gelman E, Johnson EL (1997) Solving large scale crew scheduling problems. Eur J Oper Res 97(2):260–268
9. Hoffman KL, Padberg M (1993) Solving airline crew scheduling problems by branch-and-cut. Manage Sci 39(6):657–682
10. Jütte S, Albers M, Thonemann UW, Haase K (2011) Optimizing railway crew scheduling at DB schenker. Interfaces 41(2):109–122
11. Marsten RE, Muller MR, Killion CL (1979) Crew planning at flying tiger: a successful application of integer programming. Manage Sci 25(12):1175–1183. https://doi.org/10.1287/mnsc.25.12.1175
12. Benichou M, Gauthier JM, Hentges G, Ribiere G (1977) The efficient solution of large-scale linear programming problems-some algorithmic techniques and computational results. Math Program 13:280–322. https://doi.org/10.1007/BF01584344
13. Karloff H (1991) Linear programming. Birkhäuser Basel, Birkhäuser Boston
14. Kuhn HW (1955) The Hungarian method for the assignment problem. Naval Res Logistics Q 2:83–97. https://doi.org/10.1002/nav.3800020109
15. Kuhn HW (1956) Variants of the Hungarian method for assignment problems. Naval Res Logistics Q 3:253–258. https://doi.org/10.1002/nav.3800030404
16. Munkres J (1957) Algorithms for the assignment and transportation problems. J Soc Ind Appl Math 5(1):32–38
17. Ahuja R, Magnanti T, Orlin J (1993) Network flows. Prentice Hall, New Jersey
18. Burkard R, Dell'Amico M, Martello S (2009) Assignment problems. Society for Industrial and Applied Mathematics, Philadelphia
19. Karloff H (2009) The simplex algorithm. In: Linear programming. Modern Birkhäuser Classics, Birkhäuser Boston, pp 23–47
20. Shamir R (1987) The efficiency of the simplex method: a survey. Manage Sci 33(3):301–334. https://doi.org/10.1287/mnsc.33.3.301
21. Bixby RE (1992) Implementing the simplex method: the initial basis. ORSA J Comput 4(3):267–284. https://doi.org/10.1287/ijoc.4.3.267
22. Dickson JC, Frederick FP (1960) A decision rule for improved efficiency in solving linear programming problems with the simplex algorithm. Commun ACM 3(9):509–512. https://doi.org/10.1145/367390.367411
23. Nabli H (2009) An overview on the simplex algorithm. Appl Math Comput 210(2):479–489. https://doi.org/10.1016/j.amc.2009.01.013
24. Maros I (2002) Computational techniques of the simplex method. Springer, London
25. Padberg M, Rinaldi G (1991) A branch-and-cut algorithm for the resolution of large-scale symmetric traveling salesman problems. SIAM Rev 33(1):60–100. https://doi.org/10.1137/1033004
26. Achterberg T, Koch T, Martin A (2005) Branching rules revisited. Oper Res Lett 33(1):42–54. https://doi.org/10.1016/j.orl.2004.04.002

Magnesium Oxide Mixture Technology for Construction Printer

A. V. Kiyanets[(✉)]

South Ural State University, 76 pr. Lenina, Chelyabinsk 454080, Russia

Abstract. Examined different compositions for a binder based on magnesium oxide for construction printing, evaluating the strength characteristics of the mixtures as well as the impact of their plasticity on pumpability and extrudability. Experiments were conducted in a laboratory per the standard methods according to GOST 5802-86, GOST 23789-79. Experiments showed the following characteristics of the mixture: the compressive strength was measured at up to 42 MPa; the curing rate on the first day was up to 38% of the 28-day compressive strength; and the mixture showed 0.44–0.78 water resistance. The shrinkage of the samples was 2.91–3.30 mm/m for aggregate-free mixtures and 0.85–1.69 mm/m for mixtures with an aggregate. The compositions with a plasticity of 55–120 mm showed distinguishing characteristics: uniform spread under the influence gravity, absence of stratification, homogeneity throughout the mixture. We obtained formulas to calculate the average flow of the material in a pipe (V) and the necessary pump drive power depending on the plasticity of the mixture (N).

Keywords: 3D-printing · Magnesium oxychloride cement · MOC · Rheology · Printable property · Pumpability

1 Introduction

Additive manufacturing technologies have become more widespread in modern industry due to a number of technical advantages over other methods of material processing and production. Due to the use of automated design systems, various complex products can be manufactured only through 3D printing. 3D printing is also one of the most promising areas of development in the construction industry. The advantages of this technology include saving material resources in the production of workpieces, enabling a high degree of automation and robotization of assembly and laying processes, the ability to create a physical version of a digital model of a building or structure (BIM technology), the ability to apply Generative Design, a significant increase in productivity, and reduced environmental pollution.

To date, several construction projects around the world have been completed through the application of 3D printers. The Chinese company Winsun is well-known because it built several objects using a frame (portal) 3D printer: several residential one-story houses in 2014 in China, two- and five-story buildings in 2015 in Suzhou Industrial Park,

and a one-story futuristic office building in Dubai, UAE [1]. American and European projects have developed the technology and equipment and have constructed demonstration houses and structures based on 3D printing technology [2]. There are also well-known Russian projects in this field. The mobile construction printer developed by the Russian company ApisSor, unlike most well-known systems, allows for the construction of houses and structures exceeding its own dimensions. In 2017, a small one-story 38 m^2 house was erected in the Moscow region using this printer. Thus, the development of additive technology in construction is a recognized global trend.

Despite variations in designs, the general layout of construction printers utilizing mixtures with a mineral binder consists of the following key systems and structural elements: a printing head positioning system in the form of a manipulator or mobile frame, a control system, and a system for preparing, transporting, and laying the construction mixture. The latter consists of a bin (or several bins) for loading the dry mixture, a continuous flow mixer, a water pump and pressure control system, a pump for the prepared mixture, a piping system, and a printing head (extruder).

By design, construction printers are divided into two main groups: portal printers, consisting of a frame that moves along guides, and manipulators with different degrees of freedom [3]. Some designs have features of both groups, therefore they are classified as "combined". Construction printers can also be categorized by the system of organization of construction operations: stationary, which print building elements and structures in factories; and mobile, which are used on the construction site. This technology is now actively developing and improving around the world; an intensive search for the best ideas and solutions is under way [4].

The effectiveness of a construction printer depends on three main components: the printer design, the software, and the mixture used. Modern mixtures proposed by various researchers for use in construction printers can be categorized by the binder used. These are mixtures based on mineral binders (cement, gypsum, etc.) [5], geopolymers [6], and various types of plastics, polymers, and metals. Taking into account the unique features of construction and operation of buildings and structures, currently, mixtures based on mineral binders and geopolymers with various types of aggregates are most suitable for a construction printer.

There are special processes and physical and mechanical requirements [7] for the mixtures used for construction printers. The process requirements include properties of the mixture which support the convenience and applicability for 3D printing: extrudability, workability, pumpability, the ability to withstand pressure from the overlying layers of the mixture without deformation during printing, and a setting time which ensures the specified duration of the process from the beginning of mixing to the beginning of structure formation processes in placed (printed) layers [8]. The physical and mechanical requirements include those set for structural materials in construction: strength, water resistance, low shrinkage, durability, etc. [9, 10]

The difficulty in choosing a mixture for construction printer is that some of the requirements are contradictory [11]. For example, the mixture should have good pumpability (fluidity) to be transported via pipes; on the other hand, it should not spread under the influence of gravity and the weight of the overlying layers during printing [12]. The mixture should harden quickly, ensuring high construction speed, but the strength gain

periods should not interfere with the construction process [13]. That is, after mixing and before the beginning of the setting time, the mixture should complete the entire technological cycle: mixture preparation, transportation from the mixer to the printing head, extrusion of the mixture through the print head, and applying the mixture in one layer.

One more problem in the development of mixtures for construction printers is the lack of generally accepted test methods; therefore, each researcher uses his/her own standards for experiments [14]. This complicates comparative analysis of the results.

Considering the above requirements, a magnesia binder-based mixture is a promising material for construction 3D printers. Magnesium oxychloride cement (MOC, magnesia binder) consists of two components: magnesium oxide MgO and a grouting fluid. The grouting fluid is an aqueous solution of salts; an aqueous solution of magnesium chloride $MgCl_2$ is most often used due to its high strength characteristics [15]. Studies on magnesia binder-based concretes and solutions have proved their high strength, high hardening rate, biological stability, and environmental safety [16, 17]. The acidity of the medium is close to neutral, making it possible use a wide range of organic, mineral, and synthetic aggregates in magnesia composites [18]. A number of additives have satisfactorily solved the problem of water resistance [19–21]. However, several processing characteristics remain unstudied [22]. This prevents the successful use of magnesium oxychloride cement-based mixtures in construction printers.

Therefore, the purpose of this study was to examine the properties of the magnesia binder-based mixture for construction 3D printers. To this end, it was necessary to solve a number of research tasks:

- study the strength characteristics of the mixture (strength, strength gain rate, water resistance, shrinkage deformation);
- determine the influence of the composition of the mixture on its rheological characteristics (determine the plasticity of the mixture);
- study the influence of the plasticity of the mixture on pumpability and extrudability.

2 Methods

We conducted an experiment to determine the physical and mechanical characteristics of the mortar mixture (Table 1). The following factors were taken as significant: the ratio of the magnesia binder to the aggregate, density of the grouting fluid solution (an aqueous solution of magnesium chloride), and the grain size of the aggregate (sand). The following characteristics were monitored: compressive strength of the solution at the age of 1, 3, 7, 28, 90, and 180 days; strength gain rate; water resistance of the magnesia solution. Water resistance was determined by the water resistance coefficient as a ratio of the strength of a sample aged in water to the strength of a sample hardened in dry conditions.

We conducted an experiment to establish the dependence and degree of influence of the magnesia mortar mixture composition on its rheological characteristics. The plasticity of the magnesia mortar mixture was determined according to the method described in GOST 23789-79 "Gypsum Binders. Test Methods" using a Suttard viscometer, which

Table 1 Mortar mixtures

No	MOC:sand ratio	Grouting fluid density, g/cm3	Grain size of sand, mm
1	1:1	1.15	0.63–0.315
2	1:1	1.15	2.5–1.25
3	1:3	1.15	0.63–0.315
4	1:3	1.15	2.5–1.25
5	1:1	1.25	0.63–0.315
6	1:1	1.25	2.5–1.25
7	1:3	1.25	0.63–0.315
8	1:3	1.25	2.5–1.25
9	1:2	1.20	0.63–0.315
10	1:2	1.20	2.5–1.25
11	1:1	1.20	1.25–0.63
12	1:3	1.20	1.25–0.63
13	1:2	1.15	1.25–0.63
14	1:2	1.25	1.25–0.63
15	1:2	1.20	1.25–0.63

is a stainless steel cylinder with a polished inner surface. The diameter of the mixture volume spread from the viscometer when raised characterizes the plasticity of the mixture.

The following factors, which most noticeably influenced the processing characteristics of the magnesia solution, were taken as significant: cement:sand ratio (by weight)—1:1, 1:2, 1:3; grain size of sand (aggregate)—0.315–0.63 mm; 0.63–1.25 mm; 1.25–2.5 mm; the ratio of the grouting fluid consumption to the magnesia cement consumption (by weight)—1:1; 1:2; 1:3.

An aqueous solution of magnesium chloride with a density of 1.2 g/cm^3 was used as grouting fluid. In addition to the plasticity of the mortar mixture, we also controlled the strength of the tested compositions (mixtures).

The dependence of the screw pump capacity on the plasticity of the mixture was studied on an experimental setup that included a bin for the dry mixture of the magnesia binder and sand with a mechanism to feed into the mixer, a water pump with a system to control the feed of the aqueous solution of magnesium chloride, a mixer, a screw pump, and a measuring tank.

The mixture was loaded into the dry mixture bin; an aqueous solution of magnesium chloride of the required density was poured into a special tank. The water pump was set to the desired capacity. When the machine was turned on, the dry mixture and bischofite were simultaneously fed into the mixer. The prepared mixture was fed into the screw pump, and then into the measuring tank. The finished mixture was transported through

a pipe with a diameter of 25 mm. Capacity was estimated as an arithmetic average of the results of three minutes of operation.

The shrinkage of the material was estimated by relative deformations of the samples with an accuracy of 0.01%. The significant factors for shrinkable deformations include the binder:aggregate ratio in the mixture and the density of the aqueous solution of magnesium chloride. The compositions for this experiment are shown in Table 2.

Table 2 Mixtures tested for shrinkage deformation

No	MOC/sand ratio	Density of the aqueous solution of magnesium chloride (g/cm^3)
1	1:3	1.15
2	1:2	1.15
3	1:1	1.15
4	1:0	1.15
5	1:3	1.20
6	1:2	1.20
7	1:1	1.20
8	1:0	1.20
9	1:3	1.25
10	1:2	1.25
11	1:1	1.25
12	1:0	1.25

3   Results and Discussion

The percentage of magnesia binder (MOC) in the mixture, which reflects the MOC:sand ratio (Fig. 1), has the greatest influence on the strength characteristics. The higher the binder content, the higher the strength. The density of the grouting fluid, on the contrary, does not have such a clear influence on strength. When the mixture has a high magnesium oxychloride cement content (MOC:S = 1:1, 1:2), there is a direct dependence of the strength gain on the increase in the density of the grouting fluid, and when the percent of the magnesium oxychloride cement content in the mortar mixture is decreased, the density of the grouting fluid does not have any noticeable influence on the strength. This can be linked with the existence of an optimal ratio of magnesite and magnesium chloride in the magnesia cement system. That is, provided that there is a sufficient amount of magnesite and magnesium chloride, the hydration reaction occurs intensively throughout the entire volume of magnesia cement, thus, we obtain high strength gain, which is observed in compositions with a high proportion of magnesia cement when mixed with solutions of different density [23].
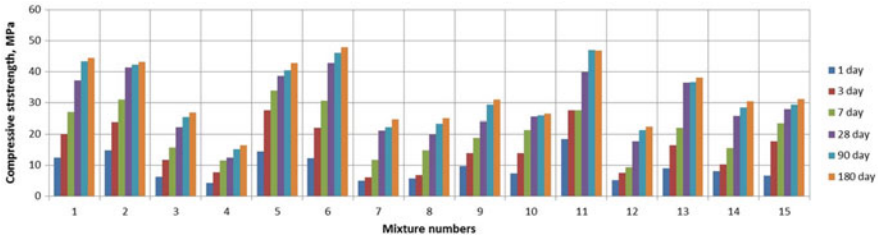
Fig. 1 Compressive strength at different ages of the studied compositions

In compositions with a relatively low content of magnesia cement, when the density of the grouting fluid is increased, oversaturation of the magnesia solution system with magnesium chloride is observed. The magnesium chloride has nothing to react with, since at a certain moment, no free MgO remains in the magnesia solution system when increasing the density of the grouting fluid (increasing the amount of magnesium chloride introduced into the system). Therefore, in this case, no matter how much the density of the grouting fluid introduced into the system increases, after it reaches the optimum magnesite:magnesium chloride ratio, the strength of the magnesia solution will not increase. This has also been noted by other researchers [24].

The strength gain rate of the studied magnesia solution compositions was 22–38% of the grade strength (28-day strength) on the 1st day, 33–68% on the 3rd day, and 50–88% on the 7th day (Fig. 2).
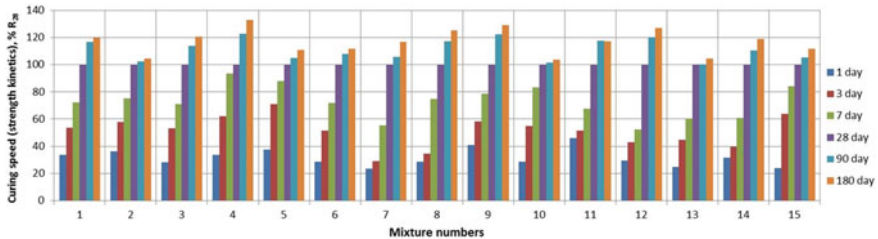
Fig. 2 Hardening speed of the studied compositions

When studying the water resistance of the magnesia solution, it has been established that, in general, it is within $Kw = 0.43$–0.78 (Fig. 3). With an increase in the density of the grouting fluid, the water resistance of the magnesia solution increases. When the density of the magnesium chloride solution is 1.15 g/cm^3, water resistance is influenced by the content of magnesia cement and the grain size of the sand: the smaller the grain size of the sand and the smaller the cement content, the higher the water resistance. If the density of the grouting fluid is 1.20 g/cm^3, water resistance does not depend on the changes in the values of the selected impact factors, and if the density is 1.25 g/cm^3, water resistance depends only on the grain size of the sand: the larger the grain size, the higher the resistance. This behavior of the material is primarily related to grain packing density and the thickness of the binder film. The smaller the thickness of the binder film

and the denser the material structure, the less the influence of water on the binder, and the less the strength decreases. In addition, the optimum $MgO:MgCl_2$ ratio also has an effect [25, 26]. If there is no unreacted caustic magnesite or magnesium chloride in the material, the water resistance increases.
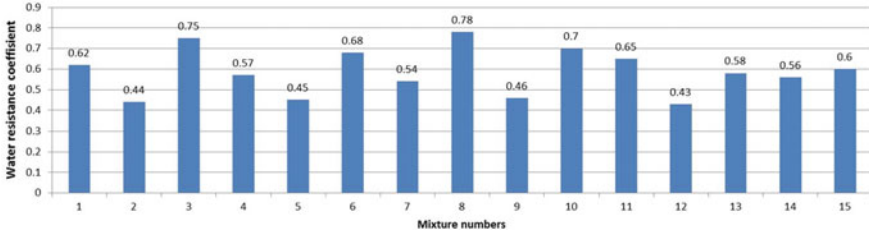
Fig. 3 Water resistance of the studied compositions from Table 2

The cement:sand ratio had the greatest influence on the development of shrinkage deformations. The samples with the lowest aggregate content in their composition were subject to maximum shrinkage. The most intense shrinkage develops in the first 7–10 days of hardening, equal to 50–60% of the maximum value. Then, the growth rate of shrinkage deformations decelerates. This pattern of deformation development relates to the processes of active curing, which take place in the initial period of hardening. The density of the grouting fluid solution had a less noticeable influence: the higher the density of grouting fluid used, the smaller the shrinkage value. The maximum value of shrinkage by the end of the studied period was: for aggregate-free compositions—0.291–0.330% (2.91–3.30 mm/m); for compositions with a 1:1 MOC:sand ratio—0.152–0.169% (1.52–1.69 mm/m); for compositions with a 1:2 MOC:sand ratio—0.113–0.123% (1.13–1.23 mm/m); for compositions with a 1:3 MOC:sand ratio 1/3—0.085–0.101% (0.85–1.01 mm/m).

The plasticity of the magnesia mortar mixture mainly depends on the grouting fluid to magnesia binder ratio, as well as the binder to aggregate ratio. When these factors change within the chosen limits of variation, the plasticity of the mixture varies from 50 to 135 mm (Fig. 4). An increase in the grouting fluid to magnesia binder ratio (an increase in the amount of the introduced grouting fluid) unambiguously lead to an increase in the mobility of the mixture. An increase in the cement:sand ratio lead to an increase in the plasticity of the mixture only with a proportional increase in the amount of the introduced grouting fluid; an increase in the MOC:S with a constant amount of grouting fluid lead to a decrease in the plasticity of the mixture.

The compositions with a low content of magnesia binder (MOC:S = 1:3) and grouting fluid (GF:MOC = 0.35–0.45) were rigid and non-plastic. Mixing these compositions in the mixer and pumping them through the pipe to the extruder would be impossible or require significant energy consumption by the mixer and pump drives. To avoid a significant increase in the hydraulic resistance of such a rigid mixture when it is pumped through the pipe, and to avoid "blocks", it is necessary to impose restrictions on bends in the pipe. The restrictions concern the quantity and quality of the angles of bending through which the mixture is pumped. The degrees of freedom of the printer arm along
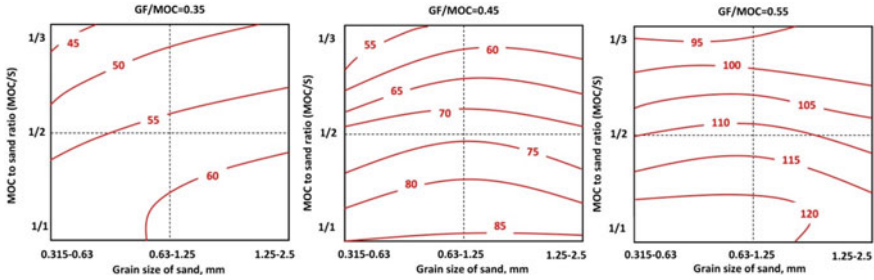
Fig. 4 The dependence of the plasticity of the mortar mixture on its composition

all axes will be significantly restricted. These compositions also showed an obvious lack of cement paste, which ensures the reliable bonding of aggregate grains, leading to low final strength and low adhesion of new layers of the mixture to the old ones.

The compositions with a plasticity from 55 to 120 mm showed differences in uniform spread under the influence of gravity, formed a figure which is closest to a geometrically correct circle, lacked stratification, and showed homogeneity throughout the mixture. If the plasticity of the mixture increases from 60 to 120 mm, pump capacity increases from 7.37 to 15.07 L per minute. This pattern of dependence is logical and can be explained by the decrease in the pump energy consumption for pumping the mixture. This is ensured by an increase in the mixture fluidity and a decrease in the shear stress. The average flow rates in a 25 mm-diameter pipe for the studied compositions were 0.09–0.18 m/s (1):

$$V = \frac{P_r}{3600\pi D^2} = \frac{0.0015P_l^2 - 0.1423P_l + 10.55}{3600\pi D^2}, \tag{1}$$

where V is the average flow rate of the material, m/s; P_r is the pump capacity, m³/h; D is the diameter of the pipe, m²; and P_l is the plasticity of the mixture, mm.

The necessary pump drive power to ensure the required capacity can be calculated using formula (2):

$$N = \frac{PP_r}{1020\eta\pi D^2}, \tag{2}$$

where N is pump drive power; P is the total force required to move the mixture through the pipe; and η is the efficiency of the screw pump.

The mixture threads produced with the above parameters will be unbroken, from 16 to 65 mm high, and from 61 to 118 mm wide. These characteristics allow us to use the mixture to print structures [27, 28].

4 Conclusions

Strength characteristics of a mixture based on a magnesia binder and sand (mortar mixture): the compressive strength was 12–42 MPa, the curing rate on the first day

was 22–38% of the 28-day strength, on the third day—33–68%, on the seventh day—50–88%, and water resistance Kw = 0.44–0.78. The shrinkage of the samples was 2.91–3.30 mm/m for aggregate-free mixtures and 0.85–1.69 mm/m for mixtures with an aggregate. The strength characteristics depend on the composition of the solution and the density of the grouting fluid. When magnesia binder consumption increases, strength increases; when the density of the grouting fluid increases, strength increases only in the compositions with a high content of magnesia cement (with a cement to sand ratio by weight larger than 1:2). The grain size of the aggregate (sand) does not have a noticeable influence on the strength of the magnesia solution.

The water resistance of the magnesia solution increases with an increase in the density of the grouting fluid, as well as with an increase in the grain sizes of the aggregate, when the density of grouting fluid is 1.20–1.25 g/cm^3.

Hardening of the magnesia solution is closely related to the development of shrinkable deformations. The cement:sand ratio has the greatest influence on shrinkage of the magnesia mortar. An increase in the amount of aggregate in the mixture reduces shrinkage. The aggregate compensates for shrinkage deformations. The grain size of the aggregate does not play a decisive role. When mixing the magnesia solution, an increase in the density of the magnesium chloride solution contributes to minimizing the development of shrinkage deformations during further hardening.

The plasticity of the magnesia mortar mixture mainly depends on the ratio of the grouting fluid to the magnesia binder, as well as the binder to aggregate ratio. Compositions with a plasticity of 55–120 mm showed distinguishing features: uniform spread under the influence of gravity, absence of stratification, homogeneity throughout the mixture. We obtained formulas for calculating the average flow rate of the material in the pipe (V) and the required pump drive power depending on the plasticity of the mixture (N).

The results of experiment allow us to recommend the following parameters for 3D construction printer mixtures: the binder to aggregate ratio by weight should be 1:1–1:2 if the grain size of the aggregate is up to 1.25 mm, and 1:3 if the grain size of the aggregate is over 1.25 mm; the amount of the grouting fluid should ensure mixture plasticity when the grouting fluid to binder ratio is 0.4:1–0.55:1, and the density of the grouting fluid should be at least 1.2–1.25 g/cm^3. The above parameters of the mixture will support printing of layers with a height of 16–65 mm and a width of 61–118 mm at an extrusion speed of 0.09–0.18 m/s, provided that the diameter of the extruder nozzle is 25 mm.

References

1. Vatin NI, Chumadova LI, Goncharov IS, Zykova VV, Karpenya AN, Kim AA, Finashenkov EA (2017) 3D-printing in construction. Constr Unique Build Struct 52:27–46. https://doi.org/10.18720/CUBS.52.3

2. Shatornaya AM, Chislova MM, Drozdetskaya MA, Ptuhina IS (2017) Efficiency of 3D printers in Civil Engineering. Constr Unique Build Struct 60:22–30. https://doi.org/10.18720/CUBS.60.2

3. Shakor P, Sanjayan J, Nazari A, Nejadi S (2017) Modified 3D printed powder to cement-based material and mechanical properties of cement scaffold used in 3D printing. Constr Build Mater 138:398–409. https://doi.org/10.1016/j.conbuildmat.2017.02.037

4. Bong SH, Nematollahi B, Nazari A, Xia M, Sanjayan J (2019) Method of optimisation for ambient temperature cured sustainable geopolymers for 3D printing construction applications. Materials 16:902. https://doi.org/10.3390/ma12060902

5. Ding Z, Wang X, Sanjayan J, Zou PXW, Ding Z (2018) A feasibility study on HPMC-improved sulphoaluminate cement for 3D printing. Materials 11:2415. https://doi.org/10.3390/ma11122415

6. Xia M, Nematollahi B, Sanjayan J (2019) Printability, accuracy and strength of geopolymer made using powder-based 3D printing for construction applications. Autom Constr 101:179–189. https://doi.org/10.1016/j.autcon.2019.01.013

7. Le TT, Austin SA, Lim S, Buswell RA, Gibb AGF, Thorpe T (2012) Mix design and fresh properties for high-performance printing concrete. Mater Struct 45:1221–1232. https://doi.org/10.1617/s11527-012-9828-z

8. Ma G, Wang L (2018) A critical review of preparation design and workability measurement of concrete material for large-scale 3D printing. Front Struct Civ Eng 12:382–400. https://doi.org/10.1007/s11709-017-0430-x

9. Barabanshchikov YuG, Belyaeva SV, Arkhipov IE, Antonova MV, Shkol'nikova AA, Lebedeva KS (2017) Influence of superplasticizers on the concrete mix properties. Mag Civil Eng 6:140–146. https://doi.org/10.18720/MCE.74.11

10. Fediuk RS, Lesovik VS, Svintsov AP, Mochalov AV, Kulichkov SV, Stoyushko NY, Gladkova NA, Timokhin RA (2018) Self-compacting concrete using pretreatmented rice husk ash. Mag Civil Eng 3:66–76. https://doi.org/10.18720/MCE.79.7

11. Yu J, Leung CKY. (2019) Impact of 3D printing direction on mechanical performance of strain-hardening cementitious composite. RILEM Bookseries 19:255–265. doi:https://doi.org/10.1007/978-3-319-99519-9_24

12. Zhang Y, Zhang Y, She W, Yang L, Liu G, Yang Y (2019) Rheological and harden properties of the high-thixotropy 3D printing concrete. Constr Build Mater 201:278–285. https://doi.org/10.1016/j.conbuildmat.2018.12.061

13. Panda B, Singh GB, Tan MJ (2019) Synthesis and characterization of one-part geopolymers for extrusion based 3D concrete printing. J Clean Prod 220:610–619. https://doi.org/10.1016/j.jclepro.2019.02.185

14. Kazemian A, Yuan X, Meier R, Khoshnevis B (2019) A framework for performance-based testing of fresh mixtures for construction-scale 3D printing. RILEM Bookseries 19:39–52. doi:https://doi.org/10.1007/978-3-319-99519-9_4

15. Zhou X, Li Z (2012) Light-weight wood-magnesium oxychloride cement composite building products made by extrusion. Constr Build Mater 27:382–389. https://doi.org/10.1016/j.conbuildmat.2011.07.033

16. Lu Z, Zhang J, Sun G, Xu B, Li Z, Gong C (2015) Effects of the form-stable expanded perlite/paraffin composite on cement manufactured by extrusion technique. Energy 82:43–53. https://doi.org/10.1016/j.energy.2014.12.043

17. Nguyen VC, Tong FG, Nguyen VN (2019) Modeling of autogenous volume deformation process of RCC mixed with MgO based on concrete expansion experiment. Constr Build Mater 210:650–659. https://doi.org/10.1016/j.conbuildmat.2019.03.226

18. Siddique R, Naik TR (2004) Properties of concrete containing scrap-tire rubber. Waste Manage 24:563–569. https://doi.org/10.1016/j.wasman.2004.01.006

19. Tan Y, Liu Y, Grover L (2014) Effect of phosphoric acid on the properties of magnesium oxychloride cement as a biomaterial. Cem Concr Res 56:69–74. https://doi.org/10.1016/j.cemconres.2013.11.001

20. Chen X, Zhang T, Bi W, Cheeseman C (2019) Effect of tartaric acid and phosphoric acid on the water resistance of magnesium oxychloride (MOC) cement. Constr Build Mater 213:528–536. https://doi.org/10.1016/j.conbuildmat.2019.04.086

21. Wang Y, Wei L, Yu J, Yu K (2019) Mechanical properties of high ductile magnesium oxychloride cement-based composites after water soaking. Cement Concr Compos 97:248–258. https://doi.org/10.1016/j.cemconcomp.2018.12.028

22. Nerella VN, Nather M, Iqbal A, Butler M, Mechtcherine V (2019) Inline quantification of extrudability of cementitious materials for digital construction. Cement Concr Compos 95:260–270. https://doi.org/10.1016/j.cemconcomp.2018.09.015

23. Li Z, Chau CK (2007) Influence of molar ratios on properties of magnesium oxychloride cement. Cem Concr Res 37:866–870. https://doi.org/10.1016/j.cemconres.2007.03.015

24. Sglavo VM, DeGenua F, Conci A, Ceccato R, Cavallini R (2011) Influence of curing temperature on the evolution of magnesium oxychloride cement. J Mater Sci 46:6726–6733. https://doi.org/10.1007/s10853-011-5628-z

25. Misra AK, Mathur R (2007) Magnesium oxychloride cement concrete. Bull Mater Sci 30:239–246. https://doi.org/10.1007/s12034-007-0043-4

26. Li Y, Yu H, Zheng L, Wen J, Wu C, Tan Y (2013) Compressive strength of fly ash magnesium oxychloride cement containing granite wastes. Constr Build Mater 38:1–7. https://doi.org/10.1016/j.conbuildmat.2012.06.016

27. Li G, Yu Y, Li J, Wang Y, Liu H (2003) Experimental study on urban refuse/magnesium oxychloride cement compound floor tile. Cem Concr Res 33:1663–1668. https://doi.org/10.1016/S0008-8846(03)00136-4

28. Mechtcherine V, Nerella VN (2019) 3D-concrete-printing by selective deposition—requirements for fresh concrete and testing. Beton- und Stahlbetonbau 114:24–32. https://doi.org/10.1002/best.201800073

Financing Housing Construction in the Russian Federation Using Escrow Accounts

L. A. Guzikova[✉] and N. V. Neelova

Peter the Great Saint-Petersburg Polytechnic University, 29, Politekhnicheskaya ul,
Saint-Petersburg 195251, Russia

Abstract. Financing is always a critical factor in construction: compliance with
the deadlines for the completion of work, the cost of the object for the customer
and the financial result of the developer depend on its organization. The paper
deals with theoretical and practical problems associated with sources of housing
construction financing in the Russian Federation. The reasons for the transition
to using escrow accounts are discussed. The positive and negative sides of this
transition are revealed and an assessment of its consequences is carried out. The use
of IFRS as the most reliable data source on the activities of construction companies
in the Russian Federation is substantiated. Changes in the construction companies
financing are analyzed on the base of their IFRS statements. The conclusion is
made about the formation of new tendencies in the structure of financing for the
activities of large developers. The results of the study can be useful for the heads,
managers and accountants of construction companies, as well as for researchers
investigating construction financing.

Keywords: Housing construction · Developer · Financing · Escrow account ·
Structure of Financing

1 Introduction

Constructing multi-apartment residential buildings is expensive and time-consuming,
which makes its financing especially important. A construction company, like any other
firm, has three main sources of financing for its activities: its own funds (authorized
capital, reserves, retained earnings), borrowed funds (bank loans, issued bonds, loans)
and advances received from buyers.

Most of the housing on the primary market in the Russian Federation is sold at the
construction stage under agreements for participation in shared construction (APSC).
Until recently, funds received immediately on the developers' accounts from the shared
construction participants (share participants) constituted the main source of construc-
tion financing. At the same time, the risks of stopping construction and bankruptcy of
the developer fell on individuals, creating the so-called "defrauded share participants"
problem [1]. To reduce these risks, Art. 3 of the Federal Law of December, 30, 2004 No.
214-FZ "On participation in the shared construction of apartment buildings and other real

estate objects and on amendments to some legislative acts of the Russian Federation", the requirements for developers raising funds from share participants were restricted.

In 2017, the Fund for the Protection of the Rights of Citizens—Participants of Shared Construction was created. In the case of the developer's bankruptcy, the Fund should make a decision on financing the completion of construction or paying compensation to share participants from the compensation fund. According to the Federal Law of July 29, 2017 No. 218-FZ "On a public law company for the protection of the rights of citizens participating in shared construction", compensation funds should be formed by compulsory contributions from developers entering into APSC without using escrow, in the amount of 1.2% of the cost of the agreement, and funds from the federal and regional budgets on co-financing terms.

Current contributions from developers do not cover liabilities to share participants: the increase in the actuarial deficit of the compensation fund from 616.2 billion rubles as of 01.01.2020 to 1,028.2 billion rubles as of 31.12.2024 is foreseen. According to the Accounts Chamber, during 2017–2019 the Fund received 102.8 billion rubles, including 42.4 billion rubles from developers, 43.6 billion rubles from the federal budget, 14.2 billion rubles from the budgets of the constituent entities of the Russian Federation [2]. As of 01.01.2020, the Fund needed 686 billion rubles to complete the construction of 3137 problematic residential buildings. In 2020, within the framework of anti-crisis measures, the Fund got 30 billion rubles of federal funds and budget subsidies for 2021–2023 have not yet been provided to the Fund. The regions plan funds for the problematic facilities completion in 2020–2022 in the amount of about 40 billion rubles. Although the "road maps" of most of the constituent entities of the Russian Federation planned to solve the problem of "defrauded share participants" in 2020–2023, at the end of February 2021, 1086 developers still had 2856 problematic objects.

According to the results of the audit of the Fund's activity undertaken by the Accounting Chamber, alongside the problem of insufficient funding, the low efficiency is also noted: as of January 1, 2020, the funds were used only by 16.6% [2].

The practice has shown, that the tightening of requirements and control of state bodies over developers attracting funds from share participants, and the mandatory contributions to the compensation fund did not completely avoid the emergence of problematic objects and the need to restore the rights of affected individuals—share participants, mostly at the expense of budget funds. To fundamentally change the current situation, the Government of the Russian Federation on December 21, 2017 approved the "Action Plan ("road map") for the phased replacement within three years of funds of individuals attracted to create apartment buildings and other real estate objects, with bank lending and other forms of financing minimizing the risk for citizens"[3].

The purpose of this study is to analyze the sources of financing for housing construction in the context of the "road map" implementation.

2   Methods and Data

The study is based on the analysis of the regulatory legal acts of the Russian Federation governing the activities of developers in financing housing construction with share participation and the IFRS reporting data of the 9 largest companies for 2018, 2019 and the first half of 2020 (Table 1). Descriptive statistics and structural analysis methods were used.

Table 1 Sources of IFRS statements of the developers

Developer	Website
PIK Group of Companies, PJSC	https://www.e-disclosure.ru/portal/files.aspx?id=44&type=4&attempt=1
LSR Group, PJSC	https://www.lsrgroup.ru/investors-and-shareholders/disclosure-of-information
Ingrad, PJSC	https://e-disclosure.ru/portal/files.aspx?id=1664&type=4
Setl Group, LLC	https://www.setlcity.ru/investors
Etalon LenSpetsSMU, JSC	https://finance.lenspecsmu.ru/debtinvestors/reporting/consolidated_statements.php
Group of Companies Samolyot, PJSC	https://samolet.ru/investors/documents/
Group of companies Pioneer, JSC	https://www.pioneer.ru/company/investors
Leader-Invest, JSC	https://www.e-disclosure.ru/portal/files.aspx?id=36668&type=4
Legenda, LLC	https://legenda-dom.ru/investoram/material-facts

3   Main Provisions and Results

To implement the "road map", amendments have been made to the legislation.

According to APSC submitted for state registration after July 1, 2019, share participants must deposit funds for paying the contract price on escrow accounts opened in the authorized banks (paragraph 1 section 15.4, Law No. 214-FZ). No interest is paid on these funds. After the developer gets a permit to put the building into operation, the developer submits it to the bank, and the latter transfers funds from escrow accounts to the developer or directs the funds to repay the target loan for construction, if stated in the loan agreement. In the case of cancellation of the agreement, its termination or unilateral refusal of one of the parties, funds from the escrow account are returned to the shared participant and (or) to the bank which provided the shared participant with the loan [4]. Thus, share participants are guaranteed to receive an apartment or to return the deposit (sections 15.4, 15.5, Law No. 214-FZ) [5, 6].

The share participants' funds are also insured against license revocation of an authorized bank in the amount of 100%, in total, no more than 10 million rubles on all escrow accounts in one bank (section 13.1, Federal Law of December 23, 2003 No. 177-FZ "On Insurance of Deposits in Banks of the Russian Federation"). The reimbursement is transferred on the share participant's escrow account in another bank opened for settlements on the same construction object (section 13.2, Law No. 177-FZ).

The "road map" provides the transition of construction financing from share participants as unqualified investors to qualified investors, in particular, to banks in the form of targeted loans [7]. This helps prevent the emergence of "defrauded share participants", to spare the budget expenditures to restore their rights, to abolish the control of developers by state bodies through transferring financial risks along with control and regulatory functions to banks, which should presumably perform these functions in a more concerned, detailed and efficient manner [8]. Permanent monitoring should contribute to the improvement of developers' business processes technological level, personnel qualifications and the quality of the projects implemented. Paying loans and opening escrow accounts only after the commissioning of the facility building stimulates not to delay the construction period. Loan funds cover cash gaps, reduce the construction progress dependence on sales: they allow selling at a higher stage of readiness, therefore, more expensively, and avoiding price reduction in case of unfavorable market conjuncture. Construction with the use of escrow causes more confidence among the population due to share participants' rights protection.

In order to transit to bank financing, "Recommendations on determining the optimal procedures for interaction between authorized banks and developers in the transition to project financing of shared housing construction using escrow accounts" were developed (Letter of the Ministry of Construction of Russia No. 13275-VYa / 07, Bank of Russia No. 01-40 / 2711, JSC "DOM.RF" No. 4373-AP of 15.04.2019). The letter recommends taking into account the "Performance standards, characteristics and requirements for developers for the purpose of lending to the construction (creation) of apartment buildings and (or) other real estate objects", developed by JSC "DOM.RF", and Bank of Russia Regulation No. 590-P of 28.06. 2017. As a result, most of the requirements for developers established by Law No. 214-FZ (subparagraph 2 paragraph 1 section 2, subsection 1.1 section 3, paragraphs 1.1–1.8 and 7 subsection 2 section 3, subsections 2.3 and 4 section 3, subsections 2, 5–7 section 9, sections 12.1, 13–15, 18, 18.1 and 18.2) became unnecessary when using escrow accounts [9], and were included into requirements of banks for obtaining target loan. To ensure the safety margin of the project, the loan life cover ratio (LLCR) should be not less than 1.2 (paragraph 6.2 of "Standards …"). To increase the transparency of activities, the developer's group should publicly disclose the audited consolidated IFRS statements (paragraph 3.4).

As of February 2021, according to JSC DOM.RF, 56.2% (51.8 million m^2) out of 92.2 million m^2. of housing under construction was financed using escrow accounts, 38.1% were completed in the former manner with the contributions to the compensation fund and 5.7%—ithout using funds from the population. 63% of housing completed in the former order is planned to be commissioned in 2021 and another 22%—in 2022. Projects without financing from the population are usually small and with a short construction period: for example, the average number of apartments in buildings under construction

using escrow accounts is 214, with contributions to the compensation fund—236, without funds from population—153.

According to the Bank of Russia, by the end of 2020, the volume of share participants' funds in escrow accounts increased 8 times compared to 2019, and the limit of loans provided to developers—3 times. As of February 1, 2021, 313 thousand escrow accounts were opened in the total amount of 1.26 trillion rubles, 2404 credit agreements were concluded for 3.084 trillion rubles with the current amount of 1.1 trillion rubles. Since October 2020, the total amount of funds on escrow accounts exceeds the developers' loan arrears.

During the transition to project financing of construction, the following problems were identified in practice [10, 11]:

1. Different authorized banks have different requirements for borrowers and call for different packages of documents, use different interaction procedures. The Bank of Russia reacted negatively to the unified comprehensive list of documents proposed by the National Association of Builders at the end of 2019 [12]. The regulator believes that this approach is contrary to market mechanisms and violates the "freedom of contract principle".

    According to the Bank of Russia, by the beginning of 2020 the number of applications for project financing increased 10 times to 3325. 40% of the applications were rejected. The main reasons for refusals are the negative business reputation of the borrower, failure to provide proper documents, inconsistency with the bank's credit policy, insufficient equity funds, lack of necessary collateral, low project margins [13].

2. Regional construction projects tend to have lower margins and their LLCR often falls below the recommended 1.2. According to Expert RA agency estimates, only 40% of regions have gross profit margins in housing construction exceeding 10% [14]. Previously, regional projects were financed mainly from the funds of share participants, and 80% of developers have no enough experience in forming other financial models and interacting with banks. The costs of auditing small regional projects and preparing documentation are commensurate with large construction projects but the margin is lower. This makes it difficult to obtain project financing in the regions.

According to the Bank of Russia, as of February 1, 2021, there were no open escrow accounts in the Jewish Autonomous Region, Kamchatka Territory, Magadan and Murmansk Regions, Chukotka and Nenets Autonomous Districts, Ingushetia, Chechnya, Karachay-Cherkessia and Tyva. In these regions, the share of individual housing construction is higher than the average for the Russian Federation. In Dagestan, Altai and Adygea, insignificant funds (0.7 million rubles, 2.1 million rubles, 166.7 million rubles, respectively) have been placed on escrow accounts and there were no concluded credit agreements.

1. The pledge of more than 75% of the developer's shares (stakes) (paragraph 7.9 of "Standards …") creates problems when financing other construction projects in other banks.

2. Funds on escrow accounts are intended exclusively for housing construction and cannot be used to create mandatory social infrastructure (kindergartens, amenities objects, etc.) [15].

3. Until November 2020, funds on escrow accounts were not recognized as targeted funding that is exempt from taxable income. As a result, the entire amount of revenue from the sale of shared construction objects was considered as income when using escrow accounts [16, 17]. This was especially critical for developers using the simplified tax system, since a sharp increase in income violates the conditions for using the simplified taxation system—no more than 150 million rubles for the year (paragraph 4 section 346.13, Tax Code of the Russian Federation) and requires a transition to a common taxation system. This tax conflict was resolved only by the adoption of Federal Law No. 368-FZ on 09.11.2020. Funds of share participants on escrow accounts from 01.01.2020 are equated to targeted financing funds that are excluded from taxable income under the general and simplified taxation system (subparagraph 14 paragraph 1 section 251, Tax Code of the Russian Federation).

In the scientific sources, a number of ambiguous effects of the mandatory use of ecrow accounts are noted:

1. It became more difficult for developers to find financing, and now it is required in a larger volume, since earlier funds were immediately transferred to a single current account, which allowed the company to solve unforeseen difficulties by transferring share participants' funds from one project to another [18].

2. The use of escrow accounts may force developers to refuse various kinds of discounts that share participants could have counted on before [10].

3. The prime cost of developers' projects may grow [19], a decrease in the volume of housing commissioning and an increase in prices may occur. However, in large cities, a slight decrease in prices is possible due to the high competition of developers [10].

4. The ability to obtain financing became more dependent on the level of prices at the place of implementation of the project [20].

5. Threat of deprivation of the developer of the right to use escrow accounts if the commissioning deadline is violated of at least one object from a large residential complex [21].

6. The developers became insecure from corrupt bank employees, a limited choice of credit institutions, a small amount of insurance payments for loss of funds [19].

7. Since the bank that approved the loan controls its intended use, the developer is restricted in using borrowed funds and cannot invest them in the construction of other objects, use them to pay off other loans, etc. From the standpoint of the share participants, this is seen to a greater extent as a positive, however, restrictions on the use of funds may worsen the general position of the developer and, thus, negatively affect the interests of the share participants [22].

8. The obligatory use of escrow accounts has not fully protected the participants in shared construction from fraud. In order to attract funds, unscrupulous developers began to use investment agreements with individuals and legal entities, on the basis of

which developers sell apartments in buildings under construction, under the pretext of investing in a commercial organization [23].

At the same time, the proper management of financial flows and the appropriate choice of a sales strategy can allow developers to significantly improve the financial performance of projects [24]. In order to minimize the amount of interest payments, the developer should use a sales strategy that provides a minimum loan rate. Since the developer is interested in the growth of profits and profitability indicators of the project, then, in addition to changing the factor of production activities' profitability due to the physical volume of sales, the sales price should be additionally varied. In [24], a mathematical toolkit for analyzing the factors of increasing the profitability of production activities in the construction industry is proposed, which allows the developer to track current financial flows promptly and to optimize financial indicators.

According to the Bank of Russia estimates, before the transition to project financing, about 4 trillion rubles were invested in housing construction in the Russian Federation. rubles, of which 650 billion rubles—funds of credit institutions, 400 billion rubles—developers' own funds, the rest—funds of share participants [25]. Now these ratios must change. Let us consider in more detail the structure of construction financing and its dynamics according to the financial statements of the largest developers.

Large construction companies often organize their activities in the form of holdings. Russian accounting statements do not provide a complete picture of the activities of such groups. The functioning of the group as a single business entity is presented only in its consolidated financial statements under IFRS. Most of the largest construction companies are bond issuers and are required to prepare annual and interim consolidated statements in the event of registration of a securities issue prospectus (paragraph 2, paragraph 4, section 30, Federal Law No. 39-FZ of 22.04.1996 "On the Securities Market") or admission of securities to organized trading by inclusion into quotation list (paragraph 8 subsection 1 section 2, Federal Law No. 208-FZ of July 27, 2010 "On Consolidated Financial Statements") [26].

We calculated the average values of the portions of the financing sources of the developers under consideration and analyzed their variation (Table 2). The dynamics of the averaged structure of liabilities of the companies is shown in Fig. 1.

The coefficients of variation exceeding 33% indicate the heterogeneity of the analyzed sample, significant differences in the structure of financing for individual companies. The smallest variation is observed for the item "Contract liabilities".

In the structure of assets of all construction holdings, the largest proportion (over 60%) is occupied by inventories, including land plots for construction, building materials, construction in progress, ready-made apartments for sale. In the structure of funding sources, the largest share (about 30%) is constituted by obligations under contracts with buyers. Thus, so far almost half of the construction costs are still financed from prepayments received from buyers. The proportion of this source is diminishing as the objects with the former financing procedure are completed.

The decrease in the proportion of liabilities to buyers from 32.6 to 26.2% is offset by an increase in raising funds on loans and issued bonds, the proportion of which in liabilities is approximately the same (11–14%) [27]. The highest growth rate is demonstrated

Table 2 Averaged indicators of the consolidated statements of the analyzed companies (compiled by the authors)

Indicator	Mean share (%)			Coefficient of variation (%)		
	31.12.18	31.12.19	30.06.20	31.12.18	31.12.19	30.06.20
Equity	20.7	21.3	22.0	60.3	58.2	58.2
Bank loans	11.3	12.0	12.1	86.3	58.0	74.8
Escrow-backed loans	0.1	1.6	2.6	300.0	180.2	173.0
Bonds issued	11.3	12.9	14.3	68.5	61.4	72.1
Non-bank loans	0.3	0.6	0.5	111.5	195.8	124.3
Contract liabilities	32.6	30.3	26.2	35.3	33.9	36.1
Other liabilities	23.7	21.3	22.3	41.8	45.4	48.7
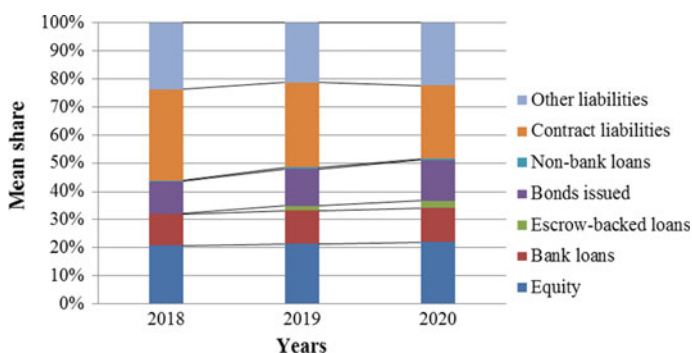
Fig. 1 Dynamics of the averaged structure of analyzed companies' financing

by loans within the framework of escrow financing, which still constitute an insignificant part of liabilities (2.6% as of June 30, 2020). This item also has the greatest variation across companies that among other reasons may be caused by the lack of information disclosure on such loans by some companies.

Analysts expect more developers to enter the bond market: by the end of 2021, the number of issuers will reach 35–40, in addition to the largest companies that have already received more than 200 billion rubles in the market new participants will borrow up to 30 billion rubles [14]. To issue bonds, fewer documents are required, no collateral is needed, funds can be used more freely than targeted loans, a public history of the issuer is formed, which can simplify further obtaining project financing. But due to high credit risks, the cost of such borrowings may exceed the lending rate. The state is ready to provide support to issuers from priority sectors, including construction. Resolution of the Government of the Russian Federation No. 532 of April 30, 2019 approved the "Rules for the provision of subsidies from the federal budget to Russian organizations—small and medium-sized businesses in order to compensate for part of the costs of issuing shares and bonds and paying coupon income on bonds offered on the stock exchange."

Actually incurred expenses on the offer of bonds can be reimbursed in the amount of 2% of the nominal value, but not more than 1.5 million rubles, and coupon payments—in the amount of 70% of the rate established by the Bank of Russia on the payment date. Of the analyzed developers such subsidies were obtained by Legenda LLC and Talan-Finance LLC.

The rest of the construction costs is financed from equity. This is consistent with the requirement for the developer's own funds (at least 10% of the project cost of construction) (paragraph 1.1 subsection 2 section 3 of Law No. 214-FZ and paragraph 7.2 "Standards …"). Within the group, the management company can raise borrowed funds and invest them in the capital of subsidiaries-developers, providing the latter with the necessary amount of their equity. In the consolidated financial statements, these funds should be presented as borrowed funds. The proportion of equity in total financing is 21–22%, its growth occurs mainly due to an increase in retained earnings and other reserves, rather than the issue of equity instruments to raise funds.

4   Conclusions and Discussion

The analysis of measures within the framework of the "road map" for the transition of financing housing construction in the Russian Federation to the qualified investors allowed identifying their positive and negative sides. The negative aspects include the difficulty of obtaining targeted loans, especially by medium-sized regional developers, and the rise in construction costs due to interest expenditures. On the positive side—increasing the transparency and improving the business process in construction activities, cleaning up unscrupulous developers using market methods, reducing risks for buyers and budgetary costs to protect their rights.

The financial statements of developers also indicate new trends in the structure of financing: a 20% decrease in the proportion of liabilities to share participants were replaced by a 25% increase in liabilities on loans and bonds. In the future, as settlements using escrow accounts expand, it seems appropriate to study in more detail their impact on other indicators of the financial statements of developers (financial results, cash flows, etc.).

Currently, Russian legislation does not provide for a phased disclosure of an escrow account for a developer. Abroad, for example, in Germany, such a model is successfully applied. In the future, this model can be applied in Russia as well. However, the conditions necessary for its implementation have not been created jet: a stable pool of bona fide developers has not been formed, banks have not enough experience in monitoring the progress of construction projects and their stages to provide fair and high-quality assessment construction results [28]. A multilevel control should exclude the possibility of misappropriation of funds from escrow accounts and other abuses by unscrupulous developers [29]. In this case, developers will have the opportunity to gradually use the funds of share participants to finance construction, and control over their activities will ensure maximum protection of the rights of participants in shared construction. The creation of a mechanism for the stage-by-stage disclosure of escrow accounts can make adjustments to the emerging trends in changes in the structure of financing for developers.

References

1. Sternik SG, Malginov GN, Lavrentiev MA (2020) Impact of the institutional reform of equity participation in construction on the primary market for multi-apartment housing. Property relations in the Russian Federation 5(224):25–43. https://doi.org/10.24411/2072-4098-2020-10501

2. Accounting chamber of RF (2020) AC: to solve the problem of defrauded share participants will help their full accounting and increase in funding. https://ach.gov.ru/checks/sp-reshit-problemu-obmanutykh-dolshchikov-pomozhet-uvelichenie-finansirovaniya-i-polnyy-uchet-takikh (access date: 20.02.2021)

3. Durnovo DV (2018) Transition to the target model of housing finance. Construction: accounting and taxation 2:15–17

4. Morozova Y (2020) Using escrow accounts in the new model of shared construction: banking process settings. Settlements and operational work in a commercial bank 1:40–52

5. Andreeva NV, Gavrichenko EV (2020) The mechanism of interaction between participants in investment and construction activities, taking into account the use of an escrow account. Int Res J 7–3(97):122–130

6. Belobabchenko MK (2019) A new approach to the procedure for attracting and using funds from participants in the shared construction of an apartment building. Law Pract 3:150–157

7. Klochkova EN, Ovechkina AI, Petrova NP (2019) Topical issues of formation and development of project financing for housing construction in the Russian Federation. Bull St. Petersburg State Univ Econ 5–1(119):33–38

8. Blokhin AA, Sternik SG, Teleshev GV (2019) Transformation of the institutional rent of multi-apartment housing developers into the institutional rent of credit institutions. Property relations in the Russian Federation 1(208):6–17. https://doi.org/10.24411/2072-4098-2019-10101

9. Koshkina TY (2018) The next changes in the shared housing construction entered into force. Constr: Acc Taxation 8:21–35

10. Ignatova NB (2019) Pros and cons of the escrow account in the participatory shared construction. Ural J Legal Res 5(6):612–620

11. Kirsanov AR (2020) Problematic issues of project financing for housing construction. Property relations in the Russian Federation 2(221):7–22

12. Aminov K, Andrianova D (2019) Developers were added to the list. Kommersant 220:7

13. Osipchuk D (2020) Money for construction: legal aspects of project financing today. Single resource for developers https://erzrf.ru/publikacii/dengi-na-stroyku-pravovyye-aspekty-proyektnogo-finansirovaniya-segodnya (access date 20.02.2021)

14. Sergienko D, Mitrofanov P (2020) Review of the housing construction industry in the Russian Federation: bonds to replace APSC. https://www.raexpert.ru/researches/development/housing_industry_2020/ (access date 20.02.2021)

15. Buzulutskiy MI (2020) Regional markets challenge in the framework of a new project financing scheme. Innov Investment 9:250–252

16. Guzikova LA, Neelova NV (2020) Agreements of participation in shared construction: relationship of legal, tax and accounting aspects. In: IOP conference series materials science and engineering, vol 962, p 022081. https://doi.org/10.1088/1757-899X/962/2/022081

17. Serova AI (2020) The Ministry of Finance has decided on the taxation of developers using escrow accounts. Constr: Acc Taxation 5:41–47

18. Bazileva SG, Linnikov KI (2020) Features of using an escrow account in shared construction. Bulletin of the Faculty of Management of St. Petersburg State University of Economics 8:19–25

19. Antifeeva VS, Romanova AM (2019) Escrow accounts and their impact on changes in real estate prices. Socio-economic management: theory and practice 4(39):88–90
20. Kogan AB, Chaetsky AA (2020) The impact of project escrow financing on housing entrepreneurship. Real Estate: Econ Manage 2:35–40
21. Magomedov MS (2019) Impact of the introduction of escrow accounts in construction activities. Science without borders 10(38):5–12
22. Sviridova MD, Popov VG (2019) Problems of using an escrow account in the segment of shared construction. Economy in the investment and construction complex and housing and communal services 2(17):164–170
23. Slepnev DV (2020) Adaptation of the rule of law in the context of the evolution of fraudulent actions in the field of shared construction. Tribune Scholar 12:707–711
24. Ketova KV, Vavilova DD (2020) A model for managing financial flows in the construction industry using escrow accounts. Intell Syst Manuf 8(2):85–95
25. Kaledina A (2019) Access to buyers' money before the end of construction is a return to the past. https://iz.ru/950351/anna-kaledina/dostup-k-dengam-pokupatelei-do-okonchaniia-stroiki-vozvrat-v-proshloe (access date 20.02.2021)
26. Neelova NV (2016) Institute of the consolidated financial statements in the Russian Federation. Auditor 2–5:19–29
27. Guzikova L, Plotnikova E, Zubareva M (2017) Borrowed capital as risk factor for large construction companies in Russia. In: IOP conference series materials science and engineering, vol 262(1), p 012206. https://doi.org/10.1088/1757-899X/262/1/012206
28. Bovsunovskaya MP, Sahakyan SS (2020) Prospects for the phased disclosure of escrow accounts in the housing construction of the Russian Federation. Bull Altai Acad Econ Law 1–2:35–39
29. Kirsanov AR (2019) "A German lesson", or a phased transition of developers to escrow accounts. Property relations in the Russian Federation 4(211):63–66

Geothermal Power Supply of Buildings in Harsh Climatic Conditions

E. Sharovarova[1]([✉]), V. Alekhin[1], S. Shcheklein[1], N. Novoselova[2], and A. Hussein[1]

[1] Ural Federal University, 19 Mira St., Ekaterinburg 620002, Russia
[2] Ural State University of Architecture and Art, 23, K.Liebknecht st, Ekaterinburg 620075, Russia

Abstract. The problem of energy saving and sustainable development in construction is especially urgent at the present time. This article describes the new concept of using renewable energy sources in buildings, which represents the efficient scheme of solar and geothermal energy use for buildings with a ventilated façade. To analyze the efficiency of geothermal energy supply to a building with multilayer facade panels, the calculation of ground heat exchanger parameters was carried out in ANSYS software. The heat exchanger parameters were calculated for heating the supply air for temperatures from –18 to 0 °C. During the experiment three variants of collector pipe diameters were analyzed at different values of air flow rates. The calculation results show that with a decrease in the flow rate in the pipe, the difference in air temperatures at the inlet and outlet increases and the specific heat removal decreases.

Keywords: Renewable energy sources · Green buildings · Sustainability · Geothermal power supply

1 Relevance of Renewable Energy Sources Implementation in Buildings

Modern architecture and energy-saving technologies set the vector of development in the construction of buildings and structures, aimed at reducing the aggressive impact on the environment. Construction is one of the strongest factors of anthropogenic impact on nature [1–5]. There are over a billion buildings in the world, and the construction and operation of buildings accounts for over 40% of all materials and energy. The problem of saving energy resources is especially urgent in the world community. In solving this problem, developed countries are focusing on reducing specific energy consumption and increasing the use of renewable energy sources. The concept of sustainable development is actively discussed, implemented and popularized all over the world. The growing demand for electricity is driving the interest into renewable energy [6–8].

The development of new technologies and structures for the construction of buildings in remote regions of the Russian Federation with extreme climatic conditions become necessary. Distinctive features of these regions are extreme climatic conditions, remoteness from the main industrial centres, low population density. As a rule, in these areas,

fossil fuel reserves are limited or difficult to access, and the construction of centralized transmission networks is often technically impossible. The territories of Russia with decentralized energy supply have a huge potential for the development of renewable energy sources [9–11]. The energy sector of agriculture in Russia is characterized by the dispersal of rural consumers, low consumer capacity, the length of electrical, heat and gas networks, and a low population density in areas without centralized energy supply, where agricultural production is carried out. These features form additional reliability requirements for power supply system due to significant wear of transmission lines and poor power quality, failures and loss of power in the lines. Rural areas have great potential for renewable energy development to address many of the energy supply problems in these areas. In some cases, the lack of fuel endangers the lives of people. The low specific capacity of power plants and their remote mutual position in vast territories ensure the maximum efficiency of the implementation of renewable energy systems. Most of the fuel and energy balance of Russia constitute the needs of heat supply. In the face of rising prices for traditional energy sources, their limited resources and aggravation of environmental problems, it seems advisable to widely develop geothermal resources. Such a choice from common list of unconventional energy sources (solar, wind, etc.) is motivated by the main advantage of thermal energy of the subsoil which is independence on climatic conditions, with comparable, practically unlimited resources.

The main consumers of geothermal resources in the near and long term there will undoubtedly be heat supply and, to a much lesser extent, power generation. Priority of heat supply in the balance of the use of geothermal energy is, which allows to outline directions of attracting investments, creating specialized equipment, choosing promising areas and priority objects.

Despite significant advances in the development of geothermal energy, its contribution to the overall energy balance of the world is still relatively small. The pace of development and the effectiveness of development geothermal energy most high in developing countries, where the share of geothermal resources in production electricity reaches 15–20%.

2   The Concept of Renewable Energy Power Supply of Buildings

An integrated approach to the implementation of energy installations based on renewable energy sources in buildings will significantly reduce energy consumption and improve their energy efficiency. There are many passive ways to use solar energy in buildings. For example, Felix Trombus's solar wall is a massive stone structure installed on the south side of the building behind a glazed façade. The wall can be covered with absorbent foil or painted black. Such a wall construction allows to accumulate solar energy, and then gives the room thermal energy at night. Douglas Balcomb's solar home concept uses the principle of residential heating using a double-height solar greenhouse on the south side. Swedish architect Bengt Varna came up with the idea of creating a greenhouse built inside a transparent glass or polycarbonate case. Reducing the wind load and the air gap between the facades allows to reduce the temperature difference between the premises and the street [12–15].

A new concept was developed for the use of renewable energy sources in buildings with the aim of increasing their energy efficiency. The concept is to create wall enclosing

structures of buildings that performs a heat-shielding function and an energy-generating function due to solar panels installed on the outside of the facade (Fig. 1). The facade system is proposed to be made of panels with a closed ventilated air gap, into which warm air is supplied, pre-heated by a ground heat exchanger [16–20]. In summer, the supply air, cooled down to ground temperature by using a ground heat exchanger, is fed into the air gap of the facade, as a result of which the required capacity of the air conditioning system is reduced.
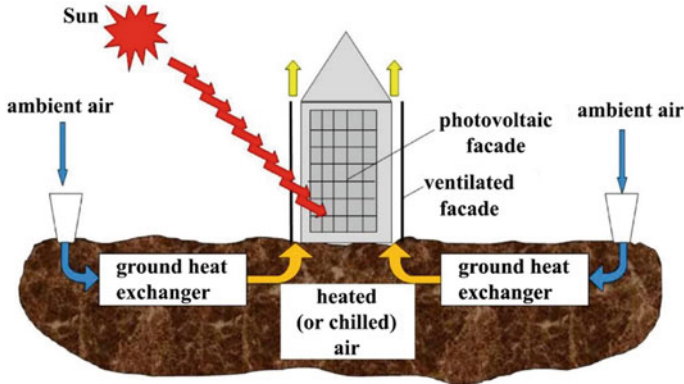
Fig. 1 Renewable energy concept in buildings with ventilated air gap façade panels

Using low temperature geothermal energy shallow depths can be considered as some technical and economic phenomenon or a real revolution in the heat supply system. The essence of the technologies under consideration is the creation of an underground heat exchanger located at a shallow depth with a closed or open circuit connected to a heat pump located inside the heated premises. In this case, the soil temperatures are in the range from 5–7 to 12–14 °C. These systems do not use only geothermal energy stored in soil or in the water, but also solar energy. The specific share of a particular energy used by the source depends on the depth of the heat exchanger, climatic and hydrogeological conditions of the area. It is assumed that for shallow horizontal heat exchangers, the main contribution is made by the share of solar energy.

Figure 2 shows a multi-layer facade panel (MFP) in layers. MFP consists of internal and external heat-insulating layers, with a frame made of perforated channels in between.

Such schemes of operation form a closed cycle of movement of air masses, as a result of which the entire volume of heated air for forced ventilation systems is aimed at maintaining a positive temperature in the ventilated gap.

3 Calculation of a Horizontal Ground Air Heat Exchanger for Buildings with Multi-Layer Façade Panel

To analyze the efficiency of geothermal energy supply to a building with multilayer facade panels, the multi-apartment three-storey residential building in Ekaterinburg was
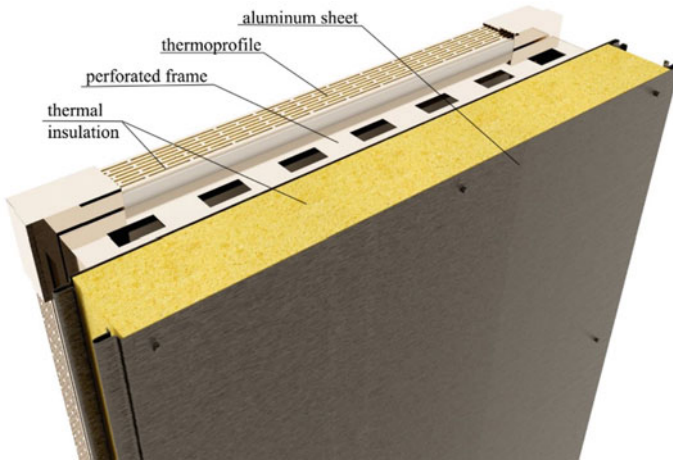
Fig. 2 Multi-layer façade panel structural design

analyzed. The scheme of operation of engineering systems in a building using a ground heat exchanger is shown in Fig. 3.
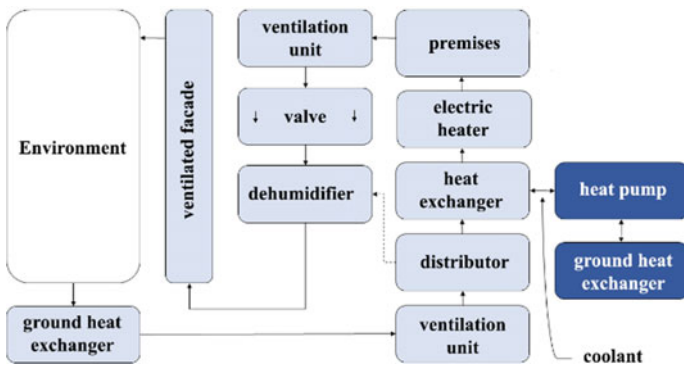
Fig. 3 The operation scheme of engineering systems

To provide mechanical ventilation of the building and the ventilated gap of the facade panels, two high-pressure fan units are used, selected taking into account the total aerodynamic resistance of the system elements.

In order to reduce energy consumption for heating the supply air, a heat pump with a thermal power of 27.6 kW and a conversion factor of 4.6 is used. For the operation of the pump, a device of 14 wells for geothermal probes with a depth of 60 m is required. Exhaust air from the premises passes through a duct condensation dryer before it enters the ventilated gap of the façade panels.

3.1 Air Heating Simulation

To preheat the supply air, a ground collector is used, installed at a depth of 3 m. The heat exchanger parameters were calculated for heating the supply air for temperatures from −18 to 0 °C. During the winter heating season, the ground heat exchanger is used only at negative ambient temperatures.

In the ANSYS software package, a fragment of a polyethylene pipe with a soil mass was modeled. The design model is shown in Figs. 4 and 5. The calculation adopted a moisture-saturated loam with a density of 1600 kg/m^3 and a specific heat of 1000 J/(kg K). The wall thickness of the polyethylene pipe is taken equal to 9.8 mm for all variants of the outer diameters.
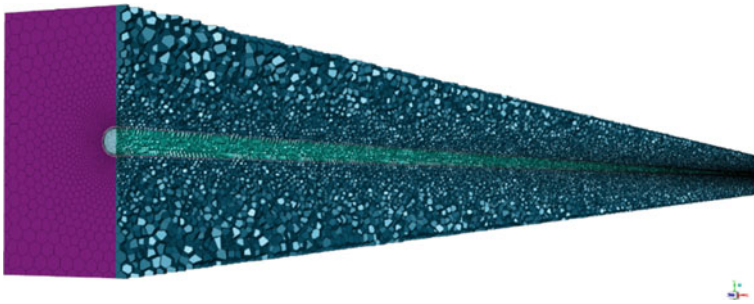
Fig. 4 Grid of the model of the ground heat exchanger in the ANSYS software
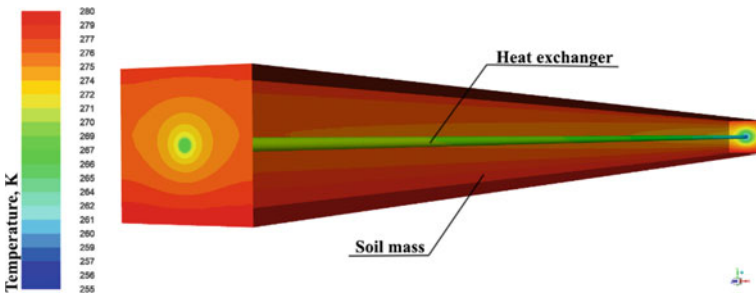
Fig. 5 The calculation model of the ground heat exchanger in the ANSYS software

A fragment of the model in cross-section is shown conventionally in Fig. 6. For the surrounding soil, the temperatures of the upper and lower layers are set to 5 °C and 7 °C, respectively. At the inlet to the collector pipe, the air speed is set with a temperature of minus 18 °C. The air velocity depends on the pipe diameter and the number of parallel collector pipes. The scheme of the ground collector is shown in Fig. 7.

The mass air flow through the collector pipe is determined by the equation

$$Q_m^p = \frac{Q \cdot \rho_{air}}{3600 \cdot N_p},\tag{1}$$
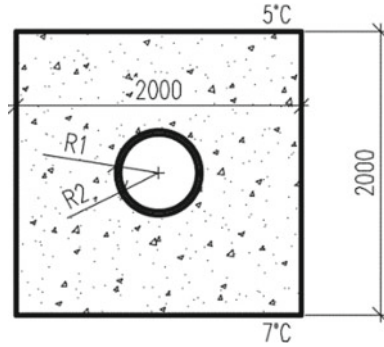
Fig. 6 The fragment of the model in cross-section
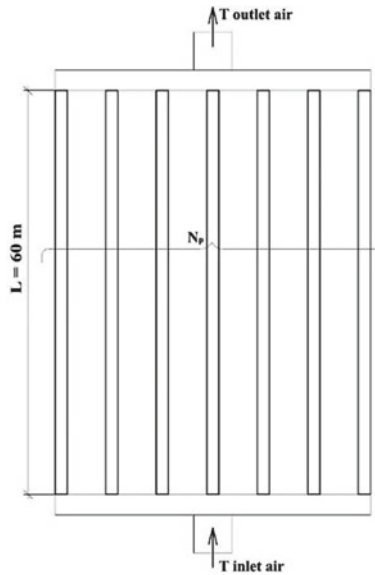
Fig. 7 The scheme of the ground heat exchanger

where Q—volumetric flow, m^3/s; ρ_{air}—density of inlet air, kg/m^3; N_p—number of parallel pipes of ground collector.

Specific heat removal from a running meter of a collector pipe is determined by the equation

$$q = \frac{Q_m^p \cdot C_{air} \cdot \left(T_{air}^{outlet} - T_{air}^{inlet}\right)}{L}, \tag{2}$$

where C_{air}—specific heat capacity of inlet air, J/(kg·K); T_{air}^{outlet}—temperature of outlet air, K; T_{air}^{inlet}—temperature of inlet air, K; L—length of the pipe of ground heat exchanger, m.

The air flow rate in the collector pipe is determined by the equation

$$V^p = \frac{4Q}{3600 \cdot 3,14 \cdot (D - 2t)^2 \cdot N_p} \tag{3}$$

where D—outer diameter of the collector pipe, m; t—pipe wall thickness, m.

3.2 The Results of Air Heating Simulation

During the experiment three variants of collector pipe diameters were analyzed at different values of air flow rates. The calculation results to determine the required parameters of the soil collector are presented in Table 1.

Table 1 The results of determination of the required parameters of the ground collector

№	D (mm)	N_p	Q_m^p (kg/s)	V^p (m/s)	T_{air}^{outlet} (K)	T_{air}^{inlet} (K)	ΔT (K)	q (W/m)
1	0.4	3	0.44	2.77	255	262.29	7.29	54
2	0.4	6	0.22	1.39	255	265.86	10.86	40
3	0.4	9	0.15	0.92	255	268.35	13.35	33
4	0.4	12	0.11	0.69	255	270.49	15.49	28
5	0.4	16	0.08	0.52	255	272.65	17.65	24
6	**0.4**	**18**	**0.07**	**0.46**	**255**	**273.68**	**18.68**	**23**
7	0.28	10	0.13	1.78	255	269.45	14.45	32
8	0.28	14	0.09	1.27	255	271.75	16.75	26
9	0.28	16	0.08	1.11	255	272.58	17.58	24
10	**0.28**	**20**	**0.07**	**0.89**	**255**	**273.77**	**18.77**	**21**
11	0.225	6	0.22	4.76	255	265.91	10.91	40
12	0.225	9	0.15	3.17	255	268.61	13.61	33
13	0.225	10	0.13	2.85	255	268.59	13.59	30
14	0.225	12	0.11	2.38	255	268.88	13.88	25
15	0.225	14	0.09	2.04	255	269.71	14.71	23
16	0.225	18	0.07	1.59	255	271.53	16.53	20
17	0.225	22	0.06	1.30	255	272.64	17.64	18
18	**0.225**	**26**	**0.05**	**1.10**	**255**	**276.4**	**21.4**	**18**

In the selected three experiments, the maximum temperature head is provided

The calculation results show that with a decrease in the flow rate in the pipe, the difference in air temperatures at the inlet and outlet increases and the specific heat removal decreases. Reducing the number of parallel collector pipes leads to a reduction in the amount of excavation work. The temperature difference of more than 18 °C is provided in experiments №6, 10, 18. The minimum number of parallel pipes of collector is achieved in case №6 with usage of pipes with an outer diameter of 400 mm.

4   Conclusions

The known averaged data of heat removal from the ground are insufficient for an accurate calculation of the parameters of a ground heat exchanger. An accurate assessment of the efficiency of the heat exchanger can be carried out in the software package ANSYS when air consumption, temperatures and soil characteristics are known. Geothermal power supply of buildings with mechanical ventilation can be efficient even in harsh climatic conditions.

Heat and cold supply systems for buildings and structures are one of the most energy-intensive consumers of fuel and energy resources in Russia. Replacement of limited reserves of fossil fuels (oil and oil products, natural gas, coal, etc.) with practically unlimited resources of renewable natural sources of low-potential heat (heat from water from underground and surface sources, soil, air, etc.) and resource conservation and environmental protection. Heat pump units used to solve problems of heat and cold supply have recently demonstrated competitive advantages in the market of heat and cooling equipment due to their ability to replace fossil fuel with low-grade heat of natural and technogenic origin. These trends are intensifying with increasing prices and tariffs of fossil fuels.

A key aspect of ground-air heat exchangers is the passive nature of their operation and their applicability to different environmental conditions. Ground-to-air heat exchangers can be extremely cost effective in both upfront and capital costs, as well as durable and low cost to maintain.

In the context of today's declining of fossil fuels, rising electricity prices, air pollution and global warming, properly designed ground collectors offer a sustainable alternative to reduce or eliminate the need for traditional compressor-based air conditioning systems, particularly in harsh climates. They also provide an additional benefit of a controlled, filtered and softened fresh air flow, which is especially valuable for small, sealed and energy efficient buildings [21–25].

References

1. Rheude F, Kondrash J, Roder H et al (2021) Review of the terminology in the sustainable building sector. J Cleaner Prod 286
2. Wen B, Musa N, Chen Onn C et al (2020) The role and contribution of green buildings on sustainable development goals. Build Environ 185
3. Wen B, Musa N, Chen Onn C et al (2020) Evolution of sustainability in global green building rating tools. J Cleaner Prod 259
4. Teng J, Mu X, Wang W et al (2019) Strategies for sustainable development of green buildings. Sustainable Cities and Society 44: 215–2261. Smith J, Jones M Jr, Houghton L et al (1999) Future of health insurance. N Engl J Med 965:325–329
5. Leyzerova A, Sharovarova E, Alekhin V (2016) Sustainable strategies of urban planning. Procedia Eng 150:2055–2061

6. Menard R, Souviron J (2020) Passive solar heating through glazing: the limits and potential for climate change mitigation in the European building stock. Energy Build 228
7. Lotfabadi P (2015) Analyzing passive solar strategies in the case of high-rise building. Renew Sustain Energy Rev 52:1340–1353
8. Peterkin N (2009) Rewards for passive solar design in the Building Code of Australia. Renew Energy 34(2):440–4439
9. Shepovalova OV (2015) Energy saving, implementation of solar energy and other renewable energy sources for energy supply in rural areas of Russia. Energy Procedia 74:1551–1560
10. Velkin V, Shcheklein S, Danilov V (2017) The use of solar energy for residential buildings in the capital city. In: IOP conference series: earth and environmental science, vol 72
11. Sharovarova E, Alekhin V, Avdonina L (2020) The potential for the development of renewable energy generation in Russian territories where the power supply system is decentralized. In: IOP conference series: materials science and engineering (MSE), vol 962(2)
12. Luo Y, Zhang L, Bozlar M et al (2019) Active building envelope systems toward renewable and sustainable energy. Renew Sustain Energy Rev 104:470–49113
13. Tan H, Lei Y, Chen Y et al (2016) Renewable energy development for buildings. Energy Procedia 103:88–9315
14. Mbungu N, Naidoo R, Bansal R et al (2020) An overview of renewable energy resources and grid integration for commercial building applications. J Energy Storage 2917
15. Hassan A, El-Rayes K (2021) Optimizing the integration of renewable energy in existing buildings. Energy Build 2388
16. Palomo Torrejon E, Colmenar-Santos A, Rosales-Asensio et al (2021) Economic and environmental benefits of geothermal energy in industrial processes. Renew Energy 174:134–146
17. Duus K, Schmitz G (2021) Experimental investigation of sustainable and energy efficient management of a geothermal field as a heat source and heat sink for a large office building. Energy Build 2358
18. Miglani S, Orehounig K, Carmeliet J (2018) A methodology to calculate long-term shallow geothermal energy potential for an urban neighborhood. Energy Build 159:462–473
19. Ghasemi-Fare O, Basu P (2018) Influences of ground saturation and thermal boundary condition on energy harvesting using geothermal piles. Energy Build 165:340–351
20. Zurmuhl D, Lukawski M, Aguirre G et al (2019) Hybrid geothermal heat pumps for cooling telecommunications data centers. Energy Build 188–189:120–128
21. Cohen J, Azarova V, Kollmann et al (2021) Preferences for community renewable energy investments in Europe. Energy Econ 100:21
22. Li R, Leung G (2021) The relationship between energy prices, economic growth and renewable energy consumption: evidence from Europe. Energy Rep 7:1712–1719
23. Potrc S, Cucek L, Martin M et al (2021) Sustainable renewable energy supply networks optimization—the gradual transition to a renewable energy system within the European Union by 2050. Renew Sustain Energy Rev 146
24. Ramsebner J, Linares P, Haas R (2021) Estimating storage needs for renewables in Europe: the correlation between renewable energy sources and heating and cooling demand. Smart Energy
25. Soeiro S, Dias M (2020) Renewable energy community and the European energy market: main motivations. Heliyon 6(7)

Improving the Methodology for Predicting the Destruction of the Heat Supply System in an Accident

E. A. Biryuzova[(✉)]

Saint-Petersburg State University of Architecture and Civil Engineering, 4, Vtoraja Krasnoarmejskaja Ul, St. Petersburg 190005, Russia

Abstract. Forecasting the heat supply system destruction caused by various reasons, such as damage, wear, corrosion, as well as the prevention of an emergency situation are actual research topics during the entire service life of heat network pipelines. Corrosion damage is the most common pipeline wear type. Forecasting the destruction development will make it possible to determine the most effective method for heat supply pipeline restoration. The method will help prevent the destruction of engineering structures, improve the environmental situation and ensure the optimal pipeline systems functioning. Regardless of how advanced the existing methods are, they are still being finalized. Their application practice shows that it is best to work them out on a real existing system, as opposed to a new one which has not previously been operated, which has its own characteristics and risk factors. Getting started, it is important to check all the technical features, make a clear action plan, which will eventually make it possible to reduce the recovery time, improve the operational characteristics and reliability of the system. The study results can be used by organizations that have heat network pipelines on their balance sheets to adjust the preventive repair work schedule.

Keywords: Predicting destruction · Failure rate · Insufficient heat release

1 Introduction

The study analyzed the destruction causes of heat supply system pipelines. As well as existing methods that allow to predict this process, which is undeniably important especially for organizations involved in the heat supply system operation. [1–7]

The analysis of the methods enable to identify the factors that are taken into account when making forecasting these factors are [8–10]:

- Pipe diameters
- Duration of pipeline operation
- Availability of additional equipment

The list of identified factors does not take into account the pipelines operating conditions and heat network operation hydraulic modes, therefore, the methodology improvement is an objective necessity allowing to increase the efficiency and reliability of the heat network [11–17].

Reliability and efficiency indicators of the heat network are interrelated. Therefore, they cannot be considered separately from each other. Only a comprehensive approach to solve the problem will help you get the maximum result.

2 Study of Factors Affecting the Rate of Corrosion Propagation

Corrosion processes have the greatest impact on the process of wear, damage and, consequently, destruction, especially during long-term operation or in the presence of a high ground water level. Corrosion is the spontaneous destruction of metal as a result of chemical or physico-chemical interaction with the environment (Fig. 1).

Carbon dioxide corrosion

Pitting corrosion

Crevice corrosion

Corrosion damage of longitudinal welded pipes

Fig. 1 Corrosion variants of thermal network steel pipelines

Pitting corrosion occurs in the lower pipe sections, where stagnant water, condensation accumulation and corrosive deposits can form. The main feature of this corrosion type is a large amount of damage, where many separate deep damage areas appear on the surface. It eventually leads to through holes, thereby a system section needs to be decommissioned.

Carbon dioxide corrosion forms when the heating medium contains normal and acidic salts of carbonic acid, that is, carbonates and bicarbonates, which form lumpy deposits on the pipe walls. Ulcers appear from 5 to 20 mm in diameter under lumpy deposits. As a rule, it is caused by a violation of the water treatment.

Crevice corrosion occurs at welded joints with poor-quality seams (with no penetration). Such a technological defect contributes to this type of corrosion, since stagnant zones are formed in these areas, where the environment becomes more acidic and concentrated.

Longitudinal welded pipelines are more susceptible to corrosion damage. Corrosion occurs along the inner side of the alloy length when the pipes are not heat-treated after automatic welding. This situation results in increased residual stress in the seam. It leads to a fracture.

Damage caused by internal corrosion on the pipeline surface leads to the coolant leakage in the corrosion pits 5–6 years after the installation work. Also, in these places, there is a heat-insulating layer gradual wetting, which leads to the next type of common damage. This is corrosion of the outer surface of the pipe, and not pointwise, but throughout the entire area of insulation contact.

External corrosion is the result of reactions under the influence of substances in an aggressive environment. When metal comes into contact with active gases and liquids, a chemical reaction occurs, and when it interacts with electrolytes, an electrochemical reaction occurs. That's why, more attention is paid to the chemical analysis of soils when designing a pipeline.

The process of internal and external corrosion development is possible both together and separately. In the first case, the process begins with the internal destruction of the pipeline wall with small ulcers, which eventually penetrate it to the through hole, forming a leak of the transported liquid, moistening the insulating layer and, as a result, there will be surface corrosion development. The causes of the formation and development of only external corrosion can be flooding by groundwater, surface moistening due to leaks from pipelines for other purposes, as well as high humidity in the heating network channel. Generally, external corrosion is characterized by localized damage, located no more than 1.5 m away.

Corrosion of steel under thermal network conditions occurs with oxygen depolarization, so oxygen has a great influence on pipeline damage. Figures 2 and 3 graphs show that as the oxygen concentration in the transported liquid increases, the corrosion rate increases.
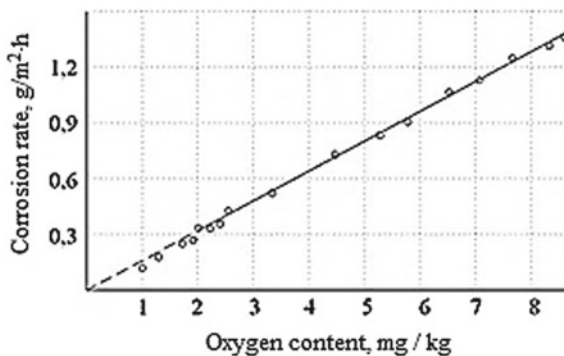
Fig. 2 Dependence of corrosion development rate on the oxygen content in the heating medium
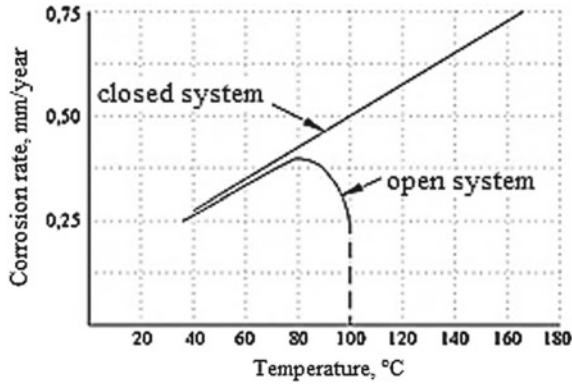
Fig. 3 Dependence of corrosion development rate on the temperature of the heating medium

When analyzing the factors affect ne the rate of corrosion in pipelines, it is impossible not to note the pressure and temperature of the heating medium. As the pressure increases, the corrosion process rate also increases, especially if the water temperature also increases.

3 Analysis of Performed Research Results

To predict the extent of corrosion damage to the main pipelines, it is necessary to calculate the reliability of the heat network.

The method used to calculate the reliability indicators for sections and elements of the central heating network helps to select or adjust the routing scheme in the design, but to improve the efficiency and accuracy of system reliability calculations and to identify a larger number of assumed vulnerable sections and elements of the heat network, the methodology should be supplemented.

When calculating such an important indicator as the failure rate of the heat network elements it is necessary to consider not only the operation duration, but also such a parameter as the corrosion rate, i.e. the ratio of the change in wall thickness to the service life (Fig. 4) [17–19].

3.1 Study of the Failure Rate Indicator of the Heat Pipeline

The failure rate of the heat pipeline, taking into account its operating time "(1)": [20–23]

$$\lambda = \lambda^{\text{the initial}} \cdot \left(0.1 \cdot \tau^{\text{operation}}\right)^{\alpha-1} \tag{1}$$

$\lambda^{\text{the initial}}$—the initial failure rate of the heat pipeline, corresponding to the period of normal operation, 1/(km h); $\tau^{\text{operation}}$—duration of site operation, years; α—coefficient that takes into account the duration of the site operation.
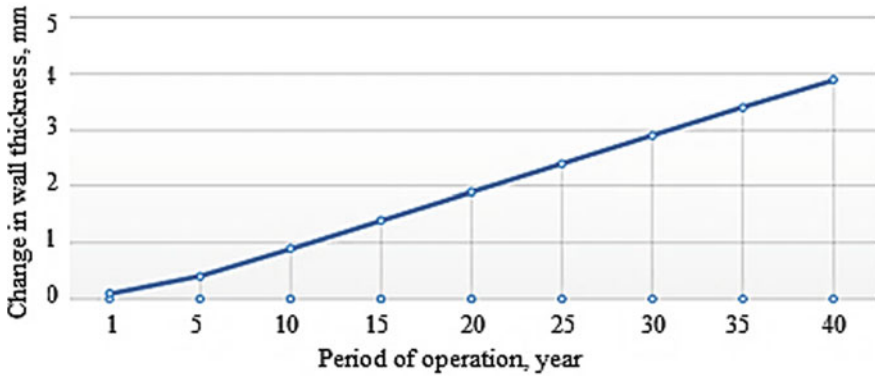
Fig. 4 Dependence of the pipeline wall thinning thickness on the service life

Figure 2 shows the dependence of steel wall thickness change on the operating time, identified on the basis of statistical data.

To add this parameter to the formula, you need to make it dimensionless "(2)":

$$v_c = \frac{x - x_{min}}{x_{max} - x_{min}} \tag{2}$$

x—change in wall thickness, mm.

$$v_c = \frac{0.09 - 0.08}{0.1 - 0.08} = 0.86$$

After that, we add the obtained parameter value to the coefficient α, which takes into account the duration of site operation. Thus, the failure rate of the heat pipeline, taking into account the time of its operation and the corrosion rate, 1/(km·h), is calculated by the formula "(3)":

$$\lambda = \lambda^{\text{the initial}} \cdot \left(0.1 \cdot \tau^{\text{operation}}\right)^{(\alpha + v_c) - 1} \tag{3}$$

Substituting this resulting v_c value into formula "(3)", we get formula "(4)":

$$\lambda = \lambda^{\text{the initial}} \cdot \left(0.1 \cdot \tau^{\text{operation}}\right)^{\alpha - 0.14} \tag{4}$$

As a result, the failure rate in the sections will increase by 1.3 times from 0.000057 to 0.0000076 ($5.7 \cdot 10^{-6}$ before $7.6 \cdot 10^{-6}$).

Two tables (Tables 1 and 2) present technical characteristics and reliability indicators of heat network sections, such as the section number, length, diameter, operation period, failure rate of the heat pipeline, average restoration time for the sections, the recovery rate and the failure probability of the heat network.

As a result of considering the effect of the corrosion rate, the values of the failure flow in the sections and the failure probability of the heat network increase.

Table 1 The calculation is made taking into account the time of its operation

Plot number	The length of the plot, m	$d_{internal}$, m	$\tau^{operations}$, years	λ, 1/(km·h)	ω, 1/h	z^v, h	μ, 1/h	P_f
Sections of the heat network T1, T2								
1	61	0.309	14	0.0000057	$3.48 \cdot 10^{-7}$	16.44	0.06	$5.72 \cdot 10^{-6}$
2	226	0.207	14	0.0000057	$1.29 \cdot 10^{-6}$	11.28	0.09	$1.45 \cdot 10^{-5}$
3	18	0.15	14	0.0000057	$1.03 \cdot 10^{-7}$	8.59	0.12	$8.82 \cdot 10^{-7}$
4	51.5	0.15	14	0.0000057	$2.94 \cdot 10^{-7}$	8.59	0.12	$2.52 \cdot 10^{-6}$

Table 2 The calculation is made taking into account the operation and the corrosion rate

Plot number	The length of the plot, m	$d_{internal}$, m	$\tau^{operations}$, years	λ, 1/(km·h)	ω, 1/h	z^v, h	μ, 1/h	P_f
Sections of the heat network T1, T2								
1	61	0.309	14	0.0000076	$4.64 \cdot 10^{-7}$	16.44	0.06	$7.63 \cdot 10^{-6}$
2	226	0.207	14	0.0000076	$1.72 \cdot 10^{-6}$	11.28	0.09	$1.94 \cdot 10^{-5}$
3	18	0.15	14	0.0000076	$1.37 \cdot 10^{-7}$	8.59	0.12	$1.18 \cdot 10^{-7}$
4	51.5	0.15	14	0.0000076	$3.92 \cdot 10^{-7}$	8.59	0.12	$3.37 \cdot 10^{-6}$

3.2 Study of the Average Total Heat Under-Discharge to the Consumer

The relative hourly heat consumption by a consumer in case of failure of one of the network elements is characterized by the ratio of the hourly heat consumption by a consumer in case of failure of a network element and the estimated hourly load of this consumer, however, does not take into account the effect of hydraulic stability at the connection site of this consumer, which shows the system ability to maintain a constant heating medium flow at the consumer input when the operating conditions of other consumers change.

The average total heat under-discharge to the jth consumer during the heating period, Gcal, "(5)": [20–23]

$$Q_j = \left(g_j^{\text{the estimated}} - \sum_{f=0} P_f g_{j,f} \right) \cdot \left(\tau_1^{\text{calculation}} - \tau_2^{\text{calculation}} \right)$$

$$\times \frac{t_j^{\text{internal calculation}} - t^{\text{average outdoor}}}{t_j^{\text{internal calculation}} - t^{\text{the calculated outdoor}}} \cdot \tau^{\text{heating}} \cdot 10^{-3} \tag{5}$$

$g_j^{\text{the estimated}}$—the estimated hourly flow rate of the heating medium at the jth consumer, t/h; $g_{j,f}$—hourly flow rate of the heating medium at the jth consumer in case of failure of the fth element, t/h; p_f—the probability of the network state corresponding to the failure of the fth element; $\tau_1^{\text{calculation}}$ и $\tau_2^{\text{calculation}}$—calculation (at $t^{\text{internal calculation}}$) water temperatures in the supply and return lines of the heat network, °C; $t_j^{\text{internal calculation}}$— calculated air temperature in the building of the jth consumer, °C; $t^{\text{average outdoor}}$—average outdoor air temperature during the heating period, °C; $t^{\text{the calculated outdoor}}$—the calculated outdoor air temperature for heating, °C; τ^{heating}—the duration of the heating period, h.

The ability of the system to maintain the required flow rate of the heating medium is characterized by hydraulic stability in case of a failure of some consumers in the event of an accident.

Hydraulic stability is quantified by hydraulic stability coefficient "(6)":

$$Y = \frac{g_j^{\text{calculation}}}{g_{j,f}} \tag{6}$$

Therefore, it is advisable to enter into the formula for determining the average total heat loss the value of the hydraulic stability coefficient for a more accurate determination of this value in the event of an emergency situation (Table 3). When introducing the hydraulic stability coefficient, Gcal, "(7)":

$$Q_j = \left(g_j^{\text{the estimated}} - \sum_{f=0} P_f \cdot \left(\frac{g_j^{\text{calculation}}}{Y} \right) \right) \cdot \left(\tau_1^{\text{calculation}} - \tau_2^{\text{calculation}} \right)$$

$$\times \frac{t_j^{\text{internal calculation}} - t^{\text{average outdoor}}}{t_j^{\text{internal calculation}} - t^{\text{the calculated outdoor}}} \cdot \tau^{\text{heating}} \cdot 10^{-3} \tag{7}$$

4   Conclusion

Based on these results, we can conclude that taking into account the hydraulic stability coefficient the average total heat loss value increases on average by 3 times (Fig. 5).

To improve the efficiency and accuracy of the used method of system reliability calculations and to identify a larger number of supposed vulnerable sections and elements of the heat network, it is necessary to supplement the calculation of such important indicators as the failure rate of heat network elements, the average recovery time for the sections and the relative hourly heat consumption by a consumer in case of failure of one of the network elements with parameters that affect the rate in an emergency situation.

The results of the research can be used as a methodology for predicting the degree of destruction and as choice options for restoring heat supply systems when developing sections on preventing emergency situations, thus it will increase the service life to 30–40 years.

Table 3 The average total heat loss to the jth consumer during the heating period

The calculation is made without taking coefficient into account of hydraulic stability	The calculation is made taking into account the coefficient hydraulic stability		
Consumer's no	Average total heat under-output for the heating period Q_j	Consumer's no	Average total heat under-output for the heating period Q_j
Consumers of the heating and ventilation system			
6	0.00004	6	0.00007
7	0.00005	7	0.00010
8	0.00005	8	0.00010
10	0.00016	10	0.00017
11	0.00011	11	0.00024
16	0.00023	16	0.00028
19	0.00007	19	0.00010
20	0.00003	20	0.00035
25	0.00011	25	0.00010
27	0.00003	27	0.00013
29	0.00014	29	0.00103
35	0.00015	35	0.00073
36	0.00019	36	0.00072
37	0.00020	37	0.00030
38	0.00003	38	0.00029

The calculation is made without taking coefficient into account of hydraulic stability

The calculation is made taking into account the coefficient hydraulic stability
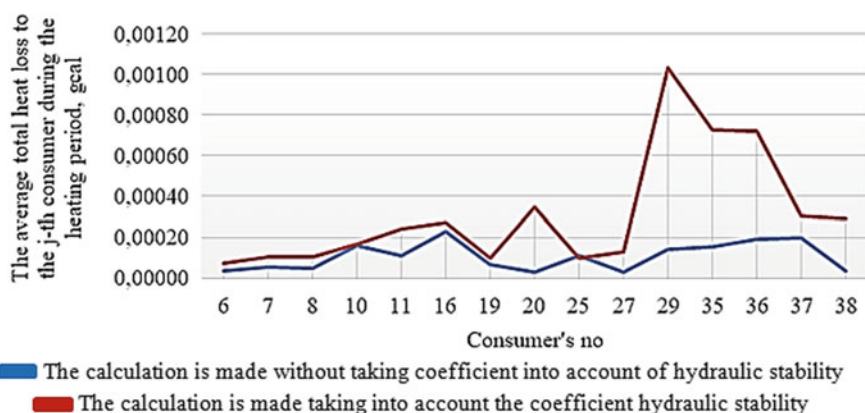
Fig. 5 Comparison of the value of the average total undersupply of heat, the calculation is made without taking coefficient into account of hydraulic stability [20–23] with the results of the calculation is made taking into account the coefficient hydraulic stability "(7)" for consumers

References

1. Buravlev AI (1995) Management of technical condition of dynamic systems Mechanical engineering, Moscow, p 240
2. Vasiliev-Yuzhin RM, Gatsak PM, Golovanov AI (2004) Development of algorithmic support for parametric diagnostics of ship internal combustion engines. Dvigatelestroyeniye St. Petersburg 1:43–46
3. Gottschalk OA (2003) Industrial controllers. Microprocessor systems of power facilities: written lectures, St. Petersburg, p 64
4. Erofeev MN, Kravchenko IN, Moskal OY, Markovchin SG, Gerasimov DV (2012) Formation of sets of means of metrological support, taking into account the criterion of adaptability of technological equipment to diagnostics Encyclopedic reference, Moscow 11:11–16, 12:18–27
5. Dmitriev AK, Maltsev PA (1988) Fundamentals of the theory of construction and control of complex systems. Energoatomizdat, Leningrad Branch, Leningrad, p 192
6. Nekrasov IN, Buyakov SN, Senchenkov VI (2014) Analysis of methods for technical diagnostics of ventilation and air conditioning systems of buildings and structures of the RKK technical position and prospects for their development. In: Proceedings of the All-Russian scientific-practical conference "Modern problems of improving the tactical and technical characteristics of rocket and space technology, its creation, testing and operation", St. Petersburg, pp 43–47
7. Senchenkov VI (2013) Models, methods and algorithms for technical condition analysis, p 377
8. GOST P 22.1.12-2005 Safety in emergencies. A structured system for monitoring and managing engineering systems of buildings and structures. General requirements, Standards Publishing, Moscow, p 27
9. GOST P 22.1.13-2013 Safety in emergencies. Civil defense measures, measures to prevent natural and man-made emergencies. A structured system for monitoring and managing engineering systems of buildings and structures. Requirements for the order of creation and operation, Standards Publishing, Moscow, p 49
10. Federal Law of December 30, 2009. No. 384-ФЗ Federal Law "Technical regulations on the safety of buildings and structures"
11. Biryuzova EA (2020) Investigation of methods for increasing of energy efficiency of hot water boilers of small and average capacity at the expense of reduction of heat losses with exit gases. In: IOP Conf. Ser.: Mater. Sci. Eng. vol 753, p 022006
12. Biryuzova EA (2019) Study of factors affecting reliability and efficiency of heat supply system. In: IOP Conf. Ser.: Mater. Sci. Eng. vol 687, p 044028
13. Nefedova MA, Biryuzova EA, Pestich SD, Aleksandrov AS (2018) Comparative analysis of the efficiency of cast iron boilers at power plants. In: IOP Conf. Ser.: Mater. Sci. Eng. vol 463, p 032047
14. Biryuzova EA (2018) Investigation of methods for determining heat losses from external cooling of surfaces of a small-capacity hot-water boiler. In: IOP Conf. Ser.: Mater. Sci. Eng. vol 463, p 032056
15. Biryuzova EA, Glukhanov AS (2020) Improving energy efficiency and reliability of heating networks through the use of multilayer thermal insulation structures. In: IOP Conf. Ser.: Mater. Sci. Eng. vol 962(3), p 032002
16. Biryuzova EA, Glukhanov AS (2021) Study of the effectiveness of the transition from an open heat supply systems to a closed one. In: IOP Conf. Ser.: Mater. Sci. Eng. vol 1079, p 032072
17. Glukhanov AS and Biryuzova EA (2021) On the question of reducing technogenic risks of accidents in the technical systems of buildings and structures. In: IOP Conf. Ser.: Mater. Sci. Eng. vol 1079, p 042096

18. Biryuzova EA, Glukhanov AS, Kobelev NS (2012) Application of modern pipeline systems in the design and reconstruction of heating networks. In: Proceedings of the South-West State University Series Engineering and Technology, vol 2(2), pp 63–68
19. Biryuzova EA, Glukhanov AS (2019) The influence of the method of laying pipelines on the energy efficiency of the heating network. PNRPU Bull Constr Archit 10(4):59–66
20. Kitaev YN (2010) Variant design of heating systems taking into account the reliability of the heating network. Young Scientist Publishing House, Kazan, pp 46–48
21. Raiser VD (1998) Reliability theory in building design. Publishing House of the Association of Building Institutions, Moscow, p 304
22. Smorodova OV, Skripchenko AS (2016) Ordinal statistics in heat supply systems. Oil and Gas Business, Moscow, pp 124–137
23. Semenov VG (2010) On improving the reliability and energy efficiency of heating networks. Energosvet, Moscow, pp 71–79

Experimental Study of Deformation of Soil Berms Retaining Pit Fence

D. R. Safin[1(✉)], R. T. Zainullin[2], and A. D. Safina[2]

[1] Kazan State University of Architecture and Engineering, 1, Zelenaya St, Kazan 420043, Russia
d.safin@list.ru
[2] OOO "Navek", 2, Tetsevskaya St., Kazan 420043, Russia

Abstract. When the sheet pile wall is deformed, a complex stress state occurs in the surrounding soil mass: the resulting compaction areas and shear areas have a mutual effect on each other. To determine the boundaries of the shear zone theoretically, it is necessary to solve a mixed problem of the theory of a linearly deformable medium and the theory of the ultimate stress state. The strict solution for such a problem is of considerable complexity, at present it is only possible to outline ways to approach its solution with the introduction of a number of simplifying assumptions. Substantial assistance in this direction should be provided by appropriately designed experimental studies. This experimental study aims to assess the deformability of soil counterweight berms, which improve the stability of deep pit enclosing structures during gradual soil excavation. The reference sources provide no methods for berm calculation, while the existing approaches are based on various safety coefficients addressing the reduction of passive pressure from the pit side when the counterweight berms are arranged. The main study results are new experimental data on the behavior of the soil counterweight berms. Certain approaches are proposed for defining the passive pressure from the counterweight berms. The research results are relevant for the construction industry because the obtained data will contribute to a more reasonable selection of the soil counterweight berm size during the deep pit design. The provided approaches addressing the passive pressure can be used in the calculations.

Keywords: Soil · Counterweight berm · Enclosing structure · Passive pressure · Active pressure

1 Introduction

A vast experience in the design and construction of structures with retaining walls confirms the opinion that flexible walls used as pit fences, in the construction of berths, coastal abutments of bridges, locks, fences to support road embankments, have the best performance. However, an obstacle to their widespread use is the lack of knowledge of the actual operation of such structures, since it has not yet been possible to create a reliable working model of a flexible wall. The calculation methods used in the design of the enclosing structures of the pit, based on the classical theory of soil pressure, assume

the presence of a certain pattern of movements, which in reality is not observed. One of the common disadvantages of the existing methods of calculating flexible walls, which designers are now forced to put up with, is, as is well known, an overestimation of the active pressure of the soil on the wall and, consequently, the calculated forces and movements of the enclosing structure.

When the sheet pile wall is strained, a complex stress state occurs in the surrounding soil mass: the resulting compaction areas and shear areas have a mutual effect on each other. To determine the boundaries of the shear zone theoretically, it is necessary to solve a mixed problem of the theory of a linearly strained medium and the theory of the ultimate stress state. The strict solution of such a problem is a significant complexity, at present it is only possible to outline ways to approach its solution with the introduction of a number of simplifying assumptions.

In most cases, the methods currently used for calculating enclosing structures do not take into account the possible change in the stress–strain state of the soil mass, the enclosing system in the process of constructing the system as a whole. In the construction practice, there are no absolutely fixed enclosing structures: they either bend under the action of loads or shift in any direction, depending on the compressibility of the foundation soil. These deflections and displacements of the walls, as well as the soil settlement behind them, lead to soil friction along the contact faces of the walls and to various displacements of the soil particles, which differ significantly from the estimated ones.

According to the Blum-Lohmeyer method, which is the most popular method for calculating tankless thin retaining walls, the wall bends and rotates relative to some point that is close enough to its lower end. As a result, the wall sections buried in the base above and below this point experience a reactive pressure directed towards the displacement directions. As shown by the research carried out by the authors [1], the possible turning point of the structure at the initial stage of soil digging in the pit occurs at shallow depths. With the further deepening of the pit, the turning point tries to shift in depth, but it is fixed by the movements of the soil mass as a result of wall bending of the wall, it stops. In the future, fixed by the soil mass displacement due to the wall bending, the turning point remains virtually unchanged.

The decrease in pressure above the point of the structure rotation is explained by the deviation of the wall from the vertical and, as a result, the soil mass unloading from the embankment side. The intensity of the soil resistance below the turning point on the side of the embankment, due to the presence of a large load from the base soil weight, increases very quickly. Thus, taking into account the gradual soil development, the turning point of the unencumbered thin retaining wall may be very close to the mark of the excavation depth. The number of stages and the depth of soil development within the stage have a decisive influence on its location.

According to the classical scheme of the stress–strain state of the soil at the level of the pit bottom from the side of the excavation, the value of the passive soil pressure should be equal to zero. However, if we take into account that the excavation mark of the pit at each subsequent stage is the zone of maximum values of passive pressures for the previous stages, then in the final phase of soil development at the level of the pit bottom, the zone of the greatest pressures is obtained. As the tests showed, the passive

soil pressure increases throughout the experiment. As a result of excavation, the soil loading is sharply reduced and the soil is decompressed and removed, which contributes to additional shear strains of the wall itself. As the soil is excavated behind the enclosing wall, the maximum bending moment zone gradually goes down, the area position with the maximum moment corresponds to the theoretical ones, but the value of the experimental maximum moment is much smaller. At the same time, in the upper zone of the enclosing structure, the experimental values of the bending moments are significantly higher than the theoretical values. That is, the decrease in the maximum moments is compensated by a more uniform distribution of them along the wall height.

The intense impact of the soil mass begins already at the first stages of the development of the soil in the form of prisms of collapse. The calculated values of deviations from the vertical throughout the experiment exceed the calculated values by up to 2.2 times. These movements of the structure top are also associated with the appearance of additional bending moments. The angles of inclination of the slip lines for all the collapse prisms agree well with the theoretical values and are in the range of 290–340. However, the wall is affected by several blocks formed at different stages, which significantly changes the strain figure of the enclosing structure. The actual maximum bending moment in the enclosing structure is 45–55% less than the theoretical values. The position of the section with the maximum moment corresponds to the theoretical values. However, in the upper part of the wall, the bending moments are several times higher than the calculated values, which should be taken into account when designing enclosing walls with different strength and stiffness characteristics in the height of the structure.

As a result of the gradual development of the soil, the position of the proposed turning point of the enclosing structure was determined below the bottom of the pit by ¼ of the height of the part being developed. This position of the turning point can negatively affect the stress–strain state of the soil mass from the side of the developed part of the pit. Also, as a result of the phased development in the final phase, the type of passive soil pressure plot changes significantly. At the same time, the stresses in the soil in the immediate vicinity of the bottom of the pit increase sharply, which contributes to the bulging of the ground surface. The maximum displacement of the top of the enclosing structure exceeded the calculated value obtained by existing methods by 25%.

In the case of cramped urban conditions, with buildings and structures in the immediate vicinity of the designed deep pit, certain difficulties arise related to ensuring the stability of pit enclosing structures during soil excavation. In some cases, when retaining systems or soil anchors are economically inappropriate or even inconceivable, the temporary stability of the pit enclosure structures can be provided by counterweight soil berms producing passive pressure along the wall perimeter [2–4]. However, despite the few available experimental and theoretical studies in this area, currently, no generally accepted mechanisms are described for the counterweight soil berm degradation, as well as no procedures for calculating their bearing ability and deformability are given in regulatory documents. The existing engineering approaches in the calculations [5–7] are based on various safety coefficients addressing the reduction of passive pressure from the pit side when the counterweight berms are arranged. In this regard, the authors of this paper conducted experimental studies of counterweight soil berms at different soil

excavation stages on a reduced scale using boxes. During the tests, the geometric dimensions of the soil berm and the types of soil were changed. The most common types of soil were used as the material of the soil berm.

2 Experimental Studies Using Boxes

Experimental studies were carried out in a square metal box with side dimensions of 1 m. A 1.5 mm steel hot-rolled sheet was chosen as the pit protective structure. These parameters of the enclosing wall were selected to form a relatively flexible structure allowing to trace the real bending behavior of the enclosing wall and the counterweight soil berm by height. Fine sand with an internal friction angle $\varphi = 32°$ was used as a back-fill. The intended soil density was $\gamma = 15 \text{ kN/m}^3$. Sand humidity in different experiments ranged from 1.55 to 1.8%. Soil pressure sensors (4) were installed on the steel sheet on the counterweight soil berm side with 150 mm step, which allowed evaluating the pressure from the berm (Figs. 1 and 2). The counterweight soil berm was built from the following materials:
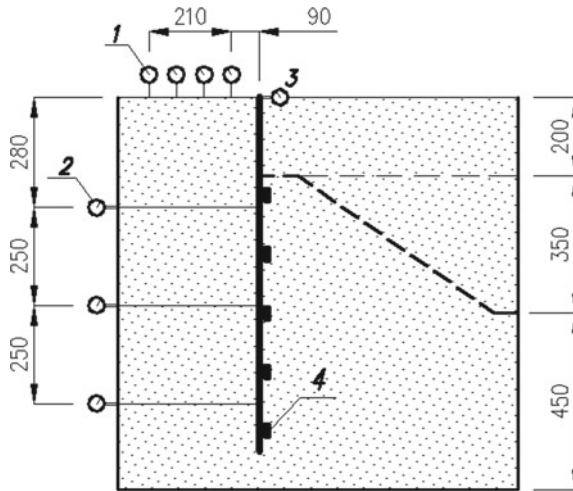
Fig. 1 Sensor and indicator locations

- Series 1—fine sand similar to back-fill with specific adhesion $c = 0.5$ kPa and the internal friction angle $\varphi = 32^0$ (12 samples);
- Series 2—sandy loam with the specific adhesion $c = 5$ kPa and the internal friction angle $\varphi = 20^0$ (3 samples);
- Series 3—clay loam with the specific adhesion $c = 20$ kPa and the internal friction angle $\varphi = 15^0$ (3 samples).

Soil pressure sensors shown in Fig. 3 were 3D-printed from plastic. Sensor dimensions were selected to ensure that the equivalent module of the structure is an order

Fig. 2 Enclosing structure and counterweight soil berm mockup

of magnitude higher than the soil deformation module. The main working element of the soil pressure sensor is a 0.2 mm flat membrane with a glued 20 mm resistive strain gauge. The deformation gauge measurements were read by an automatic deformation meter. The gauges were pre-calibrated on a test bench at different soil pressures. The calibration process consisted of multiple loading and unloading cycles.
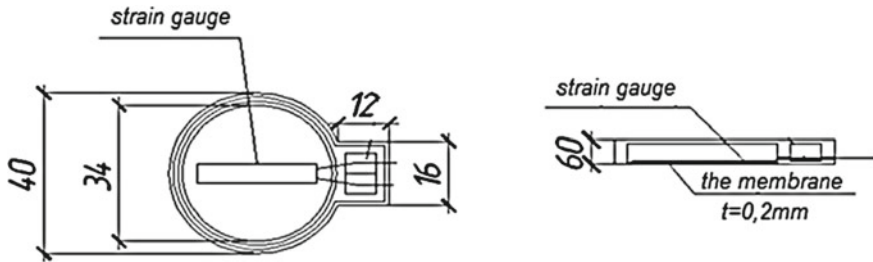
Fig. 3 Soil pressure sensor design

The vertical strains of the soil surface were taken from dial gauges (sensor group 1) fixed on a rigid metal frame. Wall displacement by height was measured using the same dial gauges (sensor group 2) connected to the wall via aluminum rods embedded in the soil (Fig. 1). The wall top displacement was measured by sensor group 3. Soil filling was performed in layers with compaction, as well as a density control by sampling and weighing.

Experiments were carried out in several stages:

Stage I. The soil was dug out to a depth of 20 cm over the entire area near the walls.

Stage II. The soil was dug out to a depth of 550 cm (with a counterweight soil berm arranged along the enclosing structure). The berm angle was taken equal to the soil internal friction angle, and the total dimensions—from the design experience [7–9].

Stage III. Application of an additional distributed load up to 1.4 kPa on the soil surface behind the wall. The load was applied to bring the counterweight soil berm to destruction.

The diagram and photo of the experimental box and counterweight soil berm with the installed system of measuring devices are presented in Fig. 4.
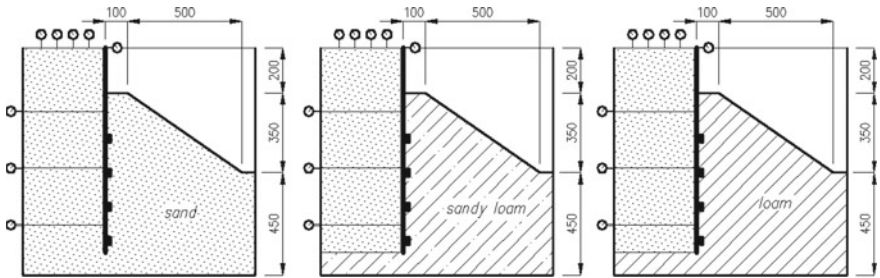
Fig. 4 Counterweight soil berm layout for 3 series of experiments

The enclosing structure displacement, vertical deformations in the soil surface, and the wall pressure on the berm were measured at each stage. All measurements were carried out by calibrated measuring devices and tools. A polyethylene film was used to exclude friction between the soil particles and the metal sheet. The berm and soil surface behind the wall was photographed during the whole experiment to study cracks and shear strains. Each subsequent stage was started after deformation stabilization. Figure 5 shows the averaged resulting values of the series of experiments conducted using the aforementioned method.
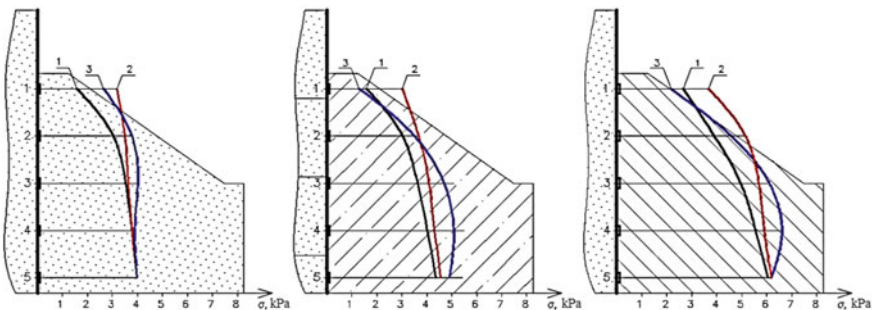
Fig. 5 Indications of soil pressure sensors: 1—stage *I*, 2—stage *II*, 3—stage *III*

3 Analysis of the Obtained Experimental Data

The field experiments and the analysis of their results allowed getting an idea of the actual stress–strain state of the soil mass within the soil berm and the enclosing pit structure. The work technology (in this case, the phased development of the pit was considered) significantly changes the stress–strain state of the soil mass and the strain figure of the enclosing structure itself.

The measurements of the soil pressure sensors (Fig. 4a) show that the wall pressure on the soil from the counterweight berm side does not change at the sensor 5 depth (85 cm), does not exceed the values of active soil pressure behind the wall and is actually a reactive counter pressure of soil. During all stages of the experiment, the pressure increases from 4.2 to 7.2 kPa at a depth of 40–70 cm (depths of sensors 2, 3, 4). However, the wall pressure on the berm increases to a certain amount and then begins to decrease between the sensors 1 and 2 (approximately at a depth of 13–28 cm from the berm surface). The specified phenomenon may indicate that the soil resistance threshold [10–12] is reached at the given depth. The enclosing structure displacement at this depth reaches 12 mm. The soil pressure on the wall is further redistributed to the lower berm layers with a greater bearing capacity. The pressure on the berm increases throughout the experiment below the –35 cm elevation, which indicates that the soil bearing capacity threshold [13–15] has not yet been reached, and the berm can bear the pressure from the enclosing structure despite the horizontal strain already reaching approximately 5 mm. Figure 6 shows the graphs of the horizontal displacement for the enclosing structure averaged along the depth, as well as soil compression near the walls at the last stage of loading (stage III) according to the indications of the sensor group 1, 2, 3. The maximum soil compression behind the wall in the immediate vicinity of the wall is about 0.65 of the wall top displacement.

As mentioned by some researchers [16–18], the active soil pressure distribution on the retaining walls directly depends on the wall displacement itself. This means that considering the wall-soil interaction only along the contact face is not enough. It is necessary to consider soil displacements in the back-filling behind the wall together with the strain of the counterweight soil berm.

Wall displacements can cause a sharp decrease in the lateral pressure of the soil on the wall. At the initial stage when the wall displacement does not exceed the diameter of the prevailing soil particles, the particle shifts occur, the limit equilibrium is established in a certain region within the sliding triangle, and the active soil pressure will virtually coincide with the values defined by the classical theories of limit equilibrium for this stage. A sharp decrease in active pressure is observed with further wall displacements. These states occur sequentially at different stages of soil development (stages I, II, III). At the first soil development stage (to a depth of 20 cm), the active pressure begins to grow. However, the pressure drops sharply after the wall is displaced, which corresponds to the moment when the counterweight berm achieves its bearing capacity at the corresponding depth. A uniform displacement occurs further with the formation of a sliding triangle, while the active pressure starts affecting the wall at full force again. The above processes are repeated sequentially during the second soil development stage (when the counterweight berm is arranged) and at the additional loading stage. A corresponding
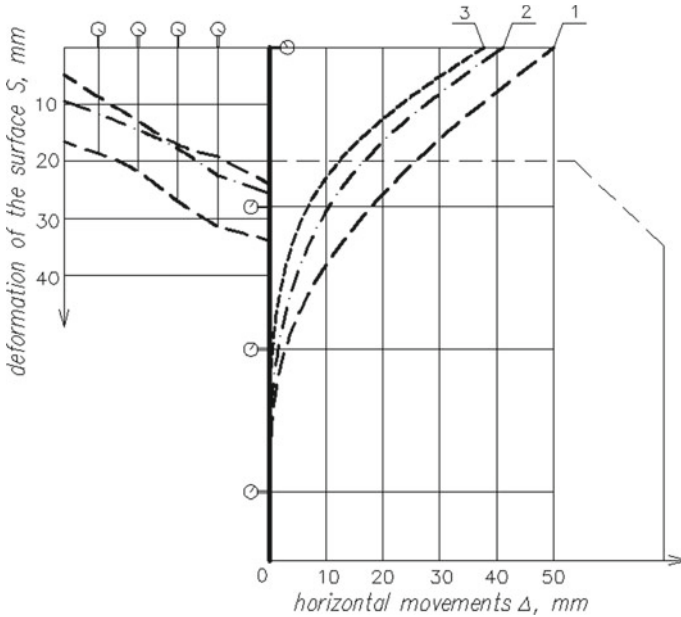
Fig. 6 Horizontal displacement of the enclosing structure by depth and soil compression near the wall: 1—for series 1; 2—for series 2; 3—for series 3

sliding area is formed resembling a wedge with different sizes for each soil development stage. Laterally, the sliding triangle boundaries behind the wall resemble a stepped fault.

The experimental observations led to a conclusion that the moments of wall active pressure reduction at different stages virtually coincide with the moment of counter-weight soil berm passive pressure reduction at specific depths. Based on the foregoing, it can be concluded that the counterweight soil berm degradation occurs with a simulta-neous decrease in passive pressure from the berms and active pressure behind the wall. This means that the enclosing structure displacements caused by shear strains inside the counterweight berm at different depths are accompanied by a temporary decrease in active pressure along the wall-soil surface behind the wall [19–23].

4 Recommendations for the Passive Pressure Determination from the Counterweight Berm

To define the bearing capacity of the berm, analytical dependences will be used to define the passive pressure of the soil behind the wall, which address pressure changes from the size and design specifics of the counterweight soil berm.

To take into account passive pressure from the counterweight soil berm in engineering calculations, the soil body is recommended to be divided into 3 calculation sections (Fig. 7):
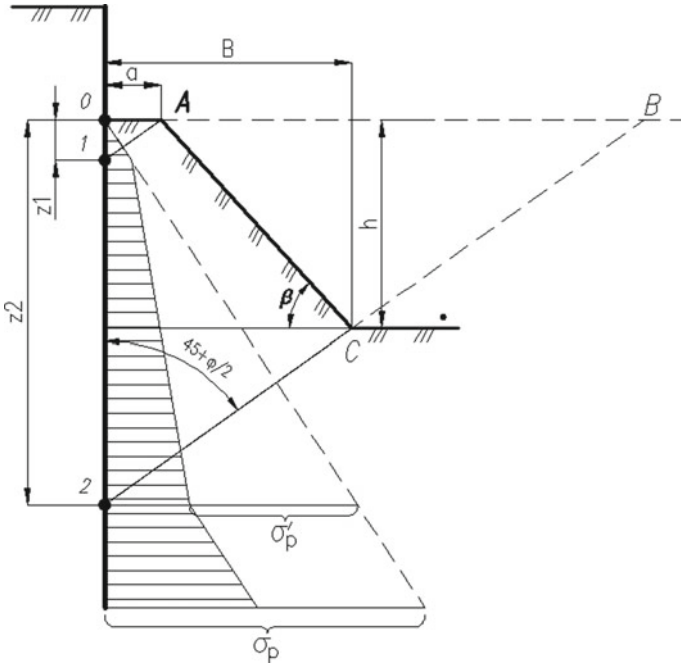
Fig. 7 Distribution of actual passive pressure from the counterweight soil berm

- the total passive pressure from the soil is recommended to be taken for section p. 0 ÷ p. 1;
- for sections p. 1 ÷ p. 2 and the section below p. 2, the actual passive pressure from the counterweight soil berm is recommended to be taken as a difference $\sigma_p - \sigma_p^1$:

where σ_p—the total passive pressure assuming that the soil surface lies on the plane A–B (i.e., berm design is not considered);

σ_p^1—passive pressure reduction due to the soil contained in the *ABC* sliding triangle.

The length of the estimated sections in the soil depth shall be determined assuming that the sliding surfaces of the bulging triangle coming from points A and C are tilted to vertical plane at an angle $\pi/4 + \varphi/2$:

$$z_1 = a \cdot \cot\left(45 + \frac{\varphi}{2}\right) \tag{1}$$

$$z_2 = h + B \cdot \cot\left(45 + \frac{\varphi}{2}\right) \tag{2}$$

The passive pressure in specific points along the depth of the enclosing structure can be determined according to the classical theory:

- in p. 1:

$$\sigma_p^1 = \gamma \cdot z_1 \cdot tg^2\left(45° + \frac{\varphi}{2}\right) + 2c \cdot tg\left(45° + \frac{\varphi}{2}\right); \tag{3}$$

- in p. 2, taking into account the function $k = f(c, \varphi, \beta)$, which addresses the decrease in the passive pressure of the soil due to the counterweight soil berm:

$$\sigma_p^2 = \left[\gamma \cdot z_2 \cdot tg^2\left(45° + \frac{\varphi}{2}\right) + 2c \cdot tg\left(45° + \frac{\varphi}{2}\right) \right] \cdot k \qquad (4)$$

Below p. 2, the value of the actual passive pressure can be determined by subtracting σ_p^1 from the total passive pressure calculated for the moment before the counterweight soil berm has been arranged.

5 Conclusions

The resulting data from the experimental studies allowed identifying and evaluating the strain and degradations behaviors of the counterweight soil berms. The stages of soil development arising due to the counterweight berm arrangement lead to the formation of separate stepped sliding triangles of soil behind the wall, which size depends on the geometric and strength properties of the counterweight soil berm.

Typically, the counterweight soil berm degradation occurs with a simultaneous decrease in the active pressure behind the wall and passive pressure from the counterweight soil berm. According to the experimental data analysis results, the value of the function $k = f(c, \varphi, \beta)$ is recommended to be taken as follows for use in practical calculations: for loose soil (sand) — $k = 0.5$; for sandy loams—$k = 0.6$; for clay loams—$k = 0.7$.

References

1. Mirsayapov IT, Safin DR (2011) Experimental surveys of deflected state of soil body consistent with rabbet in the process of graded excavation of ditch. Izvestiya KGASU 17:79–84
2. Wei D, Xu D, Zhang Y (2020) A fuzzy evidential reasoning-based approach for risk assessment of deep foundation pit Tunnelling and Underground Space Technology 97:103232
3. Goh ATC, Zhang F, Zhang W, Zhang Y, Liu H (2017) A simple estimation model for 3D braced excavation wall deflection. Comput Geotech 83:106–113
4. Mirsayapov IT, Khasanov RR, Safin DR (2015) Design fence of deep foundation pit of the residential complex in a congested urban area. Izvestiya KGASU 32:183–191
5. Grigorev YS, Fateev VV (2020) Geodetic deformation monitoring of a residential building constructed on a sloping site. Soil Mech Found Eng 5:17–21
6. Konyushkov VV, Urazaeva NY, Kirillov VM, Kondrat'eva LN (2018) To the issue of studying the diaphragm wall as an enclosing and load-bearing construction of buildings and structures. Bull Civil Eng 66:68–74. https://doi.org/10.23968/1999-5571-2018-15-1-68-74
7. Nikonorov A, Terleev V, Pavlov S, Togo I, Volkova Y, Makarova T, Garmanov V, Shishov D, Mirsche W (2016) Applying the model of soil hydrophysical properties for arrangements of temporary enclosing structures. Procedia Eng 165:1741–1747
8. Bogov SG, Bochkerev NP (2015) Geotechnical monitoring during zero cycle of constructing buildings with underground space. Hous Constr 1:36–41
9. Nikonorov A, Pavlov S, Terleev V, Arefiev N, Badenko V, Volkova Y (2015) Use of enclosing and temporary special structures under the reconstruction of hydraulic facilities in Saint-Petersburg. Procedia Eng 117:258–263

10. Lv J, Li Z, Xie X, Fu B, Fu H, Zhao H, Li X, Li Z, Tang Y (2020) Segment stress characteristics and ground deformation caused by constructing closely spaced parallel tunnels under a complex geological condition. Adv Civil Eng 1725210. https://doi.org/10.1155/2020/1725210

11. Siraziev LF (2017) Experimental studies of the stress-strain state of the three-layer soil base under short-term plate-bearing test and the presence of the water saturated layer. Izvestiya KGASU 42:228–236

12. Zhou J, Gong X, Zhang R (2019) Model tests comparing the behavior of pre-bored grouted planted piles and a wished-in-place concrete pile in dense sand. Soils Found 59:84–96

13. Mirsayapov IT, Khasanov RR (2011) Experimental studies of stress-strain state of flexible barriering design with bracing in the process of the phased excavation of the soil. Izvestiya KGASU 16:129–135

14. Sapin DA (2015) Settlements of foundations of adjacent buildings when arranging the trench "slurry wall." Hous Constr 4:8–13

15. Safin DR (2020) Experimental studies of a weak clay base reinforced with sand piles. In: IOP Conf. Series: Materials Science and Engineering, vol 962, p 032020. https://doi.org/10.1088/1757-899X/962/3/032020

16. Matos Paucar GD, Gutierrez Lazares JW (2020) Numerical modelling and geotechnical monitoring of an anchor wall system for a deep excavation in Lima conglomerate. In: Proceedings of the LACCEI international multi-conference for Engineering, Education and Technology. https://doi.org/10.18687/LACCEI2020.1.1.451

17. Minakov DK (2020) Analysis of monitoring results of technological settlements induced by the diaphragm wall installation. Geotechnics 1(1):46–48. https://doi.org/10.25296/2221-5514-2020-12-1-46-58

18. Luo Z, Li Y, Zhou S, Di H (2018) Effects of vertical spatial variability on supported excavations in sands considering multiple geotechnical and structural failure modes. Comput Geotech 95:16–29

19. Zhou Y, Ye W-N, Gao S (2018) Deformation characteristics of excavation of deep foundation pit at a metro station in Lanzhou Yantu Gongcheng Xuebao/Chinese. J Geotech Eng 40:141–146. https://doi.org/10.11779/CJGE2018S1023

20. Chen Y, Zhao W, Jia P-J, Han J-Y (2018) Proportion analysis of ground settlement caused by excavation and dewatering of a deep excavation in sand area. Indian Geotech J 48:103–113. https://doi.org/10.1007/s40098-017-0249-3

21. Xu W, Tang D, Tan R, Zhang Q (2015) Application of digital foundation pit system in a deep excavation. Yanshilixue Yu Gongcheng Xuebao/Chin J Rock Mech Eng 34:3510–3517. https://doi.org/10.13722/j.cnki.jrme.2014.0246

22. Mirsayapov IT, Aysin NN (2021) Evaluation of subgrade vertical deformations of the building with the influence of a deep pit. Lecture notes in civil engineering, vol 126, pp 51–58. https://doi.org/10.1007/978-3-030-64518-2_7

23. Mirsayapov IT, Aysin NN (2020) Subgrade vertical deformations of a building in the zone of a deep pit influence. In: IOP Conference Series: Materials Science and Engineering, vol 890(1), p 012071. https://doi.org/10.1088/1757-899X/890/1/012071

Problem-Solving for Moisture Transport in Loess

I. Yu. Dezhina[✉]

Don State Technical University, 1, Gagarin Square, Rostov-on-Don 344000, Russia

Abstract. This article presents the key resolving equations for the nonstationary filtration problem in soils with incomplete water saturation. When deriving the equation for moisture transport, we used Polubarinova-Kochina's equation for incomplete water saturation, as well as Darcy's law and Averyanov's formulae for physical correlations. We present a non-linear initial boundary value problem for moisture transport. The variational equation of the linearized problem was used to find the solution through the finite element method within an arbitrary time frame. We present the defining moisture transport equation as a matrix per period, including the water permeability, moisture transport, and nodal filtration rate matrices. The developed calculation procedure allows us to forecast base humidity changes in case of localized moisturizing or changes in underground water level. It views the soil as a heterogeneous filtration anisotropic medium in case of incomplete water saturation. The results of the computer simulation of loess soil moisturizing were compared to the moisturizing obtained from the pilot trench.

Keywords: Loess soils · Moisture transport · Variational equation · Finite-element formulation · Solution algorithm · Non-saturated media · Round trench

1 Introduction

The intensification of construction projects in areas with loess collapsing soils makes the forecasting of the stress and strain state of the bed crucial in view of possible moisturizing due to human activities. Subsidence loess soils include silt-loam spoils that are homogeneous and mostly macroporous. In terms of grain-size composition, they are over 50% silt particles (0.05–0.005 mm in size), high and medium soluble salts, and calcium carbonates. When soaked, they subside, become soggy and easily washed away. Under complete water saturation, they may enter into a quick state. These soils differ in color (dun, pale-yellow, straw-colored) and lithological type (loess-like sandy clays, loams, clays, loesses) and feature a rather low moisture content ($S_r < 0.8$), porosity $n = 44$–53%, and dry subsidence soil weight $\rho_d = 1.2$–1.6 t/m^3. Loess soils differ in their mineral composition, structure properties, salt composition, and relative subsidence. The total strain modulus, Poison's ration, specific cohesion, and internal friction angle depend on the moisture content [1].

When beds are waterlogged, the soil's strain and stress properties are reduced and buildings and structures may be deformed. Waterlogging can take various forms. They may include the increase in humidity due to the lack of normal aeration of developed territories, numerous water leaks from water supply lines, etc.

The study of the impacts waterlogging has on loess beds in terms of their physical, mechanical, and structural properties, as well as the study of the strain–stress state of foundation beds in case of waterlogging, is a relevant problem [2]. Filtration in loessic collapsing soils have been studied by Mustafaev [3], Prikhodchenko [4], Mirzaev [5], Chernyi [6], Sobolev [7], Volkov [8], Sitnikov [9], Broodwidebridge [10], De Roo [11], Boer [12], Chen et al. [13].

Following the existing regulations, the gravity or imposed load subsidence of a building can be determined based on the complete water saturation of the soil. Subsidence, however, begins much earlier [14]. The rate of strain is also significant and it depends on the moisture transport and the filtering ability of the soil.

The author's works deal with the improvement of calculation procedures using the second group of limit states through non-linear mechanical and mathematical models, with complete and incomplete water saturation, and under the interactions of non-stationary stress fields and humidity. This being said, we take into account that loess deposits are heterogeneous, filtrating, and anisotropic and that the water filtration in soil and subsidence can occur under incomplete water saturation. Wetting zone boundaries are not preset but determined for each period during the load soaking.

2   Defining Equations for Filtrating Transport of Moisture

Below are the key resolving equations for the non-stationary filtration problem in soils with incomplete water saturation. We assume that pressure, water permeability coefficient, and diffusion coefficient depend on saturation.

When deriving the moisture transport equation, we use Polubarinova-Kochina's equation for incomplete water saturation [15]. We can also apply Darcy's law and Averyanov's formulae [15]:

$$K(w) = K_1 \left[\frac{w - w_0}{m - w_0} \right]^{3.56} \tag{1}$$

where K_1 is the filtration coefficient under complete water saturation, m is the soil porosity, w_0 is the amount of bound water per soil volume unit (volumetric bound water content).

$$P_W = -\frac{P_0 \cdot w_0}{w} \cdot \frac{w_n^3 - w}{w_n^3 - w_0^3} \tag{2}$$

where P_0 is the pressure at bound water humidity w_0, w_n is the humidity of complete water saturation.

Bound water content value w_0 can be calculated using this formula

$$w_0 = w_{vs} + w_{rs} \tag{3}$$

where w_{vs} corresponds to the air-dried moisture (the amount of water per sample at the relative humidity of 55% and the temperature of 19–20°). According to Larionov [16], this value for loess soils is within 0.012 (loess) and 0.037 (heavy loess loam) (Rostov-on-Don). w_{rs} is the content of spongy-bound water determined through drying, vacuuming, and adsorption curves. Experiments show that this value was between 0.116 and 0.128 for loess loam.

The use of an empirical equation for suction pressure [4] instead of Averyanov's formulae allows for a better consideration of loess soil properties.

Initial boundary moisture transport is expressed as follows:

$$
\begin{aligned}
-B^T kJ - B^T DBw + \dot{w} &= 0, & &\in V; \\
-B_S^T kJ - B_S^T DBw - V_S &= 0, & &\in S_3; \\
w - w_S &= 0; & &\in S_4; \\
w - w_0 &= 0; & &\in V, S, t = 0.
\end{aligned} \tag{4}
$$

where B is the differentiation operation matrix, D is the diffusion coefficient matrix, V is the filtration speed, w is the water content change rate.

Darcy's law is applied in case of incomplete water saturation:

$$
V = -DBw - kJ, \qquad \in V \tag{5}
$$

Filtration coefficients k and fluid pressure P were determined using formulaes (1) and (2).

To obtain subsequent solutions in relatively small periods $\tau \in [0, \Delta t]$, we assume that the diffusion coefficient $[0, \Delta t]$ is constant and equals D^n, calculated using w^n at the beginning of the period. The system of Eq. (4) is linearized in an arbitrary period. We use the variation convolutional equation [17] and the finite element method [18] to calculate a solution within an arbitrary period.

The matrix of the defining moisture transport equation for the period Δt looks as follows:

$$
\begin{aligned}
&\left(\theta \cdot \Delta t \cdot K^n \cdot 3 \cdot C \right) \cdot q^{n+1} + \left[(3 - \theta) \cdot \Delta t \cdot K^n - 3 \cdot C \right] \cdot q^n \\
&+ \left[P^n \cdot (3 - \theta) + \theta \cdot P^n \right] = 0
\end{aligned} \tag{6}
$$

where θ is the stability of the computation sequence (assumed to be $\theta = \frac{3}{2}$ following the Crank-Nicolson scheme).

The water permeability matrix

$$
K^n = \int_V \Phi^T D^n \Phi dV \tag{7}
$$

The moisture transport matrix

$$
C = \int_V \varphi \cdot \varphi^T dV \tag{8}
$$

The nodal filtration rate vector

$$P = \int_V \Phi^T K^n I dV + \int_V \varphi V_S dS \tag{9}$$

where V_S is the filtration rate.

To obtain stable forth integration sequences for moisture transport equations, we used the method of pinpoint invariant preservation (PIPM) proposed by Vasilkov [19].

For conservative moisture transfer problems, the total moisture content in the porous medium in question is the preserved parameter. A problem is deemed conservative if it lacks nodal moisture sources and drains in the finite-element model, i.e. a conservative problem is described by a homogeneous moisture transfer equation

$$g * (Kq + C\dot{q}) = 0 \tag{10}$$

Let us review the solution of Eq. (10) for the *(n + 1)* timeline as a sum of the conservative and non-conservative parts

$$q^{n+1} = q_1^{n+1} + q_2^{n+1} \tag{11}$$

We obtain the approximate solution of the problem using the Crank-Nicolson method with a "frozen" water permeability matrix whose elements are determined via the nodal moisture values $w^n(t = t^n)$.

The conservative part of the equation:

$$\left(K^n + \frac{2C}{\Delta t}\right) q_1^{n+1} = \left(-K^n + \frac{2C}{\Delta t}\right) q^n - 2P_1^n \tag{12}$$

The non-conservative part of the equation:

$$\left(K^n + \frac{2C}{\Delta t}\right) q_2^n = -2P_2^n - 2P_2^{n+1} \tag{13}$$

$$P_1^n = \int_V \Phi^T K^n I dV \tag{14}$$

$$P_2^n = \int_S \varphi V_S^m dS \tag{15}$$

The solution q^{n+1}, in the physical sense, corresponds with the moisture movements in the V porous medium with waterproof boundaries.

Following the law of matter conservation, the total moisture content is constant at any time in the given medium with waterproof boundaries. Thus, the total moisture content for the finite element model is as follows:

$$W = \sum_{r=1}^{m} \int_{(v1)} W_r dV_r = const \tag{16}$$

where V_r is the volume of finite element r; W_r is the moisture distribution function in finite element r; m is the total number of elements of the discrete model.

We can use expression (16) to develop a stable forth-integration chart.

The solution sequence for moisture transport problems using the PIPM is as follows. From Eq. (11), we determine q_1^{n+1}. Condition testing:

$$q_0 \leq \tilde{q}_1^{n+1} \leq q_0^{sat} \tag{17}$$

If condition (17) is fulfilled, we calculate the humidity vector for the next period using formula (11). Otherwise, we calculate the correcting module

$$\gamma = \frac{W(q_1^0)}{W(q_1^{n+1})_{const} + W(q_1^{n+1})} \tag{18}$$

Clarifying the humidity vector using this formula:

$$\tilde{q}_1^{n+1} = \gamma \cdot q_1^{n+1}; \tag{19}$$

Solving non-linear equations using a forth integration sequence consists of performing consecutive steps along the time axis.

The moisture transport was validated by the author by comparing the results of the numerical experiment and the results of large-scale field studies using one-curve and two-curve moisturizing in Grozny [20]. The analysis of the results obtained shows that, apart from θ, the stability of the forth integration sequence depends on the period Δt, moisturizing time, the volume of water injected into the soil, as well as the physical and mechanical properties of the soil.

3 The Statement and Solution of an Axially Symmetric Problem for Moisture Transfer Using the Finite Element Method

Let us consider the finite-element digitalization of an axially symmetric problem using triangular elements.

Let us denote the following: W is the required nodal moisture function. We will use approximation W as a linear polynomial.

$$\begin{aligned}
W_i &= a_0 + a_1 r_i + a_2 z_i \\
W_j &= a_0 + a_1 r_j + a_2 z_j \\
W_k &= a_0 + a_1 r_k + a_2 z_k
\end{aligned} \tag{20}$$

Or

$$\{W\} = [rz]\{a\}, \text{ where } \{a\} = \{a_0 \ a_1 \ a_2\}, [rz]^T = \{1 \ r \ z\}$$

Constant values a_0, a_1, a_2 are determined through solving the system of equations (20).

$$a_0 = \frac{1}{2S}\left[(r_j z_k - r_k z_j)W_i + (r_k z_i - r_i z_k)W_j + (r_i z_j - r_j z_i)W_k\right]$$

$$a_1 = \frac{1}{2S}\left[(z_j - z_k)W_i + (z_k - z_i)W_j + (z_i - z_j)W_k\right]$$

$$a_2 = \frac{1}{2S}\left[(r_k - r_j)W_i + (r_i - r_k)W_j + (r_j - r_i)W_k\right] \tag{21}$$

Area of triangle

$$S = \frac{1}{2}\left[(r_j - r_k)(z_k - z_i) - (r_k - r_i)(z_j - z_k)\right]$$

Moisture at any point on the element can be expressed as follows:

$$W = \{rz\}^m[a]^{-1}\{q\} = \{\phi^m\}\{q\} \tag{22}$$

where $\{q\}$ is the nodal moisture flow vector; $\{\varphi^m\}$ is the coordinate function matrix of a finite element.

At the barycenter of the triangle $r = \frac{r_i + r_j + r_k}{3}$; $z = \frac{z_i + z_j + z_k}{3}$.

Let us denote

$$[\Phi] = \{B\}\{\varphi\}^T \tag{23}$$

where $\{B\}$ is the differentiation matrix.

Coordinate function matrix

$$\{\varphi\} = \left(\tfrac{1}{2S}\right)\left\{\begin{array}{c} (r_j z_k - r_k z_j) + (z_j - z_k)r + (r_k - r_j)z \\ (r_k z_i - r_i z y_k) + (z_k - z_i)r + (r_i - r_k)z \\ (r_i z_j - r_j z_i) + (z_i - z_j)r + (r_j - r_i)z \end{array}\right\} \tag{24}$$

Then

$$[\Phi] = \left(\frac{1}{2S}\right)\begin{bmatrix} zj - zk & zk - zi & zi - zj \\ rk - rj & ri - rk & rj - ri \end{bmatrix} \tag{25}$$

The balance equation looks as follows:

$$[K]\{q\} + [C]\{q\} + \{P\} = 0 \tag{26}$$

The water permeability and moisture transfer matrices respectively are

$$[K] = \int_V [\Phi]^T[D][\Phi]dV = \frac{r\pi}{2S}[\Phi]^T[D][\Phi] \tag{27}$$

$$[C] = \int_V \{\varphi\}\{\varphi\}^T dV = \frac{\pi r}{2S}\{\varphi\}\{\varphi\}^T \tag{28}$$

where $[D]$ is the diffusion coefficient matrix. Nodal moisture flow vector

$$\{P\} = \int_S \{\phi\}\{V_S\}dS + \int_v [\Phi]^T[K_{zz}]\{I\}dV; \tag{29}$$

Or

$$\{P\} = \left(\frac{2\pi S}{12}\right)\left\{\begin{array}{c} K_{zz}(2r_i + r_j + r_k) \\ K_{zz}(r_i + 2r_j + r_k) \\ K_{zz}(r_i + r_j + 2r_k) \end{array}\right\} \tag{30}$$

where $[K]_{zz}$ is the vertical water permeability coefficient.

4 Numerical Solution of Moisture Transport Problems

To solve practical problems, the author prepared a calculation algorithm and a program that forecasts bed humidity changes during local moisturizing and underground water level changes. Soil is modeled as a heterogeneous filtering and anisotropic medium under incomplete water saturation.

The initial data comprise the following values: horizontal filtration coefficient k_f^g, vertical filtration coefficient k_f^v; humidity under complete water saturation w_{sat}; porosity factor e; initial humidity w_{est}; volumetric bound water content w_0; bound water humidity pressure P_0; period Δt; computational domain parameters. The solution algorithm stipulates the formation of the physical and mechanical properties of finite elements and the geometrical dimensions of the computational domain, the division of the computational domain into nodes and triangles, determining the filtration and diffusion coefficients, forming equation parameters using the Crank-Nicolson method, solving the system of equation using the compact exclusion method and the formation of the humidity vector.

5 Determining Humidity Change While Moisturizing the Trench (an Axisymmetric Problem)

It is required to determine the change of humidity within the subsidence layer when finite-element formulation 10 m in diameter and 0.4 m in depth in Grozny.

The physical and mechanical characteristics of the soil are given in Table 1 [20].

Table 1 The physical and mechanical characteristics of the soil in Grozny

–	ρ	W	e	S_r	ρ_s	W_L	W_p
W_{est}	1.53	0.08	0.93	0.26	2.7	0.226	0.168
W_{sat}	1.88	0.33	0.93	0.97	2.7	0.226	0.168

The experimental plot comprises light loess-like loams that turn into sandy clay. The subsidence deposit is 8–9 m thick and has an underlay of sand. The relative soil subsidence under 0.2–0.3 mPa reachers $\xi_{sl} = 0.11$–0.12, which is very high, thus signifying almost destruction of the soil structure when moisturized. Work [20] presents observations of moisture distribution in-depth at various periods (Table 2).

To solve the problem using the method of finite elements, we divided a plot of 16-m radius and 8-m depth into triangles. Based on the calculation results, we built humidity isolines for various periods (0.2–5 days). For the calculation, we assumed that $w_0 = 0.1$; $k_f^v = 0.7$ m/day; $k_f^g = 0.538$ m/day; $w_{vol}^{est} = 0.126$; $w_{vol}^{sat} = 0.48$.

The calculation confirms that if the water surface is large enough in highly porous soils and there are no watertight layers in the passage of the filtration flow, the pellicular front shifts from the trench down in an almost plane-parallel manner, and the sideway water distribution is low (Fig. 1).

Table 2 Moisturizing depth of the loess depos it at different times, m (from the bottom of the trench)

T, day	Experiment	Calculation
0.40	–	1.25
1.00	2.00	2.40
2.00	4.00	4.10
3.00	6.00	5.65
4.00	7.50	7.10
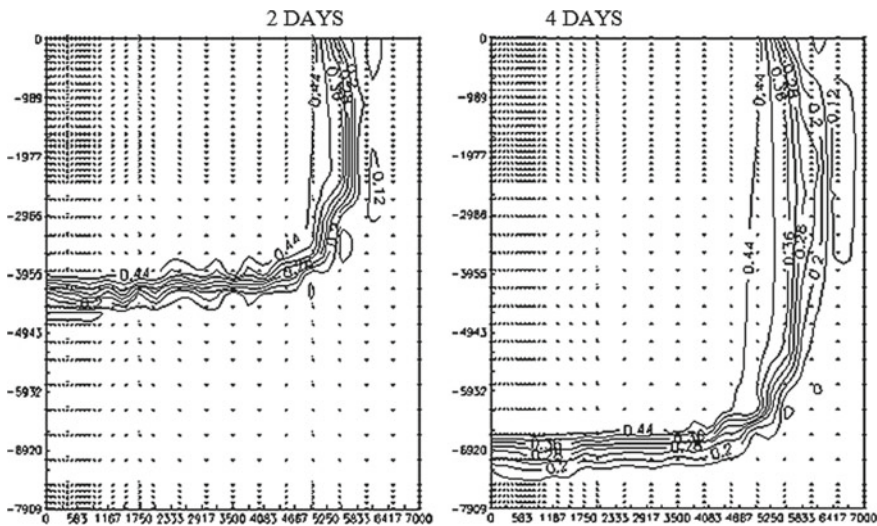
Fig. 1 The location of humidity isolines (from the soil surface, mm) after 2 and 4 days of moisturizing (of a trench in Grozny); $\Delta t = 0.005$ days

6 Summary

We presented a set-up and finite-element formulation of moisture transport problem solution for non-saturated media (as exemplified by subsidence loess soils) without consideration of the stress and strain state. The suggested calculation procedure using numerical methods showed a good correlation with the results of moisturizing a pilot trench.

References

1. Li Y, Shi W, Audin A et al (2018) Loess genesis and worldwide distribution. J Earth-Sci Rev. https://doi.org/10.1016/j.earscirev.2019.102947
2. Dezhina IYu (2018) IOP Conf Ser: Mater Sci Eng 451:012106. https://doi.org/10.1088/1757-899X/451/1/012106

3. Mustafaev AA (1989) Foundations on subsidence and swelling soils. Vysshaya Shkola, Moscow
4. Prikhodchenko OE, Peredelsky LV (1979) Soil water suction in loess soils and methods of its measurement. In: Base beds and foundations. Building on subsidence soils. Rostov University Press, Rostov-on-Don, p 115–119
5. Mirzaev AG, Yakubov MM (1986) On measuring the moisturizing of loess soil deposits. J Izvestiya AN UZSSR Ser Phys Math 2:91–93
6. Cherny BI (1970) Calculating the moisturizing regime for the loess bed. The problems of soil mechanics and loess bed construction. Chechen and Ingush Publishing House, Grozny, pp 157–162
7. Sobolev AA, Shvetsov GI, Glubokova EA (2006) The experimental research of filtration anisotropy of loess macropore soils. In: Polzunovsky Vestnik 1, 2. Barnaul, p 112–113
8. Volkov IA (1978) On the mathematical modeling of non-stationary filtration in fractured porous media. In: Water filtering in porous media. Naukova Dumka, Kyiv, p 61–89
9. Sitnikov AB (2009) The recommended procedure for the mathematical modeling of non-linear moisture transport in non-saturated and saturated soils. J: Geol Zhurnal 2:77–85
10. Broodwidebridge P, White I (1988) Constant rate rainfall infiltration: a versatile nonlinear model 1. Analytic solution. J Water Resour Res 24:145–154. https://doi.org/10.1029/WR024i001p00145
11. De Roo APJ, Th RH (1992) Infiltration experiments on loess soils and their implications for modeling surface runoff and soil erosion. CATENA 19(2):221–239
12. Boer R (2000) Theory of porous media, p 187–330. https://doi.org/10.1007/978-3-642-59637-7_4
13. Chen X, Fridman A, Kimura T (1994) Nonstationary filtration in partially saturated porous media. Eur J Appl Math 5(03):405–429. https://doi.org/10.1017/S0956792500001522
14. Krutov VI, Bulgakov VI, Korotkova ON (1980) The impact of humidity increase on the relative subsidence and compaction of loess soils. J Soil Mech Found Eng 1:19–21
15. Polubarinova-Kochina PYa (1977) The theory of groundwater movement. Nauka, Moscow
16. Larionov AK (1971) The methods of researching soil structures. Nedra, Moscow
17. Rozin LA (1978) Variational problem set-up for elastic systems. Publishing House of Leningrad University, Leningrad
18. Singiresu R (2017) The finite element method in engineering. Butterworth, Heinemann
19. Vasilkov GV, Imedashvili NG (1997) The pinpoint invariant preservation method in solving non-stationary mechanical problems. News of higher educational institutions, vol 4. Construction, Novosibirsk, pp 60–68
20. Kravtsov GI (1970) The stress-strain state of the moisturized loess bed of a rigid round stamp (axisymmetric problem). The problems of soil mechanics and loess bed construction. Chechen and Ingush Publishing House, Grozny, pp 108–124

Application of BIM-Technology in Developing a Two-Room Apartment Interior Design Project

O. Finaeva[✉] and V. Osadchaia

South Ural State University, 76, Lenina Av., Chelyabinsk 454080, Russia
finaevaov@susu.ru

Abstract. The article presents our experience of using building information modeling (BIM) in the development of a remodeling and interior design project for a two-room apartment in an existing building. The introduction provides a brief overview of current trends in design and an overview of the situation of BIM design in Russia and abroad. A brief overview of the history of the development of information modeling of buildings is provided. The main section provides a description of the project and lists the structure and basic principles of information modeling of buildings when working with existing objects. Information on the regulatory framework and the structure and composition of the construction information classificator providing interoperability when designing spaces using BIM is considered and summarized. A comprehensive approach to design planning is considered, taking into account the requirements of ergonomics and anthropometry. The initial data and design task, the accepted design decisions for remodeling, and the basic concept of interior design are given. The lighting scenarios, BIM tools, and the advantages of BIM in the development of apartment interior design are described. The results section provides a list of the works carried out during the remodeling and functional zoning of the space, in accordance with which the lighting scenario was developed. The project elements created using BIM are described. In conclusion, the need for new approaches to the residential interior design due to requirements for improving the quality of design and design techniques, including the development of BIM is noted.

Keywords: BIM · Building remodeling · Interior design

1 Introduction

The modern approach to design planning involves the consideration of many different parameters. When developing an apartment interior design project, the preferences of the customer must be accounted for. The optimal technical, technological, and design requirements must be guaranteed through design methods while ensuring compliance with environmental standards. Optimal planning solutions must be sought after. The integrated design method solves these issues best. Building Information Modeling (BIM) reflects the maximum benefits of the integrated design approach. BIM is a technology for

information modeling of buildings and structures, which involves the creation, editing, and subsequent use of a virtual copy of buildings and structures [1].

The BIM concept originated in the United States in the 1970s [2] and is one of the most advanced methods of design today. It allows the user to automatically make and track changes in various structural elements [3] and monitor the state of the object at all design levels [4, 5] and when the object is in operation [6]. This makes it possible to reduce errors in the work of related specialists [7] and reduce labor costs for their implementation [8]. The efficiency and flexibility of such design systems is best demonstrated when changes to the design must be made due to technological requirements introduced into the project at the development stage, changes in the construction conditions, or the wishes of the customer.

One of the stages of project development is the creation of a 3D model [9]. When applying information models to existing real estate objects, their reconstruction, and their operation, BIM can optimize the design processes, making it possible to:

- simulate changes in building structures;
- design upgrades and renovations to the utilities of a building or structure;
- change the building (structure) parameters and assess its suitability and usefulness for specific conditions;
- predict the performance of the object [10].

BIM can be applied to solve problems of use of space, form making, and visualization of a project. The distinctive features of BIM are its tools for project presentation and resolution of conflicts in the mutual arrangement of objects [11]. This facilitates the design process, saves time, and significantly improves the quality of the project in terms of maintaining ergonomic parameters and ensuring optimal use of apartment space.

2   Computer Modeling and Design Technology

Various standards have been developed in BIM which regulate all stages of information modeling and the implementation of the corresponding processes: organization of work at all stages of the object's life from design to demolition, interoperability in BIM technology [12], requirements for components and their information models, development of classification systems, creation of information platforms and data libraries, guidelines for design management, and much more [13, 14].

Various companies offer options for BIM design in Russia [15, 16] and abroad [17, 18]. They have a different set of characteristics and offer options for working in different areas of design. Each of them has certain advantages and disadvantages. The list of supported functions varies, as does their ability to load certain databases, typical objects, and automatically create specifications for certain types of work [19].

One of the first BIM programs was GRAFISOFT ArchiCAD. It was originally created for the development of architectural and design projects. Its advantages include: the team collaboration function, the presence of certain helpful tools (such as Layout Book, CineRender) and several other functions. The disadvantages of the program are its narrowly focused construction site: its toolkit is aimed exclusively at modeling buildings, other forms of design such as urban development are not possible.

In the development of interior design projects, special attention is paid to the issues of ergonomics: the influence of color [20, 21] and light on the perception of space [22–24] and the creation of a comfortable living environment [25, 26]. One of the principal objectives in mini apartment design is visually expanding the internal space. Design techniques aimed at mini apartment spacial remodeling serve a means of creating personal space for comfortable living in an urban environment [27]. Conducive living conditions provide reducing physical exertion and enhancing the relaxation of the inhabitants [28].

An integrated approach to solving the assigned project tasks takes priority: attention is paid to the individual needs of the customer and their anthropometric, sociopsychological, psychophysiological, physiological, psychological, hygienic and factors when developing the functional zoning of the space of an apartment and design concepts.

To carry out the above-mentioned tasks, the following methods can be used: developing a thorough lighting scenario and placing the lighting equipment and its operating and control elements according to the needs and parameters of a certain individual [29], selection and disposition of the kitchen and sanitary equipment, selection of furniture and interior finish materials based both on their aesthetic value and maintainability.

Thus, the right approach to developing an apartment interior design project will lead to providing all necessary conditions for comfortable living of an individual by applying modern techniques and smart systems, taking into account the individual's pace of life, without destroying the stylistic and compositional unity of the interior design [30].

3 Development of a Remodeling and Interior Design Project for a Two-Room Apartment

3.1 Architectural and Designing Planning Specification

It is necessary to develop a design project for the interior of a two-room apartment in a brick multi-apartment building with an average number of stories. The building is located in climatic region 4, in the city of Miass (Chelyabinsk Region). The space includes: a living room, a kitchen-niche, a bathroom, a bedroom, a hallway, and a walk-in closet. The total area of the apartment is 45.6 m^2.

The interior design project includes several tasks:

- renovate the apartment without changing (disrupting) the structure of the load-bearing walls (changing the configuration of the bathroom, allocating space for the dressing room from the total area of the bedroom);
- replace the plumbing fixtures of the kitchen and bathroom;
- account for the requirements of functional zoning, ergonomics, and anthropometry;
- create an electrical plan (develop lighting scenarios, determine the placement of electrical equipment, install heated floors).

3.2 Interior Concept

The interior is created for one person. The apartment is long with small windows—there is not enough natural light in the space. We decided to design the entire interior in light

colors and increase artificial lighting. For the same reason, the kitchen sink and the dining table were placed adjacent to the windows. This is an area to attract guests; we visually enlarged it with mirrors.

The bedroom is large, so we moved the closet to the bedroom. The walk-through closet is separated from the general space with a sliding door, which significantly saves space.

The bathroom was remodeled in accordance with the wishes of the customer. Since the customer's age does not allow for the use of a bath, we replace it with a shower. This allows us to place a washing machine in the bathroom (see Fig. 1).
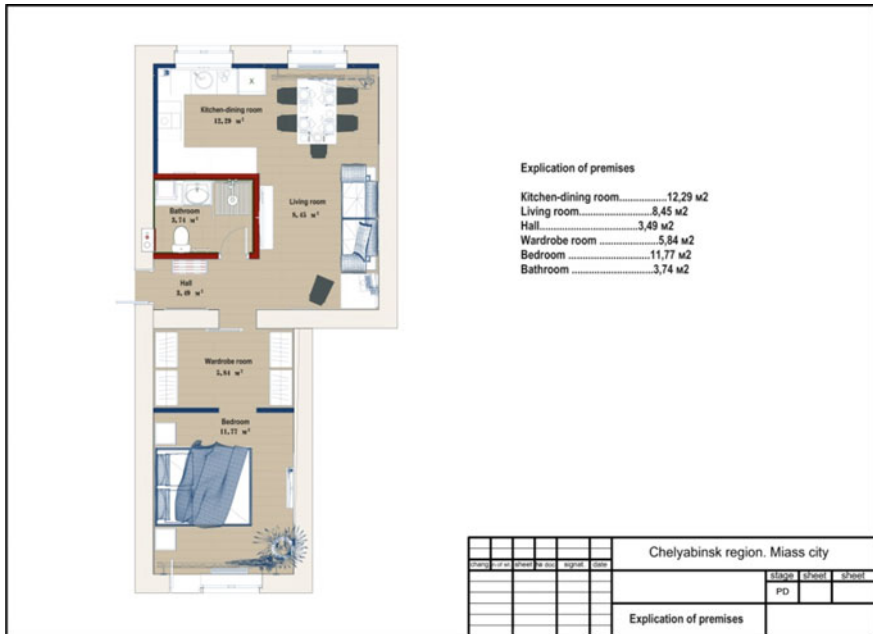
Fig. 1 Layout of the apartment with furniture arrangement

We chose a floral wallpaper for the accent walls, which serves to break the space of the rectangular room. We chose fine textured and light wallpaper for the remaining walls. We painted the ceilings in light colors to visually increase the height of the rooms.

We choose quartz vinyl as the flooring material. This is a versatile material, allowing it to be placed in the hallway, in the kitchen, and in the living room without t-molding, which gives us a visually continuous space and minimizes flooring transitions. For comfort and additional heating, we included electric heated floors in the hallway and bathroom, thus providing dry shoes in the hallway and a comfortable microclimate in the bathroom.

3.3 Lighting Scenario

The project includes two way light switches located at the entrance and in the living room so that the customer does not need to return to the entrance (where floors might be

dirty) to turn off the lights. The switch allows for the light to be turned on when moving towards the walk-in closet and turned off at the front door when leaving the home.

The ceiling height is 2500 mm, so we choose surface-mounted and flat luminaries. We only use suspension lamps in the bathroom by the mirror, thereby visually stretching the interior vertically. The living room is illuminated by one ceiling lamp, while the dining area is lit by a pendant lamp, which descends over the table to create a cozy atmosphere and delineate the table space. The kitchen is illuminated by spotlights to evenly distribute the light throughout the room. The ceiling light would cast a shadow on to the kitchen counter if the customer is cooking, so we added under counter lighting for illumination and visual comfort.

The bedroom has two lighting options: a chamber light from a sconce by the bed and a pendant lamp above the bed for general lighting. In the bathroom there is a ceiling light and an additional button for a lamp near the mirror, which can be turned on as needed.

The dressing room is lit by functional spotlights evenly distributed over the perimeter, with the lamps directed towards the cabinets.

3.4 Application of BIM in Design

We created an interactive model of the apartment in ArchiCAD. The model includes the floor plan, furniture, plumbing and electrical, and finishing materials. The interactive model allows you to view the object in 3D or create interactive elevations and interactive sections. Changes made to a section (for example) are automatically made in the plan, in the 3D model, in the schematics.

According to the BIM system, during the creation of our interior design project, we will create:

- interactive sections
- a set of plans with a description of the object
- a list of doors
- a list of electrical appliances
- a list of flooring, wall, and ceiling materials
- a list of plumbing fittings.

The interactivity of the model allows for finishing materials to be selected during the design stage (Fig. 2) and to view and evaluate the result on a 3D model (Figs. 3 and 4). For example, we chose a Rada Doors model Agilta DG5 in white enamel for the bathroom and sliding doors mirrored on both sides for the walk-in closet. Changes can be made at any stage of the design process. When coordinating the interior design with the customer, it is possible to demonstrate the intended result, including a VR demonstration.

3.5 Advantages of BIM in the Development of Apartment Interior Design

BIM helps to store all information about an object in the model, including the price of realization. The user can:
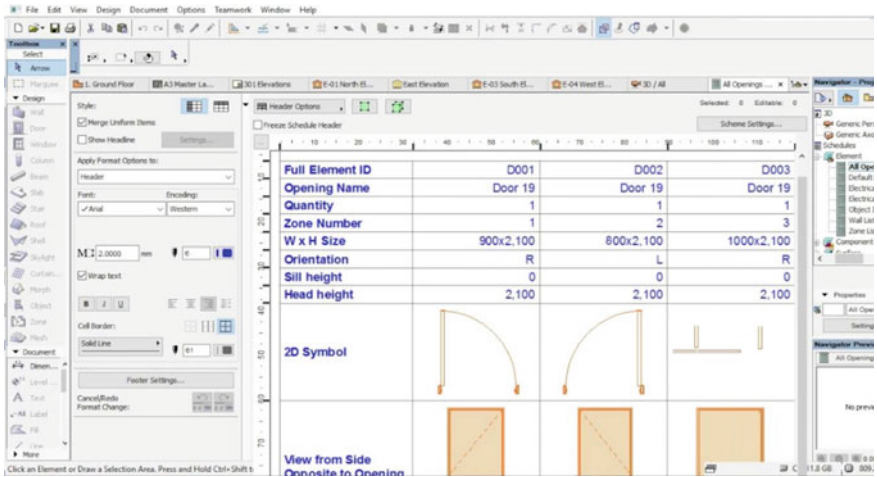
Fig. 2 Screenshot. The list of doors

Fig. 3 Kitchen

Fig. 4 Living room

- count the volume and area of the required materials;
- see the result in the sections and in the 3D model;
- change the location of an element once (in a section, for example) and everything which has changed in the model will change in the schematics automatically, which significantly reduces the chance of errors and saves time;
- use the human model provided in the library of elements to solve issues of ergonomics and visually indicate sharp angles in the layout for the customer.

Creating lighting scenarios and an electrical plan in BIM can significantly reduce the labor of developing project schematics. The interactive model allows for the designer to visually demonstrate the result to the client and immediately make changes to the project if the client so desires, including changing their color scheme and the placement of furniture in the apartment without additional labor costs to change working schematics.

For example, the bathroom schematic is formed from interactive views. There are three fragments per sheet. The designer can drop in to each schematic to make changes (Figs. 5 and 6). By highlighting an object, we can see certain information on it: layer, height, ID number.

4   Results

As a result of the work carried out with the help of BIM, we developed a design project for the interior of a two-room apartment. First, a minor remodel of the apartment was completed without changes to the load-bearing walls:

Fig. 5 Bathroom. General view
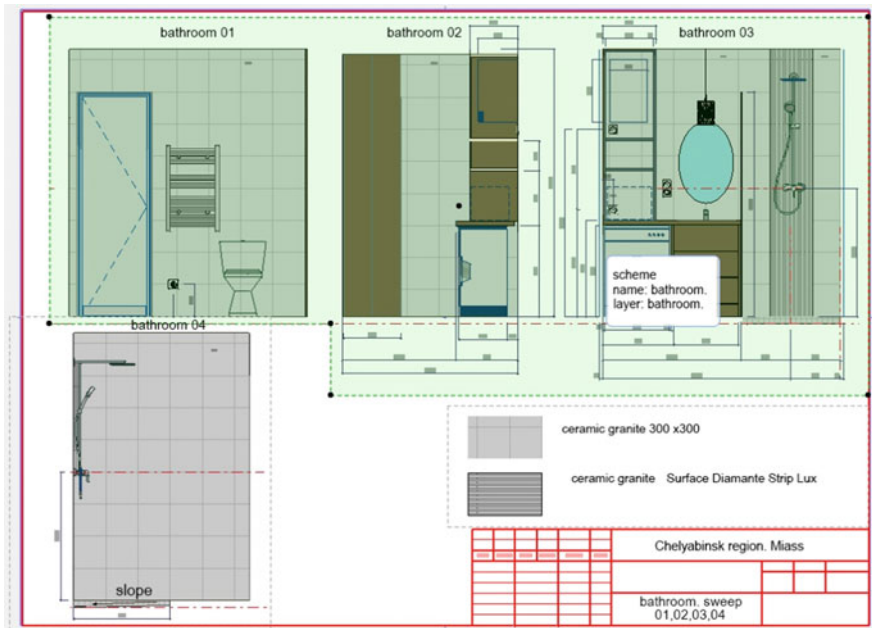
Fig. 6 Screenshot. Bathroom schematics

- the configuration of the bathroom and the plumbing was changed;
- floor space from the bedroom was reallocated as a walk-in closet;
- the kitchen space was reorganized, the sink was moved to the window.

Secondly, functional zoning was performed and lighting scenarios were developed accordingly. Color combinations were chosen, accents (prints and mirrors) were placed. Finishing materials and lighting equipment were selected.

Thirdly, an interactive 3D model of the apartment was developed and the following elements of the project were formed:

- interactive sections;
- a set of schematics with a description of the object;
- a list of doors;
- a list of electrical appliances;
- a list of finishing materials—flooring, walls, ceiling;
- a list of plumbing materials and fixtures.

5   Conclusion

Changing the approach to design allows the architect and designer to concentrate on the creative side of the design. Automatic generation of schematics of various elements after changes are made to the project (both at the request of the customer and at the request of the designer), eliminating the need to spend time and effort on reworking the complete set of technical documentation. This is a significant change from the standard approach to the design and preparation of schematics. It also reduces the chance of inconsistencies in the schematics of various related specialists, which is almost inevitable in the standard design approach. The use of BIM allows architects and designers to improve the quality of design while reducing the costs of coordinating the project with the customer and making changes to the design documentation throughout the entire design process.

References

1. Petrov KS, Morozova SG, Zantaria RR, Shustova AV (2019) Osnovnye principy i struktura informacionnogo modelirovaniya. Innovacii v nauke: puti razvitiya: Materialy XI Vserossijskoj nauchno-prakticheskoj konferencii (Basic principles and structure of information modeling. In: Innovations in science: ways of development. Materials of the XI All-Russian Scientific and Practical Conference), CHeboksary, pp 73–76
2. Sheina SG, Petrov KS, Fedorov AA (2019) Issledovanie etapov razvitiya BIM-tekhnologij v mirovoj praktike i Rossii. (Investigation of the stages of development of BIM technologies in world practice and in Russia). Stroitel'stvo i Tekhnogennaya Bezopasnost' 14(66):7–14
3. Rybin EN, Ambaryan SK, Anosov VV, Galtsev DV, Fakhratov MA (2019) BIM-tekhnologii (BIM-technologies). Izvestiya Vuzov. Investicii. Stroitel'stvo. Nedvizhimost' 1(28):98–105. https://doi.org/10.21285/2227-2917-2019-1-98-105

4. Petrov KS, Shvets YuS, Kornilov BD, Shelkoplyasov AO (2018) Primenenie BIM-tekhnologij pri proektirovanii i rekonstrukcii zdanij i sooruzhenij (The application of BIM technologies in the design and reconstruction of buildings and structures). Inzhenernyj Vestnik Dona 4(51):173

5. Travush VI (2018) Digital technologies in construction. Acad Architect Constr 3:107–117

6. Travush VI, Shakhramanian AM, Kolotovichev YuA, Shakhvorostov AI, Desyatkin MA, Shulyat'ev OA, Shulyatiev SO (2018) Lakhta Center: automated monitoring of bearing deformations structures and bases. Acad Architect Constr 4:94–108

7. Vozgoment NV (2020) Modern challenges and prospects for development of BIM-modeling in Russia in the era of digitalization. E-Management 3(3):20–27

8. Utkina VN, Gryaznov SYu, Babushkina DR (2019) Problemy i perspektivy vnedreniya tekhnologij informacionnogo modelirovaniya v sfere stroitel'stva v Rossii: problemy i perspektiv vnedreniya (Problems and prospects for implementing information modeling technology in the field of construction in Russia: problems and prospects for implementation). Osnovy Ekonomiki, Upravleniya Prava 1(19):57–61

9. Shemyakina TYu (2020) Ekonomicheskie osobennosti ispol'zovaniya informacionnogo modelirovaniya v stroitel'noy praktike (Economic features of the use of information modeling in construction practice). Sovremennaya Nauchnaya Mysl' 3:159–164

10. Loenko AS, Tuskaeva ZR (2020) Primenenie BIM-tekhnologiy pri proektirovanii i rekonstrukcii zdaniy i sooruzheniy (The application of BIM technologies in the design and reconstruction of buildings and structures). V sbornike: Sovremennye tendencii razvitiya informacionnyh tekhnologiy v nauchnyh issledovaniyah i prikladnyh oblastyah. Sbornik dokladov I Mezhdunarodnoy nauchno-prakticheskoy konferencii. Vladikavkaz, Mart 2020:56–60

11. Korabelnikova SS, Korabelnikova SK (2019) Cifrovye tekhnologii kak element snizheniya riskov v stroitel'stve (Digital technologies as an element of risk reduction in construction). Diskussiya 2(93):18–27

12. Ginzburg AV, Kulikova EN, Pavlov AS, Weinstein MS (2019) Obespechenie interoperabel'nosti pri proektirovanii s ispol'zovaniem tekhnologij informacionnogo modelirovaniya (Ensuring interoperability in design using information modeling technologies). Vestnik Evrazijskoj Nauki 11(6):69–78

13. Skvortsov AV (2016) Obzor mezhdunarodnoj normativnoj bazy v sfere BIM. (Review of the international regulatory framework in the field of BIM). SAPR i GIS Avtomobil'nyh Dorog 2(7):4–48

14. Kuzhakova ZU, Bayburin AKh (2020) Obzor normativnoy dokumentacii v oblasti BIM-modelirovaniya v Rossiyskoy Federacii (Review of normative documentation in the field of BIM-modeling in the Russian Federation), Vestnik YUzhno-Ural'skogo Gosudarstvennogo Universiteta. Seriya: Stroitel'stvo i Arhitektura, vol 20(3), pp 70–79

15. Parshina SV, Nizina TA (2019) BIM-kompleks RENGA—Rossijskij programmnyj produkt (BIM-complex RENGA—Russian software product). Osnovy Ekonomiki, Upravleniya Prava 1(19):53–56

16. Dubinin DA, Nabok AA, Kharin VA, Lavrentyeva LM (2017) Preimushchestva ispol'zovaniya i razvitiya otechestvennogo BIM: sistemy dlya trekhmernogo proektirovaniya RENGA (Advantages of using and developing domestic BIM: systems for three-dimensional design RENGA). Inzhenernyj Vestnik Dona 3(46):57

17. Pertseva AE, Volkova AA, Khizhnyak NS, Astafieva NS (2017) Osobennosti vnedreniya BIM-tekhnologii v otechestvennye organizacii (Features of the implementation of BIM technology in domestic organizations). Naukovedenie 9(6):51–58

18. Burova OA, Bozhik AS, Shevtsov AV (2020) Primenenie BIM-tekhnologij v stroitel'stve: otechestvennyj i mirovoj opyt (Application of BIM technologies in construction: domestic and world experience). Vestnik Moskovskogo Finansovo-Yuridicheskogo Universiteta 2:84–90

19. Volkodav VA, Volkodav IA (2020) Razrabotka struktury i sostava klassifikatora stroitel'noy informacii dlya primeneniya BIM-tekhnologiy (Development of the structure and composition of the classifier of construction information for the use of BIM technologies). Vestnik MGSU 15(6):867–906

20. Griber YuA, Samoilova TA, Dvoynev VV (2018) Cvetovye predpochteniya pozhilyh lyudey v razlichnyh tipah zhilogo inter'era (Color preferences of older people in different types of residential interiors). Urbanistika 4:36–49

21. Galyautdinova EN, Milova NP (2020) The influence of color on the visual perception of the space of a small apartment. Globus 5(51):5–10

22. Ryzhikov VO, Kharitonova DM (2019) Sovremennye tendencii v svetovom dizayne zhilogo inter'era (Modern trends in lighting design of residential interiors). V sbornike: Iskusstvo cveta: dizayn, arhitektura, hudozhestvennoe i proektnoe tvorchestvo, Moskva, Oktyabr', pp 78–82

23. Agaev NA (2019) Issledovanie vliyanie priemov osveshcheniya na sub"ektivnuyu ocenku kachestva svetocvetovoy sredy (Investigation of the influence of lighting techniques on the subjective assessment of the quality of the light-color environment). V knige: Mezhdunarodnaya vystavka dekorativnogo i tekhnicheskogo osveshcheniya, elektrotekhniki i avtomatizacii zdaniy. Sbornik Dokladov XXV Nauchno-Tekhnicheskoy Konferencii, Moskva, Sentyabr' 2019:7–11

24. Vasilyeva MO, Pyzhova EN (2018) The principle of universality in interior lighting. Gaudeamus Igitur 1:32–35

25. Korotkova SG (2015) Ergonomicheskiy podhod v arhitekturnom proektirovanii (Ergonomic approach in architectural design). Izvestiya Kazanskogo Gosudarstvennogo Arhitekturno-Stroitel'nogo Universiteta 4(34):113–119

26. Budarin EL, Saprykina NA (2016) Osobennosti principa ergonomichnosti v arhitekture i dizayne sovremennogo zhilishcha (Features of the principle of ergonomics in the architecture and design of a modern home). Ontologiya Proektirovaniya 2(20):205–215

27. Sorokina VN (2017) Dizayn malogabaritnogo zhil'ya kak sredstvo formirovaniya lichnogo prostranstva dlya komfortnogo prozhivaniya v gorodskoy srede (Design of small-sized housing as a means of forming a personal space for comfortable living in an urban environment). V Sbornike: Bezopasnost' Gorodskoy Sredy. Materialy IV Mezhdunarodnoy Nauchno-Prakticheskoy Konferencii, Omsk, Noyabr' 2016:296–298

28. Vasilyeva MO, Galich MV (2018) Ergonomika elementov upravleniya v dizayne inter'ernyh svetil'nikov kombinirovannogo osveshcheniya (Ergonomics of control elements in the design of interior lamps for combined lighting). Trudy Akademii Tekhnicheskoy Estetiki Dizayna 2:27–30

29. Proshunina KA, Ovcherenko IA (2018) Teoreticheskaya vzaimosvyaz' ergonomicheskih principov i konceptual'noy arhitektury zhilogo prostranstva (Theoretical relationship of ergonomic principles and conceptual architecture of living space). Inzhenerno-Stroitel'nyy Vestnik Prikaspiya 4(26):12–23

30. Dzhanakhmetov UK, Bayganova AS (2021) Interior design of residential buildings taking into account modern stylistic trends. Sci Heritage 62:3–6

Methodology for Development of Building Information Model to Automate the Process of Obtaining Estimates

K. V. Avdeeva^(✉) and A. Y. Bukalova

Perm National Research Polytechnic University, 29, Komsomolsky Prospect, Perm 614990, Russia

Abstract. Modern software makes it possible to create a three-dimensional model of a building, and also to supplement it with all kinds of information on elements of the project. This paper describes the necessity of using building information modeling at various stages of object design. The relevance of the subject area of this study is beyond any doubt, since the introduction of the BIM technologies allows to solve a number of problems: reducing the design time, automating the design process, minimizing the number of human errors. To automate obtaining estimate and cost information by the BIM model, the authors have analyzed products implementing the idea of information modeling and software. The paper describes creation of the information model of a veterinary clinic in the *Autodesk Revit* software package to prepare and further export it to the *Hector: 5D-Estimate* software package. It will make it possible to get estimates for the capital construction of the objects. Based on the results, the advantages of using software packages for building information modeling and 5D modeling, in particular, have been revealed. This approach certainly saves time of the designer and quantity surveyor, which will have a positive impact on the economic side of the project.

Keywords: Information modeling · BIM-design · Building model · LOD · *Autodesk Revit* software package · *Hector: 5D-Estimate* software package

1 Introduction

The software market currently offers a variety of solutions, that allow partial or complete use of the Building Information Modeling—the BIM.

Information modelling implies object-oriented design. Engineers, architects, designers do not work with 2D objects (lines, hatches, etc.), but with parameterized elements: walls, beams, columns, etc. Together with the geometrical information these will help to form specifications, when scheduling and obtaining estimates for construction [1]. In other words, the building model is a database for the entire lifecycle of the object, where data on all sections and stages of design is stored.

2   Relevance and Problem Statement

At the moment, the design process has reached a more advanced level where it is possible not only to build a three-dimensional model with all the necessary properties of elements and to avoid collisions (intersections), but also to automatically create specifications, bills of quantities, time schedules and obtain construction cost estimates [2–4].

The point is that modern software makes it possible to obtain a large amount of information at different stages of design, but this requires a design engineer to have additional software packages [5, 6].

This fact determines the expediency of conducting research, aimed at designing a model of a veterinary clinic building in the *Autodesk Revit* software package and its preparation for further export to the *Hector: 5D-Estimate* software package in order to automatically obtain estimates of construction cost.

To achieve this goal, the following tasks were set and solved within the framework of the research:

1. To review and analyze software tools in the field of construction design, making it possible to create a 3D-model of the object and automate creation of estimate documentation.
2. To create the information model of the veterinary clinic building using various LODs (Level of Detail) in the *Autodesk Revit* software package.
3. To supplement the model with necessary information (input parameters) to obtain more accurate construction cost estimates, preparing it for export to the *Hector: 5D-Estimate* software package.

3   The Scientific Significance of the Methodology for Developing the Building Information Model to Automate the Estimating Process

In the initial stages, review and analysis of works on solving problems of structural design was conducted. Modern software packages that provide the use of automation tools to create elements of building structures were used.

In Refs. [1, 7–12], the authors describe the software packages in detail, analyze them and come to conclusions about the expediency of a particular software in a particular case.

Having analyzed a wide range of software packages and applications in the field of information modeling, the authors of this paper have come to conclusion that the *Revit* product from Autodesk takes the leading position. This choice may be due to the software popularity in the Russian construction market because of the competent implementation by Autodesk. Moreover, a parallel is drawn with another well-known product, AutoCAD, which is studied and applied everywhere. Also, Ref. [9] presents statistics on the use of the BIM design software in 2017. As can be seen from the statistics, the most popular BIM solution that almost completely embodies the idea of information modeling on a single platform is the *Revit* software package by Autodesk. It is worth nothing that it leads by a large margin.

Also, analysis of software packages implementing the idea of 5D-modeling (automatic obtaining of estimate documentation) was carried out [13–16]. Currently, there is a wide variety of software packages that can "translate" the BIM model into an estimate. The authors of the paper [13], Davydov and Priduzhin, describe in detail the main products, which at the moment of creating the paper, were leading competitors on the domestic market of automating the production of estimate documentation for the BIM model.

Based on the analysis, Davydov and Priduzhin come to conclusion that the software product *Hector: 5D-Estimate* software package is the easiest to use, because it focuses on the work in the *Autodesk Revit* software package. Also, to work in *Hector: 5D-Estimate* software package it is not necessary to purchase additional software for the production of estimate documentation.

On the basis of the results, the following most common software packages for three-dimensional modeling in combination with software packages that implement the idea of 5D modeling were identified:

1. *Autodesk Revit* with Dynamo add-on.
2. *Hector: 5D-Estimate* software package.

4   Practical Significance and Results of the Technology for Designing the Information Model of the Veterinary Clinic Building

Based on the initial data, an information model of the veterinary clinic building was designed.

The overall dimensions of the 4-storey building are 45×12 m.

The building is designed with strip foundations made of concrete wall blocks and reinforced concrete foundation slabs. The slabs are 220 mm thick reinforced concrete hollow-core ones.

The external walls are three-layer masonry with effective insulation inside the masonry, while the internal walls are made of 380 mm thick ceramic hollow bricks. Eighty mm thick tongue-and-groove plates are used for partitions. The exterior finishing of the building is yellow and brown facing bricks.

Windows are double glazing in paired bindings with solid selective coating. Windows' size meets the insolation requirements of the premises.

The whole territory of the veterinary clinic includes the clinic itself and the surrounding territory with recreation area, car parking driveways and green spaces.

The size of the land plot allocated for the design and construction of the veterinary clinic is 70×105 m, the area is 7350 m^2. There are a lot of green spaces.

There are sidewalks along the facades of the veterinary clinic building, the width of which meets the regulatory requirements. The construction site is covered with paving slabs, while driveways are made of asphalt concrete.

The process of constructing a three-dimensional model of the building was carried out by adding architectural and structural elements, called families, to the project. Families in *Revit* are a kind of analogue of libraries and catalogues [17, 18].

Families allow designers to provide additional information about the structure of the building and the interaction of structures with each other [19]. It is through the families that the completeness of the object information is achieved, which depends on the LOD.

Thus, in the *Autodesk Revit* software package, a general three-dimensional model of the veterinary clinic building was assembled from the families. The result of this work is shown in Fig. 1.

Fig. 1 Information model of the designed object, veterinary clinic

5   Levels of Detail for Building Information Model Elements

As mentioned above, the completeness of object data depends on the building information model elements—the LOD.

The LOD is a characteristic that describes levels of graphical and informational detailing of structural elements and systems as parts of a building or structure [9]. The graphical component of this concept implies the degree of graphical elaboration of the elements. The information component of the LOD implies the completeness and detail of the information specified in the properties of the model elements, starting from their spatial and functional affiliation and ending with reference to technical documentation. In other words, the LOD has three main aspects: geometric data, visual display (appearance, color, hatching (shading), etc.) and level of attributive data elaboration (article, cost, manufacturer, etc.).

Actually there are five basic levels of detail in information modeling of building objects, from the conceptual one to matching the actual sample: LOD 100, LOD 200, LOD 300, LOD 400, LOD 500, although the sixth level of detail (LOD 350) is sometimes given. As a rule, three of the five levels of detail are mainly used: LOD 100, LOD 200, LOD 400.

The main purpose of the LOD is to determine the cost of construction at various stages of the project: from estimating the approximate cost at the conceptual stage (LOD 100) to determining the exact cost at the stages of issuing working documentation and performing construction and installation works (LOD 300-LOD 500) [20, 21]. That is, the levels of detail should meet the specific needs of all project participants at each stage [7].

The basic levels of detail of the veterinary clinic information model are described below.

When using LOD 100, a model element can be represented as three-dimensional shape-forming elements with approximate dimensions, shape, spatial position and orientation, or as a 2D symbol. A graphic representation of the LOD 100, as it was developed for the information model of the veterinary clinic, is shown in Fig. 2.
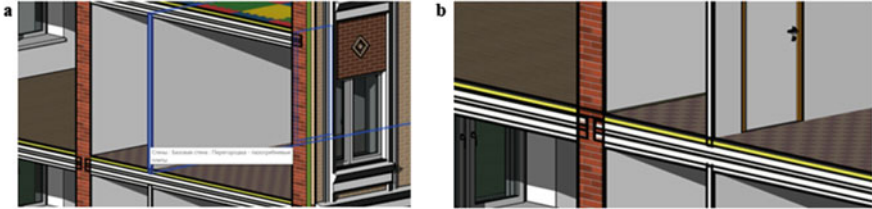
Fig. 2 a Graphical representation of the LOD 100, the partitions are made of tongue-and-groove plates; **b** graphical representation of the LOD 200, the interface of the floor slab and the brick wall

The specific feature of the LOD 200 is that the model element is represented as an object or assembly with preliminary dimensions, shape, spatial position, orientation and all the necessary non-graphical (attributive) information. Example of the LOD 200 is shown in Fig. 2a.

The specific feature of the LOD 200 is that the model element is represented as an object or assembly with preliminary dimensions, shape, spatial position, orientation and all the necessary non-graphical (attributive) information. Example of the LOD 200 is shown in Fig. 2a.

The LOD 300 is different in that the object or assembly representing the model element belongs to a specific building system with precise dimensions, shape, spatial position, orientation, connections and all the necessary non-graphical information. Graphical representation of the LOD 300 is shown in Fig. 3.
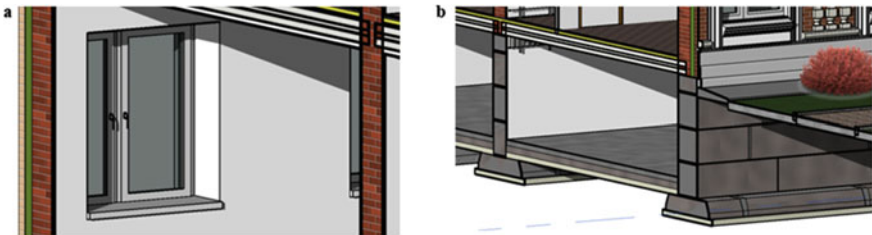
Fig. 3 a Graphical representation of the LOD 300, window opening; **b** graphical representation of the LOD 400, building foundation (foundation blocks and slabs)

When creating a model using the LOD 400, an element is presented as a specific assembly with precise dimensions, including dimensions of node elements, shape, spatial

position, orientation, node connections (bolts, rivets, welds, shaped elements, etc.), manufacturing and installation data, as well as other necessary non-graphical information. Example of the LOD 400 is shown in Fig. 3b.

With the LOD 500 the model element is presented as a specific assembly with actual dimensions, shape, spatial position, orientation and non-graphical information sufficient to put the model into operation. Graphical representation of the LOD 500 is shown in Fig. 4.

Fig. 4 Graphical representation of the LOD 500, the facade of the building with the surrounding area

As can be seen, the toolkit of the *Autodesk Revit* software package makes it possible to develop all the necessary elements of the project. Besides it takes into account the LOD for each stage of the information model designing. In this work, the LOD 300 was chosen as the main and the most suitable one.

6 Preparation of the Information Model for Work in the Hector: 5D Estimate Software Package: Description of the Input Parameters of the Model

All the elements of *Autodesk Revit* software package represent the concept of the "family" [19]. The information contained in the properties of parametric objects is used to create specifications, bills of quantities, as well as to obtain time schedules and the estimated cost of the project.

Figure 5 shows a cross-section of the BIM model of the veterinary clinic with many parameterized elements—"smart" families, each of which contains certain information grouped by categories.

Figure 5 shows the dialogs of two different families: FBS (foundation wall blocks) and doors, which already have some information—the basic attributes of the elements: element material, geometric dimensions, the State Standard (the GOST), etc. These basic attributes have already been created in all elements of the model. It is convenient to form
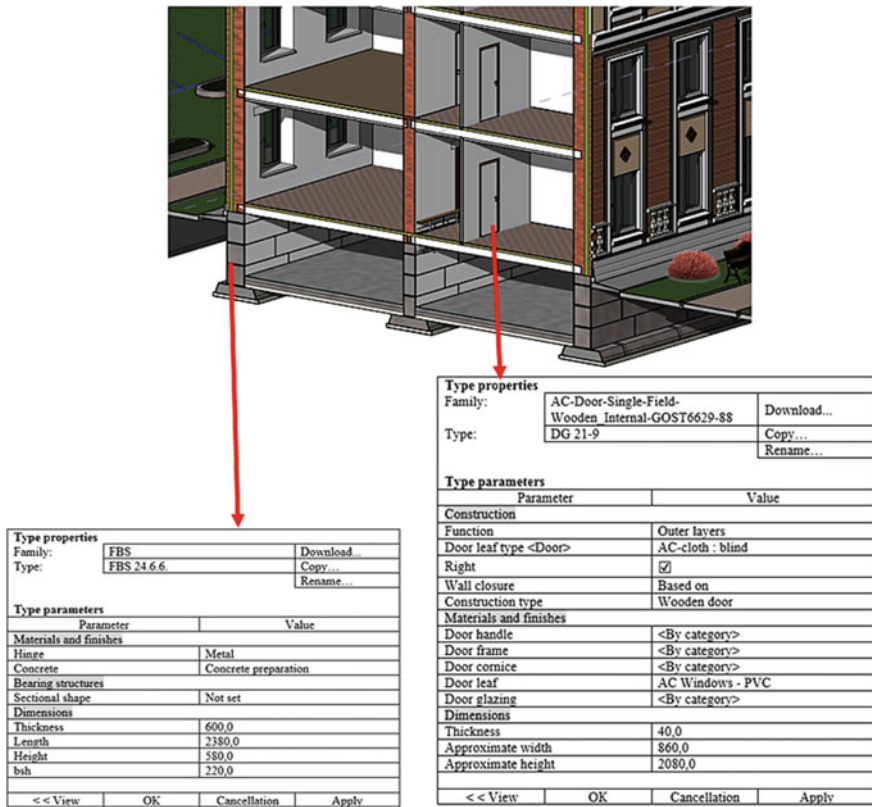
Fig. 5 Dialogs for "smart" family properties in *Revit* with base attributes

correct specifications from such information, which significantly reduces the number of errors in the formation of specifications in the traditional way, accelerates the issue of project documentation and increases the efficiency of the entire project.

However, to obtain a more accurate estimated cost of the project, a wider range of attributes is required, such as cost, manufacturer and a link to the manufacturer's website (Fig. 6). Such information was input into each family manually (model element) at the design stage.

Thus, the information model of the veterinary clinic building, created in *Autodesk Revit*, was prepared to obtain estimates for the capital construction of objects using the *Hector: 5D Estimate* software package.

7 Conclusion

The study showed that the interrelation between software packages is possible and has a number of positive effects. Implementation of the 5D-modeling principle is one of them. It consists in automated calculation of the scope of work and assignment of estimated

Type properties

Family:	FBS		Download...
Type:	FBS 24.6.6.		Copy...
			Rename...

Type parameters

Parameter	Value
Materials and finishes	
Hinge	Metal
Concrete	Concrete preparation
Bearing structures	
Sectional shape	Not set
Dimensions	
Thickness	600,0
Length	2380,0
Height	580,0
bsh	220,0
Identification	
Description	FBS-1
Size Comments	GOST 13579-85
Manufacturer	OOO «Complex-C»
URL	http://www.complexs.ru/jbi/view/pid/
Cost	3597.00
Size marking	FBS 24.6.6
Other	
ADSK_Mass	1960.00
ADSK_Volume	0.828

<< View	OK	Cancellation	Apply

Type properties

Family:	AC-Door-Single-Field-Wooden_Internal-GOST6629-88		Download...
Type:	DG 21-9		Copy...
			Rename...

Type parameters

Parameter	Value
Construction	
Function	Outer layers
Door leaf type <Door>	AC-cloth : blind
Right	☑
Wall closure	Based on
Construction type	Wooden door
Materials and finishes	
Door handle	<By category>
Door frame	<By category>
Door cornice	<By category>
Door leaf	AC Windows - PVC
Door glazing	<By category>
Dimensions	
Thickness	40,0
Approximate width	860,0
Approximate height	2080,0
Identification	
Manufacturer	OOO "Weather in the House"
Description	Wooden internal blind door
URL	http://pogoda-dom.ru/dveri-mezhko
Cost	6315,00
Size marking	3

<< View	OK	Cancellation	Apply

Fig. 6 Dialogs for "smart" family properties in *Revit* with attributes created to obtain the estimated project cost

norms to the elements of the BIM model. Consequently, the information can be uploaded to any estimated programs in order to make estimated calculations [13].

It is also important to note that the information model practically excludes human errors in these processes, since all data are automatically loaded into the estimate program from the BIM model and then only supplemented by the quantity surveyor. Implementation of such technologies into the construction industry of Russia will primarily result in a more reasonable cost of construction [13].

However, it should be emphasized that despite all the advantages of 5D modeling, there are a number of problems associated with the introduction and use of this technology. In order to eliminate them, it is necessary to further study the existing international and domestic practices of using the BIM technologies in the construction industry.

References

1. Novikov AI (2018) Methodology for preparing an information model for transfer to the operation service. Dissertation, Peter the Great St. Petersburg Polytechnic University. Civil Engineering Institute
2. Vladimir Popov (2011) BIM - Building Information Model: Time or Not Time. Available via Google. https://scadsoft.com/download/BIM2011.pdf. Accessed 18 Mar 2021
3. Chegodaeva MA (2018) Optimization of the technical operation of a building based on its information model. Dissertation, Togliatti State University
4. Gamayunova OS (2019) Formation of an organizational and technological mechanism for improving the quality of the issued project documentation. Dissertation, Peter the Great St. Petersburg Polytechnic University. Civil Engineering Institute
5. Kimetova NR (2017) Integration of settlement complexes into the field of information modeling of buildings. Dissertation, Peter the Great St. Petersburg Polytechnic University. Civil Engineering Institute
6. Lushnikov AS (2018) Ensuring the quality, cost and timing of investment and construction projects based on the implementation of information modeling. Dissertation, St. Petersburg State University of Architecture and Civil Engineering
7. Golosova TS (2018) Organizational and economic mechanisms for the transition to information modeling in architectural and design detail. Dissertation, Russian Economic University named after G.V. Plekhanov
8. Garshin AD (2018) The effectiveness of information technology in construction. Dissertation, Peter the Great St. Petersburg Polytechnic University. Institute of Industrial Management, Economics and Trade
9. Nikolaev DI (2019) Methods for building a BIM model of the CM section using Autodesk Revit. Dissertation, Peter the Great St. Petersburg Polytechnic University. Civil Engineering Institute
10. Abaltusov YuV, Chaturov VV (2019) BIM technologies. Problems of their implementation and development prospects in construction and design. Young Scientist. Archit Des Constr 20(258)
11. Shakirov RM (2018) Methodology for using the information model at the stage of reconstruction of the attic floor. Dissertation, Peter the Great St. Petersburg Polytechnic University. Civil Engineering Institute
12. Bukunov AS (2017) Development of training processes for construction specialists for the use of information modeling of buildings in construction. Dissertation, Peter the Great St. Petersburg Polytechnic University. Institute of Computer Science and Technology
13. Davydov NS, Pridvizhkin SV (2018) The introduction of BIM technologies in terms of pricing through the use of automation systems for the release of estimate documentation. In: Materials of the All-Russian scientific and practical conference on March 29–30, 2018, pp 8–13
14. Mineeva AV, Kochneva ME (2019) Problems of introducing BIM technologies in the construction industry in order to issue estimate documentation. Eurasian Sci Assoc 12–1(58):53–57
15. Petrochenko MV, Stolnikova KA (2019) Automated calculation of the scope of work and the assignment of estimated norms to the elements of the BIM model. SPbPU Sci Week 273–275
16. ISICAD (2019) Accurate budgeting in industrial design. The experience of the successful application of the 5D estimate program at the All-Russian Research Institute of Galurgia. isicad.ru/ru/articles.php?article_num=20555. Accessed 16 Apr 2021
17. Papushina KS (2018) Technological sequence of end-to-end design of a public building. Dissertation, Peter the Great St. Petersburg Polytechnic University. Civil Engineering Institute
18. Ozhigin DA (2006) Working with parametric components of autodesk revit. CAD Graph 4:86–90

19. Lyalin DO, Mashtaler SN, Dmitrenko EA (2017) Application of the Autodesk Revit software package in design activities. Bull Donbass Natl Acad Civ Eng Architect 3(125)
20. Stepanov AV, Gilmiyarova YuV (2016) Development of levels of detail (LOD) of objects in the PC Autodesk Revit. Polzunovsky Almanac No 2, T 2
21. Perepelitsa FA, Kalimullina AYu (2017) Levels of detail of the information model at different stages of the life cycle. Almanac of scientific works of young scientists. In: XLVI scientific and educational conference of ITMO University, vol 4, pp 189–191

Scan to HBIM Technology Problems: A Case Study of Holy Cross Exaltation Cathedral in Solikamsk, Russia

A. Semina[1(✉)], A. Shamarina[2], and F. Picchio[3]

[1] Perm State National Research Polytechnic University, 29, Komsomolsky Prospekt, Perm 614 990, Russia

[2] Moscow State University of Civil Engineering (MGSU), 26, Yaroslavskoye Shosse, 129337 Moscow, Russia

[3] University of Pavia, 3, Via Adolfo Ferrata, 27100 Pavia, Italy

Abstract. Building Information Modeling is gradually becoming the standard in architectural heritage. The article discusses a method for converting point clouds into a three-dimensional information model. The point clouds for the cathedral were obtained by photogrammetry and terrestrial laser scanning methods. The current trend is a combination of Digital Photogrammetry with Laser Scanning. The combination of ground and aerial photogrammetry allowed the building to be digitally displayed in the best possible way. The model of the Cathedral of the Holy Cross Exaltation is the case study described in this paper. Modeling was carried out on the basis of such a combined point cloud. The modeling took into account the real state of both the building as a whole and its individual elements. Problems with the use of BIM modeling for historical objects can be considered difficulties with including all the inaccuracies of the real object. On the basis of historical photos, the historical view of the architectural monument has been recreated. BIM models play an important role in the documentation process. All information collected about the building becomes a single database, collected in one file. This is important for the subsequent work. Such knowledge bases about architectural monuments are aimed both at solving applied problems in the field of reconstruction and construction, and at spreading knowledge about architectural heritage.

Keywords: Architectural survey · BIM model · Information model · Historic appearance · Architecture heritage · Photogrammetry

1 Introduction

The architectural survey, both traditional and digital, is the primary tool for architects and restorers. Fixing the architectural monuments current state provides input to improve the physical state of the object and subsequent analysis, as well as the possibility of virtual reconstruction.

The official requirements for the methodology of the architectural survey and virtual historical reconstruction have yet been formed for the current state. In world practice there are generally accepted methods for digitalizing architectural heritage and creating 3D models. Building Information Modeling (BIM) is the leading technology for building objects models development. BIM accumulates information about architecture in a single file. It describes not only geometry and appearance, but also providing other attribute information for each element. This makes the 3D-model "smart" and workable for further analysis.

Some authors consider BIM modeling as a process but not technology. It is determined by the essence of the resulting model: the 3D parametric model represents a set of interconnected parametric elements [1–3].

Heritage preservation requires another approach that differs from design information modeling. Historic Building Information Modeling (HBIM) is an approach to modeling existing buildings [4]. The source material for the most accurate modeling is the point clouds obtained by photogrammetry and laser scanning. The current trend is a combination of Digital Photogrammetry with Laser Scanning [5–8].

The process is based on the combined point cloud processing. The descriptions and obtained photographic materials were used to create textures and refine details. The point cloud captures the fuzzy geometry, damage, and colours. It is also important to record all damages of the coatings, plasters and materials of structures for the most complete condition representation of the individual structures and the building as a whole structure [6].

The survey and digitalization of architectural heritage in Russia are becoming a more and more relevant issue, considering high rates of destruction processes. There are 721 monuments (876 objects) of architecture and urban planning located in the Perm Region according to the Monuments Protection Regional Center. These monuments are under state protection, including 48 monuments (87 objects) of federal significance. These figures include objects in decaying and ruined condition due to anthropogenic influences and ownerlessness.

Solikamsk is one of the cities of the Perm Region, which is clearly and concentrated represents the architectural heritage of the region. Architectural monuments here were maintained in operational mode due to the constant use of most of the buildings and the restoration workshops work in Soviet times. This prevented the complete destruction of the architecture monuments. Nowadays the request for architectural heritage digitalization comes not only from reconstruction specialists. Digitalization is considering as an opportunity to preserve buildings that cannot be physically preserved for various reasons.

The European project PROMETHEUS in which these documentation activities are included involves three universities, University of Pavia (coordinator), University of Perm, University of Valenzia and two European enterprises. The objective of the international and interdisciplinary project is to build collaborative intersectional protocols for the low-cost methodology to develop reliable 3D databases and Information Models of the Architectural Heritage of this cultural route of Upper Kama.

2 Historical Background

The architectural complex of the Solikamsk historical center contains several objects of religious architecture: the Trinity (summer) cathedral with a cathedral bell tower on the "chambers" that served as a belfry for the Exaltation of the Holy Cross (winter) cathedral, the Resurrection of the Christ Church, the Voevoda's House, the Epiphany Church (Fig. 1). These buildings are in different conditions. All objects except the Cathedral of the Exaltation of the Holy Cross are in the use of the local history museum. They are properly maintained, reconstruction, and are kept in operational condition. Despite this, the buildings suffer a lot of damages.

Fig. 1 General view of the central ensemble of the city of Solikamsk

Despite the fact that the Cathedral of the Holy Cross Exaltation plays a considerable role in the central architectural ensemble, nowaday it has no functional purpose. The church is not used as a building. This largely determines its current destroyed state.

The Cathedral of the Exaltation of the Holy Cross is a religious architecture monument of the late seventeenth early eighteenth centuries (built in 1700). This monument has federal significance status. The cathedral was a central winter temple, as evidenced by its squat compact exterior type. The building planimetry dimensions are 50×21.6 m. The spatial composition is common for the Upper Kama region. It is a one-storey "ship" type temple in the basement. It has a linear structure: the narthex, refectory, main temple and altar parts (Fig. 2) [9].

At the end of the eighteenth century instead of a large cupola covered with a roof lemech (wooden Russian tile) arranged a wooden belvedere with a dome replaced the upper part of the hipped roof of the main church (the belvedere and the dome were demolished in the 1920s) [10].

In different periods of its existence the temple had a different functional purpose. During the Soviet period the temple lost its original religious function and was used as a civil building. In the 1920s and 1930s, the basement of the church was used as a warehouse for the general supply department of Usollag (one of the gulag camps). In 1940 an internal redevelopment was made. The interfloor ceilings were constructed.

Fig. 2 a View of the cathedral from the river; **b** general view of the cathedral

The doorways had been placed. The brick vaults were partially removed. The building is rented by the brewery since the beginning of the 1940-s [11].

Restoration work on facades, roofs, vaults, foundations was carried out in 1952–1960. It was made according to the project and under the guidance of Toltsiner and Katsko. In 2005–2007 restoration work was carried out. The belvedere with the dome was reconstructed, and the roof was partially replaced.

The decoration of the facades is the particular interest. It is rich decorative work with the use of curved and figured bricks. The ornament is large and heavy with complex figured palmettes. The large icon cases with keeled top play an important role in the decoration.

The facade is designed in the style of the provincial baroque. The arcature-columnar belt is highlighted on the facade. At the corners it is based on beams of five hanging three-quarter columns. At the wall it based on beams of three three-quarter columns. Between the beams there are double arches with weights: the usual ones on the eastern and western facades, and made in the form of palmettes on the southern and northern facades. The temple part is crowned with a profiled cornice on crenellated brackets, a bug (zhuchkovyj) belt and a belt consists of the flat crenellations along the perimeter.

3   Field Survey and Data Acquisition

Field surveys were carried out using a DJI Phantom 4 quadricopter, a Canon digital camera, and a FARO laser scanner (interior scan).

Field surveys have shown that at the moment the floors inside the cathedral are partially collapsed and there are no stairs. A contributing factor for the condition is the location in the lowland on the river bank. It overflows abundantly during spring floods. Long-term use near the river of the winter Holy Cross Cathedral with basement piles eventually led to a significant building sag. The building has evenly sagged to the east. Cracks appeared in the northern wall of the refectory (Fig. 3).

The method of photogrammetry was used to obtain a point cloud. The design of 3D models by the SfM (Structure from motion) methodology is based on determining the objects size using stereopairs [8]. With the combination of two types of photography

Fig. 3 **a** Condition of internal structures; **b** condition of decoration and openings of the altar part; **c** condition of the north facade

(ground and aerial) the most visual result has appeared. It allowed to accurately model the geometry of the building and the decor of the facades [12, 13].

Aerial photography was carried out using a DJI Phantom 4 quadcopter, which made it possible to use predetermined flight paths to obtain anti-aircraft and perspective frames. In total, about 160 photographs were taken.

The ground photogrammetric survey was carried out for certain window openings, for the altar part and some protruding elements. For the subsequent photogrammetric processing, about 150 images of the exterior were taken, and about 70 for the interior.

Cameral processing of images was carried out in the Agisoft PhotoScan program (Fig. 4). The program allows to get a volumetric point cloud. Photo processing is in a semi-automatic mode. The results of aerial photography and ground photography are processed separately due to the difference in shooting settings.
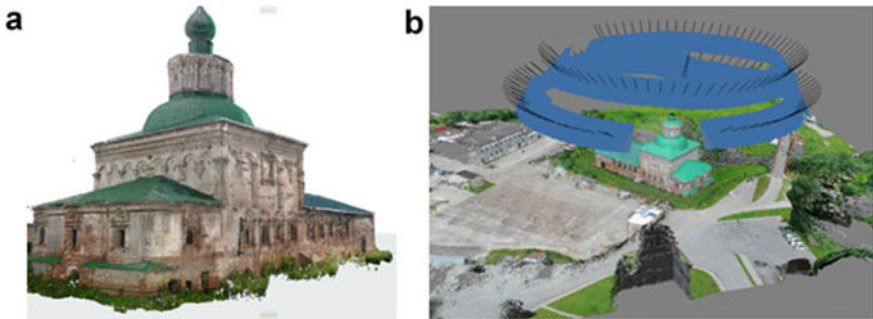
Fig. 4 **a** General view of the point cloud; **b** processing of aerial photographs of the cathedral

The next step of work with point clouds is to optimize the point cloud. The point cloud was optimized using the Leica Cyclone software. At this stage of the work it is important to remove noise and unnecessary elements. This optimization lightens the weight model and also allows a better understanding of the modeled object.

4 Scan to HBIM

A feature of historical buildings is deviations from the ideal geometric shape, heterogeneity of the material, different damages. The point cloud captures with enough accuracy all damage and deviations. The error of the point cloud taken by laser scanners can reach 3–4 mm. Point clouds obtained by photogrammetric survey methods have an error of 1 cm, depending on the type of digital camera and scaling.

The modeling process is the point cloud import into the BIM program. After that conducts the modeling element-by-element of each part of the building taking into account the real dimensions of the object. In this case the texturing of the model takes place on the basis of photographs. A seamless texture for the model elements is created from the photographic materials (Fig. 5).

Fig. 5 The process of modeling decor and texture

There is a problem that occurs during subsequent point cloud-based modeling. The parametric modeling method is well applicable for ideal shapes. To model geometrically uneven structures it is necessary to determine which deviations and damages need to be fixed, and which will be modeled with deviations from the real object.

The point cloud of the Holy Cross Cathedral was processed in Graphisoft Archicad. Then the model was saved in the Industry Foundation Classes (ifc) format for compatibility with other BIM programs. This is an open specification data format that is now the standard for working with BIM models.

The parametric 3D model was developed taking into account the existing damage to the building. Materials and composition of structures of walls, floors, coatings and other elements are specified on the basis of field surveys. The destroyed state of the building made it possible to see the composition of the materials of the structural elements.

The resulting model of the cathedral reflects the existing state with some errors. Damage to decorative elements, openings, unevenness of the wall surface in the BIM model could not be recorded. There are several reasons for such inaccuracies. All reasons appear in the principles of model development using information modeling programs.

Decor elements can be created in several ways. Typically, unique shapes are modeled using family generation. In this way, objects are created and further they can be replicated and distributed in other buildings model. Another option is to create each element separately. Then they can also be copied if these elements are repeated. But it can be within the same model. The second option for modeling decor is more labor-intensive, but it provides opportunities for modeling each damaged fragment.

The methods similar to those described above for modeling decor are used to model openings, doors and windows. In each case, the simulation is carried out depending on the goals and application of the developed model. Families are used to creating a model and library that can be used for further work. This approach often neglects the real geometry of the object—insufficient orthogonality of structures, uneven walls, and elements damage. For the most accurate representation of reality in BIM modeling manually element modeling is used. During this process it needs to check the compliance with real geometry and the point cloud.

For the current state of the Holy Cross Cathedral model the real geometry of the walls was taken into account. Wherever possible, the model was brought closer to real geometric shapes (Fig. 6).

Fig. 6 General view of the model in comparison with the real view

The second task when working with the Cathedral of the Exaltation of the Cross was the reconstruction of the historical view of the cathedral. The reconstruction of the historical image was carried out for the appearance at the beginning of the twentieth century. The reconstruction was carried out on the basis of archival data provided by the local history museum of Solikamsk. The lack of archival drawings or plans made it impossible to obtain the dimensions of the missing parts of the building. Therefore, historical photographs were used from different angles. The approach consisted of examining the object from different angles and identifying changes in the building, which made it possible to restore the appearance of the temple (Fig. 7).

5 Conclusions and Discussions

BIM has a number of advantages and also a number of challenges faced by researchers in the field of historical building information modelling.

The advantages of this technology are widely considered in the articles of researchers [14–17] and are as follows: element-by-element (parametric) modelling allows to consider the building model as a whole, in which a change in one element entails changes in related other elements; the model contains information not only about the geometry of

Fig. 7 General view of the model in comparison with the historical photo

the object, but also other related data, such as: the material of structures, the thickness of the layers in the structure, the relationship of elements with each other; the BIM model allows to conduct further analysis, such as structural analysis; the ability to create libraries of data that you can later conveniently work with, for example, libraries of decorative elements that are often repeated in buildings of the same geographic region.

Problems with the use of BIM modelling for historical objects can be considered difficulties with including all the inaccuracies of the real object. The geometry of walls, ceilings, openings, decor, the inability to know the composition and material of structures, as well as the presence of a large number of different damages-all this becomes an obstacle to create the most accurate three-dimensional object model.

Despite the shortcomings of the considered technology, the development of BIM modelling in the field of historical and architectural heritage has the great potential [18–20]. The scope of application of parametric information models lies not so much in the plane of visualization of architectural monuments, but in the possibilities of subsequent work with the resulting models. When this approach is applied to an existing monument, such as the Holy Cross Cathedral in Solikamsk, the collected data becomes an information-filled digital repository. Such knowledge bases about architectural monuments are aimed both at solving applied problems in the field of reconstruction and construction, and at spreading knowledge about architectural heritage. The digitalization of architecture gives a powerful impetus to the development of museum technologies, as well as virtual and augmented reality as applied systems for the preservation of cultural heritage.

References

1. Pocobelli DP, Boehm J, Bryan P et al (2018) BIM for heritage science: a review. Herit Sci 6:30. https://doi.org/10.1186/s40494-018-0191-4

2. Azhar S, Khalfan M, Maqsood T (2012) Building information modelling (BIM): now and beyond. Australas J Constr Econ Build 12(4):15. https://doi.org/10.5130/AJCEB.v12i4.3032

3. Worrell LL (2015) Building information modeling (BIM): the untapped potential for preservation documentation and management, Clemson University. https://heritagesciencejournal.springeropen.com/articles/10.1186/s40494-018-0191-4. Accessed 28 May 2021

4. Arayici Y (2008) Towards Building Information Modelling for existing structures. Struct Surv 26(3):210–22. http://www.emeraldinsight.com/doi/abs/10.1108/S1479-3563%282012%29000012B007. Accessed 28 May 2021

5. Maxwell I (2014) Integrating digital technologies in support of historic Building Information Modelling: Bim4conservation (HBIM). http://www.cotac.org.uk/docs/COTAC-HBIM-Report-Final-A-21-April-2014-2-small.pdf. Accessed 28 May 2021

6. Costantino D, Pepe M, Restuccia A (2021) Scan-to-HBIM for conservation and preservation of Cultural Heritage building: the case study of San Nicola in Montedoro church (Italy). Appl Geomat. https://doi.org/10.1007/s12518-021-00359-2

7. Pepe M, Costantino D, Crocetto N, Garofalo AR (2019) 3D modeling of roman bridge by the integration of terrestrial and UAV photogrammetric survey for structural analysis purpose. Int Arch Photogramm Remote Sens Spat Inf Sci 42:249–255

8. Novel C, Keriven R, Graindorge P, Poux F (2016) Sravnenie metodov ajerofotogrammetrii i trehmernogo lazernogo skanirovanija dlja sozdanija trehmernyh modelej slozhnyh obektov (Comparison of aerial photogrammetry and 3D laser scanning methods for creating 3D models of complex objects). http://www.cadmaster.ru/magazin/articles/cm_84_20.html. Accessed 12 May 2021

9. Danilov VA, Fedorov AV, Bezvershenko LS (2019) Sravnenie metodov fotogrammetrii i lazernogo skanirovanija dlja sozdanija trehmernyh modelej obektov i territorij arheologicheskih Gis (na primere arheologicheskogo raskopa Uvekskogo gorodishha) (Comparison of photogrammetry and laser scanning methods for creating three-dimensional models of objects and territories of archaeological Gis (on the example of the archaeological excavation of the Uvek settlement). Izv Sarat un-that New ser Ser Earth Sci 19:2

10. Kaptikov AJu (1990) Kamennoe zodchestvo russkogo Severa, Vjatki i Urala18 v.: problema regional'nyh shkol (Stone architecture of the Russian North, Vyatka and the Urals of the 18th century: the problem of regional schools) Sverdlovsk, pp 41–50

11. Kostochkin VV (1988) Cherdyn', Solikamsk, Usol'e. Strojizdat, Moscow

12. El-Hakim SF, Beraldin JA, Picard M, Godin G (2004) Detailed 3D reconstruction of large-scale heritage sites with integrated techniques. Comput Graph Appl 24(3):21−29. Castagnetti C, Dubbini M, Ricci PC, Rivola R, Giannini M, Capra A (2017) Critical issues and key points from the survey to the creation of the historical building information model: the case of Santo Stefano Basilica. Int Arch Photogrammetry Remote Sens Spatial Inf Sci XLII-2/W5. 2017 26th International CIPA symposium 2017, 28 August–01 September, Ottawa

13. Pepe M, Costantino D, Restuccia Garofalo A (2020) An efficient pipeline to obtain 3D model for HBIM and structural analysis purposes from 3D point clouds. Appl Sci 10(4):1235

14. Dore C, Murphy M, McCarthy S, Brechin F, Casidy C, Dirix E (2015) Structural simulations and conservation analysis-historic building information model (HBIM). Int Arch Photogrammetry Remote Sens Spatial Inf Sci 40(5):351

15. López FJ, Lerones PM, Llamas J, Gómez-García-Bermejo J, Zalama E (2018) A review of heritage building information modeling (H-BIM). Multimodal Technol Interact 2(21)

16. Parrinello S, Dell'Amico A (2019) Experience of documentation for the accessibility of widespread cultural heritage. Heritage 2(1):1032–1044

17. Inzerillo L, Turco ML, Parrinello S, Santagati C, Valenti GM (2016) BIM and architectural heritage: towards an operational methodology for the knowledge and the management of cultural heritage. Disegnarecon 9(16):16.1–16.9

18. Parrinello S, Dell'Amico A (2020) From survey to parametric models: HBIM systems for enrichment of cultural heritage management. In: Bolognesi C, Villa D (eds) From building information modelling to mixed reality. Springer tracts in civil engineering. Springer, Cham
19. Parrinello S, Picchio F, De Marco R, Dell'Amico A (2019) Documenting the cultural heritage routes. The creation of informative models of historical Russian churches on Upper Kama region. Int Arch Photogrammetry Remote Sens Spatial Inf Sci
20. Dell'Amico A (2020) H-BIM: information flows and data digitization process, Dn 7/2020 pp 54–67

Risk-Based Monitoring of the Condition of Industrial Buildings

A. Kh. Baiburin(✉) and D. A. Baiburin

South Ural State University (National Research University), Lenin Ave. 76, Chelyabinsk 454080, Russia

Abstract. The purpose of the study is to develop a method for monitoring the condition of industrial buildings into account the risk of an accident. The research object is a method for monitoring the condition of industrial buildings. The main methods of risk assessment are analyzed. The method is based on monitoring the technical condition of structures and the determination of various scenarios of accident damages. The model has a number of differences from the well-known risk analysis models. The difference lies in the matrix calculations of the relative risks, taking into account the errors of expertise and maintenance. The monitoring results are drawn up in the form of maps zoning of technical condition of structures. Then make a damage map taking into account material and social losses from possible accidents. The affected areas are found for each accident scenario. These maps impose on the plan of the building and get zoning priority repair. An example of compiling these maps to risk-based monitoring of the condition of an industrial building is given. The technical result is to increase the operational reliability of buildings and reduce the damages risk of possible building accidents.

Keywords: Industrial buildings · Technical condition · Monitoring · Damage · Accident risk · Structural safety and reliability

1 Introduction

The most comprehensive review of research papers dealing with risk assessment methodologies from a sample of over 400 articles published by six representative Elsevier scientific journals shows that quantitative methods have a higher relative frequency (65.6%) than qualitative ones (27.7%) [1]. The main risk assessment methods are:

Preliminary Hazard Analysis (PHA);
Hazard and Operability Study (HAZOP, IEC 61882:2001);
Failure Mode and Effect Analysis (FMEA, IEC 60812:2006);
Failure Tree Analysis (FTA, IEC 61025:1990);
Event Tree Analysis (ETA, IEC 62502:2010).

The classification of risk assessment methods is given in ISO/IEC 31010:2009. In Russia, risk assessment methods are outlined in the state standards for "Risk Management", "Industrial Product Dependability", and "Functional Safety of Systems". The release of Sanitary Regulations (SP) 296.1325800.2017 "Buildings and Structures. Special Impacts" classified as an emergency the following loads and effect arising as a result of defects in materials; unsatisfactory work performance; design errors; and violations of the operation of buildings and technological processes. The action of special emergency effects is taken into account by analyzing structures for progressive collapse.

Modeling is widely used to study accident scenarios, the expansion of risk assessment for business continuity, and the use of big data for risk assessment based on condition monitoring, security assessment and protection of cyber-physical objects [1–4]. [1, 5–7] note the need to study the joint effect of worsening structural resistance, the system modeling method, and the correlation between the modes of structural failure in terms of the reliability and the safety of complex systems.

In recent years, considerable success has been achieved in the modeling, analysis, and design of structural systems for civil engineering, and new approaches have been proposed for life-cycle assessment, maintenance planning, and the optimal design of buildings and structures [1, 2, 5, 8, 9]. [1, 8–11] discuss the role of inspections and monitoring, the impact of maintenance and repair activities, and the identification of cost-effective building maintenance strategies.

The uncertainties connected with modeling degrading structures strongly affect inspections, maintenance and repairs [1]. Condition monitoring and calculation methods for determining structural failure risks are used to reduce uncertainty. The failure probabilities of various scenarios are assessed separately through the use of different approaches [1, 10, 12]. The probabilities of failures, risk functions and probability-density functions of the time to the failure are assessed for each hazard [1, 13, 14]. Methods for assessing the impact of wear on the safety indicators of reinforced concrete and metal structures of bridges are the most developed [1, 9, 13, 15, 16].

The scientific community in Russia recognizes the need to develop methods for assessing and controlling the hazard magnitude of buildings and structures [17–28]. The relevance of the problem is confirmed by the growing number of accidents in construction [19, 26, 28], wear-out failures of hazardous production facilities, the lack of risk management systems in construction companies, and the training of specialists in risk management in construction. The theoretical foundations of risk assessment [26–28] and intellectual methods of automating surveys of building projects [20, 28] are being developed based on information theory and fuzzy logic. However, risk-oriented methods for the operational control of industrial buildings are insufficiently developed.

The purpose of the study is to develop a method for monitoring the condition of industrial buildings into account the risk of an accident. The objectives of the study were: analysis of regulatory methods; assessment of the impact of examination and operation errors; development of a new method of operational control.

2   Methods

The method for assessing the technical condition of buildings and structures implemented according to state standard 31937–2011 has some disadvantages. The first is

associated with the lack of standards for assigning structures to the established technical condition categories; which percentage values of the decrease in the bearing capacity correspond to the technical condition categories: standard, operable, limitedly operable, and emergency. The solution to this problem is generally within the competence of an expert and depends on his/her knowledge and experience. Any lack of knowledge or experience can lead to errors, both in assessing the technical condition and in the content, cost and priority of restoration, repair and reinforcement.

The second drawback in the normative survey methodology is associated with risk. The risk of and damage caused by structural accidents are not taken into account when assigning stages of repair works by the technical condition categories. The survey customer is often limited in financial resources (especially during economic crises) and is forced to perform surveys and repairs in stages, not taking into account the overall condition of the building or the potential risks of construction accidents.

For example, the repair of a covering reduces the collapse risk of the covered elements generally within the area of the covering element. A delay in the reinforcement of such critical structures as columns increases the risk of larger accidents in the area of all structures resting on this column. In this case, it is also necessary to take into account possible damages from the loss of equipment, injury and/or death in the collapse area. It may turn out that a larger (in terms of the collapse area) accident will cause less damage compared to a local, isolated collapse in an area with more people and expensive equipment.

Based on this, the proposed method for controlling the operation of a building or structure is reduced to the sequential implementation of the following stages:

1. building survey according to the applicable standards;
2. determination of the risk of errors when surveying the facility by means of an expert assessment;
3. determination of the risk of errors during operation by means of the facility operation service assessment;
4. creation of a financial and social risk map (damage map) indicating the potential material and moral damage on the building plan, based on the production documentation and the location of equipment and workplaces;
5. creation of a spatial risk map on the building plan, indicating the damage zones from the collapse of load-bearing structures (columns, walls, beams, trusses, slabs) according to various accident development scenarios;
6. zoning of the load-bearing structures on the building plan by the technical condition categories based on the survey results;
7. prioritizing the repair and/or reinforcement of structures by overlaying the damage, accident risk and technical condition maps on the building plan for load-bearing structures;
8. calculations of the probable collapse of structures according to different scenarios. Clarification of the priority of repair/reinforcement of various types of structures, depending on the calculation results.

The damage map is compiled based on the production documentation, depending on the value of the equipment, unreleased products, and the number of staff in the collapse

area. The spatial risk map shows areas with different risk values for a structural collapse according to different scenarios. The time sequence and the technical content of the building operation inspection are linked to these risk maps.

Based on the risk maps, we can predict possible damage from collapsing structures and develop a sequence of actions to restore their operable condition by the types of structures and sections of the building. The latter can be assigned taking into account structural zoning (temperature, sedimentary, anti-seismic blocks) or technological features (production areas). As a result of scheduled operational inspections, surveys and examinations, we can compile cartograms of defects and damage for the areas of the facility, which are laid on the zoning maps by the risk of failure of certain structures. When these maps are combined, we can create a spatial service model by the technical condition, which takes into account the "damage/accident damage" ratio at each local section of the facility's structural system.

The larger the damage and the higher the accident damage, the more intensive the required maintenance activities (in terms of their scope and time). The gradation by the maintenance and repair periods is visually marked with different colors (possibly automatically). Thus, we exercise the risk-based monitoring of the condition of buildings, ensuring minimum potential damage from possible structural failures.

3 Example of Using the Method

We will show the results of the method using a simple example. We surveyed a production workshop with 24 × 42 m axial dimensions in the form of a two-span one-story building of a frame structural system. The reinforced concrete frame consists of columns, roof beams, and 3 × 6 m roof slabs. The arrangement of the equipment with zoning depending on the cost, and the localization of the workshop staff, are shown in Fig. 1.
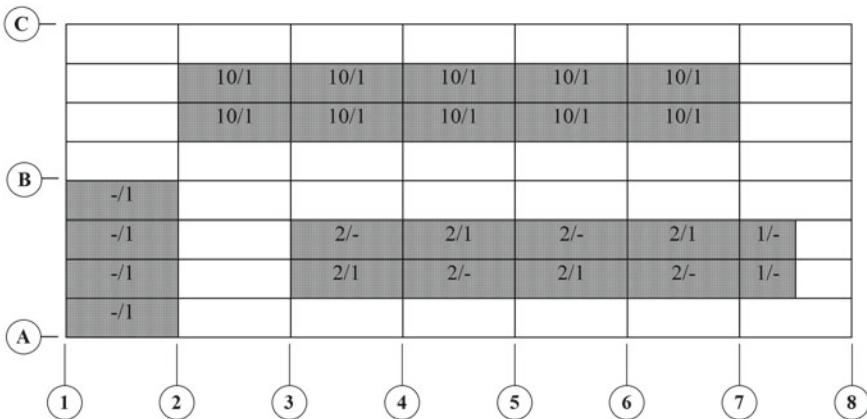
Fig. 1 Zoning of equipment and localization of the workshop employees: in the numerator—the cost of equipment, million rubles; in the denominator—the number of workplaces

According to Fig. 1, the main equipment, worth 100 million rubles, is located in the span B–C. Ten people work with the main equipment. Auxiliary equipment, worth 18

million rubles, is located in span A–B. Four people work with the auxiliary equipment. Four engineers work in the administration building, which is located in the workshop in axes A–B/1–2. The employees of the workshop work in 3 shifts and spend 2 h in the administrative building, which houses changing rooms, showers, a toilet, a canteen, engineers and meeting rooms. The probability of their being in the workshop is 22/24, and in the administrative building is 2/24.

The survey of the workshop building structure resulted in a map of damage to the roof slabs with zoning by the technical condition category (Fig. 2). The slabs were damaged only in the span B–C from roof leaks. Slabs with traces of soaking are operable; those with slight corrosion of the concrete and reinforcement are limitedly operable; significant corrosion of concrete and reinforcement indicates the emergency condition of the slabs.
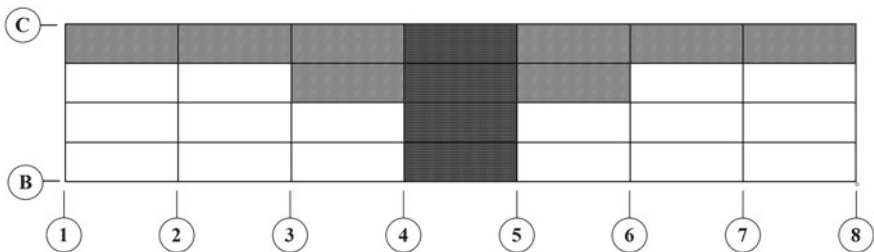
Fig. 2 Zoning of the roof slabs according to the technical condition category: white—operable; gray—limitedly operable; dark—emergency

Combining the damage map (Fig. 2) with the map of possible damage from a structural collapse in the span B–C (Fig. 1), we obtain the span zoning by the priority of repair operations (Fig. 3).
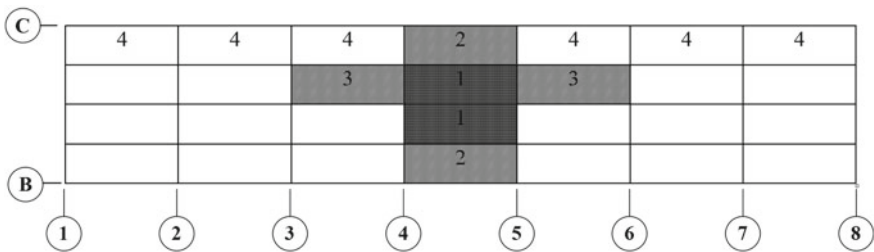
Fig. 3 B–C span zoning by the priority of repair operations

In this example, the area affected by a collapse of the emergency slabs coincides with the area of these slabs (we do not take into account the horizontal movement of the slabs during the fall). If we consider other types of supporting structures (columns, beams, trusses), the affected area will depend on the structural system. In this case, after the zoning of these structures by the technical condition categories, we perform zoning by the affected area after the damage map (Fig. 2), and then build a map of possible damage and zoning by repair/reinforcement priority.

It follows from the joint consideration of Fig. 2 and 3 that the collapse of the emergency slabs in axes 4–5 will result in a failure of the main equipment worth 20 million rubles, the probable death of two workers, and losses connected with unreleased products. If the thermal circuit of the building opens if four roof slabs collapse, it can lead to the defrosting of the workshop heating system in winter.

4 Theoretical Justification

The total relative economic damage from the i-th accident scenario in the form of the load-bearing structural collapse is:

$$U_i = T_i + c_{pt,i} L_i. \tag{1}$$

or, in general for the building, in matrix form:

$$\begin{bmatrix} u_{11} & \dots & u_{1n} \\ \dots & u_{ij} & \dots \\ u_{m1} & \dots & u_{mn} \end{bmatrix} = \begin{bmatrix} t_{11} & \dots & t_{1n} \\ \dots & t_{ij} & \dots \\ t_{m1} & \dots & t_{mn} \end{bmatrix} + c_{pt} \cdot \begin{bmatrix} l_{11} & \dots & l_{1n} \\ \dots & l_{ij} & \dots \\ l_{m1} & \dots & l_{mn} \end{bmatrix}. \tag{2}$$

For the considered example, m is the number of slabs along the letter axes, n—along with the numerical ones.

The relative indicator of the economic damage caused by interruption to the technological process is:

$$T_i = T_d / T_s, \tag{3}$$

where T_d is the possible damage caused to the technological process by a collapse with the area A_d; Ts is the possible damage caused to the technological process by a collapse of the entire building with the area A_s.

According to Fig. 1, the possible damage to the technological process caused by a collapse of the entire workshop is $T_s = 118$ million rubles. In this example, we did not take into account the loss from unreleased products or the costs of cleaning, dismantling and installation. The possible damage to the technological process from a collapse in axes B–C/4–5 is equal to $T_d = 20$ million rubles.

Let us find the relative indicator of the economic damage caused by interruption to the technological process from a collapse of the roof slabs by Eq. (3) $T_1 = 20/118 = 0.169$.

The relative indicator of the social damage is:

$$L_i = L_d / L_s. \tag{4}$$

The social damage indicator, depending on the frequency of the people being under the collapse area, is calculated as follows:

$$L_d = \sum_i n_i \cdot t_i / 24, \tag{5}$$

where ni is the number of people under the possible collapse area; t_i is the time the people spend under the possible collapse area per 24 h, in hours; i is the number of people being in the collapse area. Taking into account the time workers spend in the workshop, the indicator of the social damage of a collapse of the roof slabs is $L_d = 2 \cdot 22/24 = 1.83$ people.

For the collapse of the entire building, the social damage indicator is calculated depending on the frequency of people being under the collapse area:

$$L_s = n \cdot t/24, \tag{6}$$

where n is the total number of people in the building; t is the time people are in the building per 24 h, in hours. Taking into account the three-shift continuous work in the workshop, the maximum value of the social damage indicator is $L_s = 18 \cdot 24/24 = 18$ people.

The relative indicator of the social damage from a collapse of the roof slabs is calculated by the formula (4): $L_1 = 1.83/18 = 0.102$.

The social risk coefficient expressed in the ratio of the damage from human casualties to the damage caused to the technological process from a collapse of the entire building is:

$$c_{pt} = Ls \cdot VSL/T_s, \tag{7}$$

where L_s is the social damage indicator; VSL is the average cost of living; T_s is the possible damage caused to the technological process by a collapse of the entire building.

According to the average cost of living in Russia ($ 27,893), the average life expectancy (72.7 years), and the statistics of insurance payments, the VSL for Russia is taken as 4.0 million rubles [24]. Then, the social risk coefficient is $c_{pt} = 18 \cdot 4/118 = 0.61$. The total relative economic damage from a collapse of the roof slabs is calculated by Eq. (1): $U_1 = 0.169 + 0.61 \cdot 0.102 = 0.231$.

Let us assume that a well-known method [25–27] was used to determine the probability of a collapse $P_1 = 2 \cdot 10^{-4}$ of the emergency roof slabs at the local section B–C/4–5. Then, the accident risk is determined by the formula:

$$R_i = P_i \cdot U_i/(K_{ex}K_e), \tag{8}$$

where P_i is the probability of an accident according to the i-th scenario; U_i is the accident damage according to the i-th scenario; K_{ex} is the indicator of the risk of survey errors; K_e is the indicator of the maintenance and repair risk.

If the coefficients $K_{ex} = 0.92$ and $K_e = 0.95$, then, the accident risk, calculated by Eq. (8), is $R_1 = 2 \cdot 10^{-4} \cdot 0.131/(0.92 \cdot 0.95) = 0.30 \cdot 10^{-4}$.

After such calculations for all types of emergency structures, we determine the final priority of repairs and reinforcements.

5   Results and Conclusion

The approach corresponds to quantitative methods of risk analysis, which are used more often [1]. Failure analysis uses FMEA (IEC 60812: 2006) and ETA (IEC 62502: 2010)

methods. The model has a number of differences from the well-known risk analysis models [3, 4, 6, 12, 16]. The difference lies in the matrix calculations of the relative risks, taking into account the errors of expertise and maintenance. Further studies are aimed at optimal design taking into account the risks of collapse (RBDO approach—Reliability-Based Design Optimization) and the choice of an effective strategy for maintenance and repair.

The new method (patent RU 2,742,081) for controlling the operation of, primarily, industrial buildings and structures assesses the technical condition of building structures and organizes their operational control. A joint analysis of the maps of damage, risk of failure allows the enterprise to build an economically sound strategy for technical inspections, surveys, and repairs of supporting structures. The technical result is an increase in the operating reliability of industrial buildings and a decrease in the risk of damage from possible construction accidents.

References

1. Marhavilas PK, Koulouriotis D, Gemeni V (2011) Risk analysis and assessment methodologies in the work sites: on a review, classification and comparative study of the scientific literature of the period 2000–2009. J Loss Prev Process Ind 24(5):477–523. https://doi.org/10.1016/j.jlp.2011.03.004

2. Zio E (2018) The future of risk assessment. J Reliab Eng Syst Saf 177:176–190. https://doi.org/10.1016/j.ress.2018.04.020

3. Hingorani R, Tanner P, Prieto M, Lara C (2020) Consequence classes and associated models for predicting loss of life in collapse of building structures. J Struct Saf 85:101910. https://doi.org/10.1016/j.strusafe.2019.101910

4. Hwang S-H, Jeon J-S, Lee K (2019) Evaluation of economic losses and collapse safety of steel moment frame buildings designed for risk categories II and IV. J Eng Struct 201:109830. https://doi.org/10.1016/j.engstruct.2019.109830

5. Zhu B, Frangopol DM (2012) Reliability, redundancy and risk as performance indicators of structural systems during their life-cycle. J Eng Struct 41:34–49. https://doi.org/10.1016/j.engstruct.2012.03.029

6. Beck AT, Ribeiro LR, Valdebenito M (2020) Risk-based cost-benefit analysis of frame structures considering progressive collapse under column removal scenarios. J Eng Struct 225:111295. https://doi.org/10.1016/j.engstruct.2020.111295

7. Hingorani R, Tanner P (2020) Risk-informed requirements for design and assessment of structures under temporary use. J Risk Anal 40(1):68–82. https://doi.org/10.1111/risa.13322

8. Biondini F, Frangopol DM (2016) Life-cycle performance of deteriorating structural systems under uncertainty: review. J Struct Eng (United States) 142(9):F4016001. https://doi.org/10.1061/(ASCE)ST.1943-541X.0001544

9. Rafiq MI, Chryssanthopoulos MK, Onoufriou T (2004) Performance updating of concrete bridges using proactive health monitoring methods. J Reliab Eng Syst Saf 86(3):247–256. https://doi.org/10.1016/j.ress.2004.01.012

10. Thöns S, Stewart MG (2020) On the cost-efficiency, significance and effectiveness of terrorism risk reduction strategies for buildings. J Struct Saf 85:101957. https://doi.org/10.1016/j.strusafe.2020.101957

11. Cavalagli N, Kita A, Castaldo VL, Pisello AL, Ubertini F (2019) Hierarchical environmental risk mapping of material degradation in historic masonry buildings: an integrated approach considering climate change and structural damage. Constr Build Mater 215:998–1014. https://doi.org/10.1016/j.conbuildmat.2019.04.204

12. Beck AT, Kroetz HM (2019) System reliability-based design optimization and risk-based optimization: a benchmark example considering progressive collapse. J Eng Optim 51(6):1000–1012. https://doi.org/10.1080/0305215X.2018.1502760

13. Deco A, Frangopol DM (2011) Risk assessment of highway bridges under multiple hazards. J Risk Res 14(9):1057–1089. https://doi.org/10.1080/13669877.2011.571789

14. Nyunn S, Wang F, Yang J, Liu Q, Azim I, Bhatta S (2020) Numerical studies on the progressive collapse resistance of multi-story RC buildings with and without exterior masonry walls. J Struct 28:1050–1059. https://doi.org/10.1016/j.istruc.2020.07.049

15. Cha G, Park S, Oh T (2019) A terrestrial LIDAR-based detection of shape deformation for maintenance of bridge structures. J Constr Eng Manag 145(12):04019075. https://doi.org/10.1061/(ASCE)CO.1943-7862.0001701

16. Dat PX, Tan KH, Yu J (2015) A simplified approach to assess progressive collapse resistance of reinforced concrete framed structures. J Eng Struct 101:45–57. https://doi.org/10.1016/j.engstruct.2015.06.051

17. Baiburin DA, Baiburin AKh (2017) Assessment of technogenic accident risk of industrial building structures. In: International conference on construction, architecture and technosphere safety (ICCATS-2017). IOP Conference Series: Materials Science and Engineering, vol 262, no 1, p 012190. https://doi.org/10.1088/1757-899X/262/1/012190

18. Feng D-C, Xie S-C, Xu J, Qian K (2020) Robustness quantification of reinforced concrete structures subjected to progressive collapse via the probability density evolution method. J Eng Struct 202:109877. https://doi.org/10.1016/j.engstruct.2019.109877

19. CHeboksarov DV, Epshtejn MS (2018) Ispol'zovanie metodiki ocenki riska avarii dlya kachestvennoj ocenki ob"ektov kapital'nogo stroitel'stva specialistami gosstrojnadzora (The use of the accident risk assessment methodology for the qualitative assessment of capital construction projects by state construction supervision specialists). In: Vestnik YUzhno-Ural'skogo gosudarstvennogo universiteta. Seriya: Stroitel'stvo i arhitektura (J Bulletin of the South Ural State University. Series: Construction and Architecture), vol 18, no 2, pp 39–44. https://doi.org/10.14529/build180205

20. Kashevarova GG, Tonkov YUL, Tonkov IL (2017) Intellektual'naya avtomatizaciya inzhenernogo obsledovaniya stroitel'nyh ob"ektov (Intelligent automation of engineering survey of construction objects). Int J Comput Civ Struct Eng 13(3):42–57. https://doi.org/10.22337/1524-5845-2017-13-3-42-57

21. Nadol'skij VV, Osipchik AV (2017) Sovremennye metody polukolichestvennoj ocenki riskov avarij zdanij i sooruzhenij (Modern methods of semi-quantitative assessment of the risks of accidents of buildings and structures). Bezopasnost' stroitel'nogo fonda Rossii. Problemy i Resheniya 1:105–112

22. Bajburin DA, Mel'chakov AP (2016) Modelirovanie riska avarij zdanij i sooruzhenij (Modeling the risk of accidents in buildings and structures). In: Safety problems of construction critical infrastructures (SAFETY 2016). UrFU, Ekaterinburg, pp 47–51

23. Patel'e M, Morozov A, Pflyug E, Sagadiev R i dr (2015) Risk avarijnogo obrusheniya zdanij i sooruzhenij (Risk of accidental collapse of buildings and structures). Energonadzor 10(74):36–37

24. Rajzer VD (2010) Teoriya nadezhnosti sooruzhenij (Theory reliability of structures). Publ. ACB, Moscow

25. Bajburin AH (2015) Obespechenie kachestva i bezopasnosti vozvodimyh grazhdanskih zdanij (Ensuring the quality and safety of civil buildings under construction). Publ. ACB, Moscow

26. Perel'muter AV (2007) Izbrannye problemy nadezhnosti i bezopasnosti stroitel'nyh konstrukcij (Selected problems of reliability and safety of building structures). Publ. ACB, Moscow

27. Tamrazyan AG, Bulgakov SN, Rahman IA, Stepanov AYU (2012) Snizhenie riskov v stroi-tel'stve pri chrezvychajnyh situaciyah prirodnogo i tekhnogennogo haraktera (Reduction of risks in construction in case of natural and man-made emergencies). Publ. ACB, Moscow
28. Bezopasnost' Rossii. Bezopasnost' stroitel'nogo kompleksa (2012) (Security of Russia. Security of the construction complex). Publ. Znanie, Moscow

Special and Unique Structures Construction

Technique to Calculate the Solar Cell Shading When Designing Solar Power Plants

L. V. Markin[(✉)]

Moscow Aviation Institute (National Research University), 4, Volokolamskoe Highway, Moscow 125993, Russia
`markinl@list.ru`

Abstract. Renewable energy sources are the main trend in modern energy. However, converting solar power into electric energy using semiconductor-based solar cells (heliostats) that do not track the Sun position requires optimizing both their design parameters and layout within a solar power plant. This is primarily associated with considering the cross-shading of the heliostats by both each other and their structural elements not involved in the power generation. It is shown that optimizing the layout of solar cells can be considered a mathematical programming problem. The possibilities of geometric modeling of insolation problems using discrete (receptor) geometric models are shown within the framework of design automation of solar power plants are shown. The numerical estimation of accuracy and productivity of the developed algorithms shows the possibility of their implementation even on modern computers of medium power. This allows us to hope for the integration of the developed layout algorithms into modern systems of solid-state geometric modeling in the form of plug-in modules.

Keywords: Solar power · Heliostat · Shading · Layout · Receptor model · Algorithm · Optimization

1 Introduction

It is known that for just three days, the Sun provides the Earth with as much energy as all explored fossil fuel reserves contain, i.e., 170 billion J per second. In energy equivalent, the annual solar energy flow towards the Earth is $38 \times \cdot 10^{20}$ kWh [1], which is 108 times more than the power currently consumed in the world [2]. Along with the ecological purity of solar energy and the practical inexhaustibility of the Sun's resources, all this makes it expedient to widely use solar energy both on Earth and in space exploration up to the Mars orbit, inclusive. Therefore, today, for both economic and environmental reasons, more and more attention is globally paid to renewable energy sources, among which solar energy ranks the first. Some studies prove the possibility of creating an aircraft operating exclusively on solar energy [3].

Obtaining (primarily electric) energy from solar radiation is based on either directly converting solar energy into electric power using semiconductors (as in orbital stations

and satellites) or generating power by heat engines (this scheme is more often used on Earth). Despite the harsh winter of 2020/21 has shown in global scales that humanity cannot yet completely abandon hydrocarbon fuels, the use of green technologies in energy is a generally recognized trend in human development.

Therefore, addressing the issue of the most efficient layout of solar cells (heliostats) is relevant when designing solar power plants on Earth. The same issue arises when placing solar cells on a spacecraft (SC) and solar augmenters in the colonization of planets [4]. The study relevance is also determined by the fact that on Earth, solar energy is a green power source.

2   Physical Statement of the Heliostat Layout Problem

Simulating the layout of augmenters is a complex issue since it requires an interrelated solution of two problems:

- calculating the effective area of solar cells (heliostats) relating to the solar energy flow,
- developing a device for optimizing the number and geometry (i.e., specific dimensions and shapes) of heliostats placed within a certain area.

The main problem is associated with the fact that the heliostats are arranged in fields and thereat, partially shade each other (Fig. 1a). On an SC, they will also be additionally shaded by the space object itself (Fig. 1b). Therefore, if a certain object contains too little or too many solar cells per unit area, then the solar energy intake will be small or the cells will work ineffectively, shading each other, respectively. Let us make a proviso that we are talking about the fields of augmenters and solar cells of an SC that does not track changes in the Sun position.
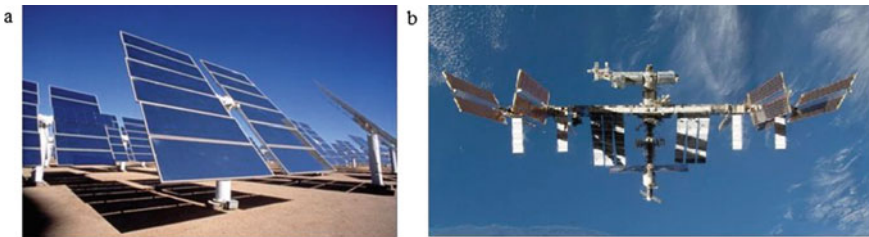
Fig. 1 The cross-shading of the heliostats

The cross-shading problem is that the shadow cast by the heliostat partially shades the next row of heliostats, reducing their efficiency. To prevent cross-shading of the heliostats, they are placed at sufficiently large distances from each other. However, preventing cross-shading in such a way requires relatively large areas to accommodate a powerful solar station. Thus, the world's largest solar station Kamuti with a capacity of 648 MW, located in India near the city of Tamil Nadu, required 10.36 square kilometers to accommodate 2.5 million heliostats (Fig. 2).

Fig. 2 The solar station Kamuti

Cross-shading can be reduced by using heliostats tracking the Sun position (Fig. 3). However, in modern technology, they are not widespread due to their high cost (determined by the need for solar sensors and decisive modules) and spending a significant percentage of the power they generate on their own needs.
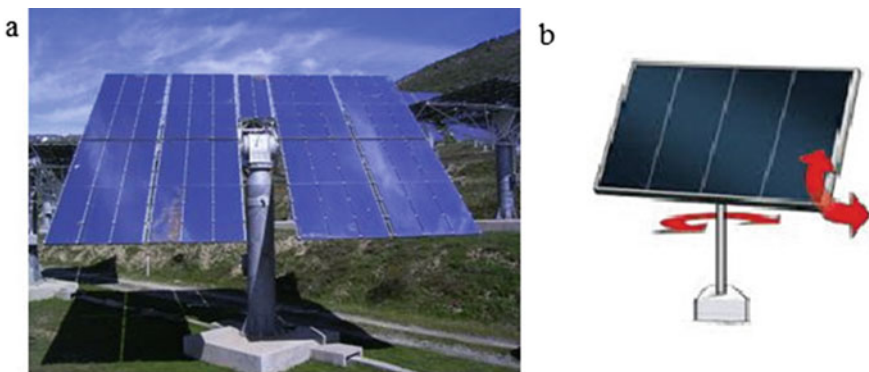
Fig. 3 a The heliostats tracking the Sun position; **b** its angles of rotation

3 Mathematical Statement of the Heliostat Layout Problem

To formulate the efficiency criteria for the problem being solved, let us reduce optimizing the layout of stationary heliostats or solar cells of the SC to a mathematical programming problem. Suppose we have space Ω to arrange heliostats (or solar cells), where n

heliostats should be placed and oriented. Let us denote the solution (one of its possible variants) by X. Considering the specific geometry of heliostats determined by this solution X and their positions relative to others within the region of feasible solutions Ω and the heliostat orientation relative to the energy flow W, at each time instant t, each of the n heliostats will have effective energy absorption area $s_i(t)$, and altogether at a given time instant—$S_\Sigma = \sum_{i=1}^{n} S_i(t)$. Our goal is to obtain the maximum Sun energy at the given time instant (i.e. for a given heliostat orientation), determined by the maximum effective area of solar cells, which can be expressed as follows:

$$\underset{P_X \to \min}{Max}\ S_\Sigma(t)\ \text{for}\ X \subset \Omega.$$

According to this expression, the maximum energy should be obtained under additional constraints—the heliostat layout option X within the region of feasible solutions Ω and minimum energy loss P_x caused by cross-shading of the heliostats by both other ones and its structural elements. Obviously, the requirement for X to belong to the region of feasible solutions Ω includes many additional ones both general restrictions (minimum area occupied) and specific determined, e.g., by the areas occupied by additional power elements not involved in the power generation, etc.

The above mathematical description should be further complicated by an additional requirement, i.e., obtaining the maximum energy not at each given time instant but for the entire time the Sun is within the heliostat visibility, and obtaining the maximum energy flow $Max\ P_\Sigma$ at a certain time instant t_0. This will be expressed as follows:

$$\underset{P_X \to \min}{Max_{t_0}}\ P_\Sigma(t)\ \text{for}\ X \subset \Omega.$$

Such a 'specific' requirement may be determined by the need to take the maximum possible amount of energy for the entire light day. Building geometric and optimization models considering all these factors are the objective of this study.

4   Geometric Models to Evaluate the Cross-Shading of Objects

Estimating the cross-shading of objects in space is a customary problem in construction and architecture (insolation problems). In technique, insolation is usually understood as the exposure of surfaces to sunlight (solar radiation). It is assumed here that a surface or space is irradiated by a parallel beam of rays coming from the current visibility point of the solar disk center. The term 'insolation' is used mainly in ergonomics, architecture, and building lighting technology. It should be noted that great attention is now being paid to the regulation and calculation of insolation. With commercializing the land use and construction, the building insolation sanitary standards have become the main factor putting a bridle on the endeavors of investors, owners, and tenants of land plots to overcrowding urban areas to maximize profits. A limiting factor for overcrowding built-up areas is the need to follow the sanitary and hygienic standards introduced in 2002 by SanPiN 2.2.1/2.1.1.1076–01, Hygienic Requirements for Insolation and Sun Control of Residential and Public Occupancies and Premises.

All the currently used insolation calculation techniques are usually divided into two groups—geometric and energy ones [5–7]. Geometric techniques allow determining the duration of insolation or shading of an area, room, or individual point, the sunbeam travel nature, etc. Developing techniques not going beyond the frameworks of classical mathematics and physics to solve these problems was mainly completed in the 70s last century. In these years, some Soviet scientists systematized the techniques for space–time calculation of insolation and shading. They have been classified geometrically into central, orthogonal, and oblique projection techniques. The orthogonal projection was chosen and recommended for manual calculation in our country. This manual calculation technique based on nomograms is still used today as a regulation prescribed for designers. To simplify calculations, they are encouraged to use tools such as the insolation ruler and solar shading protractor (Fig. 4). However, the accuracy of such manual calculations is low.
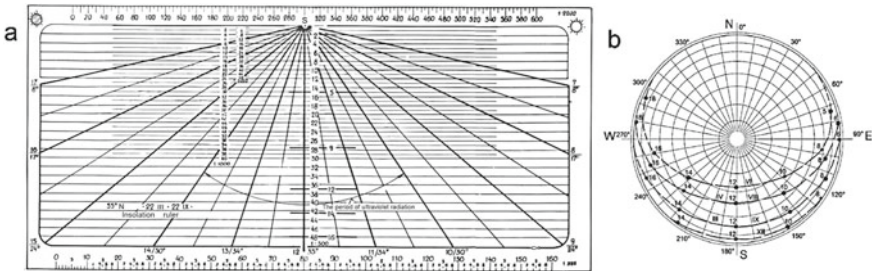
Fig. 4 **a** The insolation ruler; **b** the solar protractor

Of course, the manual technique for calculating the duration of insolation, described in the regulatory documents, became outdated in the twenty-first century. However, the descriptive geometry technique used herein formed the basis of modern computer algorithms. An example of the insolation software interface is given in Fig. 5. Before using such software, a scene should be simulated in one of the computer graphics systems. This approach has been used in the studies known to us [8, 9] and some others. In such problems, the source data is the sunbeam direction relating to the object under study. The beam direction, in turn, is determined by the Sun position, which under the conditions of the earth's surface is unambiguously defined by three parameters— the geographical latitude, date, and time. The appropriate algorithms were written in AutoLISP as a software application to the AutoCAD package to automate the calculation of the insolation duration.

Energy techniques [10, 11] are aimed at directly calculating solar radiation (solar energy) and allow defining the amount of thermal and light energy of sunbeams at each time instant in an area with a certain geographic location. These insolation calculations allow determining the flux density, the irradiance generated by it, and the exposure in radian or effective (light, bactericidal, etc.) units of measurement.
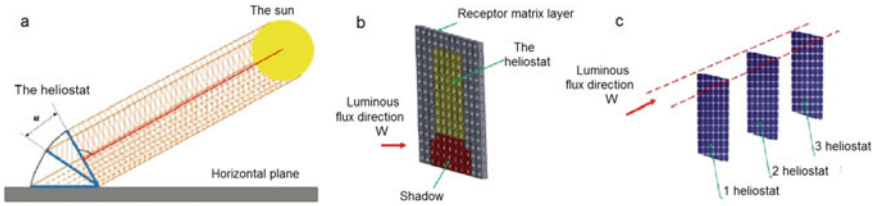
Fig. 5 Discrete geometric models to evaluate the cross-shading of heliostats

5 Discrete Geometric Models to Evaluate the Cross-Shading of Objects

In our approach to heliostat layout automation, a simulation technique discretizing the computational space was chosen. It is known that the most accurate formal description of a three-dimensional object such as a geometric body is identifying it with the area of space it occupies (a point set). We will use a space E^3 consisting of separate cubes, which in this case is called discrete or receptor, and the geometric model built in such a space is, respectively, a discrete or receptor model [12–14]. The term 'voxel' (an abbreviation of the terms 'Volumetric' and 'piXEL'), i.e., three-dimensional pixel used in foreign scientific literature is an English analog of the term 'receptor'. In the literature, the receptor technique has other names (matrix, binary, space element roster method, etc.). The use of receptor (voxel) models in solving various applied problems is described in [15–18].

Figure 5a illustrates our desire to take as much energy as possible from a unit area of the heliostat, which is limited by many factors: the specific Sun position (which does not stand still), the overall dimensions of the heliostat itself, it's plane inclination angle α relative to the solar energy flux, and its shading by other heliostats. Let us transfer our scene to the receptor matrix and analyze our solar cells by layers. Since many factors should be considered, we will use not the customary receptor matrix (filled with '0' and '1' codes) but a three-valued one with additional '2' codes added—the space already occupied by other solar cells (Fig. 5b). However, such a calculation scheme has a drawback as well: if the cells are placed strictly one behind another, then their area will be ambiguously added to the expected effective area result. To eliminate this probable error, we add a block to the calculation algorithm, which does not allow reconsidering the once-absorbed part of the energy flow (Fig. 5c). Therefore, starting from a certain receptor matrix slice, everything that follows it after the element with the '2' code is forcibly marked with the prohibiting '3' code, which does not allow using receptors with this code in any calculations. It should be noted that in the modified (4-digit) receptor model, receptors with the '3' code are not involved in any area calculations.

Based on such a model, a software package has been created in C# to simulate the effective area of solar augmenters. Herewith, a graphical shell has been developed that allows viewing the numerical values of the results obtained. This study has been performed by the post-graduate student from the Republic of the Union of Myanmar Kui Min Khan at the Moscow Aviation Institute under the thesis research [19, 20].

Although this technique is very versatile with respect to many factors affecting the heliostat shading, implementing it requires transforming the entire scene of placed heliostats into a receptor (voxel) form. Previously, this has been a certain difficulty since receptor matrices are an intra-machine presentation of the geometric object shape, while a designer thinks in parametric models. However, we have currently developed a technique for automatic transformation of a solid geometric object model built in any CAD system into a receptor matrix [21, 22].

The above description of using a discrete geometric model to calculate the effective solar cell area at given design parameters of heliostats, their layout, and orientation relative to the Sun allows plotting the change in the effective areas of both each individual heliostat and their total effective area. Thus, we have obtained the result of a verification calculation of the effective solar cell area for a heliostat system at a given Sun illumination angle. This result has independent scientific and practical value, but herewith, the issue of the obtained result optimality arises—how successful is the shape and layout of solar cells X_i we have investigated from among the set of feasible solutions Ω?

Therefore, the next study problem is to choose a technique for optimizing a function (strictly speaking, a functional) X from among an admissible set of design parameters Ω, described by a set of independent parameters a_1, a_2, …, a_n. Obviously, considering the problem complexity and the variety of possible layout options, we cannot build continuous analytical target functions and use gradient optimization methods in the calculations. Our task is to determine the global extremum (or the value close to it) of a multi-extremum function in the space $\Re^n$, for which finding the values of the function itself is relatively easy but describing it analytically and performing a complete enumeration of local extrema are impossible due to their large number. An approximate form of the target function X for the simplest two-dimensional case is shown in Fig. 6. The lack of an analytical description of the function under study excludes the use of gradient methods to find an extremum, therefore, the only way to do this is blind random search [23]. In it, a set of parameters $\{a_{ij}\}$ is randomly chosen from the range of admissible parameter values and played. For this set of parameters, the target function value is calculated, and the record target function value from a set of source data combinations is stored together with the set of relevant parameters.
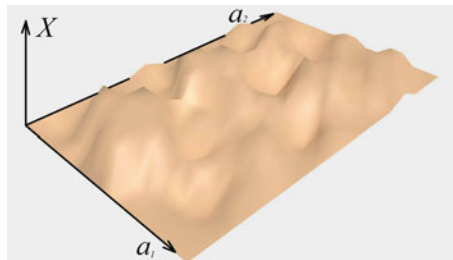
Fig. 6 An approximate view of the goal function X for 2 variables

Considering the unpredictable behavior of the function optimized, we will search for feasible solutions from among the simulation techniques. Attempts are known to

modify the blind search, of which the decremental neighborhood method seems to be the most successful for our problem [24, 25]. The method is based on randomly chosen combinations of variables a_{1i} and a_{2j}, for which the target function X_{ij} value is calculated. From among the set of the target function X_{ij} values, a record one is selected, and further target function X values are already searched near this record value. Thus, in this method, the solution is refined by narrowing the variable changing range around the solution found. This procedure is repeated several times. If at a given number of tests, not a single point is found within the admissible region, then this number gradually increases. The described optimization technique does not guarantee achieving the global optimum of the target function, so we can talk about obtaining not the global optimum of function X but one of the local optima this way. Thus, we will get a not optimal but rational solution to the problem posed.

Obviously, due to their discreteness, the receptor geometric models are approximate, and the geometric shape description accuracy degree is determined by the receptor size. To evaluate the implementation accuracy, we will investigate a test model for estimating shading, the geometric parameters of which allow predetermining the effective solar cell area. This will allow running our model through a geometric model implemented in C# with previously known parameters of the effective illuminated area (in our case, 30 m^2). The verifying calculation results are shown in Fig. 7.
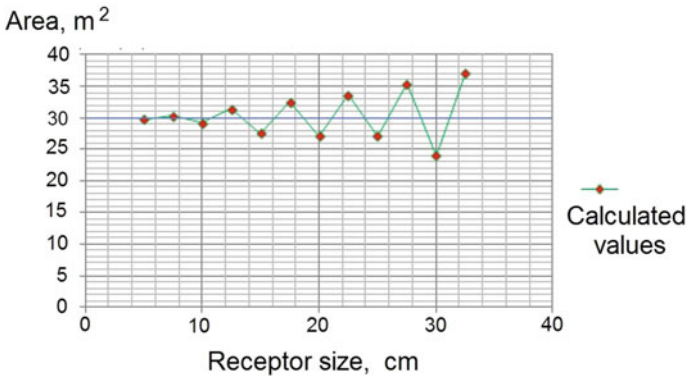
Fig. 7 Calculated values of the effective area of heliostats in test examples

Figure 7 shows that in the test example, the regression curve does not deviate from the theoretical solar cell area, which indicates the correctness of the geometric model proposed. With an increase in the receptor size, the calculated effective area deviates more and more from the theoretical value, which is quite expected. We cannot explain so strangely symmetrical location of the calculated values to the theoretical reference curve. Apparently, this is associated with the predetermined discrete algorithm for calculating the effective solar cell area.

With a decrease in the receptor size, not only the calculation accuracy but also the computation time increases. However, it does not exceed 5…12 min even for a computer of average power.

6 Conclusion

Optimizing the layout of solar cells on an SC can be described mathematically as a mathematical programming problem. Based on receptor (voxel) geometric models, scanning algorithms have been developed to calculate the surface shading areas for solar cells (heliostats) that do not track the Sun position.

Building a geometric model using quaternary logic is an effective technique for dividing the effective surface area of both solar cells and their shading structural elements. A technique based on the decremental neighborhood method has been developed to optimize the set of design parameters for the layout of external solar cells according to the criterion of their maximum efficiency (minimum shading of solar cells by both each other and their structural elements).

The software for evaluating the effective solar cell illumination area proposed in the receptor geometric model has been implemented in C#, and the results have been verified.

References

1. Vissarionov VI, Deryugina GV, Kuznecova VA, Malinin NK (2011) Solnechnaya energetika (Solar energy). Izdatel'skij dom MEI, Moscow
2. Mhitaryan EM (1999) Energetika netradicionnyh i vozobnovlyaemyh istochnikov (Energy of unconventional and renewable sources). Naukova dumka, Kiev
3. Samojlovskij AA, Lisejcev NK (2015) Metodika opredeleniya osnovnyh proektnyh parametrov bespilotnyh letatel'nyh apparatov, ispol'zuyushchih dlya poleta energiyu solnechnogo izlucheniya (Methodology for determining the main design parameters of unmanned aerial vehicles using solar energy for flight). Bull Moscow Aviat Inst 22(3):9–18
4. Grilihes VA (1986) Solnechnye kosmicheskie elektrostancii (Solar space power plants). Nauka, Leningrad
5. Obolenskij NV (ed) (1998) Arhitekturnaya fizika (Architectural physics). Strojizdat, Moscow
6. Baharev DV, Orlova LN (2006) O normirovanii i raschete insolyacii (About normalization and calculation of insolation). Svetotekhnika (Light Eng) 1:18–27
7. Karataev VA, Adonkina EV, Ten MG, Nefedova SA (2013) Insolyaciya pomeshchenij i territorij (Insolation of premises and territories). Sibstrin, Novosibirsk
8. Grilihes VA, Orlov PP, Popov LB (1984) Solnechnaya energiya i kosmicheskie polety (Solar power and space travel). Nauka, Moscow
9. Hejfec AL (2007) Sistema avtomatizirovannogo rascheta prodolzhitel'nosti insolyacii (System for automated calculation of the duration of insolation). Bull South Ural Univ Ser: Constr Archit 14(86):9–18
10. Gusev NM (1961) Estestvennoe osveshchenie zdanij (Natural lighting of buildings). Gosstrojizdat, Moscow
11. Shtejnberg AY (1975) Raschet insolyacii zdanij (Calculation of insolation of buildings). Strojizdat, Moscow
12. Egorov EV, Nartova LG (2012) Konstruktivnaya geometriya (Constructive geometry). Izdatel'stvo MAI, Moscow
13. Han KM, Markin LV, Tun EV, Korn GV (2016) Receptornye modeli v zadachah avtomatizirovannoj komponovki tekhniki (Receptor models in the problems of automated layout of equipment). Lambert, Saarbryuken

14. Tolok AV (2016) Funkcional'no-voksel'nyj metod v komp'yuternom modelirovanii (Functional voxel method in computer modeling). FIZMATLIT, Moscow
15. Korn GV (1990) Metody formirovaniya receptornyh geometricheskih modelej i ih primenenie pri reshenii inzhenerno-geometricheskih zadach (Methods for the formation of receptor geometric models and their application in solving engineering geometric problems). Dissertation, Moscow Aviation Institute
16. Lin S (2011) Razrabotka metodov i geometricheskih modelej analiza nezapolnennyh prostranstv v zadachah razmeshcheniya (Development of methods and geometric models for the analysis of empty spaces in placement problems). Dissertation, Moscow Aviation Institute
17. N'i N'i Htun (2014) Razrabotka i issledovanie receptornyh geometricheskih modelej telesnoj trassirovki (Development and research of receptor geometric models of body tracing). Dissertation, Moscow Aviation Institute
18. Han KM, Markin LV, Tun EV, Korn GV (2016) Diskretnye modeli geometricheskogo modelirovaniya komponovki aviacionnoj tekhniki (Discrete models of geometric modeling of the layout of aircraft). In: Electronic Journal "Proceedings of the MAI", no 86. http://trudymai.ru/published.php?ID=66465. Accessed 30 May 2021
19. Han KM, Markin LV (2017) Raschet vzaimnogo zateneniya solnechnyh antenn kosmicheskih letatel'nyh apparatov (Calculation of mutual shading of solar antennas of spacecraft). In: Electronic Journal "Proceedings of the MAI", no 93. http://trudy.mai.ru/published.php?ID=80474. Accessed 30 May 2021
20. Han KM. Matematicheskoe i programmnoe obespechenie rascheta zatenennosti solnechnyh batarej kosmicheskih letatel'nyh apparatov (Mathematical and software for calculating the shading of solar panels of spacecraft). Dissertation, Moscow Aviation Institute
21. Tun YW, Markin LV (2019) Universal'nyj sposob postroeniya receptornyh geometricheskih modelej ob"ektov slozhnyh tekhnicheskih form (A universal method for constructing receptor geometric models of objects of complex technical shapes). In: 18-th International conference "aviation and cosmonautics-2019", Moscow, MAI, 18–22 November 2019, p 187; 486
22. Tun YW, Markin LV (2019) Methods of formation of receptor (voxel) geometric models for automated layout tasks. 2019 IOP Conf Ser: Mater Sci Eng 687:044050. https://doi.org/10.1088/1757-899X/687/4/044050. Accessed 30 May 2021
23. Shennon R (2010) Imitacionnoe modelirovanie sistem—iskusstvo i nauka (System simulation—art and science). Mir, Moscow
24. Stoyan YG, Sokolovskij VZ (1980) Reshenie nekotoryh mnogoekstremal'nih zadach metodom suzhayushchihsya okrestnostej (Solution of some multiextremal problems by the method of tapering neighborhoods). Naukova Dumka, Kiev
25. Stoyan YG, YAkovlev SV (1986) Matematicheskie modeli i optimizacionnye metody geometricheskogo proektirovaniya (Mathematical models and optimization methods for geometric design). Naukova Dumka, Kiev

A Sierpiński 3D-Fractals in Construction. An Alternative to Topological Optimization?

L. A. Zhikharev[(✉)]

Moscow Aviation Institute (National Research University), 4, Volokolamskoe shosse, Moscow 125993, Russia

Abstract. In modern architecture, the task of creating light-weight and durable structures that allow you to build more durable and openwork buildings, as well as save construction materials, is relevant. Within the framework of this study, this problem is solved by geometric methods, which means creating a ration-al geometry. At the same time, two modern methods were used. They are optimization of topography and 3D-fractals based construction. The comparison of the methods is carried out on the example of increasing the related to weight strength of a wall console. Topology optimization was carried out using the SIMP method, which was applied according to a multi-stage scheme. Fractal constructions were created on the basis of three-dimensional analogues of the Sierpiński triangle with a different number of iterations. Their effectiveness was compared with each other, and they also were additionally tested at different weights, which made it possible to determine the stability gain that the design acquires when it becomes more complex by one pre fractal iteration. According to the results of the computer simulation, it was possible to increase the strength of the console many times, as well as to determine some criteria for choosing a particular geometric method to solve the problem of increasing the specific strength of the structure, depending on the requirements.

Keywords: Specific strength · Topology optimization · SIMP-method · Sierpiński fractals · 3D-fractal constructions

1 Introduction

Since the end of the last century, the method of topology optimization has been promising for many areas of science and technology. Using this method, it is possible to generate complex shapes of parts that best meet operational requirements. When optimizing the topology, the areas with the lowest stress arising from the specified load exerted on the part are removed from the optimized part. However, if it is necessary to lighten the part very much, standard topology optimization methods may stop working, because too thin load-bearing elements begin to buckle and collapse. In this case, it may be advantageous to replace parts of the part with structures having a fractal organization.

In the article [1], an algorithm for constructing structures using the geometry of the Serpinsky fractal was proposed and its theoretical efficiency was confirmed by the

example of flat fractals. This study is devoted to further testing the algorithm and comparing its effectiveness with an alternative way of effectively reducing the mass of structures—optimization of topology.

2   Scientific Significance

Modern architecture and construction require the introduction of new engineering solutions to increase the strength of structures. The creation of design structures often involves the use of light and durable materials. They allow us to embody the creative vision of the architect in a functional form [2–6].

High-rise buildings are no less demanding for their lightness and strength. The one in addition to their own mass, must withstand increased loads under the influence of wind and have seismic stability. This problem is investigated in many modern articles [7, 8]. Simply increasing the strength of the load-bearing elements by increasing the size of the first ones is not rational, since this will increase the mass and the strength will be insufficient. Therefore, in the construction of high-rise buildings, advanced developments in the field of research of high-strength building materials and composites are used [9, 10], as well as new geometric solutions to the problem [11].

An effective way to create a geometry of structures with outstanding mechanical properties is to the topology optimization (TO). There are many methods of TO, but they all boil down to removing the "excess" material from a certain area, which is called the optimization area. The identification of "excess" material occurs by the distribution of internal stresses that arise under the action of loads applied to the optimization area. To determine the stress distribution, the optimization area is divided into a large number of finite elements (FE), in which the stress is considered constant. During the implementation of the TO, part of the FE is removed, and the remaining ones form an optimized geometry.

The presented topology optimization mechanism leads to a number of features of the optimized geometry. First, the distribution of the material in the optimization region tends to be optimal, from the point of view of the uniformity of the distribution of stresses arising under the action of applied loads. This indicates the strength characteristics of the part can sharply decrease with a slight change in the loading scheme. Secondly, the final result is not completely determined by the conditions of topological optimization and the imposed restrictions, and therefore the shape of the obtained elements forming the product of can be quite complex. The boundary surface of the resulting parts may not be described analytically in full, since they are an approximation over a large number of vertices and faces of the FE. This complexity of the shape makes it difficult to determine many strength indicators, for example, the buckling stability of the part. In this regard, the buckling is not taken into account in any TO. And thirdly, improving the optimization of the form requires an increase in the number of finite elements. This leads to large expenditures of computing power in TO, so it is necessary to use supercomputers [12], or modifications of TO methods that allow reducing the amount of processed data [13].

Another way to create light and strong structures is to model regular geometric structures. There are many articles devoted to the study of architectural materials [14–17] that effectively perceive the load. A special type of regular structures is hierarchical

structures, the structure of which is subject to periodically recurring patterns of construction. In the article [18], Daniel Rayneau-Kirkhope end others give a classic example of the introduction of fractal hierarchical structures to reduce the mass of the materials structure. This example is the Eiffel Tower, one of the most recognizable architectural structures in the world. Due to the use of hierarchical patterns, the architects managed to achieve impressive results in the combination of strength and lightness of the structure. In the articles [19, 20], the authors confirm the effectiveness of using fractal structures to increase the specific strength of the structure. Another algorithm for creating strong and light fractal structures has shown its effectiveness in our study [1]. In the future, we will call fractal structures such structures, parts of which are described by regular hierarchical patterns, and they can be attributed to pre fractals. According to this involved definition, fractal constructions can contain non-hierarchical parts in their composition. In Figs. 8 and 10, the consoles contain supports-disks and suspension rings, which are not fractal. The hierarchical structures studied in the article [19] also have non-fractal supports, without which it is difficult to make the necessary experiments with them. The specific strength will be considered the strength per unit mass.

Despite the sufficient popularity of the research of geometric methods for increasing the strength of the structure, such as computer optimization of geometry and the creation of hierarchical structures, the topic of the general comparison of these groups of methods is insufficiently developed, which prompted the writing of this article.

3 Formulation of the Problem

Topology optimization and the design of hierarchical structures refer to geometric methods for increasing the specific strength of structures. The first one is called to optimally select the parameters of the shape of the part so that it can withstand the target load, for which optimization is being carried out. The result is a complex geometry that requires complex calculations. When creating hierarchical or fractal constructions, the final form is determined by choice of a fractal algorithm for its creation. This makes it possible to create a form that is simpler from the point of view of strength calculations.

To compare the above methods of creating a geometry, the SIMP method (Solid Isotropic Material with Penalization) [21, 22] for optimizing the topology, and the algorithm for creating structures of increased strength based on the Sierpinski triangle, described in [1], were chosen. The comparison is carried out on the example of creating a geometry of a console similar in weight and size characteristics to a product with a traditional geometric shape (Fig. 1).

The dimensions of the console: the height, width and length of the suspension were 340, 400 and 340 mm, respectively. The analysis of strength characteristics is carried out using computer simulation methods in the SolidWorks and Fusion 360 programs based on finite element analysis [23, 24].

Within the framework of this study, the effectiveness of the first and second methods is determined by increasing the specific strength of the console, relative to the strength of a conventional console (Fig. 1).

The task is to test the effectiveness of the methods by the example of solving an applied problem under various conditions, as well as determining the requirements under
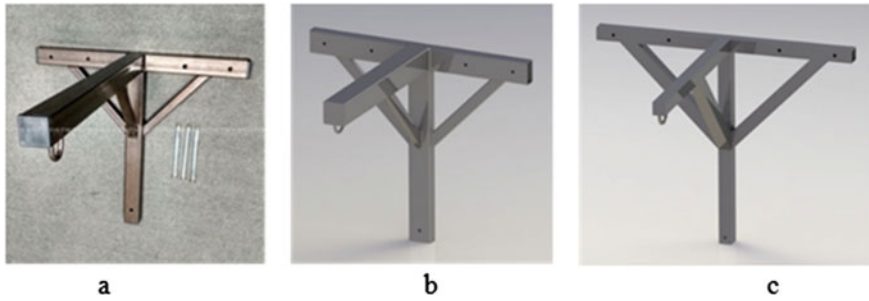
Fig. 1 An example of a console welded of pipes square and rectangular cross-section (**a**) and on the basis of which developed two models of pipes of different cross sections: 40 × 40, 40 × 20 and 20 × 10 with a wall thickness of 1 mm (**b**) and from equal pipe cross section 20 × 20 mm, with a wall thickness of 1.5 mm (**c**)

which the advantages of the first or second method are most clearly manifested. The latter will allow us to justify the choice of the method depending on the operational characteristics and requirements for the product, the geometry of which needs to be upgraded.

4   Theoretical Foundations

The SIMP method is based on working with a virtual model, during which the characteristics of the material in various areas change. The role of this characteristic can be the density of the real material. In the Fusion 360 used, the SIMP method is implemented on the basis of the finite element method. Due to the change in the density within the FE, its rigidity changes. At each step of the density change, the stress distribution is redistributed over the entire optimization area, and the density changes so that the maximum stress value decreases at the same time. The permissible density values are limited. After any change in density ceases to reduce the stress, the threshold value of the density is determined, and all FE of lower density is removed. The remaining FE form an optimized geometry.

In order to avoid a drop in the strength of parts with an optimized geometry caused by the occurrence of defects forming dangerous sections, TO should be carried out with FE of different sizes [25].

Within the framework of the tasks set, the TO, which was carried out using the SIMP method in the Fusion 360 program, turned out to be effective only within the limits of reducing the mass of the optimization area by 80–85%. In this case, the required mass of the console should be less than 1% of the mass of the optimization area. This problem was solved due to several stages of optimization, in which the geometry of parts with already optimized geometry was optimized (Fig. 2).

It is advisable to simplify the complexity of the optimized geometry of parts by approximating the obtained surfaces with their simpler analogues, such as cylinders, prisms and torus surfaces (Fig. 3). The main simulation experiments were conducted with consoles modeled according to the results from SolidWorks and Fusion 360.
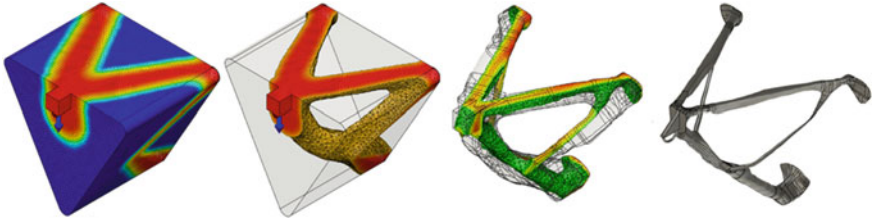
Fig. 2 Multi-stage topology optimization

Fig. 3 Simplification of topology optimization results

The console of the fractal design is based on an irregular tetrahedron assembled from cylindrical rods, the lengths of which are selected so that the dimensions of the console correspond to the accepted values. The algorithm for creating structures of increased strength based on the Sierpinski triangle is based on the idea that with a sufficiently small mass (to the left of the point K, Fig. 4) the rods, which in [1] were called base rods, begin to collapse due to buckling.
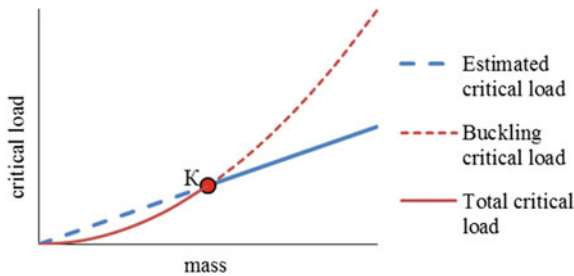
Fig. 4 Graph of the ratio of strength and stability of a rod of constant length under the influence of a compressive load

Under the base rods, the rods carrying the target load are understood, while the rest are designed to prevent loss of stability of the base rods and belong to the supporting frame. The mass of the supporting frame should be minimal and sufficient to perform

its main functions. The buckling is determined by the Euler formula:

$$P_b = \pi EJ \times (KL)^{-2}, \tag{1}$$

where E is Young's modulus of the rod material, J is the minimum area moment of inertia of the cross-section, L is the unsupported length of the rod, and K is the rod effective length factor.

Determination of the optimal ratio of the radii of the rods in the fractal console was carried out using a graph of its stability.

Figure 5 shows an example of the dependence of the console stability on the supporting frame rods radius: when it deviates to a smaller side of the sub-optimal value, the stability of the entire structure sharply decreases due to local loss of stability in the supporting frame, and when it deviates to a larger one, it decreases due to a drop in the stability of the base rods.
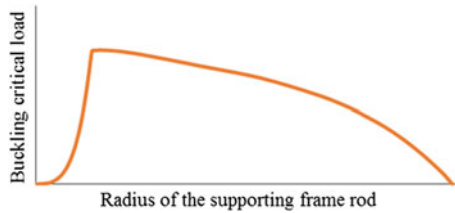
Fig. 5 Graph of the stability dependence of the console on the radius of the supporting frame rods

All studies were carried out under the influence of a force of 1000 N on the ring of the console along the plane of its fastening. The material used is aluminum alloy 7075.

5 Experimental

The topology was optimized when fixing the zones around the mounting holes. The places of application of forces and the size of the optimization area remain unchanged in all simulation experiments. The consoles obtained during the TO are indicated by the letter B.

The models have a rational geometry, but their surface turned out to be unnecessarily complex (Fig. 3). Computer simulation of strength studies shows that the approximation of these surfaces by the simpler ones increases the specific strength up to two times. This is due to the alignment of the cross-sectional areas along with the power elements. In the future, only consoles with simplified geometry will appear in the comparisons.

The final shape of the consoles of type B depends on the size of the FE, which is justified in [25]. When switching from a grid with a FE of 10 mm to a grid with a FE of 4 mm, the form becomes more complicated (Fig. 6).

The simulation results indicate that at the first stage, the complication has a positive effect, since additional elements increase stability. But with further complication, elements appear whose strength is low. This reduces the strength of the entire console.
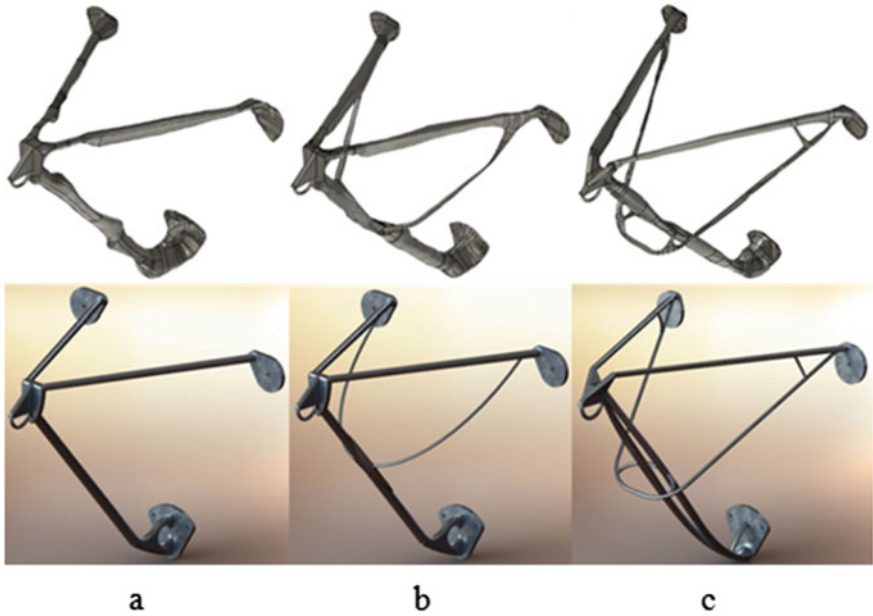
Fig. 6 Results of topology optimization with grid sizes of finite elements of 10 mm (**a**), 7 mm (**b**) and 4 mm (**c**)
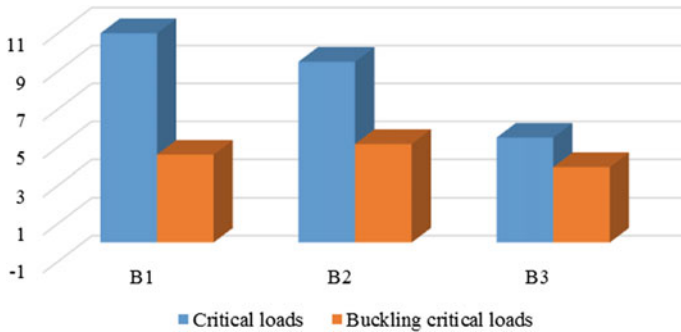
Fig. 7 Comparison of the strength and buckling stability of B1, B2 and B3

Figure 7 shows a comparison of the strength characteristics of the consoles B1, B2 and B3.

The results of simulations conducted with consoles C1, C2 and C3 (Fig. 8) confirmed the correctness of the assumptions made in Ref. [1], but for spatial fractals: with an increase in the number of iterations of the prefractal, the strength of the console decreases due to the fact that at a constant mass, an increasing part of the material is spent on the supporting frame, which means that the diameter of the base rods decreases. However, due to increased buckling stability, the *stable* total strength of the console increases from
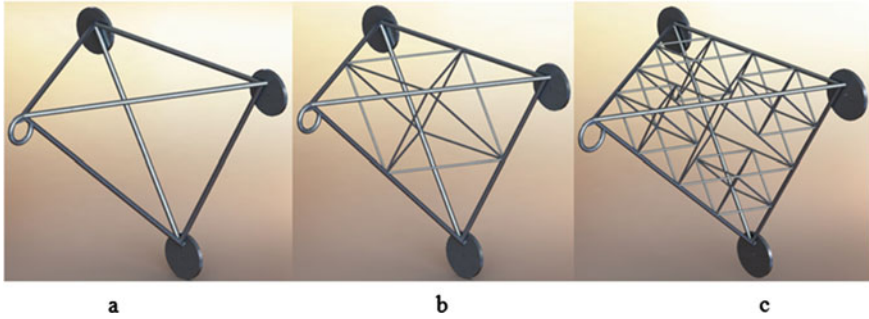
Fig. 8 The fractal consoles of the zero (**a**), first (**b**) and second (**c**) iterations, respectively, C1, C2 and C3

C1 to C3. Total strength is the actual strength, that is, the ability of the part not to collapse and bend under the action of the applied load.

The consoles of type C are slightly inferior to the consoles of type B in terms of total strength, since the rods of the triangle connecting the three mounting disks do not take the target load. At the same time, fractal structures still turned out to be much stronger than consoles A. The results of simulations confirming this are presented in the general diagram in Fig. 9.
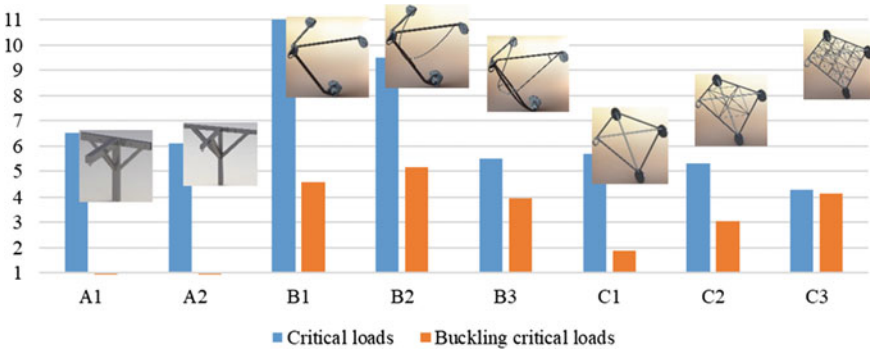
Fig. 9 General diagram of the strength and buckling stability of all console's options

It also follows from the presented diagram that the consoles A1 and A2, although they have sufficient strength, are still relatively easy to collapse with buckling—the walls of the pipes are crushed, unable to withstand heavy loads.

All the presented simulation results are relevant for consoles with a volume of 180 ms^3, that is, a mass of about 500 g. At the same time, the graph in Fig. 4 shows that with a smaller mass, the stability of structures becomes increasingly important, which means that fractal structures will be more effective. Consider the fractal console of the next iteration of C4 (Fig. 10).

According to the graphs comparing the stability and strength of C3 and C4, it can be seen that for any masses, the stability of C4 is higher than the stability of C3, and the
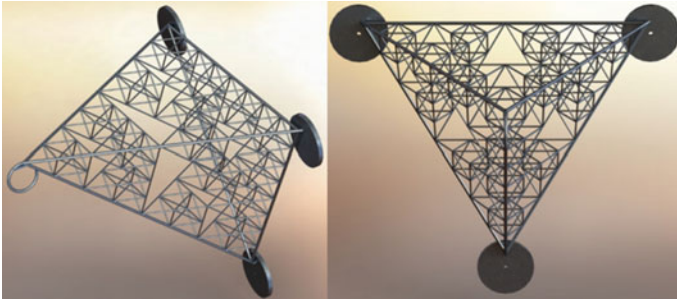
Fig. 10 The fractal console of the third iteration—C4

strength, on the contrary, is less. But when the volume of the material is less than 119 cm^3 (point K in Fig. 11a), the total strength of C4 is greater than C3. With a material volume of about 106 cm^3 (the point of intersection of the strength and stability graphs C4), the fractal console turns out to be almost 15% stronger than B3.
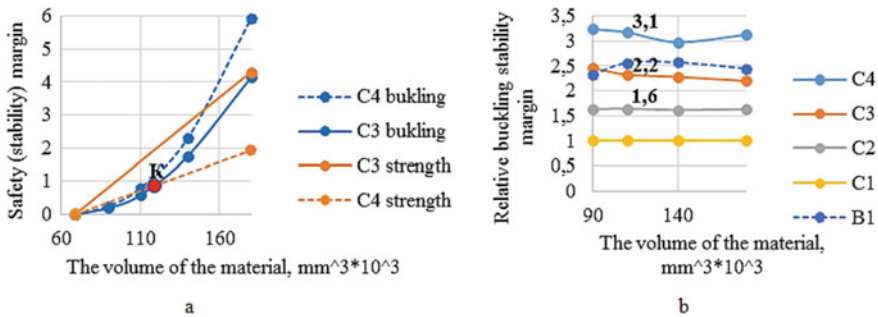
Fig. 11 Graph of the comparison of stability and strength of C3 and C4 (**a**) and graphs of C1-normalized buckling stability of C1, C2, C3, C4 and B3 (**b**)

To assess how much the stability of the fractal structure increases with each new iteration, we turn to Fig. 11b. It presents the stability graphs C1, C2, C3, C4 and B3, normalized by the stability of C1, that is, by a non-fractal structure. It can be seen that the gain in stability is approximately equal at different masses, and at the transitions from C1 to C2, C2 to C3 and C3 to C4 is 0.6 ± 0.4%, 0.6 ± 3% and 0.9 ± 2% respectively. The stability of B3 is exceeded by three iterations of the fractal structure.

The graph in Fig. 12 shows a linear or even exponential increase in relative stability with an increase in the number of iterations of the pre fractal.

6 Summary and Conclusion

The results of simulations in CAE systems presented in this article have shown the possibility of a significant increase in the strength of products with a traditional geometric shape due to the optimization of the topology and the use of fractal structures. The
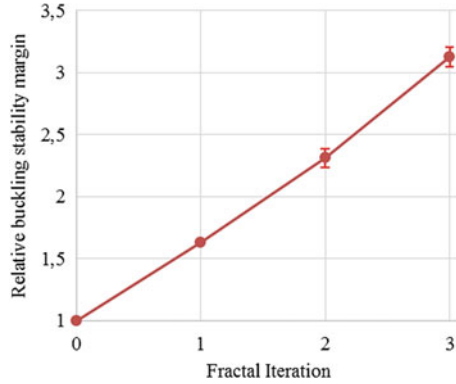
Fig. 12 Graphs of relative buckling stability with the increasing number of iterations of the pre fractal

resulting shape needs to be refined—this allows you to simplify and facilitate the part. Both topology optimization and the use of fractal structures are promising for solving applied problems in construction and architecture.

According to the results of comparing the optimized and fractal structures, for the described case (for a given weight and dimensions), optimization of the topology was more effective in increasing the specific strength of the console. However, with a decrease in the permissible material consumption for a similar part, fractal structures turn out to be more durable. Thus, the choice of a method for increasing the specific strength of a part is determined by the ratio of the mass of the material to the dimensions of the product, and the smaller this ratio is, the more effective are the structures created on the basis of volumetric analogues of the Serpinsky fractal. For the pre fractal of each iteration, there is a certain interval of the mass of the consumable material, within which it is most effective. In this case, an increase in the number of iterations unnecessarily reduces the strength, while a decrease the one reduces the stability.

A combination of comparable methods for increasing the specific strength seems promising: the load perceived by various base rods or elements of the supporting frame is not uniform, therefore the optimization of their radii will save material and thereby reduce the weight of the part. Further research will be devoted to this issue. When solving such problems, it is rational to create more variable parametric models specified using a mathematical or software description [26, 27].

The graph shown in Fig. 11b allows us to reasonably assume that the theoretical gain in total strength due to the use of fractals may be infinite when the mass of the structure tends to zero. In this case, the actual strength of the structure with zero mass will be zero in any case. To further substantiate this statement, it is necessary to study the strength of pre fractals with a large number of iterations.

References

1. Zhikharev LA (2021) A Sierpiński triangle geometric algo-rithm for generating stronger structures J Phys: Conf Ser 012066. https://doi.org/10.1088/1742-6596/1901/1/012066
2. Szolomicki J, Golasz-Szolomicka H (2019) Technological advances and trends in modern high-rise buildings. Buildings 9(9):193. https://doi.org/10.3390/buildings9090193
3. Rian IM, Sassone M, Asayama S (2018) From fractal geometry to architecture: designing a grid-shell-like structure using the Takagi-Landsberg surface. Comput Aided Des 98:40–53. https://doi.org/10.1016/j.cad.2018.01.004
4. Rian IM (2019) FracShell: from fractal surface to a lattice shell structure. In: Digital wood design. Springer, Cham, pp 1459–1479. https://doi.org/10.1007/978-3-030-03676-8_59
5. Burger J, Lloret-Fritschi E, Scotto F, Demoulin T, Gebhard L, Mata-Falcón J, Flatt RJ (2020) Eggshell: ultra-thin three-dimensional printed formwork for concrete structures. 3D Print Add Manuf 7(2):48–59. https://doi.org/10.1089/3dp.2019.0197
6. Kromoser B, Pachner T (2020) Optiknot 3D—free-formed frameworks out of wood with mass customized knots produced by FFF additive manufactured polymers: experimental investigations, design approach and construction of a prototype. Polymers 12(4):965. https://doi.org/10.3390/polym12040965
7. Gong S, Zhou Y, Ge P (2017) Seismic analysis for tall and irregular temple buildings: a case study of strong nonlinear viscoelastic dampers. Struct Design Tall Spec Build 26(7):e1352. https://doi.org/10.1002/tal.1352
8. ю Ыⅰрут Об Кут Чб Ярфтп Нб Срут О (2019) Nonlinear dynamic analysis of frame-core tube building under seismic sequential ground motions by a supercomputer. Soil Dyn Earthq Eng 124:86–97. https://doi.org/10.1016/j.soildyn.2019.05.036
9. Gharehbaghi K, Georgy M, Rahmani F (2018) Composite high-rise structures: structural health monitoring (SHM) and case studies. Mater Sci Forum 940:146–152. https://doi.org/10.4028/www.scientific.net/MSF.940.146
10. Babaytsev A, Dobryanskiy V, Solyaev Y (2019) Optimization of thermal protection panels subjected to intense heating and mechanical loading. Lobachevskii J Math 40(7):887–895. https://doi.org/10.1134/S1995080219070059
11. Ibragimov A, Danilov A (2018) Curvilinear steel elements in load-bearing structures of high-rise building spatial frames. E3S Web Conf 33:02028. https://doi.org/10.1051/e3sconf/20183302028
12. Aage N, Andreassen E, Lazarov BS, Sigmund O (2017) Giga-voxel computational morphogenesis for structural design. Nature 550(7674):84–86. https://doi.org/10.1038/nature23911
13. Liu C, Zhu Y, Sun Z, Li D, Du Z, Zhang W, Guo X (2018) An efficient moving morphable component (MMC)-based approach for multi-resolution topology optimization. Struct Multidiscip Optim 58(6):2455–2479. https://doi.org/10.1007/s00158-018-2114-0
14. Pham MS, Liu C, Todd I, Lertthanasarn J (2019) Damage-tolerant architected materials inspired by crystal microstructure. Nature 565(7739):305–311. https://doi.org/10.1038/s41586-018-0850-3
15. Schaedler TA, Jacobsen AJ, Torrents A, Sorensen AE, Lian J, Greer JR, Carter WB (2011) Ultralight metallic microlattices. Science 334(6058):962–965. https://doi.org/10.1126/science.1211649
16. Berger JB, Wadley HNG, McMeeking RM (2017) Mechanical metamaterials at the theoretical limit of isotropic elastic stiffness. Nature 543(7646):533–537. https://doi.org/10.1038/nature21075
17. Tang Y, Guoying D, Fiona ZY (2019) A hybrid geometric modeling method for lattice structures fabricated by additive manufacturing. Int J Adv Manuf Technol 102(9–12):4011–4030. https://doi.org/10.1007/s00170-019-03308-x

18. Rayneau-Kirkhope D, Mao Y, Farr R (2013) Towers of strength. Phys World 26(08):35
19. Rayneau-Kirkhope D, Mao Y, Farr R, Segal J (2012) Hierarchical space frames for high mechanical efficiency: fabrication and mechanical testing. Mech Res Commun 46:41–46. https://doi.org/10.1016/j.mechrescom.2012.06.011
20. Rayneau-Kirkhope D, Mao Y, Farr R (2012) Ultralight fractal structures from hollow tubes. Phys Rev Lett 109(20):204301. https://doi.org/10.1103/PhysRevLett.109.204301
21. Ferrer A (2019) SIMP-ALL: a generalized SIMP method based on the topological derivative concept. Int J Numer Meth Eng 120(3):361–381. https://doi.org/10.1002/nme.6140
22. Bruns TE (2005) A reevaluation of the SIMP method with filtering and an alternative formulation for solid–void topology optimization. Struct Multidiscip Optim 30(6):428–436. https://doi.org/10.1007/s00158-005-0537-x
23. Kader MA, Hazell PJ, Brown AD, Tahtali M, Ahmed S, Escobedo JP, Saadatfar M (2020) Novel design of closed-cell foam structures for property enhancement. Addit Manuf 31:100976. https://doi.org/10.1016/j.addma.2019.100976
24. Jiang H, Le Barbenchon L, Bednarcyk BA, Scarpa F, Chen Y (2020) Bioinspired multilayered cellular composites with enhanced energy absorption and shape recovery. Addit Manuf 36:101430. https://doi.org/10.1016/j.addma.2020.101430
25. Zhikharev LA (2020) Fractal graphs of the efficiency of topology optimization in solving the problem of strength versus mesh. Geom Graph 8(3):25–35. https://doi.org/10.12737/2308-4898-2020-25-35
26. Beglov IA (2021) Mass-centering characteristics of solids within quasi-rotation surfaces. J Phys: Conf Ser 1791(1):012035. https://doi.org/10.1088/1742-6596/1791/1/012035
27. Boykov AA (2021) Development and application of the geometry constructions language to building computer geometric models. J Phys: Conf Ser 1901(1):012058. https://doi.org/10.1088/1742-6596/1901/1/012058

Urban Engineering and Planning

Analysis of Landscape and Urban Planning of the Coastal Areas

N. Burilo[✉]

Novosibirsk State University of Architecture and Civil Engineering (Sibstrin), 113, Leningradskaya Street, Novosibirsk 630008, Russia
itc@sibstrin.ru

Abstract. There are numerous theoretical and applied studies of urban open and pedestrian spaces, which cover the topic of the pedestrian network formation in the city at the level of observation, theoretical description and study of features. Therefore, the architectural and planning structure of pedestrian spaces along the coastal territories of a large city is chosen as the subject of this article. Architectural and planning principles of pedestrian spaces formation in the central part of the city and on the coastal territories are considered in the article. The features of the conceptual apparatus are revealed. The prerequisites for the urban open spaces formation intended for pedestrian traffic are shown in the article. The modern aspects of pedestrian flows organization are determined. The features of the design and improvement of pedestrian spaces are considered in the Swedish model's example of the "city on the water" in Stockholm. The analysis of the existing principles of designing urban pedestrian spaces is carried out.

Keywords: Coastal territories · Recreational spaces · Pedestrian spaces · Urban planning

1 Introduction

Movement is an integral part of human life, as the basis for life's preservation on earth and the development of all living organisms. In order to fully realize the abilities and natural abilities, a person should develop, move both spiritually and physically.

In a modern city, traffic is often carried out exclusively by means of vehicles, but the role of pedestrian traffic remains invariably important. The problem of organizing this movement together with the traffic flows should be solved in conjunction with a number of important urban planning tasks in difficult environmental conditions. One of them is the interaction of the framework, developed many centuries ago, and the new conditions for the attraction objects' formation, which can not occur without a partial transformation of the existing environment. In some cases, the transformation may be of a fundamental nature (expansion of existing streets, punching galleries and passages in the first floors of buildings). But the existing framework of many cities represents an extremely valuable historical and architectural environment, which is either impossible

to change for reasons of protecting monuments of material culture, or it is economically impractical [1].

This makes it necessary to search for solutions to transform the existing environment without taking measures to radically change it. Modern elements of landscaping have sufficient means to complete or partially reconstruct the urban environment without violating its integrity. Their competent use can solve a wide range of issues related to the communication spaces organization (the formation of a barrier-free environment, etc.).

The main goal of the study is to identify the principles in the formation of pedestrian spaces along the coastal part of a city and to develop solutions and schemes that allow creating an integral pedestrian system, organically included in the structure of a city [2].

The existing numerous theoretical and applied studies of urban open and pedestrian spaces cover the topic of the pedestrian network formation in the city at the level of observation, theoretical description and study of its components. Therefore, the subject of this study is the architectural and planning structure of pedestrian spaces in the central part of a large city. It is necessary to conduct a comprehensive study of urban planning, social, functional and environmental features of the city's pedestrian communications, taking into account the analysis of experience (domestic and foreign) and modern provisions of environmental and systemic approaches.

Despite numerous vehicles, pedestrian traffic remains a popular means of transportation. Moreover, its importance is emphasized by modern medicine, psychology and sociology. This proves that the problem of pedestrian traffic organizing in the city and the issue of interaction and interdependence of open urban spaces and pedestrians is very important. Modern experiments on the separate sections creation of landscaped territories intended exclusively for pedestrian traffic do not always justify their use. It is necessary to reconsider both the approach to the pedestrian communication routes formation and their individual elements, paying special attention to the creation of extended continuous links between individual objects and all urban spaces [3].

The relevance of this work is also determined by the changing requirements for the level of the pedestrian communications environment comfort, the lack of specific methodological documents that take into account the pedestrian network formation within the street and road network: unsatisfactory state of open urban spaces in modern cities, difficult environmental situation; lack of a comprehensive methodology for assessing and analyzing the state of the existing pedestrian spaces. These problems require a revision of the interactional principles between transport and pedestrian flows in order to form components of an environment, characterized by the high activity of residents.

Pedestrian spaces (PS) are transport-free zones [4].

In the coastal territories, where the most significant unique and attractive citywide structures and spaces are located, transport needs to be forced to change the historical layout, destroy and move structures, disrupt pedestrian connections between the main cultural and everyday objects and the population. Therefore, it is no accident that in order to solve the multifaceted problems of the city functioning, where social, environmental, and transport problems are the most sharply manifested in the modern city, transport-free zones and pedestrian streets are increasingly beginning to be arranged.

As a rule, pedestrian streets appear in cities with a relatively compact center and a simple transport and planning situation characteristic of small and large cities, where

the most favorable conditions exist for the organization of pedestrian streets that do not require preparatory work, as well as significant technical and material costs. For example, in Germany 330 belong to this type of city out of 450 cities with pedestrian streets and zones.

In large cities, like Moscow, Prague, Vienna, London, as well as large Siberian cities: Irkutsk, Tyumen, Omsk, etc. the successful operation and functioning of pedestrian streets in the historically established structure of coastal territories becomes possible only after significant capital expenditures on the transformation of the public transport system, the allocation of significant territories for parking lots and the creation of streets and zones with different transport modes, after significant landscaping of the territory [5].

In large cities, pedestrian spaces have a complex nature of interaction with each other and the planning structure of the city as a whole, forming transport-free zones.

In recent decades, the major cities of the world have been struck by a real boom in the creation of pedestrian zones. Some cities have found, others continue looking for their own way to solve common problems: transport, environmental, social and protecting cultural heritage and historical originality of the environment. From ambitious projects to a balanced approach—this is the evolution of joint experience in this area, focused on sustainable development, the balance of conservation and renewal tasks, and the integration of modern objects into the existing architectural context [6, 7].

Along with solving the problems of comfort and safety, improving environmental indicators and living conditions, promoting the tourist and investment attractiveness of the environment, the idea of pedestrian spaces has become a kind of tool for the interconnected preservation of architectural heritage (from individual monuments to vast territories, restoring the integrity of ensembles and urban fabric, adapting existing structures to modern functions). Along with historical architectural objects and spatial links, new ones play the role of nodal and connecting elements of the system, ensuring its viability and development.

Pedestrian systems concentrate architectural sights, traditional and new types of environments, landscapes and views. They most clearly embody the principles of attitude to heritage, the value orientations of urban culture. In modern architecture and design, the organization of pedestrian spaces is one of the priority areas and can serve as evidence of the ability to reconcile creative ambitions; social and commercial efficiency with respect for all that has been created for centuries.

2   Materials and Methods

Every year, in EU cities, such as Paris and Vienna, the authorities are trying to make the streets more environmentally friendly and convenient for pedestrians and cyclists, while creating problems for car owners.

So, in recent years, dozens of settlements in Germany have joined the network of so-called "nature protection zones"—only cars with low carbon dioxide emissions are allowed here. In Copenhagen, huge sections of streets are closed for automobile travel, and in Stockholm they charge a high fee for moving to the city center. Parking spaces are disappearing, and even Munich, once crowded with cars, is turning into a paradise for pedestrians.

It is worth noting that at the same time, the reverse policy is being conducted in the USA cities are trying to make them comfortable for cars. With the help of the synchronization of traffic lights, a "green wave" is created; applications for parking search are offered. Creating pedestrian streets is the exception rather than the rule. For example, a certain public response was caused by the decision of the New York Mayor to transfer Times Square and some other squares of the city to a "pedestrian mode" [8].

The situation in Zurich is completely different. Here, the local traffic management is actively fighting with cars with the support of public opinion: underground passages are closed, traffic is closed in many blocks adjacent to Levenplatz, one of the most crowded squares in the city [9]. On the other streets, there are so serious speed limits that pedestrians can safely cross the street almost at any time. The "green" traffic lights are reduced, while the "red" light is on longer and longer.

The Head of the Zurich Traffic Department, Andy Fellman: "The traffic turns out with constant stops, which is what we are trying to achieve. Our goal is to win back public space for pedestrians, not to simplify the life of drivers".

The new Sihl City mall in Zurich is three times larger than the Atlantic Mall (Brooklyn), but there are twice as many parking spaces, so most buyers get to it using public transport. 91% of the Swiss Parliament delegates come to work in the same way. Actually, this method of moving around the city is better developed in Europe than in America, but the costs of motorists per kilometer in the EU are two to three times higher than in the United States.

With all the variety of "designing" pedestrian systems' ways, a number of the most characteristic and successfully tested ones can be identified.

Firstly, these are whole fragments of development with the maximum use of the existing planning network and the allocation of the main pedestrian directions. Transport is carried out outside the territories, on the "reference highways". Public and excursion transport stops, parking lots, and service facilities are located on the nodal sections of the external borders. This scheme is used in the historical centers of cities and architectural complexes of special value.

Secondly, it is used as a basis of the established links' number (streets, squares, embankments, esplanades), where traffic is limited or excluded. The system is developed due to the reconstruction of buildings and blocks, the transformation of intra-block spaces, development of lacunae and underground space, vertical zoning, regeneration of deformed territories, including the adaptation of former industrial facilities. The key importance here is the preservation of ensembles unity and historical color of the environment, context synthesis and means of modernization together with the interconnected organization of pedestrian and transport traffic [10, 11].

Thirdly, it is the formation of alternative systems—pedestrian understudies of transport highways. Practice shows that simultaneously with the use of territorial reserves and certain structural transformations, existing green recreational spaces—parks, squares, boulevards, courtyards, combined through additional pedestrian links into a single route, are perfectly exploited in this quality [12]. This way is recognized as one of the most promising means of ecological improvement of the urban environment.

Finally, it is the creation of new spatial systems in the structure of public and business zones, cultural and shopping centers, residential complexes. The latest technologies and

architectural concepts are implemented in open, closed, multi-tiered spaces. At the same time, traditional types of environment (quarter, street, square, and forum) often receive a new interpretation here. Such a kind of "city within a city", as a rule, has a landscape component, which often combines the innovations of design and art with the cult of "wild" nature, characteristic of an urbanized society. Each city has its own history, experience in creating and prospects for the development of pedestrian space systems [13, 14]. One of them is Stockholm.

3   Results and Discussion

Stockholm, which grew up on dozens of islands among "skerries", between bays and channels, is more marked by its proximity to water than any other European capital. From any point of the city, one can easily get to a large body of water. The unique pedestrian system with its diversity and integrity has developed historically in Stockholm and is being enriched with new links. Its location, settlement traditions, the "Swedish social model" and environmental priorities play a decisive role in this process.

Of course, the Swedes love their native northern nature, history and hiking.

The plan for the reconstruction and development of urban areas, which implementation began in the 1960th, the central areas were practically freed from transit traffic flows, and traffic was concentrated in a system of highways and interchanges, as isolated as possible from the surrounding development. There are well-maintained walking trails along the coastlines of the Saltschen Bay, Lake Melaren, the Stirrup Strait, numerous channels and bays, thanks to which both, historical ensembles and the modern life of the city are turned to beautiful water panoramas. The most famous view platforms are the terraces lying by the water in front of the town hall and on the west coast of the "Knight's Island". The sky, the lake, architecture and sculpture create not only a magnificent urban landscape, but also a background for festive and sports spectacles.

Stadsholmen is the heart of "pedestrian" Stockholm. It is unique and typical, like any medieval city. Along the "long" Western and Eastern streets there are shops, restaurants, and galleries that are especially popular with tourists. This is the realm of artists, musicians, and antique dealers. The center of cultural life is the Sturtoriet (Large Square)—the venue for concerts, festivals, fairs. Narrow alleys descend to the pedestrian embankment of Scheppsbrun, where there used to be shopping piers.

Six bridges connect the island with the northern and southern parts of the city. The walking routes are continued by the one-and-a-half-kilometer Drottniggatan shopping street and the adjacent Hetoriet (Sennaya) and Sergelstor squares. The latter was formed as a result of the reconstruction of the 1970th in the form of a multi-level space, associated with the demolition of historical quarters. Today, the Swedes regret the loss, but the square is very popular with young people.

A favorite place for citizens to walk is a chain of embankments on the southern side of Norrmalm and Kungsholmen, connecting the main city squares, parks, theaters, museums, and recreation places. The fashionable Blasienholmen and Strandvegen are connected by bridges to the islands, each of which is an open-air museum. The "Stockholm Bois de Boulogne"—Djurgården-has been known for three centuries as the main place of folk festivals and entertainment. There are walking embankments, paths for

cyclists and horse riding, hiking trails, yacht clubs' marinas, a landscape park, a children's town, a museum complex including the Northern and Biological Museums, the Vasa ship museum, the Rusendal Palace and the famous Skansen.

There are walking routes of a different kind along the rocky coast of the southern part of the Swedish capital—Södermalm. These are recreated streets of the former city suburbs with picturesque low-rise buildings that have preserved the atmosphere of the XVIII-early twentieth century. In the nineteenth centuries, the "city on the water" revealed itself in all its beauty from the equipped walking trails and viewing platforms.

The Fatburspark complex in the very center of Södermalm, on the site of the former railway station, was built in 1988 by the Spaniard Riccardo Bofill. A huge round square-parterre, although removed from the water, but itself resembles a "green pool" surrounded by monumental buildings. The "Space for life", as the author called it, combines the functions of a pedestrian route in the structure of a public and business center, as well as a courtyard and a park, more precisely, a "sculpture park": an exposition of modern plastics is located along the busy paths.

The residential quarter of St. Eriksonredet, built in 1997 in the city center, in the northern part of the island in Kungsholmen, is a whole ensemble that includes a suite of pedestrian spaces. The spectacular three-part composition consists of a vast oval meadow surrounded by semicircular buildings, a terrace and an amphitheater descending to the picturesque embankment of the Karlsberg Canal. An organic part of the environment is the building of an ancient chapel and a modern sculpture. The internal spaces of the quarter are publicly accessible. Their relationship with both the urban planning context and the private residential area has been successfully solved.

In the residential complex under construction in the Liljeholmen district in the southwest of Stockholm, nine-storey residential buildings form the front of the coastal development, opened by kurdoner courtyards with huge arches to the pedestrian embankment, piers. Transport traffic is provided by a parallel street connected to the embankment by through boulevards to the walking embankment of the lake Melaren, connected to the park, is also connected to the new Luxury quarter on the island of Lillaessingen.

The most ambitious project of recent years is the Hammarby residential area to the south-east of Södermalm. Its pedestrian frame is formed by the axis of an artificial canal surrounded by boulevards together with picturesque embankments. The living environment is clearly structured and, at the same time, "dissolved" in the landscape [15–17].

4   Conclusion

At the present stage, the task is no longer to create separate pedestrian streets and zones, but to comprehensively develop a pedestrian spaces' system of various types (zones, streets, squares, alleys, overpasses, crossings, etc.). Master plans for urban development should include special sections on the system of organizing pedestrian traffic in cities-both in newly developed territories and during the reconstruction of existing development zones [18]. It should be noted that the analysis of foreign practice was useful for forming "your own way" in this direction.

Special attention should be paid to the current regulatory documentation: it widely considers the physical parameters of sidewalks and paths and thoroughly develops a

method for creating a barrier-free environment for physically weakened persons. However, the need for a systematic and integrated approach to the construction of a pedestrian network is mentioned only in the generalized phrase "…on the continuity of the pedestrian network…" The way this network has to be built, and even more optimized, there is no answer in the standards [19].

In the course of the research, the internal structure and characteristics of PS are determined in the first section—geometric (physical) objects and connections and architectural, artistic, visual qualities of the environment and connections:

- communication framework of PS system (path, node, objects of exposure/support);
- urban equipment;
- borders;
- view frames, paintings (visually perceived space).

A typology has been developed that organizes the variety of PS, from the point of complementary functions view: "shopping", entertainment of social contacts, cultural education, recreation, communication with the natural environment.

In the city center, there is a layering of various types of PS. This is due to the" functions of the place "of PS in the city center, as well as the complexity of the functional-spatial and architectural-artistic organization of its environment.

The concept of a "pedestrian zone" entered urban planning practice in the middle of the twentieth century as a response to the growing level of urbanization, the deterioration of living conditions in the city. In modern urban planning, the formation of pedestrian zones has become one of the most fashionable and relevant topics: thanks to these multifunctional spaces, a special atmosphere and flavor are created, and interesting walking routes increase the attractiveness of the city. The European practice of the last decades gives many successful examples of the creation of such zones. So, new satellite cities were built and adjacent cities were reconstructed in France in the 1970th, during the implementation of the Grand Paris master plan: the basis of their centers was a specially designed pedestrian space [20]. A lot of work was done in these cities to link cultural traditions with projects development. After all, the walking routes were all the more interesting, the closer the connection with the historical part of the city was.

An important factor is that urban planning becomes profitable for both the city authorities and residents, implementing the concepts of pedestrian streets. After all, tourism on pedestrian streets significantly replenishes the city treasury.

Barcelona provides a great example of creating pedestrian spaces: it managed to create a comfortable environment, put the historical center in order and organize interesting walking routes, linking the general plan of the city's development, development projects of individual districts and the ambitions of the authorities into a single whole. Munich and Rotterdam, Kaunas and Vilnius can boast excellent pedestrian zones.

Today, the experience of European cities allows us to identify a number of general principles to create the practice of pedestrian systems:

- Flexible interpretation of the concept, a variety of the organizational forms (pedestrian streets and spaces, territories of "comfortable" and "calm" traffic);

- No isolation of local zones, but the development of interconnected systems between objects of mass attraction, recreation places, on pedestrian transit and tourist and walking routes;
- Extensive typological gradation of the urban environment elements included in pedestrian systems, including intra-block spaces and landscapes;
- Functionality that provides, first of all, the convenience of movement, clear zoning, wide possibilities of use;
- Social attractiveness of the environment, combining traditional values and the dynamics of modern life; balance of public, collective, private zones;
- Protection of the urban landscape integrity: the nature of landscaping and urban equipment that is correct in relation to the historical basis, the inadmissibility of placing large-format advertising, the regulation of color and other modern components' characteristics of the environment, thoughtful lighting design;
- Special attention is paid to the architecture of the earth, which combines the properties of the pedestrian surface, the landscape component, and in the territories with a historical sub-basis-and the object of "urban archeology";
- Comprehensive solution of urban orientation information, including historical information about places, streets, buildings;
- The cultural mission of pedestrian spaces as public centers of contemporary art, concert and exhibition halls, venues for holidays, festivals, and art events.

The basis of the generalized practical experience has highlighted the need to classify the movement by the following features:

- purpose: to nodes in the city and external transport; to public services; work (business track); to the entrances of residential buildings, recreation facilities, city and country values (recreation track);
- by the nature of the movement: organized movement of significant human masses (demonstrations, processions, parades); impulse movement (flows to work and study); walking movement (this is a free process of movement, a walk);
- according to the method of transportation: actually pedestrian, including for physically weakened persons; bicycle-roller; recreational and entertainment (electric cars and horse-drawn sleds) [21]; mixed type.

More than half a century ago, the scientific community of Urban & Planning specialists came to the conclusion that a two-circuit structure of the transport network is necessary for cities: the first circuit is driveways and streets with direct access from the development site, the second one is urban highways designed for high-speed continuous traffic between parts of the city [22]. We can add another important principle for pedestrian traffic, drawing an analogy with traffic:
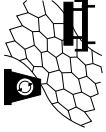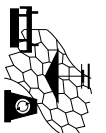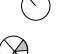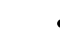
- by importance in the structure of the city: citywide continuous pedestrian routes— "pedestrian highways" (which are convenient to move not only on foot, but also by bicycle) and local pedestrian paths. However, unlike highways, local and citywide pedestrian paths are inseparable and form a single network [23].

On the basis of the studied materials, theoretical provisions were constructed, where the main typological characteristics of pedestrian paths were compared: according to the purpose, method of movement, time and intensity, architectural and environmental conditions, the structure and composition of the arrangement means [24]. The result is shown in the table of typological features (Table 1).

Therefore, we should draw a conclusion: when its own tracing methods and its own architectural and urban planning means of arranging transportation routes are required, which are determined by a complex of urban planning factors.

In the proposed classification of planning structures, according to the outline of the street network, cities are taken as examples, giving the most visual picture in support of these conclusions. In most cases, a combination of types can be easily identified in the existing urban development. This is natural, since the street network formation took place over a long period and was influenced by the socio-economic conditions of a particular region [25]. At the same time, the identified types of planning structures give a clearer idea of the peculiarities of the pedestrian spaces formation in the center of a large city and its further development, taking into account the established traditions.

Table 1 Table of the typological techniques' features applied to pedestrian paths

Typology of pedestrian paths by goal	Commercial paths To the places of application of labor	Transit routes To transport hubs	Public paths To public objects	Recreational paths	Communication paths To adjacent housing
The nature of the trace	Straight-line tracing	Straight-line tracing	Advanced mixed tracing	Curved flexible tracing	Mixed tracing
Possible ways of movement	Adapted for people with disabilities Walking on specialized types of transport	Adapted for people with disabilities Walking on specialized types of	Adapted for people with disabilities Walking	Adapted for people with disabilities Walking on specialized types of	Adapted for people with disabilities Walking
The level of arrangement I. Minimum II. Middle III. Tall	II	I	III	III	I
Intensity and time of use Weekdays/weekends					
Priority characteristics	Bandwidth, information saturation	Straightness, speed of movement	Bandwidth, information saturation, aesthetics	Environmental friendliness, aesthetics	Number of paths, security

References

1. Soloviev LA (2015) Integrated strategic development of a millionaire city: model, mechanism, principles. Russian Entrepreneurship 16(21):3789–3800
2. Ketova EV, Burilo NA (2018) Influence of environmental factors on the formation of coastal zones in Siberian urbanized territories. MaTEC Web of Conferences. International scientific conference SPbWOSCE2017 "Business technologies for sustainable urban development", vol 170, p 6. https://doi.org/10.1051/matecconf/201817004010
3. Shesterneva NN (2007) Architectural typology and principles of development of existing pedestrian communications of the largest city: on the example of St. Petersburg. Dissertation, St. Petersburg, p 220
4. Velev P (1983) Pedestrian spaces of urban centers. Stroyizdat, Moscow, p 192
5. Burilo NA (2021) Sustainable development of coastal territories of large Siberian cities. Potapov readings: collection of materials. Publishing House of MISI-MGSU, Moscow, pp 30–35. http://mgsu.ru/resources/izdatelskaya-deyatelnost/izdaniya/izdaniya-otkr-dostupa/
6. Bakutis VE, Gorokhov VA, Lunts LB, Rastorguev OS (1979) Engineering improvement of urban territories: textbook for universities on spec. Urban Planning, 2nd edn. Pererab and additional. Stroizdat, Moscow, p 239
7. Lavrov VA, Solofnenko NA, Smolyar IM et al (1978) Designer's guide: urban planning: reference book of the designer: urban planning. Stroizdat, Moscow, p 367
8. Lunts LB (1974) Urban green construction: a textbook for universities on the specialty "Urban Planning." Stroizdat, Moscow, p 280
9. Demidova TO, Burilo NA (2021) The method of formation of image cultural objects with the introduction of the principles of renovation of industrial buildings. Russian cities: problems of construction, engineering support, landscaping and ecology. Collection of articles of the XXIII International scientific and practical conference, Penza, pp 47–53
10. Potaev GA (2014) Urban Planning. Theory and practice: training manual for students of higher educational institutions studying in the specialties "urban planning", "Urban and regional planning", "State and municipal management". Forum, Moscow, p 431
11. James C (1999) Restoring the landscape: essays in contemporary landscape architecture. Princeton Architectural Press, New York
12. Maleeva TV (2015) The formation of factors and conditions for the sustainable development of a large city based on the effective use of land resources: abstract of the dissertation: place of defense. St Petersburg State University of Economics and Engineering, St Petersburg, p 38
13. Abramova AA (1979) Analysis of socio-cultural functions and architectural composition of pedestrian spaces of the city center of historical cities. In the book: the role of scientific research in the practice of urban planning design, Moscow
14. Nefedov VA (2015) How to return the city to people. Art-XXI century, Moscow, p 159
15. Nefedov VA (2002) Landscape design and environmental sustainability = Landscape design and environmental sustainability. Polygraphist, Saint Petersburg, p 295
16. Krasheninnikov AV (1988) Residential quarters: study guide. Higher School, Moscow, p 87
17. Kozyreva EI (2006) Pedestrian spaces: European experience. ARDIS. Architecture. Restoration. Design. Investment. Construction. Electron. Dan. Saint Petersburg, 1(29). http://d-c.spb.ru/archiv/29/30-33/30-33.htm
18. Berezin MP (1975) Space-perception-behavior. Constr Archit Leningrad 7:39–42
19. Ketova E, Lesotova Yu (2018) Recreational areas as a basis of the municipal and urban territories' ecological framework. MATEC Web Conf 170:04099. 10.501/matecconf/201817004099
20. Zabelynansky GB, Minervin GB, Somov GY (1985) Architecture and the emotional world of a person. Stroyizdat, Moscow, p 208
21. Potaev GA (2018) Landscape urbanism: new opportunities. Archit Constr 1:22–26

22. Vuga PG, Shelkov YuD (1980) Organization of pedestrian traffic in cities. Higher School, Moscow
23. Vergunov AP (1979) Architectural and landscape organization of pedestrian spaces in the centers of large cities. Problems of big cities. Overview information, vol. 26. Gosinti, Moscow
24. Kalpakova YuA, Logachev YeS, Burilo NA (2021) Creating a comfortable aesthetic and psychological environment for low-mobility groups of the population and maintaining equality between healthy people and people with. In: Bulletin of the Donbass national academy of construction and architecture. Buildings and structures with the use of new materials and technologies. Problems of big cities. Overview information. 2021–2023 (149). DonNACA, Makeyevka, pp 27–31
25. Burilo NA (2021) Sustainable development of coastal territories of large Siberian cities. POTAPOV READINGS. In: Collection of materials of the All-Russian scientific conference dedicated to the memory of doctor of technical sciences. Moscow, pp 30–35

Study of Urban Environment Safety in a Residential Area in Yekaterinburg

E. R. Polyantseva[✉]

Ural State University of Economics, 62, 8 Marta Street, Yekaterinburg 620144, Russia
notneb@ya.ru

Abstract. The work is devoted to the study of the residential urban environment in a separate district of Yekaterinburg. The author explores the existing problems related to the security of the urban environment, analyzes the residential environment and offers methods for solving problems based on the theory of crime prevention through environmental design. The theoretical part of the work is based on the principles of CPTED and defensible space (dividing public and public spaces, access control, surveillance, target hardening) taking into account the Russian conditions (multi-storey buildings, large block sizes). The author examines the problem of urban environment permeability by the example of a neighborhood with unfavorable conditions. The site was found to have unacceptable features—ruined buildings, free access and passage through courtyards, lack of public spaces for meetings of residents, low street lighting, and poor landscaping. Based on the principles of CPTED, a proposal was made for the reconstruction of the neighborhood with typical buildings of the Soviet period.

Keywords: Urban development · Safety · Cpted · Sustainable development · Crime prevention

1 Introduction

Social ecology and urban ecology are closely linked. Eco-friendly materials, planting and landscaping affect safety. The principles of crime prevention and the architectural means that support them change from time by time and from place to place. Architecture is always based on local conditions and, therefore, it is important to treat the urban and natural environment carefully, changing it for the better.

Green spaces and the use of natural forms and means have a positive impact on the safety and ecology of cities, including social ones. However, all these tools should be used in Russian cities taking into account local conditions. The problems of Russian built-up environments are:

- standard designs used throughout the Soviet time not suited to modern safety requirements;
- monotony of the environment;

- modern buildings accommodated without taking local needs into account;
- high level of urbanization and population density;
- abandoned industrial places;
- unrestricted and unlimited access to residential areas and yards;
- sense of neglect and impunity inspired by the urban conditions.

Another problem is the lack of historical analysis of built environment safety in Russian circumstances and lack of crime prevention requirements in Russian architectural legislation [12].

That is why the number of criminal cases provoked by the urban environment is increasing. The most common types of these crimes are theft, assaults, vandalism, etc. Modern social sciences: penology, architecture, urbanism, sociology, criminology were combined into crime prevention theory (CPTED) that evolved to prevent these crimes. The CPTED principles include first and foremost target hardening, access control, territoriality, surveillance, and maintenance.

The second generation of the theory involved the development of basic assumptions and social measures. The intention was to adopt legal activities to decrease criminal behaviour and illegal activities in localities [3]. Early attempts to deter crime though target hardening were not as successful as expected. Fortress design suppresses and increases fear in ordinary people but does not always stop criminals. The current position is that architects and urban planners should reinforce desirable behaviours rather than punishing undesirable ones [9].

2 Theoretical Basis

According to the crime prevention theory as it stands now, the revitalization of every urban area must arise from local conditions. Crime prevention design is focused on physical factors outside the crime location. Modern methods include big data analysis that helps to reveal the influences between the adjacent areas and the selected one. This approach is called geographical juxtaposition. Crime factors operate in areas from those proximal to the crime location to ones physically most distant to the crime location [7].

Some investigations have revealed that areas with residential and commercial uses exhibit lower crime rates than commercial ones. Purely residential areas are safer than mixed use ones. Where residential forms are added to an area, crime rates are lower than in places that have not been changed. Investigators have found some land-use types that attract crime within short distances while others deter crime. They conclude that the functions and contexts of some facilities generate crime. Also, a lesser percentage of crime attractors generate most of the crime risks. These attractors usually can be described as abandoned and neglected buildings; other typical crime attractors are alcohol shops, closed convenience stores, and industrial facilities and warehouses. Commonly, all of them are excluded from residential areas and multi-family houses; if not, the residential area acts as a positive factor [6, 7].

Another study suggests that there are three levels of residential area liveability: basic, moderate and advanced level of neighbourhoods. While the basic level is associated with bare minimum services, poor infrastructure and high level of fear and crime in

the community, the advanced level embodies integration of safety and sustainability. Authors show that a gated community is the most universal answer to the problems of crime and fear: gates do not make a significant difference in the increase or decrease of crime or deterrence to criminals. In advanced level neighbourhoods, aesthetics and urban forms play a major role. They contain some features that preserve the history of the place and support legitimate activities [10].

Criminology researchers believe that crime is driven by the environment, and the crime scene contributes to the formation of crime patterns. Here, the ways in which criminals move and whether they have a choice become important [4]. The presence of a choice of path from a variety of options positively correlates with the safety of the area. Connectivity (the number of roads, pedestrian paths, and transport routes) is significantly and negatively related to the projected number of crimes, so that an increase in connectivity was associated with a decrease in crime [15]. The criminal's opinion about the convenience/inconvenience of the territory for committing a crime is important: the limited space, its openness or closeness to special or social control; the distance to security objects (police strongholds, photo and video recording systems, etc.) or objects with appropriate security markers (the presence of special signs about ongoing surveillance, the presence of security systems, etc.). The criminal evaluates the possibilities (impossibility) of merging with the environment, because his presence in this place should not attract attention or arouse suspicion. Of importance is the degree of traffic to the territory, the ability to move on it (methods, number of directions, ease of use of transport), and the ability to easily conceal the crime. It is also important to establish the victim's perception of the territory as dangerous or safe [13]. It becomes essential to analyse crime data and map it. This technology allows one to identify hotbeds of crime and dangerous places that need to be reconstructed [1, 2, 5, 8, 11, 14, 16–20]. Police stations are best placed near such potentially dangerous locations. They should be included in the police patrol routes. In other cases, police posts should be located near the center of the urban area for the best possible accessibility. Visibility and transparency are another important factor that affects the orientation of people inside the urban environment and inside buildings, and improves surveillance [1, 11, 18]. Surveys show that it is necessary to inform specialists in the field of urban planning and the police about environmental criminology and the principles of this theory [17].

3   Problems of Russian Cities and Ways to Solve Them

What needs to be done to protect Russian residential places and make them safer, sustainable and well maintained? The answer is in applying natural elements that can be used as both security and ecology measures. All crime prevention measures can be divided into organisational (social), mechanical, and natural. The latter help to save energy that is used for CCTV and alarms and should be widely used in the design process. Natural measures are not only renewable and local materials but materials that give a possibility not to use expensive mechanical control measures. Planning and design should take security into account as early as possible, so that walls and landscaping, rather than fences and mechanical barriers could be used to protect against vandalism and theft.

The greatest effect will be provided by considering examples from modern design practice in the Scandinavian countries that have a similar climate (Sweden, Norway,

Denmark) and in Asian countries that have a similar level of urbanization (China, South Korea). The general point is that all the examples show linkage between the image of the territory and the reduction of crime, while the recommendations relate to improving lighting, surveillance and control in the residential area [8]. Residential areas may not necessarily have a fence on their borders. A natural boundary can be a difference in terrain, landscaping, water boundary and building form.

There are some forms of access control provided by natural measures:

- water boundary;
- forming closed or semi-closed private zones of residential courtyards with building forms;
- forming closed or semi-closed private zones of residential courtyards with landscaping and green walls;
- forming a residential courtyard with artificial relief terrain;
- mix of different measures.

Researchers suggest that it is important to create a system of restrictions in the urban environment, protecting residential areas, and the main goal is the humanization of Russian urban spaces [20].

In South Korea, urban spaces are similar to Russian multi-storey residential areas. In the first study, crime prevention measures, such as maintenance and surveillance, were implemented by paving marked safe roads for woman, arranging public places for meetings, memory fences and signs, etc. The second study includes visual crime-preventive elements such as LED streetlamps for pedestrians, floor patterns and various sculptures. The principles of CPTED – surveillance, reinforcement of activity, maintenance, and reinforcement of territoriality – were applied to problem areas and led to a reduction in the number of crimes [19].

Studies have shown that changing the use of the urban environment reduces crime because the usual patterns of behavior in this environment are destroyed, and criminals cannot behave in the usual way [2]. But the choice of specific means is left to the specialist, since they must proceed from the characteristics of the place when reconstructing the urban environment. A potential target must be identified, offenders must be deflected and property boundaries identified [5].

A separate problem is pedestrian traffic through the courtyards of residential buildings, which turns them from a semi-private space into a public one. Public spaces are less controlled, and residents will be more interested in protecting them if they understand the area for which they are responsible [14].

4   The Study of the Current Built Environment in the District

The development of the site as a whole is homogeneous and belongs to the 1970–80s: these are five-and nine-story buildings, two schools and six kindergartens, constructed according to standard designs. Most of these buildings are in good or satisfactory condition (Fig. 1).
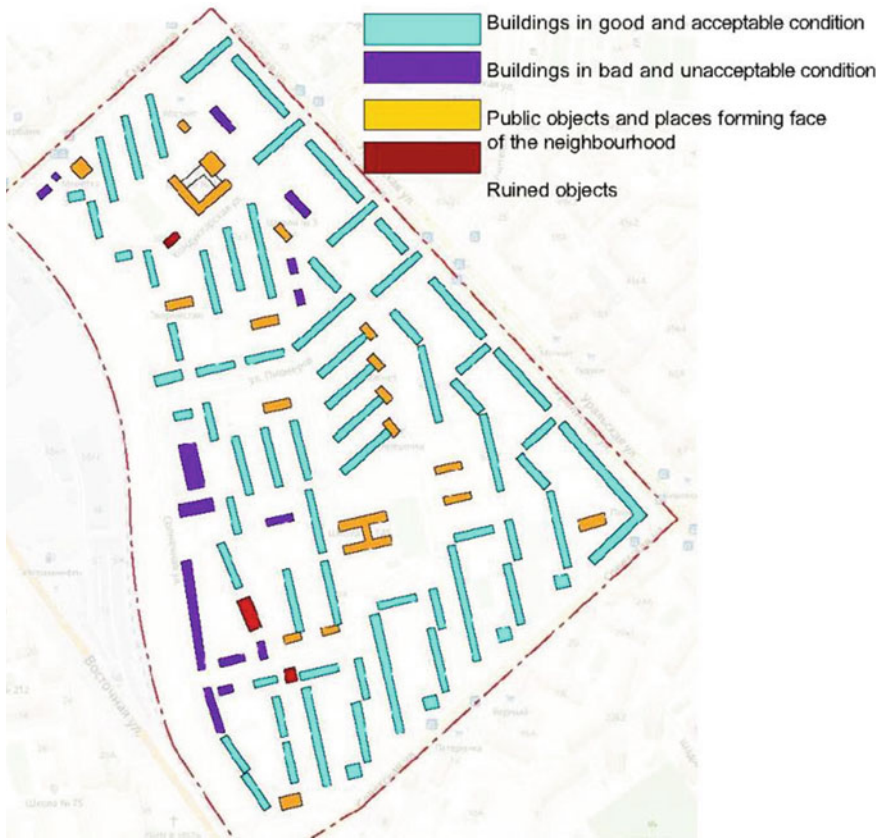
Fig. 1 Analysis of the built environment in the area between Sovetskaya and Uralskaya streets

The disadvantage of the residential yards is the proximity of a marginalized territory along the railway tracks. The bad reputation of the places leads to an outflow of better-off residents, whose apartments are occupied by less well-off people; in the end, this is reflected in the appearance of buildings and the living environment itself. Thus, the railway as a border attracts desolation, and this area along the south-western border of the district needs special attention. Another problem with this street, which runs parallel to the railway tracks, is that it cannot be identified as a street. The lack of a well-maintained sidewalk, lighting at night, overgrown bushes and trees, lack of development, fences of closed businesses—all these worsen the situation and make this area unsuitable for pedestrians who consider it dangerous. The preferred use of the vacant land in this place would be parking lots. The residential buildings face the street, so it has no face of its own. This environment was developed in keeping with the spirit of the time, the "principles of new architecture" of LeCorbusier, but time has shown that sparse buildings make the street greener but not safer. The yards are almost all passageways (Fig. 2). They are quite large, and if there are no well-maintained sites, they become a decadent territory. As for the image of the street, it is possible that the "gaps" between

the ends could be compensated by one- or two-story inserts or landscaping and fencing, decorative/symbolic. The positive quality of the Soviet building is its closeness to the human scale, a small number of floors, and large landscaped courtyards. All this, taking into account the possible reorganization of the internal structure of the neighborhood, could make it more comfortable and safe for residents.

Fig. 2 Analysis of the ways of movement in the district between Sovetskaya and Uralskaya streets

An analysis of the road transport network indicates that visitors to the block and delivery services may have difficulty navigating and moving around it. Internal passage-ways are devoid of signs and other means of orientation. They do not have such street attributes as a dedicated sidewalk, landscaping, lighting, and building facades often face them. The large size entails a problem of transport accessibility. Many streets and pas-sageways end in dead ends. Pedestrian accessibility is provided by the permeability of residential courtyards. Pedestrian paths also need dedicated sidewalks and lighting. The pedestrian network is quite well developed, but it is worth remembering that the courtyard driveways along the five-story buildings do not have dedicated sidewalks for pedestrians, and therefore are potentially dangerous places (Fig. 3).

Fig. 3 The pedestrian paths look unkept, the street view is ruined by overgrown trees

5 A Proposal for Possible Reconstruction

The goal of the article was to determine the role of crime prevention principles in the sustainability of urban spaces, which, as discussed, consists in the use of specific architectural features that help support the human scale of urban spaces. These architectural features are sustainable anti-vandal materials like stone, timber, and gardening and landscaping. Working with criminalized urban spaces includes an analysis of local environment characteristics and history of the place. The next step is to determine the vulnerabilities of the place and the most common types of crime. And the third one is to select the necessary protective measures and materials.

Natural measures provide a high level of humanity and sustainability. According to Russian circumstances, it means that foreign practices should be adapted to local conditions. Careful treatment does not mean complete preservation of the city's monotonous environment; rather, it involves gradual transformation in accordance with the above levels of protection. Reconstruction of Russian cities should not mean a complete replacement of the old buildings by multi-storey apartments without preserving historical memory and genius loci.

The transformation of a residential area's architectural forms is an important stage in creating a safe urban environment. Another important stage is to work with abandoned industrial zones. Warehouses and factories should be revitalized if they are not in use. Both stages should be implemented keeping in mind the creation of a spatial hierarchy of urban spaces, and a hierarchy of access levels, from public to private (Fig. 4).

Sustainable and green urban places give an opportunity of crime reduction and surveillance. These planning features help to avoid the feeling of abandonness and lack of surveillance. Urban areas structured by level of access and anti-vandal renewable materials can solve the problem of unlawful behaviour and vandalism. Crime prevention is promoted by advances in cognitive, behavioural and environmental sciences, such as sustainability, social information processing, research into how people perceive their environment and their satisfaction with it, and advances in neurological and cognitive sciences.

Fig. 4 Proposal for the organization of courtyards and public areas between Sovetskaya and Uralskaya streets

6 Conclusion

Firstly, security needs were met by means of target hardening and other rough methods that deter criminal attacks, but now more and more soft and natural methods are being used. Sustainable development theory says that modern cities are places intended to merge nature and culture. That is why natural methods are becoming more relevant. Green spaces, landscaping, lighting, and natural materials are becoming important tools in architecture and design.

It has been shown that the use of natural environments and materials help mitigate the negative impact of the urban environment and reduce the impact of crime and fear of crime. Russian cities need close attention and a change in the approach to ensuring their security. They can be implemented in architectural practice, as well as the use of protective materials.

Sustainable development demands advances in cognitive, behavioural and environmental sciences, combining data analysis and development of digital methods with natural elements in architecture. Landscaping and green spaces can make cities more human and reduce the fear of crime.

References

1. Adani W, Adianto J et al (2020) Analysing implications of visibility for crime occurrence in low income vertical rental-housing complex. J Fac Archit 17(3):79–88. https://doi.org/10.5505/itujfa.2020.89266
2. Anderson J (2013) Reducing crime by shaping the built environment with zoning: an empirical study of Los Angeles. Univ Pennsylvania Law Rev 699–756
3. Atlas RI (2008) 21st century security and CPTED: designing for critical infrastructure protection and crime prevention. CRC Press, Taylor and Francis Group, Los Angeles, p 279–306. http://zonebook.me/go/read.php?id=1420068075
4. Brantingham P (2017) Environment, routine, and situation: toward a pattern theory of crime: advances in criminological theory. In: Routine activity and rational choice, p 259–294. https://doi.org/10.4324/9781315128788-12
5. Clarke RV (1992) Situational crime prevention: successful case studies. Albany. NY, Harrow and Heston
6. Cozens P, Love T (2015) A review and current status of crime prevention through environmental design (CPTED). J Plann Lit I-20:8–9. https://doi.org/10.1177/0885412215595440
7. Cozens P, Love T (2019) Geographical Juxtaposition: a new direction in CPTED. Soc Sci 8:252. https://doi.org/10.3390/socsci8090252
8. Ha T, Oh G (2014) Comparative analysis of defensible space in CPTED housing and non-CPTED. Int J Law Crime Justice 43(4). https://www.researchgate.net/publication/270053319_Comparative_analysis_of_Defensible_Space_in_CPTED_housing_and_non-CPTED_housing
9. Jeffery C (2000) ICA Newsl 3:1–2
10. Mihinjac M, Saville G (2019) Third-generation crime prevention through environmental design (CPTED). Soc Sci 8:182
11. Othman F (2019) Identifying risky space in neighbourhood: an analysis of the criminogenic spatio-temporal and visibility on layout design. Environ-Behav Proc J 4(12):249–257. https://doi.org/10.21834/e-bpj.v4i12.1908
12. Pirozhkova I (2020) Koncept sredovoj bezopasnosti: kategorial'nyj apparat i sovremennoe sostoyanie (Environmental safety concept: categorical apparatus and current state). Gos Prav Issl 3:333–337
13. Radosteva Y (2021) Zhertva i prostranstvo (Victim and Space). Pravoporyadok: Istoriya Teoriya Praktika 1(28):90–93.
14. Reynald D, Elffers H (2009) The future of Newman's defensible space theory. Eur J Criminol 6(1):25–46. 1477-3708. https://doi.org/10.1177/1477370808098103
15. Summers L, Johnson J (2017) Does the configuration of the street network influence where outdoor serious violence takes place? Using space syntax to test crime pattern theory. J Quant Criminol 33(2). https://doi.org/10.1007/s10940-016-9306-9
16. Tang Y, Zhy X et al (2017) Non-homogeneous diffusion of residential crime in urban China. Sustainability 9(6):934. https://doi.org/10.3390/su9060934
17. Wartell J, Gallagher K (2012) Translating environmental criminology theory into crime analysis practice. Policing 6(4):377. https://doi.org/10.1093/police/pas020
18. Worthley R, Mazerolle L (2009) Environmental criminology and crime analysis: situating the theory, analytic approach and application. In: Wortley R, Mazerolle L (eds) Environmental criminology and crime analysis. Willian, Cullompton, UK

19. Yongwook J, Dahee K (2019) Crime prevention effect of the second generation crime prevention through environmental design project in South Korea: an analysis. Soc Sci 8:187
20. Yankovskaya Y, Merenkov A (2015) Formirovanie sistemy ogranichenij v sovremennoj gorodskoj srede (Formation of a system of restrictions in the modern urban environment). NIONC, 2

Identifying the Mismatch Between Land-Use and Transport Development in Russian Cities

E. Saveleva^(✉)

Perm National Research Polytechnic University, 29, Komsomolskiy Prospekt, Perm 614990, Russia
e.saveleva@pstu.ru

Abstract. The idea of sustainable urban mobility is slowly making its way in Russian cities, which is reflected in most recent strategic documents at the national and sometimes local level. The need to coordinate transport and land-use policies in order to reach a more sustainable mobility model is also increasingly recognised in both scientific and professional communities. The most progressive Russian cities now try to incorporate the principles of integrated transport and land use in their development plans. Yet these, still rare, efforts are often undermined by the deficient and limited plan implementation. The paper reviews the normative base for integrating transport and land-use planning as well as the experience of Russian cities in this direction pointing out the gap between theory and practice. It gives a closer look at the case of Perm, one of Russia's million-plus cities, and its (not entirely successful) attempt to introduce the integrated approach to land-use and mobility in the development strategy. The paper thus aims to raise the issue of land-use planning being largely carried out in isolation with transport planning in Russian cities, proposing some recommendations for overcoming the identified mismatch between the development of these two domains.

Keywords: Transport planning · Russian cities · General plan

1 Introduction

It has been several decades now since the economic and environmental implications of traffic congestion have been first linked to the lack of coordination between land-use and transportation planning both by researchers and planning practitioners [1]. Globally, there is a prevailing understanding of the need to integrate transport and land-use planning in order to reach more sustainable, that is economically successful and environmentally sound, solutions.

The bi-directional link between mobility and spatial development has long been analysed and confirmed by various studies [2–4]. The idea of sustainability in urban travel has brought about the shift from the preoccupation with raising the speed of movement to enhance the accessibility of places. The latter is secured not only by the improvements of transportation network but also via increasing the proximity between locations reached

with the help of compactness and functional diversity. Compact urban structures can help shorten travel distances, thus lowering emissions and fuel consumption, while at the same time promoting non-motorised modes of transport [5].

Thus, the change in urban spatial structure towards more compact, dense and mixed-use development is an essential element in the effective implementation of the strategy targeted at reaching a more sustainable mobility model. This is especially important for Russian cities with their extended and fragmented urban structure, where the established spatial organisation already creates additional barriers to sustainable and efficient mobility (all the deficiencies of the post-Soviet urban structure were analysed amply in Ref. [6]). Overcoming Soviet period legacies in urban spatial structure (peripheral clusters of high density, unreasonably stretched urbanised areas, high degree of monocentricity and underdeveloped transport network) may become a tough and time-consuming task for local authorities but an enhanced focus on integrated urban planning and land-use policies is required to ensure that cities are developed to encourage environmentally sustainable mobility patterns.

Given the proven mutual influence between mobility and urban structure it is essential to coordinate transport and land-use strategies, as confirmed by the European cities' experience [7, 8]. Some of the progressive city-planners and policy makers in Russian cities are also aware of the positive effects of transport and land use integration and try to incorporate these principles into planning documents. Yet moving from rhetoric to reality is not easy and most cities continue to replicate the same development patterns generating a growing mismatch between travel demand and transport services. This paper discusses the issues that Russian cities now face, stemming from the inability to harmonise their transport and spatial development. It gives a closer look at the case of Perm, one of Russia's million-plus cities, and its attempt to introduce the integrated approach to land-use and mobility in the development strategy.

2 (Dis)integration Between Spatial and Transport Development in Russian Cities

2.1 Theory

The project of the Transport Strategy of the Russian Federation until 2035 for the first time formulates the primary aim as "territorial connectivity" instead of "population mobility" (as it was in the previous strategy of 2013) and prioritizes public transport, even considering the possibility of making it free of charge. It signals that the need to move towards more sustainable mobility has been recognized at the national level in Russia. Yet the Strategy, developed by the transport experts, ignores the interconnection between the models of urban mobility and spatial development of the city as well as the potential of the effective alignment between transport and land-use planning.

The document that is to provide the base for linking transport and land-use development in Russia is the main national regulation in the field of urban planning—SP 42.13330.2016 "Urban development. Urban and rural planning and development" [9]. It requires, inter alia, to ensure "the balanced development of the territory and transport network" and "design of the network in conjunction with the urban structure of the city

and the territory adjacent to it, providing convenient, quick and safe transport links with all the functional areas, with other settlements of the settlement system, objects located in the suburban zone, and wider road network" [10]. Yet this document, although updated, is still methodologically similar to its predecessors of the Soviet period, when the single town planning code determined everything "necessary and sufficient", being a mixture of provisions with various legal status: from strict requirements to recommendations. Used largely out of inertia, the SP remains too broad and lacks direct requirement or guidance on developing integrated planning strategies.

At the local level the direction of the spatial development of a city is defined by its General plan establishing zones for different types of development and uses. The General Plan necessarily contains a section dedicated to transport. It is in this planning document, where urban planning and transport policies are first of all to be integrated ensuring a decent level of accessibility for existing and prospective areas. Yet the decisions General plans contain are often based on outdated information or simply transferred from the earlier plans, sometimes dated to the Soviet period. In addition, the planning horizon is very long, usually up to twenty years, most of the information in the plans is rarely updated and the amendments made are mostly confined to the functional zoning map.

Some of the leading cities do have well executed general plans declaring the principles of mutual integration of land use and transport. Yet the implementation of these principles is somewhat limited. Despite the overall turn towards more sustainable mobility that occurred in some cities, the measures performed are mostly confined to improvements to transport network and traffic management. The next section of the paper reviews the experience of Russia's leading cities in the field of transport planning assessing the level of integration of transport and spatial development.

2.2 Practice

One of the most contradictory examples of land-use and transport development is presented by the Russian capital city Moscow. The 2010 General Plan was put aside soon after it was enacted due to the change of Moscow's mayor. Urban development planning has essentially been in 'manual mode' with every project considered individually by the special commission up until 2017, when the new zoning law was approved. The zoning law, being put together without any strategic document to lean on, set its own goals including the large-scale development of transport hubs [11, 12]. This focus on public transport development was marked even earlier with the 2011 Transport strategy that was said to be developed in compliance with the latest trends in the field of transport planning [13]. The strategy included such measures as construction of new metro lines coupled with the major infrastructure project of the Moscow Central Circle, implementation of the intermodal ticket and tariff solutions, the introduction of paid parking, etc. The introduction of the Moscow Central Circle, the modernised route making use of the existing rail facilities, was supposed, inter alia, to give an impetus to the development of the adjacent brownfield sites. Yet the subsequent study of the projects' impact showed only modest effects on the rent growth and the land-use change as well as an insignificant decline in load level of Metro Circle line and radial lines in the city centre [14].

Along with the efforts to reform the transport system according to the best world practices, in 2012 Moscow made a step which caused bewilderment among the majority

of foreign, as well as local, experts [15, 16]. As a result of the administrative borders' expansion, the area of the city increased by about 2.4 times. Despite the fact that the 2017 General plan of 'New Moscow' was based on the principle of 'balanced development of the territory' [17], in practice these new territories became the site for another manifestation of the early capitalist approach, when the most profitable piece of the market—housing—was taken by the developers without provision of proper transport and social infrastructure. While employing the state-of-the-art practise in the field of transport planning, Moscow authorities pursue inconsistent and controversial spatial development policies that could simply undermine all the efforts.

Kazan, the capital of the Tatarstan republic, is another Russia's high achiever in the modernisation of the transport system. Encouraging more sustainable mobility patterns in Kazan is based on two components: stimulating the use of public transport (priority lanes, integrated ticketing system, the development of electric land transport and so on) and discouraging travel by personal transport (paid parking). In terms of the transport network the General plan of Kazan, based on the assumption of significant population growth, proposes the development of transport infrastructure that outpaces the spatial development. Particular attention is paid to undeveloped areas remote from the centre, which is to be provided with engineering and transport infrastructure in a priority manner [18]. The decisions, incorporated in the Kazan General plan appear to be quite reasonable and coordinated in terms of land use and transport (provided that the projected growth occurs in reality) but their effectiveness is largely dependent on proper implementation including due timing, resource allocation and adherence to all the plan's aspects.

The more so that there are already numerous sensible proposals and documents executed in according with the latest concepts in transport and land-use planning that remain only on paper, like happened in the case of the 2015 Complex Transport Scheme of Nizhniy Novgorod [19] or in the case of Perm General plan, which is reviewed below. Most major Russian cities try to implement certain measures for improving the transport situation with varying degrees of success: most of them made some steps in the field of traffic management, like dedicated lanes for public transport, or restricted their parking policy. Nevertheless, these steps are usually uncoordinated and bring only local relief, doing little to improve the situation in the city as a whole. Likewise, there is no proper coordination among various authorities and the link between transport and land-use policies is particularly weak [20].

Many cities also have some kind of transport model for the forecast of the transport demand. All these models, however, only include the data on the transport infrastructure and public transport routes, disregard the effects of land use and enable a purely traffic engineering approach measuring street capacity, road congestion, the efficiency of the route network, etc. They facilitate developing strategies that take current or proposed land-use patterns as a given ignoring the reverse influence that transport interventions may have on spatial development.

Despite the existence of some positive examples, transport and land-use planning in most Russian cities tend to function as separate worlds. These two domains of city development have their own institutions, disciplinary and cultural backgrounds, planning procedures and concepts. It leads to the many inconsistencies between the development of land use and the transport system, which are discussed in the next section.

2.3 Discrepancies Between the Development of the Land-Use and the Transport System

One striking example of transport interventions being out of tune with the spatial development is the introduction of underground metro systems in some of the largest cities, which dates back to the Soviet period but still remains an aspiration for all the major cities of Russia. While in Moscow and St. Petersburg, the underground metro covers most of the cities' territories and functions as the main transport mode supported by other means, in other cities (Samara, Kazan, Yekaterinburg, Nizhny Novgorod and to a lesser degree Novosibirsk) this kind of transit is far from being dominant transport mode. Instead of being the 'backbone' of the public transport system providing the main intercity transportation and tying the whole city together, most of the Russian cities' metros are only one of the many types of transport. Moreover, the metros are typically poorly integrated with the rest of the transport system and now carry only a small share in the total passenger flow of the cities. The efficiency of the metro systems is often undermined by their ill-thought location. For instance, in Samara the only metro line does not cover the most densely populated areas of the city and some stations are hidden somewhere in the quiet streets. As a result, the Samara underground may be considered as the most inefficient metro system in Russia with operating costs exceeding the revenues 3.3 times [21].

There are also numerous examples of the opposite situation when high-density urban development is occurring at locations, which offer poor accessibility by public transport and is not supported by appropriate infrastructure development. With the widespread replication of the Soviet development model extensive high-density housing at the outskirts of the cities now creates high transportation demand in places where it cannot be met by any mode other than the private car. One such development is the new neighbourhood in the Rusanovka district of St Petersburg, pictured in Fig. 1. It is a recent high-density residential development at the edge of St Petersburg, which is connected with the city's street network via the only street. Other links are formed by the confusing system of narrow inner driveways in the tradition of Soviet microrayons' peculiar layouts. The neighbourhood is served only by minibuses with the terminal station located at the neighbourhood's entrance.

Fig. 1 Example of high-density residential development with inadequate transport provision [22]

3   The Case Study of Perm

3.1   Justification of the Case Selection

As already seen, even if the integration of land-use and transport decisions appears as a goal of urban planning and territorial management, it is relatively little implemented in practice. This section analyses the changes in the spatial and transport development of Perm 10 years after the approval of its General plan [23]. The General plan of Perm was based on the Strategic masterplan developed by the group of international experts led by the Dutch company KCAP and became the first planning document in Russia that was fundamentally different from typical general plans in its vision and priorities.

As stated in the 2010 General plan of Perm, the transport system was considered by the authors together with the spatial organization of the city as being in close interaction with all the components of the urban system. After all the sections of the plan were scrutinised, it appears that planning for the development of transport infrastructure facilities was indeed carried out in accordance with the strategy of the spatial organization of the city. The 2010 Plan withdrew the previous direction of extensive territorial development and corresponding infrastructure upbuilding, typical of the previous general plans and other earlier planning documents of Perm.

The transport section of the 2004 General Plan, for instance, intended to increase the volume of transport infrastructure by about one and a half times. The main direction of development was the expansion of the main road network of the city and the network of public transport, taking into account the need to strengthen transport links for the territories of the existing development and ensure the development of new territories outlined in the General Plan. Transport planning was aimed at adapting urban infrastructure to the needs of growing motorization, at the increase in transport mobility and at the improvement in the passenger transportation system.

The decisions laid out in the 2010 General Plan became a major retreat from the previous practice. The transport sections distinguished two types of intervention. Although having conventional transport planning measures as its part, the transport strategy prioritized interventions are urban structure to promote a mobility model that meets the needs of public transport and other sustainable means of transportation. These interventions included an increase in the building density in and around the centre, promoting the role of secondary urban centres, stimulation of mixed development. Thus, for its time and geographical setting, the Perm General plan was a revolutionary document based on the principles of sustainable mobility and proper integration between land use and transport. This section aims to analyse to what degree the principles of the Plan were implemented in practice.

3.2   Methodology

The study includes analysis of such components of city development, as building density growth, population density growth and changes in urban street network expressed via the share of land allocated to streets (LAS).The main objective envisaged by this research—examining the mutual development of street network and urban structure of Perm—is accomplished by using the GIS tools. The changes of network and densities' distribution

have been analysed based on the General plan and Open Street Map dataset. Modelling of the population density distribution was performed with the help of the database of the State Corporation "Fund for assistance to reforming housing and communal services" [24].

The analysis was performed across 8 different types of residential districts identified in the General plan. The types of residential districts for analysis and their description are summarised in Table 1.

Table 1 Types of residential districts for analysis

Type	Description
STN A	The central zone, most of it is reserved for high-density public and business development
STN B	A zone adjacent to the centre, which combines a high proportion of residential and public business areas
STN C	The territory near the central zone, the structure of the territories continues the logic of a decrease in the share of public and business territory and an increase in the share of residential buildings
STN D	The residential zone around the centre, the dominance of high-rise residential buildings
STN E	A multi-storey residential development remote from the centre with weak maintenance functions
STN F	Peripheral city centres, the most diversified zones cities that combine the entire set of functions
STN G	Low-density peripheral residential areas, including service areas; low-density residential buildings prevail, there are public and business zones
STN H	Residential areas on the outskirts of the city, dominated by low-rise residential buildings

3.3 Analysis of the General Plan Implementation

Comparative analysis of the forecasted values of population and building densities with calculated values of corresponding indicators showed that actual population growth almost closely corresponds to the forecasted one while the building density increase that occurred in reality significantly lags behind the planned values. The difference between the prognosed and actual values is illustrated in the diagrams in Fig. 2. The distribution of the building and population densities across the districts should have become the result of a consistent policy of the city authorities aimed at stimulating the reconstruction of the built-up areas of the central part of the city and avoiding the development of additional green-field sites. The results indicate that the actual spatial development of Perm did not follow the scenario proposed in the General Plan.
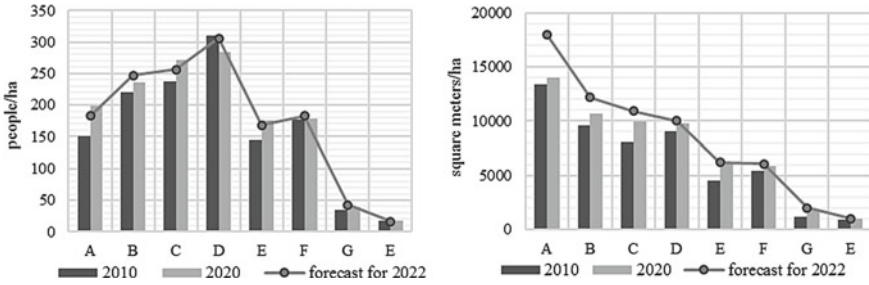
Fig. 2 Population densities (left) and building densities (right) in different years across different types of residential districts

At the same time the performed analysis did not reveal a substantial change in the share of land allocated to the street network (LAS) since 2010. Figure 3 shows a bar chart of street network distribution across the districts combined with the graphs of actual building densities in the years 2010 and 2021 as well as forecasted building densities for the year 2022 and for the distant future (according to the General plan target indicators).
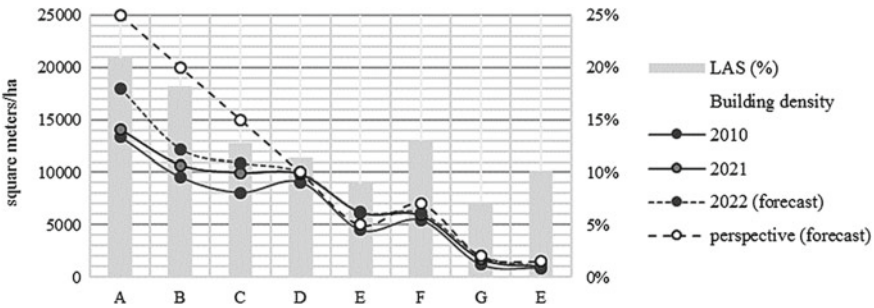
Fig. 3 Relation between the share of land allocated to streets (LAS) and the building density in different years across different types of residential districts

At the time of the plan development, the main transport issues included, apart from the congestion on some parts of the network, insufficient transport provision of certain areas of the city with a high population density. The central part of the city, formed by the district types "A" and "B", as well as by the territories of the middle zone (district type "C") were recognised as areas with high transport accessibility. The unsatisfactory level of communication with the city centre was revealed in the districts "D" and "E". According to the GIS modelling results, the planned level of building density in the central part of the city best equipped with infrastructure was not achieved, while the values of density in districts "D" and "E" exceeded the predicted values. If the level of densities corresponded to the ones set by the plan, the distribution of the network density would become more balanced.

Furthermore, in the light of the current government policy for urban development this discrepancy is likely to intensify. In an effort to balance the provision of social infrastructure, the local authorities have restricted the development in the city core. The

introduced amendments to the zoning law imply height and density limits for residential development: 4 to 10 floors in the central parts, 4 to 8 floors in other parts and various density coefficients ranging from 0.3 to 2.5 (the ratio of the building area to the plot area). Developers will be able to bypass the new restrictions upon the agreement with the municipality to provide residents with social facilities. Depending on the volume of the deficit of places in schools and kindergartens within the territory, the developer will have to build these or replenish the city budget with a certain contribution per square meter in excess of what is permitted by the zoning law. So, the density of development in Perm is now regulated mostly for reasons of the provision of social infrastructure. Such a policy, regretfully, may lead to the active development of high-density residential buildings outside of the city's core.

The analysis also made it possible to identify foci of an anomalous increase in building density and population density, while not being supported by the corresponding increase in the density of the road network. The examples include the residential development Griboedovskiy—several towers at the edge of the built-up area not properly served by public transport—or the recent residential development Krasnye Kazarmy designed ignoring the local context including the network of streets: its internal streets are not connected with primary streets or adjacent network having only one exit from the whole neighbourhood.

Thus, in the case of Perm the efforts to integrate spatial and transport development of the city were undermined by the plan's inappropriate implementation. Local authorities' inability to adhere to the original spatial development strategies laid down in the plan led to the growing mismatch of the transport provision across the city's districts with the densities in these districts that is with the amount of the transport system potential users.

4 Conclusion

The importance of linking land use and urban form to mobility is increasingly recognized in Russian cities. This induces the need for a holistic and integrated approach to urban policy considering the relationship between urban structure and travel and emphasizes the need to integrate transport and land-use planning. To ensure the success of the sustainable mobility policies, they should be supported by creating urban forms that are highly conducive to public transport ridership and/or non-motorised travel. Even if the major Russian cities are to introduce some kind of modern high-speed transit (much needed in many of them), the efficient performance of public transport system is only guaranteed subject to the consistent government's efforts to form an appropriate settlement pattern that includes directing of all urban growth along the routes.

Unfortunately, local authorities often lack the resources and institutional capacity necessary to coordinate land-use and transport development so that they generate a more effective mobility model. Institutional fragmentation present in Russian cities does not allow bringing land-use and transport policies into a harmonious or efficient relationship. The fact that municipalities do not control all aspects of urban transport makes it difficult for cities to prepare and, especially, implement long-term integrated strategies. The harmonization of transport and land use may take decades before one can see any

results. One major problem that is present in all the Russian cities is the lack of political continuity. The experience of the leading world cities shows that sustained political commitment to the once accepted vision, supported by like-minded leaders who built on the work of their predecessors, is an important pre-requisite of successful implementation of any plan aimed at the change in the current course of development towards more sustainable and effective mobility model.

Below are the recommendations for overcoming the mismatch between transport and land-use development in Russian cities. At the national level government should develop some sort of guidance stating their aspiration towards integrated planning. The new Transport strategy has become an important step away from a car-centred approach that dominated until recently but does not even touch upon the issues of integrating transport planning with land use. At the local level authorities can stimulate developing urban form conductive of forming the desirable travel patterns. Planning policies reflected in General Plans of cities can influence the scale of urban compactness and land-use mixing. In line with the strategic aims set by the General plans local authorities should maintain the desired densities, support infill development through infrastructure provision and reduce infrastructure support for development outside preferred areas. Other measures include the already ubiquitous traffic management, enhanced public transport provision and so on. In many cases these individual initiatives can be synergistic, strengthening each other through joint implementation. As regards the planning process, projects may be more effective and can be delivered more quickly when experts are brought together in multidisciplinary project teams. To avoid the failures in the plan's implementation it is important to ensure constant monitoring of its target indicators, which would ideally be carried out by the special interdepartmental administrative body combining the functions of different relevant authorities including those in charge of land-use and transport development.

Thus, the main contribution this paper aimed to make was to increase the awareness of the need for the integration of land use and transport to be properly performed at different stages and different levels of urban development planning. Only the adoption of the integrated approach to land use and mobility in planning documents and its implementation in day to day planning practice may determine spatial development trends that facilitate forming more sustainable mobility patterns in Russian cities.

References

1. Banister D (1999) Planning more to travel less: land use and transport. Town Plann Rev 313–338
2. Newman PG, Kenworthy JR (1989) Gasoline consumption and cities: a comparison of US cities with a global survey. J Am Plann Assoc 55(1):24–37
3. Ewing R, Cervero R (2001) Travel and the built environment: a synthesis. Transp Res Rec 1780(1):87–114
4. Ewing R, Cervero R (2010) Travel and the built environment: a meta-analysis. J Am Plann Assoc 76(3):265–294
5. Rode P, Floater G, Thomopoulos N et al (2017) Accessibility in cities: transport and urban form. In: Meyer G, Shaheen S (eds) Disrupting mobility. Springer, Cham, pp 239–273

6. Saveleva E (2019) The Soviet legacy in the urban morphology of major Russian cities. In: Urban form and social context: from traditions to newest demands: Proceedings of the XXV ISUF International Conference, p 259–272
7. Geerlings H, Stead D (2003) The integration of land use planning, transport and environment in European policy and research. Transp Policy 10(3):187–196
8. Bertolini L, Le Clercq F, Kapoen L (2005) Sustainable accessibility: a conceptual framework to integrate transport and land use plan-making. Two test-applications in the Netherlands and a reflection on the way forward. Transp Policy 12(3):207–220
9. UNECE (2020) Handbook on sustainable urban mobility and spatial planning. https://unece.org/transport/publications/handbook-sustainable-urban-mobility-and-spatial-planning. Accessed 25 May 2021
10. Minregion Rossii (2016) SP 42.13330.2016. Urban development. Urban and rural planning and development. Moscow
11. Nabatnikova O (2017) Obnovleniye genplana Moskvy stanet aktual'nym voprosom posle 2020 goda (Updating the general plan of Moscow will become relevant after 2020). In: Nedvizhimost' RIA Novosti. https://realty.ria.ru/20170227/408381689.html. Accessed 21 May 2021
12. Lyauv B (2016) Moskovskie Vlasti Ne Budut Menyat' Genplan Luzhkovan (Moscow Authorities are Not Going to Change Luzhkov's Genplan). Vedomosti. https://www.vedomosti.ru/realty/articles/2016/11/21/666213-moskovskie-menyat-genplan. Accessed 21 May 2021
13. Liskutov M (2015) Development priorities of urban transport system in Moscow agglomeration. International Transport Expert Council 2015. http://transport.mos.ru/common/upload/docs/1445948334_Liksutov.pptx. Accessed 25 May 2021
14. Kotov E, Muleev E, Koncheva E et al (2019) The effects of introduction of the Moscow Central Circle rail passenger service: transport, urban, economic and travel behaviour consequences. In: Towards human scale cities—open and happy. 15th biennial NECTAR conference, 5–7 June 2019. Helsinki, p 23
15. Pogorelova Y (2012) Bol'shaya Moskovskaya Utopiya [Greater Moscow Utopia]. Gazeta.ru. https://www.gazeta.ru/realty/2012/05/12_a_4581137.shtml. Accessed 22 May 2021
16. Pogorelova Y (2013) Zachem Vy Sdelali Etu Novuyu Moskvu? (Why Did You Do This New Moscow?). Gazeta.ru. https://www.gazeta.ru/realty/2013/12/13_a_5801969.shtml. Accessed 22 May 2021
17. Institut Genplana Moskvy (2017) General'nyy plan goroda Moskvy do 2035 goda. https://genplanmos.ru/project/generalnyy_plan_moskvy_do_2035_goda/. Accessed 22 May 2021
18. Institut Genplana Moskvy (2020) Genplan Kazani (do 2040 goda). https://genplanmos.ru/project/genplan-kazani-do-2040-goda/. Accessed 21 May 2021
19. Rasskazova I (2018) Mer Panov: deystvuyushchaya transportnaya sistema goroda ne sootvetstvuyet KTS (Mayor Panov: the current transport system of the city does not comply with the CTS). GIPORT: Nizhniy Novgorod. http://www.giport.ru/news_city/121621. Accessed 28 May 2021
20. Blinkin M, Zalesskiy N (2016) A forecast for transport system development in Russia. In: Blinkin M, Koncheva E (eds) Transport systems of Russian cities. Springer, Cham, pp 273–293
21. Zyuzin P, Ryzhkov A (2016) Urban public transport development: trends and reforms. In: Blinkin M, Koncheva E (eds) Transport systems of Russian cities. Transportation research, economics and policy. Springer, p 67–99
22. Valdin V (2021) Rusanovka, Leningradskaya Oblast', Russia. https://www.facebook.com/1063125265/posts/10222711085420105/?d=n. Accessed 22 May 2021
23. Perm City Administration (2010) General'nyy plan Permi (General plan of Perm). http://permgenplan.ru/generalnyij-plan,-dokumentyi/. Accessed 22 Apr 2021
24. Reforma ZHKKH (2021) Fund for assistance to reforming housing and communal services. https://www.reformagkh.ru/opendata. Accessed 11 May 2021

Simulation of Aerodynamic Processes in the City to Create a Comfortable Environment

V. D. Olenkov[(✉)], A. D. Biryukov, A. O. Kolmogorova, V. A. Sukhorukov, and A. V. Alemanov

South Ural State University, 76 Lenin Avenue, Chelyabinsk 454080, Russia
olenkovvd@susu.ru

Abstract. The article presents general principles for modeling and calculating wind speeds in urban areas. The main methods of calculating and modeling the location are disclosed with appropriate examples. The experience of scientists in determining the comfort factor in urban development is studied. New ways to optimize the processing of the computational model are considered. As an example of the calculation, we took existing buildings in the city of Chelyabinsk in order to build a virtual model of them. After that, the obtained models were investigated in virtual wind tunnel with CFD methods in four directions: north, south, west, and east. The obtained wind speeds for each wind direction were evaluated according to the presented wind comfort criteria. Conclusions are drawn on the work carried out and the further direction of research is formed.

Keywords: Wind comfort · Computational fluid dynamics (CFD) · Wind environment · Climate modelling · Urban climate · VR postprocessing

1 Introduction

Urban residential development includes a combination of various factors that affect a person. The wind factor has a great influence on a person, especially when combined with other factors [1, 2]. For example, in hot weather, the wind can have both positive and negative effects. It all depends on the speed and intensity of the wind. Therefore, the task of modern urban planning is to ensure the comfort of urban residential development.

There is no clear answer to the need for wind in urban built-up areas, because you need an individual approach for each part of the urban development. For example, in congested places with cars, it is necessary to ventilate them to avoid gas contamination of the air, because it is well known that exhaust gases contain a large number of heavy metals, including lead. Children's sports and playgrounds are an example of a lack of wind, where the presence of wind is not recommended, because it can lead to children getting hypothermia and cause various diseases. In addition, when the wind speed is ≥5 m/s, it starts the movement of small particles (dust, pollen from plants, etc.), which can cause various allergic reactions, diseases [3]. Moreover, dust particles and fine sand can get into the eyes, which makes it inconvenient for children and adults to be on the playground.

For these reasons, it is necessary to install structures or vegetation in certain places. But how do you know in which places it is necessary to install structures to increase or slow down the wind speed, and in which it is not? This problem is solved by the simulation of the urban environment.

2   Methods of Studying the Microclimate of Urban Development

Studies of bioclimatic comfort and aeration of urban structures can be carried out in two ways: calculated and experimental. The combination of these two methods provides the most accurate information about the level of adaptation of the environment to human life [4, 5]. The process of conducting computational and experimental studies is divided into stages and should be performed in the following order:

- Climate analysis of the territory, including analysis of topographic and meteorological data;
- Performing preparatory work for a series of experimental works: developing and creating a reduced-scale model that includes an assessment of the object's geometric characteristics;
- Creating an object model (three-dimensional and large-scale-physical);
- Experimental studies in a specialized wind tunnel and processing of the results obtained;
- A series of numerical tests of a computational model in certified software;
- Verification of the results of computational and experimental studies;
- Analysis of the obtained data and development of conclusions and recommendations on ensuring the bioclimatic comfort of urban areas.

One of the advantages of the wind tunnel is the ability to test smaller models of complex shapes installed at any angle to the direction of flow velocity. One of the modern methods of visualizing flows and measuring their velocities is the Particle image velocimetry (PIV), which belongs to the class of "non-contact" methods for measuring velocity in flows. The method is based on high-frequency illumination of a cloud of sputtered particles and measuring their movement between flashes. This method takes a special place because of its ability to record instantaneous spatial velocity distributions and allows obtaining information about the dynamics of structures, scales, calculation of differential characteristics, spatial and spatio-temporal correlations, as well as statistical characteristics of the flow. The use of these technologies makes it possible to significantly improve classical aerodynamic tests and give them a more "digital" vector of development. The flow structure in modern wind tunnels corresponds to wall turbulence and is formed due to the same mechanisms as in full-scale conditions, i.e., as a result of interaction with the underlying surface (floor) of the wind tunnel and due to the flow around the roughness elements located on it. By changing their size and relative position, it is possible to obtain a gradient of the flow velocity along the height in the form of a wind profile corresponding to different localities.

Numerical computer simulation is the newest and most actively developing method for studying and modeling the city's microclimate [6–8]. This method can significantly

supplement and expand the results of experimental modeling, and in some situations, even partially replace it [9]. As a rule, CFD (computational fluid dynamics) modeling methods are most often used in the framework of problems of microclimate assessment and wind regime modeling dynamics. CFD modeling is one of the subsections of continuum mechanics. This section is intended to calculate the characteristics of flow processes and dynamics of liquids and gases using computational methods based on solving the Navier–Stokes's equations. CFD modeling allows to estimate the temperature and simulate the movement of air flows in buildings or indoors. The biggest advantage of modeling using CFD methods in comparison with other experimental methods is that not only the values at sample points are determined, but also the totality of all physical quantities is simultaneously recorded, and thus it becomes possible to verify the correctness and adequacy of the selected model.

Thus, currently, researchers are increasingly resorting to computational and digital CFD- methods for modeling the climatic parameters of aerodynamic processes in urban development, as a rule [10, 11]. It happens due to the lower cost and resource requirements of these methods. In current studies, scientists strive to obtain results as close as possible to the real simulated prototype. To achieve maximum similarity and reliability in the modeling process, it is necessary to take into account the maximum possible number of factors, such as:

- Terrain geometry.
- Geometry of the studied and surrounding buildings.
- Surface temperature and other satellite-based data.
- Data on the state and vegetation and the percentage of green areas.
- Data on the shading of the underlying urban surface.
- Retrospective data on the characteristics of the urban heat island.

As a result of modeling, taking into account the maximum number of conditions, it is possible to obtain comprehensive information about the microclimate parameters in the built-up area, including the aeration regime of the territory and air temperature. In the future, these data will be required to analyze and evaluate the obtained map of the aeration regime of residential development in order to determine the bioclimatic comfort of the territory or assess wind comfort. According to [12], the favorable or optimal aeration regime of the territory determines not only the wind comfort of the population but can also significantly affect the temperature parameters of the territory. Also, the optimal aeration mode allows you to improve the ventilation performance of high-rise dense buildings from exhaust gases, smog and harmful emissions.

3 Microclimate Visualization Using VR Technologies

In the course of research, it is necessary to obtain readable research results. For example, for the ANSYS FLUENT software package, there are various visualization methods; the most advanced way to visualize the microclimatic and aerodynamic parameters of a building is to use virtual reality tools, which is described in [13]. This example describes the process of creating a software and hardware solution used for postprocessing and

visualization of data obtained during aerodynamic modeling of the processes of air flow around a building. This complex allows you to visualize the following air parameters: speed, pressure, temperature, humidity. To implement visual representation of vector data obtained during modeling in the ANSYS Fluent complex, a three-dimensional Unity-3D editor was used, which allows using built-in tools to process and visualize air parameters in an interactive form [14]. In the considered complex, 4 main data visualization tools were implemented:

1. Vector-based visualization system is used for visualizing individual cells as vectors with a specific direction and magnitude, indicated by a color gradient (Fig. 1a).
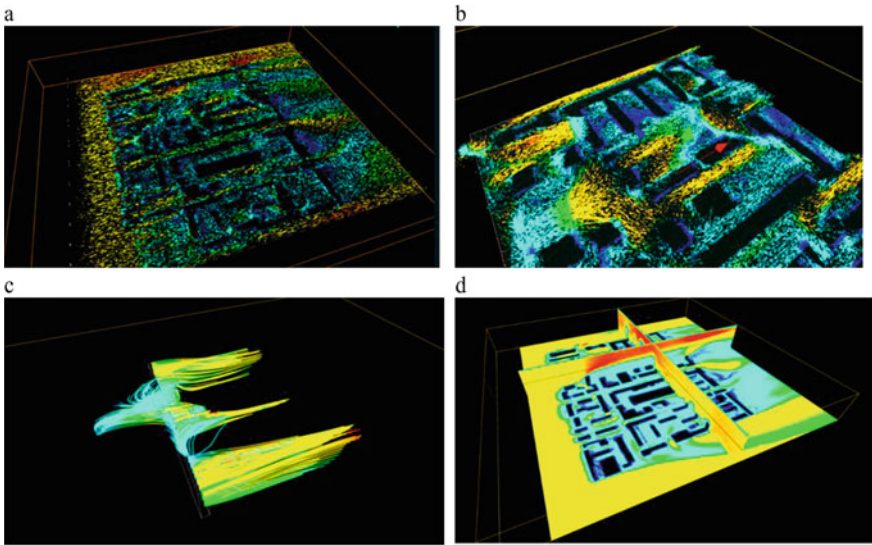
Fig. 1 Visualization of results **a** using a system of vectors; **b** using a system of particles with trace tracing; **c** using a system of streamlines; **d** using cut contour planes

2. Particle-based visualization system, which allows you to visualize the current of air masses using a configurable emitter (source) of particles with adjustable geometric dimensions. The particles emitted by the emitter follow the direction of the vectors at each point in the space of the calculated case and take the velocity and color according to the result file. The system allows setting the lifetime of a single particle in seconds to limit the flight range. As an additional mode for this module, the mechanism of trail rendering (drawing a visual trace of a particle) was implemented in the form of particle track tracing in space (Fig. 1b).

3. Streamline visualization module is the component, which is designed for drawing three-dimensional flight lines of an object of zero mass, for forming a picture of vortices and mixing flows with modulating the color of current tubes according to the air velocity at a given point (Fig. 1c).

4. The cut plane visualization module is a standard and most familiar visualization tool. It is designed for obtaining flat image maps of the flow velocity distribution within a plane with an arbitrary axis and coordinates (Fig. 1d).

This complex allows you to use the listed tools for the sessions of joint network VR visualization and research of the results of problems of hydrodynamic simulation of the microclimate. Wind tunnel testing is not something that every research center can afford, and the use of numerical computer simulations to solve even the simplest problems of building aerodynamics can provide a starting point for research and field measurements (Fig. 2).
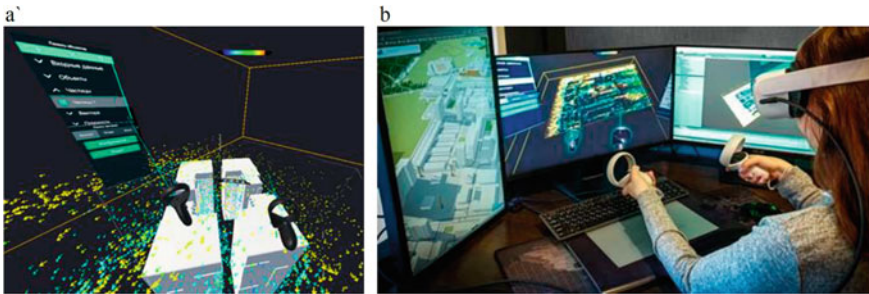
Fig. 2 Example of how the system works: **a** view from a VR headset; **b** appearance of the system

Working in a network mode using virtual reality tools allows scientists to work together during a pandemic, as well as increase the visibility and accessibility of the results of hydrodynamic simulation for the population. The technical implementation of this mode consists in creating a virtual room in which it is possible to find several virtual "avatars" of users, each of which uses visualization of only three reference points: a head and two limbs. To identify users, as well as to visually indicate the place of interaction, each user has a virtual pointer in the form of a "laser" beam of the corresponding color emitted from the controllers. With the help of these beams, users enter data on the stand-in interface, which completely duplicates the control panels from the desktop version of the complex [13]. Once all remote users confirm readiness, the session administrator starts network synchronization mode for interaction. To start, the results file initializes the received parameters and is loaded for all remote users. Then users appear in a synchronized area where they can view other users' avatars, as well as data visualization modules. In accordance with the general architecture of the complex, when one of the users changes the visualization parameters, data is synchronized for all clients, so specialists can simultaneously observe changes in the visualization parameters by one of the researchers and indicate points of interest using VR controllers and voice chat.

4   Wind Comfort

Using the calculated and experimental method, it is possible to obtain wind speeds in different building zones. Locally accelerating wind flows and turbulence resulting from

the interaction of buildings with the air flow form the local wind regime of development. At the same time, turbulence and high wind speeds caused by the presence of channeling effects and the Venturi effect between buildings cause discomfort for pedestrians in areas near buildings [15]. Mainly, the flow field causes unpleasant sensations at the height of the pedestrian (about 2 m above the ground). In particularly difficult cases, the presence of high wind speeds also increases the risk of sudden falls or "blow-off" for pedestrians and cyclists.

The criteria for evaluating wind comfort began to be thought about in the last century [16]. Certain criteria have been developed to prevent wind hazards and mitigate their effects over time. The most well-known of these are the Lawson, Davenport limits [17] and the relatively new NEN 8100 standard [18, 19], introduced in 2007 by the national standard of the Netherlands, which contains both safety criteria and the required comfort criteria. An interesting fact is that this standard is the only current regulatory document in the world for assessing wind comfort in urban development. Wind comfort in a particular location can be assessed using these criteria based on meteorological data and local wind conditions. Meteorological data in the field of research show the emerging wind speeds in the direction and their repeatability. Such data sets are often displayed as a so-called wind rose (Table 1).

The NEN8100 standard is currently the most popular in the scientific literature, although it is not mandatory and is recommended for buildings above 30 m. The standards present the calculation method and the effects of certain wind conditions on various activities. The wind comfort criterion in the Netherlands is based on the probability of exceeding the limit value of the average hourly wind speed Uoc = 5 m/s for any type of activity. From these conditions, 5 quality classes are formed (A-favorable; E-bad) for a certain type of activity (Table 2). In order to calculate the probability of exceeding the Uoc, we need to make the following step-by-step calculations for 12 wind directions in this project:

1. Determine the coefficient of the ratio of wind speeds (γ = Uped/Urv, 60 m) at the pedestrian level Uped-to the reference value of wind speed in a given territory at an altitude of 60 m Urv, 60 m;
2. Bring the wind speed limit indicator for pedestrians Uoc to the overriding criterion at an altitude of 60 m Uoc, 60 m = Uoc/y;
3. Using wind statistics for a specific area, calculate the percentage of excess (over time) of the limit indicator of the average hourly wind speed at an altitude of 60 m. In the Netherlands, statistics for 12 wind directions are provided in NPR 6097 [18, 19].

5 Example of Determining Wind Comfort

As an example, we chose a building located in the center of Chelyabinsk: an area separated by Sonia Krivoy, Smirnykh, Lesoparkovaya and Entuziastov streets. A three-dimensional terrain model was obtained (Fig. 3) and this model was used for CFD modeling of the wind comfort. Methods for obtaining a three-dimensional terrain model are described in the article [20].

Table 1 Beaufort scale

# On the Beaufort scale	Description	Wind speed interval (m/s)	Wind effect
0	Calm (calm)	0–0.25	–
1	Light air	0.25–1.55	Wind is not noticeable
2	Light breeze	1.55–3.35	Feel the wind on your face
3	Light breeze	3.35–5.45	Disheveled hair, swaying clothes, it's hard to read the newspaper
4	Moderate breeze	5.45–7.95	Picks up dust and fine paper, hair is dishevelled
5	Fresh breeze	7.95–10.75	Wind force is felt on the body, danger of tripping
6	Strong wind	10.75–13.85	Umbrellas are difficult to use, hair is disheveled, it is difficult to walk steadily, the wind noise on the ears is unpleasant
7	Light storm	13.85–17.15	Inconvenience felt when walking
8	Storm	17.15–20.75	Makes movement difficult, it is difficult to balance in gusts of wind
9	Strong storm	20.75–24.45	People are blown away by the wind

Table 2 Comfort criteria for NEN8100

P (Uoc > 5 m/s), h/year, %>	Quality class	Activity type		
		Moving around	Walk	Sitting
<2.5	A	Favorable	Favorable	Favorable
2.5–5.0	B	Favorable	Favorable	Satisfactory
5.0–10	C	Favorable	Satisfactory	Bad
10–20	D	Satisfactory	Bad	Bad
>20>	E	Bad	Bad	Bad

Fig. 3 The original three-dimensional terrain model obtained from the OSM service

As an example, this article will show results for the wind in only two directions: south and north. The assessment will be made according to the Dutch standard NEN8100. CFD modelling was carried out at a wind speed of 10 m/s. This wind speed was assumed conditionally. It is necessary to take the wind speed taking into account the roughness that operates in this area indeed. Roughness is accounted for using conversion factors. The method of accounting for conversion factors is described in [12].

The CFD modelling results were obtained at a height of 2 m (Fig. 4). According to the results of the study, when exposed to wind, there are zones with a decrease and increase in wind speed. In this study, special attention is paid to the designated area (zone 1), as this area is the place for playgrounds and playgrounds of preschool institutions. In addition, there is an underground parking lot in this area.
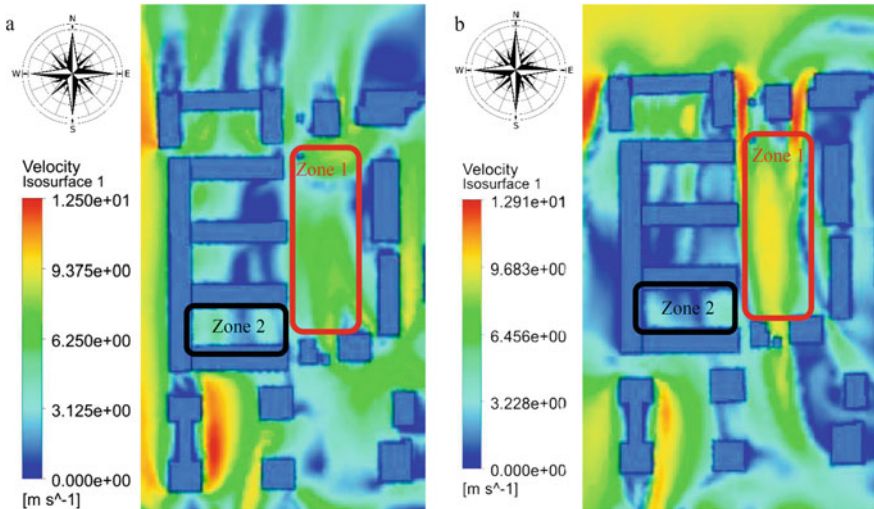
Fig. 4 Gradient of wind speeds in urban development **a** south wind direction, **b** north wind direction

In this territory (zone 1), the average speed of 6.25 m/s operates in the south direction of the wind, while the speed of 9.683 m/s mainly operates in the north direction of

the wind. Let's analyze this section using NEN8100. According to this standard, at current wind speeds, sedentary activities are not recommended, walking is rated as satisfactory, and movement in this area is allowed. However, we need to keep in mind that the requirements for preschool children should be higher, so you can exclude walking from the permitted activity. In addition, at these speeds, there is a transfer of solid particles (sand, foliage, dust, etc.) and possible hypothermia of the body. Therefore, placing playgrounds in this area without a wind protection device is unacceptable. Wind protection is unlikely to be installed in this area, as planting trees and shrubs is not possible due to the presence of underground parking. Artificial wind protection structures will be required.

As a result, it is not recommended to place playgrounds in this area (Zone 1). It is best to move playgrounds to a low-air area (Zone 2). But there are places for temporary parking of cars in this zone. Therefore, there is an air pollution with gas that enters the apartments through open windows. As a final note, it is recommended to move playgrounds to the low-air zone (Zone 2), and to move temporary car parking to the high-wind zone (Zone 1).

6   Conclusion

Modern buildings are becoming increasingly dense, so it is necessary to analyze the wind speeds of the projected development during the project development process. It is also necessary to correctly identify areas where it is best to place parking lots for cars, children's playgrounds and sports grounds, recreation areas, walking areas, etc. Such tasks will have to be performed by urban planners, so they need to create modern methods for calculating and evaluating the wind regime of buildings, training complexes based on modeling tools. For these studies, there are various software packages for modeling and analyzing the wind regime of buildings. Standards have also been developed that specify recommended speeds. All this makes it possible to fully assess the wind regime of development. The development shown as an example of determining the wind regime is not fully explored. In addition, this area is being built up with new buildings. Therefore, it is necessary to analyze this area, taking into account new buildings and all possible wind directions. Therefore, research on the wind regime of urban development will continue. The aim of further research is to develop recommendations and techniques for designers, as well as model examples that simplify the selection of optimal solutions for designers.

References

1. Peng Y, Feng T, Timmermans HJP (2021) Heterogeneity in outdoor comfort assessment in urban public spaces. Sci Total Environ 790:147941. https://doi.org/10.1016/j.scitotenv.2021.147941

2. Andrade H, Alcoforado MJ, Oliveira S (2011) Perception of temperature and wind by users of public outdoor spaces: relationships with weather parameters and personal characteristics. Int J Biometeorol 55:665–680. https://doi.org/10.1007/s00484-010-0379-0

3. Vaysman AA (2000) Urban planning and wind. Publishing House of Bukovsky, Saint Petersburg

4. Perén JI, van Hooff T, Leite BCC, Blocken B (2015) CFD analysis of cross-ventilation of a generic isolated building with asymmetric opening positions: impact of roof angle and opening location. Build Environ 85:263–276. https://doi.org/10.1016/j.buildenv.2014.12.007

5. Dunichkin I, Poddaeva O, Churin P (2016) Assessment of the bioclimatic comfort of urban development. Publishing House of the National Research University MGSU, Moscow

6. Montazeri H, Toparlar Y, Blocken B, Hensen JLM (2017) Simulating the cooling effects of water spray systems in urban landscapes: a computational fluid dynamics study in Rotterdam, The Netherlands. Landsc Urban Plan 159:85–100

7. Toparlar Y, Blocken B (2017) The effect of an urban park on the microclimate in its vicinity: A case study for Antwerp, Belgium. Int J Climatol 38(Suppl. 1):e303–e322. https://doi.org/10.1002/joc.5371

8. Blocken B, Stathopoulos T, Beeck J (2016) Pedestrian-level wind conditions around buildings: review of wind-tunnel and CFD techniques and their accuracy for wind comfort assessment. Build Environ 100:50–81. https://doi.org/10.1016/j.buildenv.2016.02.004

9. Poddaeva OI, Dunichkin IV (2017) Architectural and construction mechanics. Bulletin of MGSU 12 No. 6 (105):602–609. https://doi.org/10.22227/1997-0935.2017.6.602-609

10. Olenkov VD, Lazareva IV, Biryukov AD (2019) Numerical simulation of wind flow around building complex with different software approaches. IOP Conf Ser: Mat Sci Eng 687:055066

11. Poddaeva O, Dunichkin I, Gribach J (2018) Conducting calculating and experimental researches of the bioclimatic comfort of the residential area territory. IOP Conf Series: Mat Sci Eng 365:022029. https://doi.org/10.1088/1757-899X/365/2/022029

12. Serebrovsky FL (1985) Aeration of populated places. Stroyizdat, Moscow

13. Olenkov VD, Biryukov AD, Kolmogorova AO (2021) Application of virtual reality technologies for visualization of computer modeling tasks in the framework of architectural and construction activities. Vestnik MGSU 16(5):557–569. https://doi.org/10.22227/1997-0935.2021.5.557-569

14. Berger M, Cristie V (2015) CFD post-processing in Unity3D. Proc Comp Sci 51:2913–2922. https://doi.org/10.1016/j.procs.2015.05.476

15. Zhang X, Weerasuriya AU, Zhang X et al (2020) Pedestrian wind comfort near a super-tall building with various configurations in an urban-like setting. Build Simul 13:1385–1408. https://doi.org/10.1007/s12273-020-0658-6

16. Lawson TV, Penwarden AD (1975) The effects of wind on people in the vicinity of buildings. Cambridge University Press, Heathrow, London

17. Lawson TV (1978) The wind content of the built environment. J Wind Eng Ind Aerodyn 3(2–3):93–105

18. Janssen W, Blocken B, Khayrullina A (2015) Wind comfort. Application experience in the Netherlands. High-tech buildings (winter 2015). ARCUS III: BREEAM certification experience, pp 24–31

19. Janssen W, Blocken B, Hooff T (2013) Use of CFD simulations to improve the pedestrian wind comfort around a high-rise building in a complex urban area. Proceedings of BS, pp 1918–1925

20. Olenkov VD, Biryukov AD, Tazeev NT (2018) Three-dimensional modeling of buildings and structures for simulation of wind effects on urban areas. IOP Conf Series: Mat Sci Eng 451:012162. https://doi.org/10.1088/1742-6596/451/1/012162

Modern Principles of Organization of Production Territories

O. A. Rastyapina[(✉)], V. G. Polyakov, and S. O. Yaschenko

Volgograd State Technical University, 1 Akademicheskaya, Volgograd 400074, Russia
O_rast@list.ru

Abstract. Modern trends in the development of urbanized systems dictate new requirements for the organization of urban space. One of the elements of such a space is the production territory, also as a source of impact on the residential area. Taking into account environmental requirements, such sources of impact must be removed from the residential environment, minimizing the negative impact. But at the same time, production territories should be located as close as possible to the residential area. This is necessary to ensure the transport accessibility of the territories and the effectiveness of the city-forming factor. The modern level of technology allows organizing the production process with minimal or zero negative impact on the environment. To improve the quality of the organization of industrial territories, it is necessary to use the basic principles of the architectural and landscape organization of the territory. The architectural and landscape organization of production territories helps to form a favorable space, including the visual one. This is well reflected in the level of perception of the quality of the enterprise from the point of view of employees. The openness of the production territory helps to form the company's safety image for the environment. The article discusses the basic principles of the formation of the architectural and landscape appearance of the production territory. The development of such principles is necessary for the formation of a new qualitative level of the production territory and the urbanized system as a whole.

Keywords: Urban spaces · Production territories · Organization · Quality of the organization

1 Introduction

The modern level of development determines new requirements for planning changes in urbanized systems. Enterprises should look for more efficient ways of territorial organization of space. Visual, layout and aesthetic requirements should be added to the general planning requirements. It is necessary to create a safe high-quality space. These requirements apply not only to the organization of residential / urbanized space, but also to production territories. Initially, it was necessary to allocate the production area and the sanitary protection zone [1–4]. Today it is necessary to preserve the ecology directly at the source of impact. The implementation of modern production technologies,

protection from gas and dust is one of the ways. Another way is to organize the space within the production territory. The production territory should become a part of the urbanized environment in the absence of a negative impact on the living environment [5–7]. Taking into account modern requirements for the formation of a safe urbanized environment, including production territory, it is necessary to use various organizational and planning measures aimed at creating a safe spaces. Such measures may include:

- using architectural forms—in order to create barrier protection for the spread of negative impact;
- using green spaces not only heals the environment, but also creates a visually favorable area;
- planning layout of facilities within the production territory, which helps to reduce the spread of negative impact;
- organization of the landscape of the production territory. This implies not only the formation of the landscape in terms of vertical planning (in compliance with the main goals of it) but also a combination of open and closed spaces of the production territory;
- using architectural measures to form a favorable visual appearance of the production territory and reduce the burden on the environment through the applying of modern materials [8].

In the 50 s, the principle of combining production processes was introduced. N. N. Kolosovsky (Soviet economist and economic-geographical) created the theory of energy-production cycles, which is the basis for the development of special zones of economic development—territorial-production complexes [9, 10]. The territorial-production complex supposes combining the enterprises according to certain principles [11, 12]. Since 1930, the following basic principles for the allocation of production territory should be noted [13]:

- allocation of the production territory at the lowest cost, taking into account natural and special conditions, the principle of maximum efficiency;
- combining management systems, maximizing overall performance;
- zoning principle;
- creating transport links between production territories.

The priorities of the territorial allocation of production were lined up depending on the economic and political interests of the state [14, 15]. Currently, a cluster approach is used to allocate production territories. The most advisable is the joint allocation of enterprises on an economic basis. There are opportunities for the integration of production, as a consequence of the synergistic effect [16–19]. With this approach, the competitive advantages of enterprises increase. Association of enterprises at one territorial site helps to save territorial resources. From the point of view of the planning organization of production territories, the merge of enterprises allows the formation of safe areas outside the production zone, by reducing the burden on the environment, since the sources of

impact are combined, and not dispersed. Also it is possible to create favorable microclimatic conditions in production territories by using architectural landscape and planning measures.

Our analysis of foreign and Russian experience in the formation of territorial zones made it possible to identify various features determined by the nationalization of production, natural conditions, the level of economic development and infrastructure development.

Based on the analysis, it is established that the main forms of organization of territorial-production complexes are:

- industrial-production zones;
- industrial parks;
- it-parks;
- technology parks.

The form of organization is determined by the type of production and the characteristics of the production process, as well as a number of economic parameters [20, 21].

Taking into account the current trends in the formation of multifunctionality of territories, as well as the need to take into account environmental requirements, regardless of the form of organization of the territorial production complex, the issue of the architectural and landscape organization of the production territory is relevant. The external appearance of the territorial-production complex should be organized in an attractive and bright way. Thus, the modern requirements that determine the principles of organizing territorial-production complexes of an urbanized area are the following:

- ensuring the safety conditions of the residential area in relation to the production source of negative impact;
- forming open social space by ensuring the visual appearance of the territorial-production complex [22].

The first requirement is ensured by taking into account the characteristics of the production technology and the placement standards. The second requirement is ensured by the architectural and landscape organization of the territory. Achievement and compliance with the requirements are possible by using architectural landscape and planning measures. The implementation of all activities involves the use of green spaces, small architectural forms, visualization tools for facilities and buildings. So, the designers of safe production territories need a detailed analysis of the measures by which the goal can be achieved.

2 Qualitative Characteristics of the Organization of Production Territories

Based on the analysis, the main qualitative characteristics were established that determine the architectural and landscape organization of the territory (Table 1) [23]. The analysis

of foreign models of territorial-industrial complexes made it possible to establish the following features of the organization of territorial-industrial zones, which must be used in landscape architectural organization:

Table 1 Qualitative characteristics of the territorial production complex

No.	Characteristics	Production allocation value
1	Quality of geotechnical conditions of construction and operation	±
2	Availability of utilities (electricity, gas, water)	+
3	Transport accessibility (railway, water transport, roads)	+
4	State of the environment	+
5	Climatic conditions	±
6	The presence of greening	+
7	Condition of greening	+
8	Mineral availability	±
9	Availability of water resources (surface, underground sources)	+
10	Opportunity to realize the recreational potential	+

- availability of a single building for the placement of industrial, energy-intensive enterprises;
- high degree of greening and landscaping;
- location in picturesque areas with favorable natural conditions;
- convenient transport links with residential areas and other production territories.

The main evaluative characteristics of the improvement of production territories are:

- sanitary condition;
- contrast of relationships;
- color scheme;
- lines;
- rhythm;
- illumination.

All characteristics can be divided into groups: "already formed" and "being formed". The "already formed" characteristics are determined by the prevailing natural and climatic features of the territory and the requirements for the specifics of production. This group of characteristics should include: geological, hydrogeological, meteorological, microclimatic conditions. Microclimatic conditions include climatic conditions that are formed under the influence of the built-up area and the landscape organization of the

territory. These characteristics determine the existing construction conditions and have a direct impact on the choice of the design solution. However, in the process of construction and operation of production territories, changes are possible: in the level and qualitative characteristics of groundwater, in the structural and qualitative composition of ground masses, in biotic factors, etc. To analyze the qualitative characteristics, an assessment of these factors is necessary. Determination of their dynamics, assessment of the impact on the territory from the point of view of providing a favorable or unfavorable impact. In conditions of unfavorable impact, it is necessary to develop a complex of architectural, landscape, planning measures to reduce it.

The "being formed" characteristics are determined by the project assignment and project solutions. They can be created and changed during the operation of the territory. The "being formed" characteristics include: transport accessibility, the state of the environment, negative sources, greening and disclosure of the recreational potential. Formation of these characteristics is possible using various measures of the architectural design of the production territory.

For each enterprise, depending on the type of production, all characteristics have a different value. Accordingly, when estimating the quality of the architectural and landscape organization of the territory, they have various weight coefficients. The weight coefficient should be determined taking into account the opinion of experts, based on the number of significant indicators for the considered production territory according to the formula

$$C_w = \frac{W_n}{1 - \sum_{i=1}^{n} W_n} \tag{1}$$

C_w—the value of the weight coefficient of the i-th indicator; W_n—the weight of the indicator according to the expert; n—number of indicators.

Employees of the enterprise, residents of the city, who daily encounter this territory and understand the importance of the specific factor for the formation of safe and high-quality territory, may act as experts in assessing the significance of indicators. Moreover, the concept of safety and quality should be perceived together. Since the production territory cannot be defined as qualitative due to the presence of hazardous factors.

The value of each characteristic from Table 1 can be positive or negative. The presence of the characteristic makes the value positive and increases the overall assessment of the quality of the production territory. In the absence of a characteristic, or an unfavorable assessment, it is marked with a negative sign, which means that the total assessment decreases.

Geotechnical conditions can be favorable and unfavorable. In the latter case, additional engineering measures are required to create optimal conditions for the construction of buildings and facilities.

For industrial enterprises, it is important to have engineering communications of the required capacity. During the construction of industrial complexes, the question of the availability of the necessary power of engineering communications and resources should be considered. Accordingly, the ability to connect to the required power of engineering resources is assessed as a positive value of the characteristic.

The transport accessibility of production territories contributes to the formation of logistics networks, affects the economic potential of the enterprise. The more developed

transport accessibility, taking into account different types of transport, the higher the value of the characteristic.

The state of the environment is a comprehensive indicator that includes analysis of the lithosphere, hydrosphere and atmosphere. Taking into account modern legislation, the analysis of the quality of soil, water and atmospheric air should be carried out at regular intervals. The analysis and assessment of this characteristic are determined on the basis of the available environmental monitoring data.

Climatic conditions contribute to the formation of favorable conditions for the dispersion of pollutants in the atmosphere. Or, on the contrary, the concentration of these components increases under the influence of air temperature and wind speed. Climatic characteristics are assessed in terms of the chance and frequency of the combination of adverse climatic factors. All territories can be divided into three groups: a conventionally comfortable climate, an uncomfortable climate and a relatively uncomfortable climate. The territories located in conventionally comfortable climate include spaces with favorable climatic, geomorphological and hydrogeological conditions. Territories of uncomfortable climate are with unfavorable natural and climatic areas in aggregate. Territories with a relatively uncomfortable climate include one of the above unfavorable factors and construction requires using special measures for the development of the territory.

The analysis of greening should estimate the qualitative composition of green spaces, compare the area of green spaces with standard indicators and assess the sanitary state of green spaces and the species diversity of greening forms. The assessment of species diversity should compare the use of different forms of greening, depending on the climatic conditions of the territory. Consideration should be given to the various functional purposes of green spaces. The main functions of green spaces are: participation in gas movement and regulation, climate-forming, prevention of the development of negative natural processes (erosion, landslides, etc.), neutralization of pollutants in the atmosphere and soil, phytoncidal activity, preservation of biodiversity and genetic resources, creating natural products and recreation.

The presence of minerals is a characteristic of certain types of industries. The value of the characteristic is determined from its relevance to the manufacturing process.

The analysis of the types of water resources is necessary when assessing water resources. The assessment is carried out from the point of the source of water supply, the capacity of water resources and the possibility of using the waterway as a transport way. The value of the characteristic is determined from its relevance to the manufacturing process.

The characteristic of the recreational potential involves the availability of natural resources for the formation of social openness of the territory. The value of it is determined by the natural potential and the impact of the production process on the environment.

All characteristics can be described by criteria: availability, condition, need/demand. Different factors can have different values for citizens, in different climates and at different levels of development of the urbanized areas. Their value must be determined for a specific production complex.

Thus, to determine the overall quality assessment of the organization of the production territory, it is necessary to determine the weighting factor, taking into account the opinion of experts. The value of the characteristic and the weight coefficient obtain an aggregate quality assessment by summing. The maximum rating for these characteristics is 1 or 100%. Accordingly, when analyzing these characteristics it is possible to determine the directions for the implementation of measures for the formation of quality conditions for the organization of production territories. The proposed measures should be aimed at improving performance with the resulting minimum score. When optimizing the characteristics of the production area, it is necessary to determine the order of implementation of measures, based on the weight coefficient. The higher the value of the weighting factor, the more significant the characteristic is for the given conditions.

3   Principles of Organization of Production Territories

These characteristics reflect the measures (Table 2) of the architectural and landscape organization of the territory of the industrial complex. The formation of these measures is possible through the use of various forms of the greening of the territory, landscape solutions and small architectural forms. Using various techniques of greening makes it possible to form not only enclosed zones, but also opened areas visually limited by low species of tree and shrub vegetation. Techniques for group and single planting of trees, vertical and mobile greening allow improving the visual perception of the territory and microclimatic characteristics. Various dendrological species of tree and shrub vegetation create different color schemes for the territory. The variety of modern small architectural forms, which can be mobile and transformable, contributes to the improvement of the production territory and have a positive psycho-emotional impact on a people.

Table 2 Recommended measures for territory organizing

Territory characteristics	Emotional condition
Free spaces. Smooth, flowing shapes and patterns. Warm vibrant colors	Joy
The consistency of the arrangement of the elements of landscaping and architecture on the territory. A combination of space, shape, color, lighting, texture. Use of materials for their intended purpose	Satisfaction
Bold shapes. Powerful constructive rhythm. Planes set at an angle. Rough natural surfaces. Massive materials. Highlighting the compositional center. Ethno-historical aspects	Dynamic action

In addition to the positive influence formed with the noted measures (Table 2), there is a negative influence on the psycho-emotional state of people at production territory. Taking into account the negative perception of the area, the following measures of improving the production territory should be avoided:

- restrictions on the territory, lack of orientation points, forming the hidden zones and space;
- frequent change of directions on the way of movement;
- obstacles in the way of movement.

To create favorable visual and whole microclimatic conditions on the territory of the industrial complex, it is necessary to use various measures [24–26]. Such measures are the color design of the territory and the use of small architectural forms, the symbols of the territory and companies, sculptural compositions.

The color scheme is used as a means of emotional self-regulation, correcting the psychological state in the right direction (Table 3). Warm colors are preferred for activation. It is recommended to use cool colors to reduce stress. With the help of color accents, it is possible to enhance and hide the role of various objects. Considering the psychological influence of color on the emotional state of a person, it is recommended to use the following colors when designing the territory: white, green, blue, yellow, red, orange, black. The sequence of colors indicates the degree of their perception by a person and the effectiveness of the influence on the psycho-emotional state [27, 28]. The first three colors in the group are present in natural conditions. They must be distinguished by various methods of shaping the architecture of the area. The use of such techniques will contribute to the formation of a favorable visual space.

Table 3 The influence of color on the psycho-emotional state of a person

Psycho-emotional state of a person	Color
Calms, inspires hope	White
Increases organization and willpower	Black
Increases self-esteem, performance	Red
Improves concentration, refreshes the mind	Blue, yellow
Increases concentration, relaxes	Green
Increases concentration of attention, relieves irritability, develops a sense of responsibility, stimulates intellectual activity	Orange

The main elements of the formation of a favorable architectural and landscape appearance of the production territory are: greening, small architectural forms, fountains, artificial reservoirs, coating materials (road and path chains and finishing of building facades). When choosing an element, attention should be paid to its main functional purpose and location. The most versatile element is greening the area of the industrial complex. When choosing a dendrological composition, the designer should be guided by the following factors: dust and gas resistance of green spaces; decorative properties of green spaces (crown type); phytoncidal properties of green spaces to create favorable microclimatic conditions. The forms and measures of greening can be different and depend on the main purpose of the area being formed and on the size of the territory. These can be group

greening with the aim of limiting and highlighting (focusing attention) of the area. Or point green objects in order to regulate microclimatic parameters in a separate area.

The criteria for evaluating the landscape architectural organization of the production territories are:

- nature of the layout—a holistic layout, regular development or spontaneously formed buildings;
- main organizing element—how much the central point of the production territory is determined (this can be a square, a fountain, etc.);
- scale of the territory—how much everything can be measured up;
- interconnectedness of spatial elements—buildings, paths, squares, etc., the advisability and sequence of the movement organization;
- sequence of the territory perception.

Basic principles for organizing production territories are:

- Using various forms of greening and a different dendrological composition of green spaces, given their resistance to potential adverse effects and climatic conditions. Recommended forms of greening are: vertical, horizontal, mobile. Vertical greening involves the traditional planting of green spaces in the production territory and greening of facades (taking into account climatic conditions and production characteristics) as well as vertical greening of small architectural forms (pergolas, arbors). For the architectural and landscape organization of the territory, it is necessary to use various options for planting green spaces. It is possible to form single plantings defining dominants of the territory, and closed spaces to delimit the functional purpose of the territory.
- Using small architectural forms, color design of buildings and facilities in accordance with the perceived general appearance and functional purpose. Small architectural forms in production territories are designed to relieve the emotional stress of employees, organize free time during leisure hours. The task of color design of the building and the production territory is the formation of a favorable psychoemotional state of employees, stimulating their performance. Therefore, it is necessary to use a color scheme according to the purpose of the building or facility and the effect of color on the emotional state of a person.
- Forming open planning structure accessible to third parties contributes to the creation of perceived safety of the production territory.

The external positive ecological image of the production territory also depends on communication between the enterprise and the public. Specialists should tell the public about the enterprise, its problems, successes and prospects. The attitude of people towards the enterprise will change clearly. It is important to organize excursions, open days in the production area, to create an image of a positive company that cares about the protection of the environment and working people.

4   Conclusion

The architectural and landscape organization of the territory of the industrial complex is an urgent issue for many modern industrial enterprises. Initially, the allocation of the territorial-production complex was determined only by economic factors and characteristics of production. The foreground was transport accessibility for the transportation of raw materials and finished products, remoteness from the main sources of energy and engineering networks. Today, the organization of the internal area of the territorial-production complex (architectural and landscape organization) influences on the positioning of this enterprise in the professional market, creates advantages for it over competitors. Using the measures of architectural and landscape organization it is possible to create favorable microclimatic conditions, reduce the impact on the environment, ensure the safety of the industrial complex and its positive perception by the people. The safety of the complex is achieved through the formation of openness and socialization of the production territory. The main principles are: transport accessibility of the territory; organization of free spaces on the territory; using various measures for greening the nearest territory and the territory of the complex (forming a sanitary protection zone); using small architectural forms, the combination of colors, textures; location of the main functional buildings and facilities in a clear, logical sequence; social accessibility of the territorial-production complex. All this contributes to the perception of the production complex as an environmentally friendly facility. These principles correspond to the requirements of the urban system and the current level of development of society and industry.

References

1. Chebanova SA, Polyakov VG, Erokhin DA (2016) Engineering systems of heat supply and working on coal as sources of air pollution by finely dispersed dust. Procedia Eng 1989–1995
2. Sharova IV (2017) Development of a project for a sanitary protection zone. Mod Res 76–77
3. Smolyakov YS, Ufimcev MG (2020) Justification of the sanitary protection zone. World Innov 27–30
4. Gorbunova YA (2009) Distinctive features of the Soviet territorial-production complexes (TPC) and modern economic clusters. Taxes Financ Law 317–321
5. Rastyapina OA (2012) Environmental safety as the basis of environmental policy. Bulletin VolgGASU, pp 178–188
6. Pogrebnyak RG, Zhukov DV, Pogrebnyak OY (2011) Environmental aspects of the functioning of industrial territorial-production complexes. Financial Anal 23–29
7. Rastyapina OA (2015) Directions for assessing urban planning security. Internet Bull VolgGASU 4(40):9
8. Degtyarev AA (2017) Influence of the urbanized environment on a person: calculation of the coefficient of visual aggressiveness of objects and methods of its neutralization. Adv Mod Sci Educ 6:13–17
9. Kolosovsky NN (1969) The theory of economic zoning. Moscow
10. Timoshenko AI (2020) Formation of territorial-production complexes in the Soviet period. Socio-Econ Hum J Krasnoyarsk GAU 132–143
11. Rastyapina OA, Merzlikina GS (2010) Development of forms of integration interaction. News of higher educational institutions. Ser: Econ Finance Prod Manage 35–43

12. Krzhizhanovsky GM (1957) Questions of economic zoning of the USSR. Collection of materials and articles, pp 1917–1929
13. Lomovceva OA, Tkhorikov BA, Gerasimenko OA, Polyakov VG (2016) The strategic nature of public-private project in solving the problems of small and medium-sized cities in Russia. The Social Sciences, Pakistan, pp 3136–3141
14. Polyakov VG (2010) Strategic management of the development of industrial construction in the region. St. Petersburg
15. Polyakov VG, Yashchenko SO (2009) Volgograd region: socio-economic prospects. social aspects of the construction of large industrial complexes. Russian Entrepreneurship, pp 121–125
16. Sapozhnikova AA (2014) Severo-Irkutsk territorial-industrial zone of federal significance: possibilities of territorial-industrial zoning. In: Proceedings of the Bratsk State University. Series: economics and management, pp 32–36
17. Golyashina EA, Chaika AA (2015) Features of the development of special economic zones in Russia (on the example of the industrial production zone "Alabuga". Science Time, pp 101–106
18. Rastyapina OA, Polyakov VG, Kalashnikova EV (2020) Methods of evaluating yard area development in the context of urbanization. IOP Conf Ser: Mater Sci Engineering
19. Rastyapina OA, Babenko KV (2017) Neccesarity to form a visual space in cities in order to ensure environmental safety. Bulletin VolgGASU, pp 384–395
20. Suchikhina AP, Kulakova YO, Ermolaeva EV (2015) Cooperation in Russia. In: Bulletin of medical internet conferences, p 1483
21. Kovalev AM (2007) On the structure of visual space. GEO-SIBERIA, pp 24–28
22. Tsivin AV (2009) Features of visual perception of urban spaces. In: Regional architecture and construction, pp 106–108
23. Gubankova ML, Lamanova RV (2015) Formation of a greening system for a cement plant. In: New ideas of the new century: proceedings of the international scientific conference FAD TOGU, pp 45–49
24. Vahtinova ON (2014) Technogenic impact of a production enterprise on the atmospheric air of an urban area. In: Problems of ensuring safety during emergency response, pp 21–4
25. Tozhiboev IM, Krivogina DN (2020) Subject-oriented methodology for assessing the quality of the city environment advanced construction technologies. Theory Pract 1:435–441
26. Babicheva AV (2009) Stress as an emotional state, its effect on the human body and on educational activity. Probl Higher Educ 1:279–281
27. Burdova AA, Borodaenko AA, Kotlyarova VV (2017) The influence of the color spectrum on the psychophysiological state of a person. Alley Sci 7:45–49
28. Galchinova TA (2020) Influence of color on the emotional state of a person. Innov Sci 5:172

The Eco-Positive Design and Planning of the Educational Facilities Network in Cottage Communities

E. S. Novitskaya^(✉) and T. N. Kolesnikova

Orel State University Named After I.S. Turgenev, 77A Moskovskaya st., Oryol 302030, Russia

Abstract. There has been a considerable increase in the single-family detached housing development over recent decades. The majority of such housing development projects, though, fall short of modern comfort requirements and fail to provide residents with primary public services which causes major inconveniences. The most important public amenities are educational institutions, and the construction of those is either not planned or is included into the further construction phases. The authors have analyzed the master site plans of the Orel region based single-detached housing communities and the basic characteristics (parameters) of their design and layout (the type of a housing development, the number and area size of the lots, etc.). This was done to define the most advantageous types of educational institutions for cottage communities. The basic factors that have been considered are: present-day social and economic conditions, small-size infrastructure facilities areas, provision of all the necessary basic services characteristic of a development-oriented environment. The study enabled the authors to propose a certain range of suitable educational institutions for different types of communities. The authors also introduced the guidelines or principles aimed at improving the master site plan structure. These principles include: comfortable access; increasing the functions of the living environment; social service facilities cooperation (this principle is advisable for a cottage community not only from a design and planning perspective, but also as an economic benefit because it implies the integration of educational, sport and development facilities).

Keywords: Educational institutions · Kindergarten · School · Network facilities · Suburban community

1 Introduction

An active impact on the growth of the number of low-rise residential buildings in suburban settlements was influenced by the state program "Affordable and comfortable dwelling for Russian citizens" implies observing certain requirements related to residents' comfortable living. According to the data provided by the Office of the Federal State Statistics Service for the Oryol Region [1, 2], at the moment there is a composition of the population by age groups. For example, see Fig. 1.
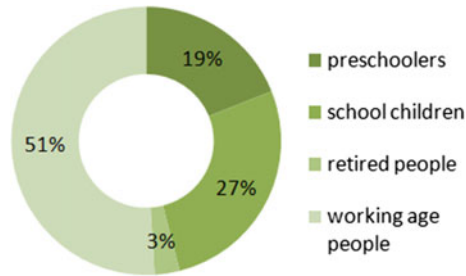
Fig. 1 The approximate age structure of residents of cottage settlements

Transportation lines and public utilities are a must for a low-rise single-detached housing development, but public amenities and social infrastructure facilities are rarely included into the master plan of a community.

Statistical data show a significant number of school-age children and preschool-age in suburban settlements of individual development.

There schools and kindergartens are being built later than the houses of residents. This situation with educational institutions creates uncomfortable conditions for residents. Such living conditions do not comply with any modern requirements, cause much trouble and do not contribute to the wellbeing or comfortable living of the residents. Comfortable living is a basic component of the biosphere compatibility concept [3–5].

This concept points out seven basic functions or services that a community should provide. These are: essential (life-sustaining, primary social) services, education, administrative functions, creation, interaction with the natural environment [6]. The most significant functions related to single-detached housing developments are providing essential services, entertainment and leisure, education, creative activities and connection with nature. The first and last requirements of this list are as a rule implemented while the others are usually not considered during the design and planning stage.

2 Methods

The major goal was to define the most advantageous types of educational institutions which can provide proper education and creative activities for the residents of single-detached housing communities. To achieve this goal the authors firstly thoroughly analyzed the master site plans of the single-detached housing communities located in the Orel region. The basic characteristics or parameters pointed out during this study then underwent quantitative and qualitative assessment.

The objects of the study were nine newest single-detached housing communities [6–15]. The basic classification characteristics (parameters) of these communities defined by the authors are presented in Table 1.

The study of the communities planning and types that we have carried out shows a great variety of the sizes of communities—from small ones to big ones with the area sizes of the housing units from 0.06 up to 0.15 ha. The area size of a housing unit increases from 0.02 ha up to 0.15 ha with the increase of the distance between a housing community and the city.

Table 1 Classification characteristics (parameters) of the single-detached housing communities located in the Orel region (erected from 2007 to 2021)

Characteristic/Parameter	Name of a community								
	Platonovo	Edelweiss	Malaya Kulikovka	Novaya Kulikovka	Zelyonye Berega	Saburovo	Mechta (4 phases)	Suburbia (3 phases)	Obraztsovo Estate
Type of a housing development									
Single-detached cottages	+	+	+	+	+	+	+		+
Townhouses, duplexes									
Mixed housing								+	
Number of housing units									
150–249	232	155		156		149			168
250–500			366		481				
1200–1600							1500	1200	
Distance from the city, km									
2–5	2			2	3		2	3	
5–10			6			5	6		
More than 10		12							
Area size of a land lot, ha									
0.02									
0.04									
0.06								+	

(*continued*)

Table 1 (*continued*)

Characteristic/Parameter	Name of a community								
	Platonovo	Edelweiss	Malaya Kulikovka	Novaya Kulikovka	Zelyonye Berega	Saburovo	Mechta (4 phases)	Suburbia (3 phases)	Obraztsovo Estate
0.08							+	+	
0,10				+	+		+	+	
0.12		+		+	+	+			+
0.15	+	+	+	+	+	+			+
Total area	60.9	42.56	92.52	39.59	76.15	31.31	162	135	44.7
Social infrastructure assets, construction phase									
Kindergarten	+	+	+			+		+	
School	+							+	
Medical facilities	ABSENT								
Public safety organizations	ABSENT								
Commercial and utility services		+						+	
Entertainment, leisure and sport buildings and facilities									

Note The sign "+" shows the presence of a characteristic

The analysis of the housing developments mentioned above also reveals significant disadvantages in their master site plans. For example, social infrastructure assets are either completely absent there or included into the future construction phases. Thus, the design and planning of social infrastructure assets (especially kindergartens or preschools and schools) in cottage communities is essential. The study enabled the authors to propose a certain range of essential educational institutions types. During the study the authors considered a great number of cottage communities characteristics (see Table 1) as well as the present-day social and economic conditions and the small-size infrastructure facilities areas suggested by the master site plans on the one hand, and the need for all the basic development-oriented services on the other hand.

The important task was to define the factors and criteria which determine the classification characteristics of the design, planning and layout of educational facilities in the communities. The basic criteria which help to determine the classification characteristics of different educational institutions types are: the number of housing units, population density (the family index), the area size of the lots surrounding houses. There is a wide range of the area sizes of the housing units lots (from 0.06 up to 0.15 ha) which complies with the Regulations for land use and development in the Orel region and other regions of the Russian Federation [15].

One of the major factors determining comfortable living is the access distance (radius) to the social infrastructure facilities which is regulated by the Set of specifications known as "Urban planning. Design and construction of urban and rural housing developments" [16]. Our further study is based on this factor. We calculated the potential capacity of educational institutions considering each of the two different options of the access distance (radius):

500 m for kindergartens; 1000 m for schools—according to the Specifications set "Urban planning. Design and construction of urban and rural housing developments" [16] for a rural development;

300 m for kindergartens; 500 m for schools—the same as for an urban development—that is a higher comfort standard accepted for suburban cottage communities which residents are used to the city life and, consequently, require the city standards of living.

The following formula proposed by the authors was used in these calculations. The formula takes into account all the factors which determine the capacity and types of the primary infrastructure facilities.

$$N_i = 0.75 \cdot \frac{S_R \cdot k_f \cdot k_p}{S_i} \tag{1}$$

with N_i—the average number of inhabitants; S_R—the area size with the specific option of the access distance (radius) (300, 500, 1000 m); k_f—the family index (3, 2) [15]; S_i—the area size of the land lot, ha; k_p—the index for the configuration of the communities master site plans (0.65)—it is accepted by the authors after the detailed study of the Orel region suburban communities master site plans, it denotes the numerical dependency relation between the capacity of educational institutions and the overall dimensions presented in the master plans of cottage communities; 0.75—the standard ratio of the residential housing land lots in residential cottage communities [16].

Thus, if we accept one of the two options of the access distance (radius) for the buildings of preschool buildings it is possible to determine the dependence of the capacity of institutions on the area of individual sites.

According to the Specifications set 42.13330.2016 "Urban planning. Design and construction of urban and rural housing developments" we must calculate the number of preschool and school places assuming that there should be 100 preschool places and 180 school places for 1000 inhabitants [16]. Table 2 presents the results of the calculations carried out to find the number of places for two different options of the access distance (radius)—access radius (preschool institutions—500 m and schools—1 km) and distance for increased comfort (kindergartens—300 m and school buildings—500 m).

Table 2 Possible estimated number of children in kindergartens and schools with different urban planning accessibility

Area size of a land lot, ha	Number of land lots, housing units	Number of inhabitants	Required number of kindergarten places, children	Required number of secondary school places, children	Standard kindergartens	
					Capacity, number of children	Number of groups
The results based on the standard access distance (radius) (preschools—500 m, schools—1 km)						
0.02	1875	6000	600	1080	350, 250	22.17
0.03	1250	4000	400	720	210, 190	16.15
0.04	937.5	3000	300	540	290	15
0.06	625	2000	200	360	190	10
0.08	468.75	1500	150	270	155	8
0.1	375	1200	120	216	125	7
0.12	312.5	1000	100	180	95	5
0.15	250	800	80	144	75	5
The results based on the higher comfort access distance (radius) (preschools—300 m, schools—500 m)						
0.02	675	2160	216	389	210	12
0.03	450	1440	144	259	135	7
0.04	337.5	1080	108	194	95	5
0.06	225	720	72	130	75	5
0.08	168.75	540	54	97	55	3
0.1	135	432	43.2	78	45	2
0.12	112.5	360	36	65	40	2
0.15	90	288	28.8	52	30	2

3 Results and Discussion

Table 2 makes it possible to define the target capacity of the educational facilities. The calculations performed with the consideration of the best possible access distances of preschool and school facilities helped us to determine the required number of places.

The study of the Table 2 data shows that the needs of the small and big cottage communities with the area size of housing land lots 0.06 ha and less within both the standard and higher comfort access distances can be covered by the existing types of secondary schools and kindergartens.

That is why the objects of our further study are single detached housing communities with the bigger area size of the land lots—from 0.08 up to 0.15 ha.

Our conclusions are based on the existing experience in the design and planning of such buildings [17–21].

The authors have defined a range of educational facilities for single-detached suburban communities depending on the size and capacity of a cottage community:

If the area size of a housing land lot is 0.15 ha:

(1A) the number of housing units is 150 to 200—a kindergarten for 55 places and a primary school;
(1B) the number of housing units is 200 to 275—a kindergarten for 75 places and a primary school;
(1C) the number of housing units is 275 to 350—a kindergarten for 95 places and a middle school;
(1D) the number of housing units is 350 to 500—kindergartens for 55 places and 135 places and a secondary school [18].

If the area size of a housing land lot is 0.12 ha:

(2A) the number of housing units is 175 to 250—a kindergarten for 55–75 places and a primary school;
(2B) the number of housing units is 250 to 350—a kindergarten for 110 places and a middle school;
(2C) the number of housing units is 350 to 500—kindergartens for 55 places and 135 places and a secondary school;
(2D) the number of housing units is 500 to 800—kindergartens for 135 places and 135 places and a secondary school [18].

If the area size of a housing land lot is 0.10 ha:

(3A) the number of housing units is 210 to 400—a kindergarten for 165 places and a middle school;
(3B) the number of housing units is 400 to 600—kindergartens for 75 places and 135 places and a secondary school;
(3C) the number of housing units is 600 to 1000—kindergartens for 135 places and 180 places and a secondary school with 2 parallel cohorts of students [18].

If the area size of a housing land lot is 0.08 ha:

(4A)   the number of housing units is 270 to 500—a kindergarten for 55 places and 135 places and a secondary school;

(4B)   the number of housing units is 500 to 800—kindergartens for 135 places and 135 places and a secondary school with 2 parallel cohorts of students;

(4C)   the number of housing units is 800 to 1200—kindergartens for 180 places and 180 places and a secondary school with 3 parallel cohorts of students [18].

If the area size of a housing land lot is 0.08 ha and higher there should be done some thoughtful planning of the primary public services facilities in the communities.

In cases B (1A)–(1D), (2A)–(2C), (3A) the cooperation and integration of preschool and school facilities would be advisable because it would enable the reasonable use of the land and utility lines and help to avoid the doubling of the maintenance units for such a type of buildings. Moreover, it would be reasonable to include family childcare groups (family kindergartens) into the master site plans of the housing development at the stage of planning. The family childcare groups would be convenient for multi-child families or for the families having hyperactive children or children with a poor health state because the latter should avoid crowded surroundings.

In cases (2D), (3B), (3C), (4A)–(4C), taking into account the unification of the kindergarten and the school into a single building, additional construction of preschool institutions is required to comply with comfortable urban planning conditions. Architectural and urban planning zoning implies the possibility of building small kindergartens, or organization of family childcare groups which create a certain network of education facilities in single-detached suburban communities.

The development of cottage communities territories is a gradual process and the increase in the capacity of preschool educational institutions should correspond to the development rate. Table 2 shows that in case of the standard access distance the construction of educational institutions should be carried out simultaneously, but really it occurs in the further construction phases. It is obvious that such a kind of the community development has certain disadvantages—firstly, it is the absence of social infrastructure assets for a long period of time (if their construction is included into the further construction phases) and, secondly, it is their scattered location (which corresponds to the rate of the cottage community development and to the master site plan. That is why the design and location planning of education facilities should be a stage by stage process.

During the stage by stage and integrated development of the cottage communities we do not face the problems mentioned above. It also increases the availability index for the functions typical of ecopositivity theory communities because the distance and time access is one of their basic characteristics [18].

Thus, accepting the higher comfort access distance—300 m (the same as for urban communities)—enables to design and construct a network of educational institutions which will include the central building—a cultural and educational center fulfilling the education, leisure and sport functions—as well as the network of small-size ungraded kindergartens or family childcare groups located some distance away and constructed when required within every next construction phase. This will both improve the quality of life in a cottage community and make the educational institution an attractive investment

since it also provides supplementary education, entertainment and sport activities. The construction also requires less land and fewer utility lines due to the integration of the equivalent zones of a kindergarten and a school.

A stage by stage development is more convenient. It implies firstly the construction of the central unit or building. In case of preschools the access distance should be 300 m and this project also includes a network of family childcare groups located 300 m away from the central unit. Such a network helps to increase the capacity of an educational institution gradually and simultaneously with the construction of a cottage housing development. The access distance (radius) for schools should be 500 m in the higher comfort zones and 1 km in standard conditions [18]. The shorter is the access distance, the more comfortable is the community; the construction of the core support unit in the central building which will cover the needs of the whole network will decrease the costs on the construction and operation of the facilities.

The author (Novitskaya E.S.) proposed a systematization of the types of educational institutions in sequence to reduce the number of students:

Center for Comprehensive Education / (CKO), it includes a kindergarten, a secondary school, a sports and leisure center.

The main block of the network of educational institutions. It represents the building in which the school, kindergarten, general developmental sports function, cultural and creative function are located [19].

A kindergarten in the same building as a secondary school.

A kindergarten combined in the same building with a primary school [19].

Type 2 and Type 3 education facilities have certain characteristics: a kindergarten and a primary school share the sports centre, the kitchen and canteen unit, the assembly hall and activity rooms.

Type 3 shows that the functional units of the kindergarten and school are separated in distance but they share such zones as the kitchen and canteen, the assembly hall and the sports centre. Such a planning and layout concept enables a gradual transition of a child from one educational stage to another. The existing succession and familiar surroundings help children to avoid stress which is very important considering the fast development of the present-day information society and the increase of the school curriculum basic study load [19].

A kindergarten combined with a residential house [19]:

1. an allotment type—in this case there is a big land lot (10–15 ares) near the house. The organization of a kindergarten can require the replanning and remodeling of the existing house (if the area size of the house is sufficient) or the construction of an adjacent building. A mini-kindergarten can also be constructed on this land lot near the house (if the owners wish, it is possible to repurpose and redesign the existing housing units if there are proper conditions and certain needs for it).
2. an ungraded kindergarten incorporated with a single-detached residential house—in this case the kindergarten is located on the ground floor while the dwellers inhabit the upper floors (the construction of such a building is suggested during the design and layout planning stage).

Such types of preschools are the components of the preschool facilities network in a community, they help to maintain the proper access distance (radius). These preschools are "satellites" or branches of the central kindergarten, and in case it is absent or located at a considerable distance they are the only options for education, supervision and socialization of preschool children [19].

Listed below are the principles guidelines of the educational institutions layout within the housing developments which should be followed to provide the proper location for the types of preschools and schools that were proposed by the authors. These principles take into consideration the whole range of the criteria which influence the location of the educational institutions in suburban communities as well as the space and layout aspects of the master site plans.

The principle of comfortable access. Nowadays in the Russian Federation the residential developments undergo some social and economic reformations which also influence certain designing and planning aspects. These reformations related to economic, legal and land use aspects also affect the implementation of the principle mentioned above which means that there should be some new approaches to the location of educational facilities, including preschools, during the housing developments planning. The communities residents need social infrastructure assets, schools and preschools in particular, on a daily basis, that is why, it is essential to provide the spatial accessibility of educational institutions and to maintain the proper access distance (radius) according to the rural and urban planning specifications [19].

The authors have proposed a model of the network structure for the preschool educational institutions layout as the most reasonable from functional, social and economic perspectives. This model should provide the proper access distance (radius) and it can vary depending on specific design and planning conditions.

The principle of social service facilities cooperation. This principle is related to the social service facilities in cottage communities. This principle is advisable for a cottage community not only from a design and planning perspective, but also as an economic benefit because it implies the integration of educational, sport and entertainment facilities.

The principle of increasing the living environment functions. The essence of this principle is combining the facilities of different functional types within the residential housing development (mixed-use buildings for both residential and business or other purposes) [20, 21].

The network structure of the master plan for single-detached suburban communities helps to avoid certain problems related to the access distance (radius) of educational institutions (also it is possible to reduce the access radius to the city development standards) and to provide the entertainment and sports facilities for the inhabitants of a cottage community.

Considering in detail the space and layout planning of the proper types of educational institutions for single-detached suburban communities it would be reasonable to point out the guidelines for creating the master plan of each facility belonging to a definite type.

One of the types of the educational institutions which we defined as necessary while analyzing the designing planning of single-detached suburban communities is a large

educational centre (EC) which includes a preschool, a school (middle or secondary) and an entertainment and sports unit.

Educational centres are the basic components of the general network planning for the housing development. Their design and planning depend on the types of the functional units that they include and comply with the major requirements applied to the master site plans. These requirements are: following the zoning rules, avoiding the overlapping of crowd and utility flows, providing the spatial continuity of a facility.

The basic principles/guidelines for devising the educational centres master site plans are:

the principle of area zoning (the spatial separation for the children of different ages);

the principle of social facilities cooperation.

A kindergarten built into the cottage.

This is a special type of a facility, its design and planning should comply with the following principle:

the principle of the area zoning (spatial separation of the kindergarten area from the residential area);

A family childcare group/ a family kindergarten can function properly only if the children supervision area is separated from the utility area which also is a health and hygiene requirement. The residents and the kindergarten children should use different entrances. The major site plan of the housing development should also include guest parking spaces for the parents who bring their children to the kindergarten. The calculation of the places should be based on the 50% of the kindergarten expected attendance [22–24].

4 Conclusions

In this article we have defined the types of educational institutions and proposed the principles of their rational layout within single-detached suburban communities as well as the improvements to their master plans.

1. We think it is reasonable to introduce the network structure of educational institutions which consists of the central educational complex (EC) including a kindergarten, a school (primary, middle and secondary), entertainment and sports facilities as well as the network of the family childcare groups/ family kindergartens which are connected with the central educational complex. Such a planning concept helps to solve the problems related to the access distance (radius) (it is also possible to reduce it) and to the lack, or complete absence of preschools in suburban communities. It also provides the community residents with entertainment and sports facilities. The model of the educational institutions network that the authors have proposed helps to solve social problems and is economically efficient because it reduces the site area due to the elimination of the some functional units and implies the multipurpose use of the entertainment and sports assets by the community residents.
2. The possibility of organizing family kindergartens will enable women who have several children to set up family childcare groups which will solve the problems of

unemployment and the lack of educational places in the central educational unit. It is also possible to organize special kindergartens which concentrate on certain spheres of children development. One more advantage is a small number of children in such kindergartens which is favorable for children's psychological state and creates appropriate health and hygiene conditions. Such a network structure does not have any major disadvantages, that is why, it is reasonable and efficient.

3. By making the educational environment accessible to both children and adults, we solve important social problems. Pedestrian and transport accessibility of institutions of the first stage of service of settlements, such as kindergartens and schools, is provided, in addition to this, a place is created for the development of physical abilities and creative potential of children.

References

1. Territorialnyi organ federalnoi sluzhby gosudarstvennoi statistiki po Orlovskoi oblasti. Rozhdaemost, smertnost, i estestvennyi prirost ubyl naseleniya v Orlovskoi oblasti (The Orel region office of the Russian Federation State Statistics Service. Birth and death rates, natural increase and decrease in the population of the Orel region). http://orel.gks.ru/wps/wcm/connect/rosstat_ts/orel/ru/statistics/population/. Accessed 08 Sept 2021

2. Rossiiskii statisticheskii ezhegodnik (The Russian Federation statistical yearbook) http://www.gks.ru/wps/wcm/connect/rosstat_main/rosstat/ru/statistics/publications/catalog/. Accessed 08 Sept 2021

3. Ilyichyov VA (2011) Biosfernaya sovmestimost: Tehnologii vnedreniya innovatsiy. Goroda, razvivayuschie lyudei (Biosphere compatibility: the technology of innovations implementation. The cities which develop people). Book House "LIBROKOM", Moscow (in Russian)

4. Bakaeva NV, Chernyaeva IV (2016) Funktsii biosferosovmestimogo goroda I ih dostupnost cheloveku (The functions of a biosphere-compatible city and their accessibility). Building and reconstruction, FSBEI HE "SWSU". Kursk, pp 64–74

5. Ilyichyov VA (2010) Printsipy preobrazovaniya goroda v biosferosovmestimyi I razvivayuschii cheloveka (The principles of biosphere-compatible and development oriented city transformations). Ind Civil Eng 6:3–13

6. Ilyichyov VA (2010) Mozhet li gorod byt biosferosovmestimym i razvivat cheloveka? (Can a city be biosphere-compatible and development-oriented?). Arhitektura i stroitelstvo Moskvy (Architecture and construction in Moscow) 2(544):8–13

7. Kottedzhnye posyolki goroda Orla (The cottage community of Orel). http://www.realtyse.net. Accessed 08 May 2021

8. Kottedzhnye posyolok Platonovo (Cottage community Platonovo]. http://invcorp.ru/plots/platonovo/. Accessed 08 May 2021

9. Kottedzhnye posyolok Edelveis (Cottage community Edelweiss). http://invcorp.ru/plots/edelvejs/. Accessed 08 May 2021

10. Kottedzhnye posyolok Malaya Kulikovka (Cottage community Malaya Kulikovka). http://invcorp.ru/plots/malaya_kulikovka/. Accessed 08 May 2021

11. Kottedzhnye posyolok Saburovo (Cottage community Saburovo). http://invcorp.ru/plots/saburovo/. Accessed 08 May 2021

12. Kottedzhnye posyolok Novaya Kulikovka (Cottage community Novaya Kulikovka). http://xn--57-6kceo0fn2eh.xn--p1ai/novaya-kulikovka/. Accessed 08 May 2021

13. Kottedzhnye posyolok Zelyonye Berega (Cottage community Zelyonye Berega). http://xn--80abggaabam5bxa3b5j.xn--p1ai/зелныеберега. Accessed 08 May 2021
14. Kottedzhnye posyolok Mechta (Cottage community Mechta). http://xn--80ajuzbag2a.xn--p1ai. Accessed 08 May 2021
15. Pravila zemlepolzovaniya i zastroyki gorodskogo okruga "Gorod Oryol" (The regulations for the land use and development of the urban district "Orel city"). http://www.orel-adm.ru/index.php?option=com_k2&view=itemlist&task=category&id=221:pravila-zemlepolzovaniya-i-zastroyki-gorodskogo-okruga-gorod-oryol. Accessed 08 May 2021
16. Design and construction specifications 42.1330 "Building regulations 2.07.01–89** Urban planning. Design and construction of urban and rural housing developments" (1994)
17. Novitskaya ES, Kolesnikova TN (2016) Improving the basic classification of the preschool educational institutions for single-detached suburban communities. In: Proceedings of the construction-2016: the 2nd Bryansk international innovation meeting, Bryansk, 1 Dec 2016, vol 2, p 264
18. Kolesnikova TN, Novitskaya ES (2012) Problemy ekopozitivnogo gradostroitelnogo razmescheniya i formirovaniya generalnyh planov detskih doshkolnyh uchrezhdeniy prigorodnyh poseleniy individualnoy zastroyki (The problems of the eco-positive layout and developing the master plans of preschools for single-detached suburban communities). Building and reconstruction. FSBEI HPE "State University—SRPC", Orel, pp 69–75
19. Novitskaya ES, Kolesnikova TN (2018) Koncepciya arhitekturno-gradostroitel'noj organizacii seti obrazovatel'nyh uchrezhdenij v usloviyah poselenij individual'noj zastrojki na osnove paradigmy biosferosovmestimosti (The concept of the architectural and urban organization of the network of educational institutions in conditions of settlement of individual development based on the paradigm of biosphere-compatibility). Biosphere compatibility: person, region, technology. Southwestern State University, Kursk, pp 27–39
20. Doxiadis CA (1968) Ekistics. An introduction to the science of human settlements. Leningrad
21. Virt L (2005) Urbanizm kak obraz zhizni. Izbrannye raboty po sotsiologii. (Urbanism as a way of life. Selected texts on sociology). Moscow (in Russian)
22. Prioritetnyi natsionalnyi proekt "Detskie sady – detyam" (National priority project "Kindergartens for children"). http://www.dumahmao.ru/right/smi/pressrelizes/2010/09/17/pressrelizes_2890.html. Accessed 08 May 2021
23. Prioritetnyi natsionalnyi proekt "Dostupnoe i komfortnoe zhilyo – grazhdanam Rossii" (National priority project "Affordable and comfortable dwelling for Russian citizens"). http://www.prime-realty.ru/new/nv29.htm#1. Accessed 08 May 2021
24. Potrebnost v detskih uchrezhdeniyah (The need for educational institutions for children). http://ria.ru/society/20130130/920555983.html. Accessed 08 May 2021

A Right to the City: Environmental Safety and Comfort in the City

N. Antonova[1]([✉]), S. Abramova[1], A. Gurarii[1], and P. Antonova[2]

[1] Ural Federal University, 19 Mira St, 620002 Yekaterinburg, Russia
`n.l.antonova@urfu.ru`
[2] St Petersburg University, 13B Universitetskaya Emb., Saint Petersburg 199034, Russia

Abstract. The article examines environmental safety as a condition for exercising the right to the city by young people. Based on the survey data (n = 800) of young people in the city of Yekaterinburg (Russia), we found that the city's natural environment is one of the factors that influences the young people's choice of territory for their future residence. Young people are ready to engage in various environmental activism practices and transform the world around them. Every fourth respondent is prepared to engage in environmental protection. Young people express an explicit request for the development of parks, gardens, green areas and squares. The aspiration to live in a clean and tidy city becomes one of the fundamental motives. The city's natural environment is perceived as an open platform for exercising the right to the city, which potentially provides an opportunity for citizens' initiatives. However, the lack of belief in the possibility of achieving positive changes becomes the main reason for the refusal of citizens to participate in urban projects. One of the practical recommendations is to establish a youth group under the architectural and urban planning council of the city of Yekaterinburg, which may contribute to the discussion of architectural and urban planning projects of particular importance for the city's social, economic, and cultural development from the viewpoint of young people. In addition, it is recommended to raise environmental awareness, further development of environmental activism, and continuing a dialogue with local government and businesses.

Keywords: Right to the city · City · Environmental safety · Environmental activism · Youth

1 Introduction

For more than a decade, environmental safety has been discussed among the research community and included in the agenda of the government agencies responsible for the development of territories [1–37]. In accordance with the Environmental Protection Act No. 7-FZ, the concept of the environmental safety is defined as the state of protection of the natural environment and vital human interests from the possible negative impact of economic and other activities, natural and technogenic emergencies, and their consequences.

The impact of nature-transforming human activities is increasing both in scale and degree. This is becoming a threat to the environment and a new challenge to human existence. The causes for the unfavourable environmental situation in Russia are as follows: an increase in the number of hazardous industrial and household waste; emissions of harmful substances into the atmosphere; discharge of harmful substances into water reservoirs; irrational land use; disposal of radioactive and chemical waste; the residual principle of financing environmental projects and activities; and weak environmental legislation.

Along with the external conditions for the development of environmental safety, it is also essential to highlight the subjective component. It manifests in the environmental conscience of the population or, in other words, an individual's awareness of the degree of protection of one's meaningful needs and interests from possible anthropogenic and natural negative impact. Such exposure can lead to poor health and a decrease in the quality of life.

The development of an environmental conscience is an essential and effective tool for the nation's survival in the face of environmental challenges and dangers. The sustainable development of society needs a paradigm shift: a transition from economic to environmental priorities. This may lead to the change of people's conscience and the 'reassembly' of the values in the context of understanding environmental challenges and the responsibility of each person in addressing them. Changing consumer behaviour towards nature may be possible through increasing environmental culture. Therefore, environmental awareness of people is becoming an effective mechanism for the prosperity of future generations.

More than half of the world's population now lives in cities. According to the forecasts, in 2050, the urban population may reach 70% [33], with urban areas expected to absorb virtually all of the world's population growth.

The increasing urban development opens a wide range of opportunities, but it also poses challenges. Today, modern cities face many problems: air, water and soil pollution, traffic congestion, noise, and others. Therefore, the current agenda moves in the direction of the city openness, safety, vitality and sustainability. Such cities become the point of attraction for young people who are seen as a key driver of the innovative development of the city.

In a situation of competition for human capital, cities need to make more efforts in creating conditions for the preservation and growth of human capital and organising the living space in such a way as to satisfy the citizens' needs. Young people are of particular importance for the successful functioning of the city, since they become a key resource for the intellectual and innovative development of a territory.

Youth is a period of planning one's future [7, 19, 36]. During these years, various scenarios for constructing the image of the future and strategies and tactics for moving towards it are being made. Modern Russian youth is characterised by pragmatism and independence; they accept and exercise responsibility for implementing their 'life projects'.

The city's natural environment is one of the factors that influences the young people's choice of territory for their future residence and achieving their life goals. The creation of favourable conditions for work, life, and leisure, along with maintaining the environment

and sanitary well-being of the population are the main criteria for the quality of life. Thus, studying the factors of the urban environment to ensure the environmental safety of the urban population, including young people, becomes an urgent issue.

2 Materials and Methods

Environmental safety can be seen as exercising of the right to the city. The right to the city is one of the topical issues in modern urban studies. According to the French sociologist Henri Lefebvre [16], the right to the city is the right of citizens to use the opportunities and resources of the city (facilities and infrastructure). It is the right of the urban population to reproduce and develop the urban environment, satisfy their needs, change the city according to these needs, and declare their interests. David Harvey rightly asserts that by changing the city a person changes oneself [12].

In line with the doctrine of the right to the city, it can be argued that the citizens have the right to a safe environment. A safe environment, in its turn, makes it possible to satisfy the diversity of the needs of young people while maintaining an urban lifestyle. In line with that, the interests of young people are 'determined' by the natural environment of a particular territory. For instance, clean water reservoirs with a developed adjacent public catering system speak for the satisfaction of the leisure needs of young people. In contrast, a polluted water reservoir can cause migration or manifest in eco-activism.

On the one hand, rapid global urbanisation provokes environmental stress, but, on the other hand, unveils the benefits for the well-being and health of the urban population (availability of hot water, electricity, a developed network of shops, medical institutions, and others) [8, 29, 34]. For example, a developed transport system can be considered an undoubted advantage of a large city. However, it can also become the cause of an environmental collapse since cars are one of the leaders in urban air pollution and the primary source of lead, zinc, cadmium, and nickel in the environment [5, 9, 22].

This is where the contradiction lies in making the city environmentally friendly while not sacrificing opportunities to maintain an urban lifestyle. An ideal city from the point of view of environmental safety, perhaps, does not exist. There are instances of eco-settlements as a new trend in spatial distribution, but they are not in high demand among young people. Young people strive for a high level of consumption, but the waste and the products of its recycling may not be environmentally friendly. Young people are focused on high mobility in everyday travel, but the developed transport network can ruin the ecosystem. Therefore, on the one hand, we are witnessing the appearance and implementation of innovative ideas aimed at the successful interaction of society and nature (for instance, alternative energy sources).

On the other hand, manufacturers, management and innovators often focus on environmental friendliness—ecological consumption and environmentally friendly transport—to deliver an environmental message to the urban space [11, 37]. Thus, today's demands are generating products and services that are claimed to be sustainable but cannot be so. There is no absolute environmental safety in the city.

The Sverdlovsk Region is one of the leading industrial and economically developed regions of Russia. According to its Strategy of Environmental Safety for the period up to 2020 [32], the state of the environment in the region is determined by the characteristics

of the regional development: high industrial pressure due to excessive concentration of industry, including predominantly environmentally hazardous production; long-term and continuous negative impact on nature, causing a significant reduction in the natural resource potential, and in some cases—their degradation; the use of outdated technologies and equipment with high resource and energy consumption of production, resulting in the accumulation of a significant amount of waste, pollution of soil, air and water basins, loss of biological diversity, and deterioration of the quality of the environment. We stress that the characteristics of the environment presented in the document indicate not its development but describe current topical environmental issues that require resolution. In other words, the Strategy reveals the key problem areas of the human environment.

Researchers found that the city ecosystem affects the health of its residents [3, 4, 10, 25, 28]. For instance, an extended stay of children in areas with a high concentration of harmful substances in the atmosphere contributes to respiratory diseases. Other environmental-related disorders such as cardiovascular diseases, congenital malformations, and others are also aggravated in an unfavourable environment.

Based on the analysis of mortality data (2000–2008), researchers from Switzerland found that the mortality rate decreases with an increase in the residence floor. In other words, the largest proportion of people with a history of respiratory diseases, diseases of the cardiovascular system, and cancer live not higher than the eighth floor [23].

A survey conducted by the Russian Public Opinion Research Centre [17] shows that for Russians in general, the more poignant challenges are the pollution of water areas: rivers, lakes, reservoirs (76%), garbage dumps (70%), air pollution (66%). At the same time, the spread of COVID-19 has become a factor that made the environmental agenda more pronounced: the pandemic made Russians think about the environment to a greater extent than before (25%). After the pandemic, people will start thinking about the environment more seriously (29%).

Researchers are actively studying the phenomenon of eco-anxiety, which is a fear of environmental disaster [6, 24]. They attribute it to a feeling of powerlessness about environmental change. The current Generation Z is characterised by a high level of concern related to climate change and the state of the environment in the world [20].

These concerns affect the planning for the future: what kind of world will I live in; in which city will I feel comfortable? The study of the future and its image is a set of typical characteristics of the life strategies of an individual or a group, projected in consciousness and behavioural practices. The image of the future is a process and result of a thought experiment; its content aspects are associated with both previous experience and ideas about the world order. The city in this regard acts as an urban geosystem.

Young people strive to choose an environmentally friendly city for their residence, on the one hand, and, on the other hand, to engage in designing an environmentally friendly and comfortable city, thus, exercising their right to the city in the spirit of Lefebvre. Young people articulate the need to develop urban space and participation in managing the territory; there is a feeling of responsibility before oneself and the next generations [2].

To study the participation of young people in practices for transforming the space around them, including those with an environmental focus, at the end of 2020, we

conducted an online survey of young people aged 18 to 30 in the city of Yekaterinburg (Russia). A total of 800 people ($n = 800$) were interviewed using a quota sampling: 60% females and 40% males. The employment characteristic was also controlled: 50% of respondents were studying, 44% working and 6% were neither working nor studying. This, in turn, determined the age distribution of the study participants: 18–22 years old—55%, 23 to 26—28%, and 27 to 30—17%. The survey consisted of 24 questions (closed-ended, open-ended, and semi-closed). The average time taken to complete the survey was 20 min. The data was analysed using the SPSS and subjected to frequency, cross-tabulation and correlation analysis to calculate a percentage and average indicators and correlation coefficients.

We also conducted 20 semi-structured individual interviews with students of the Ural Federal University named after the first President of Russia, Boris Yeltsin. We interviewed six males and 14 females enrolled in undergraduate programmes in humanities and social sciences. The students were in their 1st or 2nd years and did not have a history of outstanding academic requirements. The interviews were conducted in the students' free time. The average interview duration was 25 min. The questionnaire consisted of 10 questions. The participants were given the opportunity to formulate their own opinion independently. During the interview, two key topics were discussed: the image of an environmentally friendly city and the student participation practices in developing an environmentally safe urban environment. The interviews were transcribed and were subject to thematic analysis. That made it possible to identify the general and specific characteristics in the participants' responses, which facilitated their interpretation.

3   Results and Discussion

A significant number of urban youth feel responsible for what is happening in their environment: in their common outdoor areas and/or houses (60%) and in the city (37%). On the one hand, we see the orientation of young people towards local practices of transforming the space around them. On the other hand, such responsibility is based on an assessment of the potential for influencing the environmental processes in large urban centres and the inclusion of these processes in the area of young people's responsibility. While at the level of 'common outdoor area and/or house' 12% of the respondents believe that they cannot influence the development of the environment in any way, at the level of 'city' 28% see no possibility of influencing that.

When choosing the domains of city life in which they could personally influence what is happening, young residents of Yekaterinburg most often chose the domains of culture and arts (25%) along with the environmental domain—environmental protection, animal protection, and others (23%). Therefore, the environmental domain is perceived as sufficiently open for exercising the right to the city and potentially providing an opportunity for the citizens' initiatives. The expansion of knowledge and ideas about the environment domain as having a high personal and social importance and potential for action, a domain which is open for the implementation of socially significant projects and allowing to reveal the individual potential of young citizens through environmental activism makes it possible to overcome a barrier for youth participation in urban projects. Thus, 62% of respondents believe that it is the lack of belief in the possibility of achieving

positive changes that become the main reason for the refusal of citizens to participate in urban projects, including environmental ones.

Participation in specific city activities also confirms this perception. Among those surveyed who have participated in urban activism over the past year, 31% chose environmental activities (voluntary neighbourhood clean-up, landscaping of courtyards, planting trees, and others). We stress that this indicator is higher than participation in the activities of public and non-profit organisations (24%), participation in rallies (17%) and actions to help citizens in difficult life situations (11%).

The most important confirmation of the importance of the environmental factor is the analysis of the motivation for the civic engagement of young people. The aspiration to live in a clean and tidy city (58%) occupies the first place in the structure of their motives. Young people, in our opinion, personify the city, 'humanise' it, and believe that the environmental friendliness of urban space is the result of not only of the work of enterprises, transport, utilities but also begins with a person and one's aspiration to make the city clean and safe.

The results of the survey of young people show that respondents are ready to engage in various environmental activism practices and transform the world around them, following their ideas about environmental safety. In responding to an open-ended question, they argue that the city needs large areas of green spaces to reduce the adverse environmental effects and the level of anxiety: "… the green colour calms …, staying in the park relieves stress" (female, 19 years). Squares with green spaces can be included in the routes of daily movement to the places of work and study. In other words, within the city limits, these "third places" [21] will be in demand by young people as transit travel.

The idea of the environmental attractiveness of the city assumes that green zones become not only an ecological factor and a visual background of the city, but also carry an emotional and associative message and, thus, become meaningful spaces [30], because they provide a venue for dates, walks with children, sports, and other activities. Parks and green squares are a factor of the present and the future of comfortable living in the city [1]. Green areas are designed to give positive emotions and to encourage feelings that are not easily attainable in the streets in everyday travel, at work, or in studies.

The participants emphasise that the goal of living in an environmentally safe city can only be achieved with civic participation: '*Everyone needs to realise that it depends on them which city they will be living in*' (female, 18 years old). The young people express that, in addition to participating in volunteer clean-ups and landscaping the territory, they are ready to engage in the awareness campaigns: '*I can organise friends through social networks for some actions for protecting the nature. I can also distribute flyers; I have the experience*' (female, 20 years).

Every second participant has taken part in environmental campaigns held at different, including international, levels. For instance, one of the participants notes: '*On March 27, 2021, in Yekaterinburg, I took part in the Earth Hour international initiative. My friends and I decided that it would be the right thing to do! First, it allowed us to join an international project; we became a part of something immense and understood that other people on the planet support the environment. Second, this is our gratitude to nature, our 'thanks' to it*' (female, 19 years old).

At the city level, the participants name such environmental projects as Green Spring, Bottle Caps for Kids, and Water of Russia. '*Environmental actions are essential; they lead to the unity of people. We are not alone; we love nature, we make our city cleaner*' (female, 18 years old).

Group types of environmental activities, according to the participants, perform a function of communication, a function of cooperation, and play a psychotherapeutic role: '*Participation in group activities makes it possible to 'feel the shoulder of a friend'. You feel less psychological tension as you understand that other concerned people are around, and you are doing the right thing together. It brings a feeling of joy and satisfaction*' (male, 20 years old).

Petukhov emphasises that it becomes vital for modern Russian society to develop the responsibility of citizens and a sense of belonging '*with everything that happens around them—from their courtyard to the country as a whole*' [26].

Along with group activities aimed at creating a safe environment, the participants also name individual practices that become routine and replicated in everyday life. According to the participants, such socially responsible behaviour leads to the development of environmental conscience, which '*will be passed on from generation to generation*' (female, 20 years old).

First, the actions related to sorting waste occupy the leading position among such practices: '*I put plastic bottles into a separate container*' (female, 18 years old); '*I always dispose of batteries separately from other waste, and I urge everyone to do so*' (male, 20 years old).

Waste collection and disposal is one of today's global challenges [13, 27]. The participants note that '*the city government should fundamentally solve the issue of separate waste collection: different waste bins should be placed in the city and different containers—in the courtyards, which is not the case now*' (female, 20 years old).

The participants indicated that at present, they have to cover considerable distances to fulfil their need for separate waste collection: '*I collect plastic bottles at home and bring them to the next courtyard because there is a plastic container*' (female, 19 years old).

Second, the students indicate that they use environmentally friendly transport in their daily travels during warm seasons: '*A bicycle is the only way I move around. It is convenient and makes the city cleaner*' (female, 19 years old).

A great deal of experience has been accumulated in the design of environmentally friendly transport: from the improvement of internal combustion engines and the use of alternative fuels to the use of an electric drive. At the same time, according to the participants, it is necessary to '*limit travel by private cars, make all parking lots in the centre paid and expensive, change to public transport, use bicycles and walk; only in this way can we show concern for nature*' (female, 18 years old).

Third, one-fifth of the participants note the importance of the transformation of consumer behaviour practices: '*I refrain from impulsive purchases*' (female, 20 years old); '*I don't use aerosols*' (male, 19 years old); '*I shop in second-hand stores*' (female, 18 years old).

In this case, they are talking about responsible consumption. Researchers emphasise that responsible consumption is based on environmental values and the social consequences of individual consumer choice [18, 35, 38].

The young people develop the environment of the city, creating comfort and safety for their lives. The practices of civic participation (both group and individual) in the production of city space should be considered a tool for exercising the right to the city, an act of socially responsible behaviour and a factor in the formation of local identity. When changing the space of the city, young people fill it with new deep meanings. As one of the participants notes: '*At school, we used to clean up the territory and plant apple trees. I didn't want to do it back then, but now I even go to school on purpose and watch how my apple tree grows. I feel proud*' (male, 20 years old).

Urban youth also expressed a willingness to participate in the design of an environmentally friendly urban environment: '*Our participation in the city planning committee should be arranged; we have our environmental requests for the city*' (female, 20 years old).

The active focus of youth's interest in citizens' influence on solving environmental safety problems can be attributed to one of the fundamental contradictions of a large industrial city. On the one hand, young Yekaterinburg residents highly appreciate the original natural conditions of the city's location (the beauty of nature, landscape, and the lakes and forests surrounding the city). On the other hand, they rank low the current state of the environmental situation and the cleanliness of urban space.

It should be emphasised that the environmental safety of the urban environment is one of the leading factors in their decision to change the place of residence. An analysis of the migration attitudes of young people showed that an adverse environmental situation in the city of residence could be the reason for migration for almost every second respondent. This is evidenced by the results of our pilot study conducted in Yekaterinburg in 2019 (n = 200) [1].

Despite a wide range of events organised by the municipal authorities of Yekaterinburg within the framework of the Year of Ecology (2017), 34% of respondents explain their readiness to engage in the transformation of the city space by the inability of the authorities to solve this challenge effectively. As was noted by one of the participants: '*Start with yourself, don't expect the government to do something for you. Ride a bicycle, don't use plastic, clean up the courtyard, plant a tree, paint a bench. If everyone makes a small contribution to the city environment, the city will become cleaner and more beautiful*' (female, 20 years old).

The participants emphasised that green park areas and separate waste collection should be considered when planning and designing new city residential areas. In addition, they note: '*All harmful industries should be taken out of the city. One should think not about economic gains but environment*' (male, 20 years old).

Interaction with the city government and its urban planning departments may contribute to addressing the environmental requests of young people and exercising their right to live in a clean, attractive and environmentally friendly city.

4   Conclusion

In general, the research data allows us to come to the following conclusions. The main goal of the environmental safety is to ensure the high-quality living of modern and future generations in the face of the increasing environmental anthropogenic, technogenic, natural threats, and preservation of the environment. The environmental factor in the life plans of young people today is one of the leading in choosing the place of future residence. An unfavourable environmental situation is a basis for the formation of fears of young people and an increase in the level of anxiety. The youth of a large industrial city is mostly ready to engage in transforming urban space according to their needs and demands, including engaging in eco-activism. The aspiration to live in a clean and tidy city becomes a leading life motive. Reducing the environmental anxiety of young people is seen as important. It is necessary to strengthen the raising of environmental awareness at the level of institutional structures (family, school, and university), along with the development of environmental activism and participation in environmental projects and movements. In addition, we suggest establishing a youth group under the architectural and urban planning council of the city of Yekaterinburg. This may contribute to the discussion of architectural and urban planning projects of particular importance for the city's social, economic, and cultural development from the viewpoint of young people.

References

1. Abramova S, Antonova N, Pimenova O (2019) Attractiveness of a city as a factor of territorial mobility in student estimates (on the example of Ekaterinburg). Educ Sci J 21(1):97–123. https://doi.org/10.17853/1994-5639-2019-1-97-123
2. Antonova N, Abramova S, Polyakova V (2020) The right to the city: daily practices of youth and participation in the production of urban space. Monitor Public Opin Econ Soc Changes 3:384–403. https://doi.org/10.14515/monitoring.2020.3.1597
3. Babisch W, Kamp I (2009) Exposure-response relationship of the association between aircraft noise and the risk of hypertension. Noise Health 11:161–168. https://doi.org/10.4103/1463-1741.53363
4. Bai X, Nath I, Capon A et al (2012) Health and wellbeing in the changing urban environment: complex challenges, scientific responses, and the way forward. Curr Opin Environ Sustain 4:465–472. https://doi.org/10.1016/j.cosust.2012.09.009
5. Cai H, Xie S (2007) Estimation of vehicular emission inventories in China from 1980 to 2005. Atmos Environ 41:8963–8979. https://doi.org/10.1016/j.atmosenv.2007.08.019
6. Galea S, Freudenberg N, Vlahov D (2005) Cities and population health. Soc Sci Med 60:1017–1033. https://doi.org/10.1016/j.socscimed.2004.06.036
7. Carabelli G, Lyon L (2016) Young people's orientations to the future: Navigating the present and imagining the future. J Youth Studies 19(8):1110–1127. https://doi.org/10.1080/13676261.2016.1145641
8. Comtesse H, Ertl V, Hengst S et al (2021) Ecological grief as a response to environmental change: a mental health risk or functional response? Int J Environ Res Public Health 18(2):734. https://doi.org/10.3390/ijerph18020734

9. Davis L (2008) The effect of driving restrictions on air quality in Mexico City. J Polit Econ 116:38–81
10. Eckert S, Kohler S (2014) Urbanisation and health in developing countries: a systematic review. World Health Popul 15(1):7–20. https://doi.org/10.12927/whp.2014.23722
11. Hannula I, Reiner D (2019) Near-term potential of biofuels, electrofuels, and battery electric vehicles in decarbonizing road transport. Joule 3:2390–2402. https://doi.org/10.1016/j.joule.2019.08.013
12. Harvey D (2008) The right to the city. New Left Rev 53:23–40
13. Henry R, Zhao Y, Dong J (2006) Municipal solid waste management challenges in developing countries—Kenyan case study. Waste Manage 26:92–100. https://doi.org/10.1016/j.wasman.2005.03.007
14. Kaletnik G, Lutkovska S (2020) Strategic priorities of the system modernisation environmental safety under sustainable development. J Environ Manage Tour 11(5):1124–1131. https://doi.org/10.14505//jemt.v11.5(45).10
15. Kelly A (2017) Eco-anxiety at university: student experiences and academic perspectives on cultivating healthy emotional responses to the climate crisis. Independent study project (ISP) collection 2642. Available via the repository is a service of the SIT Graduate Institute/SIT Study Abroad Libraries. http://digitalcollections.sit.edu/isp_collection/2642. Accessed 15 Mar 2021
16. Lefebvre H (1996) Writings on cities. Blackwell, Oxford
17. Life after Greta Thunberg, or consumption amid global warming (2020). Russian Public Opinion Research Center. https://wciom.ru/analytical-reports/analiticheskii-doklad/zhizn-posle-grety-tunberg-ili-potreblenie-na-fone-globalnogo-potepleniya. Accessed 25 Mar 2021
18. Lindenberg S, Steg L (2007) Normative, gain and hedonic goal frames guiding environmental behavior. J Soc Iss 63:117–137. https://doi.org/10.1111/j.1540-4560.2007.00499.x
19. Lundqvist C (2019) Time horizons in young people's career narratives—strategies, temporal orientations and imagined parallel futures negotiated in local settings. Edu Inq 4:379–396. https://doi.org/10.1080/20004508.2019.1601000
20. Morgunov B, Bagin A, Kozeltsev M, Terentiev A (2017) Problems of environmental safety of Russia in the light of the «green» growth concept. Ekologiya cheloveka (Hum Ecol) 4:3–11. https://doi.org/10.33396/1728-0869-2017-4-3-11
21. Oldenburg R (1999) The great good place: cafes, coffee shops, bookstores, bars, hair salons, and other hangouts at the heart of a community. Marlowe, New York
22. Olszewski P (2007) Singapore motorisation restraint and its implications on travel behaviour and urban sustainability. Transport 34:319–335. https://doi.org/10.1007/s11116-007-9115-y
23. Panczak R, Galobardes B, Spoerri A et al (2013) High life in the sky? Mortality by floor of residence in Switzerland. Eur J Epidemiol 28(6):453–462. https://doi.org/10.1007/s10654-013-9809-8
24. Panu P (2020) Anxiety and the ecological crisis: an analysis of eco-anxiety and climate anxiety. Sustainability 12(19):7836. https://doi.org/10.3390/su12197836
25. Pedersen E (2015) City dweller responses to multiple stressors intruding into their homes: noise, light, odour, and vibration. Int J Environ Res Public Health 12:3246–3263. https://doi.org/10.3390/ijerph120303246
26. Petukhov V (2019) Civic participation in Russia today: interaction of social and political practices. Sotsiologicheskie Issledovaniia 12:3–14. https://doi.org/10.31857/S01321625000 7743-0
27. Nyumah F, Charles J, Bamgboye I, Aremu A, Eisah J (2021) Generation, Characterisation and management practices of household solid wastes in Cowfield, Paynesville City, Liberia. J Geosci Environ Protect 9:113–127. https://doi.org/10.4236/gep.2021.94007
28. Rocha L, Thorson A, Lambiotte R (2015) The non-linear health consequences of living in larger cities. J Urban Health 92(5):785–799. https://doi.org/10.1007/s11524-015-9976-x

29. Rydin Y, Bleahu A, Davies M et al (2012) Shaping cities for health: Complexity and the planning of urban environments in the 21st century. Lancet 379:2079–2108. https://doi.org/10.1016/S0140-6736(12)60435-8

30. Simmel G (1984) Das Individuum und die Freiheit. Essais. Wagenbach, Berlin

31. Statuto A (2020) Overview of the of Arctic shipping role and ensuring of its environmental safety. Russian Arctic 9:5–16. https://doi.org/10.24411/2658-4255-2020-12091

32. The concept of environmental safety of the Sverdlovsk region for the period up to 2020 (2009) Available via Ministry of Economy and Territorial Development Sverdlovsk Region. http://economy.midural.ru/content/koncepciya-ekologicheskoy-bezopasnosti-sverdlovskoy-oblasti-na-period-do-2020-goda. Accessed 30 Mar 2021

33. United Nations, Department of Economic and Social Affairs, Population Division (2019). World population prospects 2019: Highlights (ST/ESA/SER.A/423). http://www.europeanmigrationlaw.eu/documents/UN-WorldPopulationProspects2019-Highlights.pdf. Accessed 19 Mar 2021

34. Vlahov D, Galea S (2003) Urban health: a new discipline. Lancet 362:1091–1092. https://doi.org/10.1016/S0140-6736(03)14499-6

35. Webster Jr (1975) Determining the characteristics of the socially conscious consumer. J Consum Res 2:188–196

36. Woodman D (2011) Young people and the future: multiple temporal orientations shaped in interaction with significant others. Young 19(2):111–128. https://doi.org/10.1177/110330881001900201

37. Zakirova M, Chuprina E (2018) Ensuring environmental Safetyin the conditions of environmental pollution by Cadmium. Urban Const Architect 8(1):59–62. https://doi.org/10.17673/Vestnik.2018.01.11

38. Zhang Q, Li X, Tian W et al (2014) Scenarios for vehicular air pollutant emissions abatement: a case study in Hangzhou, China. J Zhejiang Univ Sci A 15:753–760. https://doi.org/10.1631/jzus.A1400013

Impact of the Pandemic on the Sustainable Development of Metropolitan Residential Complexes

I. N. Maltseva[1]($\boxtimes$), E. S. Zhilyakova[1], and K. A. Tkachuk[2]

[1] First President of Russia B. N. Yeltsin, Ural Federal University, 19 Mira str., Yekaterinburg 620002, Russia
i.n.maltceva@urfu.ru
[2] Technical University of Munich, 21 Arcisstraße, 80333 Munich, Germany

Abstract. The article reviews sustainable architecture formation principles of the residential complex in Russia in the post-covid period. The situation has changed in three sociological coordinates: the usual way of life has been destroyed, the quality of life has been reduced with the threat of its radical fall, goals have changed and the possibility of long-term planning is lost. The authors conduct an analysis of the post-covid situation and derive new demands of citizens. It's about the cult of productivity has been replaced by a cult of health care, both physical and mental. Consequently, all vital structures should be within walking distance: centers for first aid and diagnostics, pharmacies, sports grounds and fitness centers. When designing residential complexes, emphasis should be placed on landscaping and improvement. New is the organization of spaces for urban agriculture. There is a return not to the pre-covid reality from which the population was expelled by the virus, but to a new state called the "new normal"—a life different from the previous one. The article reveals the concept and formulates the basic principles of the architectural design of quarter residential buildings, typical for large cities in different countries in modern conditions. The authors of this article confirm the need to unite the infrastructure in the space of the residential complex, which will ensure the satisfaction of the needs of all residents living in the residential unit. The new practice of urban planning implies the ability to live, work and spend leisure time within the same accessible territory. Architecture contributes to both the physical and emotional recovery of a person.

Keywords: Sustainability · Sustainable development · Pandemic · Residential complex · Architectural form · Comfortable urban environment

1   Introduction

The coronavirus pandemic has been a tremendous shock to the entire world. It has changed our lives, and it will definitely leave its marks on people's minds. Under the influence of the pandemic, a number of trends have emerged worldwide. The cult of productivity has been replaced by a cult of health care, both physical and mental. The

pandemic has accelerated digitalization, and the topic of sustainability and conscious consumption has taken a new stage of development. Increased attention is being paid to the aesthetic component of the surrounding environment.

Changes in people's consumption patterns entail new approaches in urban development. Some trends of post-covid architecture are given in articles by the Ukrainian architect Sergey Makhno and the founder of the architectural studio IND architects Amir Idiatulin [1, 2].

The format of multifunctional residential complexes, designed according to the "mixed-use" principle, is becoming dominant. The infrastructure of the residential complexes incorporates functionality that corresponds to a new way of life and thinking. Agriculture and biophilic architecture are integrated into the urban space, extending the topic of sustainable housing constructed with natural building materials and renewable energy sources [3].

The first project of post-covid housing was presented by Guallart Architects [4]. The project is positioned as a self-sufficient complex designed to provide its residents with everything they need. Similar typologies are used in competition projects for the development of a former industrial site in the city of Nachod (Czech Republic) [5], and Mid-Sity from AUX architect in Los Angeles, USA [6].

In Russia, there are not many residential complexes that take into account the new needs, or they are expensive and belong to a business or elite classes. Based on foreign experience, it is possible to create a model of a residential complex that reflects new values and needs [7].

2 Research Methodology

In the spring of 2020, architects, urbanists and sociologists made predictions about how urban architecture might change under the influence of the pandemic. Two main approaches to the formation of the residential architecture of the city could be distinguished. The first and most popular approach was the concept of deurbanization, advocated by the American urbanist Joel Kotkin, who predicted the acceleration of the era of megacities ending [8]. The second group of experts spoke about the transformation of the city while maintaining the urban density, in particular, this mentioned Richard Florida, an American sociologist and economist [8]. Both groups based their predictions on historical facts and experiences from past pandemics.

Today, a year and a half after the start of the pandemic, it is clear that we will not leave urban spaces, but a new approach to the formation of the urban environment should appear, motivated by a change in people's behavior patterns. Proof of the need for changes can be found in the studies carried out by the CoronaFOM association, which are based on the method of sociological surveys, as the primary source of collecting information about the way of life from citizens during a pandemic [9, 10].

There is a clear direction of the residential architecture development—multifunctionality, pedestrian accessibility and socially focused. Urbanists are massively turning to the concept of a 15-min city, the founder of which is the Franco-Colombian urbanist Carlos Moreno [11]. The concept is based on the pedestrian accessibility of all vital locations and a variety of buildings and functional content, see Fig. 1.

Fig. 1 15-min city scheme for Paris. *Source* https://medium.com/

This approach is also valid for special cases of designing residential complexes and is elaborated in the "mixed-use" typology. Robert Winkel, head of the Dutch architectural bureau Mei Architects and planners, has shown the validity of this approach in practice, using it in his projects. "An important aspect of the success of residential projects is the mixing of functions. Thanks to such a variety of uses, the building is teeming with life" are the words of Robert Winkel [12].

An advocate of living architecture is the mathematician and architectural theorist Nikos A. Salingaros. Salingaros proposed an alternative theoretical approach to architecture and urbanism that is more adapted to human needs and combines rigorous scientific analysis with a deep intuitive experience. Salingaros talks about the direct impact of architecture on human health and the pernicious effect of modernist architecture. This is why it is so important to create a healthy urban environment. Nikos A. Salingaros draws on mathematical logic and gives a set of tools and algorithms that can be applied to design a vibrant and healthy urban environment that obeys the ideas of sustainable architecture [13]. Based on these algorithms, a mathematical model of a sustainable residential complex can be proposed. Combining this model with the necessary social content, which is set by new needs, we get the formula for a post-covid residential complex [14].

2.1 Lifestyle Changes and New Needs

The pandemic changes the living conditions of people and, as a consequence, the situation changes along with three major sociological coordinates:

- Way of life—its habitual structure is shattered
- Quality of life—achieved quality of life is declining and threatened by a further radical decline
- Meaning of life—previous goals and plans change, the possibility of long-term planning is lost

The restrictions imposed on urban residents during the period of self-isolation, for the most part, led to negative social consequences. Today, as the crisis recedes, there is a return not to the pre-covid reality from which the population was expelled by the virus, but to a new state called the "new normal"—a life different from the previous one [9].

According to the latest sociological studies, Russians continue to significantly limit social contacts and visits to crowded places, regardless of the vaccination factor, see Fig. 2. The income of the population continues to decline, which causes a sense of instability, mental ill-being in the face of the current situation.

SOCIAL CONTACTS
■ More often ■ Less often ■ Same as before ■ Don't know
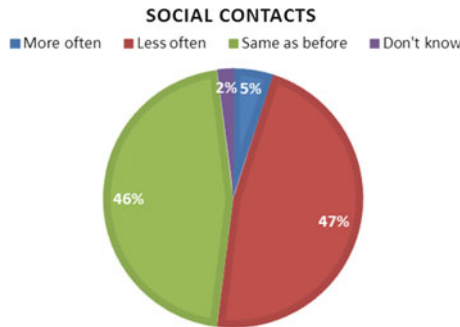
Fig. 2 Dynamics of social contacts for the period March–April 2021

Remote work became an option for the "new normal". During isolation, satisfaction with remote work increases, but limited social contacts remain a major problem.

At a time when the fear of illness persists, it is not the medication that becomes fundamental in health care, but the prevention of illness and strengthening of immunity through a healthy lifestyle, including a balanced diet, sports activity, and stress reduction. This is followed by the preference for walking and the use of individual mobility means of transport. And not only cars, but also bicycles, scooters, scooters, etc. Awareness and demand for ecological consumption are growing.

There are increasing requirements for surrounding visual content as one of the main factors influencing the emotional background and the creation of a comfortable living environment. Today, high demands are imposed not only on business and elite class housing, but also on economy class housing.

3 The Solution—Multi-functional Housing

A new way of life leads to the emergence of new human needs, which, in turn, require the development of new standards for infill of residential buildings and adjacent spaces. From the above data, it follows that it is necessary to combine the infrastructure in the space of the residential complex, which will ensure that the needs of all residents living in the residential unit are met. The concept of a multifunctional residential building takes on new meaning. The prevailing circumstances make it necessary to design the entire basic social structure within walking distance so that the space is comfortable both during the pandemic and after it, meeting the new emerging needs of residents [15].

Under the influence of the pandemic, "mixed-used development" becomes the most researched and implemented. As a result, in almost all megacities of the world, the idea of "the necessary is always there" is embodied. The new practice of urban planning implies the ability to live, work and spend leisure time within the same accessible area. In the worlds, it has long been the norm to combine more than three functions in one object [16–18]. We still have a few projects with more than two functions conceived at the starting point.

In Russia, similar principles of housing arrangement were applied in the architectural concepts of constructivism and functionalism for the construction of communal houses, in which an attempt was made to transform architectural solutions for the new concept of everyday life organization: saving apartment space and organizing infrastructure by transferring functions to public spaces: canteens, bath houses, cultural centers, etc.

However, the organization of these houses came from the socialist utopians' idea of creating a "new mass man". In the context of the ideology of industrialization, this concept of Soviet life was aimed at solving the problem of optimizing the distribution of domestic needs in order to free up as much energy as possible for production tasks.

In the new reality, these ideas become a solution to the problem of providing a comfortable living. The residential complex and its content should be shaped by the lifestyle and needs of the dweller [19, 20].

In the contemporary model, we must see the content that provides a comfortable living environment in the conditions of the "new normal". Two interconnected logical tasks that define the transformation of buildings and streets are multifunctionality and sociality. As many processes as possible must be integrated into a building. Therefore, mandatory attributes of modern urban housing are:

1. Retail. Commercial spaces to provide the necessary goods and services. This should include the provision of food and household goods, beauty salon services, etc. This aspect should be thought out by the developer at the stage of project preparation.
2. Integrated workspace. Coworking is becoming a new necessary component that should be included in the residential complex similar to retail retail on the ground floor.
3. Elements ensuring the health of residents. Pharmacies and medical centers for first aid and diagnostics. Sports facilities are integrated into courtyards and fitness centers to provide basic physical activity.

4. Safety, including security and access control. Also, this can include health and safety elements, including environmentally friendly finishing materials, easy-to-sanitize materials and good ventilation to reduce the concentration of harmful substances.
5. Environmental sustainability, provided by a range of measures, from eco-friendly building materials to energy-efficient technologies.
6. Landscape design and pedestrian focus. 15 min walking distance. Urban agriculture. The first foreign concept of a post-covid residential complex reflects all the necessary principles, see Fig. 3. [10].

Fig. 3 Post-covid residential complex, Arch. Bureau Guallart Architects, project, 2020., Xiong'an, China. *Source* https://archi.ru/world/87046/gorod-na-samoobespechenii

7. Aesthetics and visual sustainability. The visual component should be designed taking into account the peculiarities of the influence of architectural forms on the human psyche.
8. Multiple typologies of housing in one complex. Combining several housing classes in one residential complex provides an opportunity to create a diverse social environment and avoid the segregation of districts. The expansion of the range of residential units in one residential formation also leads to a development variety.
9. Kindergartens and educational facilities within the residential complex. An essential component for families with children.
10. Communication and socialization. Neighborhood centers will bring back a culture of neighborliness, which will also increase the security of the residential complex and its adaptivity to foster creative space.

All of the presented components are interconnected and cannot be mutually exclusive. This is what the new mixed-use concept represents. The functionality affects how the residential complex will look like. At the same time, it is necessary to provide for the possibility of adapting premises for different functionalities. In Yekaterinburg, the

project that most clearly reflects the presented principles is the Forum City residential complex, see Fig. 4.

Fig. 4 Forum City, Arch Bureau LEVS architecten, 2021, Yekaterinburg Russia

4 Creating a Healthy Urban Environment Through Architectural Form

People are still in a state of stress or adaptation to the existing crisis. The formation of a psychologically comfortable, healthy urban environment is more important than ever.

A comfortable urban environment is as much about form as it is about function. In his book Sustainable Design Algorithms. Twelve Lectures on Architecture Nikos A. Salingaros writes: "A healthy mind in a healthy body—in a healthy environment!" [12]. In a positive environment, a person develops a positive emotional response, which affects stress reduction and disease resistance.

Architecture can provide a person with emotional recovery. It is possible to influence the incidence of disease and the rate of human recovery by creating a healthy, vibrant environment. It is within the power of an architect to do so. People need contact with the geometry of natural forms. Experiments show that sick people recover much faster if trees and the sky are visible from their windows, which confirms the importance of proper landscaping, and also leads to the need to limit the building's height.

Post-covid architecture should have the attributes of living structures as described by Nikos A. Salingaros in his book. The architectural environment must have connections that match the characteristic of the living system's internal structure, which are stable. The architecture must be biophilic. Biophilic architectural forms resonate with our physiological structure and are perceived with the same ease as natural, living forms [21]. Specifying it, N. Salingaros shows the connection at the genetic level of a man and

the geometry of biological structures. He claims that human health depends on the surrounding shapes and geometries. The proximity of the architectural forms surrounding a man to biological structures makes it easy for them to process these forms, and therefore contributes to their well-being. It is important to understand that we are not talking about a primitive set of architectural elements, but about the concept of creating entire buildings and cities that obey the rules of biophilia. This explains its restorative effect. Moving away from biophilicity is painful and detrimental. To design a healthy urban environment, it is necessary to move away from the principles of modernist architecture, which completely excludes biological forms and creates forms that are not friendly to humans. The ideas of Nikos A. Salingaros are already finding followers [22, 23].

One of the conditions for a sustainable building model is universal scaling—having large and small scale elements in the building structure connected to each other. Emotional recovery begins with recursive structures of each scale and the right mix of them. Biophilic ornament implies the presence of small-scale elements, which form a coherent network and result in large-scale fragments. The scaling should be performed according to the rules of scaling: division according to the Fibonacci sequence, the golden ratio, the rule of three.

Modern buildings should be free of anti-gravity, including vertical stretching and expansion towards the top, overhanging massive parts. Such elements give rise to anxiety. Instead, use stable forms that expand to the bottom, which occurs during vertical compression.

Universal legal morphologies are proposed for design. Fifteen fundamental properties were derived by Christopher Alexander from the observation of "living" structures. These properties are reflected in the 3 laws of the architecture of Nikos A. Salingaros. Solutions for creating a sustainable and vibrant architectural environment are also presented by Christopher Alexander [24]. According to the universal laws, the concept of adaptive design can be introduced. It began with the architecture of ancient civilizations, which is considered the most sustainable. The adaptive design emerged as a response to the physiological structure of humans. It should provide an escape from the monotonous architecture that has become a disease of the Russian cities landscape. By adhering to the principles of adaptive design, it is possible to help people reduce stress and feelings of social disadvantage.

5   Conclusion

Sustainable development will further strengthen its status as an integral component of each approach, and projects will become even more self-sufficient. In order to create a modern residential complex, two fundamental principles must be combined: the provision of a functional content that meets all human needs, and an architectural form based on the properties of living biophilic architecture. This is the only way to form a healthy and sustainable living space that meets the conditions of the new reality.

The new challenge for designers, architects and residential planners is to create spaces that are not only attractive and comfortable, but also safe, allowing them to adequately respond to various infections. In the future, humanity will pay more attention to the impact of architecture on health. Design for health will be the new norm. The vector

of development of the urban environment will be such phenomena as the fight against pollution, overpopulation, a more attentive attitude to the distance between people. Now it is difficult to draw far-reaching conclusions, but it is obvious that in one way or another the changes will affect the infrastructure of the residential complex and the urban environment in general.

References

1. Bushukhin I (2020) Our cities are designed for a social distance of 50 centimeters—An Interview with Amir Idiatulin. RBC—News Agency. https://realty.rbc.ru/news/5f5766ac9a79 47d421b41d52. Accessed 11 Apr 2021
2. Makhno S (2020) Architecture after a pandemic: an architect's forecast. J TEHNE.com. http://tehne.com/event/novosti/arhitektura-posle-pandemii-prognoz-arhitektora-sergeya-mahno. Accessed 25 Dec 2020
3. Makhno S (2020) 7 things that will change the world after the pandemic. J Archidea. https://archidea.com.ua/ideas/ecotechnologies/2246875-7-veschej-kotorye-izm enyat-dom-posle-pandemii. Accessed 25 Apr 2021
4. Frolova N (2020) Self-sustaining city. J Archi.ru. https://archi.ru/world/87046/gorod-na-sam oobespechenii. Accessed 11 Apr 2021
5. Sadova P (2020) New identity. J Archi.ru. https://archi.ru/world/92934/novaya-identichnost. Accessed 11 May 2021
6. Mid-City Mixed-Use (2020) J Architect. https://www.architectmagazine.com/project-gallery/ mid-city-mixed-use. Accessed 01 Apr 2021
7. Self-sustaining city (2020) J Archi.ru. https://archi.ru/world/87046/gorod-na-samoobespech enii. Accessed 08 Apr 2021
8. Saprykin M (2020) 12 world experts discuss whether we will go to the office and build new cities after quarantine (2020) STRELKA MAG—Published by the Institute "Strelka". https:// strelkamag.com/ru/article/kak-izmenitsya-gorodskaya-zhizn-posle-pandemii. Accessed 18 Apr 2021
9. CoronaFOM Project (2021) https://covid19.fom.ru. Accessed 11 Apr 2021
10. Project coronaFOM Ruk (2021) Oslon CAA (ed) Sociology of a pandemic. Institute of Public Opinion Foundation, Moscow, pp 235–267
11. The 15 minute city—No cars required-is urban planning's new utopia. dloomberg.com. 2020-11-12. Retrieved 2021-03-12
12. Vinkel R (2020) Scenario of the future: post-covid trends from dutch architects. J Repa. The Association of Real Estate Professionals, 30 Nov 2020
13. Salingaros N (2017) Anti-arhitektura i dekonstrukciya. Triumf nigilizma (Anti-architecture and Deconstruction: The Triumph of Nihilism). Bystrova T, Duylovskaya E, Makarova A (eds) Kabinetnyj uchenyj, Ekaterinburg, Moscow, p 296
14. Bystrova TY, Rodnova OY (2020) Sustainability assessment of residential building architecture in terms of Nikos A. Salingaros's criteria. B: IOP Conf Ser: Mater Sci Eng 944(1):012003
15. Cohen A (2020) City and virus. In: Construction Ind J 5:44–45. http://ancb.ru/files/pdf/pc/ Otraslevoy_zhurnal_Stroitelstvo_-_2020_god_05_2020_pc.pdf. Accessed 18 Apr 2021
16. Everyone mixes up: how the trend towards integrated development is developing in Russia. J Forbes 28 December 2020. https://www.forbes.ru/partnerskie-materialy/416741-miksuyut-vse-kak-v-rossii-razvivaetsya-trend-na-kompleksnyy-development. Accessed 08 May 2021
17. Kmita M (2020) How public spaces and our life in the city will change after the pandemic. J Buro247.ru. https://www.buro247.ru/culture/architecture/14-apr-2020-urban-landsc ape-after-covid.html. Accessed 11 Apr 2021

18. Frolova N (2019) Self-sustaining city. J Archi.ru. https://archi.ru/world/87046/gorod-na-sam oobespechenii. Aaccessed 17 Apr 2021
19. Strelka KB (2020) What shortcomings of housing revealed self-isolation and how to fix them. STRELKA MAG—Published by the Institute "Strelka". https://strelkamag.com/ru/art icle/nedostatki-zhilya-issledovanie-kb-strelka. Accessed 18 Apr 2021
20. Krits AM, Gazizov Kh (2021) Designing a multifunctional residential building within a comfortable living environment in a pandemic. J Innov Invest 2:163–166
21. Fromm E (2010) Dusha cheloveka, eyo sposobnost' k dobru i zlu (The heart of man: its genius for good and evil). In: Zaksa VA (ed). AST, Astrel', Moscow, p 256
22. Downton P, Jones D and Zeunert J (2016) Biophilia in urban design: patterns and principles for smart Australian cities international urban design conference (Canberra), p 168–183
23. Amirova N, Stasinopoulos TN (2017) Faces of biophilia in contemporary Turkish architecture living and sustainability: an environmental critique of design and building practices, locally and globally. AMPS Proc 9:115–127
24. Alexander C, Ishikawa S, Silverstein M (2014) Template language/transl. from English I. Syrovoy. House of Art. Lebedev Studio, Moscow, p 1096

University Campus as a Model of Sustainable City Environment

O. Ye. Zheleznyak[✉] and M. V. Korelina

Irkutsk National Research Technical University, 83, Lermontov Str., Irkutsk 664074, Russia

Abstract. This study analyzes the existing research and practices for the introduction of a sustainable, "non-depleting" city and campuses development, being a key trend in modern culture, urban planning, and urban environment life. This study covers important sustainability problems at the current civilization development stage and interprets the university campuses as original models of sustainable environment development, which allows using the campus design and operation experience for the sustainable cities creation. The study includes theoretical research into the sustainable city and urban environment development, main sustainability factors and current development stage specifics, the creation and operation experience for university campuses as examples of balanced and eco-friendly development of the environment, as well as design proposals for the Irkutsk National Research Technical University (INRTU) campus. An important result is the experimental concepts suggested for the Irkutsk city aimed at the development of public areas and urban interior images of the INRTU campus as part or form of a sustainable environment, which shows the practical significance of the work.

Keywords: Design · University campus · Sustainable city environment · Irkutsk

1 Introduction

Becoming increasingly artificial, modern life generates significant gaps in the natural relationships created over the lifespan of our civilization [1]. Here, it is important to discuss the sustainable development of cities, which are the main foci of an artificial world [2]. As the cities are the places where the main human, cultural and production resources are concentrated, and, at the same time, sources of gaps between artificial and natural environments.

The modern practice of university campuses creation and operation is an almost perfect city sustainability model, requiring a detailed study and understanding that campuses are a space for the sustainable environmental development.

2 Research Relevance and Objectives

Various aspects of sustainability are actively studied by experts both in theory and practice. Being an important trend of modern culture, urban planning, joined functioning of

urban and natural environments, the sustainable city development play a key role in the development in terms of territorial arrangement [2, 3], "non-depleting development" and sustainable design, which ensures meeting the needs of the society and preservation of ecosystems. Considering university campuses as cases of sustainability concepts implementation and unique examples of sustainable environment allows representing them as resource use models [1], as a part of the general structure of urban sustainability, as well as sustainable environmental centers. This shapes the relevance of the study.

Accordingly, the objective is to study the sustainability specifics of modern cities and university campuses as models of a sustainable environment, to analyze and develop the concepts for the development of Irkutsk National Research Technical University (INRTU) campus, to create urban interior images as a form and means for creating a sustainable environment.

3   Theoretical Part

3.1   Sustainable Development of Cities as an Important Trend of Modern Culture, Urban Planning and Functional Urban Environment

- Sustainable development of cities and urban environment—fundamental concepts

The study of sustainable development and implementation of new methods and technologies is an important topic for experts in various fields [1–11]. Sustainable development concept forms a basis for a general scientific paradigm, integrating natural, social and human sciences [4]. Combining the issues of restoration and environmental protection, as well as consistency of the humanity interests with the general laws of ecosystem existence [6], "sustainable development" implies balancing the development of artificial environment and the preservation of the natural world in all areas of human life including meeting the people's actual and future demands, observing the regional specifics [1], and guaranteeing the civilization safety. The ideology of sustainable development implies a "preserving" behavior [7] and survival of civilization, preventing environmental degradation and improving the quality of life.

An important part of this discourse considers transforming the existing cities into rationally organized and sustainable systems. At the same time, the industry-related approach established in the regulatory framework of domestic urban planning should be revised in terms of city environment planning and design. When the main objective is to ensure sustainable and safe development conditions, it is advisable to switch to a comprehensive management of the city as a sustainable system, as well as to take into account the differences between the ideology of sustainable city development and the conventional urban environment management [12]. As any territory has a huge number of functions [13], the sustainable city development can be considered as a comprehensive process of achieving the consistency of various development functions and forms, which is equally efficient both in the context of new construction and reconstruction of the historical environment.

Consequently, the cities' development aimed at creating a friendly urban environment requires applying the sustainable development concepts, since the cities have the majority

of problems and, at the same time, the majority of population and have to ensure a certain quality of life level and meet basic demands [4].

- Main sustainability factors and modern specifics

Fundamental principles and factors of the sustainable city development are based on the fundamental principles of sustainable society. The principles proposed by the UN reflect the respect for social values, principles aimed at quality of life improvement, preservation of sustainability and biodiversity, reduction of non-renewable resource usage, providing opportunities for city communities to take care of their natural environment, and other directions [1]. The main factors of sustainable development include environmental equilibrium, economic stability and social well-being [8].

A special features of the current stage include the friendliness of interaction between human and nature, the civilization development based on innovations (while preventing any harm to the natural environment), the protection and revival of historical cities and cultural identity, and the creation of a unique authentic environment.

Based on the existing concepts and research, the upcoming stage can be described as a period of global environmentalization and the transition to a sustainable "environmentally friendly development" [1]. It turns the conformity to natural laws and eco-friendly (biopositive) environment into a key sustainability factor limiting the depletion of natural resources based on the productive potential of the Earth's ecosystem. This is largely dictated by the fact that one of the priorities of the modern city functioning is the creation of a healthy, environmentally friendly, and vibrant urban environment, which has a direct positive effect on the city stability and quality of life, and the population. Being close to humans and in balance with the natural environment, the sustainable and biopositive buildings, structures and urban environment are organically integrated into the ecosystem and perceived as natural components [1].

Another significant sustainable city development factors and essential attributes of modern city functioning are the technologies and digital transformations that have already changed the world. Being one of the conditions for the survival of modern cities, the introduction of innovative technologies [9] aiming at the emergence of "smart" cities, becomes today an important means of improving the quality and efficiency of city functioning and competitiveness. Moreover, a new term—a "smart sustainable city"—is proposed by a group of ITU Telecommunication Standardization Sector given the critical relevance of resource-saving approaches, the dependence of sustainable development on innovative technologies for the formation of the distinct features, and the principles of integration and interaction of systems of "sustainable environmentally friendly cities" and "smart" cities.

An equally relevant component of the urban environment restoration and sustainable development is the protection and revival of historical cities and cultural identity spaces, as well as the formation of a unique authentic environment and lifestyle. The activities aimed at the protection of historical heritage and the revival of historically significant territories are characterized by the increased importance of building reconstruction, renovation and revalorisation of historical environments, and reduced new construction, as well as identification of the genetic codes of certain "places" and environmental gentrification. This can be accompanied by city environment modernization programs

and investments aimed to improve sustainability and energy efficiency (introduction of innovative and efficient street lighting systems, providing modern furnishing of historical spaces and environments, providing new functions to the buildings, etc.). The progressive city environmentalization is also associated with environmentally friendly landscape restoration activities, restoration of equilibrium between the artificial city environments and the natural environment [1].

- "Non-depleting development" and sustainable design

The concept of "non-depleting development" and the processes of sustainable design and construction can be considered as an objective and means for the "implementation" of a sustainable city environment, which is able to satisfy all the vital demands of the modern generation, while preserving resources for the descendants and creating an aesthetically attractive, healthy and comfortable artificial environment organically built into a natural context to ensure the preservation of the Earth's ecosystem and enhancing its potential, and etc.

Specific "indicators" of sustainable and non-depleting development are used to monitor sustainability, representing a system of indicators for system sustainability monitoring. 27 indicators of sustainable development are grouped into four main categories—energy; ecology; politics, economics, institutions; society and culture [1].

Ensuring all demands is an absolute condition for meeting the sustainability criteria requirements. And this is not only the opportunity to use the material comforts of "non-depleting" development (reduced energy costs, improved quality of service, creation of a comfortable urban environment, generation of resources for economic activity development, etc.), but also meeting the socio-cultural, spiritual needs, which include social, ethnic, psychological (ethological and behavioral), educational, and other needs. The conditions and indicators of the implementation of the necessary needs include the freedom of knowledge and self-education, the possibility of organization of various groups for communication, the existence of "native nature" landscapes, as well as architecture and cultural landscapes preserved in the ethnic memory.

The sustainability indicator is significant for the "Society and Culture" category and focused on the implementation of educational demands. It includes the creation of the space for cultural continuity and reproduction, the creation of an aesthetically attractive environment (important for education), as well as physical and virtual social spaces, along with traditional children and adult education.

At the same time, the implementation of the sustainable development ideology in each particular city requires finding individual approaches to emphasize the differences between all the cities. Such "unique sustainability" can be manifested through sustainable design and construction, which ensure the formation of a healthy sustainable environment, contribute to the creation of conditions for the communication of residents and organization of their joint activities to build a beautiful and comfortable city—all these being important qualities of sustainable environmental development. To a large extent, sustainable design and construction are related to the environmentalization of cities and with biopositive qualities of buildings and structures, with renovations aimed at improving the environmental friendliness, the preservation and restoration of natural landscapes, and maintaining biodiversity. Furthermore, the design of a sustainable

and beautiful city includes paying respect to historical heritage, improving the aesthetic qualities of the city, and perceiving the city as an organic component of the natural environment.

3.2 University Campus is a Model of the City and Urban Environment Sustainability

- Functions of a university campus as a part of the general urban sustainability structure

Campuses can be considered as nearly perfect models of city sustainability. They often serve as a sustainability core, and forming specific standards and codes for the creation and functioning of the urban environment, its preservation and renovation, being places for innovation and approbation of new technologies relevant for the city, as well as the space for various communication forms.

Modern campuses are not only places of study and research, but also recreation and leisure territories with a developed system of "green" areas for both the participants of the educational process and ordinary citizens [14–21]. Transforming an educational space into a comfortable, multifunctional, and sustainable campus environment contributes to the creation of a self-developing core of constant transformation and improvement in the city.

As the campuses are a center of intellectual life and communication, their development leads to the formation of an effective infrastructure including education, health care and sports objects as well as an attractive urban environment, creating areas of attraction and activities.

The consistent implementation of new visions of educational environment organization turns a campus into a supplier of resource for regional development, an point of access to the most demanded educational programs, a center for priority research, the key factor in attracting talents and retention of young people in the region, which ensures the sustainable development of the "place".

Enhancing the interaction between science and practice, education and businesses, modern campuses provide high-quality research infrastructure, create a sustainable environment and comfortable conditions for work and life in various conditions.

Being part of the social and cultural city infrastructure, campuses become sources of development, saturating the urban environment with activity and diversity, ensuring interaction with city communities, being a specific center for the modernization and technological development of the city, and a discussion platform for ecology, ethnic and cultural heritage issues.

Campuses are spatially arranged with no strict borders between the campus and the city, sharing public areas (cafes, galleries, art studios and centers, libraries, coworking spaces, sports facilities, etc.), and providing places for city events.

To summarize all the above, acting as a model of sustainable city development, a campus should be an eco-friendly, natural environment, the source of scientific development and civilization growth based on innovative technologies, the space for communication and implementation of educational needs, as well as the space for cultural continuity and identity reproduction.

- The experience in the creation and operation of university campuses as centers of sustainable environment development

Conventional campuses are the most vivid examples of sustainable development, being spaces of cultural continuity reproducing the natural environment, spaces for communication and implementation of educational needs.

In particular, having a wide variety of resources, the campuses of top USA universities are actually the models of urban environment sustainability allowing the system to maintain its integrity and viability, as well as providing unique, comfortable and sustainable conditions for the city life. For instance, the Yale University campus located in the center of New Haven includes 12 residences, a natural science museum, several art galleries, and an art center. Also, the university owns the natural reserve territory and a well-developed sports infrastructure. The building architecture is quite diverse, incorporating many styles—from Victorian to modern. All this turns the campus into a center for educational, cultural, sports and entertainment city events.

The Columbia University campus is an important part of the urban structure of New York. The campus occupies six Manhattan quarters with unique historical buildings, which incorporate 25 libraries, various sports facilities, dozens of student organizations, as well as a radio station, two newspapers, a magazine, television studio and the best orchestra in New York.

The Harvard University campus in Cambridge stretches for more than 2000 hectares having scientific laboratories outfitted with the latest technologies, sports centers, museums, libraries, cafes, as well as a multitude of various student organizations and 42 popular city clubs.

The Princeton University campus located in the central part of Princeton includes many historic buildings with libraries, a theater, a museum of arts, a fitness center with a swimming pool and a tennis court. The campus holds events covering a wide range of urban interests, which integrates the campus into the city life, forming a model of sustainable interaction between the university and the city.

The campus of the University of Chicago occupies a territory to the south of the main business district incorporating a dozen research institutes and 113 centers. Student buildings in the Neo-Gothic style, residences at the Hyde Park on the Michigan shore, a botanical garden, own observatory, one of the largest libraries, the famous University Publishing House (Chicago Press), and more than 350 clubs create a unique historical, cultural and natural (biopositive) environment that serves as a source of active activity and technological innovations for the university environment and the city as a whole, which is organically incorporated in the social and cultural city space.

The most vivid example of a modern campus corresponding to sustainable development principles is the new campus of the Vienna University of Economics and Business. The campus layout created by BUSarchitektur, BOA Office and Landschafts Architektur, includes an educational building, a student center, residences, administrative offices and public spaces (libraries, restaurants and cafes, a landscape park, fountains, and etc.). An important part of the campus structure is the six entrance zones, public areas and the main Forum interconnected by pedestrian and cycling paths ("campus—for pedestrians"), and a green belt around the perimeter bordering the city park (Prater). A distinctive

visual reference to the natural environment of Prater Park and the development of the eco-scenery is the decorative style of D3 building facades made of raw fir planks. The central architectural object is the "auditorium", called an "educational platform" by the authors serving for "regular and spontaneous communications".

The city-integrated campus of the Vienna University of Economics and Business represents the balance between the university within the city and the "city within city", which concepts imply having a full-fledged infrastructure within each territorial unit.

The ideology of the modern campus being a sustainable structure, the foundation of urban development, was formulated by Professor den Heijer [21] in the framework of Delft University of Technology campus modernization concept. The key development strategies include stimulating various sustainability components—recycling and environmental approaches, as well as sustainable behavior and sustainable technologies.

The educational function implementation implies rethinking of the academic presentation of a workplace, enriching the campus with "non-academic functions", creating a flexible educational environment, investing in the creation and modernization of modern laboratories [21].

An essential part of the strategy is addressing the historical heritage and cultural traditions, trying to give a new life to old buildings, accepting the "academic history" and using heritage for branding. Additionally, "smart tools" and innovative technologies are introduced.

The concept of campus design as "city within city" implies high accessibility and intensive use of the best locations, improvement of the design for the quality of space, improving the attractiveness of the environment, stimulating social and intellectual interactions between all participants of the educational process, as well as between students and citizens, which expands the role of campus as an important public city space.

Following the proposed strategy, the Delft Technical University campus modernization after the fire of 2008 included the restoration of historical buildings, creation of additional public places for meetings and communications, the introduction of flexible technologies for mixed space use providing the transparency of processes. Special attention has been paid to "visible quality", a kind of "showcase decoration", creating a visual image of the campus and a unique, author's decoration of its own workplace forming a "home-like" environment.

In the domestic tradition, campuses often inherit the organizational and spatial structures of conventional spaces of student quarters, gradually transforming the educational and scientific directions, modernizing the object and spatial environment in accordance with the modern requests and trends. Simultaneously, new campuses are created with the strategic goal of building the centers of the innovative city and regional development, which is ensured by the presence of modern scientific and educational infrastructure, as well as by the concentration of intellectual potential in campuses. Most often the main activities within a campus are related to the formation, innovative development, research and preservation of the environment.

4 Results

4.1 INRTU Campus—Sustainable Environmental Development Strategy. From the Old Student Quarters Area to the Modern University Campus

The history of the student quarters area in Irkutsk originates in 1930 with 6 student dormitories built in Proviantskaya Square. In 1956, large-scale construction started over the territory previously occupied by the campus—the university building, dormitories, residential buildings, and a large-scale catering establishment were built. Since then, the student quarters area (and INRTU campus now) has been a historically stable territorial and cultural unit within the Irkutsk structure with the current development trends based on the concepts of sustainable development.

The Spatial Development Concept for the campus of Federal State-Owned Publicly-Funded Institution of Higher Education INRTU proposed by the Siberian Laboratory of Urban Planning includes public and recreational spaces, the modernization of the university's internal spaces, objects of new construction, a technology park and business area. Public and recreational spaces are combined into a single system and constitute a front square of the main building, an amphitheater forum, a boulevard with the green terraced slopes, a city embankment including a river station, a park territory, pedestrian bridges and platforms, as well as a series of recreational microspaces. Modernization of the university's internal spaces is focused on providing multiple functions, expanding the public areas, creating new scientific locations, improving the environmental quality, sensory and visual variability, accessibility for mobility-impaired persons, and introducing technological innovations. Special attention is paid to the development of the INRTU Technology Park and business area. Following the sustainable development strategy, the newly constructed objects of the INRTU campus include educational and laboratory buildings, a library building, a complex of public buildings and structures (palace of youth, water and sports center, medical center, kindergarten, general education school, etc.).

The created INRTU Campus Formation Concept allows preserving the existing student quarters area as an internal sustainable social and cultural, scientific and educational, and highly-technological space, as well as an important structural part of Irkutsk, which maintains the balance of interests of society, nature, technology and economics.

4.2 INRTU Campus Public Area Development Concept

A part of the process of INRTU campus formation as a sustainable environment is a special design concept of INRTU student quarters area (campus) territory reorganization and the development of a system of public spaces. Focused on solving the problems of sustainable operation of INRTU as an integral university system, with buildings scattered on the student quarters area, this special design project organically incorporates the university environment into the general system of urban development of the left-bank Irkutsk, and also allows increasing the recreational potential of the territory and forming the INRTU campus presentation space. The problem of creating the University's main square as the entrance area and key representation space is solved by arranging an amphitheater facing the main INRTU building facade. The unified structure including

an amphitheater includes a system of overhead pedestrian passages and a new parking building forming new composition axes and organically incorporating into the existing context.

Considering that public spaces are part of the strategy of sustainable environmental development, their new interpretations and forms (such as coworking spaces) take an increasingly important role. Being a modern communication space, a new type of "third place", a form of comfortable environment organization and high-quality design, coworking spaces are actively introduced into the life of cities and universities becoming important components of any campus.

The authors propose the concept of INRTU coworking cluster formation, which will become a new space of the student quarters area and correspond to modern ideas about the comfort of environment, its sustainability and viability. The cluster structure reflects various forms of territory functioning, ensures the urgent needs of its inhabitants, which are used as a base for the development of coworking network, includes an open-air anti-office, sports coworking space, art residence, VIP coworking space, business incubator and coworking space for digital nomads, coworking space for education of children and parents. A flexible system of hybrid spaces will contribute to the creation of a sustainable campus environment and actively work for the city's prosperity, an increase in the comfort and viability of the urban environment.

4.3   Urban Interior Images and Concepts for the INRTU Campus as a Form and Means of Sustainable Environment Development

Processes of sustainable design of a comfortable, biopositive and dedicated city environment now are based on strategies for restoring the uniqueness and urban environment preservation, concepts of sustainable campus development including the ideas of "process transparency", "reassessment of academic rituals", "reinventing the past", working environment and space "decoration", making the public environment home-like, creation of a "home when far from home ", etc.

The design developments performed under the guidance of authors are aimed at the uniqueness, comfort, and cultural codes of the environment as one of the mandatory conditions for creating a viable, sustainable urban environment and conservation of traditions.

The search for the urban interior concepts for individual INRTU campus areas includes searching for image and stylistic features and a concept for INRTU campus improvement, which set the semantic and stylistic context for subsequent design, increasing the status of the territory and the general gentrification of the INRTU campus environment.

The design includes developing layout solutions and design codes in accordance with the functional zoning of the space and the common principles of sustainable and comfortable object and spatial environment of a modern university campus, creating concepts of the environment and design examples based on the case of the INRTU Institute of Quantum Physics.

The development of unique environment concepts for key zones of the student quarters area (campus) and sustainable development spaces form a special system of design codes, object and spatial arrangement, as well as unique urban interiors.

5 Conclusions

Sustainable, "non-depleting" city development is focused on providing a comprehensive solution to the city problems, improving the quality of life through the rational use of resource potential and the achievement of the balance of social, economic and environmental development. Campuses actually embody the existing models of rational resource usage, interaction between people and the nature, and innovation-based civilization development not limited by the economic system and including regulation in science and education, cultural and social areas, as well as the development of technologies and innovation. The study of this model is suited for theoretical research of the problem, as well as practical application of these results in the design, including the dedicated INRTU campus concept development.

References

1. Tetior AN (1999) Sustainable city development. Moscow
2. Papenov KV (2019) Small cities of Russia: past, present, future. Sustainable development of cities, Faculty of Economics, Moscow State University named after Lomonosov MV, Moscow, p 288
3. Nikonorov SM (2016) The role of the ecological factor in the strategy of socio-economic development of cities in Russia. De Econ 11:50–63
4. Denevizyuk DA (2012) Sustainable development of the city: theory and assessment methods 2, regional problems of transformation economy. Moscow, pp 103–112
5. Ursul AD (2005) Sustainable development: a conceptual model. National interests, vol 1, Moscow
6. Sheina SG, Starodubtseva AS (2017) Sustainable urban development. An integrated approach to the transformation of the urban environment. Engineering bulletin of don, vol 2/45, Rostov-on-Don, p 104
7. Ursul AD (2013) National idea and global processes: security, sustainable development, noospherogenesis. Natl Secur 2:1–66
8. Starchevus VK, Shchitinsky VA, Romanovskaya NV (2002) Habitat project "Sustainable human settlements"—the next step. Ind Civil Eng 5:56–59
9. Knyazeva GA (2019) Sustainable development of northern single-industry towns: tools and management models. Sustainable development of cities, Faculty of Economics, Moscow State University named after Lomonosov MV, Moscow, pp 267–282
10. Tetior AN (1998) Sustainable development. Sustainable projection and construction. NIA-Nature, Moscow, p 310
11. Bobylev SN (2017) Sustainable development: a paradigm for the future. World Econ Int Relat 3:107–113
12. Martynova EV (2014) Methodological foundations of energetically effective reconstruction of urban development: Ph.D. thesis, Rostov-on-Don, p 208
13. Golovanova LA (2002) The main aspects of territorial energy saving. Khabar Publishing House. State tech. University, Khabarovsk, p 115
14. Puchkov MV (2011) Experience in the spatial organization of modern university complexes. Univ Manag Pract Anal 2:30–39
15. Hoeger K, Christiaanse K (2009) Campus and the city. Urban design for the knowledge society
16. Melent'eva AA, Shvets AV, Merenkov AV (2017) The concept of a modern educational space in the city of Yekaterinburg (on the example of a medical campus). New Ideas New Century 1:283–290

17. Zobova MG (2015) Modern aspects of architectural and urban planning design of university campuses. Bull Orenburg State Univ 3(178):243–248
18. Belotserkovsky AV (2015) Universities as generators of regional development. Higher Educ Russia 1:5–10
19. Damyanova LT (2013) Experience of European countries in creating a new type of universities. Creative Econ 12(84):95–101
20. Zheleznyak OYe, Korelina MV (2020) University environment today: problems and prospects of spatial organization. INRTU. In: International conference on construction, architecture and technosphere safety (ICCATS 2020) 6–12 September 2020, IOP conference series: materials science and engineering 962:032051
21. Magdaniel FC (2019) Campuses, cities and innovation. https://www.hanze.nl/assets/kcnoor derruimte/Documents/Public/NoorderRuimte-lunches/pdf. Accessed 27 Mar 2019

Engineering Structure Safety, Environmental Engineering and Environmental Protection

A Technical and Economic Evaluation of Gas Pipeline Construction in Perm Karst Region

A. Grishkova[1]([✉]) and A. Minibaev[2]

[1] Perm National Research Polytechnic University, 29, Komsomolsky av, Perm 614990, Russia
[2] Gazprom Gazoraspredelenie Perm" JSC, 43, Petropavlovsk str, Perm 614000, Russia

Abstract. Perm region is the area of developing karst. There is a significant risk in installing gas pipelines in this area. However, gas is used for heating buildings, cooking and heating water in the region settlements. Violation of the gas pipeline integrity can lead to serious environmental consequences, as well as the risk of explosion and fire. Therefore it is urgent to make a preliminary assessment of geological conditions to develop anti-karst measures when designing and installing gas pipelines. Preliminary calculations of pipelines possible stress should be carried out to determine the laying type and the method to strengthen a site. The site in the Kungursky district of the Perm Region was selected for the feasibility study. Based on earlier research and the authors' inspection, the current study examines the scale of karst in the proposed trail route and suggests the alternative route with less karst development. 10 karst forms were recorded on a 1.5 km long section. The selection of the underground gas pipe with tampon cement mortar was founded on the calculation of the stresses in the pipeline. The gas pipeline construction cost was estimated against the favourable conditions.

Keywords: Karst · Anti-karst activity · Natural gas transport on the karst territories · A gas pipeline construction cost in the karst territory

1 Introduction

It is urgent to provide measures that exclude the possibility of karst deformations and significantly reduce the risks of engineering piping when gas networks are designed in karst-covered areas. Violation of the gas pipeline integrity leads to natural gas leaks, which negatively affects the environment, and can cause explosions and fires. So, the cost of implementing projects in karst areas increases significantly.

The specific landforms composed of soluble rocks, such as rock salt, gypsum, limestone, dolomite, and others are called karst [1, 2]. Karst (the German wording) is one of the most dangerous natural processes on the Earth due to the suddenness of the manifestation in the sinkholes form and earth's surface subsidence, sometimes reaching 50–100 m or more in diameter and depth. In the active phase, karst manifestations are the formation of sinkholes on the earth's surface. The essence of karst processes is the dissolution of the rock by atmospheric, thawed or underground water. Access to the surface or the soluble rocks, the resulting cracks and cavities complicate the karst territories development.

Any construction requires a comprehensive and thorough study of the karst phenomena and the potential karst formation. The engineering networks design and underground construction are regulated by the existing legislation of the Russian Federation: Federal Law No. 7-FZ of January 10, 2002 "On Environmental Protection" and Federal Law No. 116-FZ of July 21, 1997 "On Industrial Safety of Hazardous Production Facilities", as well as by special regulatory and recommendation documents [3–7].

2 Problem Statement

In the paper, we considered the technological features of gas supply systems and the change in the gas line installation cost in the karst area. A significant budget share is allocated for the gas pipeline system development in Perm Region. About 400 million rubles were invested in the municipal gas distribution pipelines construction in 2019. The amount of funds required for engineering networks construction depends on many factors, such as the network length, pipes material, laying method, pipes diameter, special equipment availability, soil type, presence of natural origin obstacles along the engineering network route.

The following tasks were set:

- get acquainted with the specifics and geographical karsts location on Perm Region territory;
- study current environmental safety requirements;
- analyze the regulatory framework for the design, construction and operation of gas pipelines for the presence of special for the design, construction and operation rules of gas pipelines by laying on the karst territories;
- determine the degree of karst processes influence on technological processes for gas supply system;
- determine the list of anti-karst measures to ensure the safe construction and gas pipeline operation;
- design a project for a gas pipeline section running through the karst territories;
- compare the construction cost of two construction options: in good soils for construction and in karsts.

According to the scheme of geomorphological zoning of the Perm region for the studied territory, the karst process plays a significant role in the natural relief formation, which continues at the present time. Perm Region is characterized by a large karst type's variety, a significant potential of the mining and processing industry and a significant man-made load on natural objects. Many Perm Region cities and districts have the most dangerous types of karst: sulfate and salt. A significant danger for buildings and engineering constructions is represented by sinkholes, which are typical for gypsum areas (Fig. 1).

The region karst rocks occupy almost a third of the territory. The total karst area of the region is 45.9 thousand km^2 [8]. The carbonate, sulfate and salt karst areas occupy 94% in Oktyabrsky district, 77% in Ordinsky, 68% in Suksunsky, 61% in Solikamsk, about 50% in Krasnovishersky, Cherdynsky, Kishertsky and Kungursky areas. Due to karst, the multi-storey building's construction is restricted there [9].
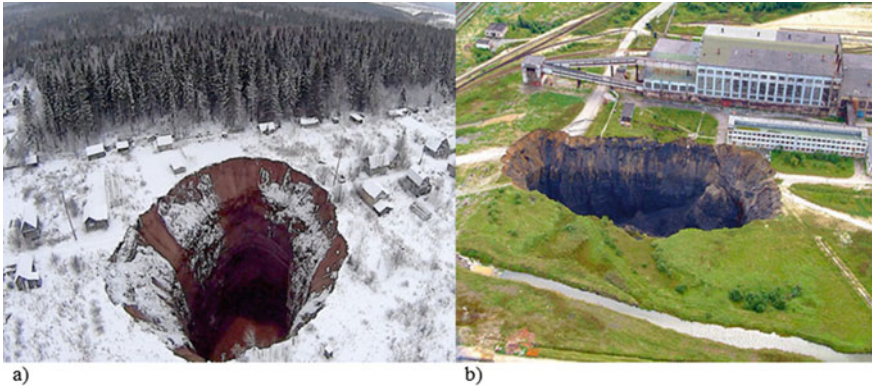
Fig. 1 Karst sinkholes in the Perm territory [8]: **a** Solikamsk, **b** Berezniki

5 zones of karst risk are identified in Perm Region karst territories. They are gypsum, carbonate-gypsum and carbonate karst zones. The most widespread is the carbonate karst [10], the total area occupies 29.6 thousand km^2 (Fig. 2a). The most disruptive influence on the region territory stability is exerted by the sulfate karst, which causes the main types of earth's surface deformations. The karst may become more active or, conversely, fade depending on the geological conditions and the type of impact in different parts of the locality. Often, the activation of the karst is associated with a specific object or technical action [11, 12].
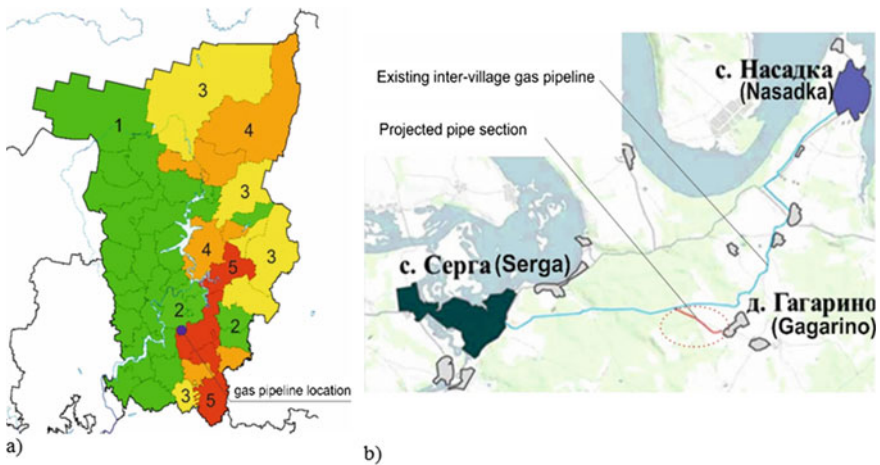
Fig. 2 Location of the gas pipeline planned section: **a** zones of karst risk (1—below 5 sq. m/(ha*year), 2—from 5 to 20, 3—from 20 to 35, 4—from 35 to 60, 6- over 60 sq. m/(ha*year), **b** gas pipeline projected section

For example, the development of Verkhnekamskoye potash-magnesium salt deposit led to man-made karst development, which caused two mines flooding and four sinkholes

formation in Berezniki. Currently, this process is in an active phase, and new destructions are expected to form. Therefore, special regulatory documents have been developed in Perm Region [13].

It is necessary to provide protective anti-karst measures at the design stage due to the risk of the high collapse during the construction and operation of engineering networks in karsts. This significantly increases the implementing project cost.

3   Theoretical and Experimental Results

The site in Kungur district was selected for the technical and economic evaluation of the gas pipeline project on the karst territory (Fig. 2b). In tectonic terms, Perm Region is located at the junction of East European Platform and Central Ural uplift. Kungursky district is an intense carbonate-sulphate karst area of the platform type. The peculiarities of karst development in carbonate-sulfate strata are related to the fact that the layers of gypsum and anhydrite in the zone of their contacts with carbonate layers are subject to relatively intensive dissolution, whereas in carbonate layers, as a rule, only the development of cavernous and secondary porosity is observed.

The pipeline for nature gas supply was construction to Nasadka In 2016 it eventually extends more than 15 km from Serga. Its path takes it underneath karst terrain in the region. It passes along the coastline of Sylva River. Serious risks have to do with securing and maintaining the structural integrity of the pipeline in a sinkhole prone terrain.

An additional section is planned to be connected to the existing pipeline. The gas pipe is going to provide gas to facilities located in the village of Gagarino with altitudes of 130–215 m (in the Baltic altitude system). The projected gas pipeline is designed for natural gas transport with:

- a capacity of 1500 m^3/h,
- a calorific value of 8189 kcal/nm^3,
- the specific weight of 0.698 kg/nm^3,
- working pressure of up to 0.6 MPa.

The completed project composition and content meets the requirements of the Urban Development Code of the Russian Federation and other regulatory documents in the field of urban development. The main part of the project included field and desk works.

Field works:

- investigate geological and hydrological factors on the gas pipeline route;
- chosen of the gas pipeline section route;
- route approval with the settlement administration.

Desk work:

- stress calculation in the pipeline;
- the karst hazard assessment;
- boundary plan formation for the gas pipeline land plot;

- zones boundaries drawing with special territory using conditions;
- analysis of the main anti-karst measures;
- execution of gas pipeline drawing.

The pipeline stress calculation data was estimated and the gas pipeline installation type was chosen. Aboveground gas lines are recommended if the design stresses do not meet the strength requirements; stress reduction by installing underground expansion joints is associated with significant costs. Aboveground installation is allowed for gas pipelines if it can lead to forming dips, cracks and develop stresses exceeding the permissible levels [13].

The strength and stability of underground gas pipelines should be ensured by increasing the mobility of the gas pipeline in the ground and reducing the influence of deforming soil on the gas pipeline. Compensators are used for this purpose. They are installed in special niches that protect against pinching. In addition, low-impact materials are used to fill the trenches after laying the pipes.

To explore the sinkhole-induced risks to the proposed pipeline and assess the potential for harm by the construction of the gas pipeline were carried out in this study. We studied the phenomenon of karst in Kungur territory. The karst hazard assessment of the investigated gas pipeline section was carried out on the basis of the karstological survey data, the archival materials of previous year's surveys, the results of drilling water wells, and studies of Perm State University [14–16]. Several routes were analyzed. The scope of the survey along the projected gas pipeline route amounted to 1.5 km. In the upper part of the section study area, there are deposits of dolomite, siliceous dolomite with layers of clay and selenite, fine-grained limestones, plate marls, clays, siltstones, sandstones that overlap the deposits of the sulfate-carbonate stratum, where gypsum-anhydrite bundles are interspersed with dolomite and calcareous bunches. No underground water was encountered during the survey period.

4 Proposed Activities and Design Results

According to the cover deposits nature, the studied area karst belongs to the closed type of karst, and there is also a bare and turfred karst. The relief of the work site is relatively flat, the absolute marks of the earth's surface range from 124 to 213 m (the Baltic elevation system) 0.10 karst forms were registered in the 24-m-wide survey strip in the studied section of the projected gas pipeline route. The total area of karst craters accounted for 7697 m^2. The average karst sinkhole size was evaluated.

Based on the karstological survey, drilling operations analysis, scientific publications, karst formation indicators, the distance from the nearest karst formations and [9, 14], the territory of the investigated section of the projected gas pipeline is characterized by:

- as **very dangerous** in the zones adjacent to karst craters at a distance to one diameter of the crater;
- as **dangerous** in the zones adjacent to karst craters at a distance from one diameter of the karst crater to 100 m from it;

- as **moderately dangerous** in the other studied area.

Table 1 shows surface karst indicators and measures to prevent accidents. A short description of some measures is given.

Table 1 The karst territory study results and the main project characteristics

	Indicators of the karst deformations intensity	Hazards category	Emergency prevention measures
1	Karst forms density	II	– Filling of all karst forms in the right part of the path of the projected structures with water-repellent pulverized clay soils with layer-by-layer ramming (24 m-for the gas pipeline route in open areas and 17 m in the forest zone, 12 m and 8.5 m respectively, to the right and left of the route axis) – The sand base for the gas pipeline is 200 mm thick and the pipeline is filled with sand to the height of 300 mm above the upper forming pipe along the entire trench length – Open ponors and cracks during earthworks are tamponed or fixed with karst and overlying rocks by cementation solutions injection with reinforcement if necessary – Polyethene pipes are accepted with the safety factor of 3.2 at least – All welded butt joints (100%) are controlled by physical methods – The installation of control tubes
2	Karst forms density with a depth index ≥0.3	IV	
3	Surface karst formation coefficient	IV	
4	Surface karst volume index	IV	
5	The intensity of the karst sinkholes formation	III	
6	Proximity to karst craters	II	

The engineering-geological and hydrological conditions of the site under investigation are partially favorable for the work. However, when performing work, it is recommended:

- consideration account for the presence of bedrock represented by limestone—when designing the construction of a gas pipeline in the bedrock, it is necessary to provide for the protection of these soils from the destruction of atmospheric influences and

water during the development of the trench. For these purposes, the backfill of the trench should be made immediately after the gas pipeline installation of the;

- karst forms presence consideration account—provide for the gas pipeline laying with a filling trench of 300 mm with non-adhesive soil (sand);
- consideration account for the peculiarities of the geological study area structure.

Gas pipeline construction should comply with the geotechnical and anti-karst rules and regulations [4, 7, 9]. According to the normative documents provisions, anti-karst measures should perform the following functions:

- prevent the activation, and reduce the activity of karst processes;
- eliminate or reduce to the necessary extent karst deformations of ground layers, or, conversely, contribute to the stabilization of construction conditions by accelerating karst deformations;
- prevent increased filtration and water breakouts from karst cavities into underground rooms and mine workings;
- ensure the possibility of normal territories operation, buildings, structures, underground premises and mine workings in case of karst manifestations.

To perform these functions it is necessary to provide for measures that exclude the possibility of the karst deformations formation or reduce their adverse impact on structures when designing gas pipelines. These include:

- provide for the depth of the foundation below the zone of dangerous karst manifestations;
- use of compensators (U-shaped, lenticular, wavy);
- filling of karst cavities;
- artificial acceleration of the formation of karst manifestations;
- creation of an artificial water barrier and anti-filtration curtains;
- fixing and compacting of soils;
- water supply and regulation of the underground water regime;
- organization of drainage.

Not all of the above measures are applicable for linear objects due to the impracticability and high implementation cost. Since an inter-village gas pipeline is an object of capital construction and its service life is 50 years, it is necessary to choose protection measures that can ensure the safety of its operation for a long time.

The gas pipeline route took into account the existing engineering communications, the existing development and the natural conditions of the site. The gas pipeline design includes existing buildings and structures and complies with the requirements [4]. The project gas pipeline is made of non-metallic polyethene (material PE 100, SDR11) with a diameter of 315×28.6 mm. A site plan is shown in Fig. 3a.

The depth of the underground gas pipeline is taken on the basis of the engineering and geological structure, taking into account the composition of the soil. Open underground gas pipelines in low puffing up of the soil should be laid at a depth of up to the top pipe not less than 1.0 m. Figure 4 shows a fragment of the gas pipeline route profile.
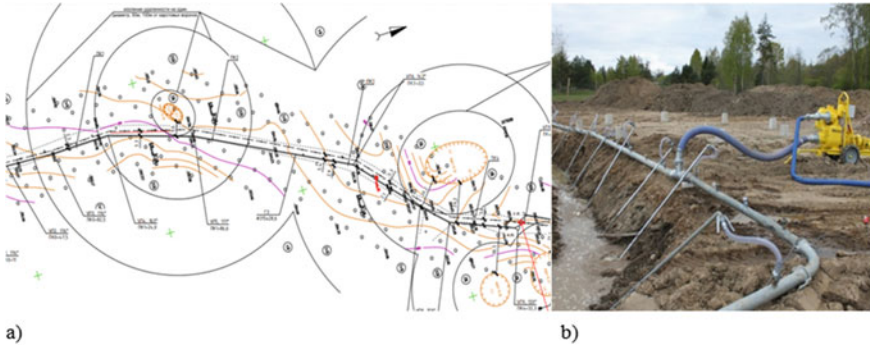
Fig. 3 Gas pipeline section: **a** the plan fragment; **b** the territory tamponing
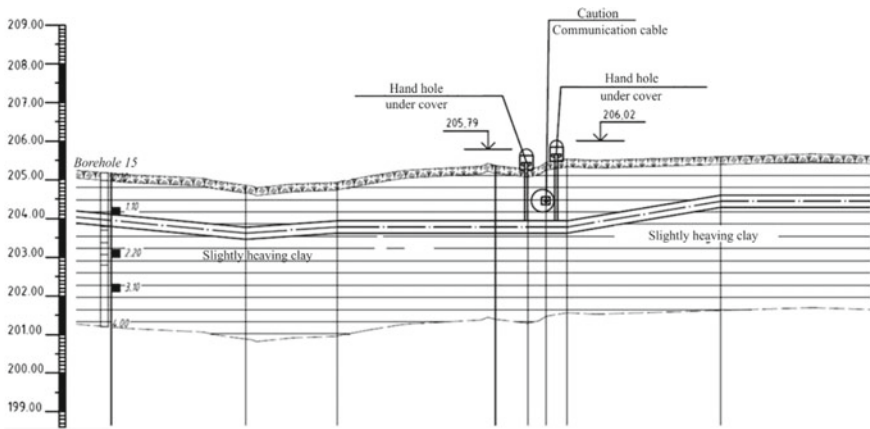
Fig. 4 Gas pipeline route—the profile fragment

Tamponing is accepted as the main anti-karst measure. The essence of the tamponing method is to fill voids, cracks and pores in the soil mass with materials that can harden for a certain time. Materials are introduced into the soil in the form of solutions. Solutions are injected through special injection tubes located according to a certain scheme in the soil mass. The mixture of several components produces the formation of a gel in the soil pores. The gel substance strengthens the soil and makes it water resistant. Grouting solution spreading to a certain distance from the trench. The solution squeezes out water or partially mixes with it, and after solidification blocks the path of ground water filtration to the trench. The method of tamponing the soil is called the method of fixing the soil. The solution hardened in the pores and cracks of the soil significantly increases its strength properties. This is a soil chemical fixing method. The material that forms the basis of the solution injected into the soil mass determines the type of filler: cementation, claymation, bitumization, silicatization or resinization. The main criteria for choosing the soil tamponing type are their filtration capacity and the requirements for soil strength [17]. The great advantage of this method is the fact that the effect of

fixing is manifested for a long time—almost the entire service life of the structure. This allows for the safe construction and further operation of the structure in relatively favorable geological conditions. The soil properties analysis indicated cementation as the best method (Fig. 3b). Cementation is usually used in fractured rocks and sandy soils, it can be used in clays and loams. As a fixing solution, Portland cement is used, which is the cheapest and most environmentally friendly material.

Two estimates for pipeline installation have been provided; with anti-karst measures and under normal conditions.

Construction estimates are made in compliance with construction rules and regulations in the Russian Federation [18]. The construction budget is based on the prices of 2011 (amended in 2017). Federal unit prices [19, 20] are used for the estimates. When converted to current prices, the inflation index of construction and installation works costs to the base prices is applied. The calculation costs are given in Table 2 in the prices of 2020.

Table 2 Estimated construction cost of the gas pipeline section

Gas pipeline construction conditions		Good soil	Karst territory
1	Construction costs	4,946,000	6150000
2	Installation cost	43,000	53000
3	Wage fund	122,500	151,000
4	Intensity of labor, man hour	1,052,701	1,300,261
5	Estimated cost	6,340,000	9,830,000

5 Conclusion

Today, the karst phenomenon and the behavior of different natural karst forms has been sufficiently studied. However, it is still not possible to fully control the formation of karst cavities and predict changes in the karst in the future. Intensive karst development along the proposed route of the gas pipeline suggest that spatial distribution of karstic features is considered to be critical in the decision process.

Detailed studies conducted on the basis of our own analysis and other authors data on the territories characteristics in the Perm Region have shown that the results of various research methods converge well in determining the zones that increase the intensity of dangerous natural and man-made processes in the ground. This ensures reliable forecasting when gas pipelines designing and making decisions during their operation. The published data were confirmed by field observations for the Kungursky district of the Perm Region. The established zones with unfavorable geological processes made it possible to choose the gas pipeline route with minimal pipeline destruction risk.

In order to explore the sinkhole-induced risks to the proposed, and assess the potential for harm by the construction of the gas pipeline, data from geological and hydrogeological studies were analyzed. Most of this data is published in print. However,

further territories development requires more extensive research, including digitizing aerial photography.

The application of anti-karst measures is a mandatory requirement for the designing of gas pipelines in karst territories. The technologies developed for these conditions require preliminary assessment and calculations before selection and application. Operating of pipelines in karst areas requires further improvement in control.

The economic evaluation of the gas pipeline project was carried out in the Kungursky district of the Perm Region. The geological study of the karst was carried out and measures to prevent accidents on the projected site were determined. The calculation showed that underground installation, which requires anti-karst measures, increases the construction cost by at least 55% compared to the construction of a gas pipeline under regular conditions.

References

1. Waele Jo De (2017) Karst processes and landforms. The International Encyclopedia of Geography. . Wiley, New York, pp 13–25
2. Popov YuV, Pustovit OE (2015) Karst textbook. Southern Federal University, Rostov-on-Don, p 64
3. Denizman C, Parrish E (2017) Assessment of a pipeline route in a Karst Terrain Florida. USA J Remote Sens GIS 6:5. https://doi.org/10.4172/2469-4134.1000210
4. Body of rules SP 62.13330.2011* Gazoraspredelitel'ny'e sistemy'. Aktualizirovannaya redakciya SNiP 42–01–2002 (Gas distribution systems. Updated version of SNiP 42-01-2002) approved by the order of the Regional Development of Russia Ministry of 27.12.2010, N780, pp 25–26
5. Body of rules SP 42-102-2004 Proektirovanie i stroitel'stvo gazoprovodov iz metallicheskix trub (Designing and construction of gas pipelines from metal pipes). Letter of the State Russian Federation Construction Committee of 15.04.2004, N LB-234/9, pp 39–40
6. Body of rules SP 42-101-2003 Obshhie polozheniya po proektirovaniyu i stroitel'stvu gazoraspredelitel'ny'x sistem iz metallicheskix i polie'tilenovy'x trub (The general provision and construction gas distribution system from steel and polyethyelene pipes approved). Resolution of the State Russian Federation Construction Committee of 26.06.2003 N112, p 29
7. Body of rules SP 116.13330.2012 Inzhenernaya zashhita territorij, zdanij i sooruzhenij ot opasny'x geologicheskix processov (Engineering protection of territories, buildings and structures from dangerous geological processes) approved 01.01.2013, N 118, pp 20–21
8. Kataev V, Maksimovich N, Meshcheryakova O (2013) Tipy' karsta Permskogo kraya (Types of Perm Krai karst). Bulletin of the BFU named after I. Kant. Publishing House of the Baltic Federal University named after I Kant, Kaliningrad 1:56–66
9. Territorial building codes TSN 11-301-2004 of the Perm region. Inzhenerno-geologicheskie izy'skaniya dlya stroitel'stva na zakarstovanny'x territoriyax Permskoj oblasti (Territorial building codes of the Perm region. Engineering and geological surveys for construction in the karst territories of the Perm region). Administration of the Perm region Press, Perm, p 122
10. Kopylov IS (2019) Estimation of Geodynamic Activity and its effect on mining-geological conditions and flooding of potassium mines. IMWA 2019 "Mine water: technological and ecological challenges", pp 16–22
11. Gaev A, Kilin Y (2018) Ob obespechenii e'kologicheskoj bezopasnosti gornodoby'vayushhix rajonov na osnove minimizacii negativny'x karstovy'x processov (On ensuring the environmental safety of mining areas on the basis of minimizing negative karst processes). Vestnik RUDN J Eng Res Peoples ' Friendship University of Russia, Moscow 1:35–51

12. Territorial Building Codes TSN 31-11-2005. Territorial'ny'e stroitel'ny'e normy' Permskogo kraya. Proektirovanie, stroitel'stvo i e'kspluataciya zdanij i sooruzhenij na zakarstovanny'x territoriyax Permskogo kraya (Territorial building codes of the Perm Region. Design, construction and operation of buildings and structures in the Perm Region karst territories). Perm Region Administration, Perm, p 50

13. Body of Rules SP 11-105-97 Inzhenerno-geologicheskie izy'skaniya dlya stroitel'stva (Engineering and geological surveys for construction). Adopted on 01.03.1998, p 86

14. Minkevich I (2003) Gidrogeologicheskie osobennosti rajonov razvitiya sul'fatny'x karstuyushhixsya porod Permskogo Prikam'ya (Hydrogeological features of the development sulphate karst rocks areas on the Permian Kama region). Thesis on the internet Scientific specialty 25.00.07, p 27

15. Gaev A, Kilin Y, Minkevich I (2013) O gidrogeologii karstosfery' na primere Urala i Priural'ya. (On the hydrogeology of the karstosphere on the example of the Urals and the near Urals regions). Bulletin of the Baltic Federal University named after I. Kant. Publishing House of the Baltic Federal University named after I Kant, Kaliningrad, pp 66–75

16. Tolmachev V, Reuter F (1990) Inzhenernoe karstovedenie (Engineering karst studies). Nedra, Moscow, p 151

17. Sposob predvaritel'nogo tamponirovaniya gruntov (The method of soils preliminary tamponing). http://vse-lekcii.ru/mosty-i-tonneli/stroitelstvo-tonnelej-i-metropolitenov/sposob-predvaritelnogo-tamponirovaniya-gruntov.html. Accessed 24 Jun 2019

18. Methodological documents in construction MDS 81-35. 2004. Metodika opredeleniya stoimosti stroitel'noj produkcii na territorii Rossijskoj Federacii (Methodology for determining the cost of construction products on the Russian Federation territory). Gosstroy, Moscow, p 61

19. Federal uniform rates FER 81-02-24-2001. Collection 24. Teplosnabzhenie i gazoprovody' - naruzhny'e seti (Heat supply and gas pipelines - external networks), p 72

20. Federal uniform rates FER 81-02-25-2001. Collection 25 Magistral'ny'e i promy'slovy'e truboprovody' (Main and field pipelines), p 94

Assessment of Industry-Related Risks for Human Environmental Well-Being

O. E. Bezborodova[✉], O. N. Bodin, and A. V. Svetlov

Penza State University, 40, Krasnaya str, Penza 440026, Russia

Abstract. The increase in the number and the capacities of industrial facilities makes the assessment of industry-related risks increasingly relevant for environmental safety management. This is because the risk theory is a versatile modeling and forecasting tool for the development of dangerous situations at industrial facilities. Besides, the risk theory allows for the consideration of risk factors of different origins. The purpose of this research is to develop a comprehensive assessment method for the impact of an industrial facility on human health that could be used to manage industrial facilities and improve the environmental well-being of people. This problem can be solved through modeling the interactions between industrial facilities and the environment and their impact on human health using the Lotka-Volterra model and the new methods of processing diverse data. The suggested method is based on comprehensive monitoring of multi-parameter object states in terms of diverse data. It helps improve the efficiency and reliability of multi-parameter object state controls. The research work proposes an algorithm for the assessment of the environmental well-being of a person residing within the industry-related risk factor area, and a Lotka-Volterra model for the interactions between the polluted environment (predator) and prey (human health). We provide an example implementation of the suggested method. The developed method may be used in the industry-related risk analysis, processing, and evaluation to manage territories and improve the environmental well-being of people and reduce the risks for their health.

Keywords: Industry-related risks · Industrial facilities · Industry-related risk · Environmental well-being of people · Environment

1 Introduction

The analysis and assessment of industry-related risks (IRR) are globally acknowledged tools for determining the impacts industrial facilities (IF) have on environmental safety, human health, and the establishment of people's environmental well-being because they allow for the consideration of risk factors of various origins.

Many authors from Russia [1–4] and abroad [5–10] use risk analysis to assess the impacts that chemical (chemical compounds and substances in the air, water, soil, and food), biological (pathogenic germs in food and water), and physical (ionizing, electromagnetic, and acoustic radiation) industry-related risk factors have on human health

(IRRHH). These factors come from IF in routine and emergency operation modes. The factors mentioned arise from production process instabilities, relatively low efficiency of environmental protection equipment, and the implementation of adverse scenarios of IF operation.

Environmental laws, standards, and regulations in Russia and the world are designed to protect human health and their living environment and based on the maximum permissible levels of adverse impacts and risks associated with them [11–15]. This approach is based on the acceptable risk concept which states that risks are never at zero, and attempts to eliminate risks at any cost may not be feasible. It is often more profitable to accept some level of risk and take rational, although not excessive, actions to minimize it. Mathematical simulations provide an opportunity to obtain a forecast for every risk development scenario analyzed and select a suitable one based on a set of criteria, as well as to rationalize the best management decision.

The purpose of this paper is to assess the industry-related risks for the environmental well-being of people (EWBP) using the Lotka-Volterra model.

2 Materials and Methods

Conducting an EWBP assessment helps solve several important problems and collect the data necessary to take a rational management decision [16]. To do this, it is necessary to determine the potential IF risks, assess the strength of evidence and their ability to bring about changes in human health under specific conditions, and select the prioritized risks that shall be studied in detail.

It is also important to determine the parameters that characterize risks (the levels, duration, frequency, and methods of impacting human health) and link the risks and their IF sources determining the ways the risks spread in the environment (ENV) and find their way into human bodies. Quality risk assessment allows establishing the connection between the risks existing in the ENV and their impacts on the human body, the changes in human health, and the consequences of these changes.

Using the data obtained, we can rank IRRHH risks and prioritize the areas of the regional environmental policy requiring adjustments according to the results of IRR assessment and develop recommendations to reduce the impacts on the health of the local residents.

The EWBP assessment for the residents of the areas under the IF risks is conducted in stages. The algorithm of this process is shown in Fig. 1. This assessment is based on determining, forecasting, and describing the IF risks.

To implement this algorithm, it is necessary to establish a database. This database must comprise the information on IF that are sources of risks (chemical, physical, and biological), their qualitative and quantitative description based on the ENV protection regulations, environmental documents of IF, the results of monitoring and calculations, as well as definitions, attributes and relations between the data and the rules for their retrieval. This requires a model for concept classification and a specific knowledge representation format, i.e. the ontology. The ontology comprises both the facts and the rules for retrieval allowing automatic conclusions about the existing or new data and thus perform their semantic processing.
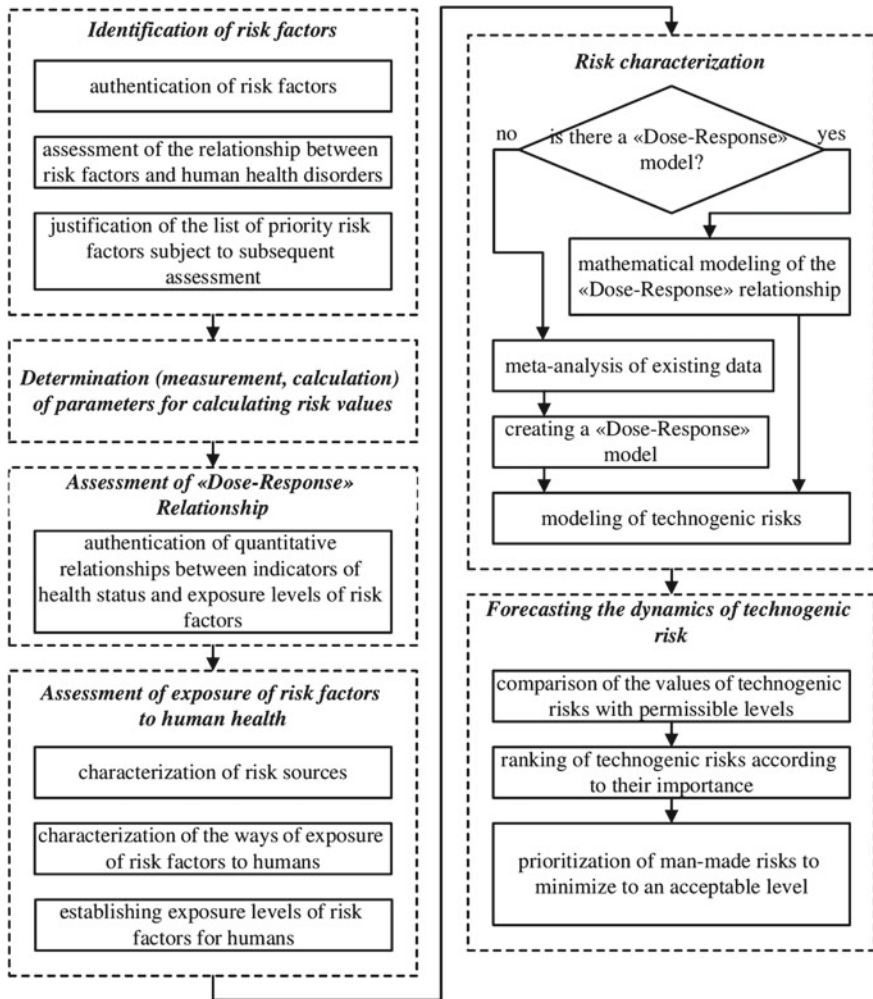
Fig. 1 The EWBP assessment algorithm for the residents of the areas under the risks from the facility

These data are used in the Identification, Exposure–Response Dependency Assessment, and the Assessment of Impacts on Health from Exposure to Risks stages. They result in the establishment of a list of risks, including the prioritized ones, and their characteristics. These data are required to organize monitoring and obtain parameters to calculate risk values and their changes over time.

A modern monitoring system for the ENV conditions operates in real-time and comprises automated fixed and mobile stations. The results of the monitoring are used as the initial data for the calculation of risk parameters [13] use in modeling and forecasting the changes in the EWBP levels.

The works on constructing an adequate mathematical model for the IRRHH assessment are quite complicated. This is due to the non-stable operation of risk sources, problems with risk parameter identification due to the scarcity of initial data, and the problems with the formalization of the quantitative assessment of modeling results that can lead to statistical uncertainty and taking wrong decisions. Thus, when rationalizing and developing risk assessment models, it is necessary to formulate the research purpose very accurately and thoroughly analyze the initial data on risk sources and factors.

Depending on the nature of the initial modeling data and the selected method of describing uncertainty, the mathematical models of risk assessment can be divided into deterministic, stochastic, linguistic, and non-stochastic. Deterministic and stochastic models are used more often as they allow for both qualitative and quantitative assessment of events.

Deterministic models are crude, they are relatively simple and effective, yet not accurate enough for final assessments and taking major decisions. The simplicity is achieved through ignoring some properties of real objects and some random factors as well. These models are used for the calculation of preliminary assessments when it is necessary to reduce the number of possible alternatives.

Probabilistic models take into account the random deviation of parameter values from their reference values due to some external and internal factors. The key advantage of probabilistic models is their high accuracy and reliability of the obtained results.

Thus, the authors suggest using a combined IRRHH analysis and assessment method that allows for obtaining more complete and detailed data on the research object and promotes the improvement of the information activity of IRR analysis and assessment.

The backbone of the suggested IRR analysis and assessment method is using the Lotka-Volterra model to process the risk data [17].

The Lotka-Volterra model applied to the interactions between the polluted ENV (predator) and prey (human health) [18] can be expressed as follows:

$$\begin{cases} \frac{dx}{dt} = (\alpha - \beta y)x, \\ \frac{dy}{dt} = (\delta x - \gamma)y \end{cases}, \tag{1}$$

where x is the EWBP parameter influenced by j-th risk factor defined as the inverse IRRHH [19];

y is the industrial load for the ENV under j-th risk factor defined as the probability of changes in the ENV due to the IF;

α is the threshold risk of the j-th factor impact on the human body defined as the probability of body resistance to the j-th risk impacts;

β is the risk for human health associated with the impact of the j-th risk factor;

γ is the territorial risk created by the j-th factor;

t is the time.

The authors bring forth a method that stipulates for using these data to analyze and assess the EWBP across the set of parameters characterizing the IRRHH [20].

This method stipulates that the IF database and the associated risks are used to establish several ranges for the IRRHH values by setting upper y_{Uij} and lower y_{Lij} boundaries for each of the controlled risk parameter $y_j (j = 1...n)$.

Taking into account the IRRHH scale (R_h) based on [11–14], the graphic representation of which is given in Fig. 2, we determined the values of controlled parameters IH_{ac}, IH_{cr}, and R_h and analyzed them using [20].
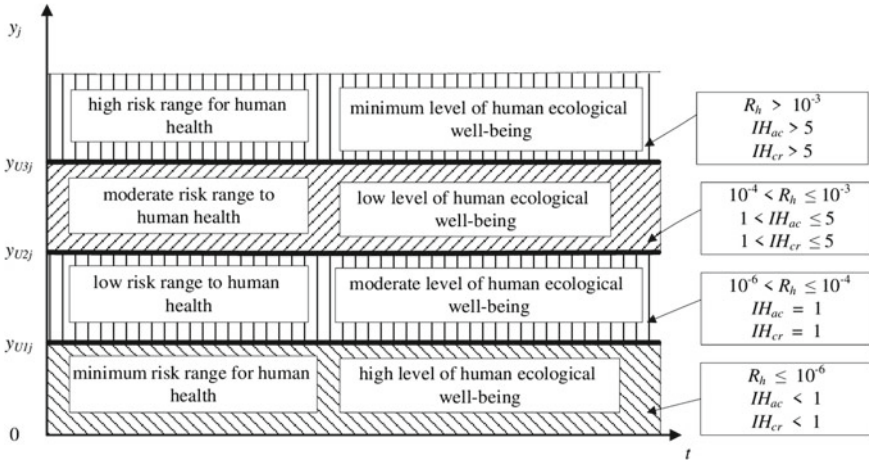
Fig. 2 Control limits for the IRRHH and EWBP levels

To do this, controlled IRR parameters are determined and calculated values are recorded $\hat{y}_j$. After this, we determined whether the calculation results for minimum, low, moderate, and high risk values δ_{ij} complied with the ranges of minimum, low, moderate, and high risks using the following formulae:

- for the low risk range:

$$\delta_{1j} = \begin{cases} 0, \; if \; y_{L1j} \leq \hat{y}_j \leq y_{U1j} \\ 1, \; if \; \hat{y}_j < y_{L2j} \; or \; \hat{y}_j > y_{U2j} \\ \frac{\hat{y}_j - y_{U1j}}{y_{U2j} - y_{U1j}}, \; if \; y_{U1j} < \hat{y}_j \leq y_{U2j} \\ \frac{\hat{y}_j - y_{L1j}}{y_{L2j} - y_{L1j}}, \; if \; y_{L2j} \leq \hat{y}_j < y_{L1j} \end{cases} \qquad (2)$$

- for the moderate risk range:

$$\delta_{2j} = \begin{cases} 0, \; if \; y_{L2j} \leq \hat{y}_j \leq y_{U2j} \\ 1, \; if \; \hat{y}_j < y_{L3j} \; or \hat{y}_j > y_{U3j} \\ \frac{\hat{y}_j - y_{U2j}}{y_{U3j} - y_{U2j}}, \; if \; y_{U2j} < \hat{y}_j \leq y_{U3j}, \\ \frac{\hat{y}_j - y_{L2j}}{y_{L3j} - y_{L2j}}, \; if \; y_{L3j} \leq \hat{y}_j < y_{L2j} \end{cases} \qquad (3)$$

- for the high risk range:

$$\delta_{3j} = \begin{cases} 0, & \textit{if } y_{L3j} \leq \hat{y}_j \leq y_{U3j} \\ 1, & \textit{if } \hat{y}_j < y_{L3j} \textit{ or} \hat{y}_j > y_{U3j} \end{cases}. \tag{4}$$

After this, we obtained and recorded complex industrial facility state parameters Δ_i for the range of minimum, low, moderate, and high IRRHH values using the following formula:

$$\Delta_i = \sqrt{\sum_{j=1}^{n} \delta_{ij}^2}. \tag{5}$$

The results of IF monitoring are presented by means of the generation of a visual image with green, yellow, red, and black colors indicating minimum, low, moderate, and high levels of IRRHH respectively.

Then we display the names and/or numbers of controlled risk parameters whose values are outside the ranges of low, moderate, and high risk levels.

3 Results and Discussion

We monitored the content of chemical substances in a residential area located close to a motor road (Industrial Facility 1) and a transport company repair shop (Industrial Facility 2). We monitored eight parameters: the content of benzene, toluene, ethylbenzene, styrene, carbon oxide, sulfur dioxide, nitrogen dioxide, and non-organic dust particles. The results of the monitoring are shown in Table 1. The table presents the average substance content values over the entire monitoring period. Besides, this table contains some monitoring results for the five checkpoints (CP), each of which represents a typical residence in the vicinity of an IF.

Table 1 Measurement results for the analyzed area

CP No	Average content, C_{cp} (mg/m^3)							
	Benzene	Toluene	Ethyl benzene	Styrene	Carbon oxide	Sulfur dioxide	Nitrogen dioxide	Dust
1	0.0276	0.0700	0.0061	0.0144	0.6039	0.0191	0.0163	0.0000
2	0.0243	0.0651	0.0081	0.0152	0.8450	0.0200	0.0162	0.1300
3	0.0217	0.0330	0.0064	0.0099	0.6846	0.0000	0.0163	0.0000
4	0.0100	0.0137	0.0050	0.0089	0.4590	0.0000	0.0170	0.1430
5	0.0100	0.0100	0.0050	0.0328	0.7529	0.0000	0.0230	0.0000

[a]For space considerations, only a portion of monitoring results is presented

The analyzed substances have both acute and chronic effects on the human body. The acute effects in Russia stand for changes in a person's condition that last up to 24 h.

The US Agency for Toxic Substances and Disease Registry (ATSDR) uses a period of 1–14 days when establishing the minimum risk levels for acute effects. The maximum duration of subacute effects is 10–12% of the average life expectancy, i.e. 8 years of a person's life. Any longer-lasting effects, i.e. those that exceed 10–12% of the average life expectancy, are considered chronic [13]. This led us to the calculation of hazard coefficients and indices for the substances that cause acute and chronic IRRHH.

The results of using the [13] methods and the Lotka-Volterra data analysis are presented in Tables 2 and 3.

Table 2 Hazard coefficients (HQ_{ac}) and indices (IH_{ac}) of the substances that have acute impacts on human health (R_h)

CP No	Coefficients HQ_{ac}								Indices IH_{ac}	R_h
	Benzene	Toluene	Ethyl benzene	Styrene	Carbon oxide	Sulfur dioxide	Nitrogen dioxide	Dust		
1	0.40	0.08	0.02	0.00	0.10	0.03	0.06	0.00	0.69	min
2	0.58	0.02	0.02	0.00	0.11	0.03	0.04	0.88	1.68	min
3	0.07	0.01	0.01	0.00	0.04	0.00	0.06	0.00	0.19	min
4	0.07	0.00	0.01	0.01	0.09	0.00	0.12	0.00	0.29	min
5	0.07	0.00	0.00	0.00	0.03	0.00	0.12	0.00	0.22	min

Table 3 Hazard coefficients (HQ_{cr}) and indices (IH_{cr}) of the substances that have chronic impacts on human health (R_h)

CP No	Coefficients HQ_{cr}								Indices IH_{cr}	R_h
	Benzene	Toluene	Ethyl benzene	Styrene	Carbon oxide	Sulfur dioxide	Nitrogen dioxide	Dust		
1	0.92	0.18	0.01	0.01	0.20	0.38	0.41	1.73	3.84	mod
2	0.81	0.16	0.01	0.02	0.28	0.40	0.04	0.00	1.76	mod
3	0.72	0.08	0.01	0.02	0.23	0.39	0.41	1.91	3.77	mod
4	0.33	0.03	0.01	0.01	0.15	0.00	0.43	0.00	0.96	min
5	0.33	0.03	0.01	0.03	0.25	0.00	0.58	0.00	1.23	mod

From the data in Table 2, we can see that the substances in Checkpoint 2 have the most obvious individual and combined acute effects on the human body. Benzene (hazard class II, $PDK_{mp} = 1.5\,\text{mg/m}^3$) and inorganic dust particles (hazard class III, $PDK_{mp} = 0.3\,\text{mg/m}^3$) make the largest contribution to this state. In all of the other checkpoints, the acute poisoning with the substances analyzed is improbable. However, if these IRR factors are ignored, changes in local residents' health may occur after eight years. Thus, with short-term exposure, the IRRHH is mostly at the minimum in the area (see Fig. 2).

As it's seen from Table 3, if the duration of the human body exposure to substances increases, health hazards also increase in four out of five checkpoints. Only in checkpoint 4, the increased level of risk remained within the minimum range. In such cases, residential areas feature moderate IRRHH.

In other words, to eliminate the chronic effects of substances, it is necessary to take prompt actions to reduce the IRRHH levels. These actions must target the reduction of substance emissions to the environments from Industrial Facilities 1 and 2 (Table 4).

Table 4 results of calculating complex industrial facility state indicators

CP No	R_h Limit value	Indices IH_{cr}	δ_{1ac}	δ_{2ac}	δ_{3ac}	Δ_{ac}	Indices IH_{cr}	δ_{1cr}	δ_{2cr}	δ_{3cr}	Δ_{cr}
1	10^{-4}	0.69	0	0	0	0	3.84	1	0	0	1
2	10^{-4}	1.68	1	0	0	1	1.76	1	0	0	1
3	10^{-4}	0.19	0	0	0	0	3.77	1	0	0	1
4	10^{-6}	0.29	0	0	0	0	0.96	0	0	0	0
5	10^{-4}	0.22	0	0	0	0	1.23	1	0	0	1

Only in Checkpoint 4, the IRRHH remained at the minimum under both acute and chronic exposure.

Decision-makers need to calculate compliance parameter values using Formulae (2)–(4), determine the complex indicators of industrial facility state Δ_i using Formula (5), and generate graphic images as shown in Fig. 3.
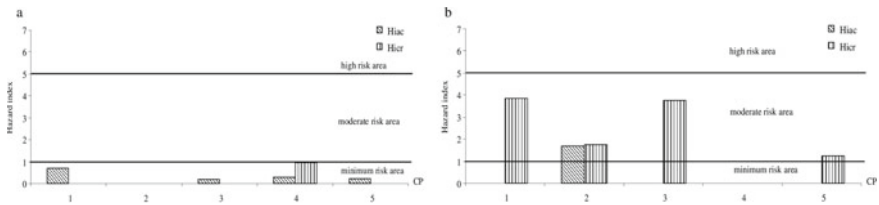
Fig. 3 IRRHH level indication: **a** acute exposure risks; **b** chronic exposure risks

Judging by the calculations, CP 2 has the highest risks of acute exposure to substances while the risks of chronic (long-term) exposure are present in CP 1, 2, 3, and 5. Only CP 4 is safe in terms of both acute and chronic exposure to substances.

Figure 3 shows the numbers of CPs whose risk parameters are outside the minimum risk range and in the moderate risk range.

Figure 3a shows CPs where the IRRHH level is within the minimum range. Figure 3b shows CPs where the IRRHH level is outside the minimum range but within the moderate range. The authors believe that this representation of data is more informative and helps interpret the results of IRRHH analysis and assessment correctly to make adequate management decisions.

4 Conclusions

Thus, the suggested comprehensive IRRHH assessment method facilitates the assessment of the IF impact on human health as well as the rational selection of management decisions based on the promptness and urgency of their implementation.

References

1. Boev VM, Boev MV, Tulina LM, Neplokhov AA (2013) Determined ecological human health risk factors in single factory towns. Health Risk Anal, 39–44. https://doi.org/10.21668/health.risk/2013.2.04
2. Chashchin V, Kovshov A. Thomassen Y, Sorokina T, Gorbanev S, Morgunov B, Gudkov A, Chashchin M, Sturlis N, Trofimova A, Odland Jon Oyvind, Nieboer E (2019) Health risk modifiers of exposure to persistent pollutants among indigenous peoples of Chukotka. Int J Environ Res Public Health 17(128). doi:https://doi.org/10.3390/ijerph17010128
3. Dushkova D, Evseev A (2012) The Russian North: environment and human health risk assessment
4. Gichev P (2002) Environmental pollution and human health. Siberian Branch of RAMS, Novosibirsk, p 320. (in Russian)
5. German Advisory Council on Global Change (2000) World in transition: strategies for managing global environmental risks. Springer, Berlin, Heidelberg; New York; Barcelona; Hong Kong; London; Milan; Paris; Singapore; Tokyo, p 384
6. Jardine C, Hrudey S, Shortreed J, Craig L, Krewski D, Furgal C, McColl S (2003) Risk management frameworks for human health and environmental risks. J Toxicol Environ Health Part B 6(6):569–718. https://doi.org/10.1080/10937400390208608
7. Shunan Z, Yuzhi Y, Weimin S (2020) Human health risk assessment of heavy metals in soil and food crops in the Pearl River Delta urban agglomeration of China. Food Chem 316:126213. https://doi.org/10.1016/j.foodchem.2020.126213
8. Ava K, Mostafa L, Mohammad K, Mohammad A, Reza S (2021) Human health risk assessment of heavy metals in agricultural soil and food crops in Hamadan Iran. J Food Compos Anal 100 103890. https://doi.org/10.1016/j.jfca.2021.103890
9. Adimalla N (2020) Heavy metals pollution assessment and its associated human health risk evaluation of urban soils from Indian cities: a review. Environ Geochem Health 42:173–190. https://doi.org/10.1007/s10653-019-00324-4
10. Eom S-Y, Choi J, Bae S, Lim J-A, Kim G-B, Yu S-D, Kim Y, Lim H-S, Son B-S, Paek D, Kim Y-D, Kim H, Ha M, Kwon H-J (2018) Health effects of environmental pollution in population living near industrial complex areas in Korea Environ Health Toxicol 33(1):e2018004. https://doi.org/10.5620/eht.e2018004
11. Guidelines for assessing human health risks from environmental hazards. Environmental health risk assessment. Department of Health and Ageing and Health Council, June 2002
12. WHO/IPCS. Environmental Health Criteria 239: principles for modelling dose-response for the risk assessment of chemicals, Geneva, 2009
13. Methodical recommendations. MosMR 2.1.9.004-03. Criteria for assessing the risk to public health of priority chemicals that pollute the environment. https://docs.cntd.ru/document/3715847
14. Guidelines for risk assessment R.2.1.10.1920-04. https://docs.cntd.ru/document/1200037399
15. AMAP Assessment 2009: Human Health in the Arctic. Arctic Monitoring and Assessment Programme (AMAP), Oslo, Norway (2009) xiv+256 pp
16. Bezborodova E et al (2021) IOP Conf Ser Earth Environ Sci 666:022004

17. Trubetskov DI (2011) The phenomenon of the mathematical model of Lotka-Volterra and similar ones. Izv. universities "PND" 2:69–88
18. Bezborodova et al (2018) IOP Conf Ser Mater Sci Eng 451:012189
19. AYu Popova NV, Zaitseva IV, (2018) On the issue of the implementation of the assessment of the quality of life of the population in the system of social and hygienic monitoring. Health Risk Anal 3:4–12. https://doi.org/10.21668/health.risk/2018.3
20. The method of complex control of the state of a multi-parameter object according to heterogeneous information: pat. 2719467 Ru. Federation. stat. 11.11.2019 ; publ. 17.04.2020, newsletter No 11

Environmental Safety Assessment of Technological Complexes for the Processing and Disposal of Oil-Containing Waste in Perm Region

O. Ruchkinova[1], S. Maksimova[1(✉)], A. Maksimov[1], and A. Ageeva[2]

[1] Perm State National Research Polytechnic University, 29, Komsomolskiy prospect, Perm 614990, Russia

[2] LLC PRIRODA-PERM, 46, Gazeta Zvezda Str., Perm 614039, Russia

Abstract. The problem of ensuring environmental safety in the processing and disposal of oil-containing and drilling waste is relevant in almost every oil-producing region of Russia. The impact of technological complexes (TCs) for the treatment and disposal of oil waste on the environment has not been actually studied. The aim of the study is to assess the environmental safety of the TCs of oil-contaminated soils and drilling waste (microbiological remediation sites). The article describes the methodology of conducting research based on environmental monitoring. The work was carried out on six TCs located in different areas of Perm Region from 2010 to 2020 to study the content of pollutants in air, in surface and groundwater, and in soils. The state of vegetation in the zone of TC influence is described. Based on the results of the research, the environmental safety of the design and engineering solutions adopted during the construction and operation of the TC is justified. It is shown that minimization of environmental impacts occurs in several directions: site selection, topography arrangement and anti-filtration protection. Examples of anti-filtration protection are given depending on geological conditions.

Keywords: Environmental monitoring · Environmental safety · Oil waste disposal · Microbiological remediation · Anti-filtration protection

1 Introduction

The oil and gas sector is the backbone of the country's economy. It has a significant impact on the environment, primarily because of the high levels of oil-containing waste generation. The official state report on environment informs that in 2019, oil companies produced 1.28 million tons of waste that needed to be disposed of [1]. The importance of the problem lies not only in the significant quantity but also in the negative impact of oil waste on almost all components of the natural environment. As a result of its impact, there is a substantial change in the natural state of the geoecological environment, a

decrease in the natural protection of underground waters, an activation of geochemical and geomechanical processes, and a change in the natural microbiocenosis.

The extent to which aspects of the problem of the man-made impact of oil production facilities on different components of the natural environment are studied, varies. The problems related to changes in water bodies [2], land cover, oil degradation processes in the soil [3, 4], air conditions [5] are best studied. The impact of technological complexes for the treatment and disposal of oil waste on the environment has not been actually studied.

Bioremediation based on natural mechanisms of the soil self-cleaning is widely used for oil waste management and is implemented at open-pit bioremediation facilities (TC) [6–10]. The process of cleaning oil-contaminated soils with different types of micro-organisms is well described in the literature [11, 12]. Factors that determine the efficiency of the bioremediation process have been studied: temperature and humidity of substrate, nutrients, pH, substrate aeration, volume fraction of the structurator, the number of hydrocarbon-oxidizing micro-organisms, hydrocarbon concentration in oil and base substrate [13–16].

There is an entire industry in Russia for the remediation of territory, and there are companies for the processing and disposal of oil-containing and drilling waste. There are currently 13 companies engaged in the processing of oil-containing waste in Perm Region [17, 18].

Despite the fact that the activities of the enterprises are of an ecological nature, TCs for processing and decontamination of oil-containing and drilling waste are production facilities that have a direct impact on the state of the environment. The aim of the research was therefore to study the impact zone of the TC using environmental monitoring tools.

The objects of the research were technological complexes of LLC "PRIRODA-PERM" which provide complex ecological services to enterprises of fuel and energy complex to which they are territorially connected. Since 2001, the company has processed and disposed of more than 722 thousand m^3 of solid oil-containing and drilling waste; more than 224 thousand m^3 of liquid oil-containing and drilling waste; 12 industrial granaries have been cleaned and rehabilitated, 136 temporary storage sites for oil-containing and drilling waste have been eliminated, and more than 286 ha. of damaged and contaminated land have been reclaimed. Over 140,000 m^3 of the tank stock was cleaned [19]. The microbiological remediation method used in the enterprises of LLC "PRIRODA-PERM" is patented [20]. Work on waste treatment, recycling and decontamination at the TCs of LLC "PRIRODA-PERM" is carried out all year round, and work on reducing the content of oil products by bioremediation is carried out usually from May to October. Work on the treatment and disposal of liquid oil-containing and drilling waste is carried out all year round, with the installation of equipment in the insulated premises (including temporary ones) allowing to maintain the temperature above 0 °C in winter.

Treatment and disposal of drilling liquid waste is carried out on technological equipment using reagent treatment (demulsifier and/or coagulant, flocculant—depending on the quality characteristics of the waste) by separating the water and oil fractions and precipitation of suspended particles.

As a result of solid waste disposal, environmentally friendly materials are obtained—soils and industrial water, which are suitable for secondary use.

The soils are used for the reclamation of disturbed land, the isolation of waste in solid household waste landfills, the elimination of barns and quarries. Industrial water is used in the reservoir pressure maintenance system (PPA), for the preparation of well silencing fluid (HGS) during routine and major well repairs, as well as for its own technological needs (irrigation of oil-contaminated soils in the process of microbiological remediation).

The research was conducted at six TCs located in different areas of Perm Region, referred to in article from 1 to 6.

2 Research Methods

Environmental monitoring is the main tool for studying the state of the natural environment. The principles and approaches for organizing monitoring and interpretation of results are well developed in both scientific [21, 22] and normative literature.

The studies were carried out in accordance with the program developed, which includes: atmospheric, surface and groundwater conditions—4 times a year: in winter, spring, summer, autumn; soil conditions—once in 3 years; geobotanical studies—once in 2 years. The length of research is 10 years.

Research activities included: field work (establishment of an observation network, field measurements as well as sampling for further analysis); laboratory work (analyses and sample studies); desk work (processing, generalization, analysis of field information).

Ambient air samples were collected downwind of the boundary sanitary protection zones (300 m). At the control points, the actual meteorological parameters (temperature, pressure, wind direction, wind speed) were determined. Ambient air samples were analyzed for the content of nitrogen dioxide (RD 52.04.792-2014), hydrogen sulfide (RD 52.04.795-2014), dioxide sulphur (RD 52.04.822-2015), hydrocarbon limit (PND F 13.1:2.23-98), benzene, toluene, xylene (PND F 13.1:2.25-99). Measuring instruments were spectrophotometer UNICO, chromatograph "Chromatec-Crystal 5000". Actual concentrations of pollutants were compared with the maximum permissible concentrations of these substances for populated areas (MPC_a).

The TC regime and observation network was used to monitor groundwater conditions. Wells for establishing background concentrations are located above the groundwater flow outside the zone of TC influence. The observation wells are located, respectively, outside the site below the topography. Hydrochemical studies included water sampling from watercourses and wells. The samples from small surface watercourses were taken on a deep stream from a depth of 0.2–0.3 m above the surface. Samples were taken from observation wells. Water samples were analyzed for the content of chlorides (PND F 14.1:2:4.111-97), petroleum products (PND F 14.1:2:4.128-98). The measuring instrument was liquid analyzer "FLUORAT-02-2M". The actual chloride concentrations were compared with the maximum allowable concentration (MPC_{cl}) in drinking and household water supplies, which is 350 mg/l. Petroleum products were compared with a maximum allowable concentration of petroleum products (cumulatively) in drinking water, which is equal to 0.1 mg/l. Soil studies for each TC were conducted at three points:

25, 100 and 250 m from the boundary of the embanking site at depths of 0–20 cm at each point. The content of chlorides and petroleum products was determined in the soil samples. Geobotanical studies were carried out on the territory from the border of TC embanking site to the border of the sanitary protection zone.

3 Results and Discussions

The assessment of the state of the natural environment main components, based on the results of long-term complex geo-environmental studies of air and water, soil cover and vegetation at technological complexes of LLC "PRIRODA-PERM" has shown the following.

For the entire observation period, the actual concentrations of pollutants in the atmosphere near the TC did not exceed MPC (Table 1). Concentrations of chlorine ions and petroleum products in surface and groundwater near all TCs are within background values and did not exceed MPC for the observation period (Table 2). The single exceedances of the MPC, which were certainly observed during the ten-year period, could be caused by reasons unrelated to the activities of the TCs (features of the hydrological regime of rivers, the use of chemical fertilizers on nearby agricultural land, etc.).

Table 1 Summary results of atmospheric chemical studies in the vicinity of the LLC "PRIRODA-PERM" TC for 2010–2020

Indicator	$MPC_n.$ (mg/m^3)	Actual concentration (mg/m^3)
Nitrogen dioxide	0.2	<0.021–0.62
Hydrogen sulfide	0.008	<0.006–0.0078
Sulfur dioxide	0.5	<0.0025–0.018
Limit hydrocarbons C1-C5	200	1.0–2.2
Benzene	0.3	<0.02
Toluene	0.6	<0.02
Xylene	0.2	<0.02

The content of petroleum products and chlorides in the soils varied within the background values for Perm Region and did not exceed the permissible chloride and oil residues in the soils of Perm Region (Table 3).

The results of the geobotanical studies (Table 4) showed the parameters characteristic of the TC area vegetation conditions: broad-leaved spruce-fir forests with a well-developed shrub layer, solid grassland and weak moss layers; south-taiga fir-spruce forests dominated by boreal species in the stand and the shrub layer with a noticeable increase in the role of grasses and a weak moss layer [23].

Tables 1, 2 and 3 show the minimum and maximum values of the indicators obtained over 10 years of measurement.

Table 2 Results of hydrochemical studies in the vicinity of the LLC "PRIRODA-PERM" TC

TC	Water sampling location	Chlorides, mg / dm^3	Petroleum products, mg/dm^3
1	The Polazna River	60–142	0.021–0.062
2	The Turka River	<10	0.011—0.034
2	4-NG underground well	<10–59	0.019–0.12
3	The Osinka River (background)	<10–36	0.01–0.053
3	The Osinka River (control)	<10–43	0.011–0.039
4	The Kolynva River	<10–16	0.01–0.087
5	Underground well 4 (control well)	10–45	0.009–0.035
5	Underground well 5 (background)	<10–44	0.006–0.12
5	The Unva River	30–44	0.009–0.027
6	The Strezh River	22–226	0.01–0.067
6	Underground well 1 (background)	<10–39	0.006–0.053
6	Underground well 2 (control well)	<10–37	0.005–0.058

Table 3 Results of soil studies in the vicinity of the LLC "PRIRODA-PERM" TC for 2010–2020

TC	Soil type	Chlorides (mg/kg)		Petroleum products (g/kg)	
		Content in the soil	Standard	Content in the soil	Standard[a]
4	Sod-slightly podzolic	17.7–192.0	360	0.08–2.5	2.3
6					
1	Sod-medium podzolic				
3					
5	Sod-strongly podzolic				2.4
2					

[a]Regional standard of permissible residual content of oil and products of its transformation in the soils of the Perm Region (Resolution of the Government of the Perm Region of 23.12.2020 N 1015-p)

Table 4 Results of geobotanical studies in the vicinity of the LLC "PRIRODA-PERM" TC

Indicators	TC1	TC2	TC3	TC4	TC5
Location zone	South taiga	Coniferous-broadleaf (mixed)	Coniferous-broadleaf (mixed)	Middle Ural taiga	South taiga
Tree tier					
Stand formula	Betula pendula, Picea obovata;	Betula pendula, Picea obovata	Betula pendula, Picea obovata, Abies sibirica;	Betula pendula, Picea obovata, Populus tremula;	Picea obovata, Betula pendula, Abies sibirica, Pinus sylvestris;
average height, m	15–18	22–25	18–20	18–20	15–20
crown closeness	0.4	0.2	0.5–0.4	0.3	0.4
Shrub layer	No	No	No	No	
projective cover					0.1
average height			-		0.5–1
Herbaceous and shrubby tier					
projection coverage	0.5	0.3	0.5	0.4	0.4
average height, cm	10–20	10–20	10–20	10–15	15–20
Moss-lichen layer		No	No		No
projective cover				0.2	
Number of species	22	24	23	21	30
Abundance	1–3	1–3	1–3	1–3	1–3

The positive results of long-term environmental monitoring are determined by the approach to the arrangement of technological complexes. Minimization of environmental impacts takes place in several directions. Hydrogeological conditions are the most important criterion for selecting the site in which production takes place, as they determine the main costs of ensuring environmental safety throughout the life cycle of the site. Equally important is the terrain, which determines the amount of excavation and the impact of the process on the ecosystem. During the operation phase, the proper layout of the base ensures the collection and treatment of wastewater. For the microbiological remediation process, gradients from 0.03 0/00 to 0.010/00 are taken towards drainage ditches. Wastewater from the processing site has, as a rule, a high index of chemical oxygen consumption, a high content of phenols, nitrates, and when mixed with lake and river waters, it sharply reduces the content of dissolved oxygen. Therefore, they are collected in a drainage system consisting of drainage ditches and pits. Then wastewater is transported to the reservoir pressure system of oil-producing enterprises. Slopes from 0.03 0/00 to 0.010/00 in the direction of drainage ditches are accepted for the technological process of microbiological remediation. Ditches and pits are equipped with anti-filtration protection.

Functional zoning of the territory takes into account the specificity of the structure and the requirements of the technological process of microbiological remediation. The sites are generally divided into working maps, in accordance with the process cycle of cleaning the oil-contaminated soil. For the reception, temporary storage and disposal of liquid waste, a storage device is provided in a specialized area. To avoid negative impacts on the hydrosphere, the site is equipped with an anti-filtration shield and a drainage system for the collection and disposal of wastewater. The design of anti-filtration shields is selected according to the geological conditions of the site (Table 5). Specialized and standard technological equipment, standard construction equipment and mechanization tools[1] are used in the process of processing, recycling and neutralization of waste (Figs. 1 and 2).

4 Conclusions

Ecological monitoring of technological complexes for decontamination of oil-contaminated waste of LLC "PRIRODA-PERM" in Perm Region was carried out during 10 years. The instrumental data obtained made it possible to assess the environmental impact of production sites as acceptable. The arrangement of the sites and constructive measures aimed at minimizing the impacts ensured the environmental safety of all components of the production activities of LLC "PRIRODA-PERM" enterprises—from decontamination of oil-containing waste to the operation of production site structural elements. The environmental monitoring systems of the hydrosphere included in the project have shown the efficiency of the anti-filtration protection of production sites and confirmed the correctness of the chosen engineering solutions.

---

[1] "Technological regulations for the processing and disposal of oil-containing waste and drilling waste to produce commercial products (materials)". Positive conclusion of the State Environmental Expertise No. 56 of 05.02.2016.

Table 5 Anti-filtration protection of the TC ground base

Name technological complex	Geological structure of the TC base	Construction of anti-filtration protection
TC 3	The filtration coefficients of K_f clay soils, which form the site all-round, are from 2.5×10^{-7} to 8×10^{-7} m/day	Measures for anti-filtration protection of the base are not required
TC 4	Clay from semi-hard to soft-plastic consistency 0.109–0.529 m/day, (1.26–6.0×10^{-4} cm/s)	A shield of compacted crushed clay with $K_f = 10^{-7}$, 0.5 m thick; a protective layer of sandy loam with a thickness of 0.15 m along the drainage layer of 0.15 m, on a compacted planned base
TC 5	Marl 0.6 m/day, (6.9×10^{-4} cm/s),	The slopes are reinforced with geotextile and high-pressure polyethylene HDPE with a filtration coefficient of 1×10^{-8} m/day
TC 6	Soils with a high filtration coefficient	A shield of compacted crushed clay with $K_f = 10^{-7}$, 0.5 m thick; a protective layer of sandy loam with a thickness of 0.15 m along the drainage layer of 0.15 m, on a compacted planned base

Fig. 1 Treatment of solid oil-containing waste [19]

Fig. 2 Solid oil-containing waste in the trial of processing and disposal [19]

It should be noted that the positive results of long-term observations indicate the possibility of long-term use of existing TC sites. This reduces the need to allocate new land plots for the decontamination of oil-contaminated soils and sludge and contributes to the conservation of land resources.

In general, the results of the long-term environmental monitoring suggest that the projections of the environmental impact of the technological complexes for the treatment of oil-containing waste by bioremediation are consistent with those made in the development of the project document and the in-situ data.

References

1. O sostoyanii i ob ohrane okruzhayushchej sredy Rossijskoj Federacii v 2019 godu. Gosu-darstvennyj doklad.(2020) (State report. On the state and environmental protection of the Russian Federation in 2019). MINPRIRODY of RF, Moscow (2020)
2. Buzmakov SA, Kostarev SM (2003) Tekhnogennye izmeneniya komponentov prirodnoj sredy v neftedobyvayushchih rajonah Permskoj oblasti. (Technogenic changes in the components of the natural environment in the oil-producing regions of Perm region). Perm State Un-ty, Perm
3. Borisayko YY (2017) Biorekul'tivaciya: mikrobiologicheskie tekhnologii ochistki nefteza-gryaznennyh pochv i tekhnogennyh othodov, Intensifikaciya processov vosstanovleniya neftezagryaznennyh pochvogruntov territorij nakopitelej othodov neftegazodobychi (Intensi-fication of the recovery processes of oil-contaminated soils in the territories of accumulators of oil and gas production waste.). J Vestnik RAES 17(5):66–69
4. Loginov ON, Silishchev NN, BoykoTF et al (2009) Biorecultivation: microbiological technologies for cleaning oil-contaminated soils and technogenic waste. Moscow
5. Kostarev SM (1995) Ocenka vozdejstviya na komponenty prirodnoj sredy v rajonah nefte-dobychi Zapadnogo Urala Problemy bezopasnosti pri ekspluatacii mestorozhdenij poleznyh iskopaemyh v zonah gradopromyshlennyh aglomeracij (SMP-95): Tez. dokl. mezhdunar.

simp. GI UrO RAN (Assessment of the impact on the components of the natural environment in the oil production areas of the Western Urals). In: Abstracts problems of safety in the operation of mineral deposits in the zones of urban industrial agglomerations SMP-95 GI UrO RAS), Moscow, pp 72–73

6. Zhang XX, Geng CX, Fang MM et al (2008) Bioremediation of petroleum contaminated soil by immobilized microorganisms. Shiyou Xuebao, Shiyou Jiagong 24(4):409–414

7. Maksimov AD, Maksimova SV (2010) Kompleksnaya pererabotka nefteothodov v kontekste antikrizisnoj politiki. «Zashchita okruzhayushchej sredy v neftegazovom komplekse (Complex processing of oil waste in the context of anti-crisis policy). J Environ Prot Oil Gas Complex 6:37–40

8. Alexandrova TV, Martynenko AV (2018) Issledovanie rynka pererabotki i utilizacii promyshlennyh othodov v Permskom krae (Research of the market of processing and utilization of industrial waste in Perm region). J Econ Bus Theory Pract 3:9–13

9. Gerzhberg YM, Pystina NB, Popov AN, Kutsil OV (2005) Koncepciya sozdaniya stacionarnogo poligona dlya obezvrezhivaniya neftezagryaznennyh othodov proizvodstva (The concept of creating a stationary landfill for the neutralization of oil-contaminated production waste). J Environ Prot Oil Gas Complex 9:72–77

10. Zhukov TN, Glushankova ES, Belik, (2015) Razrabotka tekhnologii utilizacii otrabotannyh burovyh rastvorov, burovyh shlamov i neftezagryaznennyh gruntov s ispol'zovaniem biopreparatov (Development of technology for utilization of spent drilling fluids, drilling slurries and oil-contaminated soils using biological products). J Transp Transp Facil. Ecol 2:31–45

11. Chen L, Zhang F, Zhang S, Ren S (2011) Experimental study on bioremediation of petroleum contaminated soil in Puyang oilfield. Adv Mater Res. https://doi.org/10.4028/www.scientific.net/AMR.233-235.693

12. Yuniati MD (2017) Bioremediation of petroleum-contaminated soil: a review. Published under licence by IOP Publishing Ltd/ IOP conference series: earth and environmental science, vol 118, Global colloquium on GeoSciences and engineering 2017, 18–19 October 2017, Bandung, Indonesia

13. Paladino G, Arrigoni JP, Satti P et al (2016) Bioremediation of heavily hydrocarbon-contaminated drilling wastes by composting. Int J Environ Sci Technol 13:2227–2238. https://doi.org/10.1007/s13762-016-1057-5

14. Li DS, Feng JQ, Liu YF et al (2019) Enrichment and immobilization of oil-degrading microbial consortium on different sorbents for bioremediation testing under simulated aquatic and soil conditions. J Appl Environ Biotechnol 4(2):12–22. https://doi.org/10.26789/AEB.2019.02.003

15. Korshunova TYu, Chetverikov SP, Bakaeva MD et al (2019) Mikroorganizmy v likvidacii posledstvij neftyanogo zagryazneniya (obzor) (Microorganisms in the elimination of the consequences of oil pollution (review). J Appl Environ Biotechnol 55:344–354. https://doi.org/10.1134/S0003683819040094

16. Zaborskaya EA, Kramm NA, Kustova AYu (2011) Izuchenie vliyaniya strukturatorov na process bioremediacii neftezagryaznennyh pochv (Study of the influence of structurators on the process of bioremediation of oil-contaminated soils). Environ Prot Oil Gas Complex 1:22–29

17. Vyatkin KA (2014) Analiz effektivnosti tekhnologij utilizacii neftezagryaznennyh gruntov na territorii Permskogo kraya (Analysis of the efficiency of technologies for utilization of oil-contaminated soils on the territory of Perm Region). Probl Dev Hydrocarbon Ore Miner Deposits 1:223–226

18. Vyatkin KA (2014) Ocenka effektivnosti sposobov utilizacii neftesoderzhashchih othodov (Evaluation of the efficiency of methods of utilization of oil containing). J Ecol Urbanized Territ 1:25–29

19. Website of LLC Nature-Perm. https://priroda-perm.ru/. Accessed 05 June 2021
20. Fuss VA et al (2002) Metod remediacii neftezagryaznennyh gruntov (Method of remediation of oil-contaminated soils). Patent No. 2224604 C1 Russian Federation, IPC B09C 1/10. No. 2002117206/13: application 27.06.2002: publ. 27.02.2004
21. Imam A, Kanaujia PK, Suman SK, Ghosh D (2019) Analytical approaches used in monitoring the bioremediation of hydrocarbons in petroleum-contaminated soil and sludge. J Trends Anal Chem 118:50–64. https://doi.org/10.1016/j.trac.2019.05.023
22. Chikere C, Okpokwasili GC & Chikere BO (2011) Monitoring of microbial hydrocarbon remediation in the soil. In: Proceeding 3 Biotech 1:117–138. https://doi.org/10.1007/s13205-011-0014-8
23. Titma OA (2018) Rajonirovanie lesov Permskogo kraya. (Zoning of forests of Perm region). Geograficheskoe izuchenie territorial'nyh system. In: Ivanova MB (ed) Geographical study of territorial systems. In: Proceeding of the XII regional scientific and practical conference of students, postgraduates and young scientists, Perm, 16 May 2018

Current State of Lands Affected by Mining Activities in Ural Region

V. E. Konovalov[1], V. A. Pochechun[1,2(✉)], and A. I. Semyachkov[2]

[1] Ural State Mining University, 30, Kuibysheva Street, Yekaterinburg 620144, Russia
[2] Institute of Economics, Ural Branch of RAS, 29, Moskovskaya street, Yekaterinburg 620014, Russia

Abstract. This study includes research and analysis of the current state of lands in the Ural Region. It is highly affected by mining activities. Nowadays, the lands affected by mining activities are disturbed lands, which include the combination of natural and man-made landscapes. The development of mineral deposits and the primary processing of raw minerals negatively impact the environment. In particular, water-engineering structures, industrial waters accumulated in abandoned open-pits, flooded open-pits, slag dumps, and other man-made objects formed after the development of mineral deposits have many negative aspects and heavily pollute the environment. This study is based on the authors' longstanding (over 20 years) monitoring of the environmental elements in the territory greatly affected by mining activities in the Middle Urals. The study presents the analysis of geochemical surveys of environmental elements conducted during the monitoring. The impact of various man-made objects—slag dumps, tailing ponds, as well as an industrial site, on these elements is shown. The research conducted is a prerequisite for the development of a methodology for a comprehensive geoecological assessment of the impact mining activities have on the environment.

Keywords: Mine · Mineral resources · Industrial area · Waste · Ural region · Landscape · Sludge storage

1 Introduction

The development of mineral deposits (MD further) has a significant anthropogenic effect on the subsoils. This causes major anthropization with the formation of artificial post-mining landscapes and conversed lands—the results of the negative impact of the mining activities (hereinafter referred to as MA) on the environment [1, 2].

Consequently, the lands affected by mining activities (hereinafter referred to as LMA) can be defined as territories exposed to the environmental impact of MA [3]. The area of LMA is defined by the number of objects related to MA, as well as the impact of MA on the environment. It should be noted that LMA include areas with territories of various types used for certain special purposes, as well as polluting different environments—air (emissions into the atmosphere), water (discharges drainage and other industrial water), soil (accumulation of contaminants due to air emissions and water discharges) [4].

The total volume of man-made mineral waste located in the territory of the Ural Region exceeds 8.5 billion tons with about 2 km^3 of all types of production waste added annually. The contribution of the Ural Economic Region to the atmospheric pollution by stationary sources in the 1990s amounted to 23–26% of the All-Russian emissions [5, 6]. A significant portion of conversed lands was formed by the mining industry.

During over 300 years of mining history in the Ural Region, more than 1,670 mining companies were active (or stopped their activities) including gold mines—1002, underground mines—566; open-pit mines—105. Currently, more than 40 gold mines, 48 underground mines, 100 open-pit mines are operating here, notably, 40 of them are large [7]. Still, the Ural Region permits developing unallocated subsoil reserves in the future.

A detailed analysis of the current state of lands affected by mining activities is required to reduce the negative impact of MA on the environment, to have a more effective subsoil resource management, as well as to re-integrate objects remaining after MD depletion into the national economy or to support the population needs.

2   Materials and Research Methods

The study applies a systematic approach, which uses abstract-logical, geographical and morphological methods, as well as a retrospective method. The study is based on the results of field observations and the analysis of a large number of documents, map data, as well as remote sensing data.

3   Results and Discussion

The considered territory, the Ural Region, is located on the border of Europe and Asia covering a mountainous country—the Urals, as well as parts of the East European and West Siberian Plains [7]. The total area of the region is 270,421.7 thousand hectares or 16.1% of the Russian Federation.

Spanning over a common location, certain lands affected by mining activities form a mining district. Mining districts united by a physiographic region or a physiographic country form mining regions. By the type of mineral resources, the territory of the Ural Region is divided into three mining regions associated with oil and gas production, solid minerals, and peat [8–10]. This study analyzes the current state of the Ural mining region associated with the extraction of solid minerals (UMR SME). The studied mining region unites the Sverdlovsk Oblast, the eastern parts of the Republic of Bashkortostan, the Perm Krai, and the Orenburg Oblast, as well as the western part of the Chelyabinsk Oblast with the total area of approximately 29,655.1 thousand hectares (11% of the Ural Region area).

A complete transformation of natural landscapes usually takes place at MD development locations, which in turn create new objects of subsoil use. These include natural and man-made objects—such man-made landscape shapes as excavations (open-pits, strip-pits), piles (waste rock dumps, spoil tips), etc., as well as various facilities (industrial buildings and structures, including water-engineering facilities) [11]. MA objects are formed and operated during the construction and production of MA, as well as primary

processing of MD, partially remaining in a form of mining landscapes after the MD are depleted [3]. Furthermore, MD mining creates new artificial geological provinces. MA disturb the geochemical conditions for the formation of surface runoff and underground flow, as well as runoff parameters, which in turn changes the hydrochemical and hydrological conditions of water objects.

Arranging dumps, landfills, and tailing ponds in drainage basins without proper sealing essentially creates new geological provinces affecting the formation of surface runoff different from runoff in non-disturbed lands in purity, and this is already pollution. The development of residential areas without proper environmental protection measures is actually a full-scale pollution of drainage basins by man-made products. It imminently results in land quality degradation. Affected by anthropogenic activities, water bodies accumulate bottom sediments, which often include ingredients not common to discharged wastewater. For instance, deposited organic matter can be a source of toxic gases, toxic organics, as well as nitrogen- and phosphorus-containing mineral and organic substances. Accumulated sulfide minerals are often a source of metals, acids, arsenic compounds. In certain regions, such secondary pollution is currently starting to prevail, posing a significant threat to water ecosystems. The use of unsustainable technologies increased water consumption. In its turn, it required change in the hydrological conditions of surface waters. Reservoir cascades were built on many rivers of the Middle Urals, which radically changed the conditions affecting surface water quality. These conditions result in intra-basin processes starting to have a significant impact, which, alongside with anthropogenic load, leads to the occurrence of large amounts of substances present in river systems at the ambient level. Water engineering structures on rivers alter their hydrological conditions, as well as hydrochemical conditions, in turn, changing the living conditions of river flora and fauna, sometimes along the entire river length. Almost in all cases, the disruption of hydrological conditions below the control structure reduces the water level, deteriorates habitats of flora and fauna, causing deterioration of water quality, as well as sanitary and epidemiological conditions even against the minimum anthropogenic load.

The main MA objects in case of open-pit mining are open-pits (strip-pits) and waste rock dumps. In case of underground mining these are industrial sites of underground mines and allotted territories, as well as industrial sites of processing plants with dry and liquid waste dumps. The distribution of areas occupied by the MA objects for open-pit mining of MD varies within the following limits: from 20 to 60% of the MA area is occupied by open-pits (strip-pits), from 30 to 70%—waste rock dumps, from 5 to 40%—processing plants. In the case of underground mining of MD, the occupied territories generally include industrial sites with a system of buildings for transportation of rocks and ores from underlying aquifers to the surface, lifting people and equipment down to underground workings, as well as the other industrial structures and waste rock dumps (spoil tips). Industrial sites occupy areas ranging from 4 to 60 ha., while the areas of allotted territories on the surface depend on the MD volume and their subsurface formation specifics.

The areas of several large operating mining facilities are shown in Table 1.

To determine the impact of slag dumps on surface waters, the dynamics of their pollution with metals were evaluated (on the example of a slag dump of Rezh Nickel Plant).

Table 1 Areas occupied by large operating mining facilities

Mining facilities	Area, ha			
	Pit(s)	Waste rock dumps	Industrial area (including processing plant and tailing ponds)	Total
Sverdlovsk Oblast				
Uralasbest JSC	1898.0	1056.2	1635.8	4590.0
Kachkanarsk mining and processing plant	931.0	2793.5	2316.0	6040.5
Republic of Bashkortostan				
Uchalinsk mining and processing plant	252.9	334.5	457.7	1042.1
Sibay mining and processing plant	182.6	711.7	399.2	1292.5
Orenburg Oblast				
Gai mining and processing plant	309.4	717.0	718.4	1744.8
Kiembay mining and processing plant	252.1	568.2	539.4	1360.0

The observation results allowed calculating the geochemical mobility of chemical elements for various water exchange conditions. The dependence of metal concentration in waters on the season has been detected for almost all metals. The highest content of Ni reaching 1006 μg/dm^3 is observed in autumn. This is caused by increased precipitation and relatively long excessive moistening of waste rock dumps. The second period of elevated contents of Ni, Cd, Fe, and partly Mn happens to be in February–March. Apparently, this is caused by a migration environment with a higher reduction potential associated with the maximum soil freezing. Acid-alkaline migration conditions exhibit a changing pH from 8.17 in winter to 7.16 in summer. Furthermore, the Eh value varies from +185 to +326 mV. The deviations into the alkaline and reducing regions are due to the composition of the water-bearing medium. The migration ability of elements is determined, for one part, by their content in slag dumps, and for the other—by the natural water circulation conditions in the "slag dump—environment" system. The following amount of substances are carried away from the dump into surface water on average per year: Ni—25.8 kg; Cr—14.4 kg; Fe—5 kg; Mn—0.8 kg; Cd—82 g. The water migration intensity row has the form: Ni > Cd > Cr > Mn > Fe.

Also, we studied the impact of part of the drainage basin in the OJSC Svyatogor diversion channel on the surface runoff contents. The studied area of the drainage basin has acidified soils (pH = 3.6–4.5) containing a significant amount of pollutants. The following concentrations were detected (mg/kg of air-dry weight): sulfur—21,177.6–116,281.94, iron—15,412.46–116,281.94, copper—436,27–10,009.61, zinc—309.93–575.01, manganese—190.07–324.14, lead—214.12–324.36. Surface runoff in this

drainage basin is over acidified (pH = 2.3–2.6) and contains a significant amount of pollutants: sulfates—15,807.6–56,724.2 mg/dm^3, iron—370.52–1128.776 mg/dm^3, copper—19.16–119.094 mg/dm^3, zinc—44.425–45.6 mg/dm^3, manganese—11.85–50.797 mg/dm^3. The surface runoff has the following contents of nickel, cadmium, lead and cobalt (mg/dm^3): nickel—0.78–1.41, cadmium—1.3–2.53, lead—0.0035–0.012; cobalt—1.536–2.86.

The specifics of land use for the extraction and processing of MD in UMR SME is that many settlements were formed due to the establishment of mining facilities, while 34 cities are considered as industry-based towns [12]. For example, 38–40% of settlements in the Chelyabinsk Oblast are closely connected to mining. This value is about 35% in the Sverdlovsk Oblast. Among these settlements, 49% of settlements on the UMR SME territory are associated with underground mining of MD, and 51% of settlements—with open-pit mining [13]. Also, the lands associated with underground mining are impacted by underground operations. For example, the north-western part of Krasnoturinsk, the southeastern part of Upper Pyshma, almost the entire territory of Berezovsky town, the central part of Bereznyaki and Solikamsk towns, and others have underlying underground workings.

In the analysis, we paid particular attention to agricultural lands of the Ural Region, which account for 28% of all land area on average. The following territorial entities of the Russian Federation in the Ural Region have more than 50% of the territory occupied by agricultural lands: Republic of Bashkortostan (50.9%), Chelyabinsk Oblast (58.4%), and Orenburg Oblast (88.4%). They include over 850 depleted and about 500 developed MD, including large (Table 1), as well as about 260 MD in the state reserve, prepared for the development or explored [14].

The analysis of over 300 years of mining history in the region conducted by the authors revealed that the following MA objects in the UMR SME territory have not yet been properly abandoned:

- Objects of former MA (prospecting pits, mine shafts, etc.).
- *Disturbed lands* with open-pits (strip-pits) and extensive land areas with waste rock dumps and other mining-related piles, including yet to be abandoned dumps of processing plants.
- *Degraded lands* having a satisfactory environmental condition due to self-regeneration (mining facilities overgrown by trees or shrubs and/or bogged, flooded mines, open-pits, etc.), reservoirs (ponds) of mining and processing facilities with water-engineering structures (dams, dutches, gateways, etc.).
- *Contaminated lands* containing toxic substances and transformed into lifeless deserts [10, 15, 16].

For instance, the territory of the Nizhny Tagil industrial hub includes the following waste dumps—slag dump of the Kuibyshev Refinery, sludge dump in the Tagil River floodplain, waste dump of a fire brick production facility, and chemical waste dump of a coke production plant.

According to our monitoring, the Kuibyshev Refinery slag dump negatively affects the atmospheric air, which is indicated by contamination of snow cover and soils. The contaminants include copper, zinc, manganese, vanadium, nickel, chrome, and iron

exceeding the maximum allowable concentration (MAC). Figure 1 shows the distribution of iron content in soils. About 2/3 of the studied area has an iron content of 0.1–02 mg/dm^3, which exceeds the MAC by 10–20 times. This area includes locations with the maximum pollution. Such plots are located to the north, south, and southeast of the slag dump. The plot with maximum pollution has iron content ranging from 0.2 to 0.3 mg/dm^3.
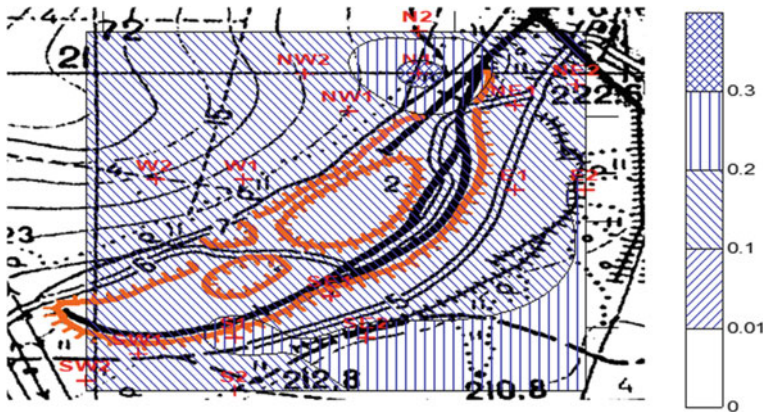
Fig. 1 Iron distribution in soils in the vicinity of the Kuibyshev Refinery slag dump (mg/dm^3), and sampling sites

The sludge dump located in the secondary landscapes of the Tagil River floodplain negatively affects underground and surface water, polluting underground water with sulfates, chlorides, manganese and increasing total dissolved solids in it. The impact of the sludge dump on surface water is manifested in the increased content of suspended substances, dry solids, sulfates, fluorides, and vanadium.

The fire brick production plant dump affects the atmospheric air and groundwater. The most severe contamination of snow cover is attributed to chrome (Fig. 2), as well as vanadium and zinc. The major contaminants of groundwater are iron and manganese.

A retrospective assessment of groundwater state in wells of the coke production plant showed no significant changes in water quality near the dump area in 3 years. The increased content of phenols (Fig. 3) and nitrates was periodically detected in individual wells.

After MD depletion, the remaining open-pits are filled up with underground and surface waters to the aquifer level. After placer mines are abandoned, the sites of dredging tailings and dumps with a changed river bed are left in river valleys, as well as cascading water bodies along the river bed.

The total number of flooded open-pits remaining after the MD depletion in UMR SME exceeds 150 locations with a total area of more than 8000 ha. Major flooded open-pits are located in Sverdlovsk Oblast (about 60 locations with a total area of about 3600 ha.) and Chelyabinsk Oblast (more than 50 open-pits with a total area of approximately 2800 ha.), as well as the Republic of Bashkortostan (more than 10 open-pits with
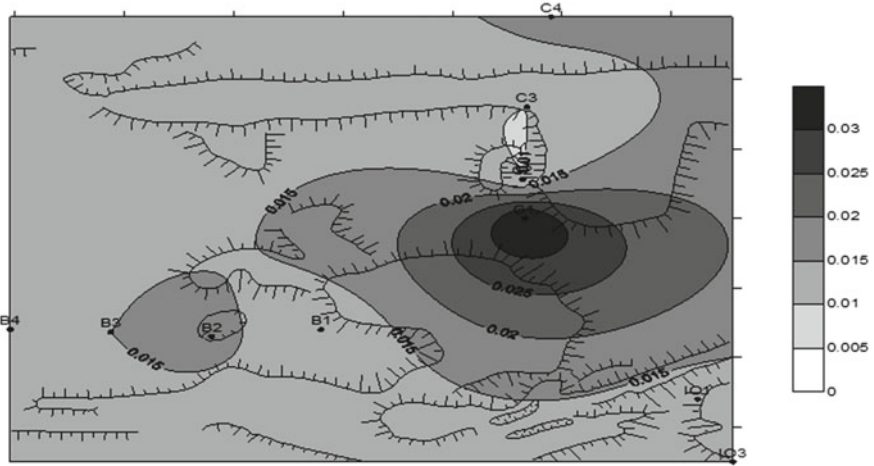
Fig. 2 Distribution of chrome from the fire brick production plant dump in snow cover (mg/dm^3), and sampling sites
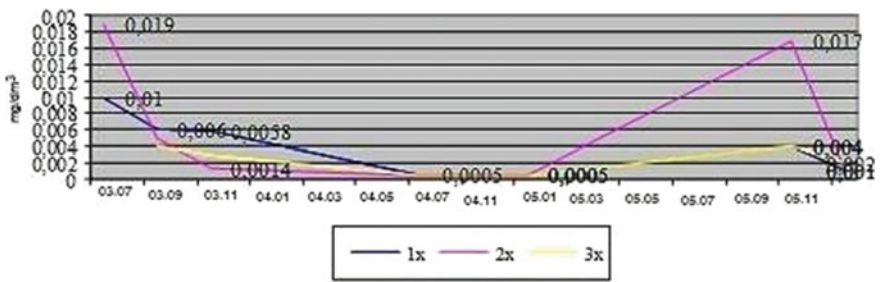
Fig. 3 Change in the content of phenols in the wells of the coke industry

a total area of approximately 1300 ha.). The areas of individual flooded open-pits range from 0.66 to 930 ha. Such open-pits are located both between and within settlements.

According to the analysis carried out by the authors using literature data [15], the placer mines affected more than 250 medium and small rivers with their tributaries, not to mention nameless streams and ravines. The scale of land conversion can be demonstrated by a couple of the following examples. Close to the Kytlym settlement, the depleted MD area is 730 ha. with the placer mine length of 13.6 km along the Lobve River, while the depleted MD area is 7140 ha. along the Is River (in the main part of the river from Shumikha settlement to Is settlement) without tributaries and ravines at a place mine length of 33.8 km and a width of the developed valley ranging from 300 to 900 m. Taking into account that landscapes of former placer mines may self-regenerate, the total area can be estimated only approximately.

The areas flooded due to overflow of mine waters reach up to 170 hectares, due to runoff from dumps—up to 1.5–6 ha., while flooded sinkhole over underground workings—up to 20 ha. For instance, the acidic mine waters of the Kizelov coal basin negatively affected the water quality of 20 small and medium rivers located in the Kama River basin, which can be traced for a long distance [17]. Other examples are mining landscapes—sources of negative impact, formed during the development of MD in the Kirovgrad orefield. The total area of the conversed (disturbed, degraded, and contaminated) lands remaining after the abandonment of 30 mines is 1165 ha. These lands include flooded open-pits, overflowing flooded mine shafts, dumps exposing host rocks and low-grad ores, sinkholes over underground working, as well as objects of Kirovgrad Hard Alloys Plant OJSC.

Both existing and mothballed or abandoned mining-related water-engineering structures [18] were constructed on the territory of more than 30 mining facilities and metallurgical plants.

For instance, one of the noteworthy facilities in the Middle Urals is a tailing pond located in the Kachkanar industrial hub. Analyze in more detail the formation of wastewater from this man-made object and its impact on the surface and underground water.

Located in the Kachkanar industrial hub, this tailing pond has raised hill-type dams and is located in the valley of the Viya River and its right-bank tributary—Rogalevka River. The tailing pond consists of three sections—Rogalevsky, Intermediate, and Viysky. Every section has a dedicated pond and drainage structures. Numerous surveys of the tailing pond territory conducted in different seasons revealed the following sources of wastewater formation (Fig. 4).

Industrial wastewater and storm waters from the overflowing Viysky section of the tailing pond form discharge point 1 releasing water to the Viya River. Discharges occur periodically during high-water periods (as a rule, in spring). Water goes through the discharge point 1 via two siphons with a diameter of 1 m directly into the bottom pool of the Viysky section, located 28.2 km from the mouth of the Viya River. Discharge point 3 is formed by seepage waters from dam 2 of the Intermediate section of the tailing pond. Currently, dam 2 of the Intermediate section of the tailing pond passes through a depression between the Lukovaya mountain and a hill with an elevation of 271 m over a meridional intra-basin drainage dividing ridge between the Viya River and its right-bank tributary—Rogalevka River. The dam body has several locations where filtrated water seeps through entering a ravine directed to the east from the drainage divide to the Viya River. The straight distance from the dam foot to the Viya River is 1.7 km (with the ravine turns included—2.3 km).

The filtrated water proceeds in several streams through the forest in the direction of the Viya River. Discharge point 4 is formed by water filtering through the dam 3 of the Rogalevsky section of the tailing pond. Water is filtered through the dam in several locations and forms several beds (up to 3–4 filtration passages), partially joining at the dam foot, which carry the filtered water across the landscape to the bogged forest. The wastewater has flooded the western side of the anticline between hills of a drainage divide with elevations 413.0 and 312.0 m and formed a small pond with a depth not exceeding 1.5 m. A gradual water level decrease is observed along the water flow due to
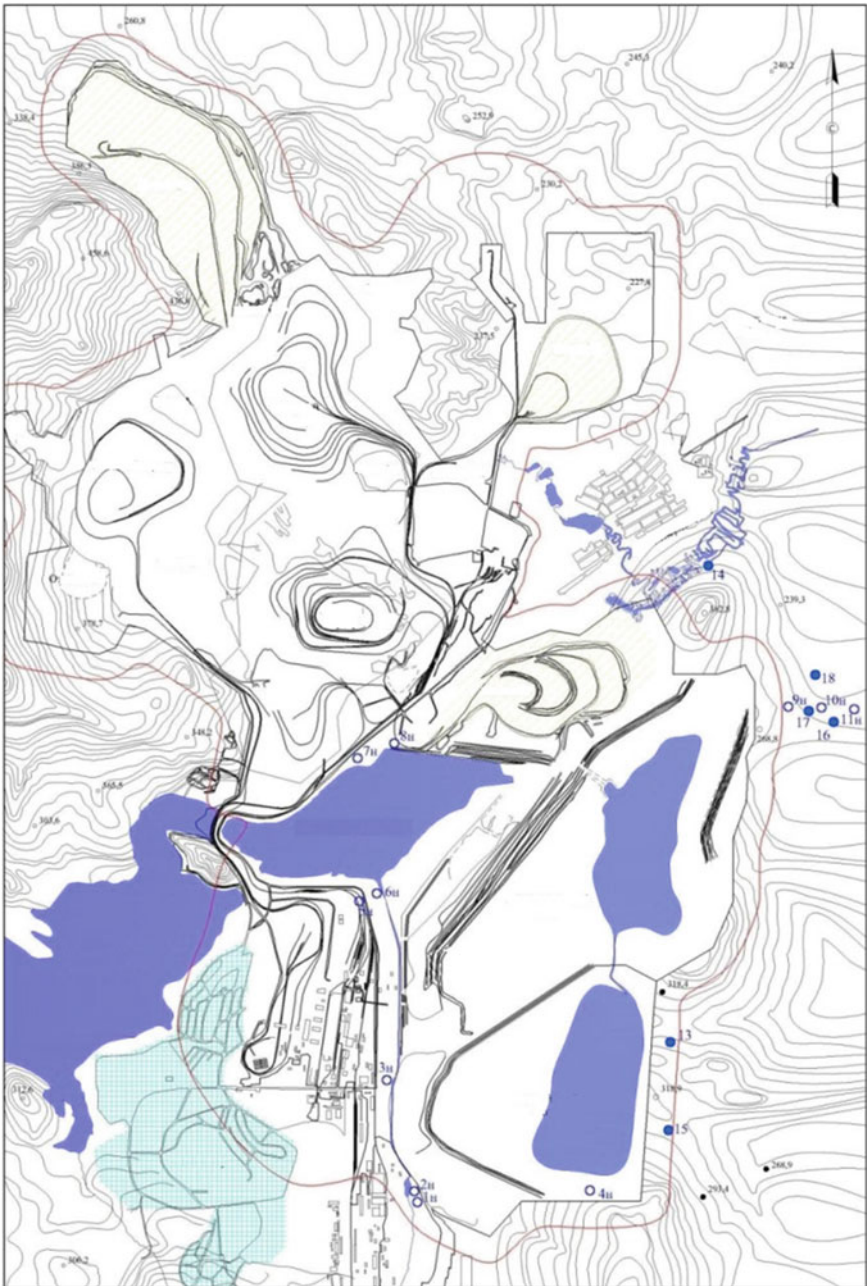
Fig. 4 Locations of points of wastewater discharge from the tailing pond into water bodies located in the Kachkanar industrial hub territory

water moving into the underflow up to a confluence with the southern river bed receiving filtrated waters from discharge point 10. In the limiting conditions of low-water periods, the upper part of the B. Medvedvka River hydrographic structure. A significant part of the wastewater goes into underlying aquifers or forms flood ice (during the winter period). Thus, most of the wastewater discharge via discharge point 4 can be considered to go into underlying aquifers. Waters filtered through the eastern dam of the Intermediate section of the tailing pond form discharge point 9. At the dam foot, wastewater forms two streams over the ridge of the anticline on the drainage divide between the Malaya Lukovaya town and a hill with an elevation of 271 m. The flow moves further along the hill slope gradually accumulating in a valley line expanding towards the Viya River near a bogged ravine. The wastewater going through discharge point 9 reaches the Viya River, draining the groundwaters, having a significant transformation during the filtering process and additional aeration on the site. Flood ice is formed during the winter period accumulating a significant amount of wastewater. It can be assumed that most of the wastewater passing through discharge point 9 goes into the underlying aquifers. Discharge point 10 is formed by water filtering through dam 4 of the Rogalevsky section of the tailing pond. Water filtered through the dam flows in several beds over the landscape to the bogged forest. Filtered water formed a pond without much growth between the dam and the anticline of drainage basin ridge between hills with elevations of 313.0 and 374.0 m. The following pollutants are brought with wastewater into the water bodies: suspended solids, sulfates, nitrogen compounds, iron, vanadium, copper, petroleum products.

On average, the areas of tailing ponds and sludge dumps range from 2.3 to 1252.25 ha., containment ponds—from 3.69 to 711.27 ha., settling ponds—from 1.67 to 45.82 ha. The total area occupied by the 69 facilities is 8283.20 ha. Their number, as well as the large volume of accumulated waste, create an environmental problem. While valuable components contained in enrichment and secondary processing tailings are secondary mineral resources that can be extracted, which is another engineering task [5, 19].

The analysis of the territories of developed and depleted MD using open-pit mining (except for certain metallurgical companies) showed that the area of land occupied by the existing mining facilities is 28,620 ha., including the area of open-pits of 9972 ha., dumps—10,593 ha., processing plants and industrial sites—8055 ha. The land area occupied by the objects of depleted MD is 30,890 ha., including the area of open-pits—9833 ha., dumps—20,127 ha., the area of waste landfills of enrichment plants and the remaining objects of industrial sites—881 ha.

4 Findings

The studies have revealed multiple types of objects of the developed and depleted MD using open-pit mining, as well as the need for remote sensing to obtain full and actual data on the state of the studied objects. The obtained data allows developing a methodology for the assessment of accumulated environmental damage to the territories and, ultimately, to propose methods for the rehabilitation of territories of depleted MD.

References

1. Milkov FN (1986) Physical geography: landscape knowledge and geographical zoning. VGU Publishing House, Voronezh, p 328
2. Isachenko AG (1991) Landscape study and physic-geographical zoning: textbook. Higher School, Moscow, p 366
3. Semyachkov AI, Pochechun VA, Konovalov VE, Ganin EV (2020) Ecological concept of mining landscape rehabilitation. Institution of economics of UrB RSA, Yekaterinburg, p 190
4. Panfilov EI (2008) Assessment of impact on the mineral resources and possible consequences while developing a mineral deposit. Min Indus 2:26
5. Mormil SI, Salnikov VL, Amosov LA et al (2002) Man-caused deposits of the middle Ural and assessment of their environmental impact SSA—Nature, Moscow, p 206
6. Slavikovskaya YO (2012) Ecological and economical aspects of developing the mineral resources on the ur-ban territories. IMA UR RAS, Yekaterinburg, p 208
7. Kolchina M, Konovalov V, Kolchina N (2019) Analyzing the state of mining towns in the Ural region. E3S web of conferences 135:04015
8. Morozova TG, Pobedina MP, Polyak GB et al (2001) Regional economy: textbook for universities. Moscow, p 472
9. Oil and gas province, basin https://neftegaz.ru/tech-library/ngk/147608-neftegazonosnaya-provintsiya/
10. Effort of the Ural into the mining of Russia during 300 years: Ural mining encyclopedia, vol. 1/ eds. Prof. Khokhryakov. VS p.h. UGGA, Yekaterinburg, 2000, p 500
11. Komaschenko VI, Golik VI, Drebenshtedt K (2010) Impact of exploration and mining activities on the environment: monograph / V.I.Komaschenko. KDU, Moscow, p 356
12. Government executive order of 29.07.2014 #1398-p (rev. of 21.01.2020) On the approval of the list of single-industry municipalities in the Russian Federation (mono-cities)
13. Konovalov VY, Koltchina ME (2016) Creating and functioning of industrial landscapes in the conditions of the Ural mining region. Environmental and technosphere safety of the mining regions. Works of IV international training conference 4 April 2016, Ural State Mining University, Yekaterinburg, pp 143–149
14. Konovalov VE, Pochechun VA, Semyachkov AI (2020) Influence of mining complexes on agricultural lands of the ural region. IOP Conf Ser Mater Sci Eng 962(4):042061
15. Albreht VG, Antufyev AA (2004) Ural precious metals: ural mining encyclopedia "Mountain Ural on the turn of the century, vol. three, part 1, p.h. USMA, Yekaterinburg, p 857
16. Ural coal and black dirt: Ural mining encyclopedia "Ural on the turn of the century", vol. five; p.h. USMA, Yekaterinburg, 2007, p 705
17. Maksimovich NG, Pyankov SV (2018) Kizelovskii coal basin: environmental problems and ways of solving them: monograph. Perm State Research University, Perm, p 288
18. Yevdokimov PD, Sazonov GT (1978) Design and exploiting of tailing facilities of the processing factories. Nedra, Moscow
19. Anisimov VN (2009) Zero-waste reworking of natural-and-technogenic deposits with mobile technological complexes "Mining industry" 4(86), p 42

Identifying Significant Safety Aspect of Lighting Systems

A. V. Kudryashov[(✉)] and Y. O. Tsurkan

South Ural State University, 76, Lenin prospect, Chelyabinsk 454080, Russia
kudriashovav@susu.ru

Abstract. The article is devoted to considering the influence of the significant indicators of lighting on the work with computer displays. An experimental installation was created to simulate various parameters of the light environment. The installation consists of a general lightning system which includes various types of lamps and a PC with special software. The lighting system allows to create different levels of illumination on the work surface (up to 500 lx) and a wide range of the flicker rate (from 0 to 40%). Moreover, it allows comparing the characteristics of different types of lamps and their connection schemes, and changing other characteristics, for example, the color temperature of light sources. It was possible to reveal their influence on the operator's visual fatigue by changing the values of the light environment parameters. A proofreading test was chosen as the most appropriate method for assessing the effect of qualitative and quantitative indicators of artificial lighting on the state of vision functions. To reduce the complexity of research in determining the significantly influencing factors, elements of the Plackett-Berman plan with 8 experiments for 7 factors were used. Based on laboratory experiments using the apparatus of mathematical statistics, it was resulted that the main factor, which influence the degree of visual fatigue, is the flicker of illumination. It can be concluded that the design of lighting systems should be conducted with minimizing of the flicker.

Keywords: Illumination · Visual fatigue · Experiment · Significant indicators · Flicker

1 Introduction

The widespread use of displays in working activities made it possible to simplify and minimize the time of performed operations but at the same time led to a change in the usual working conditions. An increasing number of workers of various specialties, ages pay attention to negative changes in health, and often associate this with the necessity to perform intensive work using a PC. The task of reducing harmful effects of computers comes to the foreground because it is no longer possible to stop using them.

Among the complaints made by operators, the first place is occupied by various visual impairments, which are typical for the majority of users. Performing working tasks with video terminals is associated with specific conditions—the perception of

information occurs from the screen and is often accompanied by the differentiation of handwritten or printed materials. Human vision is poorly adapted to working with images on a computer display. The screen image differs from the natural one, it does not reflect light, but emits it, has a lower contrast compared to the printed one, the image is flickering. Unfortunately, light environment tests often do not comply with regulatory requirements. Hygienic control for a long time was carried out formally, which led to total non-compliance with the requirements concerning working conditions by designers of lighting systems, persons involved in their service and labor protection specialists. To solve the problem of minimizing visual fatigue of operators when working with displays, it is necessary to clearly understand which lighting parameters are significant.

2   Relevance of Lighting Safety Issues

The experience of the industrial use of electric light has revealed that abnormal lighting has a negative effect on well-being, leads to visual disturbances, fatigue and a decrease in work efficiency. Subsequently, state orders, norms and directives arose [1–3], lighting became the topic of occupational medicine, one of the most important factors in the arrangement of the workplace.

It is important to note that not only the level of illumination but all aspects of the quality of illumination play a role in the prevention of accidents. It is enough to mention that irregular lighting can create adaptation problems and reduce visibility. Excessive gloss also leads to individual adaptation problems, in addition, in situations where it is important to accurately see the moving parts of machines, the stroboscopic effect can be dangerous. Finally, illumination with a poor color rendering index can be the reason for misjudging potentially hazardous situations [4]. Fluctuations in the voltage of the lighting network can lead to flickering of lamps, which causes fatigue of vision and the body of workers as a whole [5–7]. It is known that developing visual fatigue leads to a decrease in the acuity and speed of difference, contrast sensitivity, stability of clear vision and other visual functions [8, 9].

It was not possible to find information on studies of visual fatigue of PC operators in available literature, therefore, the task was set to select the most appropriate method for assessing the effect of qualitative and quantitative indicators of artificial lighting on the state of visual functions of PC operators. It is known that the work of an operator is extremely heterogeneous in terms of the nature and conditions of work, tasks to be solved, and time indicators, but at the same time there are many common features. Therefore, it is necessary that the definition of visual performance includes the effect of the resulting function of the brain and eye [10]. Based on this, the most acceptable test for the integral assessment of visual fatigue in various working conditions is the proofreading test. Such studies are carried out using special printed forms, but since the object of the study is a PC operator this method cannot be used, so it is necessary to use a test in the form of a computer program. As a result, special software was created, which is a computer version of the proofreading test.

There was created an experimental installation in purpose to carry out the research that makes possible to simulate various parameters of the light environment at the workplace of the PC operator. The experiments were carried out in a chamber isolated from

natural light by a curtain made of dark opaque material. The brightness of the chamber walls in the operator's field of view was the same during all experiments and was no more than 200 cd/m^2.

The installation consists of a general lightning system, which includes various types of lamps (fluorescent and LED) and a personal computer with special software that makes it possible to assess the operator's visual fatigue. The lighting system allows to create different levels of illumination on the work surface (up to 500 lx), provide a wide range of the flicker of illumination (from 0 to 40%), compare the characteristics of different types of lamps and their connection schemes and change other characteristics, for example, the color temperature of light sources. By changing the values of the parameters of the light environment, it is possible to reveal their influence on the operator's visual fatigue. To reduce the complexity of research, we use the theory of experiment planning.

3   Planning and Implementing a Screening Experiment

The basis of the mathematical theory of experiment planning is mathematical statistics, which is applicable to the analysis of an experiment in cases where its results can be considered as random variables or random processes. This condition is met in most studies since experimental results are associated with some uncertainty. The reasons for this uncertainty are: the random nature of the investigated processes; the influence of uncontrollable factors; uncontrolled changes in the experimental conditions and observation errors. This also includes measurement errors, the reasons for which lie in the imperfection of instruments and measurement methods. The influence of these factors on the observation result can in many cases be considered as accidental [11–14].

To assess the influence of factors of the light environment on the fatigue of PC operators, it is necessary to consider a system consisting of the operator's workplace, a person, and the surrounding light environment, which is characterized by various parameters (illumination, brightness, glare, etc.).

All factors that determine the state of the system can be divided into 3 groups:

1. Group $X = (x_1, x_2,..., x_n)$. This group includes factors that affect the behavior of the system, and a person can actively change them during the experiment (variable factors).
2. Group $Z = (z_1, z_2,..., z_n)$. Factors affecting the behavior of the system, but a person refuses to control them due to certain limitations (technical, technological, financial).
3. Group $Q = (q_1, q_2,..., q_n)$. This group includes factors that affect the behavior of the system, but a person is not able to control them at this stage of the development of civilization.

The value of visual performance (fatigue) is taken as the response Y, which is equal to the time spent on the correction test.

For the correct display of the object, it is necessary that its mathematical model includes all factors that significantly affect the final result. The absence in the model of at least one of the essential factors can lead to an erroneous interpretation of the phenomena occurring in the system under study. The factors affecting the studied system, as well as their levels, are presented in Table 1.

Table 1 Factor levels

Factor number	Factor designation	Factor level	
		-1	+ 1
X1	**E, lux**—illumination of the working surface	400	200
X2	**F$_f$, %**—flicker rate	0	25
X3	**E$_d$, lux**—display illumination	100	200
X4	**L, Cd/m^2**—brightness of glare on the PC screen	0	40
X5	Lamp type (**LED/ fluorescent**)	LED	Fluorescent
X6	Fictitious factor	–	–
X7	Fictitious factor	–	–

The task of the mathematical theory of experiment planning is to use appropriate methods to identify significant, dominant factors at the lowest possible cost (the minimum number of experiments).

Conventional methods for constructing mathematical models, for example, regression analysis, which includes checking the significance of parameters, turns out to be unacceptable for a large number of factors. Therefore, special methods have been developed that, when certain prerequisites are fulfilled, make it possible to reveal essential factors with the help of a small number of experiments [14–16]. These methods include the following:

1. Analysis of variance [14, 17];
2. Saturated fractional factorial designs [14];
3. Saturated Plackett-Berman Experimental Plans [14];
4. Random balance method [14, 18, 19].
5. A survey of experts in order to rank factors according to the degree of their influence on the output value or a combination of a survey of experts and an experiment, as well as other methods [14].

Within the framework of this work, it is inappropriate to describe in detail the content of the listed methods, especially since others that are not indicated here can be cited, therefore, we will limit ourselves only to the argumentation of the choice of the method.

The random balance method (or Sutterswight's method) contains oversaturated designs and is used when the number of factors is very large. Analysis of variance is characterized by a relatively large number of experiments and is time-consuming. By constructing special design matrices, Plackett and Berman were able to reduce the number of necessary experiments [14, 18]. Thus, to solve the problem posed, the most appropriate theory of the screening experiment should be recognized according to the Plackett-Berman plan.

This research method belongs to the methods of orthogonal planning. The essence of the orthogonal planning methods is to select for each experiment such values of the variable factors $x_1, x_2, ..., x_n$, which make up the vector of conditions, so that, ultimately,

when the plan is exhausted, the parameter vectors are mutually orthogonal, that is, their product would be equal to zero [20].

To determine the significantly influencing factors, the Plackett-Berman plan with N = 8 experiments for 7 factors was used.

The variance of observation errors is estimated using special experiments, for example, by duplicating observations or by introducing fictitious factors into the plan, therefore (according to Table 1), 2 fictitious factors were added to the existing 5 variable factors.

According to the Table 2, the screening experiment matrix consists of two blocks. The first block is obtained by the method of randomization—random selection of the order of measurements, for example, using a drawing of lots, tables or a random number generator. Randomization is carried out mainly to exclude the influence of variables that change uncontrollably over time [18].

Table 2 Screening experiment matrix according to Plackett-Berman plan

Experiment number	Random			Factor levels						
				1	2	3	4	5	6	7
1	21	19	20	+ 1	+ 1	+ 1	−1	+ 1	−1	−1
2	14	22	17	−1	+ 1	+ 1	+ 1	−1	+ 1	−1
3	7	11	16	−1	−1	+ 1	+ 1	+ 1	−1	+ 1
4	6	2	4	−1	−1	+ 1	+ 1	+ 1	+ 1	−1
5	13	23	24	−1	+ 1	−1	−1	+ 1	+ 1	+ 1
6	5	10	12	+ 1	−1	+ 1	−1	−1	+ 1	+ 1
7	9	3	1	+ 1	+ 1	−1	+ 1	−1	−1	+ 1
8	8	15	18	−1	−1	−1	−1	−1	−1	−1

According to the presented matrix of the experiment, influencing factors can be presented at levels + 1 and −1, in Table 1 shows the decoding of the levels.

A feature of the implementation of the experiment plan is the repetition of experiments with different people (the number of subjects $m = 4$), that is, duplication of experiments in each line of the plan 4 times.

The experiment involved 4 male volunteers with normal vision (according to annual medical examinations), aged from 21 to 24 years.

Measurements of the level of visual fatigue for each of the eight combinations of factors were duplicated three times by each volunteer. As a result, 24 measurements of visual fatigue were taken with each subject. The order of performance of 24 experiments was randomized according to Table 2 using a random number generator.

The experimental results shown by each volunteer are presented in Table 3. The response levels correspond to the total time to complete the control task, measured in seconds.

Table 3 Final results of the experiment

Random		Factor levels							Response levels					D_j
		X1 E, lux	**X2** Fr, %	**X3** E_d, lux	**X4** L, cd/m^2	**X5** Type lamp	**X6** f.f	**X7** f.f	$\overline{y}$ m = 1	$\overline{y}$ m = 2	$\overline{y}$ m = 3	$\overline{y}$ m = 4	$\overline{y}$	
21	19	20	200	25	100	0	FL	–	–	125.2	114.5	125.8	129	123.6	39.79
14	22	17	400	25	100	40	LED	–	–	119	115.2	124.2	127	121.6	27.88
7	11	16	400	0	100	40	FL	–	–	109	93.8	111.4	109.8	106	67.15
6	2	4	200	0	200	40	FL	–	–	106	90.2	105.7	106.2	102	62.19
13	23	24	400	25	200	0	FL	–	–	115.4	103.6	123.9	119.6	115.6	76.31
5	10	12	200	0	100	0	LED	–	–	111.4	101.9	117.5	116.4	111.8	50.6
9	3	1	200	25	200	40	LED	–	–	120	117.7	128.7	129.5	124	36.01
8	15	18	400	0	200	0	LED	–	–	105.6	89.1	106.7	105.1	101.6	70.17

The last columns of the tables show the average response values for each row:

$$\overline{Y} = \frac{Y_1 + Y_2 + Y_3}{3} \tag{1}$$

Table 4 shows the final results of the experiment, including the assessment of the variance in each line D_j necessary to assess the reproducibility of the experiments. Evaluation of reproducibility (uniformity of results) can be made according to the Cochran test (if the samples are of equal size) or by the Bartlett test (if the samples are of different sizes) [15, 17]. Since in this case the number of repeated experiments in each line is the same, Cochran's test should be used.

Following the implementation of the experiment plan, its results are processed, which consists of the following operations:

1. Calculation of the effects of individual factors.

The estimate of the effect B_i is equal to the difference between the sums of the values of the objective function for factor X_i at levels $+ 1$ and $–1$, divided by N:

$$B_i = \frac{\sum_{j=1}^{N} y_j x_i^j}{N}, \tag{2}$$

where B_i—i-th factor effect, y_j—response value in j-experiment, x_i^j—level of the i-th in the j-experiment, N—the number of rows of the matrix of the design under consideration.

Table 4 Factor effects and their significance for each of the 4 experiments

Factors	X1 E, lux	X2 Fr, %	X3 Ed, lux	X4 L, cd/m²	X5 Lamp type	X6 f.f	X7 f.f
m = 1							
Effect, B_i	1.7	5.95	2.2	−0.45	−0.05	−1	0
$t_{кр}·S_i$	3.04						
Significance	No	**Yes**	No	No	No	–	–
m = 2							
Effect, B_i	2.825	9.5	3.1	0.975	−2.7	−0.525	1
$t_{кр}·S_i$	3.4365						
Significance	No	**Yes**	No	No	No	–	–
m = 3							
Effect, B_i	1.44	7.66	1.71	−0.49	−1.29	−0.16	2.38
$t_{кр}·S_i$	7.28						
Significance	No	**Yes**	No	No	No	–	–
m = 4							
Effect, B_i	2.45	8.45	2.725	0.3	−1.675	−0.525	1
$t_{кр}·S_i$	4.4365						
Significance	No	**Yes**	No	No	No	–	–

2. Checking the significance of the parameters.

To identify significant factors, the t-criterion is used, and the fulfillment of the condition is checked:

$$|B_i| \geq t_{cr}S_i, \tag{3}$$

where B_i—i-th factor effect, t_{cr}—the critical value of the t-distribution for the significance level $\alpha = 0{,}05$ and $\varphi = 2$ degrees of freedom, S_i—an estimate of the variance of the coefficient B_i.

$$S_i = \sqrt{\frac{S_l^2}{4k}}. \tag{4}$$

To estimate the variance of observation errors, 2 fictitious factors were added. The effects of these fictitious variables will be zero only if there are no interactions and the measurements are perfectly accurate. Since this is usually not the case in practice, they can be used to estimate the variance of observations S_l:

$$S_l^2 = 4k\left(B_{l+1}^2 + \ldots + B_{N-1}^2\right)/(4k - l - 1), \tag{5}$$

where S_l—variance of observations, $4\,k = N$—number of lines of the plan in question,$B_{l+1}\ldots B_{N-1}$ – effects of fictitious factors, l—number of significant factors.

The significance of the factors is checked by condition (3) for all four experiments with each of the volunteers and for the average value.

For $m = 1$: $t_{cr}{\cdot}S_i = 3.04$.

For $m = 2$: $t_{cr}{\cdot}S_i = 3.4365$.

For $m = 3$: $t_{cr}{\cdot}S_i = 7.28$.

For $m = 4$: $t_{cr}{\cdot}S_i = 4.4365$.

For averaged values: $t_{cr}{\cdot}S_i = 3.79$.

Table 4 presents the results of processing the experiment, the effects of factors for four experiments with each of the volunteers are calculated, the significance of the factors is shown.

According to the Table 4 in all four experiments, only one factor X2 turned out to be significant—the coefficient of illumination flicker.

According to the Table 5, the results of processing the averaged values do not contradict the results of individual experiments, which confirms the correctness of the conclusions drawn.

Table 5 Factor effects and their significance for averaged values

Factors	X1 E, lux	X2 Fr, %	X3 Ed, lux	X4 L, cd/m^2	X5 Lamp type	X6 f.f	X7 f.f
Effect, B$_i$	2.11	7.89	2.44	0.09	−1.44	−0.56	1.11
$t_{кр}{\cdot}S_i$	3.79						
Significance	No	**Yes**	No	No	No	–	–

In Fig. 1, the results of assessing the significance of factors are presented in graphical form. Only the factor whose assessment exceeds the critical value equal to 3,79 (units) can be considered significantly influencing.

3. Evaluation of the reproducibility of experiments.

As a test of the hypothesis about the homogeneity of variances, we take the Cochran criterion—the ratio of the maximum line variance to the sum of all line variances:

$$G = \frac{D_{j\,max}}{D_N},\tag{6}$$

where $D_{j\,max}$—maximum value of line variance,D_N—sum of lowercase variances.
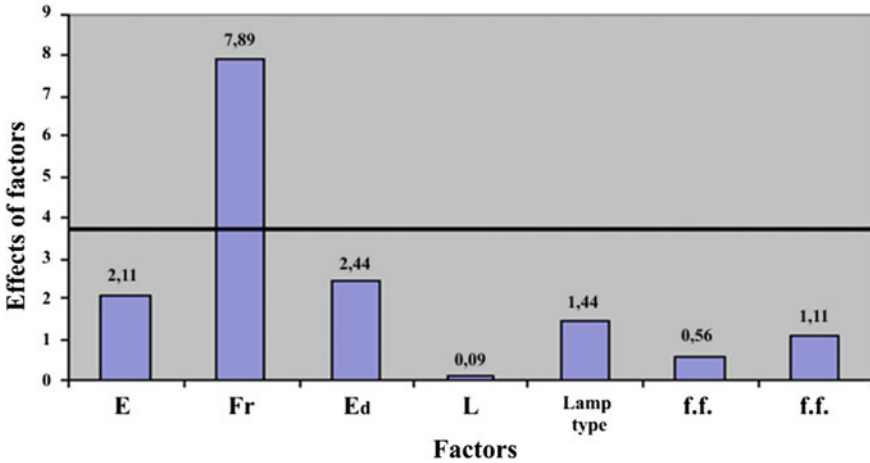
$$D_N = \sum_{j=0}^{N} D_j.\tag{7}$$

Fig. 1 The results of assessing the significance of factors

The values of the lowercase variances D_j are determined in accordance with the expression:

$$D_j = \frac{1}{m-1} \sum_{l=1}^{m} (Y_j - \overline{Y}_j) \tag{8}$$

The obtained variance values in each row are indicated in the last column of the Table 3.

In order to test the hypothesis about the homogeneity of variances at a given level of significance, it is necessary to calculate the observed value of the criterion and find the critical value of G_{cr} from the table.

The observed value of the criterion $G_{obs} = 76.31/430.1 = 0.18$. The critical value of the criterion at the significance level $\alpha = 0.05$, the number of degrees of freedom m—1 $= 2$ and the number of samples $N = 8$, $G_{cr\,(0.05;\,3;\,8)} = 0.4377$.

Since $G_{obs} = 0.18 < G_{cr} = 0.4377$, the hypothesis of the homogeneity of dispersions is confirmed, that is the experimental results are reliable and reproducible.

4 Conclusion

Suchwise, as a result of the implementation of the screening experiment it was found that among the studied parameters of the light medium, only factor X2, the flicker rate, is significant. Other parameters of the light environment: the illumination of the working surface, the brightness of the glare on the screen, as well as the illumination of the surface of the PC screen and the type of artificial light sources do not significantly affect the operator's visual fatigue. Naturally, such results will be valid only for the levels of factors indicated in Table 1. For example, for the factors "screen illumination" at levels from 100 to 200 lx and "working surface illumination" at levels from 200 to 400 lx, effect values were obtained that were close to significant. Such levels were selected based

on the characteristic values established in the study of working conditions at various workplaces. In the case of expanding the boundaries of the levels, it is quite possible that these factors will become significant, but at present, the attention of the creators of lighting systems should be focused on minimizing the flicker of illumination.

References

1. EN 12464–1 Light and lighting—Lighting of work places. Part 1 Indoor work places
2. SanPiN 1.2.3685–21 Hygienic standards and requirements for ensuring the safety and (or) harmlessness to humans of environmental factors
3. SP 52.13330.2016 Natural and artificial lighting
4. Van Bommel V, Van Den Beld G, Van Oujen M (2003) Industrial lighting and labor productivity. Lighting Technol 1:8–12
5. Yagovkin GN (1972) Study of the influence of some indicators of the quality of electrical energy on performance. Abstract dissertation. Cand Tech Sci
6. Kudryashov AV, Kalinina AS and Yagovkin GN (2017) Pulse width modulated LED light control and vision adaptation. 2017 Int Conf Indus Eng Appl Manuf 8076145. https://doi.org/10.1109/ICIEAM.2017.8076145
7. Kudryashov AV, Kalinina AS and Yagovkin GN (2017) Pulse width modulated LED light control and vision adaptation. Int Conf Indus Eng Appl Manuf 8076145. https://doi.org/10.1109/ICIEAM.2017.8076145
8. Abramov LV (1993) On a methodological approach to assessing the hygienic efficiency of high-frequency lighting installations. Lighting 5–6:17–19
9. Begemann SHA (1997) Daylight, artificial light and people in an office environment. Overview of visual and biological responses. Int J Ind Ergon 20:231–239
10. Dyadichkin VP (1990) Psychophysiological reserves of increasing efficiency. Minsk Publishing house, Higher school, p 119
11. Yudin YuV, Maisuradze MV, Vodolazsky FV (2018) Organization and mathematical planning of the experiment. Ural University Publishing House, Yekaterinburg, p 124
12. Morgunov AP, Revina IV (2014) Planning and analysis of experimental results. Publishing house of OmSTU
13. Moiseev NG, Zakharov YuV (2018) Theory of planning and processing an experiment. Volga State Technological University, Yoshkar-Ola, p 124
14. Hartman K, Letsky E, Schaefer E (1977) Planning an experiment in the study of technological processes. Mir
15. Gorsky VG, Yu AP (1974) Planning of industrial experiments. Metallurgy, p 264
16. Johnson N, Lyon F (1981) Statistics and experiment planning in engineering and science. Mir, Experiment Design Methods, p 520
17. Gmurman VE (2001) Probability theory and mathematical statistics. Textbook for universities, Higher school p, p 479
18. Nalimov VV, Golikova TI (1980) Logical foundations of experiment planning. Metallurgy, p 152
19. Krug NK, Marusova MN (1985) Planning of psychophysiological experiments in lighting engineering. Lighting 8:9–10
20. Musina ON (2015) Planning and setting up a scientific experiment: teaching aid. Direct-Media, p 88

Analysis of Associated Petroleum Gas (APG) Utilization in Russia and Abroad

A. Ch. S. Gomes[1], V. A. Shcherba[1,2], K. A. Vorobyev[1,3(✉)], and T. V. Chekushina[1]

[1] Peoples' Friendship, University of Russia, 6, Miklukho-Maklaya str, Moscow 117198, Russia
kirill.vorobyev@stud.thga.de

[2] Sergo Ordzhonikidze Russian State University for Geological Prospecting, 23, Miklukho-Maklaya st, Moscow 117485, Russia

[3] Technische Hochschule Georg Agricola, 45, Herner St, 44787 Bochum, Germany

Abstract. The article analyzes the current state and prospects of associated petroleum gas (APG) utilization, the main components of which are methane and other low-molecular-weight alkanes. When separated from crude oil, APG contains such hydrocarbons as ethane, propane, butane and pentane, as well as water vapor, hydrogen sulfide (H_2S), carbon dioxide (CO_2), nitrogen (N_2) and other components. Associated petroleum gas containing such impurities cannot be used without purification. The authors noted that, the shortage of APG processing capacities both in the Russian Federation and in the world as one of the reasons for the high level of gas flaring at the oil fields. Rational methods of associated petroleum gas utilization, which depend on oil production conditions, such as field characteristics, oil/gas ratio (gas-oil factor), as well as market opportunities for the recovered gas, were identified. An algorithm was proposed for choosing a technology for the rational utilization of APG in oil and gas companies. An overview of all APG utilization methods is given, in which the main attention is paid to unit costs, economic benefits and the nature of the environmental impact. The innovative experience of the effective use of APG in the USA and Canada is analyzed. Particular attention is paid to the need to solve the problem of effective use of APG in the world, especially to reduce the flaring volume.

Keywords: Associated petroleum gas · APG utilization · APG flaring · Environmental pollution · Deep processing · Electricity generation

1 Introduction

Associated petroleum gas (APG) is a type of natural gas that is either dissolved in oil, or as a free "gas cap" above oil in a reservoir. Regardless of the source, when the gas is separated from crude oil, it usually consists of hydrocarbons such as methane, ethane, propane, butane and pentane; in addition, APG contains water vapor, hydrogen sulfide (H_2S) and carbon dioxide (CO_2), nitrogen (N_2) and other mixtures. Associated petroleum gas containing such impurities cannot be transported or used without purification [1–7].

Depending on the production site and on the specific properties of the field, during production and separation of 1 ton of oil, it is possible to obtain from 25 to 800 m^3

of associated gas [8]. The choice of the best method for the associated petroleum gas utilization depends on the conditions of oil production, such as the geological structure of the field, the gas-oil factor, as well as the market opportunities for the recovered gas. Some of this gas is purified and sent for further processing or stored because governments and oil companies in many countries have made significant investments in its production. However, some companies are flaring APG due to technical, regulatory or economic constraints. As a result, according to the World Bank's 2019 APG research data, more than 17,000 flares at oil production facilities around the world burned about 150 billion cubic meters of APG, resulting in more than 350 million tons of CO_2 released into the atmosphere, as well as a large number of various pollutants, including very dangerous [4].

For a long time, oil companies have simply burned this unwanted by-product. The term "gas flaring" refers to the combustion of gas in an open flame that burns continuously at the top of flare units in oil production areas.

Burning occurs for two (2) main reasons:

- emergencies: limited flaring for safety reasons may always be necessary for short periods of time even after connecting the gas gathering pipeline;
- lack of gas utilization capacity - isolated APG flaring due to lack of connection to gas collection systems or other gas utilization technology. In this regard, part or all of the associated gas from the oil well will be flared.

The amount of inorganic substances emitted during the burning of the associated gas (metals, metalloids and their derivatives) is exclusively associated with the components of the APG and can only be determined in laboratories. The amount of combustion products emitted from alkanes (carbon black, CO_2, CO, 3,4-benzopyrene, H_2O) as well as unburned methane, nitrogen oxides and sulfur dioxide can be calculated in principle using a method developed in 1997 for a specific APG composition, flash design and operational characteristics, combustion mode and weather conditions [9]. The impact of APG burning on the environment is shown in Table 1, compiled by the authors based on data from WWF reports [6, 9].

The deterioration of the natural environment leads to a decrease in the population life quality, which is expressed in an increase in the incidence of various types of diseases among the population and in the accelerated degradation and destruction of infrastructure facilities.

2   Global Data on APG Flaring

It is estimated that billions of cubic meters of associated petroleum gas are flared annually in oil production facilities around the world. Studies have shown that burning this gas is a waste of a precious energy resource that should be used for its growth and economic progress.

Since 2012, the World Bank's Global Gas Flaring Reduction (GGFR) Community, in partnership with the US National Oceanic and Atmospheric Administration (NOAA) and the Colorado School of Mines, has developed global estimates of gas flaring in 2020

Table 1 Impact of APG flaring on the environment

Environment	Impact
Air	• APG flaring produces soot, nitrogen oxides, carbon monoxide, 3,4-benzpyrene, "leaked hydrocarbons", benzene, phosgene, toluene, heavy metals (mercury, arsenic, chromium), sulfur dioxide, sometimes hydrogen sulfide, carbon disulfide, mercaptans. As well as greenhouse gases, primarily carbon dioxide • Flaring is one of the main sources of air pollution in regions where the oil industry is developing and developed
Soil	• The total area of disturbed soils from the impact of emissions from burning torches is approximately 110 thousand hectares. And within a radius of 20–200 m, organic matter is almost completely burned out • The accumulation of toxicants in soils due to combustion causes the formation of geochemical anomalies—a kind of "chemical time bombs
Water	• During APG flaring, depending on the nature of the pollutant, it is localized either in a sediment, or in a dissolved and emulsified state • The presence of an oil slick on the water surface leads to the process of "clogging" of water, which limits the access of oxygen and leads to the destruction of aquatic ecosystems • When entering water reservoirs, heavy fractions of oil partially settle to the bottom, which leads to a change in the composition of bottom sediments; and buried bituminous substances in bottom sediments can be an additional source of water pollution for many years • Decrease in the number and species diversity of animals, insects and microorganisms, especially for marine animals

based on satellite observations. The satellite's sensors detect the heat generated by gas flares as infrared radiation from global oil and gas facilities. The Colorado School of Mines and GGFR quantify and calibrate these infrared emissions to provide reliable estimates of global gas flaring [10–16].

Regarding the year 2020, there was an 8% decrease in global oil production (about 82 million barrels per day (b/d) in 2019 to 76 million b/d in 2020), with the quantity of flared gas also being reduced by 5% (from 150 bcm in 2019 to 142 bcm in 2020) [5] (Fig. 1).

The top 7 of the countries with the highest amount of gas flaring is occupied by the same countries for 9 years, namely: Russia, Iraq, Iran, United States, Algeria, Venezuela and Nigeria remain (see Table 2). With oil production equivalent to 40%, the leading countries are responsible for an amount equivalent to two-thirds (65%) of global gas flaring [17]. Ranking of countries by associated petroleum gas flaring in 2016–2020 is shown in the Table 2, compiled by the authors based on GGFR Report (in billion m³) [3, 5].

According to the data presented (see Table 2), it can be seen that the United States was responsible for a reduction equivalent to 70% of global gas flaring (with gas flaring falling 32% from 2019 to 2020). This is due to an 8% drop in oil production, together with the new infrastructure to use the gas that would otherwise be flared.
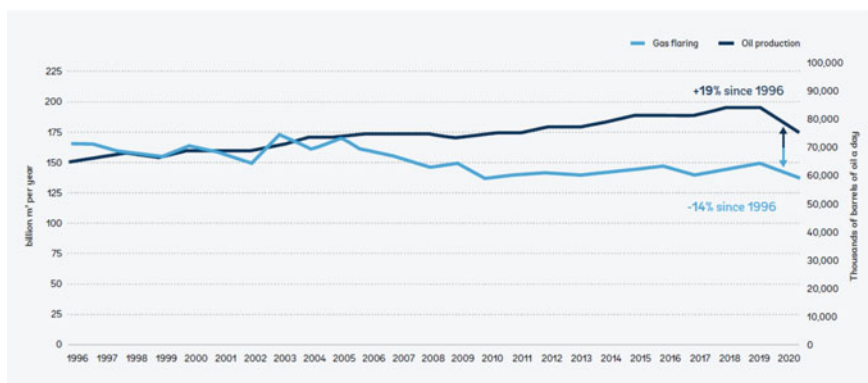
Fig. 1 Global gas flaring and oil production: from 1996 to 2020 [5]

Table 2 Ranking of countries by associated petroleum gas flaring in 2016–2020

	2016	2017	2018	2019	2020	Change 2020–2019
Russia	22.372	19.916	21.280	23.212	24.88	1.66
Iraq	17.730	17.843	17.821	17.914	17.37	−0.54
Iran	16.405	17.670	17.278	13.781	13.26	−0.52
USA	8.862	9.475	14,069	17.294	11,81	−5.48
Algeria	9.100	8.803	9.009	9.343	9.32	−0.02
Venezuela	9.350	6.997	8.225	9.541	8.59	−0.95
Nigeria	7.315	7.646	7.435	7.825	7.20	−0.63
Mexico	4.776	3.789	3.893	4.484	5.77	1.28
China	1.96	1.56	1.82	2.02	2.72	0.70
Oman	2.816	2.601	2.536	2.631	2.52	−0.11
Libya	2.353	3.908	4.672	5.124	2.47	−2.65

Meanwhile, in Russia, the leading country in gas flaring since data collection began, annual gas flaring increased by 8% from 2019 to 2020. Russia's largest oil and gas producing region, Khanty-Mansiysk Autonomous Okrug (KMAO), has been continuously working on expanding its gas utilization infrastructure in recent years and currently contributes only 20% of Russia's total flaring. Burning in KMAO is estimated to have reduced from more than 20 bcm in 2000 to less than 5 bcm in 2020 [5].

On the other hand, in Eastern Siberia, where there has been an increase in oil production in a small number of fields, there was an increase in gas flaring equivalent to 23% (or 4.8 bcm) of the total value in the country in 2018 to 33% (or 8.2 bcm) in 2020. A region also known as "the middle of nowhere", Eastern Siberia, despite having huge oil reserves, is is a mostly desert region, with little gas utilization or preparation infrastructures and very low local demand for gas or by-products. In this context, reducing

gas flaring in that region will require a large investment in new gas infrastructure, or conservation through the reinjection of gas into the reservoir (Fig. 2).
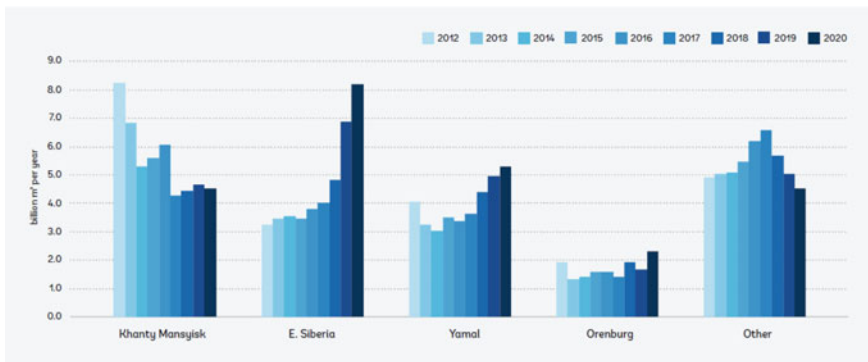

Fig. 2 2020 Flare volumes, Russian regions [5]

Due to the fact that during this period the oil production conditions did not undergo significant changes, it could be assumed that the volume of APG recoverable will change in proportion to the volume of oil produced. But we see, however, different results. In fact, it refers to the waste of an energy resource of great value, which can be used to stimulate the sustainable development of hydrocarbon producing countries. It is estimated that the 142 billion m^3 of associated petroleum gas burned during 2020 by producing countries could be transformed into 750 billion kWh of electricity, which surpass the total annual consumption of all countries on the African continent [4].

3   Rational Methods for APG Utilization

Currently, there are other possible alternatives to flaring for the associated gas; including, but not limited to, the following:

- The re-injection of associated petroleum gas into the reservoir, in order to preserve reservoir pressure and enhance oil recovery, or for its possible preservation as a resource and use in the future;
- The utilization of the APG as an energy source in the field and nearby facilities;
- The most effective method is to process it at the gas processing plants, in order to obtain to obtain the dry stripped gas (DSG), a broad fraction of light hydrocarbons (NGL), liquefied natural gases (LNG) and stable gasoline (SGB).

The following is an overview of the main methods of associated petroleum gas utilization, focusing in such parameters as unit costs, economic benefits and environmental impact (see Table 3, compiled by the authors based on reporting data from the SIBUR Company [14]).

Table 3 Comparison of data for all APG utilization methods

Utilization methods	Capital investments, rub/m^3	Economical effect, rub/m^3	Lost profit, rub/m^3	Environmental damage, mln tons of CO_2-equivalent / bln. m^3
Flaring	0.1 (construction of a flare unit and supply pipelines)	−2.8 (damage in the amount of a fine for gas flare)	From −2.8 to −22.6 (range from savings on fines to income from sales of petrochemical products)	7.1 (emissions of harmful substances into the atmosphere)
Re-injection	4.4 (collection system and gas injection wells)	0 (possible increase in oil recovery)	From −3 to −19.8 (range from savings on fines to income from sales of petrochemical products)	0 (ecological effect is taken equal to zero)
Deep processing	13.8 (maximum capital costs for the creation of the entire infrastructure complex: the APG collection system, compressor stations and gas processing facilities, transportation of dry gas and natural gas liquids, costs for further processing)	19.8–20.1 (average economic effect—monetization of methane (dry stripped gas) as a fuel gas, monetization of NGL as a feedstock for petrochemicals with further production of final products from polymers and synthetic rubber)	0 (there is no profit lost (deeper processing within the framework of the model is impossible))	0 (typical greenhouse gas emissions CO_2, CH_4, Nox from gas processing plants and petrochemical plants (according to RUPEC data), taking into account the greenhouse effect coefficients of each gas)

Table 3 (*continued*)

Utilization methods	Capital investments, rub/m^3	Economical effect, rub/m^3	Lost profit, rub/m^3	Environmental damage, mln tons of CO_2-equivalent / bln. m^3
Electricity generation	54.2 (APG collection system, gas turbine units)	3.6—5.2 (income from own power generation)	from -2.4 to -14.6 (range from revenues from utilization at mini-gas processing plants to revenues from the sale of petrochemical products)	1.2 (environmental risks with carbon emissions from large-scale power generation)

The choice of the optimal option for the use of associated petroleum gas depends on the oil production conditions, such as the geological structure of the field, the gas-oil ratio, as well as the market opportunities for the recovered gas [18].

During the years of 2005 and 2015, the volume of APG flared in the Russian Federation has decreased. The increase in the volume of deeply processed APG is covered by a decrease in the volume of shallow processing (see Figs. 3 and 4).

4 Analysis of NGL Pro Technology

When APG is supplied in small volumes, one of the directions of its utilization is the innovative technology for the liquefied natural gas production, called NGL-Pro [19, 20]. The NGL Pro process integrates dewatering, compression, refrigeration and conditioning, eliminating by this way the necessity for expensive glycol and refrigeration systems. Hydrate formation is eliminated by the thermal integration system (see Fig. 5). The technology was developed by ASPEN and is used in many fields in the USA and Canada.

The advantages of this technology: (a) production of valuable LNG; (b) ice and hydrate formation are eliminated; (c) portable, mounted on a slippery system; (d) Safe and easy maintenance—no moving parts. The method is used in the North Dakota field, the level of LNG production is 379 barrels per day, which leads to a 42% reduction in APG flaring. The method is used in conjunction with other methods in order to increase the level of LNG production and thereby eliminate combustion [10].

5 Conclusion

Analysis of the current state and prospects for APG utilization showed that due to APG flaring, a noticeable deterioration in the quality of the natural environment is observed, as
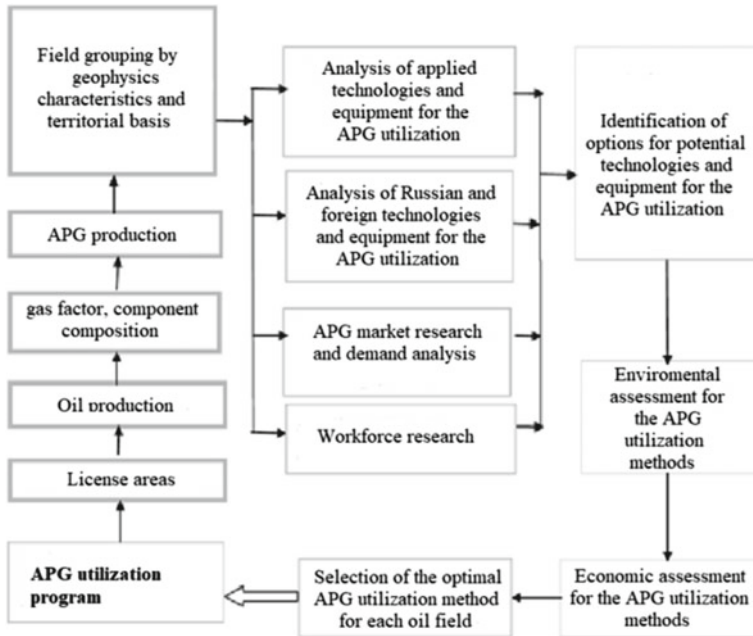
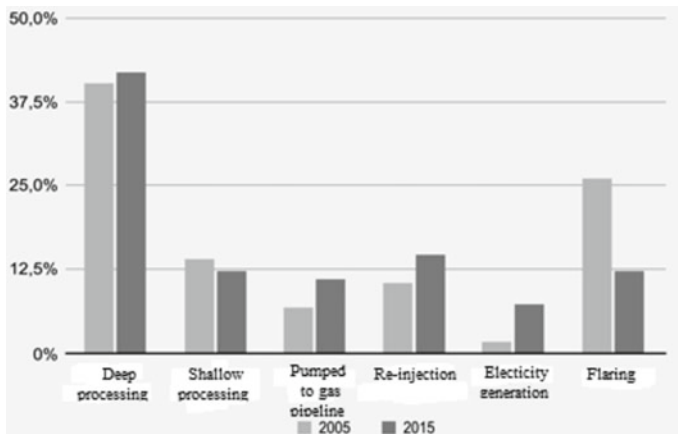**Fig. 3** Algorithm for a rational APG utilization in the oil fields [12, 13]

Fig. 4 Comparison of the APG utilization methods in 2005 and 2015 (in%) [13]
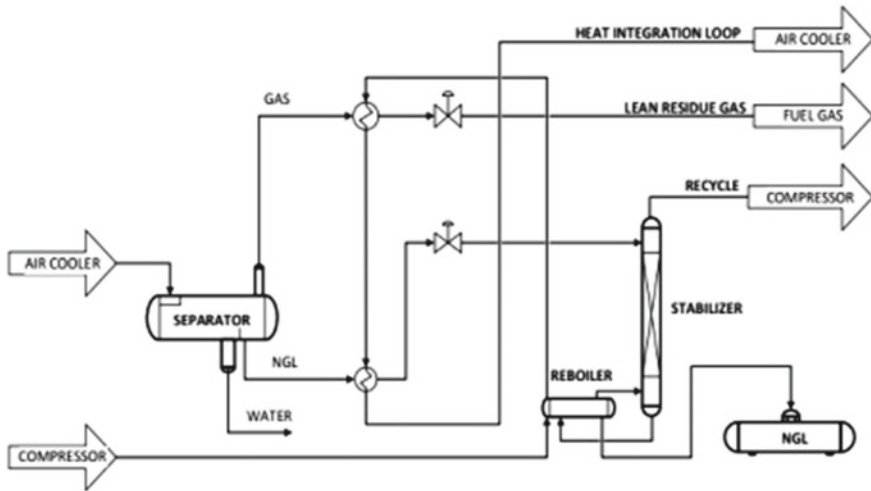
Fig. 5 System of operation of NLG-Pro technology [10]

a result of which: environmental pollution by combustion components; degradation and withdrawal of a land part from economic circulation, due to thermal effects; decrease in the number of animals and plants species. The analyzes carried out made it possible to prove that in the medium and long term, the APG flaring leads to lost profits and direct economic damage. Any of the alternative (rational) methods of APG utilization allows you to get a positive economic effect—from simple zeroing of penalties (re-injecting APG back into the oil reservoir) to receiving money from the sale of the resulting refined products (electricity and heat energy, dry gas, fuel, polymers).

Therefore, a recommendation for associated petroleum gas utilization, depending on the volume of its production, are:

- for small volumes—covering own energy needs;
- with increased volumes—electricity generation and primary processing of APG to obtain SOG as fuel for the boiler house and NGL for discharge into the oil reservoir;
- with resources from 50 to 150 million m^3/year—processing to obtain dry gas, as well as biogas, LPG and electricity;
- with APG volumes exceeding 150 million m^3/year, processing into dry gas, LPG (or LPG), BGS is recommended.

References

1. Filippov AV (2013) Komponentnyy sostav poputnogo neftyanogo gaza (Component composition of Associated Petroleum Gas). http://www.avfinfo.ru/engineering/e-06/
2. Flaring Gas: How Not to Waste a Valuable Resource (2016) By Columbia center on sustainable investment. http://blogs.ei.columbia.edu/2016/09/16/flaring-gas-how-not-to-waste-a-valuable-resource. Accessed 02 Mar 2021

3. Global Gas Flaring Data (2021) The World Bank. https://www.ggfrdata.org. Accessed 02 Mar 2021
4. Global Gas Flaring Jumps to Levels Last Seen in 2009 (2017) The World Bank. https://www.worldbank.org/en/news/press-release/2020/07/21/global-gas-flaring-jumps-to-levels-last-seen-in-2009. Accessed 28 Feb 2021
5. Global Gas Flaring Reduction Partnership (2021) Global Gas Flaring Tracker Report.The World Bank, Washington D.C
6. Gomes A, Ch S, Vorob'yev KA, Shcherba VA (2019) Osobennosti ispol'zovaniya poputnogo neftyanogo gaza v Rossiyskoy Federatsii (Features of the Associated Petroleum Gas utilization in the Russian Federation). Izd-vo RGPU im. A. I. Gertsena, Saint Petersburg, pp 82–87 (In Russ.)
7. YeS K, Ivanchenko DS (2017) Poputnyy neftyanoy gaz i problema yego utilizatsii (Associated petroleum gas and the problem of its utilization). Molodoy uchenyy 25:120–124
8. Kiryushin PA, Knizhnikov AYu, Kochi KV, Puzanova TA, Uvarov SA (2013) Poputnyy neftyanoy gaz v Rossii: "Szhigat' nel'zya, pererabatyvat'!" Analiticheskiy doklad ob ekonomicheskikh i ekologicheskikh izderzhkakh szhiganiya poputnogo neftyanogo gaza v Rossii ("No flare, recycle!" An analytical report on the economic and environmental costs of flaring associated gas in Russia). Vsemirnyy fond dikoy prirody (WWF), Moscow
9. Knizhnikov AY, Il'in AM (2017) Problemy i perspektivy ispol'zovaniya poputnogo neftyanogo gaza v Rossii (Problems and prospects of associated petroleum gas use in Russia). WWF Rossii, Moscow (In Russ.)
10. NGL PRO Low-Cost Flare Reduction, NGL Recovery, Gas Conditioning, Power Generation and Artificial Lift (2017) Aspen Engineering Services. http://aspenesco.com/uploads/3/4/8/5/34851592/ngl_pro_brochure_--_aspen.pdf. Accessed 06 Mar 2021
11. Ob"yemy szhigayemogo v fakelakh gaza stali sopostavimy s eksportom "Gazproma" (The volumes of gas flared are now comparable with the amount exported by Gazprom) (2020) EurAsia Dialy (In Russ.) https://eadaily.com/ru/news/2020/08/04/obemy-szhigaemogo-v-fakelah-gaza-stali-sopostavimy-s-eksportom-gazproma. Accessed 05 Mar 2021
12. Ozdoyeva AKh (2016) Vybor tekhnologiy poleznogo ispol'zovaniya poputnogo neftyanogo gaza na osnove ekonomicheskikh otsenok (Selection of technologies for the useful use of associated petroleum gas on the basis of economic estimates). Dissertation, Moscow (In Russ.)
13. Shcherba VA, Gomes AChS, Vorobyev KA (2019) Problemy i perspektivy utilizatsii poputnogo neftyanogo gaza v Rossiyskoy Federatsii (Problems and prospects of associated petroleum gas utilization in the Russian federation). Zhurnal Problemy regional'noy ekologii 1:139–145
14. Sposoby utilizatsii poputnogo neftyanogo gaza v Rossii (Methods of utilization of associated petroleum gas in Russia) (2017) Vsemirnyy fond dikoy prirody (WWF). Kompaniya Sibur. (In Russ.) https://www.sibur.ru/upload/iblock/a70/a70036cc7e90e0b2be004a04efb7bf3a.pdf. Accessed 01 Mar 2021
15. Bamji Z, Sucre F (2017) The World Bank/GGFR. An international partnership: The "Zero Routine Flaring by 2030" Initiative. 6 Dec 2017. http://www.olade.org/wp-content/uploads/2017/12/PANEL-2-World-Bank-Presentation-Buenos-Aires-OLADE-Ministerial-1.pdf. Accessed 01 Mar 2021
16. Shcherba VA, Vorobyev KA (2018) Utilizaciya poputnogo neftyanogo gaza v aspekte geoekologicheskoj zashchity okruzhayushchej sredy (Utilization of associated petroleum gas in the aspect of geoecological environmental protection). Vestnik Atyrauskogo instituta nefti i gaza 2(46):102–104
17. Shcherba VA, Vorob'yev KA, Gomes AChS (2018) Utilizaciya poputnogo neftyanogo gaza: ekologicheskij aspect (Utilization of associated petroleum gas: environmental aspect). Problemy i perspektivy kompleksnogo osvoeniya i sohraneniya zemnyh nedr, pp 325–328

18. Shcherba VA, Gomes AChS, Vorobyev KA (2018) Problemy i perspektivy utilizacii poputnogo neftyanogo gaza v Respublike Angola (Problems and prospects of associated petroleum gas utilization in the Republic of Angola). Geologiya, geoekologiya, evolyucionnaya geografiya 17:372–376
19. Abdulkerimov RF, Chekushina TV, Vorobyev KA (2020) Increasing efficiency of use of dryers at the gas-processing enterprises. IOP Conf Ser: Mater Sci Eng 962:042060
20. Shcherba VA, Vorobyev KA (2018) The development prospects of the shale industry in the world. Eurasian Sci J 4(10):3–12

Assessment of the Degree of Reliability
of Thermoelectric Power Sources

I. Yu. Shelekhov[1]([✉]), E. I. Smirnov[2], and M. I. Shelekhov[1]

[1] Irkutsk National Research Technical University, 83, Lermontova street, Irkutsk 664074, Russia
[2] LLC «Termostat+», 4, 8 March street, Irkutsk 664011, Russia

Abstract. The purpose of this work was to study the parameters of thermoelectric sources of electrical energy installed in water supply systems and sewerage systems of apartment buildings. A new design of a thermoelectric module is being investigated, where various composite materials are used. Investigations of the parameters of new thermoelectric modules are carried out depending on the composition of the composite material and operating conditions. The tests are carried out in the operating life support systems, the value of the thermoEMF is fixed by the OWEN device of the IMS-F1.Sh1 brand, in addition, this device controls: voltage, current and power. Temperature control of thermoelectric elements, hot and cold sides of thermoelectric module, as well as sources of "heat" and "cold" is carried out by thermocouples, the data was recorded by the TRM138 meter-regulator. The presented work shows that the use of thermoelectric devices in engineering systems is a promising area of scientific research. It is shown that with a decrease in the polymer binder below 10%, thermoelectric modules cannot be used in rooms with high humidity, and with an increase in the polymer binder above 20%, the EMF value increases during long-term operation. Based on the results of the above studies, the authors conclude that the investigated new designs of thermoelectric modules can be used to provide emergency and standby power supply. Analysis of technical parameters showed that these devices can be used as the main power source for automatic control systems of engineering systems, including the "Smart House" system.

Keywords: Thermoelectric generator · Engineering system · Hot water supply · Ventilation system · Energy saving · Useful work

1 Introduction

The concept of "alternative source" of energy implies that, together or separately with a classical energy source, it is possible to use another energy source. Usually, in the form of an alternative energy source that can replace the traditional energy source, renewable resources are used, in the form of solar energy, wind energy, and the heat of the earth.

The field of science, which deals with alternative energy, is engaged in the search for energy sources and the development of effective ways to convert this energy into "useful work" [1, 2].

One of the energy sources is located next to us, it is heat losses that occur during the operation of buildings. Much attention is paid to this energy source, since when evaluating the efficiency of any engineering system, this value is considered in a negative value. One of the promising directions in the field of converting heat losses into useful work is the method of converting heat losses into electrical energy using thermoelectric devices. Modern advances in this area give us hope for the widespread use of this method of converting one type of energy into another type [3, 4].

Heat losses in buildings can be divided into two groups: permanent and periodic.

Constant and stable heat losses are carried out in such engineering systems as sewerage and water supply. The amount of heat loss from these engineering systems does not depend on the season. Heat losses from heating and ventilation systems occur during the period of time when there is a need for an additional power source. During this period of time, for the operation of thermoelectric systems, an additional source of energy appears, this is an environment with a negative temperature. In addition, the greatest need for energy resources in buildings is the period of time when negative temperatures outside the building prevail. In the Irkutsk region, this period is long, we spend energy to heat the air and the objects around us to a favorable temperature. We do not think that somewhere this air and surrounding objects need to be cooled to a favorable temperature, while spending the same amount of energy. Energy is spent on heating and cooling air or water in engineering systems, and in fact, water or air, in this case, are energy accumulators. Using thermoelectric devices, we set ourselves the task of obtaining an effective method for extracting this energy and converting it into another type of energy that can be used for human life, for example, into electrical energy. Electricity is the most convenient form of energy that can be easily used in almost any technological process, both at home and at work. Electricity is the main form of energy into which the energy of wind, water and sunlight is converted. Thermoelectric generators generate electrical energy due to the temperature difference between the junctions, which are located on opposite surfaces. The more one side heats up or the other side cools, the greater the amount of electricity generated. The use of a natural resource, in the form of ambient temperature, for cooling one side of a thermoelectric module, considering the fact that this resource is possessed by a large territory of Russia, is economically feasible.

Many scientists, both in Russia and abroad, are engaged in the development of designs and technologies for the manufacture of thermoelectric modules. Such well-known Russian scientists such us Holtzman, Kudinov, Smirnov noted in their works [5] that the main limitation in the variety of structural elements is the lack of technology with which it is possible to manufacture thermoelectric modules in large quantities. There are many design solutions [6], but a significant factor in their implementation is the use of manual labor for the final formation of the thermoelectric system, which not only increases the cost of the product, but also seriously reduces its reliability. The size of the standard substrate, which is used in microelectronics for the production of microcircuits, was taken as the main standard for the manufacture of thermoelectric modules. Thus, the area of the thermoelectric module is limited and only one quantity appears, using which the developers could change, this is the height. In fact, the height of the thermoelectric module was limited by the size of the thermoelectric module. Model calculations presented in various works [7] showed that, depending on the operating conditions, the design

of the thermoelectric module with temperature drops and mechanical stress should be designed in limited dimensions. A special contribution to these studies was made by employees of the Moscow State Technical University named N.E. Bauman [8]. Literary studies in this field of science [9–11] have shown that the efficiency of thermoelectric systems is more influenced by technical solutions during design than by the electrophysical characteristics of thermoelectric junctions. Using the methodology proposed by the scientists of this institute, in comparison with the methods of foreign scientists [12–15], we assessed the degree of reliability of thermoelectric systems assembled using new designs of thermoelectric modules.

2   Materials and Methods

To study the parameters of thermoelectric modules, an installation was created in which six modules with different ratios of thermoelectric material and polymer binder were installed. Thermoelectric modules were manufactured in accordance with the patent for invention No. 2611562 [16]. The manufacturing technology is called "thick film technology" or "screen printing technology". The essence of this technology is to push a paste with certain properties through a stencil applied on a mesh. Depending on the thickness of the mesh and the topological pattern, you can change both the width and the thickness of the applied layer, and you can also vary the geometric shapes.

Unlike the classical technology, we transfer the volumetric figure to a plane and create a module on this plane, on a part of the plane n-type semiconductors on the other p-type part. In this case, the size of the plane can be large, the planes can be spatially oriented, the parts of the planes may not be the same, the distance between the parts of the planes can be different.

Taking into account the fact that the efficiency of thermoelectric systems operation to a greater extent depends on technical solutions during design, since external technical losses in real systems are comparable to internal losses in thermoelements. The main technical losses are due to the mutual influence of the heat transfer plates and the thermal conductivity of thermoelectric joints. The design of a classic thermoelectric module consists of two heat transfer plates, which are connected by thermoelectric elements. The distance between the plates is determined by the technical capabilities of the technologies used for the manufacture of semiconductor columns and ranges from 1 to 3 mm. The area of heat transfer plates is not significant, therefore, design solutions in the design of heating and cooling radiators do not give significant results in expanding the range of applications and increasing the efficiency of thermoelectric systems.

Using our technology, we obtain a three-dimensional figure, where the heat-transferring sides are at a distance much greater than that of classical thermoelectric modules. For the manufacture of thermoelectric modules according to our technology, connecting and switching tracks are applied to the glass-textolite plate with silver paste. The barrier tracks are then applied with dielectric alumina paste to create grooves between the connecting and switching tracks. All application cycles are done on a screen printing machine, after each application cycle, a heat treatment process is carried out at a temperature of 130° C. Then a thermoelectric material made on the basis of n-type and p-type semiconductors is applied to the recesses, which is subjected to preliminary

drying at a temperature of 65 °C, and then the process is subjected to a sintering process under pressure at a temperature of 130 °C. Figure 1 shows thermoelectric modules manufactured using this technology.
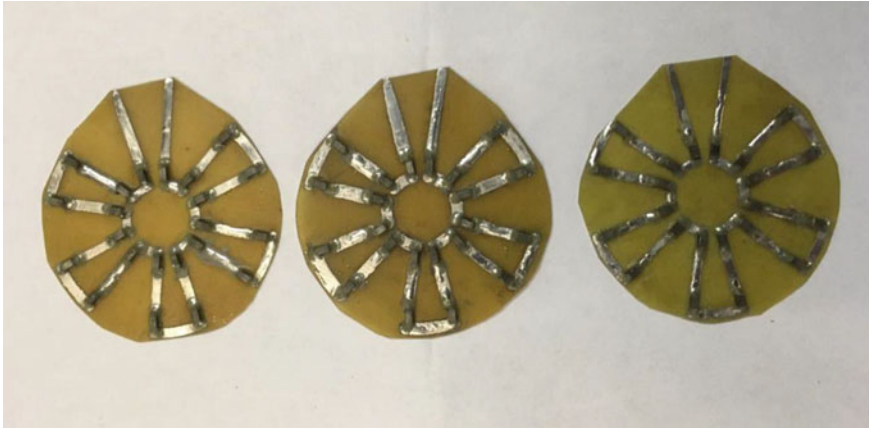

Fig. 1 Thermoelectric modules of a new type

Thermoelectric material was made from ultrafine powder of bismuth telluride (Bi2Te3) and a polymer binder (copolymer of methacrylic acid and methacrylic acid butyl ester). The ratio of thermoelectric material and polymer binder varied from 95%–5% to 70%–30%. Thermoelectric material was prepared from ultrafine n-type and p-type bismuth telluride powders in a drum mill for 24 h. After that, current-carrying wires are soldered to the first and last connecting track and we have a chain of series-connected thermoelements. The process of connecting thermoelectric modules is shown in Fig. 2.

The transition of n-type thermoelements to p-type thermoelements occurs on one side of the plane, and the transition of p-type thermoelements to n-type thermoelements occurs on the other side of the plane. The elements of the same name are connected to each other by connecting paths inside the plane, which makes it possible to space the heat transfer zones at a considerable distance. Using this technology, we can produce thermoelectric modules of various geometric shapes. After manufacturing, thermoelectric modules are assembled into a thermoelectric battery and installed in an engineering system. Figure 3 shows the process of combining thermoelectric modules into a thermoelectric battery.

Thermoelectric batteries are calculated and designed for each engineering system individually. After that, they are connected to a voltage regulator and installed in the case. Figure 4 shows a thermoelectric installation installed on a pipe of a sewage system. The generated energy of this installation is sufficient to illuminate the basement where the sewerage system is laid.

Figure 5 shows a block diagram of the stand for monitoring the parameters of thermoelectric modules.
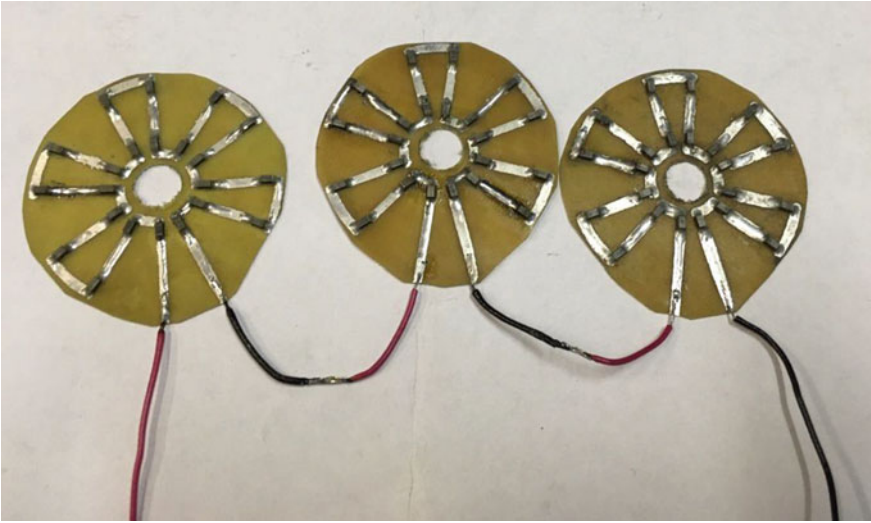
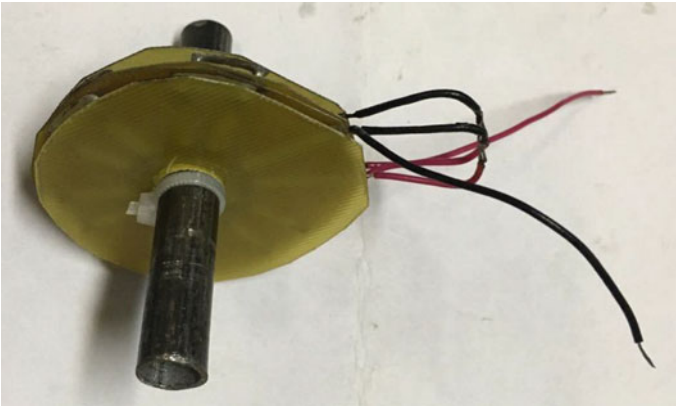**Fig. 2** The process of connecting thermoelectric modules

Fig. 3 The process of connecting thermoelectric modules

3 Research Results

During the experiments, the installation with thermoelectric modules was installed on the sewer pipe, the other side was cooled with outside air. The generated power of the generator, according to the averaged indicators, was about 200 W., no change in the operation of the sewage system was detected. Similar experiments were carried out between pipelines for hot and cold-water supply, studies have shown that the installation of a thermoelectric generator with a capacity of up to 200 W in a hot and cold-water supply system does not have a significant effect on consumers, since during operation heat is inevitably lost through the walls of pipelines, fittings and elements constructions. The ratio of the amount of energy spent on heating water for the hot water supply system

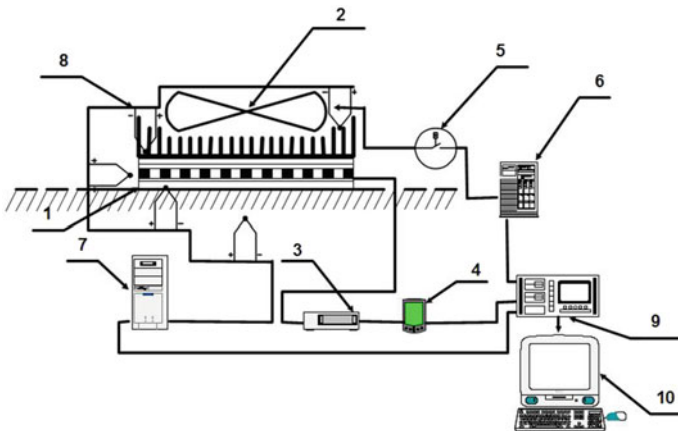**Fig. 4** Thermoelectric generator for the sewerage system

Fig. 5 Stand for researching the parameters of thermoelectric modules. Description of the stand: a thermoelectric generator is installed on the surface (1), where heat losses occur (sewer pipe, ventilation duct, etc.). The second side of the thermoelectric generator is cooled by a fan (2) combined with a radiator, which was calculated in accordance with the methodology described in the article by the authors Ivanov, Tsarev, Chugunkov [17], signal from of the thermoelectric generator enters the resistance bridge (3) and is fixed by the device of the "OWEN" brand IMS-F1.Sh1 (4), the data from the device through the modem (9) goes to the personal computer (10). Temperature control is carried out by the TRM138 meter-regulator using thermocouples (8), the data is also fed to a personal computer. The humidity sensor (5) controls the humidity in the area of thermoelectric modules and through the device MPR 51—Sh4.01 (6), it also transmits data to a personal computer

to the amount of converted energy does not exceed 1%, and the average coefficient of heat loss from one square meter of uninsulated pipeline for multi-storey buildings is 12 W / (m^2 K), respectively, the amount of converted energy is commensurate with the magnitude of the error from the total amount of pipeline losses.

Figure 5 shows the graphs of changes in the value of the generated EMF during long-term operation, at a current load of 15A and humidity of 40%. It can be seen from the graphs that the maximum EMF value at a ratio of thermoelectric material and polymer binder of 95% is 5%, despite the fact that during long-term operation the value decreased by 10%, its value is higher than at other ratios. Stable EMF characteristics are observed at a ratio of 80–20%, while it was noticed that with an increase in the dielectric binder, the EMF value increases during operation. This fact is consistent with the general theory of the formation of electrical conductivity [18]. From the graphs, it can be concluded that with a dielectric component from 10 to 20%, the EMF parameters have stable values during long-term operation, with lower ratios, the process of reducing the EMF is not completed.

Figure 6 shows the graphs of changes in the value of the generated EMF during long-term operation, at a current load of 15A and a humidity of 80%. It can be seen from the graphs that the maximum EMF value at the ratio of thermoelectric material and polymer binder 80–20%, while the EMF value during long-term operation increased by 20%. Stable EMF characteristics are observed when the value of the dielectric binder is from 10 to 20%. The EMF value at a dielectric binder of 5 and 10% is steadily decreasing, while it can be concluded that this ratio cannot be used in the manufacture of thermoelectric modules that are used in engineering systems. When the values of the dielectric binder are more than 20%, the EMF parameters are stable and, during long-term operation, increase due to the formation of new current-carrying bridge (Fig. 7).

4 Discussion and Conclusions

In addition to full-scale thermal engineering studies of systems with a thermoelectric generator, we searched for studies on the emergency supply of heat points with electric energy using alternative energy sources. It was found that research in this area has not received sufficient attention. In our region, and other regions of our country, in the conditions of a harsh winter, it is impossible to maintain a housing stock without high-quality heating and water supply. High-quality operation of engineering systems is ensured by additional actuators controlled by automatic control systems, with minor failures in electrical networks, serious problems arise during the operation of buildings.

Moreover, for lighting basements and attics in residential buildings, it is advisable to use a safe voltage of up to 36 V. In cases where a standard industrial voltage of 220 V is used, the cost of measures to ensure electrical and fire safety in these premises is very high. Stable DC sources can not only ensure the operation of electronic equipment, but also, in accordance with regulatory documents, in multi-storey buildings can be used for emergency lighting of possible evacuation routes in case of emergency (SP52.13330.2011; SNiP 23–05-95). In multi-storey residential buildings, along with emergency evacuation lighting, emergency lighting in elevators should be provided (GOST R 53,780–2010), and in buildings classified as "high-rise" there should simply be emergency lighting (SP-267.1325800.2016; SP 253.1325800.2016).

Fig. 6 Dependence of EMF during long-term operation on the value of the dielectric binder, humidity 40%: 1—ratio 95%—5%; 2—ratio 90–10%; 3—co-ratio 85–15%; 4–ratio 80–20%; 5—ratio 75–25%; 6—ratio 70–30%
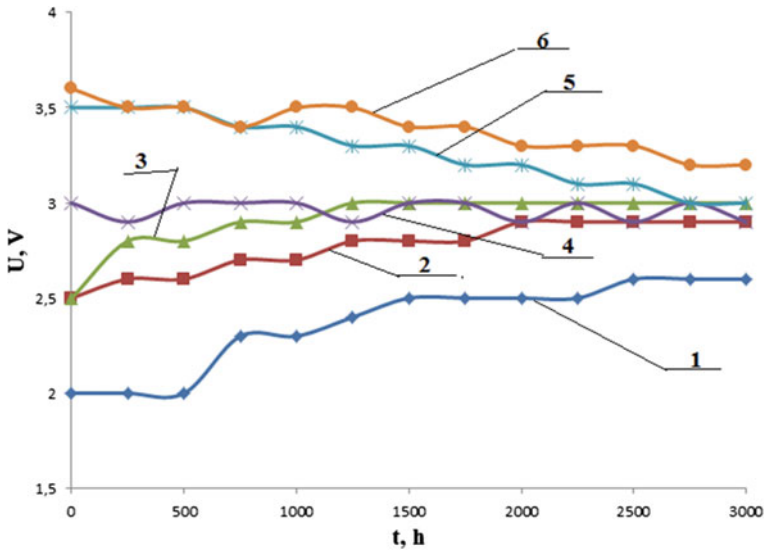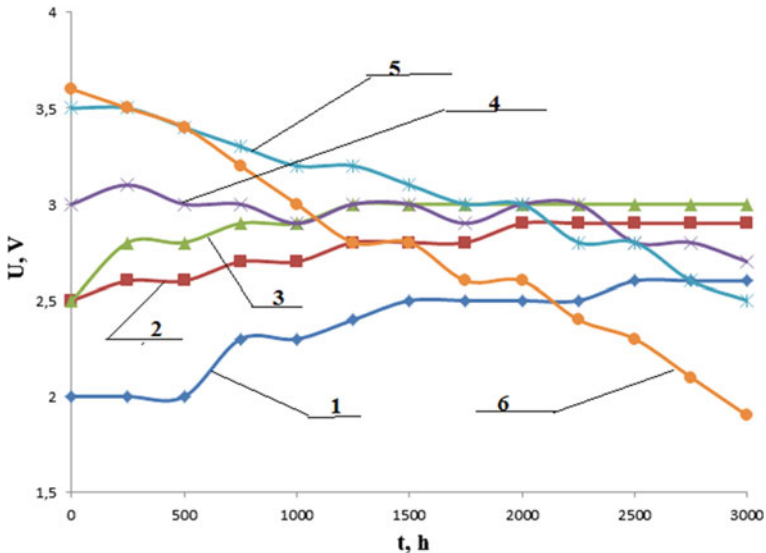

Fig. 7 Dependence of EMF during long-term operation on the value of the dielectric binder, humidity 80%: 1—ratio 95–5%; 2—ratio 90–10%; 3—co-ratio 85–15%; 4—ratio 80–20%; 5—ratio 75–25%; 6—ratio 70–30%

The thermoelectric device described in the article is an autonomous energy source that generates a safe voltage.

Studies have shown that a new technical solution for the creation of thermo-electric modules from composite materials can provide a stable generation of electrical energy, but it is necessary to consider the nature of the operation of these devices. When operating thermoelectric devices in a humid atmosphere, the ratio of the dielectric binder should be in the range of 20%. The investigated thermoelectric generators can be used as an emergency or standby power supply, as well as a stable DC source for powering automation devices in Smart Home systems or other devices that ensure the operation of engineering systems.

Research and development work in the field of improving thermoelectric devices related to improving heat dissipation from the area of the heat transfer sides have exhausted their capabilities. Therefore, further work to increase the efficiency of thermoelectric systems should be carried out in improving their designs and technologies for their manufacture. Using our technology for the manufacture of thermoelectric modules, it becomes possible to completely remove the mutual influence of the hot and cold sides, it is possible to increase the heat dissipation area within a very wide range. With an increase in their efficiency, thermoelectric modules will be able to compete with traditional heat pumps in the field of higher capacities and will be able to expand their range of applications.

References

1. Köysal Y, Özdemir AE, Atalay T (2018) Experimental and modeling study on solar system using linear fresnel lens and thermoelectri moule. J Solar Energy Eng Trans ASME 140(6):061003
2. Sokolov MM (2015) Use of renewable and non-traditional energy sources: textbook. Allowance Nizhegor State Architectures—Builds un-t. NNGASU, N. Novgorod, p 116
3. Shelekhov IYu, Smirnov EI, Ruposov VL, Shishelova TI (2013) Experience in using thermoelectric generators. Journal "Fu Damental Research" 11(part 5):919–923
4. Shelekhov IY, Ruposov VL, Smirnov EI (2020) Scientific and economic substantiation of the use of thermoelectric modules: monograph. Publishing house IRNNITU, Irkutsk, p 164
5. Goltsman BM, Kudinov VA, Smirnov IA (1972) Semiconductor thermoelectric materials based on Bi2Te3. Science, Moscow, p 320
6. Snyder GJ (2003) Design and optimization of compatible, segmented thermoelectric generators. Proc. of the 22nd International Conference on Thermoelectrics. Hérault (France), pp 443–446
7. Hasegawa Y, Oike T, Okumura H, Sato K, Nakamura K, Yamaguchi T, Iiyoshi A, Yamaguchi S, Asano K (2001) Thermoelectric Property Measurement For a Peltier Current Lead. Proc of the 20th International Conference on Thermoelectrics. Beijing (China), pp 507–510
8. Yoo C-Y, Kim Y, Hwang J, Yoon H, Park SH, Cho BJ, Min G (2018) Impedance spec-troscopy for assessment of thermoelectric module properties under a practical operating temperature. Energy 152:834–839

9. Jianzhong Z, Tiemin W (1998) Application of the thermoelectric cooler in theth seventeenth chiniesse retrievable satellite. Abstracts of the 17 Int. Conf. on Thermoelectrics, Nagoya, Japan, p 81

10. Marchenko AS, Sulin AB (2016) Efficient heat exchanger solutions for thermo-electric heat transformers. Bulletin of the Dagestan State Technical University. Tech Sci 43(4):63–72. https://doi.org/10.21822/2073-6185-2016-43-4-63-72

11. Ismailov TA, Mirzemagomedova MM (2016) Study of stationary modes of operation of thermoelectric heat exchangers. Bull Dagestan State Tech Univ. Tech Sci 1(40):23–30. https://socionet.ru/~cyrcitec/json/spz/neicon/vestnik/y:2016:i:1:p:23-30.pdf

12. Christopher W, Sinton1 Richard Winnett2—Solar powered water pumping systems in n New York state. New York state for energy research and development authority national renewable energy laboratory website. http://www.nrel.gov/clean_energy/solar.html

13. Micheli L, Sarmah N, Luo X, Mallick TK, Reddy KS (2013) Opportunities and challenges in micro and nano technologies for concentrating photovoltaic cooling. Renew Sustain Energy Rev 20:595–610. www.elsevier.com/locate/rser

14. Benn SP, Poplaski LM, Faghri A, Bergman TL (2016) Analysis of thermosyphon/heat pipe integration for feasibility of dry cooling for thermoelectric power generation. Appl Therm Eng 104:358–374. https://www.journals.elsevier.com/applied-thermal-engineering

15. Date A, Date A, Dixon C, Akbarzadeh A (2014) Theoretical and experimental study on heat pipe cooled thermoelectric generators with water heating using concentrated solar thermal energy. Solar Energy 105:656–668. https://www.journals.elsevier.com/solar-energy

16. Shelekhov IYu, Smirnov EI, Kashko KP, Shelekhova IV (2017) Spatially oriented thermo-electric module and a method for its manufacture. Patent for invention No. 2611562, Patentee: Thermostat + LLC. http://www1.fips.ru/fips_servl/fips_servlet

17. Ivanov MF, Tsarev AV, Chugunkov VV (2014) Modeling of parameters of thermoelectric cooling devices. Electronic scientific and technical journal "Engineering Bulletin" El.№FS77–51036, Publisher: Academy of Engineering Sciences im. A.M. Prokhorov 11:93–103. http://engbul.bmstu.ru/doc/745021.html

18. Nikitenko VR, Tameev AR, Vannikov AV (2009) Mechanism of metallic electrical conductivity in organic nanostructures. Proc Higher Educ Inst. Phys 52(11):28–35

Comparison of UV Fluences (365 nm) for Water Treatment by Photo-Fenton-Like Process

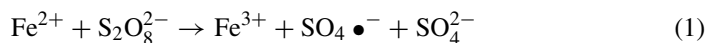G. Matafonova[(✉)], S. Popova, I. Tsenter, N. Garkusheva, and V. Batoev

Baikal Institute of Nature Management SB RAS, 6 Sakhyanovoy St, Ulan-Ude 670047, Russia
ngal@binm.ru

Abstract. The integration of water treatment and disinfection processes is beneficial for reducing energy requirements. The photo-Fenton-like process using UVA light-emitting diode (365 nm) and peroxydisulfate (PDS) was investigated in terms of light fluence (dose) requirements for concurrent degradation of 20 μM emerging organic contaminant (bisphenol A) and inactivation of 10^5 CFU/mL bacteria (*E. coli* and *E. faecalis*) in aqueous solution. The photo-Fenton-like oxidation system {UVA/PDS/Fe^{2+}} was the most efficient for degrading bisphenol A without co-existing bacteria and inactivation of *E. faecalis* in the absence of bisphenol A. The highest UV fluences of up to 5.7 J/cm^2 were obtained for 90% degradation of bisphenol A in the presence of bacteria. These fluences concurrently inactivated 100% co-existing bacterial cells due to their lower fluence requirements for total inactivation (up to 2.1 J/cm^2). The lowest fluences were needed for total inactivation of *E. coli* regardless of the presence of bisphenol A (~1 J/cm^2). The obtained fluences are comparable with the literature values for separate degradation or inactivation by other photo-induced advanced oxidation processes at 365 nm. Results show the feasibility and energy-efficiency of the integrated processes for efficient elimination of both chemical and biological contaminants from water.

Keywords: Photo-Fenton-like process · UV LED · Persulfate · Water treatment · Degradation · Inactivation

1 Introduction

Pollution of aquatic ecosystems with emerging organic contaminants and pathogenic microflora is of a global environmental concern. To date, advanced oxidation processes (AOPs) are regarded as one of the most efficient means of removing them from wastewater effluents and reducing their level in water bodies. Specifically, the homogenous photo-Fenton-like processes have attracted a significant research attention for water treatment and disinfection. Peroxydisulfate ($S_2O_8{}^{2-}$, PDS) and ferrous (Fe^{2+}) ions are efficient and environmentally friendly reagents for producing hydroxyl radicals (•OH) and sulfate radical anions (SO_4•$^-$) in water through Fenton-like reactions (1–5):

$$Fe^{2+} + S_2O_8^{2-} \rightarrow Fe^{3+} + SO_4 \bullet^- + SO_4^{2-} \tag{1}$$

$$SO_4 \bullet^- + H_2O \rightarrow \bullet OH + HSO_4^- \tag{2}$$

$$SO_4^{2-} + \bullet OH \rightarrow SO_4 \bullet^- + OH^- \tag{3}$$

$$Fe^{3+} + S_2O_8^{2-} \rightarrow Fe^{2+} + 2SO_4\bullet^- \tag{4}$$

$$Fe^{2+} + SO_4\bullet^- \rightarrow Fe^{3+} + SO_4^{2-} \tag{5}$$

Ultraviolet (UV) light is employed for activating peroxydisulfate and enhancing the production of $SO_4\bullet^-$ (6):

$$S_2O_8^{2-} \xrightarrow{\text{UV}} 2SO_4\bullet^- \tag{6}$$

The radicals can be used for concurrent water treatment and disinfection due to their dual ability of degrading organic contaminants and inactivating microbial cells. The integration of degradation and inactivation processes is beneficial for reducing the total energy consumption. Over the last few years, there has been a growing research interest in concurrent removal of organic contaminants and pathogenic microorganisms from water and wastewater by different AOPs. Most works focused on the solar-assisted photo-Fenton processes using hydrogen peroxide [1–5]. Regarding photo-Fenton-like processes, recent research showed that the addition of Fe^{2+}, PDS or peroxymonosulfate significantly enhanced the solar degradation of organic contaminants and inactivation of microorganisms in drinking water under mild conditions [6, 7]. It should be pointed out that the target organic pollutants and microorganisms were not treated in a mixture in the above investigations. However, under optimized operating conditions, the photo-Fenton-like treatment with low-pressure mercury lamp (254 nm) provided the concurrent removal of bacteria and organic contaminants from urban wastewater [8].

Meanwhile, switching to energy-efficient and mercury-free light sources, such as UVA/visible light-emitting diodes (LED), is crucial to saving energy and supporting the Minamata Convention on Mercury (2013). To date, UVA diodes (315–400nm) have become rather cost-effective and have a relatively high wall-plug-efficiency [9]. Recently, it was found that the photo-Fenton process with UVA LED was efficient for elimination of propranolol and bacteria from agricultural effluents [10]. However, the photo-Fenton-like systems using PDS towards concurrent degradation and inactivation remain less investigated. Moreover, the energy requirements in terms of light fluences (doses) have been rarely reported in the related literature.

This study aimed at calculating and comparing the UV fluences for degradation of endocrine disrupting compound bisphenol A (BPA) and inactivation of bacteria *Escherichia coli* and *Enterococcus faecalis* in the photo-Fenton-like system {UVA/PDS/Fe^{2+}} using UVA LED (365 nm).

2   Materials and Methods

Bisphenol A (99%, Sigma-Aldrich), potassium peroxydisulfate (Vekton, Russia), iron (II) sulfate and sulfuric acid (Khimreaktivsnab, Russia) were used as received. All

stock and working solutions were prepared in MilliQ-water (Simplicity®UV system, Millipore). The solvents acetic acid and acetonitrile for HPLC were supplied by Khimreaktivsnab and Cryochrom (Russia), respectively.

The stock suspensions of *E. coli* K-12 and *E. faecalis* B 4053 strains (SRIGSIM, Russia) were prepared from the overnight cultures after centrifugation, double washing out and resuspension in phosphate buffered saline (Gibco® Life technologies, UK). The overnight cultures were grown by aerobic incubation in nutrient broth (SRCAMB, Russia) and tryptic soy broth (Merck), respectively.

Experiments were conducted in a thermostabilized glass photoreactor under magnetic stirring. A UVA LED array (Yonton, 100 W, China) was positioned above the open reactor and also thermostated by a circulating water. The LED emission spectrum with a maximum at 365 nm is shown in Fig. 1.
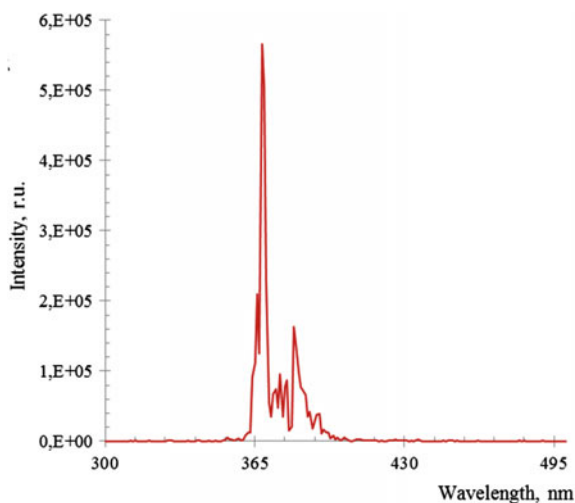

Fig. 1 Emission spectrum of UVA LED (365 nm)

The incident irradiance (at the surface of the sample), measured with a polychromatic ferrioxalate actinometry [11–14], was 2.46 mW/cm^2 over the 300–400 nm range. The model aqueous solution, contaminated with 20 µM BPA and/or 10^5 CFU/mL *E. coli* (*E. faecalis*), was irradiated by UVA LED in the photo-Fenton-like system at pH 5.0 in the presence of PDS and Fe^{2+} ions. Control experiments were performed under sole UVA irradiation, UVA/PDS and PDS/Fe^{2+} (dark) treatments. To monitor the degradation and inactivation kinetics, the samples were taken at selected times and analyzed by HPLC (BPA) and plating technique (bacteria) for residual concentrations and counts of survived cells, respectively. The BPA analysis details were described previously [15].

The absorbance spectra for fluence calculations were measured using a Shimadzu UV-1800 spectrophotometer. The fluences were calculated as the product of the average irradiance throughout the water volume (mW/cm^2) and the corresponding treatment times (s). In turn, the calculation of average irradiance accounted for the water absorbance and the relative emission spectrum of the LED across the UVA spectrum [16].

3   Results and Discussion

Initially, the efficient Fe^{2+} dosage was selected in the photo-Fenton-like system {UVA/PDS/Fe^{2+}} by varying the molar ratios at a fixed PDS concentration of 84.5 mg/L (312.5 μM) [17]. The obtained plots of BPA degradation showed that the measurable kinetics was observed at the lowest tested Fe^{2+} concentration of 1 mg/L (17.4 μM) (Fig. 2). Therefore, a molar ratio of 18:1 (312.5 μM PDS: 17.4 μM Fe^{2+}) was used in further experiments.
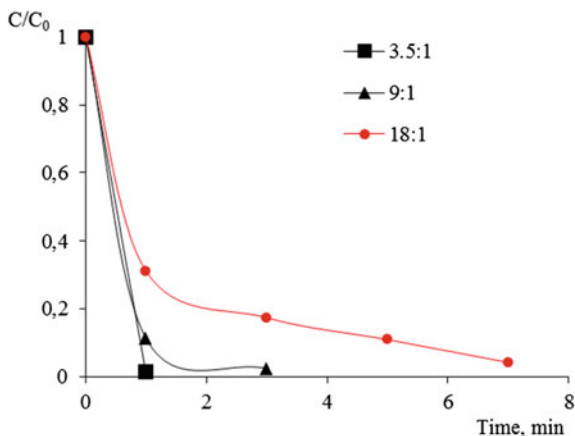

Fig. 2 The plots of bisphenol A degradation by photo-Fenton-like process at different molar ratios of PDS and Fe^{2+}. [BPA]$_0$ = 20 μM, [PDS]$_{fixed}$ = 312.5 μM, [Fe^{2+}]$_{variable}$ = 17.4 μM (18:1), 34.7 μM (9:1), 89.3 μM (3.5:1), pH = 5.0

Further on, degradation experiments were conducted in the oxidation systems, namely, {UVA} (direct photolysis), {PDS/Fe^{2+}} (dark Fenton-like), {UVA/PDS} and {UVA/PDS/Fe^{2+}}, and the obtained plots are shown in Fig. 3. BPA with two absorption spectrum peaks at 225 and 276 nm was not photolyzed by sole UVA irradiation. Addition of peroxydisulfate lead to generation of $SO_4^{\bullet-}$ and complete BPA degradation in 30 min ($k_{BPA,\ SO4^{\bullet-}} = 1.37 \times 10^9$ [18]). The highest degradation rate was observed in the UVA/PDS/Fe^{2+} system, which was 3.7 times higher than that found in the UVA/PDS system. Dark treatment (PDS/Fe^{2+}) resulted in removing approximately 30% by the Fenton-like reaction.

The experiments on BPA degradation in the presence of bacteria were conducted in the most efficient UVA/PDS/Fe^{2+} system. The pseudo-first-order fluence-based rate constants, which were obtained from the corresponding fluence-based linear plots (not shown), are given in Table 1. Evidently, the degradation rates significantly decreased after adding bacteria. This is consistent with the literature data on inhibition effect of co-existing microorganisms on the degradation of organic contaminants at relatively high initial concentrations at mg/L level [19–23]. These organic substrates are competed with each other for •OH and $SO_4^{\bullet-}$, thereby decreasing the radical levels and exposures.
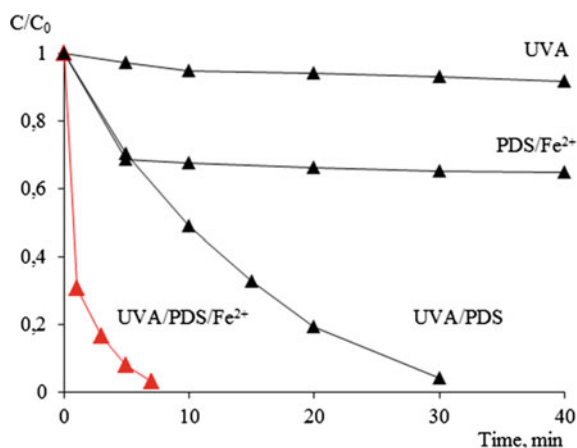
Fig. 3 The plots of bisphenol A degradation in different oxidation systems without co-existing bacteria. $[BPA]_0 = 20\ \mu M$, $[PDS]:[Fe^{2+}] = 18:1$, $pH = 5.0$

Table 1 The fluence-based rate constants (k) of bisphenol A degradation by photo-Fenton-like process. $[BPA]_0 = 20\ \mu M$, $[Bacteria]_0 = 10^5$ CFU/mL, $pH = 5.0$

System	$k \times 10^{-2}$ (cm^2/mJ)	R^2
UVA/PDS/Fe^{2+}	0.27	0.99
UVA/PDS/Fe^{2+} + E. coli	0.05	0.98
UVA/PDS/Fe^{2+} + E. faecalis	0.04	0.95

Additionally, the sorption of compound molecules onto bacterial cells also contributes to the inhibition. This was supported by control experiment (BPA + bacteria), which showed 8–12% BPA decay in 20 min stirring without any exposure.

The UV fluences required for 90% degradation were determined from the corresponding fluence-based constants. As shown in Fig. 4, the fluences for BPA removal in the presence of E. coli or E. faecalis are expectedly higher than those obtained without bacteria, increasing to 5.7 J/cm^2.

Mostly, the obtained UV fluences were within the range of the previously reported values for degrading organic contaminants by UV_{365}-induced AOPs. Specifically, the fluences for degrading BPA (along with other emerging contaminants) by LED/NO$_2^-$ and crotamiton by UVA/Fe^{III}-NTA/Oxone were 3.66 [24] and 3.9 J/cm^2 [25], respectively. LED/Chlorine treatment required 1.9 J/cm^2 for removing 96% acetaminophen [26]. Other literature fluences, which were estimated by multiplying the given irradiance by irradiation time, reached 9.4 J/cm^2 for degrading acetamiprid by LED/Fenton [27] and varied in the range of 30.6–122.4 (60–240 min) for decomposing p-hydroxybenzoic acid by LED/TiO$_2$ process [28]. Another estimated fluence of 2.36 J/cm^2 (0.15 kJ) was also reported for photocatalytic elimination of sulfamethoxazole, oxytetracyline and 17-α-Ethynylestradiol [29].
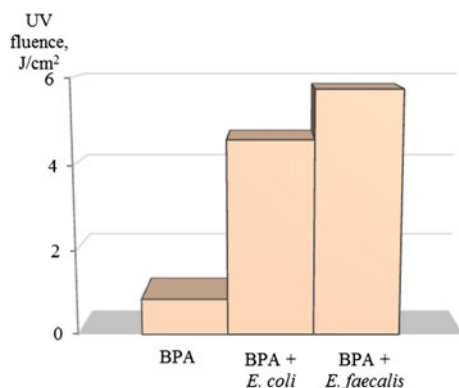
Fig. 4 The UV fluences required for 90% degradation of bisphenol A with and without co-existing bacteria by photo-Fenton-like process. $[BPA]_0 = 20\ \mu M$, $[Bacteria]_0 = 10^5$ CFU/mL, pH = 5.0

Unlike degradation, the plots of *E. coli* and *E. faecalis* inactivation did not follow the pseudo-first-order kinetics and some exhibited the lag time, during which no measurable inactivation was observed. Comparing the inactivation rates by sole UVA, UVA/PDS, PDS/Fe^{2+} and target UVA/PDS/Fe^{2+} processes, the latter was the fastest for total inactivation of *E. faecalis* (10 min). Its efficiency for *E. coli* was similar to the UVA/PDS treatment, achieving the total inactivation in 7 min by both processes. This suggests the predominant contribution of high-intensity UV radiation to inactivation of gram-negative *E. coli*, which is more sensitive to UV light than gram-positive *E. faecalis*. Indeed, *E. coli* was inactivated faster than *E. faecalis* under sole UVA irradiation (10 versus 20 min). Dark treatment (PDS/Fe^{2+}) did not cause a measurable inactivation of both species.

When BPA was present in the solution, the inactivation rates also decreased that support the statement of competition for radicals between co-existing chemical compounds and microorganisms (Fig. 5). Notably, the inhibition effect of BPA was more pronounced during *E. faecalis* inactivation.
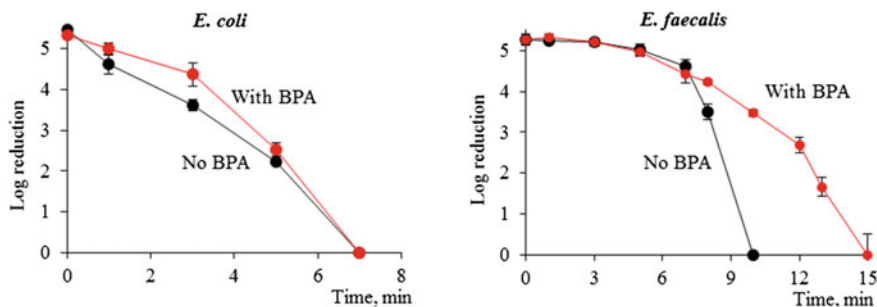

Fig. 5 The plots of *E. coli* and *E. faecalis* inactivation with and without co-existing bisphenol A by photo-Fenton-like process. $[BPA]_0 = 20\ \mu M$, $[Bacteria]_0 = 10^5$ CFU/mL, [PDS]:[Fe^{2+}] = 18:1, pH = 5.0

The UV fluences required for total (100%) bacterial inactivation are depicted in Fig. 6.
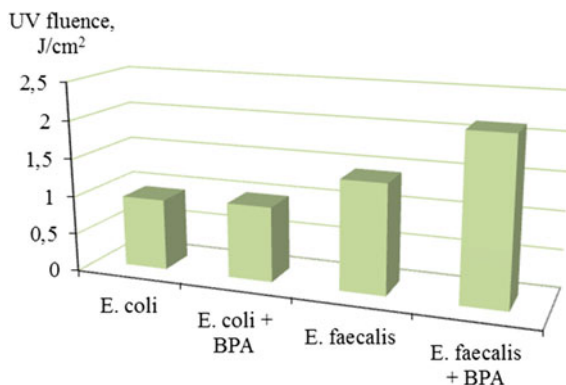

Fig. 6 The UV fluences required for 100% inactivation of *E. coli* and *E. faecalis* with and without bisphenol A by photo-Fenton-like process. $[BPA]_0 = 20\ \mu M$, $[Bacteria]_0 = 10^5$ CFU/mL, pH = 5.0

Overall, the UV fluences for *E. faecalis* were higher and reached 2.1 J/cm^2. The concurrent presence of organic contaminant prolonged the total inactivation and increased the final fluence by ~30%. Since BPA did not cause the significant inhibition of *E. coli* inactivation, the corresponding fluence was the same regardless of co-existing contaminant (~1 J/cm^2, 7 min). The obtained fluences are substantially lower that those reported in the literature with UVA LED alone. However, only a few studies reported the UV fluences at 365 nm for microbial inactivation by photo-based AOPs. Specifically, the fluences of 0.688–0.870 and 0.105 J/cm^2 were needed to attain 3-log [30] and 0.4-log reductions of *E. coli* by UVA/TiO$_2$ treatment [31]. The reported values are comparable with the obtained fluences for *E. coli*. Overall, the UV fluences for total inactivation of *E. coli* and *E. faecalis* are considerably lower than those found for BPA degradation.

4 Conclusions

The homogenous photo-Fenton-like process using UVA LED and peroxydisulfate is efficient towards the concurrent degradation of BPA and inactivation of *E. coli* and *E. faecalis* in model aqueous solution. Although the degradation rates substantially decreased in the presence of bacteria, the required fluences (doses) are comparable with the previously reported values for degradation of organic contaminants by other UV$_{365}$-based advanced oxidation processes without any co-existing microorganisms. The UV fluences required for degradation of 90% BPA in the presence of bacterial cells provide their concurrent inactivation. In this regard, degradation and inactivation in a single treatment step appear to be a promising energy-effective process for further up-scaling.

References

1. Gutiérrez-Zapata HM, Sanabria J, Rengifo-Herrera JA (2017) Addition of hydrogen peroxide enhances abiotic sunlight-induced processes to simultaneous emerging pollutants and bacteria abatement in simulated groundwater using CPC solar reactors. Sol Energy 148:110–116. https://doi.org/10.1016/j.solener.2017.03.068

2. Villegas-Guzman P, Giannakis S, Rtimi S et al (2017) A green solar photo-Fenton process for the elimination of bacteria and micropollutants in municipal wastewater treatment using mineral iron and natural organic acids. Appl Catal B 219:538–549. https://doi.org/10.1016/j.apcatb.2017.07.066

3. Alvear-Daza JJ, Sanabria J, Rengifo Herrera JA et al (2018) Simultaneous abatement of organics (2,4-dichlorophenoxyacetic acid) and inactivation of resistant wild and laboratory bacteria strains by photoinduced processes in natural groundwater samples. Sol Energy 171:761–768. https://doi.org/10.1016/j.solener.2018.07.026

4. Ioannou-Ttofa L, Raj S, Prakash H et al (2019) Solar photo-Fenton oxidation for the removal of ampicillin, total cultivable and resistant *E. coli* and ecotoxicity from secondary-treated wastewater effluents. Chem Eng J 355:91–102. https://doi.org/10.1016/j.cej.2018.08.057

5. de la Obra Jiménez I, Giannakis S, Grandjean D et al (2020) Unfolding the action mode of light and homogeneous vs. heterogeneous photo-Fenton in bacteria disinfection and concurrent elimination of micropollutants in urban wastewater, mediated by iron oxides in Raceway Pond Reactors. Appl Catal B 263:118158. https://doi.org/10.1016/j.apcatb.2019.118158

6. Rodríguez-Chueca J, Giannakis S, Marjanovic M et al (2019) Solar-assisted bacterial disinfection and removal of contaminants of emerging concern by Fe2+-activated HSO5- vs. S2O82- in drinking water. Appl Catal B 248:62–72. https://doi.org/10.1016/j.apcatb.2019.02.018

7. Marjanovic M, Giannakis S, Grandjean D et al (2018) Effect of µM Fe addition, mild heat and solar UV on sulfate radical-mediated inactivation of bacteria, viruses, and micropollutant degradation in water. Water Res 140:220–231. https://doi.org/10.1016/j.watres.2018.04.054

8. Rodríguez-Chueca J, García-Cañibano C, Lepistö RJ et al (2019) Intensification of UV-C tertiary treatment: Disinfection and removal of micropollutants by sulfate radical based advanced oxidation processes. J Hazard Mater 372:94–102. https://doi.org/10.1016/j.jhazmat.2018.04.044

9. Matafonova G, Batoev V (2018) Recent advances in application of UV light-emitting diodes for degrading organic pollutants in water through advanced oxidation processes: a review. Water Res 132:177–189. https://doi.org/10.1016/j.watres.2017.12.079

10. López-Vinent N, Cruz-Alcalde A, Malvestiti JA et al (2020) Organic fertilizer as a chelating agent in photo-Fenton at neutral pH with LEDs for agricultural wastewater reuse: micropollutant abatement and bacterial inactivation. Chem Eng J 388:124246. https://doi.org/10.1016/j.cej.2020.124246

11. Calvert JG, Pitts JN Jr (1966) Photochemistry. Wiley, New York

12. Jin S, Mofidi AA, Linden KG (2006) Polychromatic UV fluence measurement using chemical actinometry, biodosimetry, and mathematical techniques. J Environ Eng 132:831–841. https://doi.org/10.1061/(ASCE)0733-9372(2006)132:8(831)

13. Kheyrandish A, Taghipour F, Mohseni M (2018) UV-LED radiation modeling and its applications in UV dose determination for water treatment. J Photochem Photobiol A 352:113–121. https://doi.org/10.1016/j.jphotochem.2017.10.047

14. Keshavarzfathy M, Malayeri AH, Mohseni M et al (2020) UV-LED fluence determination by numerical method for microbial inactivation studies. J Photochem Photobiol A 392:112406. https://doi.org/10.1016/j.jphotochem.2020.112406

15. Popova SA, Matafonova GG, Batoev VB (2019) Removal of organic micropollutants from water by sonophotolytic activated persulfate process. IOP Conf Ser: Mater Sci Eng 687:066051. https://doi.org/10.1088/1757-899X/687/6/066051

16. Beck SE, Ryu H, Boczek LA et al (2017) Evaluating UV-C LED disinfection performance and investigating potential dual-wavelength synergy. Water Res 109:207–216. https://doi.org/10.1016/j.watres.2016.11.024

17. Popova S, Matafonova G, Batoev V (2019) Simultaneous atrazine degradation and *E. coli* inactivation by UV/S2O82-/Fe2+ process under KrCl excilamp (222 nm) irradiation. Ecotoxicol Environ Saf 169:169–177. https://doi.org/10.1016/j.ecoenv.2018.11.014

18. Sánchez-Polo M, Abdel daiem MM, Ocampo-Pérez R et al (2013) Comparative study of the photodegradation of bisphenol A by HO(•), SO4(•-) and CO3(•-)/HCO3 radicals in aqueous phase. Sci Tot Environ 463-464:423–431. https://doi.org/10.1016/j.scitotenv.2013.06.012

19. Moncayo-Lasso A, Mora-Arismendi LE, Rengifo-Herrera JA et al (2012) The detrimental influence of bacteria (*E. coli*, Shigella and Salmonella) on the degradation of organic compounds (and vice versa) in TiO2 photocatalysis and near-neutral photo-Fenton processes under simulated solar light. Photochem Photobiol Sci 11:821–827. https://doi.org/10.1039/c2pp05290c

20. Timchak E, Gitis V (2012) A combined degradation of dyes and inactivation of viruses by UV and UV/H2O2. Chem Eng J 192:164–170. https://doi.org/10.1016/j.cej.2012.03.054

21. Barrera M, Mehrab M, Gilbride KA et al (2012) Photolytic treatment of organic constituents and bacterial pathogens in secondary effluent of synthetic slaughterhouse wastewater. Chem Eng Res Des 90:1335–1350. https://doi.org/10.1016/j.cherd.2011.11.018

22. Subramanian G, Parakh P, Prakash H (2013) Photodegradation of methyl orange and photoinactivation of bacteria by visible light activation of persulfate using a tris(2,2'-bipyridyl)ruthenium (II) complex. Photochem Photobiol Sci 12:456–466. https://doi.org/10.1039/C2PP25316J

23. He J, Zeng X, Lan S et al (2019) Reusable magnetic Ag/Fe, N-TiO2/Fe3O4@SiO2 composite for simultaneous photocatalytic disinfection of *E. coli* and degradation of bisphenol a in sewage under visible light. Chemosphere (2019) 217:869–878. https://doi.org/10.1016/j.chemosphere.2018.11.072

24. Zhou S, Li L, Wu Y et al (2020) UV365 induced elimination of contaminants of emerging concern in the presence of residual nitrite: roles of reactive nitrogen species. Water Res 178:115829. https://doi.org/10.1016/j.watres.2020.115829

25. Wang Z, Zhu K, Chen J et al (2021) Oxone activation by UVA-irradiated FeIII-NTA complex: Efficacy, radicals formation and mechanism on crotamiton degradation. Chem Eng J 408:127324. https://doi.org/10.1016/j.cej.2020.127324

26. Li B, Ma X, Li Q et al (2020) Factor affecting the role of radicals contribution at different wavelengths, degradation pathways and toxicity during UV-LED/chlorine process. Chem Eng J 392:124552. https://doi.org/10.1016/j.cej.2020.124552

27. de la Obra I, Esteban García B, García Sánchez JL et al (2017) Low cost UVA-LED as a radiation source for the photo-Fenton process: a new approach for micropollutant removal from urban wastewater. Photochem Photobiol Sci 16:72–78. https://doi.org/10.1039/c6pp00245e

28. Ferreira LC, Fernandes JR, Rodríguez-Chueca J et al (2020) Photocatalytic degradation of an agro-industrial wastewater model compound using a UV LEDs system: kinetic study. J Environ Manage 269:110740. https://doi.org/10.1016/j.jenvman.2020.110740

29. Malkhasian AYS, Izadifard M, Achari G (2014) Photocatalytic degradation of agricultural antibiotics using a UV-LED light source. J Environ Sci Health B 49:35–40. https://doi.org/10.1080/03601234.2013.836871

30. Xiong P, Hu J (2013) Inactivation/reactivation of antibiotic-resistant bacteria by a novel UVA/LED/TiO2 system. Water Res 47:4547–4555. https://doi.org/10.1016/j.watres.2013.04.056

31. Montenegro-Ayo R, Barrios AC, Mondal I et al (2020) Portable point-of-use photoelectro-catalytic device provides rapid water disinfection. Sci Tot Environ 737:140044. https://doi.org/10.1016/j.scitotenv.2020.140044

Parametric Skeletal 3D Modeling
of an Underground Water Aerator

M. G. Novosjolov and M. Yu. Belkanova$^{(\boxtimes)}$

South Ural State University, 76, Lenin ave, Chelyabinsk 454080, Russia
`belkanovami@susu.ru`

Abstract. The article describes the process of creating a model of an underground water aerator based on the parametric skeletal modeling technology using the Autodesk Inventor Professional software product. An underground water aerator is intended to be used in process schemes for the purification of underground waters from dissolved gases (radon, carbon dioxide, hydrogen sulfide) and the oxidation of dissolved forms of iron and manganese. The model is parameterized using the internal functionality of the program; assembly components have a common coordinate system. The paper proposes a method for creating and optimizing a model range by the criterion of geometric similarity. The 3D model has passed the test for its ability to transform, that is, to take any shape when changing parameters in a given range. Thus, two models of devices are ready for serial production. A set of drawings was created for only one model, while drawings for the second model were obtained automatically. Analysis of the modeling results shows that the optimization problem is a mandatory procedure for parametric modeling of assemblies. Based on the experience gained in modeling, the authors propose a procedure for creating a parametric skeletal model, which can be used for simple assemblies, in particular, for technological equipment for water treatment and water purification. The number of components in the current model is 118.

Keywords: Parametric modeling · Skeletal modeling · Aerator · Autodesk inventor

1 Introduction

Scientific and technological development strategy of the Russian Federation [1] sets the following tasks for the construction industry and science: improving the quality of life of the population, increasing the share of products of new high-tech and knowledge-intensive industries in the gross domestic product, which can be achieved by the transition to digital technologies, new materials and design methods. On the other hand, the development of Building Information Modeling (BIM) technology and 3D modeling in the architecture and construction industry is both a challenge and an opportunity for technological development in Russia. When designing water and wastewater treatment facilities in the BIM concept, the designer's task is to create a library (family) of assembly

components (typical elements, parts and nodes), parametric 3D models of technological equipment and general assembly [2].

Parametric modeling is actively used for parts of mechanisms, and its use in assemblies has some peculiarities. The works [3–6] are devoted to parametric modeling technologies. The modeling object proposed by the authors is a simple assembly and is suitable for learning modeling technologies. The principle of skeletal modeling is reduced to building a model in one coordinate system using the parameters from the parent file. Skeletal 3D modeling is considered in [7–9]. Models created using parametric skeletal modeling technology are good for industrial manufacturing [10] and smart manufacturing [11]. Comparative analysis and capabilities of Autodesk Inventor are analyzed in papers [12–15]. The works [16–18] are devoted to the issues of automation of parametric modeling using Excel, iLogic tables and programming.

The purpose of this paper is to study and apply practically the technology of parametric skeletal 3D modeling of water treatment and water purification equipment, implemented using Autodesk Inventor Professional (AIP) for its use in industrial production. The objective of the study is to apply parametric skeletal modeling technology to create a 3D model of an underground water aerator (UWA), and then create a library component in AIP assemblies [9] or Revit families based on this model.

1.1 Materials and Method

A UWA is intended to be used in process schemes for the purification of underground waters from dissolved gases (radon, carbon dioxide, hydrogen sulfide) [19, 20] and dissolved forms of iron and manganese [21]. When designing a UWA, it is necessary to create a simple structure that is easy to use and install. The UWA's field of application is individual housing construction. The UWA is constructed out of plastic and consists of a column with conical bottom head, cover, water flow divider, bubble aerator, check valves, overflow section and pipes. South Ural State University (national research university) holds a patent for the UWA with the number RU204563U1, which is valid from March 16, 2021.

1.2 Parametric Modeling

Parametric modeling allows automatically modifying the size of the model and reduces design time [3]. The parameterization of the UWA model is carried out to obtain a line of product standard sizes, optimize the model range and reduce the time for the release of drawings. The parameterization of the UWA model and its components is performed using the internal AIP functionality by the method of parametric ranges (parameterization without codes). The classification of parameterization methods is given in [4], and the principle of the parameterization method is outlined in [5].

The main parameters of the model describing the geometry are presented in Table 1. The designer sets the initial parameters V1, d1, d2, d3, t1, t2, and a2 on the basis of technological and hydraulic calculations. The parameters h1, h2, h3, V2, V3, and a1 are calculated by the computer. When the initial data changes, the model recalculates the calculated parameters automatically.

Table 1 Model parameters

Parameter	Units of measurement	Formula	Value	Parameter description
a1	deg	90	90	Opening angle of a bottom cone
V1	m^3	0.4	0.4	Water volume
d1	mm	600	600	Inner diameter of the container
d2	mm	217	217	Conical bottom diameter
t1	mm	5	5	Wall thickness, 5 mm sheet
t2	mm	20	20	Wall thickness, 20 mm sheet
h1	mm	$\frac{4}{\pi} \cdot \frac{V3}{d1^2}$	1319.5	Height of the cylindrical part of the column
h2	mm	$\frac{(d1-d2)}{2}$	191.5	Height of the conical part of the column
h3	mm	h2 + 163	354.5	Height of the supporting structure
V2	m^3	$\frac{\pi \cdot h2}{3}\left(\left(\frac{d2}{2}\right)^2 + \frac{d2 \cdot d1}{4} + \left(\frac{d1}{2}\right)^2\right)$	0.027	Volume of the conical part of the supporting structure (bottom)
V3	m^3	V1–V2	0.373	Volume of the cylindrical part of the column

Figure 1 shows the parametric geometry of the model, which is a cross section of the UWA. One may notice that the solid model is based on a simple theoretical drawing, that is, the 3D model is preceded by a 2D model. This modeling technique allows maintaining the connection between computer modeling and the classical solution to the problem of designing a device.
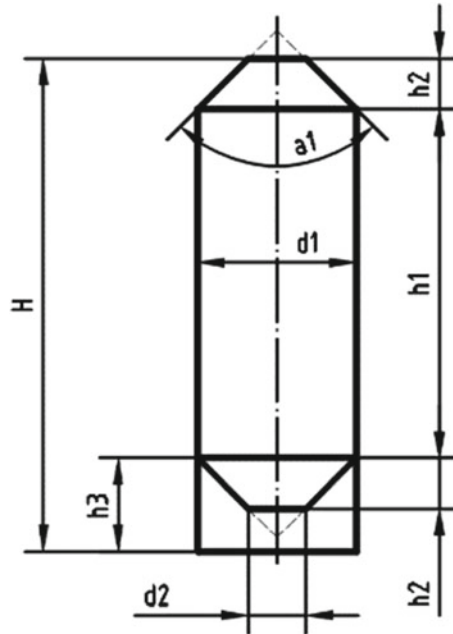
Fig. 1 Parametric model sketch

1.3 Skeletal Modeling

Skeletal modeling is a type of top-down modeling, in which assembly components have a common coordinate system with the skeleton [7, 8]. In the AIP, a skeleton is an Inventor part file (.ipt) that contains a table of user parameters and sketches (other geometry) of the UWA longitudinal section in sectors that coincide with the axes of the nozzles. This is how the geometry of the product is described. Assembly components are derived from skeleton using the Derive tool. The skeleton is created in the general assembly with the Make Layout tool. As a result of modeling, a single-level skeleton in the form of a star is obtained, which defines the structure (skeleton), has the ability to transform the general assembly and, as the author of [7] writes, ensures the survivability of the project as a whole.

1.4 Model Range

It is necessary to have a number of the UWA's standard sizes for the design of typical process water treatment schemes. The creation of a model range is carried out using a parametric table (parameter array). Optimization of the model range is carried out by the method of conditional multivariate optimization. Solving such problems demands much effort. The essence of the problem is to compare models with a reference one and select those models that meet the selection conditions. The reference model is the original one. Thus, several optimal models can be obtained from the array.

The sought models are generated [9] from the reference model by varying the parameters in the intervals d1 (500–600) mm with a step of 50 mm and V1 (300–400) liters with a step of 50 L. In the array of generated models (see Table 2), it is necessary to find the optimal models that satisfy the criterion of geometric similarity to the reference model and the constraint conditions by searching solutions. Let us introduce a criterion for the geometric similarity of the reference and the investigated models as the ratio of the internal volume of the cylindrical part to the internal volume of the conical part of the column: $k = \frac{V3}{V2} = \frac{V3'}{V2'} = const.$

Table 2 Model range

		$V1_j$		
		1	2	3
$d1_i$	1	M_{11}	M_{12}	M_{13}
	2	M_{21}	M_{22}	M_{23}
	3	M_{31}	M_{32}	M_{33}

If the similarity condition is not met, then the physical processes are violated in the model, and the model does not correspond to the reference one. The objective function is the modulus of the difference between the criterion of geometric similarity of the investigated model and the criterion of similarity of the reference model, which is written by the expression: $K_{ij}(d1_i, V1_j) = |k_{ij}(d1_i, V1_j) - k_{11}(d1_1, V1_1)| \to 0.$

The constraint conditions include: overall height dimension H (no more than 2000 mm) and product weight m (must be minimal). In a formalized form, the optimization problem will take the form:

$$M_{ij} \sim \begin{cases} H_{ij}(d1_i, V1_j) \le H \\ m_{ij}(d1_i, V1_j) \to min \\ K_{ij}(d1_i, V1_j) \to 0 \end{cases}$$

$$d1_i \in (a, b), \; i = \overline{1, I}; \; V1_j \in (c, d), \; j = \overline{1, J}$$

1.5 Testing the Model

The 3D model cannot transform, if AIP spits out errors when changing the skeleton's parameters. The creation of a model range and its optimization allows for identification of errors in sketches, connections, dependencies and other inconsistencies. Eliminating the identified errors improves the model. Thus, the skeletal model is checked for its ability to transform without errors.

2   Results and Discussion

It is worth noting that the device is being prepared for serial production under license at a small business enterprise that specializes in plastic processing. Therefore, the model contains only plastic components. Compressor, pump and other equipment are calculated and selected when designing a process scheme for underground water treatment. The modeling result is presented in Fig. 2, which shows a parametric sketch of the model and the completed 3D model. The number of components in the current model is 118; the number of active documents is 91. Components made of plastic sheet materials are converted to sheet metal components and contain flat patterns for shop drawings. Pipes and nozzles are created based on a 3D sketch with parameterization and can be easily transformed with the model. All parts are manufactured on a CNC boring machine from sheet plastic using the computer-aided manufacturing system.
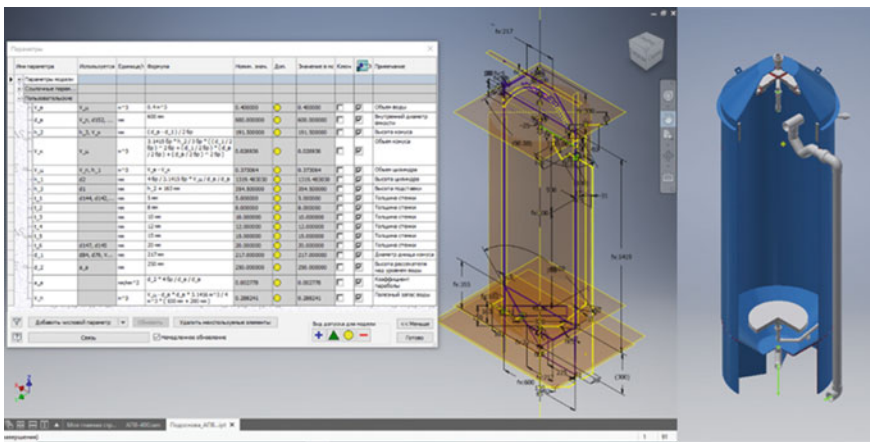
Fig. 2 Parametric skeletal 3D model of the UWA

Table 3 shows the results of generating the model range. The table shows that three models M12, M13 and M23 satisfy the optimization condition (1), and one model M23 satisfies the condition (2).

Let us find the value of the objective function of the M23 model and check it for compliance with the optimization condition (3). $K_{ij} = \left| k_{ij} - k_{11} \right| = |14 - 13, 8| = 0, 2 \approx 0$. The M23 model satisfies all the conditions and is the optimal solution. The model range in a given range of parameters consists of two models − M11 and M23.

The search of the model parameters revealed errors in the sketches of the layout and in the definition of welded joints. Defects in welded joints were eliminated by redefining the welding surface. The following errors were found in the sketches of the layout: when setting the parameter change from a larger value to a smaller one, for example, the inner diameter of the container varies in the range from 600 to 500 mm, there is a "jump" of some dimensions over the base surface in the parametric sketch. Initially, the dimension is laid off below the base surface. Lowering the base surface while decreasing the parameter causes a "jump". However, if the range of parameters is set from a smaller

Table 3 Model parameters values

Model	H, mm	M, kg	V1, m^3	V2, m^3	k = V1/V2
M$_{11}$	2000	27.3	0.373	0.027	13.8
M$_{12}$	1824	25.6	0.323	0.027	12
M$_{13}$	1647	23.9	0.273	0.027	10.1
M$_{21}$	2229	27.5	0.38	0.02	19
M$_{22}$	2018	25.6	0.33	0.02	16.5
M$_{23}$	1808	23.7	0.28	0.02	14
M$_{31}$	2542	28.1	0.385	0.015	25.6
M$_{32}$	2287	25.9	0.33	0.02	16.5
M$_{33}$	2032	23.8	0.285	0.015	19

value to a larger one, that is, using the example of an inner diameter of 500, 550, and 600 mm, then an error in the sketches of the layout does not occur. The defect is easily corrected manually in a parametric sketch. Perhaps the dimension should be set relative to a fixed reference surface. The general view of the reference model M11 is shown in Fig. 3.

The two UWA models are static, meaning that the model parameters will remain unchanged at the end of the modeling. In the practice of designing unique products, it is necessary to adapt the size of the equipment to the external conditions, for example, when creating a layout solution. In such conditions, the parametric modeling method is indispensable, since it allows calculating the best shape and creating a model range.

The final step in the UWA modeling is to create a shrink wrap part using a Shrink Wrap command. This will simplify the model and improve the performance of the computer when working with large assemblies, for example, creating an assembly for a water purification system. Next, using the functions of the BIM Components menu, the simplified model is prepared and exported to Revit MEP. In this way, the UWA models are becoming unified.

3   Conclusions

Parametric skeletal 3D modeling is a complex process that requires a highly skilled engineer. The preparation includes the following stages: development of a parametric sketch of the model (design scheme), assignment of initial and design parameters, interrelationship between parameters and formulas, setting the boundaries for changing parameters, testing a 2D model for its ability to transform without errors. Skeletal modeling of assembly components can be started only after successful testing.

The skeletal model should not contain components and elements that prevent it from freely transforming. For example, joints are best welded at the end of the modeling. The skeletal model should be executed using tools and methods that exclude errors during its transformation. For example, inserting a component and constraining a surface. Testing
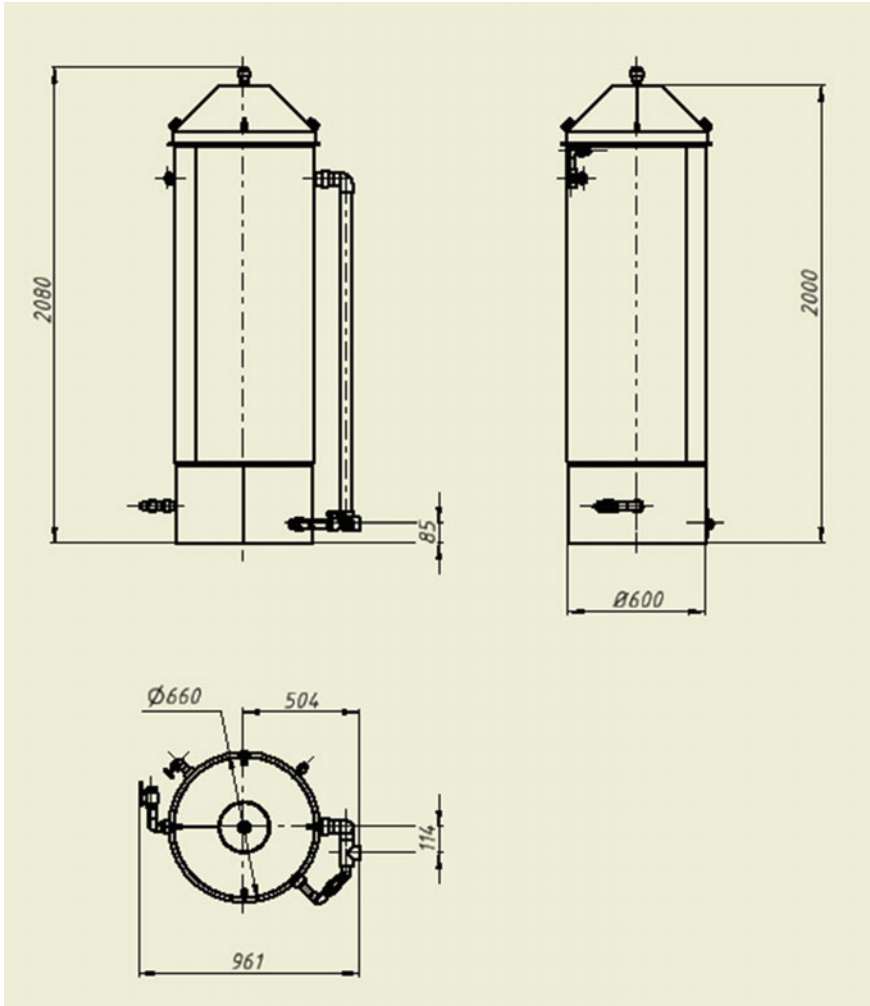
Fig. 3 General view of the UWA

of the 3D model for its ability to transform without errors is required, preferably for each component.

The task of optimizing a model range is a mandatory procedure for debugging a skeletal model, testing the model for its ability to transform. At this stage, it is advisable to conduct a study of the model for its manufacturability (assemblability) and identify the minimum residues when cutting materials.

A set of drawings in the reference model is prepared after determining the optimal parameters and eliminating defects. The model, along with the drawings, is copied and transformed for optimal parameters. Modern design methods significantly reduce the time for preparing drawings. So, as a result of creating one model, 26 sets of working drawings or 33 sheets of A3 and A4 format are formed.

The next level of modeling is the development of parametric 3D skeletal models for large water-purification plants and/or systems. In such assemblies, the parametric sketch can be an equipment layout plan. The skeletal model in such assemblies can be multilevel. Generic components are created as library assemblies.

References

1. Strategy of the scientific and technological development of the russian federation. Approved by the Order of the President of the Russian Federation on 1 December 2016 No. 642
2. Shishkin N, Shchuckin I (2020) Application of BIM technologies in the design of an industrial building. Modern technologies in construction. Theory Practice 1:172–176
3. Petrakova E, Kholmuratov U, Yu B (2019) The functionality of CAD-programs for the development of electronic 3D-model parts according to GOST 2.056–2014. Vestnik MSTU "Stankin" 3:87–91
4. Petrakova E, Samoilova A (2020) Application of iLogic Technology in Autodesk Inventor to create parametric 3D-model of a gear wheel and conduct research. Nauchno-tekhnicheskiyvestnikBryanskogogogosudarstvennogouniversiteta 1:109–119. https://doi.org/10.22281/2413-9920-2020-06-01-109-119
5. Dzhunkovskiy A, Kholodov D, Chikunov I (2019) Usage of autodesk inventor API for automatic parametric modelling of engineering parts. Modern High Technol 9:75–79
6. Borowski G, Jankowska A, Pasnikowska M (2015) Using parametrization of objects in Autodesk Inventor in designing structural connectors. Adv Sci Technol Res J 26:157–160
7. Anan'ev V, Staroverov A (2008) Skeleton modeling or the benefits of second derivatives. CADmaster 5:24–27. http://www.cadmaster.ru/articles/article_17948.html
8. Belokopytov S (2010) Top-down design in AutoCAD Inventor Suite 2010. CADmaster 1:12–20. https://www.cadmaster.ru/magazin/articles/cm_51_02.html
9. Wei L, Xiaobing Z (2017) Towards product design automation based on parameterized standard model with diversiform knowledge. National Engineering Research Center of Die and Mold CAD, Shanghai Jiao Tong University, 200030, China. AIP Conference Proceedings 1829. https://doi.org/10.1063/1.4979734
10. Soonhung H (2020) A review of smart manufacturing reference models based on the skeleton meta-model. J Comput Des Eng 7(3):323–336
11. Jinsang H, Soonhung H, Duhwan M (2009) Representation and propagation of engineering change information in collaborative product 2009 development using a neutral reference model. Concurr Eng 2:147–157. https://doi.org/10.1177/1063293X09105339
12. Yu B, Petrakova E, Rivkin A (2019) Comparative analysis of the functional capabilities of T-FLEX CAD and Autodesk Inventor when creating parametric designs. VESTNIK MSTU "STANKIN" 3:82–86
13. Kharaim M (2016) Three-dimensional modeling CAD Autodesk Inventor aware of engineering draw. In: The collection is based on the materials of the international scientific and practical competition "The best student Article 2016" in Penza, 27–33 May 5, 2016
14. Totalina A, Dolotova R, Dolotov A (2016) Features of solid-state modeling and drawing in Autodesk AutoCAD and Autodesk Inventor. In: Youth and modern information technologies. Proceedings of the XIII International Scientific and Practical Conference of Students, Postgraduates and Young Scientists: in 2 volumes. National Research Tomsk Polytechnic University, Institute of Cybernetics (IC):208–209, 09–13 November 2015
15. Koriagina M, Koriagin V (2018) Modeling assembly units and creating their drawings in the autodesk inventor program environment. CLOUD OF SCIENCE. Moscow Institute of Technology (Moscow) 5(1):60–73

16. D'jakonov N, Janishevskaja A (2017) Methods for automating the design of non-standard metal structures in the petrochemical industry. Magazine young Russia-advanced technologies in industry. Omsk State Tech Univ 2:57–61
17. Bozhenkov V, Kudrytskaya E, Sleptsov D, Litovchenko N (2018) Parametric model mirror offset antenna. Problems of infocommunications. Belarusian State Academy of Communications. Minsk 1(7):77–86
18. Alshakova E (2016) Program realization of the parametrical components of CAD software. In: Informatics and Technologies. Innovative technologies in industry and informatics. Collection of scientific papers of the international scientific and technical conference Moscow Technological University, Institute of Physics and Technology. Tom. Issue 2 (XXII):218–221, 04–06 April 2016
19. Rushnikov A (2015) Effect of aeration on carbon dioxide equilibrium in water. Part 1. Sanitary, Heating, Conditioning 11 (167):32–35
20. Rushnikov A (2016) Effect of aeration on carbon dioxide equilibrium in water. Part 2. Sanitary, Heating, Conditioning 2 (170):30–35
21. SkolubovichJu VE, Skolubovich A, Frolov A (2011) Studies of underground water treatment in an aerator-degasser. Water Purification. Water treatment. Water supply 8:44–47

The Microwave Heating Features of Wastewater and Sludge

A. M. Fugaeva[(✉)], M. V. Obukhova, and E. I. Vialkova

Industrial University of Tyumen, 38, Volodarskogo Street, Tyumen 625000, Russia

Abstract. In connection with the ecological situation deterioration caused by the discharge of insufficiently treated wastewater, a search is underway for the new effective methods of wastewater and sludge treatment. The up-to-date information on the parameters of microwave heating of the wastewater and sludge is presented in the article. The observations of the microwave heating process of the water samples were carried out using a thermal imager. It is noted that water heating by microwaves has a volumetric character; the heating rate is 2.5 times higher than in an oven or on a stove. The dependence of temperature on the microwave heating time of water is revealed. A comparison of two heating types of wastewater sludge is carried out. Because of the experiment, the polynomial equations showing a high degree of research adequacy were obtained. Calculations have shown the energy consumption of sludge convection heating is 1.8 times higher than with microwave processing at equal volumes.

Keywords: Microwave treatment · Wastewater · Sludge · Thermal imager

1 Introduction and Review

Because of the active growth of population and industry, world water consumption is increasing every year. According to published data [1], the 5-top countries consuming the largest amount of water include India (761 billion m^3/year), China (601.6 billion m^3/year), the USA ($\approx$444.3 billion m^3/year), Indonesia ($\approx$222.6 billion m^3/year) and Pakistan ($\approx$183.5 billion m^3/year). Russia also occupies a high position in terms of water consumption (about 80 billion m^3/year), consuming about 2% of all water reserves of the country [2]. At the same time, the environment of modern settlements is becoming more and more polluted. One of the reasons for the deterioration of the environment state is the discharge of untreated or insufficiently treated wastewater (approximately 70% of the total) into water sources. The total amount of wastewater sludge formed at WWPTs is 0.1–0.05% of wastewater volume. In the USA, for example, the annual sludge volume is 7000 million tons, in Russia—up to 100 million tons [3, 4]. The wastewater sludge (raw sediment of primary sedimentation tanks and active sludge of secondary sedimentation tanks) that cannot be disposed of occupying vast areas around cities and towns, disrupting the sanitary and ecological well-being of the territories.

In connection with the above, the search for the best available technologies for efficient and economical wastewater and sludge treatment is relevance. In recent years, more and more research has been carried out on the possibilities of microwave irradiation (MW, microwave) in technologies for liquid and solid municipal waste treatment. The microwave reactors are used as an efficient thermal method for the treatment of wastewater and sludge, mainly due to their rapid and selective heating, energy efficiency, ability to increase productivity and product quality, and reduce the formation of hazardous products [5].

Microwave irradiation (MW) is a part of the electromagnetic spectrum that occurs in the frequency range from 300 MHz to 300 GHz [6]. Microwave energy can be absorbed by the microwave absorbers and is usually dissipated as thermal energy; a process called the microwave thermal effect. In general, microwave energy-conversion mechanisms have three paths: (I) heating with dielectric losses, (II) heating with conduction losses, and (III) heating with magnetic losses.

Microwave heating with dielectric losses (I) is typical for many media, including the aqueous solutions. In this case, the main mechanisms of microwave heating are dipole polarization. Water is a molecule (or dipole) that is positively charged at one end and negatively charged at the other. Dipole polarization occurs due to intermolecular inertia, which is responsible for much of the microwave heating seen in liquids. The rapid change in the microwave electric field causes the water molecules (or dipoles) to rotate. In this case, the rotation rate (reversal) of the dipole cannot adequately correspond to the rate of change in the electric field direction. This is the cause of the "internal friction" of the water molecules, which leads to direct and uniform heating of the reaction mixture. However, the reflections and refractions at the local boundaries between phases lead to the appearance of so-called "hot spots" and the effect of "overheating", which can cause the opposite effects [7–13].

A simplified scheme of the microwave heating mechanism for the polar solvents is shown in Fig. 1 [13]. The scheme shows the change in the polarization of the electric field of the water molecules during the time of sample microwave irradiation.
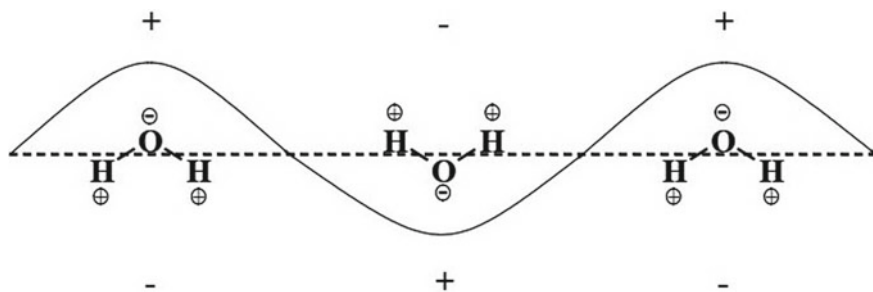

Fig. 1 A simplified scheme of the microwave heating mechanism for the polar solvents

The absorption of microwave energy by the medium depends on the dielectric properties of the heated substance, that is, how much the medium prevents the passage of microwaves through it [14]. A measure of this ability is the relative dielectric constant,

which affects the amount of loss and has a certain value for each substance. For water it is quite high and is equal to 80.08 at the temperature of 20 °C.

Considering the physical meaning of the process, it turned out that MW can provide rapid heating of materials depending on the material's scattering coefficient (or the tangent of the loss angle) or energy loss (ε"), attributed to the dielectric constant (ε') of the material (Eq. 1):

$$D = \tan\delta = \frac{\varepsilon''}{\varepsilon'} \tag{1}$$

The dielectric constant is a relative measure of the density of microwave energy in material or medium, and the dissipation factor (D) takes into account the mechanisms of internal losses, that is, the amount of microwave energy that is lost in the material or medium as heat. Consequently, a material (or medium) with high losses e " is easily heated by MW energy [6]. The scattering coefficient in aqueous solutions depends on the microwave frequency and the viscosity of the reaction medium. The water scattering coefficient decreases with increasing temperature, i.e. the absorption of microwave energy by water deteriorates with increasing temperature. At the same time, the depth of penetration of microwave radiation increases [14].

The decomposition efficiency of the wastewater pollutants and sludge can be influenced the several parameters, such as power, frequency, duration and temperature of microwave treatment. As a rule, the efficiency of a microwave system gradually increases with increasing the microwave power and irradiation time [15].

MW energy causes polarization of the molecules, resulting in electronic vibration, which entails heat release. Therefore, an increase in the power leads to a proportional increase in the reaction temperature. The relationship between the power consumption and the rate of increase in reaction temperature in an MW system is shown in Fig. 2a. In addition, the effect of the MW power on the efficiency of H-acid (Aminonaphthol disulfonic acid) mineralization and petroleum refinery wastewater is shown in Fig. 2b [6]. These two figures demonstrate that increasing the MW power proportionally increases the rate of heating and reaction. Therefore, the processing time required to remove the target pollutant can be reduced by increasing the MW-power.
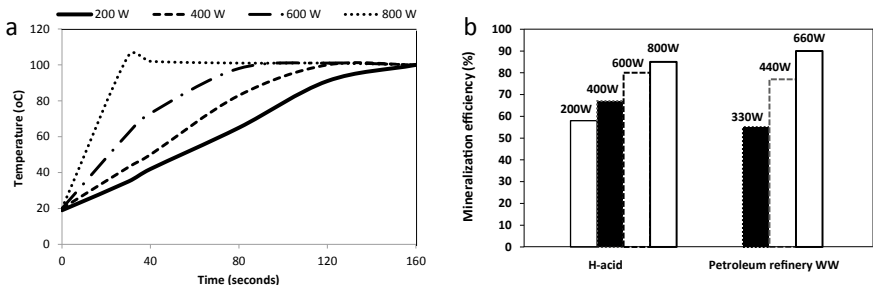

Fig. 2 a influence of the MW treatment time and power on the reaction temperature in the water-system with alternating current; b mineralization efficiency of the Aminonaphthol disulfonic acid (total organic carbon TOC) and petroleum wastewater (chemical oxygen demand COD) [6]

An increase in the time and/or power of MW-irradiation increases the degradation efficiency of the various pollutants in wastewater, for example, the organic substances (in terms of biological oxygen demand BOD and COD), oil products, ammonium, phenols and dyes [6, 13].

In some cases, it has been found that the efficiency of the microwave system decreases at very high temperatures due to the evaporation of water and an increase in the viscosity of the medium. Thus, it is necessary to determine the optimal reaction power and temperature for the decomposition of a particular target pollutant.

It should be noted that currently there is an active analysis of the efficiency of microwave heating for water environments from a technical and economic point of view by comparing it with other methods of heating and processing.

In the article [16, 17], a comparative study was conducted between microwave heating and conventional demulsification during the heating of crude oil. By the experimental results, it was found that microwave dielectric heating obtained a better separation efficiency (100%) in a short time compare with convicting heating. The optimal state for microwave dielectric heating was the irradiation time is 3 min, and the microwave power is 360 W.
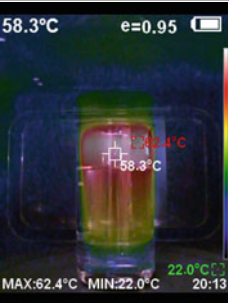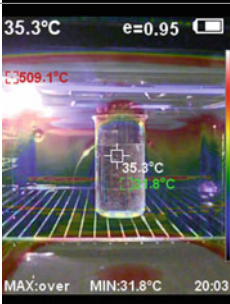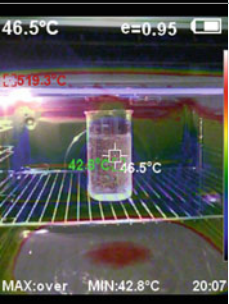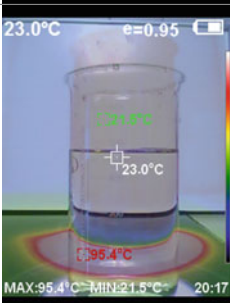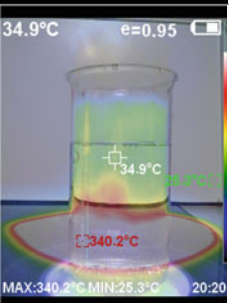
The sewage sludge treatment leads to a change in their properties: the moisture yield, degree and speed of compaction; resistivity and capillary suction. After microwave heating, the metal ions are more easily transfer into the decanting water [18, 19]. After microwave treatment for 5–10 min and subsequent compaction of a domestic sludge mixture (raw sediment of primary sedimentation tanks and active sludge of secondary sedimentation tanks), the release of some metal ions into decanting water (water over sludge) increases by about 1.2–2 times.

Many researchers have noted the disinfecting effect of the microwave. Disinfection of water occurs at a microwave power of 300 W and higher (frequency 2450 MHz) when heated from 45 to 100 °C. The processing time depends on the sample volume and the power of the microwave heating[20, 21]. It is noted that microwave irradiation is capable of destroying the pathogenic bacteria in the wastewater sludge samples in 5–10 min [20, 22]. For example, the research [23] studies an experimental MW-reactor as a possible alternative to rapid sludge treatment. The reactor performance was verified by conducting a series of periodic tests using centrifuged waste activated sludge, non-centrifuged waste activated sludge, fecal sludge, and septic tank sludge. Four kilograms of wastewater sediment of each type were subjected to MW treatment at a power of 3.4 kW for various time periods from 30 to 240 min. It was found that the treatment of MW was successful in achieving complete bacterial inactivation and reducing the weight/volume of the sludge by more than 60%, and a high level of dry matter in the dried sludge was also achieved (up to 98%). In addition, the process produced valuable end products (condensate/water and dry sludge) that can be recovered and reused as fuel and soil fertilizers.

2   Description of Studies

The article authors carried out the field observations of the MW-heating process of the water samples using a thermal imager "Hti". Table 1 shows the results of the photographic records where the water samples, which were heated by different methods, were

Table 1 The photo-fixation results of the water samples heating

Heating conditions	Start moment	End moment
Heating water in a microwave oven for 3 min: temperature interval $\Delta t = 27.4°$ C		
Heating water in an electric oven for 4 min: temperature interval $\Delta t = 11.2°$ C		
Heating water on an electric stove for 3 min: temperature interval $\Delta t = 11.9°$ C		

presented. During heating in a microwave oven, the sample (200 mL) was heated from 30.9 to 58.3 degrees Celsius in three minutes. During heating in an electric oven, the sample (200 mL) was heated from 35.3 to 46.5 degrees Celsius in four minutes. The sample (200 mL) was heated on an electric stove from 23.0 to 34,9 degrees Celsius in three minutes. In the first case, the water heating rate was 9.13 deg/min; in the second case—2.8 deg/min; in the latter—4.97 deg/min.

Analyzing the data obtained was noted that heating by microwaves has a volumetric character. The MW-heating rate is 3.26 times higher than in an oven, and 1.84 times higher than on a stove.

When processed by microwaves, a sample of water in a volume of 200 mL reaches the boiling point in 2.5–8 min; it depends on the MW power. Figure 3 shows a dependence

graphs of the temperature T = f (t) on the time of microwave treatment at a constant power (200, 600 and 1000 W).
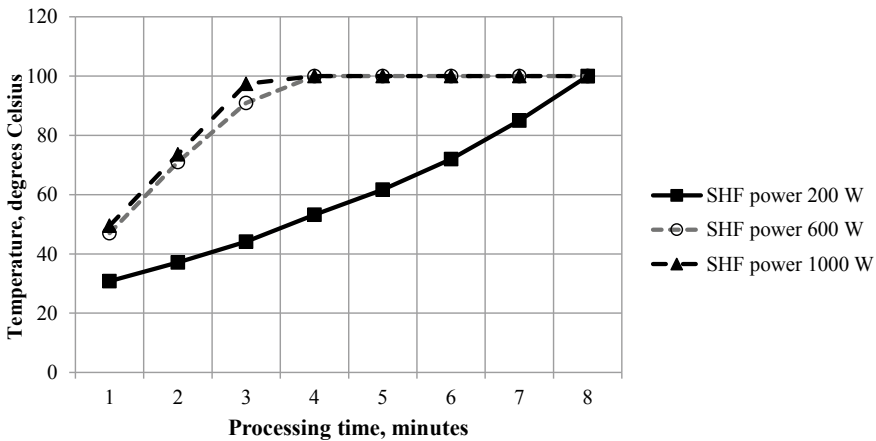
Fig. 3 Dependence of temperature on the processing time of the water samples

In order to compare the two types of sewage sludge heating, the maximum duration of heat treatment of the samples was determined. There are procedure and conditions of the experiment:

- A sampling of the wastewater sludge (a mixture of sludge: raw sludge and activated silt in a ratio of 1: 2, Wastewater Treatment Plant, Tyumen); volume (V) of the samples— 200 mL.
- Measurement of the initial temperature of the samples (+15° C).
- Heating the first sample in an industrial design microwave oven with an installed power (W) of 600 W, the temperature was recorded with a thermometer.
- Heating the second sample on a laboratory electric stove with a power of 600 W. The area of the heating surface of the electric stove was 176.6 cm^2 with a heating element diameter of 15 cm; the area of the bottom of a metal dish was 44.15 cm^2.

In both cases, the heating was carried out until the boiling point of the sample. A thermometer with a graduation value of 0.1 °C recorded the sample temperature.

Based on the measurement results, a summary graph (Fig. 4) of the dependence T = f (t) was built at a constant equal power of the microwave oven and electric stove (W = 600 W).

Next, the specific energy consumption was calculated for simple surface heating and microwave heating of the sludge samples. When calculating the energy consumption with simple surface heating until boiling, a reduction coefficient was taken into account, determined by the ratio of the heat transfer (heating surface) and heat the transfer surfaces (bottom area of metal dishes): 44.15: 176.6 = 0.25.
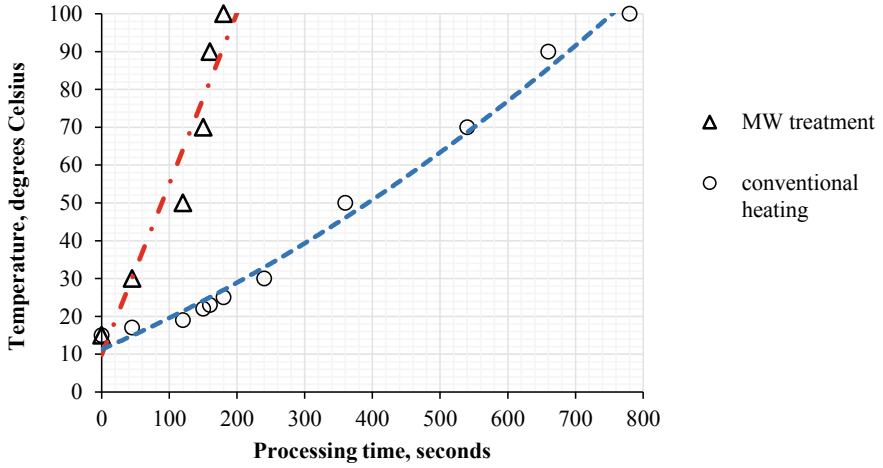
Fig. 4 Dependence of the sludge samples temperature on the processing time

The results of the experimental study and calculations are presented in Table 2. Based on the calculation results, a summary graph (Fig. 5) of the dependence of specific energy consumption (kWh/L) on processing time to boiling (seconds, hours) was built.

Table 2 Results of experimental heating of the wastewater sludge samples

No	Heating time		Temperature (°C)		Specific energy consumption (kWh/L)	
	s	h	MW	electric stove	MW	electric stove
1	0	0	15	15	0	0
2	45	0,013	30	17	0,039	0,016
3	120	0,033	50	19	0,100	0,042
4	150	0,042	70	22	0,125	0,052
5	160	0,044	90	23	0,133	0,056
6	180	0,050	100	25	0,150	0,063
7	240	0,067		30		0,083
8	360	0,100		50		0,125
9	540	0,150		70		0,188
10	660	0,183		90		0,229
11	780	0,217		100		0,271

In the software product Excel, the polynomial equations are obtained that describe the graphs in Fig. 5 with a high degree of adequacy.
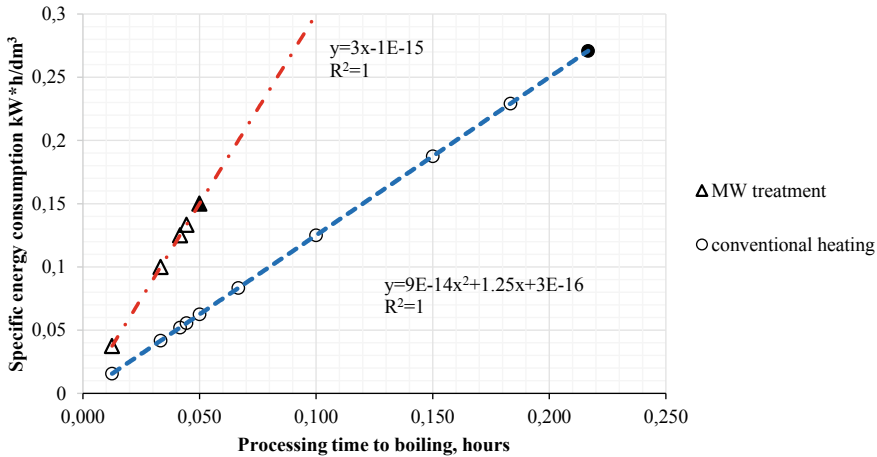
Fig. 5 Specific energy consumption for two types of treatment depending on the heating time

The studies and calculations have shown that the energy consumption of surface electric heating of the sewage sludge mixture is 1.8 times higher than with microwave treatment at the constant volumes and powers. The required boiling point of the wastewater sludge samples during microwave heating is reached 4.3 times faster.

In Russia, there are attempts to create MW-reactors designed for heating water and sewage sludge in order to disinfect them and improve their properties [24–28]. These are portion units of low productivity. These devices need significant improvement in order to gain widespread distribution. For example, the method of the treatment and neutralization of the wastewater and sewerage sediments [27] includes a two-stage sequential exposure to ultrahigh-frequency electromagnetic radiation at a total radiation power of 2.0 kW, a radiation frequency of 2450 MHz, and the treatment is carried out in a flow mode, with the duration of exposure being 4–8 min until the liquid medium temperature reaches 50–85 °C.

3 Conclusion

Thus, the experiences carried out have confirmed the high efficiency of microwave treatment of wastewater and sludge. Based on the above, the following conclusions can be done:

1. Microwave heating has a volumetric character; the heating rate is 3.26–1.84 times higher than in an electric oven or on an electric stove.
2. When processed by microwaves, the water samples in a volume of 200 ml reached the boiling point in 2.5–8 min, depending on the microwave power.
3. The energy consumption of surface electric heating of the wastewater sludge samples is 1.8 times higher than that of microwave processing at a constant volume.

4. The required boiling point of the sludge samples during microwave heating is reached 4.3 times faster than the convection heating method.

Microwave irradiation is a promising method in the current wastewater and sludge treatment technologies. The main advantage is the fast heating, which let to reduce the time for processing liquid municipal wastes, and therefore to decrease the volume of WWTP facilities and equipment. However, problems remain that prevent the widespread application of the method. This is the absence of high-capacity flow-through industrial plants.

References

1. Khetagurova R (2020) The last drop: top 5 countries that consume the most water. https://greenbelarus.info/articles/17-03-2020/poslednyaya-kaplya-top-5-stran-potreb lyayushchih-naibolshee-kolichestvo-vody. Accessed 10 March 2021

2. Adzhienko G (2012) Water Consumption. https://water-rf.ru/Glossary/951/Water Consumption. Accessed 10 March 2021

3. Tikhonova I (2020) Utilization of silt deposits in the economy of a closed cycle—the experience of Germany. http://www.otxod.com/files/materials/article%20silt%20sludge_3004% 20on%20site.pdf. Accessed 10 Mar 2021

4. Nikovskaya G, Kalinichenko K (2014) Biotechnology of utilization of municipal wastewater sediments. Biotechnologia Acta 3:21–32

5. Vialkova E, Zemlyanova M, Danilov O (2018) Energy efficiency in municipal waste treatment. MATEC Web of Conf 170:04020

6. Neelancherry R, Lin J-G (2011) Current status of microwave application in wastewater treatment—a review. Chem Eng J 166:797–813

7. Hidaka H, Saitou A, Honjou H, Hosoda K, Moriya M, Serpone N (2007) Microwave-assisted dechlorination of polychlorobenzenes by hypophosphite anions in aqueous alkaline media in the presence of Pd-loaded active carbon. J Hazard Mater 148:22–28

8. Kappe C (2004) Controlled microwave heating in modern organic synthesis. Angew Chem Int Edit 43:6250–6284

9. Wei R, Wang P, Zhang G, Wang N, Zheng T (2020) Microwave-responsive catalysts for wastewater treatment: a review. Chem Eng J 382:122781

10. Mishra R, Sharma A (2016) Microwave-material interaction phenomena: heating mechanisms, challenges and opportunities in material processing. Compos Pt A Appl Sci Manuf 81:78–97

11. Clark D, Folz D, West J (2000) Processing materials with microwave energy. Mater Sci Eng A-Struct Mater Prop Microstruct Process 287:153–158

12. Horikoshi S, Serpone N (2009) Photochemistry with microwaves: catalysts and environmental applications. J Photochem Photobiol C-Photochem Rev 10:96–110

13. Baghurst D, Mingos D (1992) Superheating Effects associated with microwave dielectric heating. J Chem Soc Chem Commun, 674–677

14. Gabriel C, Gabriel S, Grant E, Halstead B, Mingos D (1998) Dielectric parameters relevant to microwave dielectric heating. Chem Soc Rev 27:213–224

15. Zhang L, Guo X, Yan F, Su M, Li Y (2007) Study of the degradation behavior of dimethoate under microwave irradiation. J Hazard Mater 149:675–679

16. Akbari S, Nour A, Jamari S, Rajabi A (2016) Demulsification of water-in-crude oil emulsion via conventional heating and microwave heating technology in their optimum conditions. Aust J Bas Appl Sci 10(4):66–74

17. Kichigin V, Zemlyanova M, Vyalkova E (2018) Study of the possibility of using microwave radiation for the treatment of liquid municipal waste. Urban Construct Architect 8(1):44–49. https://doi.org/10.17673/Vestnik.2018.01.8
18. Qiang Y et al (2010) Physical and chemical properties of waste-activated sludge after microwave treatment. Water Res 44:2841–2849
19. Wojciechowska E (2005) Application of microwaves for sewage sludge conditioning. Water Res 39:4749–4754
20. Mawioo P, Rweyemamu A, Garcia H, Hooijmans C, Brdjanovic D (2016) Evaluation of a microwave based reactor for the treatment of blackwater sludge. Sci Total Environ 548–549:72–81
21. Mawioo P, Hooijmans C, Garcia H, Brdjanovic D (2016) Microwave treatment of faecal sludge from intensively used toilets in the slums of Nairobi, Kenya. J Environ Manage 184:575–584
22. Karlsson M, Carlsson H, Idebro M, Eek C (2019) Microwave heating as a method to improve sanitation of sewage sludge in wastewater plants. IEEE Access 7:142308–142316
23. Mawioo P, Garcia H, Hooijmans C, Velkushanova K, Simonič M, Mijatović I, Brdjanovic D (2017) A pilot-scale microwave technology for sludge sanitization and drying. Sci Total Environ 601–602:1437–1448
24. Stenanov SF, Ahmedova OO, Soshimov AG (2012) Sewage treatment installation. RU Patent 116851U1, 10 Jun 2012
25. Gunich SV, Malycheva TI (2015) Method of processing of domestic and industrial wastes to furnace fuel and hydrocarbon substance and device to this end. RU Patent 2552259C2, 10 June 2015
26. Levin EV (2016) Installation of microwave processing of sewage sludge. RU Patent 2582415C2, 27 April 2016
27. Zemlyanova MV, Vialkova EI, Obukhov LV (2019) Method for treatment and decontamination of waste water and sediments thereof, and device for method implementing. RU Patent 2693783C1, 7 April 2019
28. Kovalev DA, Kovalev AA, Sobchenko YuA (2019) Method and plant for anaerobic processing of liquid organic wastes. RU Patent 2687415C1, 13 May2019

Change of Liquid Waste Temperature in Open Wastewater Treatment Plants

A. Kruglikova[(✉)]

Novosibirsk State University of Architecture and Civil Engineering (Sibstrin), 113, Leningradskaya str, Novosibirsk 630008, Russia

Abstract. The issues of changing the wastewater temperature are considered. It is established that the wastewater temperature is influenced by climatic parameters, namely, the outside air temperature, wind speed, relative humidity and atmospheric pressure. The studies' results on the open-type site of wastewater treatment plants with 27 thousand m^3/day capacity are presented. The results highlight how much the water temperature changes during the winter and summer periods of the year. Based on the statistical data, obtained during the collection at wastewater treatment plants, a cluster analysis was performed to identify natural groupings in the data set, hypotheses about the equality of the average values of parameters in the obtained clusters were tested, and a step-by-step multi-factor regression model was constructed. The result of the study shows that atmospheric pressure does not affect the extent that it is taken into account, predicting the wastewater temperature for the selected site of wastewater treatment plants. However, the most influential factor was the wastewater temperature, as it was established during the analysis and construction of regression models. Unfortunately, today, designing wastewater treatment plants, the change in the wastewater temperature during its treatment is not taken into account, and the temperature entering the receiving chamber is taken as the calculated one. The obtained models make it possible to predict the temperature and, respectively, give an opportunity to determine the wastewater quality when it changes.

Keywords: Primary tank · Aerotank · Liquid Waste · Temperature · Cleaning quality

1 Introduction

Today, the regulatory document SN 32.13330.2012 "Sewerage, Outdoor networks and construction" is used; calculating wastewater treatment plants (WWTPs), which is recommended the values of the minimum and maximum calculated wastewater temperature be taken as an average for two weeks with the corresponding extreme values for three years of observations. However, this document does not contain any comments on changes in the temperature of wastewater during its treatment in open facilities. And also nowhere does it say anything about the fact that the temperature can also be influenced by climatic factors.

The structures, designed before the release of these recommendations, were designed generally for the average annual temperature of the wastewater that entered receiving chamber.

At the same time, most of the structures are open-type. Considering the main ones: primary sedimentation tanks, aeration tanks and secondary sedimentation tanks, which have large areas of contact between the wastewater and the outside air, it can be assumed that its temperature will change significantly inside.

The aim of the work was primarily to obtain statistical data that confirmed the influence of climatic factors, namely, the influence of outdoor air temperature, wind speed, relative humidity and atmospheric pressure [1, 2] on the change of the wastewater temperature in open-type plants, depending on the seasons of the year [3–6], as well as to obtain regression dependencies after their mathematical processing.

Also, it should be noted that to date, it is the influence of the wastewater temperature on the processes that occur in open primary and secondary tanks, as well as aerotanks, that have been studied and described in some sources [7–15], but the reasons for the change in the wastewater temperature itself are almost nowhere described, which makes this study relevant.

2 Materials and Methods

In order to obtain statistical data, a functioning site of wastewater treatment plants in Iskitim (Novosibirsk region) was selected. These structures belonged to the category of large-capacity structures and were considered as a comparison with the WWTPs Novosibirsk site, since they were located in the same climate zone, but had a different performance. The plants of Iskitim city currently receive wastewater in the amount of 27 thousand m^3/day, and the facilities of Novosibirsk 450 thousand m^3/day. The determination of measurement points and the equipment, used for conducting research, are described in detail in [16, 17]. However, it is worth noting that the measurement points could not be changed during the entire period of data collection. Detailed results, namely the statistical data were obtained at the WWTPs. The search results and their mathematical processing are described in detail in [16]. The statistical package SPSS 17.0 was used for data processing. Since the data was collected at different times of the year, the sample was heterogeneous, and in order to achieve its uniformity, a two-stage cluster analysis procedure was used, at the first stage. Then, using the Student's t-test [18], the hypotheses about the significance of the difference in the average values of the measured parameters in the already homogeneous subsamples were tested. At the last stage, multivariate regression dependencies were constructed [19]. The dependencies were constructed using the step-by-step method, since it was the most acceptable method for selecting factor features. The essence of the step regression method is to implement algorithms for sequential inclusion, exclusion, or inclusion–exclusion of factors in the regression equation, followed by checking their statistical significance.

For the first stage (cluster analysis), the package "Two Step Cluster Analysis" was used [20–22], which could be used to identify natural groupings in the data set. The algorithm, used in this procedure, has several desirable features that distinguish it from traditional clustering methods [23].

It is especially in this package that the algorithm differs from classical clustering in that it can process continuous and categorical variables [24], automatically select the number of clusters and produce scalability.

Both the seasons and the main structures (primary sedimentation tanks, aeration tanks and secondary sedimentation tanks) were used as data. The quantitative indicators, obtained during collection, include the wastewater temperature, the temperature of the outside air, wind speed, relative humidity and atmospheric pressure.

3 Results and Discussion

In the course of conducting a study on the issue of the wastewater temperature change, depending on various climatic factors, 252 measurements were obtained at the selected WWTPs site in three structures over five years.

Consider the warmest day and the coldest one, where significant changes in the wastewater temperature are reflected depending on various climatic factors (Table 1).

According to the data in Table 1, it can be seen that the temperature on the coldest day, decreased by 3 °C, passing through the structures and on the hottest day-by 0.5–0.6 °C. It is clear that in the warm period this is not a significant change, but such a decrease in the winter time will clearly lead to a significant change in the quality of the wastewater.

As it was noted above, since the statistical data were obtained in different periods of the year, the data were first subjected to clustering, which resulted in 3 clusters: cluster 1 (spring), cluster 2 (summer–autumn) and cluster 3 (winter). The breakdown analysis is shown in Table 2.

The analysis of the cluster partition (Table 2) shows a significant decrease in the main meters variation in clusters 1, 3, compared to the general sample. That is, the outdoor air temperature was characterized by the greatest fluctuations, as well as the relative humidity of the air in these seasons of the year.

Then we compared the sample averages in the obtained clusters, using the Student's t-test.

It is worth noting that the comparison was made with the superimposed filters on the structures, where the measurements were made. So, for structures 1, primary sedimentation tanks were taken, for structures 2—aeration tanks, and for structures 3—secondary sedimentation tanks.

After that, we tested the hypotheses about the equality of the parameters' average values in the obtained clusters. Table 3 shows the statistical characteristics of the measured parameter on the WWTPs, and Table 4 shows the testing results of the hypothesis of comparing the average values of the measured parameters in clusters.

The testing results of the hypotheses about the equality of the parameters' average values in the obtained clusters, which are shown in Table 4, indicate that the hypothesis about the average values equality of climatic and technological factors (the temperature of WWTPs wastewater) in the clusters is confirmed with a high degree of reliability. That is, climatic factors equally affect one of the main indicators of the WWTPs—the wastewater temperature in the winter and spring periods.

Table 1 Changes in the wastewater temperature on the warmest and coldest day at WWTPs Iskitim

Measuring point	Measurement time	Outdoor air temperature, °C	Wind speed, m/s	Relative humidity, %	Atmospheric pressure, mmHg	The temperature of the wastewater, °C
Entrance to the primary tank						
First point	10–00	− 33.0– + 23.4	1.0–4.0	69.0–40.0	779.0–755.0	+ 10.5– + 20.2
	12–00	− 25.0–24.6	1.0–5.0	62.0–38.0	779.0–755.0	+ 10.6– + 20.1
	14–00	− 23.0– + 26.0	1.0–6.0	60.0–37.0	779.0–755.0	+ 11.2– + 20.5
Exit from the primary tank						
Second point	10–00	− 33.0– + 23.4	1.0–4.0	69.0–40.0	779.0–755.0	+ 10.4– + 20.3
	12–00	− 25.0–24.6	1.0–5.0	62.0–38.0	779.0–755.0	+ 10.6– + 20.4
	14–00	− 23.0– + 26.0	1.0–6.0	60.0–37.0	779.0–755.0	+ 10.9– + 20.7
Exit from the aerotank						
Third point	10–00	− 33.0– + 23.4	1.0–4.0	69.0–40.0	779.0–755.0	+ 9.2– + 21.1
	12–00	− 25.0–24.6	1.0–5.0	62.0–38.0	779.0–755.0	+ 9.6– + 21.0
	14–00	− 23.0– + 26.0	1.0–6.0	60.0–37.0	779.0–755.0	+ 9.9– + 21.3
Exit from the secondary tank						
Fourth point	10–00	− 33.0– + 23.4	1.0–4.0	69.0–40.0	779.0–755.0	+ 7.5– + 20.9
	12–00	− 25.0–24.6	1.0–5.0	62.0–38.0	779.0–755.0	+ 7.9– + 20.7
	14–00	− 23.0– + 26.0	1.0–6.0	60.0–37.0	779.0–755.0	+ 8.4– + 21.0

The climatic factors influence one of the main parameters of the WWTPs—the wastewater temperature—was studied by constructing multivariate regression models. Models were built for each selected cluster of observations, as well as for the entire set of measurement data (the total sample).

Table 2 Statistical characteristics of the resulting clusters

Cluster	Number of observations	Outdoor air temperature, °C		Relative humidity, %		Wind speed, m/s		Atmospheric pressure, mmHg		The temperature of the wastewater, °C	
		μ	σ	μ	σ	μ	σ	μ	σ	μ	σ
1	108	6.60	7.92	64.25	19.25	3.65	1.95	753.22	7.03	13.66	2.18
2	63	6.50	14.33	73.33	17.20	2.52	1.86	753.48	9.55	17.09	4.03
3	81	− 17.10	7.67	72.85	9.04	1.44	1.14	768.26	8.89	10.50	1.72
General selection	252	− 1.04	14.79	69.30	16.62	2.66	1.95	758.12	10.85	13.50	3.62

Note μ—average, σ—mean square deviation

Table 3 Statistical characteristics of the measured parameters in clusters

Parameters	Type of structure	Number of observations	μ	σ
Outdoor air temperature, °C	1	84	13.8750	3.05700
	2	84	13.5738	3.59726
Outdoor air temperature, °C	1	84	13.8750	3.05700
	3	84	13.0488	4.12721
Outdoor air temperature, °C	2	84	13.5738	3.59726
	3	84	13.0488	4.12721

An important step in constructing the multiple regression equation is the selection and subsequent inclusion of factor features in it. The problem of selecting factor features for constructing relationship models can be solved on the basis of intuitive-logical or multidimensional mathematical-statistical methods of analysis.

The most acceptable method for selecting factor features is step-by-step regression (step-by-step regression analysis). The essence of the step regression method is to implement algorithms for sequential inclusion, exclusion, or inclusion–exclusion of factors in the regression equation, followed by checking their statistical significance. Table 5 shows the construction of the model in 3 steps.

The model is quite high-quality. It explains, as it can be seen from the Table, 4,75% of the variation in the wastewater temperature is due to the inclusion of climatic factors. In this case, the standard error of the model does not exceed 1.81 °C. Although the error is quite large, but given its error, it is significantly reduced. As a result, it can reliably predict temperature fluctuations with fluctuations in the values of climatic factors.

The construction of a stepwise multivariate regression model of the WWTPs wastewater temperature for the total sample is shown in Table 6.

The resulting linear multivariate regression model will look like this:

$$y = 0.942 \cdot T_{outsideair} - 0.155 \cdot v + 0.087 \cdot \varphi \tag{1}$$

where

$T_{outsideair}$ outdoor air temperature, $^{\circ}$C;
v wind speed, m/s;
φ relative humidity, %.

Table 6 shows that the most influential factor is the outdoor temperature, which is estimated by standardized (dimensionless) parameters of the model.

The resulting clusters were analyzed, namely the cluster "spring", "summer–autumn" and "winter", According to the same algorithm for processing the obtained statistical data.

In cluster 1 "spring", a review of the accuracy characteristics and their comparison with the accuracy characteristics of the model, based on the general sample of observations showed that, the difference is that the coefficient of determination is high, and

Table 4 Testing the hypothesis of the average values equality of the measured parameters in clusters under different assumptions about the equality of variances

Parameter	Type of structure	Verification condition	Variance comparison test		t—criterion for equality of averages	
			F-criterion	Significance level	t-criterion	Number of degrees of freedom
Temperature of the wastewater, °C	1	The variances are equal	1.359	0.245	0.585	166.000
	2	The variances are equal	–	–	0.585	161.790
Temperature of the liquid waste, °C	1	The variances are equal	4.061	0.046	1.474	166.000
	3	The variances are equal	–	–	1.474	153.002
Temperature of the wastewater, °C	2	The variances are equal	0.809	0.370	0.879	166.000
	3	The variances are equal	–	–	0.879	162.961

Parameter	Type of structure	t—criterion for equality of averages			95% confidence bounds for the difference	
		Significance level	Average difference	Standard error of the difference	lower	upper
Temperature of the wastewater, °C	1	0.560	0.30119	0.51508	− 0.71576	1.31814
	2	0.560	0.30119	0.51508	− 0.71595	1.31833
Temperature of the wastewater, °C	1	0.142	0.82619	0.56039	− 0.28022	1.93260
	3	0.142	0.82619	0.56039	− 0.28091	1.93329
Temperature of the wastewater, °C	2	0.381	0.52500	0.59736	− 0.65440	1.70440
	3	0.381	0.52500	0.59736	− 0.65456	1.70456

Table 5 Changes in the accuracy characteristics of the step regression model for the total sample

Modeling step	R^2	Adjusted R^2	Standard regression error	Changing statistics		
				R^2	Fischer's criterion F	Significance F
1	0.727	0.726	1.8958	0.727	666.179	0.000
2	0.747	0.745	1.8289	0.020	19.642	0.000
3	0.753	0.750	1.8124	0.006	5.529	0.019

Note: R^2– coefficient of determination

Table 6 Stepwise multivariate regression model of the WWTPs wastewater temperature

Step	Model Parameters	Model coefficient (not standardized)		Model coefficient (standardized)	t-Student	Significance
		B	Standard error	Beta		
1	Free member	13.176	0.120	–	114.569	0.000
	Outdoor air temperature, °C	0.209	0.008	0.853	25.810	0.000
2	Free member	14.456	0.203	–	71.218	0.000
	Outdoor air temperature, °C	0.219	0.008	0.895	26.900	0.000
	Wind speed, m/s	− 0.274	0.062	− 0.174	− 4.432	0.000
3	Free member	13.189	0.575	–	22.929	0.000
	Outdoor air temperature, °C	0.231	0.009	0.942	24.432	0.000
	Wind speed, m/s	− 0.288	0.020	− 0.155	− 4.672	0.000
	Relative humidity, %	0.019	0.008	0.087	2.351	0.019

the standard error of the regression has significantly decreased unlike the model of the general sample. The model was built in 4 steps (formula 2):

$$y = 1.130 \cdot T_{outsideair} + 0.204 \cdot v + 0.139 \cdot \varphi + 0.166 \cdot D \qquad (2)$$

where D is the measurement date.

In this case, the wastewater temperature began to depend on another parameter, namely, the measurement date. The measurement date is a quantitative variable; it is determined by the converting method of the date from the format "DD. MM. YY." to the numeric format.

For cluster 2 "summer–autumn", the regression model was built in 3 steps, as was the general sample model. The model is presented according to the formula 3:

$$y = 0.704 \cdot T_{outsideair} - 0.083 \cdot v - 0.300 \cdot D \tag{3}$$

In order to build a model for cluster 3 "winter", it took two steps, the equation is given by formula 4:

$$y = 0.460 \cdot T_{outsideair} + 0.279 \cdot \varphi \tag{4}$$

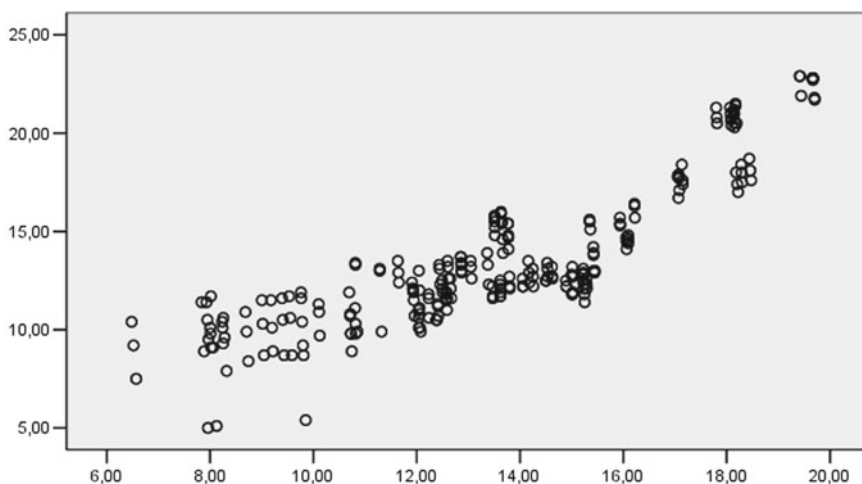Figure 1 shows the scattering diagram for the general sample model.

Fig. 1 Scatter plot for a general sample model with a dependent variable (wastewater temperature)

4 Conclusion

After mathematical processing of the obtained statistical data, it was found that the climatic parameters, namely the outdoor temperature, relative humidity and wind speed, have a significant influence on the wastewater temperature.

It is worth noting that during the data collection, atmospheric pressure was also recorded, but as a result, it was found that it was not a wag factor at the selected WWTPs site.

The obtained mathematical dependencies can be used as a recommendation for the calculation of structures at the design stage of new WWTPs, and the reconstruction of existing structures for the possibility of taking into account climatic parameters. In addition, the regression equations will be used in the software package that is being developed to calculate sewage treatment plants at the design, reconstruction and operation stages, taking into account the influence of climatic factors.

References

1. Khalkhali M, Mo W (2020) The energy implication of climate change on urban wastewater systems. J of Cleaner Production 267:121–905

2. Bayo J, Olmos S, López-Castellanos J (2020) Microplastics in an urban wastewater treatment plant: the influence of physicochemical parameters and environmental factors. J Chemosphere 238:124–593

3. Zakkour PD, Gaterell MR, Griffin P (2001) Anaerobic treatment of domestic wastewater in temperate climates: treatment plant modelling with economic considerations. J Water Research 35:4137–4149

4. Abdulla F, Farahat S (2020) Impact of climate change on the performance of wastewater treatment plant. case study central irbid WWTP (Jordan). J Procedia Manufacturing 44:205–212

5. Wang X, Kvaal K, Ratnaweera H (2017) Characterization of influent wastewater with periodic variation and snow melting effect in cold climate area. J Computers & Chemical Engineering 106:202–211

6. Langeveld JD, Schilperoort PRS, Weijers SR (2013) Climate change and urban wastewater infrastructure: there is more to explore. J of Hydrology 476:112–119

7. E'L' MA, E'L' YaF, Veber IF (1977) Naladka i ekspluataciya ochistnyh sooruzhenij gorodskoj kanalizacii (Commissioning and operation of municipal sewage treatment plants). Stroyizdat, Moscow

8. Evilevich MA, Braginsky LN (1979) Optimizaciya biohimicheskoj ochistki stochnyh vod (Optimization of biochemical wastewater treatment). Stroyizdat, Leningrad

9. YaM L, YaV V, Kalitsun VI (1987) Primery raschetov kanalizacionnyh sooruzhenij: uchebnoe posobie dlya vuzov (Examples of calculations of sewer structures: textbook for universities). Stroyizdat, Moscow

10. Kolobanov SK, Ershov AV, Kigel ME (1977) Proektirovanie ochistnyh sooruzhenij kanalizacii (Design of sewage treatment plants). Builder, Kiev

11. Bolotina OT, Bolkhovitinova MN, YaP B (1977) Metodika tekhnologicheskogo kontrolya raboty ochistnyh sooruzhenij gorodskoj kanalizacii (Methods of technological control of the work of municipal sewage treatment plants). Stroyizdat, Moscow

12. Naidenko VV, Kulakova AP, Sherenkov IA (1984) Optimizaciya processov ochistki prirodnyh i stochnyh vod (Optimization of natural and waste water treatment processes). Stroyizdat, Moscow

13. Shelomkov AS, Shelomkov SA (2014) Rukovodstvo po proektirovaniyu kanalizacionnyh ochistnyh sooruzhenij gorodskih stochnyh vod i blizkih k nim po sostavu stochnyh vod promyshlennyh predpriyatij (Guidelines for the design of sewage treatment plants of urban wastewater and industrial enterprises close to them in terms of the composition of wastewater). Mosvodokanalniiproject, Moscow

14. Stephan K (2005) Bemessungsregelnfür Nachklärbecken. WWT: Wasserwirt. Wassertechn.: Das raxismagazin für Entscheidungen im Wassermanagement 2:22–24

15. Bartova LV, Avdeeva MA, JaS L (2018) Opredelenie prodolzhitel'nosti obrabotki stochnyh vod v aerotenkah po razlichnym metodikam (Determination of the duration of wastewater treatment in aerotanks by different methods). PNRPU Bull Construction Architecture 9(3):99–107. https://doi.org/10.15593/2224-9826/2018.3.10

16. Kruglikova AV (2019) Sovershenstvovanie ucheta vliyaniya prirodnyh faktorov pri ekspluatacii ochistnyh sooruzhenij kanalizacii (Improvement of accounting for the influence of natural factors in the operation of wastewater treatment plants) News of Higher Educational institutions. Construction 12:56–63. https://doi.org/10.32683/0536-1052-2019-732-12-56-63

17. Kruglikova AV (2020) Vliyanie klimata na rabotu ochistnyh sooruzhenij kanalizacii g. Novosibirska (Influence of climate on the operation of sewage treatment facilities in Novosibirsk). Water Ecol 2(82):37–44
18. Zaks L (1976) Statisticheskoe ocenivanie (Statistical evaluation). Statistics, Moscow
19. Zhang X, Tian Y, Zhang X, Bai M, Zhang Z (2019) Use of multiple regression models for predicting the formation of bromoform and dibromochloromethane during ballast water treatment based on an advanced oxidation process. J Environmental Pollution 254 (Part A)
20. Ayvazyan SA, Mkhitaryan VS (1998) Prikladnaya statistika i osnovy ekonometriki: uchebnik dlya studentov ekonomicheskih special'nostej vuzo (Applied statistics and fundamentals of Econometrics: textbook for students of economic specialties of universities). UNITY, Moscow
21. Durand B, Odell P (1977) Klasternyj analiz (Klasternyj analiz). Statistics, Moscow
22. Gitis LH (2003) Statisticheskaya klassifikaciya i klasternyj analiz (Statistical classification and cluster analysis). Moscow State University, Moscow
23. Newhart KB, Holloway RW, Hering AS, Cath TY (2019) Data-driven performance analyses of wastewater treatment plants: a review. J Water Research 157:498–513. https://doi.org/10.1016/j.watres.2019.03.030
24. Newhart KB, Holloway RW, Hering AS, Cath TY (2019) Data-driven performance analyses of wastewater treatment plants. J Water Research 157:498–513

Experimental Research About Ceftriaxone Interaction with Metal Ions Cu, Ni, Pb in Model Solutions

A. Abramova[✉]

Kalashnikov Izhevsk State Technical University, Studencheskaya 7, Izhevsk 426069, Russia

Abstract. This article presents the results of interaction between antibiotic ceftriaxone with metals (Cu, Ni, Pb).Obtained levels of optical density and absorption lengths of solutions of antibiotics with metals can be used in the development of a method for detecting antibiotics in urban wastewater. Received levels of the optical density and absorption lengths of antibiotic's solutions with metals can be used for development of a method for detecting antibiotics in urban wastewater, and it means that it will be possible to solve an important task of the existing sewage treatment facilities—to assess the effectiveness of treatment and develop a set of measures for more effective antibiotics removal from wastewater. The relevance of researches about antibiotics in wastewater is indirectly confirmed by the fact that from 2000 to 2020 the number of scientific articles with the topic "antibiotics in wastewater" increased by almost 70 times (according to a leading discovery platform ScienceDirect). Article's analysis showed that cephalosporin antibiotics (cefotaxime, cefuroxime, ceftriaxone, etc.) are most often found in wastewater. According to the shift of the optical density peak of the antibiotic solution with copper (A = 0.06 at λ = 278) compared to the model copper solution (A = 0.023 at λ = 308 nm), it can be concluded that a complex compound of copper and ceftriaxone is formed. Therefore, it is possible to use its interaction with the specified metal for antibiotic'sdetection in waste water.

Keywords: Antibiotic · Ceftriaxone · Waste water · Optical density

1 Introduction

Nowadays there is an increase of water bodies' pollution by pharmaceuticals, including antibiotics. It happens due to increase of drugs consumption and their ineffective disposal at sewage treatment plants. Between 2000 and 2015, antibiotic consumption increased 39% in low- and middle-income countries and 4% in high-income countries, according to research by a team of scientists from the United States, Switzerland, Sweden and Belgium [1]. Authors characterized the dynamics of antibiotic consumption in the Russian Federation over 15 years, and received an increasing of 18–20 specific daily doses of antibiotics per 1000 people. They also predicted a 15% increase of global antibiotic usage if current antibiotic use remains unchanged.

The relevance of researches about antibiotics in wastewater is indirectly confirmed by the fact that from 2000 to 2020 the number of scientific articles with the topic "antibiotics in wastewater" increased by almost 70 times (according to a leading discovery platform ScienceDirect) (Fig. 1). Article's analysis showed that cephalosporin antibiotics (cefotaxime, cefuroxime, ceftriaxone, etc.) are most often found in wastewater [2–27]. There are 104 publications in Russian Science Citation Index with keywords "antibiotics, wastewater", and 19 from them since 2019. And it is not correct to compare the international systems that reflect the articles of many countries with the RSCI, which includes only domestic scientists and scientists from the CIS countries.
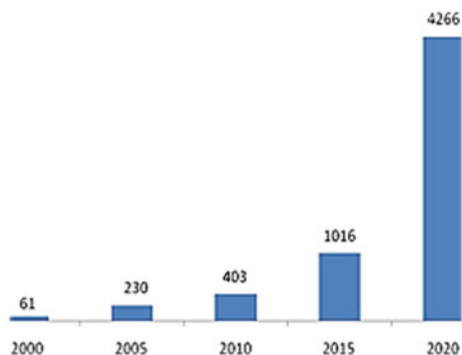

Fig. 1 Number of scientific researches about «antibiotics in wastewater», units (according to https://www.sciencedirect.com/)

However, domestic scientist's studies about assessment the content of antibiotics in wastewater were held only at two largest cities in Russia–Moscow and St. Petersburg, that leads to the conclusion that in other cities, due to the smaller number of residents, antibiotics were not found in wastewater, or similar studies were not carried out in other cities of Russia [28–44]. This determines the relevance of detecting antibiotics in the wastewater of our country. Since urban wastewater is multicomponent, it is proposed to develop a method for their detection according to their interaction with metals.

The main task of this article is to do an experimental research about identifying the interaction and formation of complex compounds of ceftriaxone with metals (copper, nickel, lead).

2 Theoreticalbasis

The antibiotic ceftriaxone was chosen as the object of research, since it belongs to one of the most important and representative groups among modern antibiotics—third-generation cephalosporin [45]. This antibiotic is an almost white or yellowish crystalline powder. It is easily soluble in water. Ceftriaxone has a broad range of action. But, unfortunately, from the point of view of chemistry, this type of antibiotic remains insufficiently explored. The structural formula of the antibiotic is shown in Fig. 2. According to previous studies, ceftriaxone forms complex compounds with copper (Cu), palladium (Pd),

vanadium monoxide (VO) (Table 1). In the article [46], it is shown the effect of pH (2, 3, 4, 5) and temperature (30, 40, 50 and 60^0C) on the kinetics of ceftriaxone hydrolysis in the presence of cations Cu^{2+}иVO^{2+}. It was found that both cations form ML complexes with antibiotics. All complexes have approximately the same stability (Table 1). It is shown that complexation accelerates the hydrolysis of antibiotics, while Cu^{2+} and VO^{2+} have the same catalytic effect. It is suggested that the complex is formed due to the coordination of betalactam (OF atom) and deprotonated amide (N atom) groups. However, the conclusion about the dissociation of the amide proton in a slightly acidic environment is rather doubtful, because a similar process in dipeptides occurs only at pH >8.
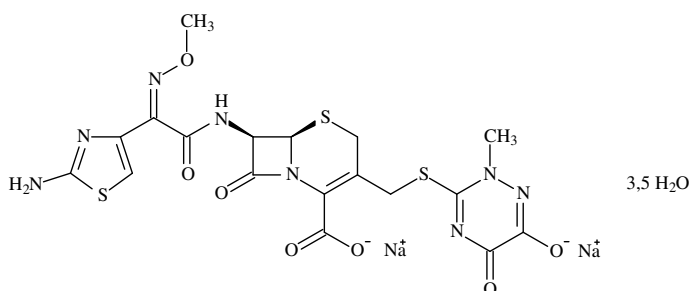

Fig. 2 Structural formula of ceftriaxone

Table 1 Formation constants of ceftriaxone metal complexes

Antibiotic	Complex	lgβ	Certainconditions $^°$C	Article
Ceftriaxone	CuL	2,5	30	30
	(VO)L	2,5	30	30
	Pd$_2$L	6,06	25, spectrophotometry	31

Also, solid complexes of ceftriaxone with Mn (II), Co (II), Cu (II), Cd (II) of composition ML (L2- is the anion of ceftriaxone) and the iron complex FeLCl were studied earlier. Complexes are insoluble in water, methanol, diethyl ether, pyridine and acetone. It is obvious that they have a polymer structure. The composition of the complexes was determined by the method of elemental analysis. Microbiological studies have shown that the Cd (II) complex is more effective than ceftriaxone. The activity of the remaining complexes is at the level of disodium salt ceftriaxone [47].

To determine the convergence of the research findings, we will carry out a spectrophotometric measurement of the optical density of antibiotic solution with different metals: copper, nickel, lead.

3 Materials and Methods

All experimental studies were carried out on a spectrophotometer PE-5400 UV, which is designed to measure the optical density of liquids and the transmittance in order to determine the components dissolved in them [46].

Research of interaction between ceftriaxone in a model solution with metals and the possibility of complex compounds formation with them has three stages:

- optical density determination of the metal solution with distilled water with $\lambda = 260–330$ nm
- determination of the optical density of ceftriaxone with metals at a wavelength $\lambda = 260–330$ nm
- make a calibration graph to determine the concentration of metal complexes of ceftriaxone in solution with $\lambda = 278$ nm.

A model solution of an antibiotic with a concentration of $C = 102$ mg/l followed by dilution to the coefficient $K_p = 100$, $K_p = 1000$, $K_p = 10\,000$, and standard metal samples with a concentration of $C = 10$ mg/l and $C = 100$ mg/l were prepared to carry out these tests. According to the displacement of the optical density peak of two solutions (1 solution—a metal solution in distilled water, 2—a solution of an antibiotic with a metal at different concentrations), it can be concluded that metal complexes of ceftriaxone are formed.

4 Results

To measure the optical density of a model copper (Cu) solution, 0.1 ml of a standard Cu solution with a concentration of 10 mg/L was taken. The results of measuring the optical density of the Cu solution with a concentration of 0.001 mg/L are shown in Fig. 3. The maximum optical density was obtained at $\lambda = 308$ nm and is equal to A = 0.023.

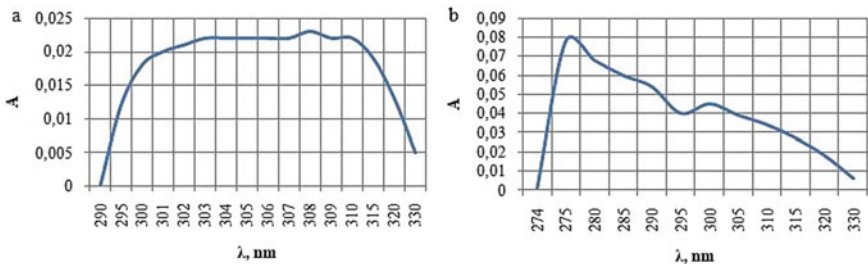**Fig. 3** **a** Optical density of a model copper solution with a concentration of $C = 0.001$ mg/l; **b** optical density of a model copper solution with ceftriaxone with its concentration of $C = 0.102$ mg/l and a ratio 1: 1

To confirm the formation of ceftriaxone complex with Cu, 3 solutions were prepared (solution of antibiotic and Cu with a concentration of 0.102 mg/l, 0.0120 mg/l, 1 mg/l
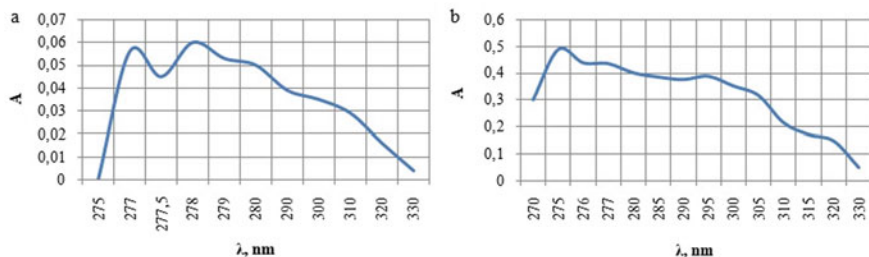
Fig. 4 **a** Optical density of a model copper solution with ceftriaxone with its concentration of C = 0,0102 mg/l and a ratio 1: 1; **b** optical density of a model copper solution with ceftriaxone with its concentration of C = 1 mg / l and a ratio 1: 1

with a ratio of 1: 1) and their spectrophotometric study was carried out at $\lambda = 270$–330 nm. The maximum optical density was obtained at $\lambda = 278$ nm and is equal to A = 0.06. Measurement results are shown in Figs. 3–4.

The shift of the optical density peak in Fig. 3–4 in comparison with the model copper solution (Fig. 3) indicates the formation of a complex compound of copper and ceftriaxone. To detect an antibiotic in waste water, it is possible to use its interaction with the specified metal. To make a calibration graph, 4 solutions of ceftriaxone with copper were prepared with a concentration $C = 0.01$ mg/l, 0.02 mg/l, 0.025 mg / l, 0,05 mg/l with a ratio 1:1. Measurement of solution's optical density was carried out with $\lambda = 278$ nm. The resulting calibration graphis shown in Fig. 5.
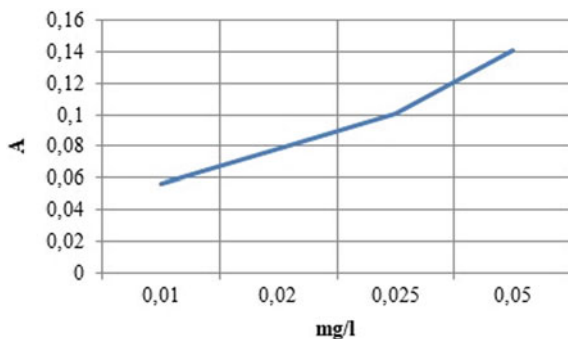
Fig. 5 Calibration graph of a copper solution with ceftriaxone at $\lambda = 278$ nm

To measure the optical density of the nickel (Ni) model solution, 0.1 ml of a standard Ni solution with a concentration of 10 mg / l was taken. The results of measuring the optical density of received Ni solution with a concentration of 0.001 mg / l are shown in Fig. 5. The maximum optical density was obtained at $\lambda = 307$ nm and is equal A = 0.022. To confirm the formation of ceftriaxone complexes with Ni, 3 solutions were prepared (solution of antibiotic and Ni with a concentration of 0.001 mg/1, with a ratio 1:2, 1:3, 1:4) and spectrophotometric research was carried out at $\lambda = 270$–330 nm. The

maximum optical density was obtained at $\lambda = 307$ nm and is equal $A = 0.051$, $A = 0.081$, $A = 0.11$. The measurement results are shown in the Figs. 6–7.

Fig. 6 **a** Optical density of a nickel model solution with a concentration of $C = 0.001$ mg / l; **b** optical density of a nickel model solution with ceftriaxone with a concentration of $C = 0,001$ mg/l and a ratio 1:2

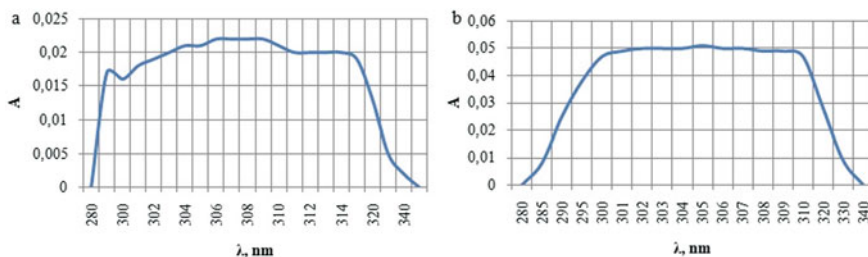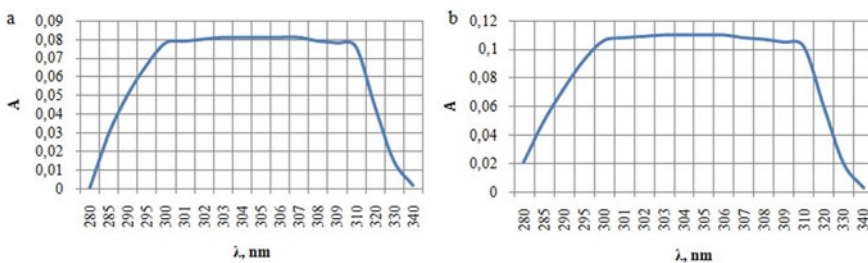**Fig. 7** **a** Optical density of a nickel model solution with ceftriaxone with a concentration of $C = 0,001$ mg/land a ratio 1:3; **b** optical density of a nickel model solution with ceftriaxone with a concentration of $C = 0,.01$ mg/l and a ratio 1:4

Figures 6 and 7 show that the optical density peak did not shift when a standard nickel solution with a concentration of 0.001 mg / l was added to the antibiotic solution. So, ceftriaxone does not form metal complexes with nickel.

To check the ability of ceftriaxone to form stable compounds with lead (Pb), 0.1 ml of a standard Pb solution with a concentration of 10 mg / l was taken. The results of measuring the optical density of received Pb solution with a concentration of 0.001 mg/l are shown in Fig. 8. The maximum optical density was obtained at $\lambda = 307$ nm and is equal A = 0.023.

To confirm the formation of ceftriaxone complexes with *Pb,*solution was prepared (solution of antibiotic and Pb with a concentration of 0.001 mg / l with a ratio of 1: 1) and spectrophotometric research was carried out at $\lambda = 270$–330 nm. The maximum optica ldensity was obtained at $\lambda = 307$ nm and is equal A = 0,025. Measurement resultsare shown in Fig. 8.

Figures 8 show that that the optical density peak did not shift when a standard lead solution with a concentration of 0,001 mg/l was added to the antibiotic solution. So, ceftriaxone does not form metal complexes with lead.
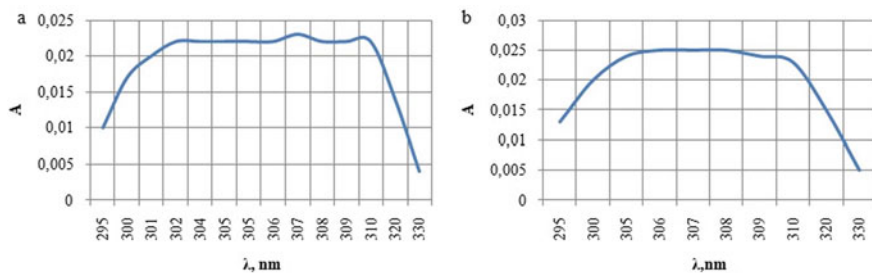
Fig. 8 a Optical density of a lead model solution with a concentration of C = 0.001 mg/l; **b** Optical density of a lead model solution with ceftriaxone with a concentration of C = 0,001 mg/l and a ratio 1:1

5 Conclusions

According tothe experimental researchofceftriaxone's interaction in a model solution with metal ions, it can be noted, that ceftriaxone can form stable complex compounds with copper, but it is impossible to make an unambiguous conclusion about the formation of metal-antibiotic complexes with nickel and lead. It is necessary to make a number of additional testsfor an accurate result. But it is possible to suggest that formation of complexes can happen in a non-aqueous environment. For example, the results of formation solid ceftriaxone complexes with *Mn* (II), *Co* (II), *Cd* (II) of composition*ML* (*L2*—cefriaxone anion) and iron complex (III) *FeLCl* [47] are shown in the article [48].

It should be noted that the antibiotic in this study has molecular form (pH = 6,4), in which it is inactive and does not form complex compounds with metals. Therefore, for further study of this issue, it is recommended to change the conditions for conducting experimental tests, and to change the pH of the environment (acidic ≤ 4, alkaline ≥ 8), temperature, and period. It is possible that in case of these parameter's changing, it will lead to an active interaction of the antibiotic with metals.

Asaconclusion, metal complexes of antibiotics of the cephalosporin group have been little studied nowadays. There is a lack of data about stability and structure of the complexes and it is impossible to make any common conclusions.

References

1. Kiein EY, Van Boeckel TP, Martinez EM (2018) Global increase and geographic convergence in antibiotic consumption between 2000 and 2015. Proc Natl AcadSci U S A. 115:3463–3470
2. Azanu D et al (2018) Occurrence and risk assessment of antibiotics in water and lettuce in Ghana. Sci Total Environ 622–623:293–305. https://doi.org/10.1016/j.scitotenv.2017.11.287
3. Becker RW et al (2020) Investigation of pharmaceuticals and their metabolites in Brazilian hospital wastewater by LC-QTOF MS screening combined with a preliminary exposure and in silico risk assessment. Sci Total Environ 699:134218. https://doi.org/10.1016/j.scitotenv.2019.134218

4. Castiglioni S et al (2020) Micropollutants in Lake Como water in the context of circular economy: A snapshot of water cycle contamination in a changing pollution scenario. J Hazard Mater 384:121441. https://doi.org/10.1016/j.jhazmat.2019.121441

5. Chiffre A et al (2016) Occurrence of pharmaceuticals in WWTP effluents and their impact in a karstic rural catchment of Eastern France. Environ Sci Pollut Res 23:25427–25441. https://doi.org/10.1007/s11356-016-7751-5

6. Dinh QT et al (2017) Occurrence of antibiotics in rural catchments. Chemosphere 168:483–490. https://doi.org/10.1016/j.chemosphere.2016.10.106

7. Gaffney V de J et al (2017)Occurrence and behaviour of pharmaceutical compounds in a Portuguese wastewater treatment plant: Removal efficiency through conventional treatment processes. Environ. Sci. Pollut. Res. 24:14717–14734. https://doi.org/10.1007/s11356-017-9012-7

8. García-Galán MJ et al (2020) Fate of priority pharmaceuticals and their main metabolites and transformation products in microalgae-based wastewater treatment systems. J Hazard Mater 390:121771. https://doi.org/10.1016/j.jhazmat.2019.121771

9. Harrabi M et al (2018) Analysis of multiclass antibiotic residues in urban wastewater in Tunisia. Environ Nanotechnol Monit Manag 10:163–170. https://doi.org/10.1016/J.ENMM.2018.05.006

10. Hernández F et al (2019) Occurrence of antibiotics and bacterial resistance in wastewater and sea water from the Antarctic. J Hazard Mater 363:447–456. https://doi.org/10.1016/J.JHAZMAT.2018.07.027

11. K'oreje KO et al (2016) Occurrence patterns of pharmaceutical residues in wastewater, surface water and groundwater of Nairobi and Kisumu city, Kenya. Chemosphere 149:238–244. https://doi.org/10.1016/J.CHEMOSPHERE.2016.01.095

12. León-Aguirre K et al (2019) A rapid and green method for the determination of veterinary pharmaceuticals in swine wastewater by fluorescence spectrophotometry. Bull Environ Contam Toxicol 103:610–616. https://doi.org/10.1007/s00128-019-02701-2

13. MirzaeiR et al (2018) Occurrence and fate of most prescribed antibiotics in different water environments of Tehran Iran. Sci Total Environ 619–620:446–459. https://doi.org/10.1016/j.scitotenv.2017.07.272

14. Pan C, Bao Y, Xu B (2020) Seasonal variation of antibiotics in surface water of Pudong New Area of Shanghai, China and the occurrence in typical wastewater sources. Chemosphere 239:124816. https://doi.org/10.1016/j.chemosphere.2019.124816

15. Park S, Lee W (2018) Removal of selected pharmaceuticals and personal care products in reclaimed water during simulated managed aquifer recharge. Sci Total Environ 640–641:671–677. https://doi.org/10.1016/J.SCITOTENV.2018.05.221

16. Parpounas A et al (2017) Assessing the presence of enrofloxacin and ciprofloxacin in piggery wastewater and their adsorption behaviour onto solid materials, with a newly developed chromatographic method. Environ Sci Pollut Res 24:23371–23381. https://doi.org/10.1007/s11356-017-9849-9

17. Renau-PruñonosaA et al (2020) Identification of aquifer recharge sources as the origin of emerging contaminants in intensive agricultural areas. La Plana de Castellón, Spain. Water 12:731. https://doi.org/10.3390/w12030731

18. Rodriguez-Mozaz S et al (2015) Occurrence of antibiotics and antibiotic resistance genes in hospital and urban wastewaters and their impact on the receiving river. Water Res 69:234–242. https://doi.org/10.1016/j.watres.2014.11.021

19. Santiago-Martín A et al (2020)Pharmaceuticals and trace metals in the surface water used for crop irrigation: Risk to health or natural attenuation? Sci. Total Environ. 705:135825. doi:https://doi.org/10.1016/j.scitotenv.2019.135825

20. Spataro F et al (2019) Antibiotic residues and endocrine disrupting compounds in municipal wastewater treatment plants in Rome. Italy. Microchem. J. 148:634–642. https://doi.org/10.1016/j.microc.2019.05.053

21. Szekeres E et al (2017) Abundance of antibiotics, antibiotic resistance genes and bacterial community composition in wastewater effluents from different Romanian hospitals. Environ Pollut 225:304–315. https://doi.org/10.1016/J.ENVPOL.2017.01.054

22. Thai PK et al (2018) Occurrence of antibiotic residues and antibiotic-resistant bacteria in effluents of pharmaceutical manufacturers and other sources around Hanoi Vietnam. Sci Total Environ 645:393–400. https://doi.org/10.1016/J.SCITOTENV.2018.07.126

23. Tran NH et al (2016) Occurrence and removal of multiple classes of antibiotics and antimicrobial agents in biological wastewater treatment processes. Water Res 104:461–472. https://doi.org/10.1016/J.WATRES.2016.08.040

24. Wang Q, Wang P, Yang Q (2018) Occurrence and diversity of antibiotic resistance in untreated hospital wastewater. Sci Total Environ 621:990–999. https://doi.org/10.1016/J.SCITOTENV.2017.10.128

25. Wang S et al (2020) Fate of antibiotics, antibiotic-resistant bacteria, and cell-free antibiotic-resistant genes in full-scale membrane bioreactor wastewater treatment plants. Bioresour Technol 302:122825. https://doi.org/10.1016/j.biortech.2020.122825

26. Zhang M et al (2018) Occurrence, fate and mass loadings of antibiotics in two swine wastewater treatment systems. Sci Total Environ 639:1421–1431. https://doi.org/10.1016/j.scitotenv.2018.05.230

27. Zhu N et al (2020) Fate and driving factors of antibiotic resistance genes in an integrated swine wastewater treatment system: from wastewater to soil. Sci Total Environ 721:137654. https://doi.org/10.1016/j.scitotenv.2020.137654

28. Analytical review: Pharmaceutical market of Russia (2019) Moscow: Issue: December DSM Group. https://dsm.ru/docs/analytics/december_2019_pharmacy_analysis.pdf. Accessed 01 Mar 2021

29. Barenboim GM, Danilov-Danilyan VI, Chekanova MA (2012) The system of ensuring environmental safety in drug pollution of the environment: tasks and principles of formation. In: Managing the development of large-scale MLSD systems. Proceedings of the Sixth International Conference, pp 29–33

30. Barenboim, GM, Chiganova MA (2012) Contamination of surface and wastewater with medicinal products. Water: Chem Ecol 10:40–46

31. Barenboim GM, Chiganova MA, Berezovskaya IV (2014) Features of contamination of surface water bodies with components of medicinal products. Water Manage Russia: Problems Technol Manage 3:131–141

32. Barenboim GM, Chiganova MA (2014) Contamination of water bodies in the Moscow region with drugs, their metabolites and other xenobiotics with pharmacological activity: problems and solutions. Bull Russian Acad Sci 2:97–103

33. Getman MA, Narkevich IA (2013) Forecasting and control of drug residues entering the environment. Remedium 5:36–44

34. Golubeva MV (2012) Physical and chemical properties and structure of complex iron (III) compounds with penicillins and cephalosporins. Tver

35. Danilov-Danilyan VI, Khramenkov SV, Poroikov VV (2012) New methods for assessing the biological activity of xenobiotics in water bodies. In the collection: methods of analysis and control of water quality. Conf Proc 10:20–25

36. Dolina LF, Savina OP (2018) Water purification from drug residues. Sci Progress Transport 3(75):36–51

37. Zhelovitskaya AV, Dresvyannikov AF, Chudakova OG (2015) Application of perspective oxidative processes for wastewater treatment containing pharmaceutical preparations (review). Bull Technol Univ 20:73–79

38. Zhuravlev EV, Alekseev VG, Feofanova MA, Ryasensky SS (2016) Complexation of copper (II) with cefotaxime in sodium chloride solution. J Inorg Chem 7:917–919
39. Kozyrev SV, Korablev VV, Yakutseni PP (2012) A new environmental risk factor: medicinal substances in the environment and drinking water. Sci Tech Bull St. Petersburg State Polytechnic University 4(159):195–201
40. Krysanova TA, Kotova DL, Vasilyeva SY, Slashcheva EA, Ryazhskikh YY, Erin OV (2015) Spectrophotometric determination of the sodium salt of cefotaxime in an aqueous solution. Bull Voronezh State University. Series: Chem Biol Pharm 2:13–16
41. Kulapina OI, Karpenko VA, Kulapina EG (2016) Investigation of the state of some cephalosporin antibiotics in aqueous media by the spectrophotometric method. Izvestiya Saratovskogo universiteta. New Series. Series: Chem Biol Ecol 2:130–135
42. Kulapina EG, Tyutikova MS (2017) Solid-contact and planar sensors for the determination of cefotaxime in aquatic and biological media. Izvestiya Saratovskogo universiteta. New Series. Series: Chem Biol Ecol 1:14–18
43. PE-5400 UV spectrophotometer. User manual. (2013). St. Petersburg
44. Ubaydullayeva ZA, Zaynutdinov HS (2015) Marketing analysis of the purchase of cephalosporin antibiotics. Bull Pharm 1(67):9–12
45. Abramova AA, Isakov VG, Nepogodin AM et al (2020) Classification of antibiotics contained in urban wastewater. IOP Conf Series: Earth Environ Sci 548(5):052078. https://doi.org/10.1088/1755-1315/548/5/052078
46. Abramova AA, Isakov VG, Grakhova EV et al (2020) Methods for detection of antibiotics in urban wastewater. IOP Conf Series: Earth Environ Sci 862:062059. https://doi.org/10.1088/1757-899X/862/6/062059
47. Alekseev V G (2009) Bio-organic chemistry of penicillins and cephalosporins. Tver
48. Doadrio AL, Mayorga A, Orenga R (2002) J Braz Chem Soc 13(1):95–100

Wastewater Treatment by Azolla Filiculoides

V. Ogasa[1([envelope])], V. Isakov[2], A. Nepogodin[2], and E. Grakhova[2]

[1] CUSS Chriwa Umwelt-Systemtechnik Und Service GmbH, Bruchweg 30, 29313 Hambuhren, Germany

[2] Kalashnikov Izhevsk State Technical University, Studencheskaya 7, Izhevsk 426069, Russia

Abstract. The article presents results of using *Azolla filiculoides* (water fern) as photoautotrophs in phyto-purification systems with their subsequent fermentation to receive biogas. The use of *Azolla filiculoides* led to high purification efficiency and, the content of ammonium (from 0.307 mg/l to 0.043 mg/l), nitrate (from 9.88 mg/l to 0.127 mg/l), nitrite (from 0.353 mg/l to 0.019 mg/l) and orthophosphate (from 0.906 mg/l to 0.027 mg/l) were decreased on the 12th day of the experiment in the purified water. The use of *Azolla filiculoides* as a substrate for biogas production also gave a positive result: in case of fermenting whole parts of *Azolla filiculoides*, the biogas yield was 302 m^3 per ton of organic dry matter, and in the case of plant grinding, the biogas yield was 242 m^3 per ton of organic dry matter. The work also presents the results achieved during the fermentation of several treatment options for *Azolla filiculoides*: when it was frozen before fermentation, the biogas yield was 238 m^3 per ton of organic dry matter; after autoclaving, the biogas yield was 134 m^3 per ton of organic dry matter; in case of dried plant's fermentation, the biogas yield was 36 m^3 per ton of organic dry matter, and fermentation of boiled plant led to 24 m^3 of biogas per ton of organic dry matter.

Keywords: Wastewater treatment · Constructed Wetlands · *Azolla filiculoides* · Biogas

1 Introduction

Since the 70 s of the twentieth century, water purification by phyto-purification systems has been actively developing in the world. They are known as Constructed Wetlands (or Treatment wetlands, Reed bed systems).

There are several vast historical reviews of using phyto-treatment systems [1–6]. These reports describe in detail the stages of development of this technology: from the first scientific research in Europe in the 1950s, and to the creation of Manuals for such systems in the USA in the late 1960s [7].

The wastewater treatment concept in phyto-wastewater treatment systems with the horizontal subsurface flow was developed in Germany in the 1970s. The first working phyto-purification system was applied in 1974 at Othfresen in Germany, and the purification process was called the "root zone method" (RZM, German Wurzelraumentsorgung) [8]. Research work about the development of phyto-treatment systems in

the United States was carried out during the 1970s and 1980s, but widespread using of phyto-treatment systems in North America began in the early 1980 s of the twentieth century. Nowadays, it continues to grow.

It must be noted that in the 1970s and 1980s phyto-treatment systems were used just for the treatment of domestic or municipal wastewater. And only from the beginning of the 1990s they started to be used for treating all types of wastewater, including leachate from municipal solid waste landfills, storm water (for example, municipal, highway, airport and agricultural drains), wastewater from livestock enterprises, industrial runoff (chemical, pulp and paper industry, etc.), mine water and even phyto-systems for excessive activated sludge.

Russia has experience in using phyto-purification systems with the open water surface. These are post-treatment ponds, bio plateau, which quite successfully purify storm drains or kept for tertiary treatment for activated sludge treatment facilities. Moreover, there are experimental phyto-purification systems. For example, according to an international project (Russia, Finland, Sweden, the Netherlands), the world's only bioplateau for wastewater treatment beyond the Arctic Circle was created in the Shongui village of the Murmansk region [9]. Some systems of subsurface and surface runoff are operated in the Tomsk region with conditions of even lower average annual temperatures (-1.5 °C) and frosty winters (up to -53 °C) [10].

Phyto-purification systems are artificial ones designed and built for wastewater treatment, consisting of elements similar to the natural landscape with built-in technical elements. The main features are:

- artificial aquatic plants for water purification
- presence of a low-speed flow of water from the source of pollution to the receiver of treated water

The second feature, despite the apparent obviousness, is very important. If the time spent by wastewater in any natural-technogenic system is weeks and months (as, for example, in a natural swamp) and there is no flow of treated water (as an object for monitoring), such a system cannot be considered as a phyto-purification one. In other words, the time spent in the phyto- purification system has a finite and well-defined value, which can be calculated quite accurately.

The most widespread classification is the division of phyto- purification systems into systems with an open water surface and subsurface; subsurface ones—with the vertical or horizontal flow or hybrid [11].

Analysis of the articles makes it possible to classify these systems also according to the following criteria:

- according to the use of natural water bodies as blocks of phyto- purification systems
- according to the location of the hydraulic project line
- according to the direction of water flow
- according to the type of filtering and loading material
- according to the use of man-made blocks built into the system
- according to the type of artificial aquatic plant.

Phyto-purification systems currently are widespread in almost all countries of the world. The largest ammount of them were built in Germany and the USA (tens of thousands). There are thousands of them in Australia, and hundreds in the European Nordic countries. The number of phyto- purification systems in Southeast Asia and China cannot be estimated accurately enough due to a lack of data. But, it is known, that phyto-technologies are actively developing in these countries.

2   Theoretical Basis

Photoautotrophs (plants) play a basic role in phyto-purification systems. This is their main difference from classical activated sludge treatment facilities (in classical wastewater treatment plants, autotrophs are only nitrifying bacteria—chemoautotrophs, as well as an insignificant part of unicellular algae). Thus, the ecosystem of phyto-purification systems is more complex and consists of autotrophs and heterotrophs. There are several "full" (stable in time) trophic levels, which can be distinguished according to the type of grazing food chains (base—photoautotrophic biomass) and detrital ones (base—detritus, a loose mass of decaying material), while—only detrital food chains exist in classical treatment systems.

Higher plants play several important roles in phyto- purification systems, which fundamentally distinguishes them from drainage ditches or drainage wells widespread in Russia, where gravel is also used as the main cleaning component. Plants are (a) an assimilator of pollutants (inclusion into biomass), (b) the load on which the attached bacterial cenoses expand: on roots—in case of partially submerged plants, on roots, leaves and stems—in case of completely submerged plants; (c) an additional source of autochthonous organic matter for processes of denitrification, methanogenesis, biochemical oxidation, which are extremely important for xenobiotics removing.

Organic compounds are decomposed in phyto- purification systems both under aerobic conditions and in anaerobic conditions—by bacteria attached to underground plant organs (roots, stems, rhizomes) and to the loading surface (gravel). Oxygen required for aerobic decomposition is supplied either directly from the atmosphere by diffusion or oxygen permeation from the roots and rhizomes of macrophytes in the rhizosphere (without aeration in case of phyto-purification systems) and/or from aeration systems (in the case of phyto- purification systems using forced aeration).

Nitrogen is removed in phyto- purification systems by nitrification/denitrification, anaerobic ammonium oxidation and plant assimilation. According to the research of processes in vertical and hybrid phyto-purification systems, it was shown that nitrification, denitrification, ammonification and anammox happen simultaneously in most of these systems [12]. However, the degree of manifestation of some processes is different.

Phosphorus in phyto- purification systems is removed using exchange reactions on the surface of the mineral load, where phosphate displaces water or hydroxyl groups from the surface of Fe and Al hydroxides. However, fine gravel, crushed stone used for vertical phyto- purification systems usually doesn't not contain large amounts of Fe, Al or Ca and therefore phosphorus removal is generally low. Aerobic conditions are more favorable for the sorption and coprecipitation of phosphorus. Therefore, the latest phyto- purification systems using forced aeration allow to comply with strict standards for phosphates level.

There are lots of reports, indicating that xenobiotics are actively removed in phyto-purification systems. Biochemical processes help to remove it, which is confirmed by research on the decomposition of aromatic compounds, oil products, pesticides and other organic pollutants [13, 14]. The efficiency of removing toxic organic matter increases with the age of the structure, which may lead to the possible formation of a specific bacteriocenosis of waste water. The newest biological methods (next generation sequencing, PCR, geochips) make it possible to assess the structure of bacteriocenosis and design it with specified properties.

The significant residence time of the water makes it possible to disinfect wastewater. Disinfection happens due to the destruction of fecal (pathogenic and conditionally pathogenic) bacteria in the process of successive changes of plants as the water moves from the entrance to the exit from phyto-purification systems, as well as due to the consumption of bacteria by fouling organisms.

3   Materials and Methods

To determine the possibility of using photoautotrophs in phyto- purification systems, an experiment was carried out with *Azolla filiculoides* at a treatment plant in the city of Suderburg (Germany) within the framework of cooperation of teachers and students from Ostfalia University of Applied Sciences, the Suderburg campus and Kalashnikov Izhevsk State Technical University.

Azolla filiculoides is free floating freshwater fern (Fig. 1), which can be successfully used for wastewater treatment, nitrite removal and waste treatment, it can grow under a wide range of environmental conditions [15–21]. Also, it can be used for biogas production, loading them into Digestion tanks as a substrate. *Azolla filiculoides* had a great effect on the fermentation process, and their advantage is the ability to purify water according to some indicators (such as phosphates, nitrates, nitrites, etc.) [22–26]. It can be beneficial if the ferns are cultivated in the wastewater treatment plant on the surface of the liquid and with the help of special devices, and an excessive amount of them are fed into the digesters for fermentation.

Small plastic containers filled with waste water were used for the experiment. The containers included a step overflow and a certain amount of fern was added to each container with a preliminary weight measurement into each container (Fig. 2).

Weight of the the fern was measured every certain period during the whole experiment (the growth of biomass was observed). Also parameters of the treated water were monitored (pH, electrical conductivity, water temperature, nitrogen, ammonium, nitrate, nitrite, orthophosphate, total phosphorus, chloride, fluoride, sulfate, phosphate, chemical oxygen demand (COD), biological oxygen demand (BOD5), total organic carbon). A lot of parameters were decreased in purified water on the fourth day of the experiment: the content of ammonium (from 0.307 mg/l to 0.036 mg/l), nitrate (from 9.88 mg/l to 4.75 mg/l), nitrite (from 0.353 mg/l to 0.195 mg/l)), orthophosphate (from 0.906 mg/l to 0.090 mg/l), but total weight of the fern was doubled.

Acheived experimental results are shown in Table 1.

As a result of the test, it was revealed that unpretentious fern reproduces extremely quickly, increasing the volume of its biomass, on average, 2 times for 5 days. According

Fig. 1 Water fern *Azolla filiculoides* in the wild life

Fig. 2 Model of phyto- purification system using *Azolla filiculoides*

to the tests it was detected that the fern improves different water quality indicators: nitrogen, orthophosphate, ammonium, nitrite and nitrate (Fig. 3).

However, it must be noted, that concentration of nitrates was sharply increased on the 17th day during the subsequent step of purification, which was repeated on the 21st and 28th days of the experiment. Increased nitrate concentration for more than two levels resulted in the growth of nitrite for 1–2 levels. This growth can be explained both by a change in the composition of wastewater, and by an increase in wastewater consumption in the experimental tank, which was installed outdoors and rainfall increased the hydraulic head and flow rate in all tanks. Also Azolla filiculoides cant purufy increased volume of effluents and, as a result, we get an increase in the concentration of orthophosphate.

Table 1 Quality of waste water after using *Azolla filiculoides*

| Parameters	Day of the test						
	1 day	4 day	10 day	12 day	17 day	21 day	28 day
pH	7.15	7.09	7.08	7.40	7.69	7.62	7.78
Temperature, ° C	21.1	20.5	25.2	25.4	19.5	19.9	18.3
Electrical conductivity, mS/cm	927	858	780	818	842	878	936
Total Kjeldahl nitrogen, mg/l	2.59	1.54	1.40	1.82	1.68	2.17	1.96
Ammonium, mg/l	0.307	0.036	0.057	0.043	0.230	0.053	0.024
Nitrate, mg/l	9.88	4.75	0.119	0.127	34.7	31.4	33.6
Nitrite, mg/l	0.353	0.195	0.046	0.019	0.713	0.867	1.081
Orthophosphate, mg/l	0.906	0.090	0.0485	0.027	1.65	0.333	0.021
Total phosphorus, mg/l	0.223	0.257	0.372	0.278	1.91	0.552	0.2177
Chloride, mg/l	155	146	128	153	102	109	122
Fluoride, mg/l	0.051	0.069	0.119	0.052	0.128	< 0.050	< 0.050
Sulfate, mg/l	49.5	54.7	39.0	44.6	44.2	44.8	43.8
COD, mg/l	49.4	49.1	28.9	51.5	54.2	62.9	51.6
BOD5, mg/l	3.00	4.62					
Total organic carbon, mg/l	10.3	13.1	12.6	12.3	9.99	12.3	14.75
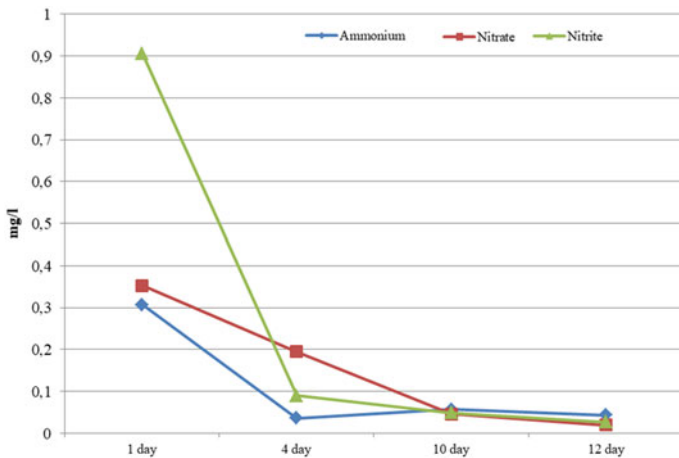
Fig. 3 Purified water parameters while using Azolla filiculoides

As a recommendation for further design of wastewater treatment facilities using Azolla filiculoides, authors point out the need to divert surface runoff to reserve tanks or install covered tertiary treatment facilities, which is an urgent issue in case of installing such facilities in northern countries.

The next step of experimental research was to determine the possibility of using *Azolla filiculoides* for biogas production in digesters, as well as the effect of the type of preparation of the fern to the level of biogas. *Azolla filiculoides* was prepared in various ways before tests [27–31]:

- frozen during the day in the freezer
- cooked in 5 min
- oven dried for dry matter determination (100 °C)
- autoclaved
- finely chopped
- fresh fern

It was done to measure their toxicity in the fermentation process and the possible impact on the amount of biogas produced.

Thermal treatment of sediments was carried out using special beakers with the studied substrate in an artificial climate chamber, where a constant temperature of 35° C (mesophilic fermentation mode) was maintained and the penetration of sunlight was not allowed. Tests were conducted for 21 days. All obtained results were recorded and analyzed every day at the same time.

Achieved experimental results are shown in Table 2 and in Fig. 4.

Table 2 Biogas yield during *Azolla filiculoides* fermentation under anaerobic conditions, which have passed through various preparation

Day and time of the tests	Fermentation time, days	Preparation type					
		full	chopped	frozen	autoclaved	dried	cooked
		m^3 biogas per ton of organic dry matter					
1 day, 12:30	0,000	0	0	0	0	0	0
2 day, 11:00	0,938	59	93	0	0	29	0
3 day, 09:00	1,854	105	153	21	40	38	13
4 day, 13:40	3,049	188	191	136	95	47	6
5 day, 09:30	3,875	223	208	176	104	50	25
6 day, 11:00	4,938	263	234	218	127	51	40
7 day, 13:00	6,021	289	239	227	128	45	30
8 day, 09:45	6,885	302	242	238	134	36	24

Tests have shown that during waste water purification and post-treatment, Azolla filiculoides grow actively and weight of the fern doubles approximately every four days, that's why they can also be used as biomass in digesters for biogas production.
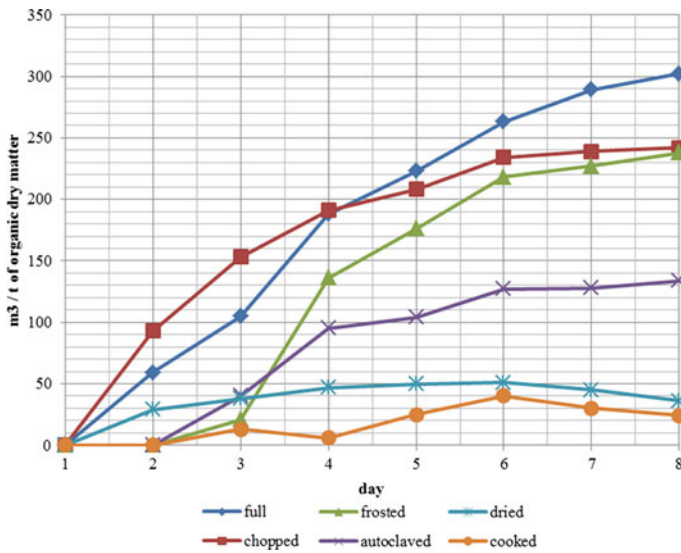
Fig. 4 Biogas yield during *Azolla filiculoides* fermentation, that passed through various preparation

The best result according to the volume of obtained biogas per weight of used raw material was obtained when fermenting Azolla filiculoides without processing and chopping. Present study result can be used in the future to design a technological process for removing excess Azolla filiculoides mass from wastewater treatment and post-treatment facilities, delivering this mass to digesters, followed by fermentation and biogas production.

4 Results

As a result of tests, it was revealed that during the fern fermentation, full *Azolla filiculoides* showed the best outcome—302 m^3 of biogas per ton of organic dry matter (m3/t ODM), and also chopped one—242 m^3/t ODM. Others have insignificant results:

- Frozen—238 m^3/t ODM
- Autoclaved—134 m^3/t ODM
- Dried—36 m^3/t ODM
- Cooked—24 m^3/t ODM

5 Conclusions

Research showed, that waste water treatment by *Azolla filiculoides* allowed in the short term to reduce the level of ammonium, nitrate, nitrite, orthophosphate and increase the total weight of the fern. It will be a profitable idea to cultivate them in secondary sedimentation tanks on the surface of the liquid and, using special devices, supply an

excess amount of the fern to the digester for further fermentation. In this case, two positive results will be achieved: increased biogas yield and additional purification of wastewater from nutrients and heavy metals using aquatic plants. It is not difficult to implement, as the ferns are unpretentious plants and grow rapidly.

References

1. Kadlec RH, Knight RL (1996) Treatment Wetlands, 1st edn. Boca Raton, Florida, CRC Press
2. Kadlec RH et al (2000) Constructed Wetlands for Water Pollution Control: Processes, Performance, Design and Operation, IWA Scientific and Technical Report No. 8. IWA Publishing, London
3. Kadlec RH, Wallace SD (2008) Treatment Wetlands, 2nd edn. Boca Raton, Florida, CRC Press
4. Vymazal J, Kröpfelová L (2008) Wastewater treatment in constructed wetlands with horizontal sub-surface flow. Springer, Dordrecht, The Netherlands
5. Dias V, Kriksunov EA, Shchegolkova N (2013) Introduction of constructed wetlands in Russia: a need. In: Abstracts of the 5th Int. Symposium on Wetland pollutant dynamics and control, Nantes, France, 13–17 October 2013, pp 276–277
6. Dias V, Kriksunov EA, Shchegolkova N (2013) MULTI-FITOX–advanced wastewater treatment system using aquatic emergent macrophytes. In: Abstracts of the 5th international symposium on Wetland pollutant dynamics and control, Nantes, France, 13–17 October 2013, p 321
7. Constructed Wetlands Treatment of Municipal Wastewaters Manual - National Risk Management Research Laboratory (Sept 1999) . Office of research and development. U.S. Environmental Protection Agency. Cincinnati, Ohio 45268 EPA/625/R-99/010
8. Seidel K (1976) Macrophytes and water purification. Biological control of water pollution. Pennsylvania University Press, Philadelphia, pp 109–122
9. Vereshchagina IY, Vasilevskaya NV (2004) Artificial bioplate in the Arctic latitudes. Production ecology 4:18–21
10. Semenov SY, Shelepova LI (2008) Vodno-bolotnaya obochistka wastewater treatment. Life safety 1:37–38
11. Kadlec RH, Wallace SD (2009) Treatment Wetlands. LLC CRC Press, Boca Raton, Florida
12. Vymazal J, Kröpfelová L (2009) Removal of organics in constructed wetlands with horizontal sub-surface flow: a review of the field experience. Sci Total Environ 407:3911–3922
13. Abira MA, Bruggen JJA, Denny P (2005) Potential of a tropical subsurface constructed wetland to remove phenol from pretreated pulp and papermill wastewater. Water Sci Technol 51(9):173–176
14. Herrera Melián JA et al (2011) Degradation and detoxification of p-nitrophenol by advanced oxidation technologies and bench-scale constructed wetlands. J Environ Manage 01:24–35
15. Bianchi E et al (2020) Improving the efficiency of wastewater treatment plants: Bio-removal of heavy-metals and pharmaceuticals by *Azolla filiculoides* and *Lemna minuta*. Sci Total Environ 746:141219. https://doi.org/10.1016/j.scitotenv.2020.141219
16. Gholizadeh AM et al (2020) Removal of Phenazopyridine from wastewater by merging biological and electrochemical methods via *Azolla filiculoides* and electro-Fenton process. J Environ Manage 254:109802. https://doi.org/10.1016/j.jenvman.2019.109802

17. Naghipour D et al (2018) Phytoremediation of heavy metals (Ni, Cd, Pb) by *Azolla filiculoides* from aqueous solution: a dataset. Data Brief 21:1409–1414. https://doi.org/10.1016/j.dib.2018.10.111

18. Mashkani SG, Ghazvini PTM (2009) Biotechnological potential of *Azolla filiculoides* for biosorption of Cs and Sr: application of micro-PIXE for measurement of biosorption. Biores Technol 100(6):1915–1921. https://doi.org/10.1016/j.biortech.2008.10.019

19. Costa ML, Santos MC, Carrapico F (1999) Biomass characterization of azolla filiculoides grown in natural ecosystems and wastewater. Hydrobiologia 415:323–327

20. Muradov N et al (2014) Dual application of duckweed and azolla plants for wastewater treatment and renewable fuels and petrochemicals production. Biotechnol Biofuels 7:30. https://doi.org/10.1186/1754-6834-7-30

21. Lumpkin T, Plucknett D (1980) Azolla: Botany, physiology, and use as a green manure. Econ Bot 34:111–153. https://doi.org/10.1007/BF02858627

22. Forni C et al (2001) Evaluation of the fern *Azolla* for growth, nitrogen and phosphorus removal from wastewater. Water Res 35(6):1592–1598. https://doi.org/10.1016/S0043-1354(00)00396-1

23. Schuijt LM et al (2021) Aquatic worms (Tubificidae) facilitate productivity of macrophyte *Azolla filiculoides* in a wastewater biocascade system. Sci Total Environ 787:147538. https://doi.org/10.1016/j.scitotenv.2021.147538

24. Dohaei M et al (2020) Integrated biorefinery of aquatic fern *Azolla filiculoides* for enhanced extraction of phenolics, protein, and lipid and methane production from the residues. J Clean Prod 276:123175. https://doi.org/10.1016/j.jclepro.2020.123175

25. Brouwer P et al (2016) Lipid Yield and Composition of Azolla filiculoides and the Implications for Biodiesel Production. BioEnergy Research 9:369–377

26. Akila V et al (2019) Biogas and biofertilizer production of marine macroalgae: An effective anaerobic digestion of Ulva sp. Biocatalysis Agricultural Biotechnol 18:101035

27. Montingelli ME et al (2016) Pretreatment of macroalgal biomass for biogas production. Energy Convers Manage 108:202–209. https://doi.org/10.1016/j.enconman.2015.11.008

28. Montingelli ME, Tedesco S, Olabi AG (2015) Biogas production from algal biomass: a review. Renew Sustain Energy Rev 43:961–972. https://doi.org/10.1016/j.rser.2014.11.052

29. Dębowski M et al (2013) Algae Biomass as an Alternative Substrate in Biogas Production technologies—review. Renew Sustain Energy Rev 27:596–604. https://doi.org/10.1016/j.rser.2013.07.029

30. Tedesco S, Barroso TM, Olabi AG (2013) Optimization of mechanical pre-treatment of laminariaceae spp biomass-derived biogas. Renew Energy 62:527–534. https://doi.org/10.1016/j.renene.2013.08.023

31. Ariunbaatar J et al (2014) Pretreatment methods to enhance anaerobic digestion of organic solid waste. Appl Energy 123:143–156. https://doi.org/10.1016/j.apenergy.2014.02.035

Development of Method and Device to Improve the Efficiency of Natural and Wastewater Treatment

O. Medvedeva[1]([✉]), T. Sautkina[1], and E. Chesnokova[2]

[1] Yuri Gagarin State Technical University of Saratov, 77, Politekhnicheskay street, Saratov 410054, Russia

[2] JSC "VNIPIgazdobycha", 4 Sacco and Vanzetti street, Saratov 410012, Russia

Abstract. The purpose of the study is to develop a method and device for intensifying the process of coagulation and precipitation in the treatment of low-turbidity waters using reagent-free technologies, to identify the effectiveness of their use and to determine the optimal technological parameters for this process. The research approach includes the main theoretical provisions of the process of coagulation water treatment, taking into account current trends in its development, modern methods of applying this process of water purification, conducting laboratory and industrial studies on natural waters, modern methods of mathematical processing and analysis of experimental data. The problem of disinfecting liquids and gases by physical methods is currently still very important. The authors plan to use the electrostatic field created by devices such as capacitors to purify liquids and gases from pathogens. As a result of previous studies of natural water purification, a device for intensifying the sedimentation of suspended particles in a liquid has been developed (patent for utility model № 170,333). The technical result consists in increasing the cleaning efficiency by accelerating the deposition of impurities in the liquid by introducing additional treatment of the liquid with an electrostatic field.

Keywords: Low-turbid waters · Water treatment · Sedimentation · Weighting additives · Electrostatic field · Water disinfection

1 Introduction

The deterioration of water quality in reservoirs is caused by various factors. During floods and heavy precipitation, the water in reservoirs becomes much worse due to the massive influx of atmospheric waters. Meltwater brings various herbicides, pesticides and residual mineral fertilizers from the fields. The unsatisfactory condition of treatment plants often leads to the discharge of wastewater into the reservoir that does not meet the regulatory documentation in its composition and properties. An equally important problem related to pollution is the uncontrolled discharge of untreated industrial wastewater into open reservoirs which exceeds 340 million cubic meters of water annually, and most of them enter the rivers untreated.

Natural and wastewater treatment is carried out sequentially at a number of facilities. All technological treatment schemes are usually of the same type. Water purification from coarse impurities is carried out under the influence of gravity during the settling process. For example, the deposition rate of fine sand with a particle diameter of 0.1 mm is 2 min/m, the deposition rate of a clay particle with a diameter of 0.01 mm is 2 h/m. The situation is different with colloidal impurities which due to their aggregate stability cannot be separated from water without any additional treatment (the deposition rate of a colloidal particle with a diameter of 0.0001 mm is 2 years/m).

Coagulation is a method of water purification based on the injection of a dose of a special reagent—a coagulant which intensifies the process of coalescing colloidal impurities to form coarse structures, followed by its release from the water by settling [1–3].

In the practice of water treatment at industrial enterprises, in municipal water supply as well as for wastewater treatment coagulants are used forming a new dispersed system with a particle charge sign opposite to the negative charge sign of natural water colloids. In this case, differently charged colloids clump together when they interact with destabilized areas. Next, the microflakes interlock, capturing coarse impurities and water, form a structure in the form of aggregates-flakes with a size of 0.5…5 mm and separate from the liquid medium. The most widely used coagulant is aluminum sulfate $Al_2(SO)_4 \cdot 18H_2O$ and ferrous sulfate $FeSO_4 \cdot 7H_2O$.

In the process of coagulation, the formation of flakes occurs in 10…30 min. During this period, the flakes, initially invisible, cause water turbidity. Then large loose structures are formed, which capture coarse impurities. The composition and formation of structures are influenced by various factors such as the water velocity in the flake formation zone should tend to zero; the optimal temperature for water coagulation is 30…40 °C; mixing of water provokes more frequent and strong collisions of coagulating particles, which contributes to their adhesion; the dose of the coagulant is determined based on the composition and amount of colloidal impurities (on average 1 mg-eq/dm^3); the pH value depends on the coagulant, for example, for the hydrolysis of $Al_2(SO)_4 \cdot 18H_2O$, the pH value should be in the range of 5…7.5.

The introduction of the coagulant into the treated water leads to a decrease in the ζ –potential (electric charge). The process of coagulation begins to occur at the value of the ζ –potential—25…30 mV, as a result of which the repulsive forces weaken, the aggregate stability of colloidal impurities and their mutual adhesion is violated. The maximum rate of coagulation is achieved when the ζ –potential is equal to 0 mV.

To choose a method for intensifying the coagulation process, it is necessary to take into account the composition and properties of the treated water. The optimal technological parameters should be determined experimentally for specific types of treated water. The solution of this issue requires special comprehensive research to study all the features of the technological process, in particular, in the treatment of low-turbidity non-ferrous waters and thatexplains the relevance of this study.

2   Theoretical Provisions of the Process of Coagulation Water Treatment

The research approach includes the main theoretical provisions of the process of coagulation water treatment, taking into account current trends in its development, modern methods of applying this process of water purification, conducting laboratory and industrial studies on natural waters, modern methods of mathematical processing and analysis of experimental data.

Sometimes chemical reagents may represent a different type of pollution or environmental threat. Therefore, it is also possible to intensify the flocculation process without the use of chemical reagents by applying an environmentally friendly electrophysical water treatment technology, which minimizes the need for any additional production of materials intended for use in the process [4–9].

The rate of water clarification characterizes the efficiency of coagulation treatment and depends on the degree of dispersion, the shape of suspended substances, the size and their density.

In the natural environment the suspension particles have different sizes and different shapes, i.e., such a suspension is polydisperse.

To characterize the deposition of polydisperse suspension, the experimentally obtained kinetic curves are used, which determine the dependence of the efficiency of water clarification (the amount of precipitated impurities) from the settling time or hydraulic fineness according to the formulas:

$$E = f(t); \tag{1}$$

$$E = f(u), \tag{2}$$

where E is the clarification effect, %; t is the settling time, min; u is the conditional precipitation rate or hydraulic particle size of the suspension corresponding to the specified effect, mm/s.

The clarification effect is determined by the following formula [10]:

$$E = \frac{C_{in} - C_{cl}}{C_{in}} \times 100\%, \tag{3}$$

where C_{in} is the initial suspension content in water, mg/l; C_{cl} is the concentration of suspension, clarified water after time t, mg/l.

The polydisperse suspension deposition curves are actually a frequency characteristic of the studied turbid liquid, showing the distribution of particles according to their hydraulic fineness. This dependence can be represented as an expression:

$$\frac{C_{cl}}{C_{in}} = \left(1 - A \cdot u^m\right). \tag{4}$$

In modern types of settling facilities the principle of thin-layer suspension deposition (separation of the flow height into thin layers) is implemented [11–13].

The efficiency of purification of low-turbid waters directly depends on the intensification of the process of sedimentation of particles in the liquid. At present, in order to accelerate the precipitation process during settling, various weighting additives are used, for example, quartz sand with a particle size of 0.05–0.14 mm, iron powder, magnetite with a particle size of no more than 0,05 mm, etc. the process of formation of flakes and contributing to the speedy settling.

The use of previously formed recycled sludge as a weighting agent for coagulant flakes leads to a more complete use of the sorption properties of the products of coagulant hydrolysis, accelerated formation of flakes in contact with the previously isolated sludge [14, 15]. This technology is implemented in clarifiers with suspended sediment, clarifiers-recirculators, as well as in schemes with the supply of the resulting sediment from flocculation chambers, and settling tanks to the mixer [16]. According to [16, 17], the coagulation of water with the addition of sediment from settling tanks reduces the dose of coagulant (up to 30%), reduces the settling time and improves the quality of treated water. The disadvantages of the water treatment method with the addition of recirculating sludge in the area where new portions of coagulant are introduced are the increased mud load on the treatment facilities, including settling tanks and filters, the increased concentration of aluminum and the reduced alkalinity of the clarified water.

Currently, priority in the development of methods for purifying liquids, is given to environmentally friendly reagent-free technologies that do not cause damage to the environment. Reagent-free cleaning technologies are based on the treatment of liquids with various physical fields: cavitation, magnetization, superimposition of electric fields, electric discharge treatment, etc.

The problem of disinfecting liquids and gases by physical methods is currently still very important. The authors plan to use the electrostatic field created by devices such as capacitors to purify liquids and gases from pathogens.

3   Experimental Studies

As a result of previous studies of natural water purification, a device for intensifying the sedimentation of suspended particles in a liquid has been developed (patent for utility model № 170,333) [18].

The device consists of a polyethylene tube twisted into a spiral coil. Water that has contamination is passed through the tube and due to the electrification by friction the particles of contamination receive an electric charge (Fig. 1). Due to the imposition of an electric field, the processes of flocculation and precipitation of the coagulated suspension are accelerated, the degree of water purification from organic and inorganic impurities by filtration is increased; for example, the separation of algae is improved [4, 19–22].

Currently, the device has been improved in order to intensify the process of liquid purification and sedimentation of impurities and to provide more effective way to improve water quality without the use of chemicals (utility model patent № 200,770). An ionizer is added to the device to create small gaps (~1 cm) and to supply significant voltages in order to intensify the deposition rate of impurities under the influence of a strong electric field generated by the power source [23].
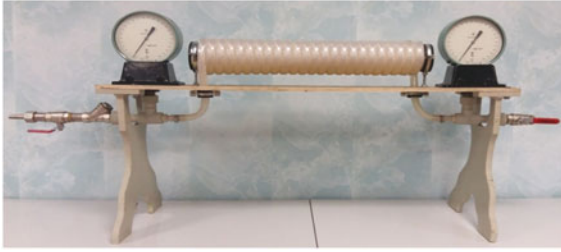
Fig. 1 Experimental model for studying the interaction of physical fields with a liquid containing impurities

The object of experimental studies on the intensification of the process of coagulation of low-turbidity waters were model solutions that simulate the quality of low-turbidity colored waters of surface sources, as well as water from the Volga River.

The first part of the research was carried out at the Gagarin State Technical University in the laboratory of the Department of Heat and Gas Supply and Oil and Gas Business.

Model solutions of non-ferrous waters were prepared from peat extract. Concentrated working solutions of peat extract were diluted with tap water to the level of color of surface sources. The quality of artificially prepared water for the period of research was characterized by the following indicators shown in Table 1.

Table 1 Physical and chemical quality indicators of model solutions

Indicators	Measure	Minimum	Average	Maximum
Temperature	° C	22.0	23.0	24.0
Chromaticity	grad	54.0	65.0	76.0
Turbidity	mg/l	19.0	25.0	31.0
pH	unit	6.3	6.75	7.2
Alkalinity	mmol/l	2.0	2.0	2.0

The quality of natural water from the Volga River at the time of the research was characterized by the indicators shown in Table 2.

The second part of the laboratory studies was carried out at the water treatment facilities of the Water Supply Complex №4 of the Municipal Unitary Enterprise «Saratovvodokanal». Physical and chemical studies of the deposition kinetics were carried out at the VK-2 station. The study of the kinetics of precipitation of the coagulated suspension during settling was carried out according to the standard method. The results were used to construct the deposition curves of the coagulated suspension.

The quality of the source water after settling and after filtration was determined by the following indicators: turbidity, color, hydrogen index (pH), alkalinity according to standard methods. Hygienic requirements for the quality of drinking water are given in Table 3 in accordance with SanPiN 2.1.4.559–96.

Table 2 Physical and chemical indicators of natural water quality

Indicators	Measure	Average
Temperature	°C	23.0
Chromaticity	grad	45.0
Turbidity	mg/l	19.0
pH	unit	5.9
Alkalinity	mmol/l	2.1

Table 3 Hygienic requirements for drinking water quality

Water quality indicators	MPC (maximum permissible concentration)
Chromaticity	grad
Turbidity	1.5 mg/l
pH	6.5–8.5 unit
Alkalinity	0.5–6.5 mmol/l

During the experiments the following reagents were used: coagulant-aluminum sulfuric acid 18-water ($Al_2(SO_4)_3 \bullet 18H_2O$) (1% solution) according to GOST 375 and, water from the settling tank.

Turbidity and chromaticity in the source water and in the water after treatment were determined using a photoelectric colorimeter KFK-3, turbidimeter 2100AN Turbidimeter, photometer Unico 2100. A pH meter was used to measure the values of the hydrogen pH index.

Neutralizer, with the help of a pump, pass at a speed of 1 m/s through a polyethylene tube (100–200 m long, 10–20 mm in diameter), rolled into a spiral. Pre-passing of the liquid through the coil of the developed cleaning device provides electrification of suspended particles, which significantly accelerates the subsequent deposition process. As a result of friction against the walls of the pipe, the particles accumulate static electricity charges and are electrified and receive some charge. In this case, the coil is placed inside a cylindrical capacitor in order to create an electrostatic field in the liquid flow. The treated liquid is passed through a polyethylene tube using a pump and an additional high voltage is applied to the capacitor plates.

Then 1 L of liquid is poured into a settling tank with a graduated ledge in the bottom and after 4 h of settling, the volume of the sediment is measured. The amount of substances that precipitate during 4 h of settling after preliminary electrification in the tube increases by 2…3 times when working on the plant tissue of coniferous wood.

The research was carried out in two stages.

The first stage of the research was carried out in order to determine the optimal conditions for the process of coagulation of low-turbidity waters during the electrification of particles in a spiral coil. The coagulation process was carried out on prepared model

solutions of low-turbidity water. Experiments on water coagulation were carried out at the temperature of the test water 22…24 °C.

At the first stage, the following parameters were determined:

- technological parameters of the spiral coil (water speed, number of links);
- optimal water settling time after coagulation.

The second stage of research was carried out in an improved device, namely, the test liquid passed through a spiral coil placed between the plates of the condenser. In particular, it was determined:

- technological parameters of the spiral coil (water speed, number of links);
- optimal electric field strength;
- optimal water settling time after coagulation.

All laboratory tests were carried out under the same conditions at least three times.

During the research observations were made on the intensity of flocculation and deposition of suspended particles. After settling, samples of clarified water were taken and turbidity and chromaticity indicators were determined.

The study of the kinetics of precipitation of the coagulated suspension during settling was carried out according to the standard method. The results were used to construct the deposition curves of the coagulated suspension.

The complex of measures to study the coagulation of river water was carried out at the complex of treatment facilities of the Water Supply Complex №4 of the Municipal Unitary Enterprise «Saratovvodokanal». A miniature pH meter of the pHPRO brand was used to determine the change in the pH of the water before and after treatment., It is possible to assess the impact of the proposed treatment by determining the hydrogen index, which serves as a quantitative characteristic of the acidity of water.

Figure 2 shows the data on the change in the hydrogen pH before and after the treatment of the test water (model liquid). Figure 3 shows the data on the change in the hydrogen pH before and after the treatment of the Volga water under study.

Figures 4, 5 show comparative graphs describing the water quality (Volga water) before and after settling.

Figures 2, 3, 4 and 5 show that the quality of clarified and decolorized water with traditional coagulation without the use of any accelerators of this process is somewhat worse than with the use of additional treatment.

Model solutions prepared specifically for laboratory studies had a higher turbidity and chromaticity than water from the settling tank.

The technical result consists in increasing the cleaning efficiency by accelerating the deposition of impurities in the liquid by introducing additional treatment of the liquid with an electrostatic field before it passes through a tube twisted into a spiral coil. The application of the electrostatic field provides orientation polarization of atoms and molecules, as a result of which there is an intensification of the process of deposition of impurities (deposition rate), a reduction in the time of separation of flakes
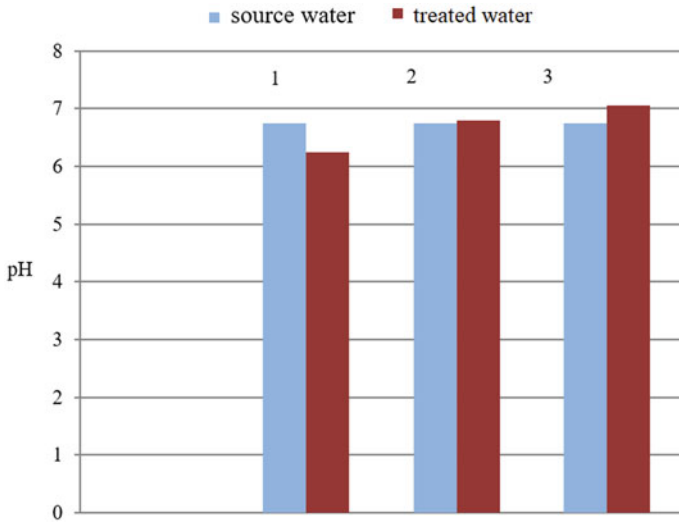
Fig. 2 Data on changes in the hydrogen pH before and after treatment of the test water (model solution): 1—normal coagulation; 2—coagulant treated in device No 1; 3—coagulant treated in device №2
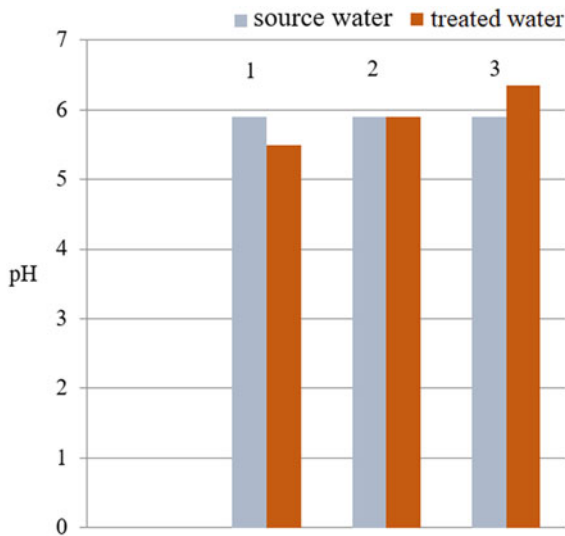

Fig. 3 Data on changes in the hydrogen pH before and after treatment of the test water (Volga water): 1—normal coagulation; 2—coagulant treated in device №1; 3—coagulant treated in advanced device №2

together with impurities of treated water, which ultimately increases the efficiency of water clarification.

This method is applicable for disinfecting both natural water and waste liquid.
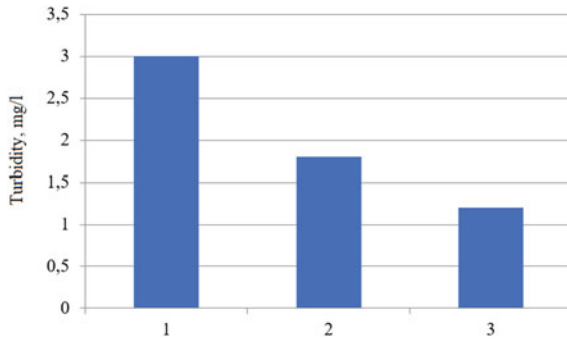
Fig. 4 Data on changes in the turbidity of the test water (Volga water): 1—normal coagulation; 2—coagulant treated in device №1; 3—coagulant treated in device №2
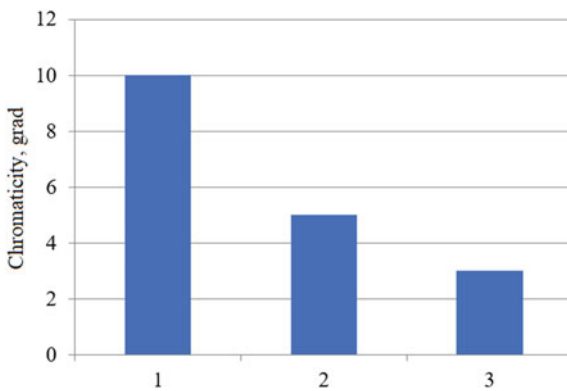

Fig. 5 Data on the change in the color of the test water (Volga water): 1—normal coagulation; 2—coagulant treated in device №1; 3—coagulant treated in device №2

Advantages of the method include insignificant dependence of its results on turbidity, pH environment, water stiffness; it can be carried out relatively easily; does not degrade the ecological condition of the environment; does not require permanent replenishment of chemicals; can be used in combination with other methods of purification of natural and wastewaters that do not have a negative impact on the environment to achieve high purification results.

The electrostatic field, constant or modulated in frequency or amplitude, affects microorganisms not only mechanically as charged particles, but also destroys them, making them not viable and biologically inactive.

In the future, as a result of tests on experimental installations developed by the authors, with the help of biological analysis of samples, it is necessary to find out the fields of what intensity affects microorganisms.

The authors aim to obtain an integral result without delving into the mechanism of interaction between the electrostatic field and microorganisms, since in this case it is practically necessary (important). This method can be applied, in our opinion, to the water and air environment, contaminated with pathogens; it can also be tested on air and water–air filters.

References

1. Hirshieva IV, Feofanov YA (2014) Povyshenie effektivnosti processa koagulyacii malomutnyh okrashennyh vod za schet vvedeniya utyazhelyayushchih dobavok (Increasing the efficiency of the process of coagulation of low-turbid colored waters by introducing weighting additives). Water Ecol: Problems Solutions 2:24–30
2. Sahu O, Dubey A (2014) Review on natural methods for wastewater treatment. J Urban Environ Eng 8:89–97. https://doi.org/10.4090/juee.2014.v8n1.089097
3. Jr-Lin L, Aldeno RI (2019) Enhanced coagulation of low turbid water for drinking water treatment: dosing approach on floc formation and residuals minimization. Environ Eng Sci 36:723–738
4. Medvedeva ON, Sautkina TN, Kalyakin AM (2020) Cylindrical condenser in a liquid cleaning device. J Phys: Conf Ser. https://doi.org/10.1088/1742-6596/1652/1/012046
5. Ivleeva AM, Obraztsov CB, Orlov AA (2010) Sovremennye metody ochistki vody (Modern methods of water purification). Tomsk, p 78
6. Ryabchikov BE (2004) Sovremennye metody podgotovki vody dlya promyshlennogo i bytovogo ispol'zovaniya (Modern Methods of Water Preparation for Industrial and Household Use). DeLi print, Moscow, p 328
7. Crini G, Lichtfouse E (2019) Advantages and disadvantages of techniques used for wastewater treatment. Environ Chem Lett (Springer) 17(1):145–155. https://doi.org/10.1007/s10311-018-0785-9f
8. Sillanpaa M, Ncibi MC, Matilainen A et al (2018) Removal of natural organic matter in drinking water treatment by coagulation: a comprehensive review. Chemosphere 190:54–71
9. Emelyanova IZ, Degtyareva NP (1968) Metod osazhdeniya vzveshennyh chastic v nejtralizovannyh gidrolizatah tkanej rastenij, stochnyh vodah i drugih zhidkostyah (Method of sedimentation of suspended particles in neutralized hydrolysates of plant tissues, waste water and other liquids). USSR Patent 218119
10. Nikoladze GI (1987) Tekhnologiya ochistki prirodnyh vod (Technology of natural water treatment). Higher school, Moscow, p 481
11. Karmazinov FV (2003) Vodosnabzhenie Sankt-Peterburga (Water supply of St. Petersburg). New magazine, St. Petersburg, p 687
12. Ivanov VG, Semenov VP, Simonov YM (1989) Primenenie tonkoslojnyh otstojnikov v cellyulozno-bumazhnoj promyshlennosti (The use of thin-layer clarifiers in the pulp and paper industry). Timber industry, Moscow
13. Babenkov ED (1977) Ochistka vody koagulyantami (Water purification with coagulants). Science, Moscow, p 356
14. Bluvestein MM (1971) Povyshenie effektivnosti raboty ochistnyh sooruzhenij vodoprovoda (Improving the efficiency of water supply treatment facilities). Stroyizdat, Moscow, p 192
15. Draginsky VL, Alekseeva LP (2005) Koagulyaciya v tekhnologii ochistki prirodnyh vod (Coagulation in natural water purification technology). Moscow, p 571
16. Novikov MG (1997) Rekonstrukciya osadka—metod povysheniya effektivnosti raboty vodoochistnyh sooruzhenij (Reconstruction of sludge - a method to improve the efficiency of wastewater treatment plants). Modern Technol Equipment Water Treatment Water Treatment Plants 1:47–50

17. Bluvestein I (1957) Koagulirovanie vzvesi s dobavleniem shlama (Suspended coagulation with added sludge). Housing and utilities 9:16–17
18. Kalyakin AM, Chesnokova EV, Semenov AP (2017) Ustrojstvo dlya intensifikacii osazh-deniya vzveshennyh chastic v zhidkosti (Device for intensifying the sedimentation of suspended particles in a liquid). RU Patent 170333
19. Yutkin LA (1986) Elektrogidravlicheskij effekt i ego primenenie v promyshlennosti (Elec-trohydraulic Effect and its Application in Industry). Mashinostroenie, Leningrad, p 253
20. Nikitenko GV (2006) Elektromagnitnye tekhnologii i tekhnicheskie sredstva dlya sistem elektrosnabzheniya (Electromagnetic Technologies and Technical Means for Power Supply Systems). AGRUS, Stavropol, p 158
21. Garcia-Seguraa S, Maesia SG, Eibanda M et al (2017) Electrocoagulation and advanced elec-trocoagulation processes: A general review about the fundamentals, emerging applications and its association with other technologies. J Electroanal Chem 801:267–299
22. Nepro Hakizimanaaf J, Gouricha B, Chafia M, Stiribab Y, Vialcd C, Droguie P, Najaf J (2017) Electrocoagulation process in water treatment: A review of electrocoagulation modeling approaches. Desalination 404:1–21
23. Medvedeva ON, Kalyakin AM, Sautkina TN (2020) Ustrojstvo dlya intensifikacii processov ochistki zhidkosti ot primesej osazhdeniem (A device for intensifying the processes of liquid purification from impurities by precipitation). RU Patent 2732864

Peat and Charcoal in Treatment of Iron-Containing Production Wastewater in Pipe Industry

M. Bryukhov[1(✉)], D. Ulrikh[1], and S. Timofeeva[1,2]

[1] South Ural State University, 76, Lenin Avenue, Chelyabinsk 454080, Russia
`briukhovmn@susu.ru`
[2] Irkutsk National Research Technical University, 83, Lermontov street, Irkutsk 664074, Russia

Abstract. The treatment of wastewater occurring at separate stages of technological processes is one of the relevant problems for metallurgical plants, in particular, pipe and tube rolling ones. Acid wastewater with a high content of heavy metals occurs at the stage of etching and thermal treatment. To neutralize them, it is reasonable to use local sorption purification with cheap sorption materials. The purpose of the paper is to test charcoal and high-moor peat as sorbents for local treatment facilities in the pipe industry. The experimental research proved that high-moor peat from the deposits in the Chelyabinsk region and charcoal can be used as sorbents to extract heavy metals from acid wastewater of the tube and pipe facilities. The technology can be implemented both by means of sorbent addition into wastewater with a subsequent separation and in dynamic conditions by means of filtration through the sorption material layer. At the building of treatment facilities it is reasonable to use composite sorbents including charcoal and high-moor peat. The article also presents the analysis for the most promising methods of wastewater treatment, such as: phytoremediation; adsorption; ion exchange; electrodialysis; floatation; electrocoagulation and other. The authors highlighted the advantages and flaws of the methods enumerated.

Keywords: Natural sorbents · Peat · Charcoal · Iron-bearing wastewater · Wastewater treatment · Sorption filtering material

1 Introduction

The wastewater treatment in industrial facilities is a relevant contemporary problem due to a high potential hazard of environmental problems' occurrence. Industrial wastewater are peculiar and, in certain cases, contain complex multi-component mixtures dangerous for the human and environment. To remove them, it is necessary to develop complex treatment facilities. When iron-bearing acid water gets into reservoirs the ferrous hydroxide contained there absorbs dissolved oxygen and gradually evolves into ferrous hydroxide during oxydation. Ferrous hydroxide precipitates on the reservoir bottom and banks forming a large amount of rust-colored precipitation. In small reservoirs such drains can fully absorb dissolved oxygen which causes the elimination of organic life [1].

In most cases the reservoirs contaminated with iron-bearing acid drain water become inappropriate as the sources of household and technical water supply; that is why water disposal and wastewater treatment should take a special place in the work of each industrial plant.

The most wide-spread methods applied today for industrial wastewater treatment are provided in Table 1. Popular methods have their advantages and drawbacks, thus, to select the treatment technology for particular wastewater basing upon their chemical composition, pollutant concentration, equipment complexity, its energy consumption and treatment efficiency.

Each of the method enumerated has its application area. For example, ion exchange is used for the wastewater treatment with the hourly consumption of up to 500 m^3/h and metal concentration of up to 50 mg/dm^3; electrodyalisis—for wastewater with metal concentration from 2500 to 15,000 mg/l; floatation—to eliminate colloid suspensoids, small hard particles and dissolved susbstances; electrofloatation—to treat wastewater from weighed substances, heavy metals, resinous substances, suspended matters; electrocoagulationis applied for water drains with the consumption of up to 80 m^3/h and metal concentration up to 30 mg/l.

Today one of the most relevant methods of deep wastewater treatment and purification from heavy metals is a sorption method which allows a significant decrease of heavy metals concentration in wastewater with a possible use of purified drains in the closed systems of plant water circulation [2]. This method is covered in numerous scientific papers [3–12]. In addition, sorbents should meet the following requirements: efficient metal sorption in acid or weak acid environments characteristic for metallurgic wastewater drains, good filtration characteristics, comparatively low cost.

Today more and more attention is being paid to natural sorbents as their virtually unlimited reserves, low cost, wide spread of deposits, quite high adsorption properties make them economically feasible in terms of wastewater treatment.

The choice of this or that sorbent as a sorption-filtering material is based on the research of sorption characteristics, in particular: optimal pH of metal sorption, sorption capacity in static and dynamic conditions, sorbent fraction composition, its filtration properties, regenerating capacity and the specific surface area.

This paper studies the opportunity to develop a local sorption technology for purifying acid wastewater occurring during pipe production where their acid treatment in the etching and thermal workshop is one of the technological stages; it is based upon the application of natural sorbents, such as charcoal and high-moor peat.

2 Research Objects and Methods

The research object is washwater of the etching and thermal workshops. Wastewater at this stage is characterized by the unstable composition largely depending on the facility workload, the steel composition and grade of the pipes processed as well as the process peculiarities as it stipulates for DC component and a recurring washwater release. After pipe treatment with working mixtures (including in the etching tanks) the technological process stipulates for the transition of remaining solutions into washwater (rinse tanks and other tanks). These remaining solutions also take into a washwater drain by means of

Table 1 The most advanced methods for wastewater treatment

Methods	Treatment efficiency (η) (%)	(+) Advantages (−) Drawbacks
Phytoremediation	$\eta \approx 90$–99	(+) eco-friendly, possibility to process the biomass of macrophytes used (−) limitation of plant use by seasons, high metal concentrations can be toxic for macrophytes, need for large areas
Adsorption/absorption	$\eta \approx 80$–95	(**+**) selective component extraction; most frequently, the absence of method implementation in most cases (−) high cost at high metal concentration in the wastewater
Ion exchange	$\eta \approx 98$–99	(+) efficiency, eco-friendly nature, clean water at the output with minimum metal concentrations (−) increased cost, complex operation, lack of ion-exchange resins, need of ion-exchanger regeneration
Electrodialysis	$\eta \approx 96$–98	(+) opportunity to utilize valuable components (−) need of preliminary waster purification from organic substances, oils, hardness salts, SAS; quite a large consumption of electric energy, membrane deficiency, operation complexity, absence of selectiveness
Flotation	$\eta \approx 98$	(+) relatively low operation costs, simple equipment, precipitation of impurities (−) use of reagents to increase the contaminant hydrophobic properties
Electroflotation	$\eta \approx 87$–95	(+) opportunity of heavy metal winning, contaminants are collected in the upper par of liquid (−) need to water down high-concentrated solution, insignificant metal content reduction in the purified wastewater, material deficiency
Electrocoagulation	$\eta \approx 60$–90	(+) no need to use reagents, compact units, low sensibility to environment change during treatment (−) increased energy consumption
Reverse osmosis	$\eta \approx 99.6$	(+) high level of wastewater treatment (−) high operation costs for maintenance, need of pre-treatment

overflows, spills or tank leakage [1]. The aggregate compositions of wastewater formed during the technological process are provided in Table 2.

Table 2 Aggregate chemical composition of the acid drain

No	Indicator	Maximum value
1	pH value (pH)	2–4
2	Total ferrum, mg/l	250
3	Zinc, mg/l	105
4	Manganese, mg/l	6
5	Nickel, mg/l	6
6	Calcium, mg/l	100
7	Copper, mg/l	14
8	Lead, mg/l	1
9	Magnesium, mg/l	100
10	Silicon, mg/l	10
11	Sodium, mg/l	600
12	Potassium, mg/l	20
13	Chrome, mg/l	15

The paper studied wastewater occurring in the facility (Table 3).

Table 3 Metal concentration in the primary drain, mg/l

Al	Co	Cr	Cu	Fe	Ni	Pb	Ti	Zn	pH
9.24	0.20	4.26	0.54	207.22	2.47	0.49	0.02	12.09	2.16

Today peat is widely applied for wastewater purification from heavy metals and oil products [13–17]. The authors selected and tested the materials easily found in the Chelyabinsk region of all the known sorption materials.

The sorption process was studied in static and dynamic conditions by known methods [18–20].

In the static mode the sorption process was studied by means of the limited volume method at the ratio hard phase—liquid equal to 1:30. The sorbent was placed into a beaker, added the studied water sample and left for 7, 14 and 28 days without mixing at the ambient temperature of 283.15; 293.15 and 303.15 К. After the sorption process completion the authors took the solution sample over the sorbent to conduct chemical analysis. The analysis was conducted by means of spectrometry with the inductively coupled plasma at the atomic emission spectrometer with an inductively coupled plasma OPTIMA 2100DV.

Under dynamic conditions the research of the system "sorbent-water" with technogenic contaminants was conducted at a specially built unit allowing one to change the dynamic mode characteristics enumerated above. The rate of water motion in the system was set by the experiment conditions (0.3; 0.6 and 1.2 l/h) and supported by the pump constant parameters. At the experiment conduct the authors used sorbents with the fraction composition of 0.5–1.25 mm. The working layer thickness made 80 mm. Before the start of tests the authors defined the sorbent mass. The water volume with technogenic contaminants, contacted with the sorbent, was measured by a volumetric cylinder.

The method of experiment conduct included the following stages: setting the rate of the simulated solution feed into the research plant; measurement of the simulated solution pH and heavy metal cations content in the filtrate in certain periods.

The pH index was measured by the ion-meter I160MI. The content of admixtures in water was measured by the atomic emission spectrometer OPTIMA 2100DV (Perkin Elmer, USA). As the base solution the authors used water with a particular treatment degree obtained at the device "Simplicity UV" (France).

3 Results and Discussion

The study of metal sorption extraction in static conditions with the sorbents under research showed that the sorption of virtually all the metal ions studied reaches the maximum value in 1.5–2 h since the start of phase mixture while the completeness of the sorbate ion exchange with sorbent superficial groups significantly depends on the solution pH and temperature.

Table 4 provides data showing the dependence of metal cations adsorption on the sorbent type and the time contact with the sorbent under various temperatures.

The authors established that the temperature increase improves the sorption efficiency by the sorption studied. The pH solution with the charcoal increased to 7.29, with peat— to 5.52.

At the dynamic mode the sorption treatment of water with technogenic contaminants the following parameters are important: solution movement rate; sorbent fraction composition; thickness of the sorbent layer; ratio of the volume of the solution purified to the granule mass. The research results are provided in Figs. 1 and 2.

The experimental data by the efficiency of heavy metals sorption with high-moor peat and charcoal provided in Fig. 1 showed that, given the filtration rate of 0.3 l/h, the efficiency of iron-bearing wastewater and, correspondingly, the amount of metal cations occluded by the sorbent mass unit are higher than at the filtration rate of 1.2 l/h. The exception can be titanium sorption which demonstrated 100% purification at all the filtration rates under study. One should point that high-moor peat has the highest aluminium sorption at the filtration rate of 1.2 l/h. Therefore, at the development of the wastewater treatment technology it is necessary to recommend the range of filtration rates from 0.3 to 0.6 l/h or the use of peat and charcoal as a composite sorbent component.

The research proved that the maximum change of the drain pH with peat use is observed at the filtration rate of 0.3 l/h and is 5.28 while at the charcoal application the solution remains acid under various filtration rates.

Table 4 Efficiency of multi-component wastewater treatment with natural sorbents under various temperatures in the static mode

No	Indicator	Treatment efficiency, %								
		283.15 K			293.15 K			303.15 K		
		7 days	14 days	28 days	7 days	14 days	28 days	7 days	14 days	28 days
Charcoal										
1	Aluminium	99.8	99.9	99.9	99.9	99.9	99.9	99.9	99.9	99.9
2	Cobalt	94.5	97.0	99.9	96.5	98.0	99.5	98.0	99.5	100
3	Chrome	100	100	100	100	100	100	100	100	100
4	Copper	96.7	97.4	100	100	100	100	100	100	100
5	Ferrum	99.9	100	100	100	100	100	99.9	100	100
6	Nickel	88.3	97.3	98.9	96.4	98.5	98.9	98.1	99.1	99.35
7	Lead	100	100	100	100	100	100	100	100	100
8	Titanium	100	100	100	100	100	100	100	100	100
9	Zinc	96.4	99.2	99.8	98.9	99.7	99.8	99.6	99.9	99.9
pH		5.99	7.00	6.98	6.84	7.27	6.83	6.88	7.29	7.11
High-moor peat										
1	Aluminium	96.8	97.1	97.4	96.8	97.5	98.3	98.3	98.4	98.5
2	Cobalt	97.0	97.5	98.0	97.5	98.0	98.5	98.0	98.5	99.5
3	Chrome	99.9	99.9	99.9	99.9	100	100	99.9	100	100
4	Copper	99.6	99.8	100	99.8	100	100	100	100	100
5	Ferrum	99.7	99.9	99.9	99.8	99.9	99.9	99.8	99.9	99.9
6	Nickel	98.4	98.7	98.7	98.6	98.9	99.0	98.9	99.2	99.3
7	Lead	100	100	100	100	100	100	100	100	100
8	Titanium	100	100	100	100	100	100	100	100	100
9	Zinc	97.6	97.9	97.9	97.7	98.3	98.4	98.2	98.5	98.9
pH		4.18	4.52	5.38	4.28	4.49	5.52	4.37	4.84	5.47

4   Conclusion

The experimental research proved that high-moor peat from the deposits in the Chelyabinsk region and charcoal can be used as sorbents to extract heavy metals from acid wastewater of the tube and pipe facilities. The technology can be implemented both by means of sorbent addition into wastewater with a subsequent separation and in dynamic conditions by means of filtration through the sorption material layer. When building local treatment facilities it is reasonable to use composite sorbents including charcoal and peat.
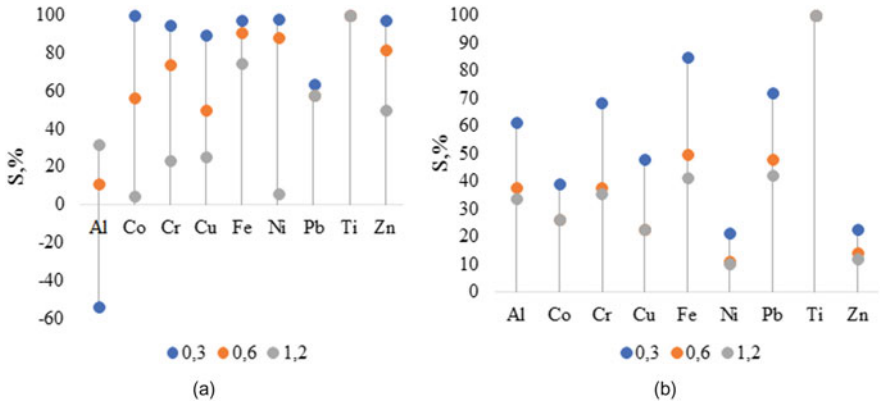
Fig. 1 Efficiency of treatment of a multi-component drain with natural sorbents (a—high-moor peat; б—charcoal) at various filtration rates (0.3; 0.6 and 1.2 l/h) in the dynamic mode
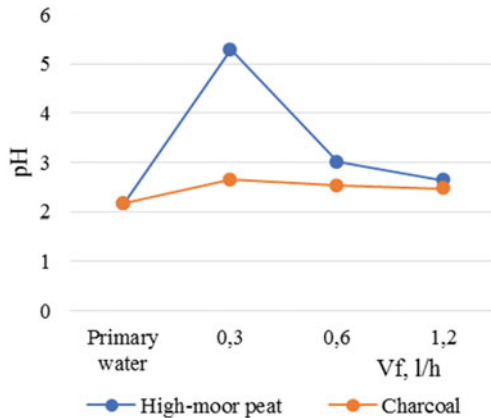

Fig. 2 pH change of the drain purified at various filtration rates in the dynamic mode

References

1. Khvang ST, Kammermeyer K (1981) Membrane separation processes/translated from English. Khimiya, Moscow
2. Laptedulche NK, Dremicheva ES (2014) Water: Chem Ecol 12:81
3. Gelfman MI, Tarasova YuV (2002) Research of sorption characteristics of natural and modified sorbent on the alumosilicate material basis. Khimicheskaya Promyshlennost 8:119–125
4. Egorova EY, Mitrofanov RY, Lebedeva AA (2007) Sorbent obtaining from pine nut shuck by low-temperature treatment. Polzunov News Bull 3:35–39
5. Zhukova IL, Khmylko LI (2009) Sorbents on the basis of cellulose-containing materials and their utilization. Ecol Indus Russia 7:30–33
6. Ulrich DV, Bryukhov MN, Zhbankov GO, Denisov SE, Timofeeva SS (2013) Measurements for advanced neutralized wastewater treatment applying the sorption method. Scienceand society: 4rd international scientific and practical conference, London, 141–147

7. Lesmana SO, Febriana N, Soetaredjo FE, Sunarso J, Ismadji S (2009) Studies on potential applications of biomass for the separation of heavy metals from water and wastewater. Biochem Eng J 44(1):19–41

8. Domracheva VA (2005) Wasterwater purification from heavy metals at application of sorbents from brown coals of Irkutsk coal field. Civil Protection 6:11–14

9. Zhang SJ, Shao T, Karanfil T (2011) The effects of dissolved natural organic matter on the adsorption of synthetic organic chemicals by activated carbons and carbon nanotubes. Water Res 45(3):1378–1386

10. Adsobent obtaining method on the peat basis. Patent RU 2102319, published on January 20, 1998

11. Epshtein SA, Meidel IM, Nesterova VG, Minaev VI (2012) Melik-Gaikazov Ya.I. Industrial wastewater treatment with peat-based reagents. Mining Inf Anal Bull 5:307–311

12. Epshtein SA, Titorova YuA, Meidel IM (2012) Recovery of precipitation from industrial wastewater treatment with peat-based reagents. Mining Inf Anal Bull 9:303–311

13. Cojocaru C, Macoveanu M, Cretescu I (2011) Peat-based sorbents for the removal of oil spills from water surface: application of artificial neural network modeling. Colloids Surf A 384(1):675–684. https://doi.org/10.1016/j.colsurfa.2011.05.036

14. Pandey S, Alam A(2019) Peat moss: A hyper-sorbent for oil spill cleanup - a review. Plant Science Today 6(4):416. doi:https://doi.org/10.14719/pst.2019.6.4.586

15. Heiderscheidt E, Leiviskä T, Lopez FC, Tesfamariam A, Postila H (2020) Suitability of natural and chemically modified peat as a sorbent material for mining water purification in small-scale pilot systems. Environ Technol Sep 2:1–12. https://doi.org/10.1080/09593330.2020.1812007

16. Brown PA, GillS SA, Allen J (2000) Metal removal from wastewater using peat. Water Res 34(16):3907–3916. https://doi.org/10.1016/S0043-1354(00)00152-4

17. Goher ME, Hassan AM, Abdel-Moniem IA, Fahmy AH, Abdo MH, El-sayed SM (2015) Removal of aluminum, iron and manganese ions from industrial wastes using granular activated carbon and Amberlite IR-120H. Egyptian J Aquatic Res 41(2):155–164

18. Timofeeva SS, Lykova OV (1986) Metal extraction from plating industry wastewater by industrial wastes of wood-processing and paper and pulp plants. Ore cleaning, Irkutsk, p 87–92

19. Timofeeva SS, Lykova OV (1990) Sorption metal extraction from plating plant wastewater. Chem Water Technol 5:440–443

20. Timofeeva SS, Lykova OV, Kukharev BF (1990) Sorbent use to extract metals from wastewater. Chem Water Technol 12(6):505–508